Bone Diagenesis: An Experimental Study of Selected Trace Elements.

by

Tracey Anne Elliott

A Thesis submitted in partial fulfilment
of the requirements for the degree of
Doctor of Philosophy

Department of Anthropology

The University of Durham
1993

Abstract

The present study describes investigations made into the diagenetic alteration of a range of trace elements in buried bone, and its relationship with physicochemical characteristics of the burial environment.

Laboratory-based uptake simulation experiments were designed to explore trace element uptake into bone. The effect of pH on spatial and temporal patterns of uptake and deposition were explored in bone with altered organic:inorganic ratios. These studies have focused on strontium and uranium because of their routine application in palaeodietary and chronometric/palaeoenvironmental studies, respectively.

The uptake of strontium into bone was found to be rapid, and resulted in its homogeneous distribution throughout the cortex, i.e. it demonstrated a cross-cortical pattern hitherto assumed to be uncharacteristic of contamination. While strontium uptake was observed predominantly in the inorganic component of bone, the mechanism of uptake appeared to be dependent on ambient pH conditions: this highlights an extrinsic source of variability, defined by the burial environment, and superimposed on biogenic strontium levels.

In contrast, uranium was taken up into both inorganic and organic components; pH conditions again determined the mechanism of uptake within each respective matrix. Furthermore, uptake was clearly more pronounced under alkaline conditions, and it is proposed that, in addition to the redox potential, the alkalinity of the burial environment is an important parameter in determining uranium levels in buried bone and thus in its subsequent archaeometric application.

Field studies were carried out in parallel with uptake simulation work for comparative purposes. Archaeological bone material was excavated from different geochemical environments, representing both terrestrial and marine burials. Examples of bone diagenesis are illustrated using the Scanning Proton Microprobe, a novel technique for such application, which revealed the diagenetic alteration of a broad range of trace elements that were not detected using more conventional instrumentation.

Certainly, both fieldwork and laboratory-based uptake experiments confirm that the trace element content of exhumed bone is essentially dependent on the physicochemical properties of the burial environment. The significance of this fact is discussed in relation to palaeochemical studies in the endeavour to derive an accurate evaluation of the past.

Acknowledgements

I welcome the opportunity to thank those who have given me guidance and support during this long but rewarding endeavour. I am grateful to Dr. Terry Williams at the Natural History Museum, London, for his continued encouragement and interest in my research, and for his valuable comments and proof-reading skills. Thanks are due both to my supervisor, Mandy Marlow, and to Professor Alan Bilsborough for their support and for proof-reading my thesis.

I should also like to thank the following for their technical assistance: Dr. Geoff Grime and the Oxford SPM Unit (Department of Physics, Oxford), and Dr. Chris Jeynes and Mickey Chan (Department of Electronic and Electrical Engineering, Surrey) for their proton microprobe wizardry; Ron Hardy (Department of Geological Sciences, Durham) for his X-ray X-pertise; Grant Staines (Department of Material Science, Newcastle) for his electron microprobe skills; Victor Din (Natural History Museum, London) for his spectrometric "aspirations"; and John Davies for introducing me to the delights of image analysis. I am also grateful to Andrea Summerson for keeping me well-equipped with laboratory supplies; and to Trevor Anderson (Canterbury Archaeological Trust), Cleveland County Archaeology, Neil Garland, and Chris Scull for kindly donating archaeological material. I should generally like to thank other members of academic and technical staff who I have encountered within Durham University's Departments of Geography, Chemistry and Biological Sciences as a result of the multi-disciplinary nature of my research.

This work was primarily supported by the Science and Engineering Research Council and thanks must also go to the Department of Anthropology, Durham, for providing additional financial support for conference purposes.

I thank my friends for their moral support and, at times, bemusement.

Finally, I salute my family - Mum, Dad and Kerry - for their unfailing encouragement and confidence in my abilities, and for their unconditional love and understanding.

Contents

Chapter I

Introduction.

1.1 The Palaeochemistry of Bone.

The chemical composition of human bone excavated from archaeological contexts has been used to provide the biological anthropologist with a wide variety of information, including palaeodiet, relative and chronometric dates, palaeohydrology, and climate.

The study of past subsistence can be directed at examining various aspects of the diet: the contribution of plant versus animal material (Schoeninger, 1979; Sillen and Kavanagh, 1982), the identification of marine and terrestrial components (Chisolm *et al.*, 1982, Schoeninger and DeNiro, 1984), and the presence of certain species in the diet (van der Merwe, 1982). While a number of research approaches have been applied to the study of diet, based on faunal analysis, palaeoethnobotany, faecal studies, dental studies of wear and caries, many of these studies possess serious deficiencies in their methodology; for example, the limitations imposed by the preservation of organic material. However, both the elemental and isotopic composition of bone is able to provide a potential wealth of quantitative information for dietary reconstruction. The basis of such reconstruction derives from the fact that certain food categories differ from others in specific aspects of their composition. For example, foods derived from animal and plant sources differ in both strontium concentration and in stable nitrogen isotope ratios (Sillen and Kavanagh, 1982; Schoeninger, 1985) which is in turn reflected in the composition of bone, registered by analysis of both inorganic and organic components.

Furthermore, information about the diet of past human populations can be used to make deductions about factors influencing dietary composition, such as cultural and agricultural factors, individual factors (including socio-economic aspects), and environmental conditions (climate, season etc.) (e.g. Runia, 1988 ; Schoeninger,

1979). In this way, dietary information concerning ancient populations can essentially characterise their trophic position, utilisation of the environment, determinants of site location, the nature of subsistence activities, status differentiation, and palaeo-climate among others.

The palaeo-climate itself has been assessed using the chemical composition of bone as an indicator (Rottlander, 1976), based on the principle that bone preservation is related to the temperature and hydrology of the burial environment. In turn, a number of researchers (Henderson *et al.*, 1987; Williams and Marlow, 1987; Williams and Potts, 1988) have used the distribution of uranium and the rare earth elements (REE's) in bone to elucidate the nature of the palaeoenvironment, specifically the hydrology, of a site.

Uranium concentration in fossil bone can also be used to date bone material, by fission track and Uranium Series (USD) dating procedures (e.g. Szabo, 1980; Korkisch *et al.*, 1982 ; Tiemei and Sixun, 1988). Other chronometric techniques utilising bone chemistry include radiocarbon dating and amino-acid racemization (reviewed by Taylor, 1987).

Therefore, the chemical composition of exhumed bone is used to obtain a wide variety of information about the lifestyle and chronological context of past populations. However, such approaches rely on a number of assumptions about the behaviour of buried bone, and the type and rate of any postmortem change during inhumation, which it is becoming increasingly evident may not always be correct. Analysis of ancient diet using, for example, strontium/calcium ratios requires that elemental levels correspond to those present at the time of death i.e. that they reflect *in vivo* conditions. In contrast, the Uranium-Series dating method relies on time-related changes: the assumption that uranium is rapidly taken up into bone around the time of its deposition, and subsequently remains stable there to undergo its natural decay pathway. However, as bone decays and is fossilized, the natural process of *diagenesis* serves to alter the chemistry of bone from its ante-mortem state via leaching and/or deposition processes.

1.2 Bone Diagenesis.

Diagenesis, or the postmortem alteration of buried bone, involves a wide range

of elements (Klepinger *et al.*, 1986), and their uptake into bone from surrounding groundwaters during fossilization is well-documented (e.g. Henderson *et al.*, 1983; Badone and Farquhar, 1982).

Elements introduced by groundwaters in the burial environment may become associated with buried bone in a number of ways. They may reside in pores, voids or microcracks; form complexes with the organic component; adsorb onto the surface of hydroxyapatite crystals; or be directly incorporated into the hydroxyapatite matrix via heterionic exchange. However, many of these processes are complex and are not well-characterised due to their unpredictability. Certainly, diagenesis is now firmly acknowledged as a problematic factor in archaeological studies that are based on both the inorganic composition of bone e.g. Henderson *et al.*(1983), Lambert *et al.*, (1985), Kyle (1986), Sillen (1989), Price (1989), and on the organic composition e.g. DeNiro (1985), Bada (1985).

While some workers have attempted to devise methods of overcoming the effects of diagenesis, e.g. Sillen (1989), Sillen and LeGeros (1991), Lambert *et al.*(1989,1990,1991), others state that the problem is insurmountable e.g. Hancock *et al.*(1989) because of contaminants introduced into bone both during burial *and* during preparation for subsequent chemical/physical characterisation.

1.3 The Study of Bone Diagenesis.

A variety of analytical approaches have been applied to the study and identification of diagenesis. Tests to evaluate the extent of diagenetic alteration have compared physical and chemical properties of modern, unaltered bone to those of archaeological samples. Physical characterisations include microscopic examination to explore microstructural preservation (White and Hannus, 1983; Grupe and Piepenbrink, 1988; Schoeninger *et al.*, 1989) and the monitoring of the crystallinity of bone mineral (Tuross *et al.*, 1989b). Chemical or quantitative characterisations include the determination of mineral:organic ratios and measurement of calcium:phosphorus ratios, and their departure from normal/unaltered values (2.33 and 2.17 atomic percent, respectively); these provide a rather crude identification of diagenesis but give no indication of the specific nature of any change.

Quantitative characterisations of more interest here depend on trace element analyses of archaeological bone. Comparison of dense long bones (usually femora) to relatively more porous rib bone may reveal differences in composition as a result of differential susceptibility to diagenesis (Grupe, 1988; Lambert *et al.*, 1985). The presence of elements commonly found in groundwaters but otherwise in immeasurably low concentrations in unaltered bone (such as uranium, yytrium and the REE's) might suggest the presence of other contaminants (Williams and Marlow, 1987; Williams and Potts, 1988; Williams, 1988). Moreover, elements have been classified into those that are typically introduced during burial, those that may be leached out over time, and those that are apparently unaffected (e.g.. Parker and Toots, 1980). Such generalisations, though in some cases controversial, serve simply as guidelines for experimental design in the evaluation of diagenetic activity. One such design comprises electron microprobe investigations of elemental cross-cortical distribution profiles within buried bone *and* the adjacent soil matrix, identifying contaminants on the basis of gradient patterns indicative of diffusion (e.g. Lambert *et al.*, 1979 and 1983).

Nevertheless, such designs are hampered by the fact that "the direction and intensity of diagenetic change is not necessarily spatially and temporally uniform" (Sandford, 1992). In approaching the problem of diagenesis from another angle, several workers have devised methods that attempt to reduce contaminatory effects prior to inorganic analysis. These include mechanical cleaning (Lambert *et al.*, 1989), chemical cleaning (Sillen, 1986 and 1989; Price *et al.*, 1992), and sequential washing (Sillen, 1986 ; Lambert *et al.*, 1990). However, there is still some concern about the effects of such procedures on biogenic composition and, indeed, their efficiency in removing contaminant material.

Therefore, many strategies have been employed to identify, evaluate and compensate for diagenetic alteration, and ideally a multi-disciplinary approach is required for any palaeochemical study on bone in order to minimise problems arising from the complexity, variability and unpredictability of diagenesis.

1.4 "The Challenge".

Diagenesis includes the processes of dissolution, precipitation, adsorption, mineral replacement and recrystallisation (Pate and Hutton,1989). These processes

and their rates of reaction will naturally depend on the physical and chemical characteristics of the burial environment. To avoid drawing false inferences about palaeodiet, chronology etc. that are made on the basis of inorganic analysis, it is necessary to understand the conditions that promote diagenesis, the mechanisms whereby it takes place, and the specific inorganic elements that it affects.

Sillen, in 1989, called for a "more aggressively experimental" approach to meet fundamental problems in palaeochemistry imposed by diagenetic alteration of bone, and while a number of studies have taken up this challenge in the form of laboratory-based exploratory investigations (e.g. Lambert *et al.*, 1985; Pate and Hutton, 1988), the potential opportunities available in this field have yet to be fully exploited.

1.5 "The Reply": The Present Study.

The following account describes a series of laboratory-based experiments that attempt to simulate the uptake into bone of trace elements judged to be of importance in palaeodietary and dating studies. The data are recorded using a number of the aforementioned approaches together with novel uptake simulation strategies designed to identify and evaluate diagenesis, and incorporating a variety of analytical instrumentation. The predominant analytical strategy, however, is concerned with microprobe analysis of bone material, so that the cross-cortical and micro-distribution of elements can be plotted, and inferences made concerning the mechanism(s) of interaction based on micro-locational detail (the intimate association of the deposited element with the bone's microstructure).

Generally, simulation experiments involve the immersion of bone samples in buffered solutions of varying chemistries maintained under different environmental conditions. Sillen (1989) indicates that the critical variables in the diagenetic alteration of bone are the duration of interment and the depositional environment. Accordingly, temporal patterns of elemental uptake are investigated to explore the effects of variable exposure to elements in solution. In order to keep the experimental system as elementary as possible, and thus more readily interpretable, the **environment of reaction** encompasses up to three variables at any one time: the **element under investigation, temperature** and **pH.** Soil pH (Gordon and Buikstra, 1981) and temperature (Von Endt and Ortner, 1984) are among the

most important variables in the chemical environment of soil-buried bone that influence diagenetic processes.

Diagenesis is also influenced by factors intrinsic to bone itself, such as bone size, density, biochemistry and microstructure (e.g. Von Endt and Ortner, 1984; Grupe, 1988). Furthermore, the diagenesis of bone is to a large extent related to the degree of preservation of the bone's structural integrity as defined by the intimate association of organic and inorganic components: as this association is compromised during postmortem decay of one or both components, the bone matrix is more vulnerable to external influences. The diagenesis of bone mineral, for example, is closely related to and influenced by the breakdown of the organic matrix (Sillen, 1989; Von Endt and Ortner, 1984). For this reason, the **organic-inorganic ratio** of bone exposed to simulated groundwaters is altered and the subsequent effect on elemental uptake noted. In a further investigation, the chemical separation of whole bone into organic and inorganic components is explored in order to determine the relative contribution of each fraction in elemental uptake.

Diagenetic effects on **bone crystallinity** are also explored using X-ray diffraction (XRD) spectrometry, a method that has itself been used to document diagenesis (Sillen, 1989; Tuross *et al.*, 1989b). Diffraction studies provide a means of identifying diagenesis on the basis of changes in crystallinity which may result from recrystallisation, ionic exchange, or the incorporation/adsorption of various mineral phases. Therefore, such studies may reveal the effects of the experimental immersion treatment and potentially distinguish between the actual mechanisms of interaction.

The simulation experiments concentrate on the uptake of two trace elements: **strontium** and **uranium**. Naturally, the importance of understanding the post-depositional activity of strontium and uranium is paramount because of their routine applications in palaeodietary and dating studies, respectively.

Strontium is the most widely studied element for palaeodietary analysis (Brown, 1973; Sillen and Kavanagh, 1982). While some studies have reported that strontium is relatively unaffected by diagenesis, and therefore provides a reliable biogenic signal (Henderson *et al.*, 1983, 1987; Klepinger *et al.*, 1986), others report a dramatic change in strontium concentration over time (Sillen, 1981; Nelson *et*

al., 1986; Sealy and Sillen, 1988). These discrepancies can almost certainly be attributed to differences in the depositional environment, and the potential for diagenetic alteration is worthy of consideration in all depositional contexts. Price *et al.*(1992) state that "there is no longer any doubt that diagenesis can modify the levels of bone strontium, either through direct changes in strontium levels or through the enrichment/depletion of other elements such as calcium and phosphorus."

Uranium is the most documented element (Henderson *et al.*, 1983; Williams and Marlow, 1987; Williams, 1988; Williams and Potts, 1988) used to examine diagenesis in the suite of elements that are commonly found in groundwater but virtually absent in bone (others include yttrium, thorium and the REE's): this property warrants their use as indicators of diagenetic activity. Furthermore, uranium in exhumed bone has chronometric applications (the Uranium Series Dating method) and can also be used to derive information about the palaeohydrology of a site (Williams, 1988). Therefore, the uranium content of archaeological bone is important in that it is used as a measurement for dating bone, as a diagnostic tool in identifying diagenetic activity, and at the same time may characterise aspects of the burial environment itself, since the mobility of uranium in groundwaters appears to be largely dependent on the redox conditions of the environment (Williams and Marlow, 1987).

In order to explore further the relationship between bone and corresponding burial environment, examples of archaeological bone material in context are provided by **field studies**. Bone excavated from a variety of burial environments, representing both terrestrial and marine sites, contributes illustrative examples of the diagenetic alteration of a suite of major, minor and trace elements in archaeological bone. A brief physical and chemical description of corresponding burial matrices are included, so that trends in elemental deposition can be monitored and those of strontium and uranium compared with experimental findings.

1.6 Summary.

To summarise, experiments are designed to artificially simulate the uptake of both strontium and uranium into bone, and to explore the influence of a number of physicochemical factors (defining the environment) on spatial and temporal patterns of uptake. Furthermore, the relative contribution of both organic and inor-

ganic components in the deposition process are considered in an attempt to clarify mechanisms of interaction. Archaeological material, the majority from characterised burial contexts, provides examples of diagenetically altered bone with which to compare experimental observations.

1.7 Thesis Plan.

The thesis is divided into four sections. The first discusses the processes controlling elemental deposition in ante- and postmortem contexts, termed by Sandford (1992) as the *biogenic-diagenetic continuum.* This necessitates a description of the biochemistry, anatomy and physiology of living bone (Chapter 2), since the chemical structure and properties of bone contribute the "intrinsic factors" influencing diagenesis, forming the connection between pre- and postmortem mechanisms of elemental deposition. Chapter 3 describes the "extrinsic factors" that influence diagenesis - those of the burial environment, including the natural geochemical abundance and distribution of strontium and uranium, and detailed accounts of the decay, fossilization and diagenesis of bone. Studies that have successfully identified diagenesis, together with current methods used both to evaluate and reduce the effects of diagenesis are reviewed in this chapter.

The second section provides an account of the research work conducted for this thesis. Chapter 4 comprises a description and justification of research design and methodology, including the analytical instrumentation employed. Having reviewed the present research work from a theoretical angle, a more practical account is presented in Chapter 5 which details experimental procedure, specifying materials, sample preparation, treatment and subsequent analytical operation.

Experimental data are presented in the third section, comprising four chapters. Chapter's 6 and 7 describe results from strontium and uranium uptake simulation experiments, respectively. Chapter 8 focuses on specific aspects of the immersion process, examining its effects on crystallinity and organic content, and explores cation exchange properties in more detail. Field studies, conducted in parallel with uptake experiments to provide case studies, are described in Chapter 9, which includes some methodology of field- and laboratory-based procedure, a description of the sites and details of qualitative and quantitative data.

Finally, the fourth section is concerned with the discussion and implications of the results detailed in Chapters 6 to 9. In Chapter 10, both laboratory and field data are collated for studies exploring (1) bone diagenesis in general, (2) strontium and (3) uranium uptake. Mechanisms of elemental deposition are considered. Furthermore, the competence and pertinence of research methodologies and technical instrumentation employed in this study are assessed, together with their applicability to further study of bone diagenesis.

To conclude, I propose recommendations and directions for future study of the evaluation and control of diagenetic effects in buried bone, to enable more accurate and realistic assessment of the human past.

Part I

Background

Chapter II

Anatomy and Physiology of Bone.

2.1 Introduction.

The *dynamic* nature of bone refers to the ability of this tissue to exist in a dynamic relationship with its immediate environment. This property, together with its unique microscopic structure, is fundamental to the understanding of variability in the elemental composition of bone, both in biological (*in vivo*) and geological contexts.

Throughout life, the skeletal system plays an essential role in maintaining mineral homeostasis (Neuman, 1980; McLean and Urist, 1955) by effectively serving as a mineral reservoir, where ions are deposited and released according to physiological demand. In this way, information about dietary constituents is recorded in the chemistry of bone, and it is this principle that provides the rationale behind palaeodietary studies. Furthermore, other dynamic processes (elemental absorption and excretion, for example), together with a variety of physiological states such as growth, pregnancy and lactation, are able to influence these constituents to shape "biogenic" concentrations of major, minor and trace elements in bone (Parker and Toots, 1980; Blakely, 1989).

Bone is no less dynamic in soil-buried, archaeological contexts. The nature of its microstructure confers a susceptibility to ionic exchange with the surrounding burial environment, such that bone is vulnerable to postmortem chemical alteration by contact with most soils (Pate and Hutton, 1988).

Therefore, the chemical composition of bone may be altered in both antemortem and postmortem contexts. The presence of minerals of dietary, physiological and/or diagenetic origin is the product of interaction between bone and its environmental milieu.

The chemical and structural nature of bone is fundamental to mechanisms of elemental uptake and deposition. In this chapter, the anatomical structure of bone, at both a macroscopic and microscopic level, is discussed in conjunction with physiological aspects of elemental uptake.

2.2 The Structure of Bone.

2.2.1 Macroscopic Structure.

The classification of bones is generally based on their function, mechanism of formation and general morphology (Bourne, 1971). On a gross level, bone tissue is built up into specific bony frameworks which are adapted to the form and function of particular bones. These frameworks are permeated with cavities and canals of varying size containing blood vessels, nerve fibres, and a variety of cells which, through their resorbing and depositing abilities, endow bone with the capacity to remodel and repair. Macroscopically, all bone tissue is composed of two basic architectural structures:

(1) cortical or compact bone, which, with the exception of microscopic channels, is a dense mass forming the outer wall (surface covering) of all bones; and,

(2) trabecular or cancellous bone, consisting of a lattice of rods, plates and arches individually known as trabeculae, which is primarily limited to the central regions of bone and contains marrow.

In fact, the two bone structures differ radically in their bone marrow or soft tissue content. The soft tissue content of cortical bone is usually less than 10% by volume, whereas it is 75% by volume in trabecular bone. Consequently, the mass of an adult human skeleton is composed primarily of cortical bone (approximately 80%) (Shipman *et al.*, 1985).

The transverse section of long bones (humerus, femur, tibia etc.) is referred to throughout the present study, and provides a simple descriptive model for the macroscopic structural arrangement of bone. Figure 2.1 shows a schematic view of the shaft of a long bone, highlighting the major anatomical features described in this study. The outer surfaces are covered by a sheath of fibrous connective tissue and an inner cellular layer of undifferentiated cells, the *periosteum*. The

marrow cavity and cavities of cancellous bone are lined by a thin cellular layer, the *endosteum*. Both these layers possess osteogenic properties and thus play an essential role in the dynamicity and plasticity of bone in gross remodelling (Frost, 1980; Bourne, 1971).

In the present study, the transverse section of bone is divided into three main cortical regions: (1) the *periosteal cortex*, representing the compact bone in the outer cortical region; (2) the *endosteal cortex*, representing the trabecular bone adjacent to and permeating into the marrow or medullary cavity; and (3) the *mid-cortex* between the two, representing the largest area in transverse section (T.S.).

2.2.2 Microscopic Structure.

Adult mammalian bone, whether compact or cancellous, is lamellated. Regularly spaced throughout lamellar bone are small cavities, or lacunae, connected by thin tubular channels called canaliculi. Both cavities and channels are occupied by bone cells or osteocytes, which may be bone-forming (osteoblasts) or bone-resorbing (osteoclasts). Canaliculi open to extracellular fluid at bone surfaces, and thus form an anastomosing network for the nutrition and metabolic activities of the osteocytes (Shipman *et al.*, 1985; Bourne, 1971).

Most human compact bone is made up of structural units called osteons or Haversian systems, each consisting of a central or Haversian canal surrounded by concentric lamellae (Figure 2.2). Each canal has a diameter between 30 and 70 microns and contains nutrient vessels, nerves and connective tissue. These canals, running longitudinally through bone communicate with the periosteum, bone marrow and each other via channels - Volkmann's canals - that run oblique or transversely through bone (Figure 2.1).

In contrast, cancellous bone consists of a network of anastomosing trabeculae with intertrabecular spaces that contain bone marrow. Trabeculae are generally less than 0.2 mm thick and are avascular. They therefore rely on diffusion processes for nutrition by canaliculi extending to the trabecular surface.

Figure 2.1: Schematic Diagram of a Long Bone in Section to Identify Major Macroscopic Features of Interest.

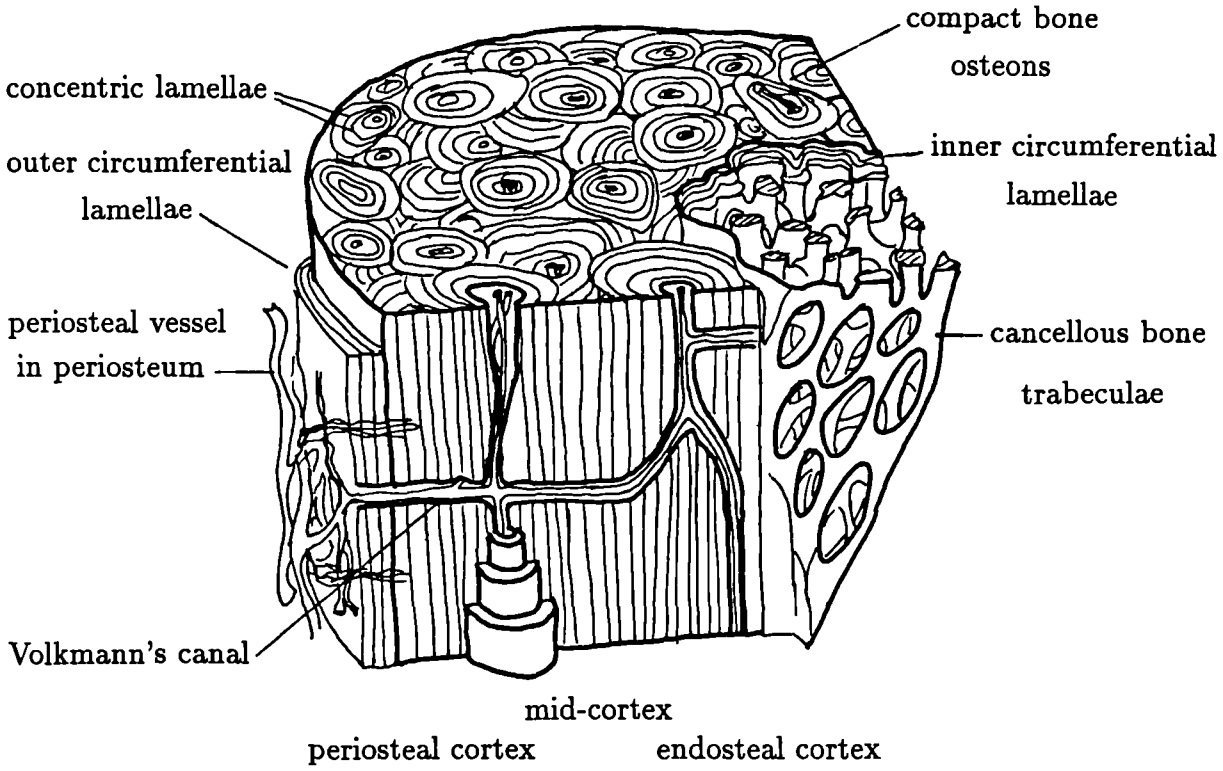

Figure 2.2: Cortical Bone in Transverse Section to Show the Microstructure of Osteons.

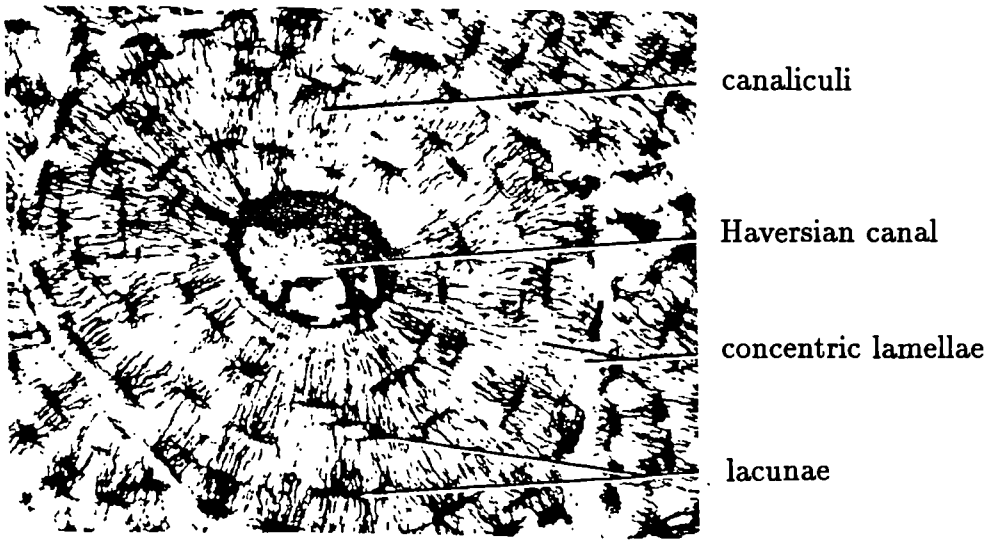

2.2.3 Blood-Bone Exchange.

The physiological processes occurring within bone are dependent on the presence of an adequate blood supply which provides nutrition and sustenance for the tissue, enabling it to perform its roles as a mineral and skeletal homeostatic mechanism. Both electrolyte and acid-base substances exchange between blood and bone tissue, and both rapidly acting (within 20 minutes or so) and slowly acting (within several weeks and years) modes of exchange exist (Willans *et al.*, 1986).

A variety of models for blood-bone exchange have been described, such as the "percolation hypothesis" (reviewed by Frost, 1981) which proposes two separate exchange phenomena:

(1) the volume phenomenon, whereby water percolates through the ultramicroscopic channels (Haversian systems) to which the canalicular network and Volkmann's canals lie oblique and transverse, thus interconnecting canals. This allows for an enormous surface area of bone mineral to be exposed to a relatively small volume of extracellular fluid, and admits small molecules and ions through the percolation bed, which probably provides the chief mechanism for the 'slow exchange' fraction between blood and bone.

(2) the surface phenomenon, whereby at any instant numerous discrete bone surface regions very rapidly turn over and exchange with their chief mineral ions and water with the blood. This phenomenon probably accounts for the 'fast exchange' fraction, and is controlled by metabolic state.

To summarise, the microstructural organisation of bone is such that it is able to respond rapidly to changes in physiological demand by maintaining an intimate association with percolating body fluids that convey metabolic "messages" or hormones (for example, calcitonin, parathyroid hormone) containing information about current metabolic state. The structural components of bone can then react appropriately, so that trace elements, for example, are either released or deposited in accordance with metabolic demand.

2.3 The Composition of Bone.

Structurally, bone is composed of an organic component and a mineral component, whose matrical structures are intimately associated. While trace elements may be associated with the organic matrix, their uptake and deposition are largely a function of the inorganic component and its physicochemical properties.

The structural organisation of both components and, as a consequence, their relative role in the metabolic regulation of trace elements are discussed in turn.

2.3.1 The Organic Component.

The organic component of bone makes up around 20-25 % of its dry weight and consists chiefly of Type I collagen (Hare, 1980). In fact, collagen accounts for approximately 90% of the organic matrix.

Collagen is made up of three polypeptide chains (α chains) folded into a rod-like, left-handed, triple-helical molecule about 300 nm long and 1.5 nm diameter: these three chains are then twisted around each other into a right-handed spiral or supercoil to form a tropocollagen molecule. The arrangement of amino-acids in these chains is essential for the assembly of these triple helical molecules into collagen fibrils. The aggregation of collagen molecules is such that each is longitudinally displaced about one quarter its length relative to its nearest neighbour: this longitudinal molecular staggering is responsible for the characteristic spacing/banding pattern of the microfibrils under the electron microscope (Hodge *et al.*, 1963).

Non-collagenous proteins (NCP's) account for approximately 5 % of total osseous protein by weight, and include glycoproteins, phosphoproteins, proteoglycans, proteolipids, sialoproteins and serum-derived proteins (Boskey and Posner, 1984; McLean and Urist, 1955). They serve a number of functions: they influence the initiation and growth of mineral crystals, mediate hormonal influences, and promote/regulate cell proliferation and tissue growth (Boskey and Posner, 1984). NCP's are important constituents of the amorphous "ground substance" that is interspersed among the collagen fibres.

2.3.1.1 Trace Elements in the Organic Matrix.

The role of the organic matrix in elemental uptake and deposition is apparently of minor importance despite its potential to form organo-metallic bonds. An organometallic compound is one where a metal is linked, usually by a covalent bond, directly to carbon. So, most organometallic bonds are polar-covalent.

Very few studies have been carried out to investigate the role of the organic matrix in elemental uptake and deposition. Perhaps the most relevant work, however, is that of Spadaro (Spadaro and Becker, 1970; Spadaro *et al.*, 1970). Spadaro and Becker (1970) explored the metal binding properties of relatively intact collagen matrices in model systems consisting of aqueous solutions of several ionic salts in order to elucidate the nature of any direct interactions between collagen proteins and metal ions. Whole sections of tendon and bone matrix whose inorganic component had been chemically removed were exposed to 24 metallic ions, and relative uptakes were determined by emission spectroscopy of the substrates.

Size-specific interactions were observed for collagen matrices: the preferentially bound ions fell predominantly into two size categories of ionic radii 0.065-0.075 nm and 0.12-0.13 nm. These categories were apparently independent of ionic charge and experimental conditions, and ions included copper and zinc in the smaller group, and lead and silver in the larger (evidence of strontium, radius 0.113 nm, uptake was not definitive).

Furthermore, a linearity was observed between uptake and ionisation potential, indicative of coordination bonding (or chelation) in collagen matrices. Indeed, many of the strongly bound (monovalent and divalent) ions readily coordinate with donor nitrogens, so bonding may potentially occur with uncharged amino, imidazole and guanidino groups on amino-acids, and are probably ion-polar or covalent in nature (Spadaro *et al.*, 1970).

Nevertheless, despite this potential, very few trace elements appear to be associated with this bone fraction. Several cations are thought to be deposited specifically in the organic matrix, such as barium, cerium, plutonium and yttrium; and while a few essential trace elements, such as iron, copper and zinc, may be deposited to

some extent in the organic matrix, most trace elements are primarily located in the inorganic fraction.

2.3.2 The Inorganic/Mineral Component.

The inorganic or mineral phase accounts for 60-70 % of the dry weight of adult bone. The principal chemical constituent of bone mineral is calcium phosphate, which is present in both crystalline and amorphous forms (Posner, 1969; Neuman, 1980). This distinction is based on the level of structural organisation displayed by the constituents of a chemical solid, or the degree of crystallinity displayed by its constituents. Crystallinity is a term which implies large crystal size and absence of structural defects (Jenkins and deVries, 1978), and can be defined as the extent to which the atomic structure has controlled the outward form of a substance, ranging from a crystallised form to an amorphous one. Crystalline solids are composed of groups of regularly repeating "unit cells" arranged in a three-dimensional pattern or "crystal lattice". In contrast, structural units of amorphous solids are arranged in a more disorganised configuration, where ordering may be present in localised areas.

The predominant *crystalline* form of skeletal calcium phosphate is **hydroxyapatite**, whose general formula (or unit cell) is $Ca_{10}(PO_4)_6(OH)_2$. The whole crystal of hydroxyapatite can be viewed as translationally periodic repetitions of this unit cell and essentially forms a right rhombic prism which, when stacked, forms a simple hexagonal lattice (Cameron, 1971).

This three-dimensional complex structure is essentially made up of a number of components, representing different propensities and locations for the uptake and/or release of ions. These essential components are: (1) interior ions within the crystal, (2) ions at the crystal surface, and (3) the surface hydration shell (Buikstra *et al.*, 1989; McLean and Urist, 1955).

The crystal structure, together with the amorphous content of the mineral presents a huge specific surface area of 100-200 m^2g^{-1}, as measured by nitrogen adsorption (Posner, 1985). 20 % of this surface area is in pores in the bone mineral that are exposed after removal of the organic matrix. The surface area allows for the adsorption, substitution and release of inorganic ions to and from interstitial fluids

and the blood supply. Since the chemical constituents of living bone can vary significantly via these processes, it is essential to delineate the normal *in vivo* properties, structure and elemental concentrations of bone before embarking on the accurate interpretation of ancient skeletal material.

Therefore, the most important features of biological apatite for consideration are the large and reactive specific surface resulting from small crystal size and their crystal imperfection and non-stoichiometry (Posner *et al.*, 1981). Bone mineral differs significantly from stoichiometry in that its calcium/phosphate ratio is lower than predicted from the chemical formula (Jenkins, 1978), relating to its poor crystallinity: the calcium deficiency confers a relatively higher reactivity on biological apatite (Sillen, 1989). Thus, hydroxyapatites not only have a high specific surface but also have crystal surfaces that are reactive to specific molecules: it is the combination of these two factors which assures that bone mineral is in metabolic interrelationship with the rest of the body through body fluids. The large surface area is a major factor in the chemical and physical properties of hydroxyapatite, greatly magnifying any effects due to substitution or adsorption of ions which can drastically alter the local composition of crystallites and thus affect crystal habit and bonding and the electronic structure.

Furthermore, the size and shape of bone apatite crystals are related to species, age and disease state. In any species, the average crystal size increases with age, often in correlation with fluoride content, until maturity, at which time there is a levelling off in growth processes. With the increase in crystal size, there is a concomitant improvement in chemical perfection with growth i.e. an improvement in crystallinity. In fact, there is considerable evidence that amorphous calcium phosphate, including dicalcium phosphate and octacalcium phosphate, is the first mineral deposited and acts as the precursor to hydroxyapatite. Certainly immature, less-calcified bone contains a higher proportion of amorphous mineral (Posner, 1969); with time, this mineral changes quickly to a poorly crystalline hydroxyapatite, which is initially calcium and hydroxyl ion deficient, and with maturation approaches, but never reaches, the perfect hydroxyapatite formula (Posner, 1969; Posner *et al.*, 1981).

The plate-like crystallites of adult bone mineral are generally 10 nanometers or

less in size and often only a few unit cells in dimension (Jackson *et al.*, 1978). The average crystal dimension is 20x20x40 nanometers, and is normally longer in the c-axis direction, so that most of the surfaces are made up of ac faces (the 3-dimensional structure of a crystal is described according to three perpendicular axes which are designated a, b and c axes). Generally each face consists of exposed calcium, phosphate and hydroxyl ions, so that the surface has highly charged positive and negative ions and is able to interact strongly with both cations and anions in solution, and with polar molecules in solution or in gas phase.

Therefore, surface areas of bone are more accessible to ions in body fluids by virtue of the *microcrystalline* nature of individual bone crystals (Neuman, 1980). Owing to their propensity for ionic exchange, surface regions have a chemical nature that is characterised as a highly dynamic system with a labile structure (McLean and Urist, 1955), and thus reflect the mineral homeostatic role of the skeletal system.

The apatite structure is tolerant of many ionic substitutions and vacancies so that the chemical composition of hydroxyapatite may vary over wide limits, while the basic apatite structure is retained. Thus, skeletal hydroxyapatite exists in a *non-stoichiometric* form (Sillen, 1989; Neuman and Neuman, 1958), with stoichiometric variations in the crystal formula arising through heterionic exchange i.e. the incorporation of various ions in the crystal, thereby displacing its normal chemical constituents (Neuman and Neuman, 1958).

The stability of the apatite lattice to ionic substitution is impressive. Trace amounts of almost any ion may be incorporated and several complete ionic substitutions are possible. For example, hydroxyl ions may be substituted by fluoride and chloride ions; while phosphate ions by carbonate, sulphate ions. Some of these are little understood, particularly the manner of charge compensation. Some substitutions may be important only at the crystal surface and may involve coupled cationic substitution. Calcium ions may exchange with several divalent ions, particularly the alkaline-earths. Therefore, strontium and barium may heterionically exchange with calcium, as may elements such as magnesium, sodium and lead (Posner, 1969; McLean and Urist, 1955). Ionic exchange tends to occur predominantly near the surface regions of crystals, since interior ions within the lattice

are more stable, having resulted primarily from contact with fluids during their formation (McLean and Urist, 1955).

Ionic substitution may alter the surface geometry as well as the chemistry of hydroxyapatite, and the extent of substitution, together with the calcium/phosphate ratio will in turn affect the surface/structural properties of hydroxyapatite (Kibby and Hall, 1972). The arrangement of the hydroxyl ions' oxygens, lying equidistant above or below the mirror plane of the crystal, introduces the possibility of considerable variability in the structure-dependent properties of hydroxyapatite (Brown and Chow, 1976); this ordering of hydroxyl groups allows reversal at vacancies or at sites containing impurities, like fluoride ions. This, and similar features have significant effects on the thermodynamic properties e.g. solubility, of the apatite crystals: the polarity imposed by a predominant orientation of hydroxyl ions in one direction along the c-axis may affect the orientation of crystallites relative to collagen, while disorder of the hydroxyl positions tend to increase crystallite entropy, thereby altering its solubility properties.

Therefore, crystallite sizes are sufficiently small that surface effects increase their solubilities (defined by the Gibbs-Kelvin equation). A small increase in crystal size will result in a measurable decrease in solubility. The non-stoichiometric nature and imperfect crystallinity of hydroxyapatite also contribute to an apparent solubility which is higher than the solubility product determined for well-crystallised, stoichiometric hydroxyapatite, in fact, 10^4 times greater (Brown and Chow, 1976). Figure 2.3 shows diffraction profiles measured using X-ray diffraction (refer to Chapter 4, sub-section 4.4.1.4), highlighting the relative acrystallinity of biological hydroxyapatite (represented by standard reference material and ashed ovine bone prepared by myself) compared to reference geological apatite (or rock phosphate); the sharper the peaks of the diffraction profiles, the more crystalline the sample.

The solubility of bone is important to understand since, after crystal formation, dissolution of the crystal and/or its surface boundaries are requisite to ionic exchange (McLean and Urist, 1955).

Figure 2.3: X-Ray Diffraction Profiles of Biological and Synthetic Hydroxyapatite and Geological Apatite to Demonstrate their Relative Crystallinities.

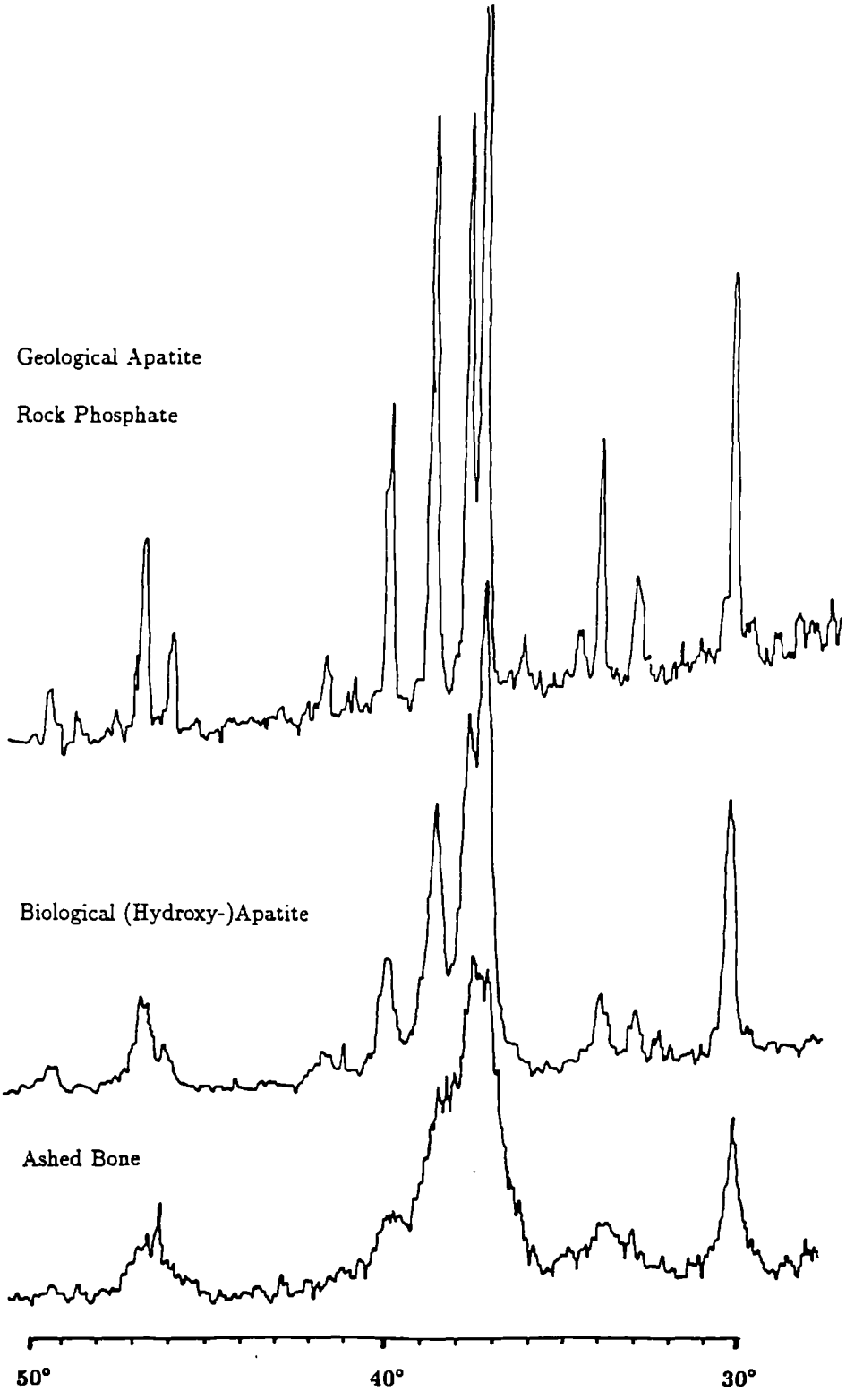

2.3.2.1 The Solubility of Bone Mineral.

Hydroxyapatite is slightly soluble in aqueous solutions; surface ions are in a dynamic equilibrium with those in solution. The position of this equilibrium is sensitive to changes in pH and ionic strength of solution, and on the presence of impurity ions. Thus, the nature of the surface may change with changes in solution. The adsorption of simple and complex ions on the crystal surface, especially those common to apatite and the solution, determines the charge characteristics of the solid/solution interface (Chander and Fuerstenau, 1983). Conversely, the surface charge is a property of the preferential dissolution or adsorption of lattice ions, produced either directly at the solid/solution interface or forming in solution and adsorbing onto the surface in amounts proportional to their concentration in solution. Thus, in some cases, the difference in the affinity of ions for the crystal surface may be attributable to differences in their hydration characteristics.

Solubility increases with the acidity of solution. Rootare *et al.*(1962) suggest that hydroxyapatite is hydrolysed in water to form a surface complex, where calcium ions are released into solution as surface phosphate ions are hydrolysed to HPO_4^{2-} ions which may then exchange with anions in solution.

$$Ca_{10}(PO_4)_6(OH)_2 + 6H_2O \rightleftharpoons 4Ca_2(HPO_4)(OH)_2 + 2Ca^{2+} + 2HPO_4^{2-}$$

Hydroxyapatite presents a highly polar surface that can therefore bind water molecules tightly. Two or three monolayers may be adsorbed and this water cannot be removed, except at elevated temperatures (Kibby and Hall, 1972). Thus, in contact with an aqueous solution, a 'hydration sphere' or adherent liquid film will cover the surface and this will contain ions in equilibrium with both the solution and the surface. Among the ions that tend to concentrate in the hydration shell are those of magnesium, strontium and carbonate (Neuman and Neuman, 1958).

Anions generally lower the solubility of hydroxyapatite at moderate pH: for example, hydroxyl, fluoride, chloride, carbonate and bicarbonate ions. These anions may act by substitution of hydroxyl and phosphate ions or more typically by adsorption on sites that inhibit the dissolution of calcium ions (Kibby and Hall, 1972). However, at high pH, carbonate ions increase the solubility.

Thus, in solution, hydrolysis reactions of surface ions and/or adsorption of the hydrolysed species from solution may take place. The hydrolysis of calcium ions is greatest at high pH where the lattice surface consequently becomes more negative, while low pH promotes the hydrolysis of phosphate ions, effecting a more positive surface. In this way, and with its high surface area, hydroxyapatite is an effective buffer and this may explain the "self-buffering" ability of bone in solution reported by Rae (1987).

Carbonate ions play a fundamental role in maintaining constant blood serum pH. They are present both as substituted ions in the apatite lattice and adsorbed onto the crystal surface. The readily exchangeable surface carbonate provides an available source of alkaline (basic) ions during acidotic stress (Posner, 1969). The most important contribution carbonate makes, however, is the increased reactivity it imparts to bone mineral by the structural disorder resulting from its substitution within the crystal (Posner *et al.*, 1981): planar carbonate ion substitution for tetrahedral phosphate groups acts to misalign the whole lattice such that its solubility and reactivity increase. Carbonate accounts for 4% of biological apatite precipitated from body fluids.

Therefore, bone apatite is characterised by a high specific surface, carbonate substitution, non-stoichiometry and relative acrystallinity.

2.3.3 Organic-Inorganic Integrity.

Surface adsorption studies have identified the existence of chemical linkage between the bone mineral surface and free polar groups in bone collagen (Dry and Beebe, 1960). This bonding is direct rather than through an intermediate hydrous system, since the presence of a hydration layer at mineral-organic interfaces would reduce the strength of polar bonding (Dry and Beebe, 1960; Posner, 1985).

The mechanical/chemical properties of bone are related to the number and strength of the bonds between mineral and organic phases. A large number of bonds is made possible by a very extensive area of interface which exists between mineral and collagen or other non-collagenous macromolecules. The mineral-organic interface predominantly consists of linkage of the mineral phase to the organic matrix by

protein-bound phosphate bonds (Glimcher, 1984). 80-90 % of mineral apatite crystals are located within the collagen fibrils.

The mineral component therefore serves the function of providing structural stability to the skeleton by infusing the organic matrix of bone to form a rigid structural material: it is the combination of mineral and organic fractions that yields the biochemical strength required for the skeletal support role which bone performs as a structural component of the body. This is reflected in the fact that bone has a modulus of elasticity intermediate to that of its mineral and organic constituents, yet its tensile strength is greater than either individually i.e. the whole bone is stronger than the sum of its parts.

Therefore, the intimate association between inorganic and organic components confers upon bone its unique mechanical properties.

At the same time, the relatively acrystalline and non-stoichiometric nature of hydroxyapatite endows bone mineral with considerable reactive and labile properties, so that it is able to operate effectively as a mineral reservoir. Trace elements, predominantly derived from dietary intake, are thus deposited in bone and released into the bloodstream, the timing and location of these phenomena influenced by a number of physiological factors.

2.4 Trace Elements in Bone.

Biogenic processes are responsible for the deposition and loss of elements throughout life. Trace element levels in bone are originally derived from dietary intakes and environmental prevalences (Parker and Toots, 1980). The actual composition of a diet may depend on a number of factors which have all been exploited in palaeodietary studies to derive as complete a picture of ancient lifestyle as possible. These factors include environmental conditions, such as climate and season, cultural and agricultural factors, and individual factors, which include socio-economic aspects such as sex, age, wealth and social ranking (Runia, 1988). Furthermore, metabolic factors such as absorption, excretion, pregnancy, lactation and growth may influence skeletal concentrations.

Therefore, the concentration of trace elements in living bone reflects physiological processes and the levels in the environment as a whole (Rheingold *et al.*, 1983). Trace elements can enter the body either through the skin, lungs or gastrointestinal tract (Runia, 1988). The majority are associated with the latter, thus reflecting the dietary (food and water) intake of an individual. Once foods have been ingested, a proportion of the elements are absorbed into the bloodstream across the intestinal wall, and are transported through the body to tissues, such as bone, that either temporarily or permanently store these elements.

Trace elements are classified as dietary essentials, possible essentials, nonessentials and toxic elements (Underwood, 1977). Most anthropological research tends to focus on essential and/or toxic elements. 15 trace elements are currently classified as dietary essentials and these include iron, manganese, zinc, copper, and fluoride. Essential trace elements function primarily in catalytic reactions and are often associated with specific enzymes as metalloenzymes or metal-activated enzymes: zinc and manganese function in this respect (Underwood, 1977). In other cases, trace elements constitute vital constituents of metalloproteins that perform metabolic functions, such as iron in haemoglobin. Toxic elements are classically lead, mercury and cadmium: these have toxic consequences at relatively low levels, although an excess of most trace elements will have adverse effects (Underwood, 1977).

Dietary studies based on the chemical composition of bone, whether in contemporary or ancient populations, rely on the fact that minor and trace elements are differentially distributed within and between trophic levels of the animal and plant kingdom, and more importantly in the extensive array of food resources available to human populations. At the simplest level, trace element analyses of bone may determine the relative contribution of plant and animal matter in prehistoric diets (Lambert *et al.*, 1979). Foods of plant origin contain higher levels of strontium, manganese, magnesium and calcium (Sandford, 1992). Conversely, foods of animal origin generally possess inherently higher concentrations of zinc and copper than those derived from plants, since these elements are more readily taken up from animal foods than vegetable (Underwood, 1977). Certainly zinc levels in bone roughly correspond to dietary levels as may be inferred from levels in herbivores, omnivores and carnivores (Rheingold *et al.*, 1983).

However, this delineation is complicated by a number of factors which may be environmental, cultural and/or physiological in nature. These effects may include differences in food preparation techniques and environmental variation in dietary intake; indeed, environmental levels, manifested in water and soil concentrations, may substantially effect internal elemental stores (Allaway, 1986). Variation in the elemental concentrations of soils may be reflected in plant levels and so make an impact at higher levels of the food chain, or they may be introduced indirectly to food material through contamination during cultivation and storage, for example (Underwood, 1977).

Physiological processes including absorption and excretion, and those governing internal storage and mobilisation of elements all play vital roles in maintaining elemental homeostasis, thereby regulating concentrations in bone. Factors influencing the initial absorption of elements include age, sex, health and nutritional status, as well as concomitant dietary components. With regard to the latter, interactions between elements may occur in conjunction with absorption, mobilisation and storage, and may be synergistic (enhancing) or antagonistic (inhibiting). Therefore, while the consequences of elemental interactions in many cases may have little discernible effect, in others secondary elemental deficiencies may arise (Underwood, 1977).

The excretory process includes direct excretion of the unabsorbed fraction of an element, together with the elimination of previously absorbed quantities. All these processes - absorption, mobilisation, storage and excretion - are fundamental to the metabolism of elements in the body, and must be understood before pertinent information can be obtained from anthropological trace element investigations.

A number of "special" physiological states also influence the levels of some elements, including those of potential interest to the anthropologist. The physiological stress imposed by growth, pregnancy and lactation, for example, influence the mechanism and degree to which an element is absorbed and/or excreted. Probably the most documented example of these phenomena is the impact of pregnancy and lactation on skeletal strontium and calcium concentrations (Sillen and Kavanagh, 1982; Blakely, 1989). The uptake and metabolism of strontium deserves special attention because of the implications for dietary reconstruction; indeed, the mea-

surement of strontium/calcium ratios in archaeological bone constitutes a popular strategy in anthropology for the reconstruction of palaeodiets (discussed in section 3.4.2).

4.1 Uptake and Metabolism of Strontium.

Although strontium resembles calcium chemically, its physical characteristics such as solubility and ionisation constants, are different. In spite of these differences, plants generally do not discriminate between strontium and calcium in their uptake and subsequent utilisation of these elements. While strontium can substitute for calcium in a variety of mammalian processes, it does not appear to be an essential element since it has no independent metabolic function, except perhaps in the calcification of teeth (LeGeros *et al.*, 1979). Calcium, however, is an essential element, forming a major constituent of hard tissues and playing a vital role in enzyme systems. For this reason, animals will preferentially absorb calcium over strontium, a phenomenon largely attributable to transfer proteins in the intestinal mucosa having a lower affinity for strontium and to its more rapid excretion by the kidneys (Walser and Robinson, 1963). This discrimination factor explains the observed difference in strontium/calcium ratios across trophic levels, the ratio decreasing as one moves up the food chain. It also accounts for the fact that adult humans absorb 40-80 % of ingested calcium, while only 20-40 % strontium (Comar, 1963); of the strontium absorbed, 99% is stored in bone.

The metabolism of strontium has been extensively studied and the relationship between strontium and dietary intake well-documented (Comar *et al.*, 1957; Blakely, 1989). However, a number of biogenic processes complicate this relationship, pregnancy and lactation for example (Blakely, 1989; Sillen and Kavanagh, 1982; Price *et al.*, 1985).

Both *in vivo* and *in vitro* experiments have shown that pregnancy and lactation elevate maternal bone strontium and depress bone calcium i.e. show elevated strontium/calcium ratios as the result of at least two physiological processes: (1) strontium is discriminated against in favour of calcium in the transport of ions to the placenta and mammary glands (effectively elevating strontium relative to calcium in the rest of the body), and (2) pregnancy and lactation facilitate absorption of alkaline earth metals (of which strontium is a member) from the in-

testine (Blakely, 1989). Thus, Blakely (1989) largely attributes the descending order of strontium/calcium ratios among the bones of reproductive-age females, post-menopausal females and adult males from two prehistoric sites to these physiological processes, while, at the same time appreciating the possibility of other variables (differences in diet) influencing this trend.

Strontium and calcium levels also fluctuate dramatically during growth and development (Sillen and Kavanagh, 1982). The rate of absorption of strontium is generally higher in young animals i.e. there is a lessened discrimination against strontium. Despite this phenomenon, infants may actually possess lower strontium levels than adults because the absolute amounts of the element available to them in their diet may be lower; this is particularly the case for unweaned infants whose diet of maternal milk is low in strontium because of the aforementioned discriminatory effect at the mammary glands. In fact, a high degree of variability is observed in the bones of growing individuals (Sillen and Kavanagh, 1982), which has methodological implications for the choice of skeletal tissue analysed to infer dietary intake.

Thus, dietary intake itself, age and reproductive physiology all influence strontium levels in the body. Palaeodietary reconstruction based on strontium measurements in exhumed skeletons must therefore control for age differences, the interactive physiology of elements, and gender-related physiological differences, together with possible sources of contamination before confidently associating strontium levels with diet.

2.4.2 Anthropological Applications of Trace Element Analysis.

The chemical composition of bone effectively provides a "biogenic signal", indicative of both physiological processes and the dietary intake of an individual. This fact has been exploited by biological anthropologists in an effort to reconstruct the diets of past populations and thus elucidate further detail about lifestyles, environmental resources etc. on the basis of the trace element description of bone. The main anthropological approaches in this field can be divided into those comprising elemental analysis, either single or multi-element, and those measuring the isotopic composition of bone.

2.4.2.1 Strontium and Strontium/Calcium Ratios.

The applications of strontium and strontium/calcium measurements in archaeological bone are self-evident based on the information reported in the preceding section: the principle that organisms take up strontium in quantities that vary inversely to their trophic position in the food chain warrants their use as a palaeodietary indicator. Pioneering work by Brown (1973) inspired many subsequent studies that have, in most cases, more thoroughly assessed the utility of this technique for dietary reconstruction, in addition to identifying associations between social stratification and differential dietary patterns (Schoeninger, 1979; Runia, 1988). For example, Schoeninger (1979) reported lower strontium levels in prehistoric skeletons interred with more grave goods, and hypothesised that higher-ranking individuals enjoyed more animal material in their diets.

Among food resources apparently higher in strontium content are fish, shellfish, nuts, leguminous plants and cereals (e.g. corn) (Sillen and Kavanagh, 1982). Thus, other studies have compared preagricultural and agricultural populations (Schoeninger, 1981), as well as archaic and modern *Homo sapiens* (Schoeninger, 1982), and documented changes in subsistence (Price, 1985; Price and Kavanagh, 1982). More recently, strontium/calcium ratios have been used to reveal the diversity of the diet of *Australopithecus robustus* (Sillen, 1992).

As the potential of strontium analysis in understanding past dietary adaptations has been realised and exploited, studies have encountered various interpretative difficulties.

These difficulties include those arising from complications imposed by the physiological processes outlined earlier, so that care must be taken when comparing the diet of individuals of differing sex, age and metabolic status. Furthermore, the application of this strategy only applies for adult bone, because mammalian discrimination does not occur to the same degree in juvenile animals.

An important qualification for observations based on strontium levels is that only biologically meaningful relationships can be detected within circumscribed geographic regions having similar underlying geology and baseline levels of alkaline-earths in soils and groundwaters (Sillen and Kavanagh, 1982), because the depo-

sition of strontium in bone can be substantially altered by variations in environmental and geological distributions of the element (Sillen, 1989; Sillen *et al.*, 1989 ; Runia, 1987,1988).

Similarly, there is considerable variability in strontium/calcium ratios *within* each trophic level, so that, for example, roots, rhizomes and seeds possess higher ratios than leaves and other vegetation within a given environment (Sillen, 1992). Thus, among herbivores, animals feeding predominantly on leaves have relatively low strontium/calcium ratios compared to those feeding predominantly on high fibre plant parts (Sealy and Sillen, 1988; Ezzo, 1992). This may create complications so that leaf-eating animals may not be distinguishable from carnivores; thus, while the general trend of reduced strontium/calcium ratio in higher trophic levels is confirmed, there may be considerable overlap between trophic groupings (Sillen, 1992).

Variability of this nature, together with physiological complications outlined earlier, underline the caution that must be exercised when comparing fossil species whose diet is unknown, and this fact justifies recent and on-going research that attempts to formulate specific predictions about strontium/calcium variability in fossil foodwebs based on investigations of modern ones (Sealy and Sillen, 1988; Sillen, 1992).

2.4.2.2 Multi-element and Single-element Studies.

A number of multi-element studies have focused on a broader array of analysed elements for dietary discrimination, delineating proportions of food categories, gender- and status-based dietary differences and dietary changes over time (Sandford, 1992; Buikstra *et al.*, 1989).

This multi-element approach has been adopted by, for example, Gilbert (1985) to look at sample populations spanning the transition from hunter-gathering to agricultural subsistence; Lambert *et al.*(1979) to document the adoption of maize agriculture; Ezzo (1992) to reconstruct the palaeonutritional status in a prehistoric site representing two different cultural horizons possessing a wealth of different floral and faunal remains; Vuorinen *et al.*(1990) examine trace and heavy metals in

juvenile skeletons to explore the possibility of toxic elements in Roman diet. Recently, multi-element studies have evidenced a broader sphere of concern, analysing remains from a more diverse spectrum of geographical and cultural contexts (Sandford, 1992).

A suite of elements may, in theory at least, be studied to identify the dietary signature of an individual within a population: strontium and barium are typically used as indicators of herbivorous dietary components (Price, 1985; Francalacci, 1989) ; while zinc and copper may provide an indication of a carnivorous diet (Rheingold *et al.*, 1983 ; Francalacci, 1989; Hatch and Geidel, 1985) ; vanadium provides information on the consumption of nuts and berries (Hatch and Geidel, 1985).

Intra-individual variability poses a major problem in such studies (Klepinger *et al.*, 1986; Grupe, 1988) and should be quantified by analysing many different bones for each skeleton whenever possible. In addition, more recent studies have included an increasing awareness of postmortem contamination, and their strategies frequently include several independent diagnostic methods within a research design (Kyle, 1986; Byrne and Parris, 1987) ; indeed, specific elements known to be common contaminants, such as manganese and aluminium, uranium and yytrium, may be utilised as markers for contaminatory activity (Lambert *et al.*, 1984; Henderson *et al.*, 1987 ; Williams, 1988). Such strategies are discussed in more detail in Chapter 3.

Other studies focus on one particular element of interest, which is usually associated with a particular disorder or disease, so that a variety of elemental deficiencies or toxicities may be addressed. Indeed, dietary deficiencies and excesses, and their pathologic consequences form a recent novel approach in anthropological studies that derive information about palaeodiets and human health on the basis of indications of disease in skeletal tissue (Klepinger, 1992). Studies combining morphological/pathological and chemical analyses may, for example, identify iron deficiency (anaemia) by porotic hyperostosis, which may be correlated with evidence of infectious disease (Fornaciari *et al.*, 1981; Klepinger, 1992). Other studies have focused on lead, often in an attempt to relate cultural practices to abnormal

lead ingestion and/or toxicity (Waldron *et al.*, 1979). Again, however, the problem of postmortem contamination complicates interpretation.

2.4.2.3 The Isotopic Composition of Bone: Stable Isotope Analysis.

Isotopic strontium ratios (Sr^{87}/Sr^{86}) have also been used as dietary indicators. Strontium isotope ratios in bone are ultimately inherited from local rocks and groundwaters, via foodstuffs. The ratio of these naturally-occurring isotopes in bone is identical to the underlying geology, since heavy isotopes do not undergo biological fractionation. If a geographical area includes more than one rock type with differing isotopic strontium ratio, then the regional source of the food material may be identified; classically, this method is applied to discriminate marine and terrestrial food resources (where ratios are clearly different) (Sealy *et al.*, 1991). Thus, bone strontium isotopic measurements provide a measure of the relative importance of foods from geologically-characteristic isotopic zones.

Similarly, the carbon (C^{13}/C^{12}) and nitrogen (N^{15}/N^{14}) isotope ratios in fresh bone collagen and the carbon isotope ratio of the carbonate component of hydroxyapatite of fresh bone are determined by the isotopic composition of the diet (Nelson *et al.*, 1986). So, carbon isotope ratios may distinguish between C_3 and C_4 terrestrial plants (van der Merwe, 1982), while the nitrogen isotopic composition of collagen may reflect legume versus non-legume consumption (DeNiro and Epstein, 1981); both isotopic ratios for collagen should distinguish the use of marine and terrestrial food sources (Schoeninger and DeNiro, 1984).

2.4.2.4 Summary of Trace Element Analyses in Anthropology.

In summary, both elemental and stable isotope analyses of bone provide a wealth of information about the dietary intake of an individual. Element analysis has been used to reconstruct relative amounts of particular plant types (e.g. nuts, grains, leafy vegetables), and animal types (e.g. fish, shellfish, herbivorous and carnivorous terrestrial animals, browsers and grazers) as well as discriminating between plant versus meat foods (Schoeninger, 1979; Price and Kavanagh, 1982 ; Sillen and Kavanagh, 1982; Byrne and Parris, 1987 ; White and Schwarcz, 1989). Stable isotope analysis may determine the relative contribution of C_3 and C_4 plants, legumes, and marine versus terrestrial animals (van der Merwe, 1982).

Palaeodietary analyses based on variations in the trace element and stable isotopic composition of both inorganic and organic phases in bone all depend on the assumption that measured values reflect *in vivo* values and are thus representative of the biogenic character of an individual. However, the postmortem alteration of buried bone may change the chemical composition of bone from its ante-mortem state. The complications and implications of this chemical activity during inhumation to the reconstruction of past populations based on *trace element* analyses are discussed in Chapter 3.

2.5 Summary.

This chapter has briefly described the anatomical structure and physiology of living bone, concentrating on its function as a mineral reservoir in the homeostatic regulation of major, minor and trace element levels in the body.

The intimate relationship between the mineral component and the organic matrix in bone ultrastructure is essential in endowing bone with its unique structural properties. These closely interdependent structural components are themselves intimately associated with a rich blood supply and the stromal and haemopoietic (marrow) tissue of bone, conferring on bone its plasticity and dynamicity in responding to physiological demands, whether structural, mechanical or metabolic/chemical: the trace element content of bone thus describes a "biogenic signal" representative of individual metabolism during life.

After death, the "non-structural" soft tissues that permeate bone are among the first materials to decay, leaving bone vulnerable and accessible to infiltration by trace elements in solution in the immediate burial environment. Such a predicament provides a wealth of opportunity for chemical interaction between bone and percolating groundwaters, and thus an alteration in the chemical character of bone, previously defined by physiological processes.

Chapter III

Bone in the Burial Environment.

3.1 Introduction.

As skeletal material enters soil and is buried, the homeostatic relationship between bone and its physiological environment is replaced by an equally dynamic interaction between bone and the immediate geochemical environment. In this postdepositional milieu, skeletal tissue is exposed "to the elements".

The postmortem history of skeletal tissue relies upon an interplay between opposing agencies of preservation and destruction. The intrinsic physical characteristics of bone, together with rate of burial, determine its preservation potential, while chemical, physical and biological agents within the burial environment may constitute either agents of preservation or destruction, depending on the particular physicochemical characteristics of the burial environment; if these are favourable, bone tissue may be preserved and fossilized.

3.2 Fossilization and Diagenesis.

3.2.1 Fossilization.

A fossil can broadly be defined as an organic trace buried by natural processes and subsequently permanently preserved. The term 'organic trace' includes impressions of organisms, excremental material, tracks, trails and borings, and, of course, skeletal material. Fossilization can take place via a number of mechanisms which may preserve organic and/or inorganic components, in either an altered or unaltered state. Examples of organic preservation include insects in amber (unaltered) and the impressions of jellyfish (altered); while those of inorganic material include calcitic shells and teeth (unaltered), and, finally, bone (altered to varying degrees). Preservation of bone occurs by petrification as the result of (a) infilling of pore spaces in the deposited structure by any number of different substances

(commonly calcite, silica, pyrite), or (b) replacement, either coarse or molecular, of the original skeletal material by similar or different substances.

Therefore, the fossilization of bone consists of a complex physicochemical process involving:

(1) the breakdown of organic components, via autolysis and microbial activity (Hare, 1980),

(2) the introduction and exchange of inorganic components (Parker and Toots, 1979),

(3) conversion of bone apatite to inorganic apatite minerals (Hassan *et al.*, 1977).

3.2.2 Diagenesis.

Physicochemical changes in both the organic and inorganic components of bone are generally described as bone *diagenesis*. Bartsiokas and Middleton (1992) discriminate between diagenesis and fossilization by defining fossilization as a naturally occurring physicochemical process that *preserves* the gross morphology of a structure (by ionic exchange, increasing crystallite size, loss of organic material and mineral pore-filling); while diagenesis at the same time includes destructive processes that may counteract fossilization.

The concept of diagenesis was originally developed in geology to describe processes affecting sediments or sedimentary rocks following their deposition while at or near the Earth's surface i.e. at low temperature and pressure. Biological anthropologists have subsequently adapted this term, directing it more specifically to postmortem alterations in the chemical composition of bone following its deposition in soil.

The interacting processes of bone decay, fossilization and diagenesis are discussed in the following sections for organic and inorganic components, respectively. Factors affecting the degree of postmortem alteration of each component are then broken down into those that are *intrinsic* to the bone (dependent on the nature of the tissue itself) and those that are *extrinsic* (dependent on the properties of the burial environment). The burial environment is then discussed in more detail.

3.3 Decay of the Organic Component.

The bone's intrinsic chemistry includes autolytic mechanisms which affect bone decay immediately after death. Biological processes supporting bone breakdown and the rigorous physiological controls of pH and processes of mineral homeostasis cease. Bone tissue undergoes rapid gross and microscopic changes: the cells disintegrate, membrane barriers are abolished, and the water content and organic matter begin to be lost (Cook, 1960). This loss is dependent on the ambient physical properties which determine the rate of hydrolysis of protein and fat.

Proteins can be broken down in both acidic and basic conditions via amide hydrolysis. However, they are generally more stable in basic conditions than acidic ones, and can therefore tolerate greater fluctuations from neutral pH conditions in the alkali range of the pH spectrum (March, 1977; O'Hagan, pers.comm.).

Proteins are hydrolysed with either acidic or basic catalysts because of the *zwitterionic* properties of their amino-acid constituents i.e. their ability to accept both hydroxyl and proton groups. At the simplest level, amides are hydrolysed to form the following products: in acid conditions, the free acid and the ammonium ion, and in basic conditions, the salt of the acid and ammonia; these hydrolyses are essentially irreversible. Elevated temperatures will accelerate protein hydrolysis (e.g. Von Endt and Ortner, 1984).

Collagen experiences a range of postmortem processes such as sub-aerial weathering, leaching by groundwater and microbial attack. Moreover, with time, bone may be contaminated by sedimentary organic matter (Hare *et al.*, 1991). Thus, the isotopic and chemical composition of archaeologically-derived bone may be compromised (Tuross *et al.*, 1989a), making dietary determination with fossil material difficult. Exogenous compounds, specifically humic and fulvic acids and adsorbed proteins and peptides, can contaminate bone and skew isotopic ratios; while diagenetic alteration of collagen (via hydrolysis) shifts the relative proportion of amino-acids, resulting in a different mass balance and consequently a different total protein isotopic composition (Hare *et al.*, 1991).

Amino-acid compositions may vary enormously according to the preferential preservation of protein components: for example, non-collagenous proteins (NCP's) are

preferentially preserved, probably via retention by their adsorption to the hydroxyapatite matrix, while collagen is degraded and lost to the environment over time (Masters, 1987). NCP's are acidic proteins, and these or their remnant peptides are retained by charge interactions with the mineral phase; in addition, they are more resistant to hydrolysis (Hare, 1980).

The extent of organic breakdown is variable: proteinaceous residues of amino-acids can persist in ancient fossil bone material (Wyckoff, 1972). In fact, the extent of organic preservation can be characterised by a number of chemical properties: amino-acid or nitrogen content, non-collagen composition, the degree of racemization (D/L aspartic acid ratio), and C/N ratio (Bada, 1985; DeNiro, 1985). Laboratory simulations of bone diagenesis have demonstrated the importance of the aqueous environment, since while fresh bone contains roughly 15% water by weight which is sufficient for initial fat and protein hydrolysis, variations in the groundwater will accelerate or retard hydrolytic breakdown (Henderson *et al.*, 1983). Indeed, March (1977) states that pure water alone is not sufficient to hydrolyse most amides because of the stability of the C-N bonding between the amine and carbonyl groups. In contrast to protein degradation, racemization rates are affected predominantly by temperature, rather than by other environmental factors such as leaching, pH and humidity (Bada, 1985).

3.4 Diagenesis of the Inorganic Component.

The dissolution of the mineral phase will occur where pH conditions are below pH 6, since the solubility of hydroxyapatite increases below pH 6.5-6.0 (Lindsay, 1979). This acidity is derived both externally, from the groundwater and depositional environment, and from within the bone itself: the organic acid byproducts of soft tissue decomposition and the microbial breakdown of collagen produce localised acidity, initiating bone demineralisation and further release of collagen (White and Hannus, 1983; Hare, 1980; Hackett, 1981). However, rather than the large-scale removal of hydroxyapatite, there tends to be a "reorganisation" of its crystals and changes in the content of the inorganic structural framework via processes of depletion, accumulation and remineralisation (Hassan and Ortner, 1977).

As the organic matter is broken down and many of its decomposing products leached out, the bone's initial dense mass becomes perforated as millions of fine ramifying canaliculi, Haversian canals and intercrystal spaces within the inorganic matrix are exposed. Groundwater moves into these spaces and carries with it all the dissolved material from the surrounding burial matrix.

A number of physicochemical reactions may take place.

3.4.1 Precipitation.

Bone appears to be a very favourable substrate for the deposition of a number of minor and trace elements; indeed, elements present in ppm amounts in bone may not be detectable in the surrounding burial matrix (Parker and Toots, 1972).

Elements may be precipitated from groundwaters or physically incorporated as as "pore-filling" mineral phases in small cracks and voids in the bone and in the natural microstructural pores, left by the decomposition of organic matter. Quartz inclusions, oxides of iron and manganese, carbonates e.g. calcite ($CaCO_3$), and sulphates e.g. barite ($BaSO_4$) are included in this category (Pate and Hutton, 1988; Parker and Toots, 1980; Hassan and Ortner, 1977). El-Kammar *et al.*(1989) report a variety of soil contaminants such as quartz, feldspars, haematite, carnalite, kaolinite and gypsum, introduced by the penetration of fine soil grains in voids and cracks. Moreover, other elements may be associated with such material; calcites, for example, may contain strontium, magnesium and manganese (Pate and Hutton, 1988). In addition, hyphae (algal growths), rootlets and charcoal fragments may be observed as physical contaminants (Hassan and Ortner, 1977).

3.4.2 Crystallographic Alterations.

During burial, microcrystalline biogenic hydroxyapatite is converted to a larger more crystalline form (Schoeninger, 1982; Sillen, 1986,1989; Tuross *et al.*, 1989 ; Bartsiokas and Middleton, 1992).

Bartsiokas and Middleton (1992) list a number of phenomena that may be attributed to improving the crystallinity of archaeological bone: ionic exchange with fluorine, an increase in crystallite size, precipitation of geological apatites, dissolution of bone and reprecipitation of its apatite (secondary apatites), accretion of

crystals or recrystallisation, and the influence of environmental water (causing the leaching or washing out of smaller crystallites and amorphous mineral phases). Furthermore, they report increases in crystallinity corresponding to the age of the material examined, and propose this phenomenon as a means of assessing the degree of fossilization, and further suggest its development as a potential relative dating method.

Biogenic apatite may serve as a foundation for the formation of diagenetically-derived crystals by its ability to "seed" new crystal formation (Nancollas and Mohan, 1970). Price *et al.*(1992) suggest that crystallinity changes are promoted during and after the decomposition of the organic matrix, and this is supported by Tuross *et al.*(1989) who have demonstrated a relationship between mineral and organic preservation by plotting calcite/apatite and glycine/aspartic acid ratios as indexes of mineral diagenesis and remaining collagen, respectively. Bone possessing good organic preservation showed little evidence of crystalline impurities (calcite and quartz, primarily), according to X-ray diffraction (Tuross *et al.*, 1989b). Indeed, some workers have reported increased crystallinity only in older samples (at least 15 ka b.p), attributing this to advanced collagen degradation (Schoeninger, 1982; Sillen, 1986, 1989).

Both the precipitation of secondary minerals and/or the recrystallisation of hydroxyapatite may involve the incorporation of ions from both soil solution and dissolved biogenic material (Pate *et al.*, 1988). Although the formation of larger crystals increases their relative stability, the absence of biological discrimination against strontium and other ions in the soil solution may result in the uptake of these elements during recrystallisation and precipitation processes.

3.4.3 Incorporation into the Matrix: Ion Exchange.

Ion exchange between bone and groundwaters is an important process in mineral diagenesis, since the large surface area of microcrystalline hydroxyapatite offers a highly reactive colloidal interface, where up to 25 % of the surface ions are available for chemical exchange (Posner, 1969, 1985). The accommodating nature of biological apatite thus offers a wide scope for elemental variability between biogenic and diagenetic mineral.

Both cation and anion incorporation processes can occur in the burial predicament by the exchange of ions in bone and the surrounding burial matrix. **Cationic substitution** for calcium generally comprises alkaline earth metals with similar ionic radius to calcium (potentially strontium, barium, radium, and possibly magnesium) and a number of other elements, notably lead (Sillen, 1989).

Anionic substitution is more complex since the positions of both hydroxyl ions and phosphate ions may be occupied. For example, fluoride ions readily exchange with hydroxyl ions, reducing crystal strain, promoting crystallinity and thereby reducing the solubility of apatite (Bartsiokas and Middleton, 1992; Oakley, 1950).

The incorporation of carbonate in buried bone is of particular importance since diagenetic carbonate will obscure biogenic carbon isotope measurements. Carbonate ions may substitute for phosphate groups and exchange with biogenic "structural" and "adsorbed" carbonates (Lee-Thorp and van der Merwe, 1991). In contrast to fluoride ions, their substitution increases the solubility of the apatite mineral.

The structural inclusion of carbonate may be coupled with sodium replacement of calcium; indeed, Buikstra *et al.*(1989) report an increase in sodium in interred bone that is clearly related to other diagenetic phenomena. In contrast, other reports have monitored a reduction in sodium levels during fossilization (Lambert *et al.*, 1984; Parker and Toots, 1974,1980) as sodium is leached from bone, largely as a property of its high aqueous solubility (Lambert *et al.*, 1985).

The incorporation of diagenetically-derived ions, and corresponding changes in the crystallinity are diagenetic processes that effectively form stages of fossilization since they serve to ultimately transform biological hydroxyapatite into geological varieties of apatite minerals (Pate and Hutton, 1988).

3.4.4 Typical Chemical Contaminants.

The variability and unpredictability of diagenetic alteration are highlighted by studies that examine chemical and physical contamination in bone from a wide range of depositional environments (Buikstra *et al.*, 1989; Price, 1989 ; Hancock *et al.*, 1989). Such studies find a high degree of variability in the major, minor and trace element contents of archaeological material in different archaeological sites.

Sandford (1992) states that "while elements may differ in terms of their susceptibility to diagenesis, there is no element that is invulnerable to postmortem alteration."

While at one extreme, manganese, iron and aluminium concentrations are subject to contamination in most geochemical environments, undergoing substantial diagenetic alteration (Parker and Toots, 1974, 1980; Lambert *et al.*, 1982, 1983, 1985), others have, over the years, been widely regarded as fairly stable in the burial context and less susceptible to diagenesis: barium, strontium and zinc, have been included in this category (Parker and Toots, 1980). Indeed, it has been suggested that barium is a more reliable dietary indicator than strontium because it is less sensitive to diagenesis (Williams, 1988; Francalacci, 1989; Ezzo, 1992), although other researchers have reported its contamination during diagenesis (Toots and Voorhies, 1965 ; Lambert *et al.*, 1985).

The diagenetic alteration of zinc is controversial. Lambert *et al.*(1982) and Buikstra *et al.*(1989) have reported similar levels of zinc (and strontium and magnesium) in rib and femoral bone from corresponding sites and concluded that zinc levels in bone are relatively unaltered in the burial environment, a view supported by Francalacci (1989) who observed the preservation of trophic discrimination in Neolithic faunal samples on the basis of zinc levels. Observations of homogeneous cross-cortical distribution of zinc, strontium, lead and calcium (Lambert *et al.*, 1984) have suggested little post-depositional contamination of these elements, in contrast to iron, aluminium, potassium, manganese and magnesium (Parker and Toots, 1970; Lambert *et al.*, 1984). In contrast, zinc levels have been correlated with manganese and copper concentrations, indicative of diagenetic activity (Price, 1989).

Recent studies have documented the postmortem alteration of strontium in widely ranging geological regions and environments (Klepinger *et al.*, 1986; Francalacci and Tarli, 1988 ; Price, 1989). Indeed, strontium differences indicative of different trophic levels may be masked, not only by diagenesis, but also by the association of faunal species from different geographical regions during transportation by fluvial deposition, for example (Schoeninger *et al.*, 1984).

In an attempt to minimise diagenetic effects, the strontium/calcium ratio is often measured on the assumption that, since strontium is able to substitute for calcium

in the apatite crystal, the diagenetic dissolution of bone will affect strontium and calcium equally; thus, the ratio will remain the same (Schoeninger, 1982).

The shift in strategy to examining strontium/calcium ratios necessitates a more careful consideration of both strontium and calcium postdepositional behaviour. Chemical weathering of hydroxyapatite may result in calcium depletion by leaching or enrichment by proton displacement (White and Hannus, 1983), enrichment by calcite and gypsum (hydrated calcium sulphate) pore-filling, and replacement by the transition metal yttrium have been documented (Parker and Toots, 1980; Pate and Hutton, 1988). Pate and Brown (1985) have therefore concluded that strontium/calcium ratios are reliable estimates of dietary intake for modern individuals, but less so in buried material due to differential diagenetic effects on the two elements in the postmortem environment.

The diagenetic alteration of strontium is examined in more detail, because of the implications for palaeodietary research.

3.4.5 The Diagenesis of Strontium.

Many workers have favoured the stability of strontium in the geochemical environment, including Wyckoff and Doberenz (1968), Parker and Toots (1970, 1974, 1980), Lambert *et al.*(1979), Vuorinen *et al.*(1990) and Schoeninger (1979) who concluded that the cationic position filled by strontium and calcium in bone appeared "to be unaffected by diagenesis over a wide range of conditions."

However, the diagenetic alteration of strontium has since been increasingly acknowledged as a significant impediment to fossil studies (Nelson *et al.*, 1986; Klepinger *et al.*, 1986; Price, 1989; Ezzo, 1992; Sillen, 1981, 1988, 1989). For example, observations that coefficients of variation across herbivores, carnivores and human omnivores in archaeological deposits became more similar with time suggested that postdepositional changes in strontium content had occurred (Sillen, 1981) causing equilibration of strontium levels in bone and the environment (Sillen and Kavanagh, 1982). In this way, diagenetic alteration obscures the natural differences that exist between taxa, together with the natural variability existing within them.

Evidence from some of the oldest human bone analysed to-date has suggested that homogenization through diagenetic alteration may be significant in very ancient remains (Price *et al.*, 1992): no significant difference in strontium content among herbivore, carnivore and human bone material (dating around 105,000 B.P., the time of *Homo sapiens neanderthalensis*) was observed by Price *et al.*(1992).

Similarly, an examination of modern and prehistoric bones from both terrestrial and marine feeders, where strontium values were predicted to be pronounced, found that only the expected differences in strontium concentrations were observed in modern material; in contrast, prehistoric samples significantly overlapped in both elemental and isotopic values, suggesting contamination of samples exposed to groundwater action (Nelson *et al.*, 1986). Certainly, Sealy and Sillen (1988) have demonstrated elevated strontium levels in human bone from marine shell middens and assigned these to chemical contamination from shells in the burial matrix.

One of the most dramatic and convincing studies demonstrating strontium diagenesis involved plotting the cross-cortical distribution of strontium in fossil and modern bone material from two archaeological sites (Williams, 1988). While distribution profiles in fossil material were relatively flat (though highly variable), there was clear and unambiguous evidence of postmortem strontium contamination as indicated by a 'U'-shaped cross-cortical profile i.e. elevated levels in peripheral cortices. Furthermore, well-preserved features, nitrogen measurements and surface colouration all indicated that the bone had been recently deposited (probably less than one year) and had only been partially buried. Strontium levels generally correlated with bone colouration, reinforcing interaction with the burial matrix; however, since strontium levels in soil associated with the bone were significantly lower than in peripheral cortices, groundwaters were considered the strontium ion source. Certainly, as Williams (1988) points out, "strontium may be rapidly incorporated into bone during very early stages of diagenesis."

Therefore, both accounts of the diagenetic alteration of organic and inorganic components of bone have highlighted the importance of the ambient physical conditions (pH, temperature etc.) and the availability of organic inorganic constituents of the burial matrix. Superimposed on these external factors are the characteris-

tics of the bone material itself which will, to some extent, determine the degree of susceptibility to diagenesis.

3.5 Factors affecting diagenesis.

The degree and direction of diagenetic alteration are influenced by the interplay of numerous factors that include both *intrinsic* and *extrinsic* variables (Von Endt and Ortner, 1984). The former arise largely from the physical and chemical characteristics of bone itself, while the latter comprise the physicochemical description of the burial environment (Parker and Toots, 1980).

3.5.1 Intrinsic Factors.

Intrinsic physical factors include the degree of mineralisation; bone size, which *tends* to be inversely proportional to decay; surface/volume ratio; and density (Shipman, 1981 ; Lambert *et al.*, 1985). In turn, all these factors are themselves dependent on the age, sex and health of an individual, showing both inter- and intra-individual variation (Kyle, 1986).

Therefore, certain categories of bone may be more predisposed to diagenesis. Juvenile bones, for example, often display relatively higher elemental concentrations than adult bone (Lambert *et al.*, 1979), probably due to the higher proportion of amorphous mineral which is more readily leached from bone. Bone density is a function of the proportions of cancellous to compact bone; the latter is less susceptible to diagenesis since it is more dense (less porous) than cancellous bone. So, the concentrations of typical diagenetic contaminants (iron, manganese etc.) are often higher in ribs than femora (Lambert *et al.*, 1982). Indeed, Grupe (1988) further demonstrates the superiority of cortical bone for elemental analysis by finding high intertrabecular variability in elemental levels, together with poor correlation with estimates of total skeletal content i.e. the chemistry of trabecular material is not necessarily representative of individual levels.

Interbone variation in elemental deposition and remodelling rates, together with age-dependent differences in living bone provides confusing variables in the interpretation and separation of biogenic and diagenetic elements (Buikstra *et al.*, 1989). Therefore, inter- and intra- bone chemistry differences may be exacerbated

by superimposition of diagenetic processes on physiological levels. Conversely, the absence of such elemental differences does not necessarily indicate the absence of diagenetic activity since the latter may effect, through an equilibration process, the dissipation of natural physiological differences that may have been pronounced originally (Sillen, 1981; Price, 1989).

3.5.2 Extrinsic Factors.

The rapidity and nature of the diagenesis of bone is controlled by the depositional environment or burial matrix, so that in addition to any morphological differentiation endowed by the bone's gross and microscopic structure, differential alteration will occur according to climate and local geology. More specifically, the physical, chemical and biological properties of the burial environment are fundamental to the postmortem history of inhumed bone.

(1) Physical decay and disintegration.

Successful bone preservation may rely initially on a quick burial since while an organism's remains lie on the ground surface they are exposed to climatic weathering (Behrensmeyer, 1978) and interference by scavengers (Hill, 1980). Thus, early postmortem change may include physical damage caused by distortion; surficial cracking and flaking ; fractures; loss of soft parts resulting in disarticulation, thus increasing the likelihood of dispersal and ultimate destruction of skeletal elements (Hill, 1980). External physical factors will still operate even after the partial/lightly-buried stage: these include sediment porosity and hence soil compaction, which is in turn affected by chemical weathering processes of deposition and erosion (Behrensmeyer, 1978).

(2) Biological decay.

In addition to the role of large predators in the disintegration and dispersion of bone operating at the ground surface, bone is vulnerable to attack by microorganisms both on and in the soil. Soil contains a vast array of microrganisms, both bacteria (up to 100 million/gramme soil) and fungi (up to 20 million/gramme soil) (Stevenson, 1982). These include *Mycelites* fungi, *Mucor* fungi (Marchiafava *et al.*, 1974) and *Actinomyces* bacteria. Their activity is intimately related to the chemical

degradation of both the organic and inorganic components of bone (Marchiafava *et al.*, 1974; Hare, 1980) ; they solubilise collagen and/or hydroxyapatite in order to utilise the energy content of the bone matrix. Consequently, they produce metabolites which create an acid microenvironment conducive to chemical weathering (Hanson and Buikstra, 1987; Grupe and Piepenbrink, 1988; Piepenbrink, 1986 ; White and Hannus, 1983). Microbial invasion proceeds from the cortical surfaces of bone via the osteons or Haversian canals. Microscopic examination reveals a series of foci or linear tunnels caused by invading microorganisms from the soil (Hackett, 1981), which produce enzymes with bone-resorbing activity. Similar enzymes may also be present directly in the soil as complexes with clay minerals. Indeed, the chemical composition of the soil determines the degree of microbial presence since many metals are actively sought in their metabolism (Hanson and Buikstra, 1987). Fungi in particular may accumulate heavy metals, essential to their metabolism, thus contaminating bone by simultaneous transportation of such metals. In this way, elements may be deposited onto the bone surface or they may be leached out of bone with the organic components via the solubilisation of hydroxyapatite and collagen respectively, causing a depletion of elements bound to both (Thornton, 1983).

(3) Chemical alterations.

Examples of chemical alterations have been reported for the diagenesis of both organic and inorganic components (sections 3.3 and 3.4, respectively). While exogenous organic compounds can contaminate bone (e.g. fulvic acids) and contaminant elements can *potentially* be taken up into the organic fraction (refer to Chapter 2, sub-section 2.2.3.1), the chemical alteration of this component tends to be a product of differential and preferential hydrolytic reactions, effectively *"shifting"* the original composition of the organic matrix. In contrast, the inorganic component is subject to a wide variety of chemical alterations that largely involve the introduction of *extrinsic* chemical entities as a function of the very nature of this fraction. For this reason, descriptions of chemical alteration in buried bone are usually confined to the inorganic component.

In summary, postmortem chemical alteration of the inorganic matrix may involve the processes of dissolution, precipitation, mineral replacement, recrystallisation,

crystal growth and ionic substitution (Pate *et al.*, 1988). The primary mechanisms of diagenesis can be classified as:

(1) the precipitation of water-soluble salts and separate mineral phases in small voids and fractures,

(2) ionic exchanges between the soil solution and hydroxyapatite lattice positions,

(3) recrystallisation and crystal maturation involving the conversion of microcrystalline (relatively acrystalline) biogenic hydroxyapatite to a larger, more crystalline form, which may at the same time enable the incorporation of extrinsic ions.

Both mechanisms of ionic substitution and the precipitation of various salts and secondary minerals are dependent on the availability of ions to the soil solution; for example, soluble salts of calcium, magnesium, sodium and potassium are common in areas with scarce rainfall and high evaporation (Pate *et al.*, 1989). In addition, the precipitation of secondary calcium phosphates is limited by the low concentration and relative immobility of phosphorus in the soil environment (Pate *et al.*, 1989); secondary calcium phosphate minerals include brushite, whose formation is accompanied by structural disintegration since brushite crystals are substantially larger than those of hydroxyapatite (Piepenbrink, 1989). Chemical reactions in the burial environment tend, however, to be dominated by the more abundant carbonates, sulphates and chlorides (Sillen, 1989).

Furthermore, the availability of these ionic forms in solution and their propensity for interaction with the bone matrix are dependent on the physicochemical nature of the depositional environment; fluorine uptake, for example, is higher in fossil bones from tropical rather than temperate climates, since environmental temperature determines its substitution rate into the hydroxyl positions of the apatite lattice (Oakley, 1950).

3.6 The Burial Environment.

Since the diagenetic source of trace elements lies in the geochemical environment (soils and groundwater), it is essential to understand the geochemical behaviour of trace elements and their relationship with the physicochemical nature of the burial environment. Pate *et al.*(1989) list the important variables to be considered at each

burial site: these include "soil pH, organic matter content, mineralogy and texture, soil solution fluoride and carbonate concentration, temperature regime, abundance and distribution of precipitation, local groundwater movement, microbial activity and duration of interment."

While a number of studies have attempted to explore chemical associations between bone and soil by comparing their elemental concentrations in respective sites (e.g. Lambert *et al.*, 1979, 1984; Kyle, 1986), Pate and Hutton (1988), Pate *et al.*(1989) point out that these values will not necessarily reflect those in soil solutions because of their differential solubilities. Instead, they recommend the measurement of soluble and exchangeable ions in solution, and suggest that both ionic substitution and mineralisation mechanisms must be considered to address diagenetic activity.

Williams (1988) has explored the alteration of the chemical composition of fossil bones by soil processes and groundwater in a number of archaeological sites. All the elements examined, including strontium, uranium and a number of rare earth elements, were found to contaminate fossil bone, and the degree of contamination was predominantly a property of (1) element availability in respective groundwaters, and (2) the redox potential of the palaeoenvironment, in the case of multivalent ions. Other studies have similarly examined the mobility and uptake of elements in conjunction with descriptions of local geochemistry and spring waters (Henderson *et al.*, 1983, 1987; Williams and Marlow, 1987), finding that element mobility, and therefore opportunity for interaction with bone, is largely a function of groundwater-rock interaction.

3.6.1 Trace Elements in Geology.

The trace element content of a soil is dependent on that of the rock from which the soil parent material was derived. Initially, the entry of trace elements in general into the crystal lattices of rocks during their formation is controlled by such factors as ionic size and charge, bond type, crystal lattice type and trace element concentration (Bear, 1964). Subsequent changes in the original levels of trace elements incorporated are then dependent on processes of rock alteration or diagenesis and weathering, and thus in the formation of soils (Bear, 1964).

Chemical weathering inevitably involves a solution process, and a number of factors may control the biogeochemical cycling of trace elements in natural waters

(fresh and marine) (Santschi, 1988): these can be divided into physical, chemical, biological and sedimentological processes which are closely interrelated. A biogeochemical description of strontium is given as a case example.

3.6.1.1 The Biogeochemistry of Strontium.

At present, around 35 strontium minerals are recognised, and in most of them strontium is bound to oxygen either as an hydroxide or in water, its valency always being 2. There are four naturally-occurring non-radioactive isotopes of strontium (Sr-84, Sr-86, Sr-87, Sr-88), whose abundances are generally constant in nature; the exception is Sr-87, where small variations exist as a function of the decay of Rb-87 (indeed, this forms the basis of Rb-87/Sr-87 chronometry) (Wedepohl, 1978).

The crystal chemistry properties of strontium determine both its behaviour and abundance in biological and geochemical systems. The size of the divalent strontium ion (ionic radius 0.112 nm) indicates that it can replace and be replaced by calcium (0.099 nm), barium (0.143 nm), potassium (0.133 nm) and lead (0.132 nm). Thus, an extensive series of isomorphous mixtures between corresponding ionic compounds of these elements can exist.

The geochemical distribution of strontium, and indeed barium, is correlated with calcium minerals e.g. aragonite, calcite, anhydrite: generally, the more calcareous a soil the higher its strontium content. Strontium and barium also form their own minerals, which are frequently dispersed in sedimentary rocks and soils as silicates, carbonates, bicarbonates or sulphates (Turekian and Kulp, 1956). The main ores are celestite (strontium sulphate) and strontianite (strontium carbonate). Strontium may also be found in phosphorites, a rock type possessing similarities to biological apatite. Strontium is able to substitute for calcium in geologic apatite: fluorapatite, for example, may contain up to 2400 ppm strontium in geological systems (Wedepohl, 1978).

Strontium is a relatively mobile element during the weathering of these minerals, and the bulk of the weathered products find their way into the sea. In sea-water, the amount of soluble strontium with respect to that of calcium is increased in comparison with soils and fresh waters, because of the higher solubility of its

salts (largely carbonates). Typically, strontium concentrations in sea-water are 6-8 ppm. These differences are clearly reflected in strontium concentrations in shells: the aragonite shells of marine mollusca contain up to 1800 ppm compared to 90-440 ppm in freshwater mollusca. Other fauna in sea-water that play a role in determining the geochemical distribution of strontium include radiolaria (*Acantharia* sp.) which extract strontium from sea-water and incorporate it into their siliceous skeletons (Wedepohl, 1978). Evaporate sediments are thus comparatively rich in strontium, and the entrance of strontium into the minerals of marine salt sediments is regulated by the calcium content of these minerals and the biogeochemical cycling of strontium. It is this difference in marine coastal and terrestrial strontium isotopic ratio that has been exploited in studies that explore means of separating biogenic and diagenetic strontium, reviewed in Chapter 2 (subsection 2.4.2.3).

Therefore, the distribution and behaviour of elements may show dramatic differences according to the nature and conditions of the environment. The sediment-water (solid-solution) interface is particularly important in influencing elemental movement, where gradients in physical properties (density), chemical (pH, Eh, ligand concentrations) and biota abundance (fauna and flora) are fundamental to their susceptibility to weathering and subsequent mobility in solution (Santschi, 1988).

3.6.2 Groundwater Systems.

Of the water that enters soil, a large part is stored as soil moisture and subsequently returns to the atmosphere by evaporation or transpiration; the remainder percolates downward in the porous rocks to the water table, where it enters the zone of saturation. Storage here, however, is temporary, as the groundwater moves under the force of gravity laterally in the direction of the hydraulic gradient toward discharge areas at the land surface. The rate of groundwater movement is very slow, commonly ranging from a few feet per year to a few feet per day (Fairbridge, 1972). Movement is complex and three-dimensional due to differences in the permeability of the rocks.

The occurrence and availability of groundwater are governed by the interaction

of numerous environmental factors, especially climate, topography, vegetation and geology. Geologic factors, principally the hydrologic properties of rocks and their stratification and structure, control the movement and storage of groundwater directly. These properties include porosity, permeability and specific yield/capacity (Fairbridge, 1972).

(1) Composition.

Groundwater can be viewed as an electrolyte solution because nearly all its major and minor dissolved constituents are present in ionic form. Davis and DeWiest (1966) classified the inorganic constituents in a typical groundwater; major constituents (greater than 5 ppm) include bicarbonate, calcium, chloride, magnesium, sodium and sulphate; minor constituents (0.01-10 ppm) - carbonate, fluoride, iron, nitrate, potassium and strontium; and trace constituents (less than 0.1 ppm) - aluminium, barium, bromide, copper, lead, manganese, phosphate, thorium, uranium, and zinc. The total concentration of the six major ions comprises more than 90 % of the total dissolved solids in water, regardless of whether the water is dilute or has salinity greater than sea-water (Freeze and Cherry, 1979). The concentrations of major, minor and trace inorganic constituents are controlled by the availability of the elements in the soil and rock through which the water has passed; geochemical constraints such as solubility and adsorption; the rates of geochemical processes; and the sequence in which the water has come into contact with the various minerals along the flow path.

Therefore, the chemistry of groundwaters is determined by a number of variables so that its physicochemical character is a property of the local/regional geology.

(2) Physicochemical character.

The various chemical and physical states of the trace elements in natural waters - their particle size, the incidence and forms of complexes and chelates- plays an important role in their movement in water and thus their availability for interaction with buried bone. Elements may exist in particulate, colloidal or soluble states, depending on mechanisms of adsorption (particle size is important here) and ion exchange (Freeze and Cherry, 1979).

Ion exchange and adsorption mechanisms are largely limited to porous geological materials that are composed of colloidal particles which have the capability to exchange ionic constituents adsorbed on the particle surfaces. This capability is quantified as the Cation Exchange Capacity (CEC), and arises from the fact that the colloidal particles have a large electrical charge relative to their surface areas. Clay minerals constitute the major colloid material in geology, and these include kaolinites, montmorillonites, illites, chlorites and vermiculites, which can all be classified as aluminosilicates. The nature of their surface charge is a function of pH: at low pH, positively charged surface prevails, while at high pH a negatively charged surface develops. The tendency for adsorption of cations and anions therefore depends on the pH of the waters.

The stability of dissolved species and minerals in aqueous environments, determining their occurrence and mobility, is to a large extent controlled by the **environmental pH and redox (Eh) conditions**. The hydrogen ion concentration of natural waters is of great significance to all chemical reactions associated with the formation, alteration and dissolution of minerals. pH values for most natural waters generally lie within the range pH 6-9, and tend to remain near constant for any given water (Stumm and Morgan, 1970). Hydrogen ion, or proton, regulation is provided by numerous homogeneous and heterogeneous buffer systems, of which the most common by far is carbonate/bicarbonate based, so that the amount of dissolved carbon dioxide predominantly determines pH. The ubiquitousness of carbonate-containing rocks allows the equilibrium reactions of carbon dioxide, bicarbonate and carbonate ions to be the basic elements in most natural waters, while other bases may include phosphate, ammonia and silicate (Stumm and Morgan, 1970; Bowen, 1979).

Organic compounds in natural waters can affect the oxidation state of trace elements, thereby exerting a strong influence on the behaviour of di- and multi-valent ions in terms of solubility, adsorption and ion exchange properties (Stumm and Morgan, 1970): examples of such elements that exist in variable oxidation states in the normal range of surface conditions include uranium, iron and manganese (Plant and Raiswell, 1983).

Microorganisms catalyse most redox reactions occurring in natural waters. Bacte-

ria are most important in groundwaters, while other types of microorganisms, such as algae, fungi, yeasts and protozoans may be important in other aqueous systems (Greenland and Hayes, 1981).

Complexation of trace elements by inorganic and organic ligands can influence their solubility, adsorption and exchange properties. Dissolved organic matter is ubiquitous in natural groundwaters, and mostly consists of fulvic and humic acids. These compounds are resistant to degradation by microorganisms, typical concentrations lying in the range 0.1-10 ppm. Organic compounds may interact with trace elements by complex and chelate formation; up to 99% of copper, for example, is associated with organic material. Complex formation of trace elements to natural organic matter is generally more important in freshwater than in seawater environments because there is less competition for organic binding and for the elements themselves by anionic forms e.g.. chloride ions. Furthermore, trace element speciation is more variable in freshwaters because compositional and pH differences are more variable (Santschi, 1988).

The pH range in most natural fresh waters is typically pH 4-9, while that of seawaters is pH 7.7 - 8.3 (Bowen, 1979), the alkalinity of the latter arising from the abundance of basic elements in solution.

3.6.3 Sea-Water.

The chemical nature of sea-water is slightly different to freshwaters. Strontium is increasingly accumulated in sea-water, together with sodium, sulphur, chloride and bromide ions, thus reflecting the differences in salinity observed between fresh and sea-water. The major constituents in sea-water are chlorine ($\approx$ 19,000 ppm) and sodium ($\approx$ 10,500 ppm), with high magnesium and sulphur values ($\approx$ 900-1,200 ppm); calcium and potassium ($\approx$ 400 ppm), bromine ($\approx$ 65 ppm), strontium ($\approx$ 8 ppm), silicon ($\approx$ 2 ppm) and aluminium ($\approx$ 1 ppm) (Bowen, 1979).

Table 3.1 directly compares fresh and sea-water concentrations of strontium and uranium, both elements of interest in fossil bone: the values shown in this table are averages of values quoted across a range of sources (Fairbridge, 1972; Rankama *et al.*, 1950; Turekian and Kulp, 1956 ; Wedepohl, 1978 ; Stumm and Morgan, 1970).

Table 3.1: A Comparison of Strontium and Uranium Distributions in Fresh- and Sea-Waters.

Element	Water source	Median (ppm)	Range (ppm)
Strontium	Freshwater	0.07	3×10^{-3} - 1.00
	Seawater	7.90	7.00 - 8.50
Uranium	Freshwater	4×10^{-4}	2×10^{-6} - 5×10^{-3}
	Seawater	3.2×10^{-3}	4×10^{-5} - 6×10^{-3}

Arnaud *et al.*(1978) explored "the fate" of archaeological bone in sea-water in a multi-disciplinary study that found enhanced calcification in samples and identified zones of fungal activity in the peripheral cortices. Generally, however, the bones studied were in good condition. The organic matrix was particularly well-preserved, perhaps by a salting process, and it was suggested that the preservation of this component had consequently facilitated apatite deposition (correlated with phosphate deposition processes in marine sediments) (Arnaud *et al.*, 1978). These observations would indicate the potential use of sea-water buried bone, although the discovery of human bone material from marine contexts has proved a rare phenomenon.

To conclude, the chemical composition of natural waters, whether terrestrial or marine, is the result of a variety of chemical reactions and physicochemical processes acting in concert (Stumm and Morgan, 1970). These include acid-base reactions; gas-solution processes ; precipitation and dissolution of solid phases; coordination reactions of metal ions and ligands; redox reactions ; and adsorption-desorption processes at interfaces (Stumm and Morgan, 1970; Bowen, 1979).

Furthermore, **the compositional, physicochemical and biological properties of the burial environment as a whole are all factors that will influence the postmortem behaviour of buried bone** (Williams, 1988).

3.7 Uranium in Archaeological Bone.

Studies of the chemical distribution patterns across bone clearly reveal chemical heterogeneity in bone (Williams, 1988). This implies that the process of elemental exchange and equilibrium takes place at different rates for different elements, in accordance with their respective mode of incorporation and the properties of the depositional burial environment and groundwater systems present throughout the inhumation period.

The diagenetic behaviour of uranium provides an ideal model of elemental uptake with which to study the combined, interactive effects of these three parameters - (1) the mode of interaction with bone, (2) physicochemical properties of the burial matrix, and (3) characterisation of the groundwater system - because its concentration and distribution profiles directly reflect the uranium abundance ratio in the surrounding medium (Henderson *et al.*, 1983; Williams, 1988).

Indeed, the presence of uranium in exhumed bone is a clear indication of diagenetic activity since modern uncontaminated bone rarely contains more than 0.2 ppm uranium by weight (Broadway and Strong, 1983). Fossil bone, however, may contain anything from 1 to 1000 ppm uranium (Bowie and Atkins, 1956) as a the result of extensive post-depositional enrichment (Hennig and Grun, 1983). Enrichment is such that concentrations in bone may be far greater than those of the enclosing sediments (Smith and Bradley, 1952).

The nature of the depositional environment largely controls the availability of uranium and hence the extent to which bones can accumulate this trace element (Rae, 1987; Seitz and Taylor, 1974). The most important factor in the burial environment appears to be the extent of groundwater percolation through bone and associated sediments (Henderson *et al.*, 1983; Rae, 1987; Williams, 1988).

3.7.1 A Brief Geochemistry of Uranium.

Geochemically, uranium is found enriched in highly evolved granitic and alkaline rocks, formed during igneous processes. While its concentration in rocks is usually low, at least 100 uranium minerals have been identified, the most common being uraninite e.g. pitchblende. The majority usually occur as hydrothermal

ering alteration products of accessory minerals (Fairbridge, 1972). The leaching of uranium as UO_2^{2+} from weathered rocks is often rapid and its concentration in surface and groundwaters is enhanced by its tendency to form complexes. Typically, the transportational environment for uranium is weakly alkaline, moderately reducing (or anoxic) groundwater with an average or higher than average dissolved carbonate species (Hostleter and Garrels 1962). In Britain, increased levels of uranium in water occur where areas have a high pH and high carbonate and phosphate levels in groundwater. A high degree of uranium enrichment tends to occur as uranium is precipitated where streams fed by slightly alkaline groundwater flow through peat bogs where pH is low and anoxic conditions exist (Szalay, 1969), so that substantial uranium concentrations in groundwater can be derived under favourable conditions.

3.7.2 The Redox Model of Uranium Uptake into Bone.

The mobility and transport of uranium into bone are dependent on the redox conditions of the burial environment which determine its oxidation state (Rae, 1987; Williams and Marlow, 1987). In aqueous solutions (groundwater) uranium can occur either in +IV or +VI oxidation states (Greenwood and Earnshaw, 1984). In the +VI state, uranium as the uranyl ion (UO_2^{2+}) or in a uranyl complex is extremely mobile. It can form several complexes with various anions; the relative stability and proportion of these species are largely dependent on the pH and Eh conditions of groundwater, and on anion concentration. Uranium is able to complex with carbonate, phosphate, sulphate, fluoride and silicate ions: the distribution and relative predominance of these uranium complexes under different pH conditions is described by Langmuir (1978). Carbonate ions are the most ubiquitous complexing agents and are dominant where pH is greater than pH 7.5, while they may be displaced at lower pH in the presence of phosphate ions, a fact that may be significant in phosphate-rich bone (Langmuir, 1978).

So, in oxidising (or oxic) conditions uranium in groundwater is found in its uranium (VI) form. The breakdown of organics in bone during the early stages of fossilization produces organic acids which are thought to produce a locally anoxic *microenvironment* (Rae and Ivanovich, 1986). Thus, as uranium in groundwater comes into contact with buried or partially buried bone it is quickly reduced to

uranium +IV, the uranous state. Uranium (IV) is thought to be stable in aqueous solution at pH < 2.9, but to give a colloid at higher pH's (Burgess, 1978).

$$UO_2^{2+} + 4H^+ + 2e^- \rightleftharpoons U^{4+} + 2H_20$$
$$\text{Eh} = + 0.62 \text{ v}$$

This enables uranium to be taken up into fossil bone as insoluble uranium IV compounds, where it is in contact with groundwater. The ionic radius of tetravalent uranium is smaller than that of hexavalent uranium and is similar to the ionic radius of calcium (0.097 nm cf Ca's 0.099 nm): consequently, uranium in its reduced form is more able to penetrate the hydroxyapatite crystal and interact with the bone matrix.

3.7.3 Uranium Interaction with Bone.

Uranium may potentially interact with bone in a number of ways (Rae, 1987).

1. **Organic complexing of uranium**: uranium ions may form weak ionic bonds with the organic ligands of degrading collagen. Certainly, geological evidence substantiates uranium-organic complexing. Doi *et al.*(1975) report that carbonaceous matter (together with zeolites, calcite and clay minerals) is the most important material for uranium fixation in geology since it is a good absorbent for uranium; poorly coalified organic matter has the highest affinity for uranium fixation from uraniferous solutions over a wide pH range. Szalay (1969) describes uranium binding to humic acids as a function of the cation exchange properties of these acids.

2. The second mode of uranium-bone interaction is via **adsorption onto the surface of hydroxyapatite crystals**, so that uranium may harbour in pores or microcracks, probably as hydrocarbon compounds (Bowie and Atkin, 1956).

3. Thirdly, interaction may occur by **uranium incorporation into hydroxyapatite by heterionic exchange with calcium**. Again, geological evidence confirms uranium interaction with apatite. Geological apatite is an important concentrate of uranium in nature: 10-66 % of the world's uranium exists in igneous apatites (Altschuler *et al.*, 1958).

Rae (1987) investigated uranium accumulation in bone by "*in vitro* fossilization simulation experiments", and found evidence for all these modes of interaction in operation, at least under the experimental conditions. Indeed, a "two-stage process" of uptake was proposed involving a combination of uranium uptake into both organic and inorganic fractions, so that the common association of uranium with the periosteal cortex may be a property of the relative preservation of mineral-organic tissue integrity and microstructure commonly reported in this cortical area (Rae and Ivanovich, 1986; Rae *et al.*, 1989). Certainly, uptake simulation work by Rae, together with fossil evidence (e.g. Bowie and Atkins, 1956) highlights the affinity of uranium for bone.

This fact was exploited by archaeological scientists who fostered the application of a series of chronometric techniques based on the isotopic composition of uranium and its decay products in archaeological material, in much the same way as geologists were dating rocks and sediments: these constitute the Uranium Series Disequilibrium dating method (USD).

3.7.4 Uranium Series Disequilibrium.

USD dating methods are applicable to material belonging to the age range 10-350 thousand years B.P. This technique therefore bridges the gap between the upper limits of radiocarbon dating and the lower limit of potassium/argon dating methods (Schwarcz, 1982). The USD method is based on the radioactive decay series of uranium-238 and uranium-235 (Ivanovich, 1982); only two of the decay pathways in this series apply to the dating of bone - Th^{230}/U^{234} and Pa^{231}/U^{235}. In terrestrial and marine weathered environments, radioactive disequilibria are set up by the differential mobility of the elements in these decay sequences. It is these disequilibria which may be used to determine absolute ages of geochemical systems.

The uranium series dating methods are based on the measurement of the activity of uranium and its various daughter nuclides. In any naturally occurring material containing uranium which has remained undisturbed, a state of secular equilibrium will exist i.e. for each decaying parent atom, one atom of each of the intermediate daughter elements also decays. However, when a sedimentary deposit is formed, various geochemical processes occur which cause isotopic and elemental

fractionation, initiating a state of disequilibrium. If no diagenetic changes or other migratory mechanisms occur after the initial formation of the deposit in this state of disequilibrium, it is possible, in principle, to determine the time of deposition (burial) by measuring the extent to which the radionuclide system has returned to the state of secular equilibrium (Ivanovich, 1982).

This dating method therefore assumes that the uptake of uranium into bone occurs early in its inhumation period around the time of deposition and is subsequently stable i.e. it assumes a closed geochemical system. However, the system is complicated by post-depositional activity that is founded on the very principles that allow the chemical fractionation of the decay series isotopes: (1) variable solubility, (2) variable capacity to hydrolyse, and (3) variable tendency to precipitate or adsorb, which all interact to produce *differential mobility*.

These phenomena would explain the reported tendency for relatively young ages to be estimated based on measurements of isotopic ratios obtained for bone surfaces, while apparently older ages are estimated for bone located in the mid-cortical regions of bone: this trend may be attributed to differential mobilities of the various uranium and thorium isotopes, and to the continuation of uranium input from percolating groundwaters later in the depositional history of the bone, causing variable activity ratios that yield inappropriate dates (Rae, 1987; Rae *et al.*, 1989).

Thus, unless a correction factor is applied to compensate for post-depositional activity, erroneous U-series dates result. Apparently successful applications of USD dating of fossil bone have been reported (Rae and Ivanovich, 1986; Rae *et al.*, 1987 ; Tiemei and Sixun, 1988) which recognise the importance of assessing the depositional environment when interpreting U-series dates.

3.7.5 Uranium as a Palaeoenvironmental Indicator.

The pattern of uranium distribution across the bone cortex, as documented by a number of workers (Badone and Farquhar, 1982; Matsu'ura, 1978; Henderson *et al.*, 1983), is not simply a reflection of the gradient associated with the gradual mineralisation of bone buried in environments possessing relatively high uranium concentrations dissolved in their groundwaters.

Rather, isotopic distributions have revealed a more complex history of actinide movement than simple diffusion, and highlighted post-depositional activity and a greater behavioural complexity than originally anticipated. Similarly, uranium distribution profiles across bone cortices, identified using such techniques as neutron activation analysis and fission track radiography, have revealed a number of different patterns, which have been interpreted in relation to changes in the physical description of the depositional environment. Cross-cortical profiles may demonstrate:

1. the normal 'U'-shaped diffusion pattern of enrichment at sediment-bone interface.

2. uranium depletion in the outer and inner cortical edges. This depletion is explained as the result of a change in the Eh of the groundwater: initially a continuous steady uptake of uranium forms a homogeneous distribution across the cortex, but a subsequent change to oxic conditions in groundwater enables uranium to be leached out from the outer rims.

3. samples showing a relatively flat profile - a cross between (1) and (2).

So, the cross-cortical distribution profile of uranium reflects fluctuations in local redox conditions and potentially provides an indication of the palaeohydrological environment (Williams and Marlow, 1987; Williams, 1988; Williams and Potts, 1988).

Furthermore, while the redox model of uranium uptake relies on the physical properties of the *microenvironment* of bone during early inhumation (Rae, 1987), the *environment of deposition* throughout its burial history is also implicated as a major factor determining uranium concentrations in fossil bone (Williams and Marlow, 1987; Williams, 1988).

Fossil bone (ranging from Pleistocene to recent in age) from Olduvai Gorge in Tanzania and from Kanam in Kenya have been used as examples to illustrate the relationship between uranium found in bone and the burial context (Williams and Marlow, 1987; Henderson *et al.*, 1983). High concentration levels of uranium have been observed in fossil bone retrieved from Beds I and II at Olduvai, corresponding to lake bottom and lake margin deposits that were generally anoxic. Fossil bone

from Bed III, on the other hand, corresponding to a fluvial deposit with an oxic environment, has demonstrated uranium levels approximately one order of magnitude lower than those of Beds I and II. Similarly, high uranium concentrations are observed in Kanam 2 fossil bone recovered from a relatively anoxic lacustrine sedimentary environment, while lower concentrations in bone located in a more oxic, less alkaline, subaerial sedimentary environment.

To summarise, the uptake and deposition of uranium in buried bone is a highly complex and dynamic process that is dependent on changes in the physicochemical properties of both the microenvironment and the depositional environment, specifically the groundwaters that come into contact with bone over time. Conversely, the sensitivity of uranium to changes in the depositional environment of bone has implications for the reconstruction of the palaeoenvironment, and in particular the nature of different groundwaters passing through a geological system. Thus, the intimate relationship between elemental uptake and the burial environment has come full circle.

3.8 A Practical Assessment of Bone Diagenesis.

This chapter has highlighted the complexity, variability and unpredictability of bone diagenesis, properties of innumerable interacting variables that are both intrinsic and extrinsic to bone. The acceptance of the inevitability of the diagenetic alteration of biogenic levels in bone has led to many strategies designed to recognise and circumvent the problem of elemental contamination (Price *et al.*, 1992; Lambert *et al.*, 1989,1990 ; Sillen, 1986,1991 ; Sillen and LeGeros, 1991). These strategies, some of which have been referred to earlier in the chapter, are summarised in the following review.

3.8.1 Methods for Identifying and Circumventing Diagenesis.

A variety of strategies have been employed to identify, evaluate and reduce diagenetic effects. These methods are generally limiting in the information that they offer and as a means of minimising contamination, again largely as a result of the unpredictability and complexity of diagenesis.

1. The identification of diagenesis.

Comparison of the physical and chemical attributes of modern, unaltered bone to those of archaeological samples has resulted in a wide variety of tests for the evaluation of diagenetic contamination (reviewed in Price *et al.*, 1992). Physical characterisations include microscopic examination of bone structure (Garland, 1988) and examination of bone crystallinity (Tuross *et al.*, 1989a,b).

Examination of bone microstructure under the light microscope can reveal post-depositional disruption by microbial activity, which may alter chemical or isotopic composition (Grupe and Piepenbrink, 1988; Schoeninger *et al.*, 1989). Furthermore, decomposition of the organic component (specifically collagen), together with possible chemical alteration of apatite, can be detected by a loss of optical orientation which is registered under polarised light (Garland, 1988). As the organic matrix is removed, the mineral becomes more exposed to the action of groundwaters and thus more susceptible to chemical alteration. This, as reviewed, tends to be correlated with an increase in crystallinity which can be monitored using X-ray diffraction and infra-red spectroscopy (Sillen, 1989; Kyle, 1986 ; Bartsiokas and Middleton, 1992). By focusing on differences in the microcrystalline structure of biogenic and geological hydroxyapatite, X-ray diffraction is able to demonstrate the interacting processes of increasing crystallinity, recrystallisation, and the incorporation of mineral phases.

Comparative skeletal studies compare the elemental concentrations in excavated material with "typical" baseline levels documented for human (or animal) species. These include measures of the calcium/phosphate mass ratio (Sillen, 1989) for the inorganic fraction, and percentage yields after ashing as an estimate of the organic fraction. Chemical alteration of bone and mineral addition can produce significant changes in these measures.

Other quantitative techniques include intrabone, interbone, interspecies and inter-populational comparisons (reviewed by Sandford, 1992). Interbone comparisons are usually made between different types of bone, such as femora and ribs (Lambert *et al.*, 1982; Grupe, 1988), but are limited by complications imposed by metabolic, sex- and age-specific physiological differences. Interspecies comparisons compare

the chemical constituents of human bone with faunal material representing different dietary patterns (Runia, 1987; Kyle, 1986; Sillen, 1981). Diagenetic activity is deduced if elemental levels deviate from values predicted on the basis of dietary intake, while biogenic concentrations of fauna, whether contemporary or modern, facilitate reconstruction of prehistoric human diets (Buikstra *et al.*, 1989; Sillen, 1988; Price *et al.*, 1985).

However, quantitative analyses in palaeochemical studies are limited by the lack of reference data for prehistoric and modern human populations (Price *et al.*, 1989). This aside, differences in the elemental compositions of soil and groundwater within and across sites may lead to substantial interpopulation differences in biological and diagenetic deposition (Runia, 1988; Sillen *et al.*, 1989), thereby questioning the validity and applicability of such a reference database.

The elemental composition of soil can itself be measured to assess diagenetic effects. Comparisons may be made between the total elemental contents of associated bone and soil samples (Lambert *et al.*, 1979, 1984, 1985). Such studies may rely on the concentration gradient theory which predicts significant contamination of elements present in higher concentrations in soil than in bone i.e. obeys the laws of diffusion (Klepinger, 1984; Lambert *et al.*, 1979). Conversely, anisotropic elemental distributions in soil and bone may be indicative of uptake and leaching processes themselves; elevated levels in the soil next to bone may reflect material that has been leached from bone into soil, and vice-versa (Lambert *et al.*, 1984). Certainly the unpredictable nature and direction of diagenetic activity (Klepinger, 1984) complicate such strategies, which are more effective in combination with other approaches. Furthermore, Pate and Hutton (1988) argue that the total elemental content of soils is not a pertinent measure for assessing potential diagenetic activity; rather, they recommend analyses for soluble and exchangeable ions, thereby accounting for differential solubilities of mineral constituents in the burial matrix.

The phenomenon of differential solubility under different physical conditions is a also a consideration in methods that utilise "indicator elements" or known contaminants to infer probable diagenetic change of other elements. This strategy employs elements that are common in depositional environments but absent/rare in unaltered bone: these include silicon, uranium, yttrium and the rare-earth el-

ements (Kyle, 1986; Williams and Marlow, 1987 ; Williams, 1988; Williams and Potts, 1988), and their presence suggests possible additions of other elements of more direct significance to archaeometry. However, Section 3.7 highlights the complexity of uranium uptake into bone and thus the caution that must be exercised when adopting such a diagnostic approach.

The characterisation of cross-cortical distribution profiles of elements, such as uranium, has been widely used to identify the diagenetic contamination of a broad range of elements. This is based on the premise that contaminants typically accumulate at the cortical edges, so that the lining of cortical surfaces and a 'U'-shaped profile indicate adsorption and diffusion processes, respectively (Badone and Farquhar, 1982: Lambert *et al.*, 1983, 1984; Klepinger *et al.*, 1986). However, this does not account for leaching phenomena that may escape detection by the electron microprobe whose detection limits are rather high for many elements (hundreds of ppm) (Lambert *et al.*, 1983); nor is it wise, based on observations for uranium, to assume automatically that homogeneity indicates an absence of diagenesis. Nevertheless, the common observation of surface accumulation of contaminants has given rise to methods that attempt to physically remove the diagenetic component of bone.

2. The circumvention of diagenesis.

Recently, a number of methods have been developed for reducing the effects of diagenesis, and their respective applicability and suitability are currently under investigation (Price *et al.*, 1992; Lambert *et al.*, 1989a/b, 1990).

The earliest attempts to overcome diagenetic contamination were chemical in nature (Sullivan and Krueger, 1981; Sillen, 1986, 1989). Sullivan and Krueger subjected finely powdered bone to a sequence of acetic acid washes, while Sillen washed the powdered bone in acetone and extracted with acetate (acetic acid/sodium acetate) buffers. Both chemical procedures depend on the dissolution of contaminants in an aqueous acetic acid phase.

Chemical washing procedures were originally designed to remove calcium and carbonate-containing contaminants since these define the most abundant mineral forms in soil solution. Thus, acid solutions in which bones are soaked typically

contain high levels of calcium and alkali elements, but are low in phosphorus, indicating the dissolution of a soluble, non-bone component.

Sillen (1986, 1989) developed a method of sequentially washing bone powder, applying a technique designed to exploit the differential solubility of biological and geological apatites; specifically the solubilities of carbonates, hydroxyapatites and fluorapatites. Differences in the composition of biogenic and diagenetic apatites confer differences in respective solubility, therefore providing a means of separating these two components. Chemical analysis of effluent solutions demonstrates a pattern of high calcium/phosphate ratios and soluble ion concentration (e.g. sodium, potassium, magnesium, strontium) in initial washes, falling slowly to a steady value. This is interpreted as the initial removal of highly soluble diagenetic components and a slow decrease to a steady value representing biogenic values. Moreover, the similarity of the extraction behaviours of strontium and barium to that of calcium, with flat elution profiles at the end of the sequence and the restoration of species by trophic level, would suggest that post-depositional effects can be minimised (Price *et al.*, 1992). Indeed, the use of a stronger, unbuffered acid has been applied in order to remove recrystallised, diagenetically altered bone mineral as well as extranneous phases and thus account for all sources of contamination (Price *et al.*, 1992).

Price *et al.*(1992) have further modified the chemical cleaning procedure by substituting dilute acid for an acid/reducing agent (hydroxylamine hydrochloride), mixture, thereby accounting for oxide forms that may not be soluble in the former. This is particularly significant for barium (Parker and Toots, 1972), but may also include aluminium, manganese and iron in oxide contaminants.

Mechanical cleaning to reduce or eliminate contaminants involves the removal of the outermost periosteal and endosteal cortices by physical abrasion (Lambert *et al.*, 1989, 1990). Such abrasion serves to remove or diminish inorganic elements that have been adsorbed onto the bone surface during burial, or filled voids left by decaying organic material, or that have entered bone apatite at the crystal surface. This abrasive cleaning method is effective in removing a suite of elements typically found in soil oxides and clays but characteristically low in unaltered bone (less than 200 ppm): these include iron, aluminium, manganese and potassium. The

removal of zinc observed at surfaces is also evident (Lambert *et al.*, 1990). However, the applicability of such a procedure, where typically 1-3 mm of the bone surface is removed, is limiting in that it does not have any effect on uniform contamination that might have pervaded the entire cross-cortical width, as observed for uranium, yttrium and the REE's (Henderson *et al.*, 1983; Williams and Marlow, 1987; Williams, 1988; Williams and Potts, 1988). This would suggest that this cleaning strategy alone is not sufficient, but might complement alternative methods.

Indeed, Lambert *et al.*(1990) recommend a combination of physical abrasion and mild chemical washings as a suitable procedure for bone preparation prior to inorganic analysis.

However, chemical cleaning, too, has a number of drawbacks. While accounting for elements that penetrate the full cortical width of bone by its uniform action, chemical washing does not affect elements that are insoluble in the acidic medium. Furthermore, this method may remove *biogenic* constituents, such as sodium, potassium, zinc and magnesium according to Lambert *et al.*(1990) who have applied different cleaning procedures to both fossil *and* modern bone material.

Similarly, acetic acid treatments designed to eliminate secondary carbonates may simultaneously cause isotopic changes and recrystallisation: Lee-Thorp and van der Merwe (1991) have found that isotopic shifts reflecting the dissolution of an adsorbed (more soluble) *biogenic* carbonate-containing phase are observed in modern mineral after treatment, together with the recrystallisation of bone apatite to brushite (dicalcium phosphate-dihydrate). These changes are not observed in well-fossilised (older) archaeological bone which is more crystalline and more resistant to acid attack. This highlights the caution that must be exercised when applying such chemical washing procedures to more recent archaeological specimens in particular, since they may simultaneously remove biogenic material in addition to secondary minerals that have been diagenetically introduced.

Nevertheless, Price *et al.*(1992) conclude that acid washing of bone effectively removes significant levels of contamination, while returning the calcium/phosphate ratio to its biogenic value and thus permitting more accurate measurement of the biogenic signal.

3.9 Summary.

Chapters 2 and 3 have focused on the dynamicity of bone in both ante-mortem and postmortem contexts in its chemical interaction with the immediate environment : the *biogenic-diagenetic continuum.* Evidence for the diagenetic alteration of a number of trace elements (strontium and uranium, for example) has been reported and consequent implications discussed. Strategies designed to evaluate and reduce contamination have been reviewed, and the practical problems associated with each highlighted.

Indeed, recent research approaches have tended to focus on the design and improvement of methods that attempt to reduce and thereby circumvent diagenetic effects. An alternative approach is surely to tackle the root of the problem more directly by endeavouring to understand the diagenetic processes themselves, and further, the conditions that promote them.

Certainly, it is clear that the problems posed for biological anthropologists by the diagenetic alteration of bone chemistry hinge on the complex and highly variable nature of this phenomenon. It is essential to investigate this variability in detail so that trace element measurements in archaeological bone provide pertinent indicators for accurate assessment of the past.

Such an objective demands systematic experimental exploration of the many facets of diagenesis in order to gain further insight and understanding into the mechanisms and differential susceptibility of elements to diagenesis, particularly those directly relevant to palaeo-reconstruction. An essential component of such a strategy is the investigation of the influence exerted by the primary physicochemical properties of the burial environment on diagenetic processes.

"The multiplicity, unpredictability, and dynamic nature of diagenetic processes demand that diverse perspectives and research strategies be used to delineate more sophisticated methods for recognising and, where possible, circumventing postmortem effects." **(Sandford, 1992).**

Part II

Experimental Design and Procedure.

Chapter IV

Strategy and Technique in Diagenetic Research.

4.1 Outline of Present Research.

For this thesis, I present a series of laboratory-based studies that investigate the potential uptake of trace elements into bone. My research work focuses on strontium and uranium because of their direct application to palaeochemical studies that attempt to determine dietary and dating information from exhumed bone.

I have designed a number of experimental methodologies to explore the uptake of these elements under variable environmental conditions, and employed a variety of analytical techniques to examine different aspects of the simulated uptake processes/mechanisms.

The large majority of experiments conducted comprise a series of **immersion** studies whose methodology and design have been progressively revised. The immersion procedure involves placing bone samples in solutions of different chemistries (strontium, uranium) maintained under variable environmental regimes. While this immersion approach has been applied in studies investigating the *medical* implications of trace element uptake into bone, little *in vitro* work has been conducted to explore bone diagenesis (section 4.2.1). Moreover, an investigation of *postmortem* uptake processes requires the incorporation of a broader range of variables, and to meet this demand research presented here includes important modifications in design and in the subsequent treatment and analysis of bone and solution (refer to Section 4.2.2).

Both elemental analysis and probe microanalysis methods have been employed to determine total elemental uptake and cortical distribution in bone, respectively. The alteration of the organic:inorganic ratio by physical/chemical means *prior* to immersion, and the chemical separation of these components in bone *after* immersion, are carried out in an attempt to characterise further the respective mechanism(s) of elemental uptake.

In addition, the effect of the immersion procedure on a number of diagenetic alterations typically observed in archaeological bone is explored: these alterations include (1) crystallinity changes in the inorganic matrix, and (2) the removal of the organic matrix, over time and against the pH of immersion. Potential ion exchange mechanisms are further investigated by measuring cation exchange properties and identifying readily exchangeable ions in bone fractions: this approach comprises a **percolation** system, rather than one of immersion, whereby solutions are passed through columns of sample material and their chemistries measured before and after percolation.

Figure IV outlines the general experimental procedures for these uptake simulation studies, identifying the treatment of bone and solution, the variables under investigation and analytical techniques employed at each respective stage of the experimental series.

This chapter comprises a descriptive account of my experimental work, discussing the rationale behind each design and the instrumentation selected, to ensure that the maximum amount of information is collected for each approach. The instrumentation is also applicable to **field studies**, carried out to supplement laboratory work and to provide "working models" with which to compare simulated uptake data. Field studies are also described here.

Uptake simulation work commences with a review of past uptake studies that have provided a grounding for the original research presented here.

4.2 Uptake Simulation Studies.

4.2.1 A Review of Past Uptake Studies.

The experimental simulation of trace element uptake into bone has been conducted in a number of investigations that have focused on living bone and the physiological consequences of their findings. Very few studies have applied this approach to explore bone diagenesis. Thus, while both *in vivo* and *in vitro* experiments have been carried out to investigate the respective uptake of strontium and uranium, these have explored the medical implications of their uptake into **living** bone

Figure IV : An Overview of the Experimental Design of Uptake Studies.

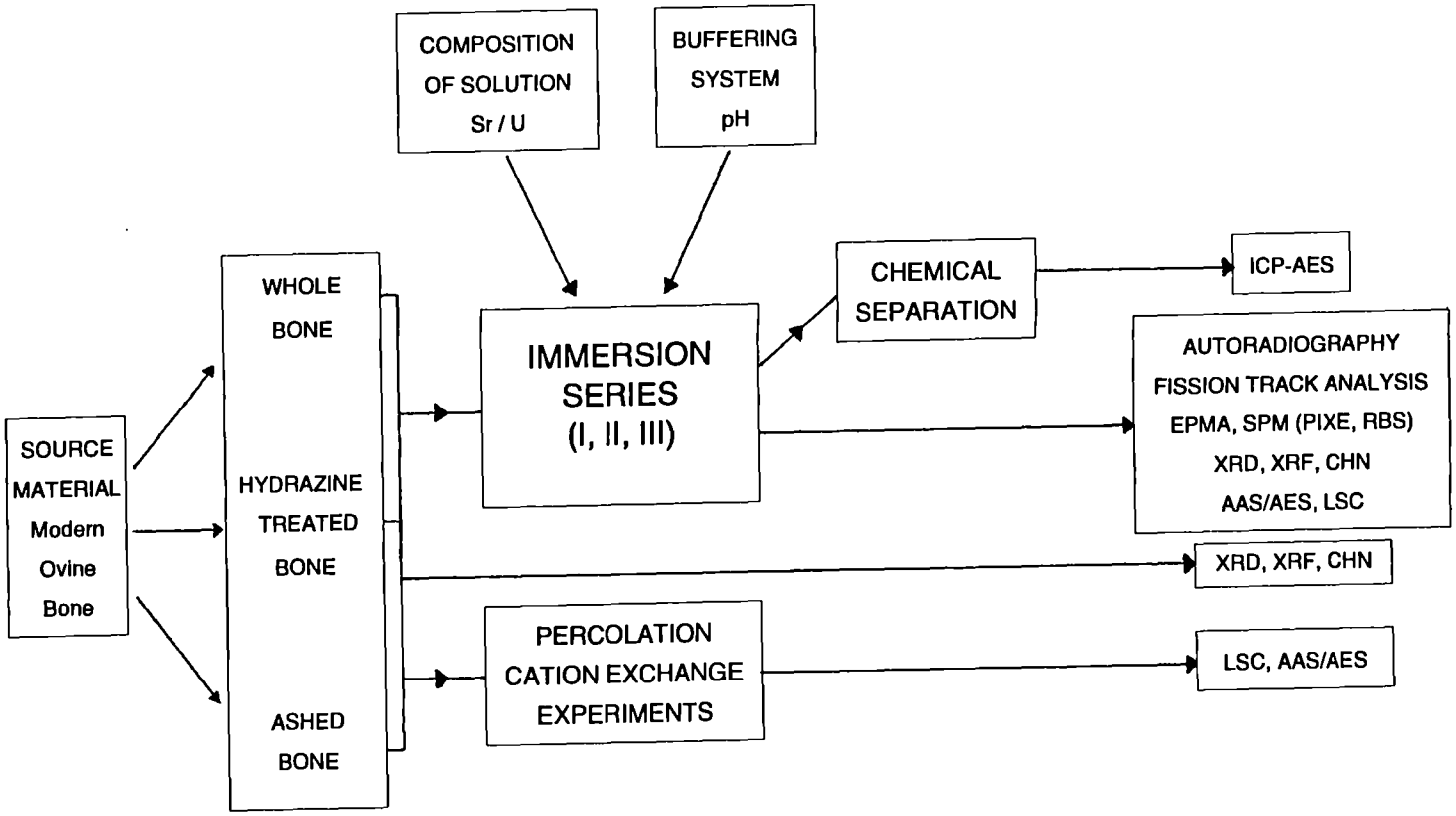

(paying particular attention to their respective radioisotopes and the consequences of radioactive exposure).

Examples of *in vivo* work include studies by Stevens *et al.*(1980) on the beagle and Priest *et al.*(1982) on the rat: these provide evidence to suggest that uranium is able to bind with organic tissue, with superficial phosphate ions in hydroxyapatite, and exchange with calcium in the inorganic matrix. However, while *in vivo* experiments provide such information on the behaviour of *living* bone, they can only give a broad indication of potential postmortem mechanisms of elemental exchange and interaction, since they cannot feasibly reflect the predicament of buried bone.

Some of the earliest *in vitro* experiments in this field include the classic studies of Neuman and Neuman in 1949. They demonstrated the importance of hydroxyapatite in the uptake of uranium which was found to be a surface phenomenon of cation exchange with calcium in the lattice. However, this study examined only powdered fresh and ashed bone, and other than stating that an increased uptake was observed in ashed bone, failed to take account of any changes in the inorganic matrix caused by the process of ashing itself and ignored any influence of the bone's organic content on uptake and subsequent distribution of uranium in bone.

Similarly, early studies on strontium uptake used fresh powdered fat-free bone and were largely concerned with strontium-*inorganic* matrix interaction. Johnson *et al.*(1970) and Harrison *et al.*(1967) employed the use of strontium radiotracer (Sr-85) solutions - the former using an immersion technique similar to Neuman *et al.*(1949), while Harrison passed the solution through a column of powdered bone in a percolation arrangement. In both these studies, immersing and influent/effluent solutions were analysed, rather than the bone powder itself, and implications again made with reference to **living** bone. Indeed, in some studies, solutions resembling extra-cellular fluid at constant pH were used in an attempt to simulate *in vivo* conditions more closely. Moreover, since the physical conditions of the *in vivo* environment are maintained within narrow limits via homeostatic mechanisms, no attempt was made to vary the ambient physical/chemical parameters (e.g. pH).

In contrast, the open system of the burial environment is subject to many geochemical, geophysical and biological influences that differ according to the local

geography, geology, groundwater and climate. *In vitro* experiments enable the manipulation of a wide range of variable controlling parameters that may artificially represent such influences. Despite this potential, experiments investigating trace element uptake, predominantly using simple immersion procedures, have been limiting in one way or another because of the need to reduce or control the many variables that can influence bone in its burial context and thus clearly identify the effects of an isolated few. For example, Hare (1980) examined the effects of water on the leaching and chemistry of organic fractions in bone, and Von Endt and Ortner (1984) examined the effects of bone size and temperature on diagenesis, but in the process neither accounted for trace element uptake and the effect of pH. Similarly, Lambert *et al.*(1985) investigated metal-ion exchange under variable pH and temperature, and, other than comparing whole and crushed bone material, failed to explore the relative contribution of organic and inorganic components.

Rae (1987) was the first worker to consider environmental factors with reference to **postmortem uranium uptake by buried bone** using *in vitro* simulation experiments. More importantly, she took account of both the inorganic and organic components in uranium uptake, and the influence of the organic fraction on Eh and pH conditions in the bone. Rae immersed metatarsal bones for 4-8 weeks in 232-Uranium solution made up in a simulated groundwater of variable pH maintained at two different temperatures. Subsequent analysis of bone and solution, together with chemical separation of organic and inorganic matrices, revealed uranium association with both organic and inorganic fractions. A number of mechanisms for uranium-bone interaction were discussed: (1) uranium-organic complexing, (2) surface adsorption and (3) incorporation into hydroxyapatite (reviewed in Chapter 3, sub-section 3.7.3). However, Rae's early work served only as a preliminary study: sample numbers were minimal and limited by the technique employed (alpha-spectrometry). Moreover, as solutions were not buffered, the effects of pH on uranium uptake were not explored.

In contrast to other workers, Rae used *whole/intact* bone and bone *slices* rather than powdered material and was thus able to observe cross-cortical distribution profiles of uranium and thorium: the importance of such an approach becomes clear in later discussion. Current research at Oxford by Millard (pers.comm.) has exposed *powdered* bone material to uranium solutions and subsequently examined

the microdistribution of uranium in individual grains of bone using the scanning proton microprobe. This has clearly illustrated surface adsorption of uranium to bone. More importantly, Millard has developed a simple mathematical model, containing parameters that allow representation of different geochemical environments and ground water hydrology, describing the uptake of uranium by bone on the basis of a diffusion driven movement of uranium into bone.

However, Rae *et al.*(1989) conclude that uranium uptake into bone is a more complex process than its simple diffusion into the cortical tissue. Rae determines this conclusion by noting the apparent inconsistency in uptake patterns between the results of case study analyses of archaeological bone and further *in vitro* laboratory studies. In this study, Rae *et al.*(1989) used slices of **archaeological** bone, again immersing them in unbuffered artificial groundwater containing radiotracer at variable temperatures and durations of immersion.

Many workers have chosen to use archaeological bone samples for uptake simulation experiments instead of modern bone. This is because fresh bone contains large amounts of lipids, polysaccharides and other organics which are hydrophobic and would therefore restrict access of the exchange solution to hydroxyapatite microcrystals. Workers such as Lambert *et al.*(1985) and Krueger (1989) have argued that in a natural burial context these organics rapidly degrade, so that 'young' archaeological bone better simulates the long-term effects of exchange between groundwater and hydroxyapatite. Of course this is a generalisation and many fossil bone specimens have been found possessing a large percentage of their original organic content, despite being thousands of years old (e.g. Randall *et al.*, 1952).

The following section outlines contrasts and modifications in my experimental design.

4.2.2 A Description of Present Uptake Studies.

4.2.2.1 Bone Material.

The preceding review describes research that has predominantly focused on the physical and chemical properties of the *hydroxyapatite* component of bone: little attention has been paid to the organic component. The bulk of *uranium* uptake

is believed to be relatively rapid, occurring early in the bone's inhumation period when the organic fraction may as yet be relatively unaltered. Certainly, work by Rae has suggested that the organic component itself plays a major role in uranium uptake.

In order to account for the organic matrix, **modern** ovine (sheep) bone has been used for this series of experiments because of its relatively uncontaminated and unaltered state, and its availability. It might arguably have been more appropriate to use archaeological bone material to examine strontium uptake, since past studies suggesting that strontium levels are little, if any, diagenetically altered might indicate that its uptake is a relatively slow continuous process compared to that of uranium. Nonetheless, I chose to examine the relative role of organic and inorganic components in both uranium and strontium uptake mechanisms. Therefore, the organic-inorganic chemical integrity of modern bone, which endows living bone with its unique physical and chemical properties, is explored in this study and its findings discussed with reference to buried bone. The term "whole" bone is used in subsequent chapters to describe bone that has not been physically or chemically compromised and thus retains its natural complement of organic and inorganic components.

However, the use of whole bone creates complications in subsequent interpretation of data and in assigning the observed phenomena as a property of either the inorganic or organic matrix or a combination of the two i.e. difficulties arise in the separation and identification of the actual mechanism(s) of bone-element interaction. In order to investigate the behaviour of the inorganic fraction, the physical and chemical properties of inorganic constituents of bone require measurement, which is often hampered by its organic fraction. Spectroscopic measurements of bone mineral, for example, are complicated by the adsorption properties of protein. Similarly, X-ray diffraction spectra, as demonstrated in this study (Chapter 8), may comprise the diffraction maxima of hydroxyapatite superimposed on an amorphous background scatter arising from protein. Therefore, it is desirable to investigate the behaviour of bone as a whole and as separate components in order to gain a complete and comprehensive account of bone-element interaction, at least under the experimental conditions of the simulation.

The isolation of the organic tissue from the mineral phase poses a number of problems since the removal of the inorganic matrix destroys the very integrity of the bone's macrostructure, thereby altering the gross morphology. Since one of the aims of this experimental study is to represent the natural predicament of buried bone as closely as possible, and, moreover, to compare cross-cortical distribution profiles obtained in the laboratory with those observed in real archaeological examples, the removal of the inorganic matrix and the subsequent breakdown of the bone's structural entity is inappropriate. Instead, the organic:inorganic ratio of bone samples is altered using two procedures *to remove the organic component*:

(1) ashing bone, and

(2) hydrazine treatment.

By comparing the uptake behaviour of whole bone with bone whose organic content has been compromised to variable degrees by progressive removal, the role of the organic and inorganic matrices in elemental uptake mechanisms can be determined. The two methods used to remove the organic component of bone in this study are discussed in turn.

(1) Ashing bone.

The ashing of bone material at temperatures ranging 500-1000 °C is routine practise as a means of removing the organic fraction prior to analysis of the inorganic component. However, in addition to burning off the organic material, the ashing process has a number of other effects which may themselves have some bearing on subsequent uptake-simulation studies. On exposure to high temperatures, bone undergoes physicochemical processes which not only strongly influence its morphologic diagnosis but also its chemical composition, potentially altering it from that of the original bone. Work by Schutkowski and Hummel (1986, 1987) has demonstrated alterations in elemental content at specific temperatures. Moreover, it has been reported that at temperatures over 800°C, physiological hydroxyapatite, because of its calcium deficiency cf. stoichiometric apatite, changes to β-tricalcium phosphate, which entails shrinkage of up to 30 % as a consequence of recrystallisation and crystal fusion (Betts *et al* , 1967). The effects of heating on bone crystallinity are briefly described in this study (Chapter 8, section

8.1). A more detailed study by Shipman *et al.*(1984) has reported an increase in bone crystallinity with increasing temperature of ashing, probably as a result of recrystallisation processes.

In summary, the heating of bone will generally affect:

(1) water content:- dehydration occurring at different levels of the bones' physical structure ie. in the crystal lattice by cleavage of hydroxyl bonds, at the crystal surface or the hydration layer, and with water bound to organic material.

(2) the organic material itself, decomposition occurring somewhere between 300 and 525 °C.

(3) the inorganic component:- the crystallinity of hydroxyapatite increasing with temperature, the conversion of hydroxapatite to β-tricalcium phosphate at higher temperatures, and fusion or melting at 800 °C upwards. In addition, selected trace elements are burnt off at characteristic temperatures (Grupe and Hummel, 1991).

An ashing temperature of **500°C** has been used in this study, although there is apparently no universal ashing temperature applicable to palaeochemical investigations. At 500°C, all organic tissue has virtually been removed by the burning off of carbon, but relatively little has occurred in terms of physical and chemical changes within the inorganic matrix (according to preliminary tests described in Chapter 5, sub-section 5.2.1.2), thereby reducing further variables which might complicate direct comparisons of uptake behaviour across whole and ashed bone samples.

Nevertheless, ashing bone at 500 °C does still have an effect on the crystallinity of hydroxyapatite. This fact is taken into consideration when comparing the uptake behaviour of ashed material with its whole bone counterpart, by acknowledging the potential ionic exchange and surface properties of hydroxyapatite in various crystalline states, ranging from the imperfect crystallinity of biologic hydroxyapatite through to geologic apatite and stoichiometric synthetic apatite (Chapter 8, section 8.1).

An alternative approach to investigating the behaviour of the crystalline matrix of bone, without altering its naturally imperfect form in the way that heating

does, is to progressively remove the organic component by chemical means, using hydrazine.

(2) Hydrazine treatment of bone.

Hydrazine (NH_2NH_2) was first used as a deproteinising reagent by Swedlow *et al.*(1972), replacing ethylenediamine organic extraction. Termine *et al.*(1973) showed that hydrazine, unlike its predecessor, does not induce substantial molecular alterations when deproteinising bone: only minor chemical changes are induced and practically no alterations in electron microscopic or physicochemical properties observed. Corresponding studies here confirm that hydrazine has little effect on the elemental composition of bone (XRF analysis: Appendix Ib) or on its crystallinity (XRD analysis, Chapter 8).

Hydrazine acts by rupturing peptide bonds within proteins. Collagenase, similarly, breaks down collagen and this enzyme has been used routinely to remove the bone's organic matrix (e.g. Rae, 1987). However, collagenase requires very specific operating and storage temperatures and is easily inactivated (denatured) outside this narrow temperature range. Hydrazine, on the other hand, rapidly and effectively deproteinises bone in a broader range of conditions, the rate of extraction depending on both the size of the sample and on the temperature of extraction. Termine *et al.*(1973) reported complete deproteinisation of bone using 95 % hydrazine with moderate heating (40-60 °C) after only 48 hours. Using these observations as a guideline, preliminary investigations have been carried out here to explore the rate and efficiency of hydrazine under the experimental conditions employed in simulation and separation studies, thus determining the required temperature and duration of hydrazine exposure (Chapter 5, sub-section 5.2.1.2).

It was anticipated that hydrazine-treated material would more closely represent 'pure' non-stoichiometric, biologic hydroxyapatite than its ashed equivalent, thereby mimicking the behaviour of the inorganic matrix early in its diagenetic history.

4.2.2.2 Solutions.

The immersing solutions used here also demonstrate important modifications in comparison with uptake studies by other workers. Rae (1987), for example, used

a *simulated groundwater* as the immersing or percolating solution. However, in the majority of experiments conducted here, ultrapure water was chosen as the bulk volume of uranium and strontium solutions. Uptake studies carried out at Harwell (Berry *et al.*, 1991) revealed a fourfold difference in uranium uptake from solution by corresponding samples in pure water, since the added complication of competition for cation exchange sites by caesium, sodium, and potassium ions was occurring in groundwater samples. Furthermore, workers at Harwell (Berry *et al.*, 1991) tended to observe both surface adsorption and incorporation phenomena in pure water samples, while only fissure- and pore-filling was observed in groundwater samples. So, pure water has been used in order to simplify the system (by reducing cation competition) and enhance uranium/strontium uptake over the relatively short experimental period adopted here.

Another important modification of the work described in this study is the introduction of *effective* and *appropriate* **buffers** to the immersion systems to maintain a desired pH regime. Previous studies attempting to simulate trace element uptake into bone have tended to use either acid/alkali addition to adjust pH (e.g. Rae, 1987), or a range of common biological buffers (e.g. Lambert *et al.*, 1985), or omitted the effect of pH altogether (e.g. Von Endt and Ortner, 1984). The limitations of these options are explained following the definition of a buffer (detailed in Dawson *et al.*, 1986; Perrin *et al.*, 1974).

- **Buffers.**

A **buffer** is defined as a substance which by its presence in solution increases the amount of acid or alkali that must be added to cause unit change in pH. From the Henderson-Hasselbach equation (Dawson *et al.*, 1986), it can be shown that optimal buffering occurs when the pH is equal to the pKa of the ionising group, and falls at an increasing distance from that value. In practise, the useful range for a buffer is its pKa $\pm$ 1 pH unit. The pKa value of any buffer, and hence its effective pH range for buffering, is affected by temperature. Many common buffers have a high coefficient of pH dependence with temperature, these buffers usually consisting of weak acid-salt or weak base-salt systems. All of these buffer systems exhibit significant deviations from the requirements of an "ideal buffer". These requirements are broadly to maintain a given pH in a particular medium

whilst not interfering with chemical and biochemical processes occurring in this medium, and not impeding in any way observations or measurements made on the system. Tris, for example, is a popular biochemical buffer: Lambert *et al.* (1985) used it in their study of ion uptake by bone. However, its appreciable solubility in organic solvents permits it to penetrate biological membranes and thus potentially interfere with biochemical processes, and it has a high coefficient of pH dependence with temperature. Similar limitations are also found with other traditional buffers such as citrate, borate, diethylbarbiturate and phosphate. Clearly, in attempting to simulate ion uptake and exchange in bone at relatively high temperatures, such properties are undesirable; buffer cations and anions themselves may interfere with any biological and/or geochemical reactions occurring.

In fact, preliminary exploratory investigations carried out by myself found that examples of these common buffers (specifically, Tris and Bis-Tris), together with simple acid/alkali addition, were not effective in maintaining solutions at the desired pH in the presence of bone ie. they were unable to counteract or buffer the bone's own buffering effects. The pH of solutions containing bone invariably tended towards pH 5-6 after only a short period of exposure (4-5 days). In contrast, appropriate zwitterionic buffers were found to be effective in keeping pH milieu constant.

Zwitterionic buffers, developed by Good *et al.*(1966), by definition contain both positive and negative ionisable groups: secondary and tertiary amine groups provide the positive charges whilst sulphonic and carboxylic acid groups, the negative. It is these highly polar, non-interacting anionic and cationic sites that make these buffers insoluble in organic solvents and thus unable to interfere with biological membranes (penetration, solubilisation, adsorption on surfaces etc.). The characteristic properties, that make them particularly suitable for this study, can be summarised as:

- good aqueous solubility
- chemical stability and non-toxicity
- insolubility in organic solvents and thus no penetration of biological membranes
- no participation in biochemical reactions

- no or only slight complex formation with cations
- minimum dependence of pH on temperature and ionic composition of medium
- pKa values and therefore optimum buffering capacities in the physiological pH range.

The physical properties of HEPES and CHES buffers are described in table 4.1.

Table 4.1: Physical properties of HEPES and CHES buffers

Buffer (abbrev.)	Formula	M.wt	pKa at 20°C	δ pKa /°C	Sol. at 0°C (mol/l)	Complex formation (log Km)			
						Mg++	Ca++	Mn++	Cu++
HEPES	$C_8H_{18}N_2O_4S$	238.81	7.55	-0.015	2.3	-	-	-	-
CHES	$C_8H_{17}NO_3S$	207.29	9.55	-0.011	1.15	n	n	n	n

where n = *unknown , and* - = *negligible*

Uptake simulation experiments have been conducted over a range of pH conditions that represent acidic, neutral and alkaline environments. This range extends from pH 4 (the rate of hydroxyapatite dissolution is too rapid below this value) to pH 10. Values outside this range (acid and alkali extremes) are considered less pertinent to such a study because generally bone is only preserved at sites with slightly acidic or alkaline soil (Gordon and Buikstra, 1981). Consequently, environmental pH regimes of pH 4, 6, 7, 8 and 10 have been studied.

While the majority of experimental work has comprised the *immersion* of bone, prepared as outlined, in solutions with variable physicochemical description, a number of associated studies have also been carried out in conjunction with immersion experiments. The rationale and methodology for each are now described.

4.2.3 Chemical Separation Study.

The main approach described thusfar to investigate the respective contribution of the organic and inorganic components in elemental uptake involves the alteration of the sample's organic:inorganic ratio *prior* to strontium or uranium exposure. In this area of study, whole bone is immersed in solution, *followed by* the chemical separation of the organic and inorganic phases after the immersion period. Since strontium and uranium levels in these solutions were predicted to be fairly low, each extraction has then been chemically analysed using inductively-coupled plasma atomic emission spectrometry, or ICP-AES (refer to subsection 4.4.2.1), for strontium, uranium, calcium and phosphorus concentrations. It was anticipated that analysis of the extractions using this sensitive technique would determine the relative extent of organic and inorganic interaction.

This strategy was briefly attempted by Rae (1987): 24 hr treatment with dilute (0.5 M) nitric acid was used to dissolve the hydroxyapatite component, and collagenase used to remove the collagen. In the present study, hydrazine has been used for the latter because, as described, it is simpler to use and does not require such specific temperature constraints and operating conditions.

These separation techniques assume that any strontium or uranium present in either the mineral matrix or organic matrix is mobilised into solution in the appropriate reagent. The extraction of both components is carried out separately on the same sample (the sample divided in two) in an attempt to compensate for simultaneous mobilisation from each source.

An alternative method for investigating organic-inorganic roles in general cation, e.g. strontium and uranium, uptake into buried bone is described below, using a Cation Exchange Capacity arrangement adapted from standard soil tests.

4.2.4 Investigation into the Cation Exchange Properties of Bone.

Here, a technique commonly used in soil science to measure the cation exchange capacity (CEC) of soil, e.g. Bear (1964), has been modified to accommodate similar studies on bone and its major components.

A small but important fraction of the total elemental content of soil minerals occurs as readily exchangeable or adsorbed ions. The supply of exchangeable ions is slowly renewed by weathering of ions from within the crystal structure of these various soil minerals. The different mineral species in soils have a controlling influence on the release of structural ions and on the chemical activity of exchangeable ions, as does the soil's content of clay and organic matter (refer to Chapter 3, section 3.6).

The determination of the concentration of cations held on soil exchange sites involves the replacement of these cations with a single species of cation from a concentrated leaching solution of known cation concentration. As the leaching solution drains through the soil, cation exchange occurs, the soil cations being replaced by those of the leaching solution. Thus the leaching solution is altered in character in terms of the species of cation present and it can be assumed that these cations have been derived from the leached soil.

The Cation Exchange Capacity (CEC) is defined as the amount of a cation species bound at a particular pH: leaching solutions are usually buffered to a standard pH (pH 7) because CEC can vary considerably with pH. Ion exchange itself can be defined as a reversible process by which cations and anions are exchanged between solid and liquid phases (and between two solid phases if in close contact with each other). From these definitions, and considering the importance of both the ambient pH and the organic content of bone in the burial situation, it was considered appropriate to apply these CEC techniques to bone, in order to investigate potential bone-groundwater interactions.

Soil has been substituted for a range of organic-inorganic bone fractions, including collagen, hydrazine-treated and ashed bone, and two phosphate standards. It was anticipated that a comparative measurement of their CEC's would give an indication of the potential participation of organic and inorganic matrices in bone-soil elemental exchange and interaction.

Samples are placed in leaching tubes and the leaching solution, buffered to pH 7, percolated through the sample column; the leachate is analysed using spectrophotometric methods (refer to subsection 4.4.2.1) to identify readily exchangeable ion forms. Standard soil CEC experiments use a concentrated solution of ammonium acetate as the leaching solution, whereby cation exchange sites become occupied

with ammonium cations. On removing the surplus ammonium acetate from the sample with pure ethanol and then re-leaching the column with a different concentrated salt solution (commonly sodium chloride), the ammonium cations are in turn exchanged. By measuring the ammonium content of the leachate an estimate of the number of exchange sites can be obtained, and the **Total Cation Exchange Capacity** calculated.

So, this procedure enables (1) the identification of cations that the bone/reference sample is able to exchange readily, and (2) the determination of respective total CEC's, using ammonium acetate as the leaching solution. In this way, the relative loss of calcium ions, for example, may be established under different experimental conditions.

The CEC properties of each sample are discussed in relation to their respective chemistries and degrees of crystallinity, since samples range from amorphous to highly crystalline substances.

The effect of uptake simulation studies - specifically the *immersion* procedure - on sample crystallinity has been explored in further detail.

4.2.5 Crystallinity Studies.

In a real burial environment, elements from soil solutions or groundwater may be introduced into buried bone in a number of ways: by association with authigenic minerals e.g. calcite that enter the bone during diagenesis; by residing in pores, voids or microcracks ; adsorption onto the surface of apatite crystals; and, finally, actual incorporation into the hydroxyapatite matrix (refer to Chapter 3, section 3.5.2).

Substitutions in hydroxyapatite may affect the following properties:

a. lattice parameters

b. crystallinity, reflecting crystal size or internal strain

c. chemical and thermal stability

Crystallinity is a term which implies large crystal size and the absence of structural defects (Jenkins, 1978).

Previous XRD studies of fossil bone have demonstrated that bone apatite progresses from the biologically imperfect crystalline state to the more perfect crystallinity of stoichiometric hydroxyapatite, a property which in itself may facilitate the incorporation of extrinsic minerals during diagenesis (Bonar *et al.*, 1983; Nelson *et al.*, 1986; Tuross *et al.*, 1989a,b).

To my knowledge, the effect of *uranium* incorporation on the crystallinity of hydroxyapatite has not been studied. However, a number of studies have investigated the effects of *strontium* incorporation over time. Shemesh (1990) studied the post-depositional recrystallisation of sedimentary apatites and found that the strontium content of ancient fish remains generally *decreased with increasing crystallinity*. In contrast, Nelson *et al.*(1986) examined prehistoric bone and found *no evidence of changes in strontium concentration* correlating with any secondary mineralisation and crystallinity changes in prehistoric bone. However, Tuross *et al.*(1989a), studying recent wildebeest bone samples, observed a slow and progressive change in crystallinity tending towards an *increase in apatite size and strontium accumulation* over a taphonomic period of 10 years. By year 10, Sr/Ca levels were significantly different as was apatite c-axis growth (defined in section 4.4.1.4), effected by changes in both crystal length and width/thickness (Tuross *et al.*, 1989b).

They suggest 2 possible explanations for these changes:

(1) As the organic matrix decomposes, the small natural crystallites are released and washed out of the bone more rapidly than the large ones.

(2) The originally small (40 nm) crystallites dissolve and reprecipitate under the influence of water, yielding an overall increase in average crystal dimension. This theory is supported by Schoeninger (1982).

So the increased crystallinity (c-axis growth) observed in fossil bone is undoubtedly the result of a combination of factors each under the influence of groundwater,

which, in turn, are presumably affected by the physical, chemical and biological conditions of the burial environment (e.g. Shemesh, 1990).

The conditions set up in the experimental simulation should, in theory, accelerate diagenetic processes by exaggerating natural weathering and groundwater effects e.g. acidic conditions (pH 4-5) at an elevated temperature. Therefore, investigations have been made on the crystallinity of a range of bone samples immersed in strontium and uranium solutions under different conditions. (section 4.4.1.4). The effect on crystallinity of the following parameters are explored:

1. organic content
2. pH of immersion
3. immersion in strontium or uranium solutions.

In the case of the latter, recorded peaks in the diffraction profiles (section 4.4.1.4) have been identified and assigned to mineral phases, either intrinsic or extrinsic to hydroxyapatite, which might indicate the nature of any strontium/uranium interaction with bone.

Earlier XRD studies on the crystallinity of hydroxyapatite have concentrated on the characteristic 002, 210, and 310 diffraction peaks because they are well-isolated and of relatively strong intensity (Bonar *et al.*, 1983; Nelson *et al.*, 1986; Tuross *et al.*1989a,b). However, peak 002, 310 and the combined 112/211 peaks are used in this study for two reasons: (1) their relative clarity, (2) they are not subject to interference from peaks representing the strontium and uranium salts used in these uptake studies.

The crystallinity indices used here comprise three separate measurements, all of which are dependent on peak breadth, or more specifically, the peak breadth measured at half the height of maximum intensity above background - $\underline{B}$. The value of this measurement decreases as crystallinity increases ie. the sharper the peak, the more crystalline the sample. This value itself does not provide explicit structural information but it is affected by crystalline size, disorder, chemical substitution, vacancies and the relatively large proportion of small bone mineral crystallites at

or near the surface - more importantly, those that are more prone to diagenetic alteration.

After correcting for the effect of instrumental factors (Klug and Alexander, 1962), the following measurements of crystallinity have been calculated:

1. the reciprocal of the corrected peak breadth (D), as used by Tuross *et al.*(1989a,b). This value is directly *proportional* to crystal size/perfection (Klug and Alexander,1962), but is not itself directly the crystal size since it does not correct for lattice strain. It does generally relate to size and lattice variation in the c-axis direction, and is useful for comparative purposes.

2. the breadth:height ratio, $\frac{B}{H}$. This ratio is often used in geological studies as an indicator of crystallinity.

3. the peak intensity, I, effectively the area under the peak (B x H).

To summarise then, X-ray diffraction patterns of the mineral content of the bone powders subjected to immersion treatment have been recorded to:

(a) identify and estimate relative abundance of mineral phases, in addition to apatite, present in the samples

(b) obtain information on the crystallinity (size/perfection) of the apatite component of the mineral under a range of variable conditions.

4.3 Fieldwork Studies.

In addition to uptake simulation work and corresponding studies, fieldwork has been conducted to provide real archaeological examples of diagenetically altered bone material and to explore the nature of this alteration in detail.

4.3.1 The Evaluation of Archaeological Bone.

A variety of analytical approaches have been employed to illustrate bone diagenesis:

(1) Microscopic examination, to assess the degree of microstructural preservation (e.g. Ascenzi, 1969), and estimate the extent of infiltration by secondary minerals

as pore-fillers,

(2) Total elemental analysis, to quantitatively monitor the degree of contamination,

(3) Probe microanalysis, to identify cross-cortical elemental profiles and microdistribution, and thus explore in detail the relationship between the bone matrix and diagenetically introduced elements,

(4) X-ray diffraction, to discriminate any changes in crystallinity and to identify evidence of secondary mineralisation or precipitation.

The bone material analysed in this study was excavated from a variety of burial sites, both terrestrial and marine, and therefore represents a broad range of environments with which to correlate observed patterns of diagenetic activity.

4.3.2 The Characterisation of Sediments.

Associated soils and sediments, where available, have also been chemically identified by their mineral (XRD) and/or elemental (XRF) composition.

Pate and Hutton (1988) were among the first workers to emphasize the use of soil chemistry data to address diagenetic activity in buried bone, acknowledging that the chemical composition of postmortem ionic substitution phases and secondary minerals in buried bone is to a large extent dependent on the availability of *ion species in the burial matrix* to groundwaters. Several studies (e.g. Lambert *et al.*, 1979, 1984; Nelson and Sauer, 1984; Kyle, 1986) have explored bone-soil chemical interactions by comparing the elemental concentrations in exhumed bone and associated soils. Lambert *et al.*(1984) investigated the dynamics of elemental interchange between buried bone and the adjacent soil by systematically analysing soil samples in and around *in situ* bone to monitor elemental profiles and thus identify flux patterns. In this way, elements were observed to be taken up into bone (e.g. iron, manganese) or leached from it (e.g. calcium); those registering a homogeneous distribution (no apparent elemental gradients) were assumed to be independent of the diagenetic process (e.g. strontium). The basic methodology has been repeated in this study, using a different analytical technique (XRF instead of AAS), and results correlated with corresponding bone data so as to construct a more complete description of diagenetic processes.

In addition to a chemical description of associated soils, two physical parameters have also been measured on-site where possible: pH and Eh. Both profoundly influence anionic equilibria in soil/groundwaters. These equilibria regulate the precipitation and dissolution of solids, the adsorption and desorption of ions and their concentrations, and the dissociation of organic acids (refer to Chapter 3, section 3.6). For example, Eh conditions may determine the valency and thus solubility of ionic species such as iron, manganese and uranium, and as a consequence govern their availability for interaction with bone. Although absolute values for soil Eh have no precise thermodynamic significance because of the difficulties in measuring true values (Stumm and Morgan, 1970), they are semi-quantitative measures of the soil's oxidation-reduction status, and therefore reveal whether a soil is aerobic or anaerobic.

pH is one of the main factors that govern the rate and degree of bone mineral decomposition (Newesely, 1987), and hence, is an important consideration with regard to the chemical stability of both organic and inorganic components. Indeed, Gordon and Buikstra (1981) reported significant correlations between osseous deterioration and soil acidity, and suggested that pH measurement, together with the individual age of the bone, be appropriately employed in anticipating the recovery potential of a site and therefore maximising the amount of osteological data to be recovered.

It was anticipated that the combination of these analyses on archaeological bone material and associated soils/sediments collected from a variety of burial environments would further elucidate the nature of bone-soil interactions under field conditions. Furthermore, data from real archaeological examples would provide useful case studies with which to compare simulated uptake observations.

- **Summary.**

These respective studies - immersion, chemical separation, cation exchange and crystallinity, together with fieldwork - employ a wide variety of analytical techniques. These are discussed in the next section with a brief description of the theory and mechanism of each, together with a review of past relevant work utilising these techniques and both their advantages and limitations. The more practical aspects (sample preparation, standards etc.) are described in Chapter 5.

4.4 Analytical Instrumentation.

The range of analytical techniques employed in this study can be classified according to a number of criteria: firstly, with regard to their applicability to bone (solid) or solution analysis; these are further divided into single element or multi-element analyses that are either quantitative or qualitative in nature.

Techniques applied to the analysis of bone material are described in sub-section 4.4.1, followed by techniques analysing solutions in 4.4.2.

4.4.1 The Characterisation of Bone.

The majority of data collected from the analysis of both experimentally exposed bone and real archaeological examples are qualitative in nature and consist predominantly of *in situ* microanalysis of major, minor and trace elements. The advantages of *in situ* analyses, in contrast to quantitative total elemental analyses and methods involving physical and/or chemical elemental (or mineral) separations, are that elemental data can be more clearly interpretated in a locational context; hence, deductions can be made concerning the likely mechanism of diagenetic reaction based on the cross-cortical distribution of elements both intrinsic and extrinsic to the bone matrix.

It was anticipated, therefore, that far more information regarding the characterisation and mechanisms of diagenesis would be obtained by *in situ* microanalysis of "intact" sliced bone material compared to absolute values for total elemental content of homogeneous powdered samples. Microanalysis can potentially distinguish between surface adsorption, incorporation and pore-filling mechanisms, limited only by the spatial resolution of the microanalytical technique. Two general approaches to microanalysis have been adopted in this study: techniques that capitalise on the nuclear properties of the sample's contents (autoradiography and fission track analysis); and techniques based on characteristic X-ray production (electron microprobe analysis and proton-induced X-ray emission (PIXE) analysis). These are comprehensively reviewed by Burnett and Woolum (1983).

A number of past studies, for example Rae *et al.*(1989), adopted the approach of locational microsampling of the cortex followed by chemical analysis. However,

this procedure is laborious and its spatial resolution very coarse: for these reasons, this rather dated "microanalytical" approach has not been attempted here.

Total elemental analyses for calcium, phosphorus, strontium and uranium have been carried out in this study on both experimentally exposed bone and archaeological material including bone and soil samples. In the case of the former, where strontium and uranium concentrations were highly exaggerated, it was anticipated that quantitative analysis would affirm microanalytical data in determining uptake trends under a variety of conditions. With regard to archaeological material, quantitative measurement of the total elemental content of these elements in bone from a range of burial sites in conjunction with elemental distribution profiles in the surrounding soil matrix would supplement corresponding microanalytical data and help provide a more complete account of natural diagenetic activity.

4.4.1.1 Autoradiography and Fission Track Analysis.

Particle track radiography provides a method of *in situ* trace element microanalysis based on the imaging of particles emitted from a sample section either by the decay of radioactivity contained in the sample (autoradiography) or by prompt radiation induced by an external bombardment of the sample (radiography). Fission track analysis is included in the latter. All nuclear techniques are reviewed by Ivanovich *et al.*(1982).

Radiographic techniques have been applied in a number of archaeological studies examining fossil bones and teeth. These range from one of the earliest employing autoradiography to map the distribution of naturally-occurring uranium and thorium in fossil bone examples (Bowie and Atkin, 1956) to fission track analyses of fossil bone (Williams and Marlow, 1987) and fossil teeth (Seitz and Taylor, 1974). Williams and Potts (1988) combined the two techniques, fission track analysis and neutron activation-induced beta-autoradiography, to examine the cross-cortical distribution of a range of elements, including uranium and the REE's, in fossil bone samples from different groundwater environments to explore palaeoenvironmental aspects of diagenetic alteration.

(1) Autoradiography.

Elemental microdistributions can be determined for naturally occurring alpha and beta emitters by alpha- and beta-autoradiography, respectively, without the necessity for neutron irradiation. Therefore, a preliminary uptake simulation experiment is set up in the present study which employs autoradiography as the principal analytical tool. Autoradiography is used to examine the uptake and distribution of uranium, a naturally-occurring alpha emitter, and a strontium radioisotope (beta-emitting strontium-90) in bone samples that have been exposed to solutions of these "tracer elements". A radiotracer is used in the case of strontium because it is not naturally radioactive. After a period of exposure to the solutions, bone samples are prepared as thin sections and reacted with a suitable detector material, here a photographic emulsion.

After development, the photographic film with the developed image is quantitatively analysed by optical density measurement (Rogers, 1979). Image density is represented by the number of silver grains present per unit area of the film; an image analyser plots the density of each image which, on cross-comparison, provides an indication of general patterns of uptake.

(2) Fission Track Analysis (FTA).

The uranium content and distribution in a range of archaeological bone examples and in a number of experimentally exposed samples have been measured using Fission Track Analysis. This method is more sensitive than simple autoradiography but requires irradiation of the sample to *induce* fission (Fleischer *et al.*, 1975). Moreover, since uranium (235) is the only naturally occurring nucleus that is fissionable by thermal neutrons, this technique is unambiguous in its findings.

Solid state nuclear track detectors (SSNTD) register the pathways, or tracks, of energetic particles produced by the decay or fission of radioactive isotopes e.g. Fleischer *et al.*(1975). The advantages of these detectors over photographic film are their cost, ease of development and their insensitivity to light. SSNTD's have been used widely to examine the distribution of trace and minor amounts of uranium in polished thin sections of geological material (e.g. Kleeman and Lovering, 1967; Duane and Williams, 1980). In this study, CA80-15 film, an alpha-sensitive

cellulose nitrate detector (reviewed by Basham and Easterbrook, 1977), has been used because of its high contrast properties. The detector is mounted on the surface of the sample and both irradiated for a period dependent on the level of activity in the sample.

After exposure (irradiation details are given in Chapter 5, subsection 5.5.1.2) and chemical etching in a suitable alkali solution, the tracks of each alpha-particle impinging on the detector describe the location of uranium in the cross-cortical section. Microlocational details are examined using optical microscopy and recorded as micrographs (photographs of microscopical images).

Microanalytical methods based on radiographic principles are relatively inexpensive and easy to use. However, the majority of microanalytical data are obtained using electron microprobe analysis which affords greater versatility in data collection and presentation, and is able to simultaneously analyse, both qualitatively and quantitatively, a wide range of elements.

4.4.1.2 Scanning Electron Microscopy (SEM) and Electron Probe Microanalysis (EPMA).

Comprehensive accounts of electron probe microanalysis methodology and instrumentation are given by Potts (1987: Ch.10) and Shinoda *et al.*(1972). A scanning electron microscope with microprobe facility was used in this study, allowing measurement of high-resolution scanning electron photo-micrographs incorporating a quantitative X-ray analysis capability. Briefly, EPMA works on the principle that when an electron beam, accelerated to 15-30 kV, is focused on the surface of a sample, sample and beam interact so that X-rays are generated that are characteristic of the atoms in the sample. The intensity of these X-rays is measured using wavelength dispersive (WD) or energy dispersive (ED) spectrometers. The former serves to isolate particular wavelengths of X-rays and record the intensity of X-rays at each, providing a more accurate measurement than the latter system which measures elemental concentrations according to the energy produced by characteristic X-rays. Both WD- and ED-microprobe analyses have been carried out in this study.

Electron bombardment generates not only characteristic X-rays but also a 'continuous spectrum' or 'bremsstrahlung', consisting of photons emitted by electrons suffering deceleration in collisions with atoms. This continuum constitutes an unavoidable background in X-ray spectra which limits the sensitivity and detection limits of this technique. EPMA is designed to measure the concentrations of major and minor elements above 0.2 percent weight for elements from fluorine and higher in the Periodic Table with a precision of the order of 1-2 % and an accuracy of 2-5 % . The potential spatial resolution of the analysis is 2-3 microns.

Back-scattered electron (BSE) images are included in the data: these represent electrons that are reflected, or back-scattered, off the target before they penetrate the surface and ionise atoms to create X-rays. The proportion of electrons that are back-scattered increases with atomic number (of the element in the sample) so that a map of the sample surface under analysis can be generated by synchronous display of the BSE intensity. The advantage of this is that the spatial resolution of the image is inherently better than the equivalent X-ray image, and an exact location and description of the cortical area under examination can be obtained.

EPMA data are illustrated as "**linescans**", or elemental profiles, and **digimaps**, or mapped areas of cortex, each under variable magnification. A linescan is a 1-D array of numbers representing the intensities of respective elements at a series of equally-spaced points along a line. In the DIGIPAD program (Link Analytical) used here, a linescan is a special case of an image: it is an image where the y-resolution has been set to 1. An image is a 2-D array of numbers representing the intensities of individual picture elements or "pixels" covering a rectangular grid over the field of view. Digimaps simply plot this area as a 2-D image to examine the intimate association of each element with the microstructure of the bone.

EPMA is predominantly employed to analyse calcium, phosphorus and strontium or uranium cortical distributions in bone material as a consequence of its immersion in a variety of solutions under variable conditions. In addition, a number of archaeological bone samples have been analysed using this method for comparison with other analytical techniques.

Electron probe microanalysis, or EPMA, has been used in the past to detect microdistribution patterns and thus identify post-depositional contamination (Lam-

bert *et al.*,1983, 1991; Parker and Toots 1980; Parker, 1967). In contrast to analysis of the total elemental content of samples, the geological significance (origin) of a given element concentration can only be effectively evaluated by determining the precise location of individual elements in the bone matrix. In this way, EPMA has successfully identified diagenetically introduced elements -

(1) by the shape of their cross-cortical distribution profiles - a 'U'-shaped profile being interpreted as one of postmortem elemental diffusion into the bone, and

(2) by their association with pores and lacunae within the bone's microstructure.

However, despite its good spatial resolution (2-3 microns), the detection limits and sensitivity of EPMA are relatively poor for a number of elements of interest to the archaeologist. Indeed, detection limits for many elements are of a similar order of magnitude to their expected biogenic levels (tens-hundreds ppm); for example, the detection limit for strontium and uranium is approximately 500 ppm.

The **scanning proton microprobe** provides an alternative microanalytical technique that offers both mapping and quantitative functions, and combines high sensitivity and good positional resolution. Studies that directly compare electron and proton microprobe analysis have found that the former is able to reveal trace elements undetected by EPMA (Grime *et al.*, 1991; Roeder *et al.*, 1987), yet its application to the study of bone diagenesis has hitherto failed to be exploited.

Therefore, the applications of the proton microprobe to the analysis of archaeological bone and studies investigating diagenesis are explored here.

4.4.1.3 Scanning Proton Probe Microanalysis (SPM).

When a nuclear particle beam, such as a proton beam, impinges on a sample many different types of interactions can take place. Measurement of the resulting reaction products (X-rays, backscattered and transmitted protons, secondary electrons, gamma-rays etc.) coupled with a scanning facility can provide a wealth of information about the sample.

The proton microscope is the most common and well-developed type of nuclear microscope, of which there are currently around 35 world-wide, offering a range of facilities. These microscopes are described in detail elsewhere (Grime *et al.*, 1991;

Traxel, 1990; Watt and Grime, 1987) and Grime *et al.*(1991a) specifically detail the facility at Oxford University used in this study.

The proton microscope employs a beam of high energy protons, that have been accelerated through electrostatic fields of several (2-5) million volts, typically via a Van de Graaff or tandem accelerator, and then focused down to a few microns or less. Using magnetic or electrostatic deflection, the finely focused beam can then be used for point analysis of selected areas at sub-micron resolution, or can be scanned across the specimen to yield detailed information about its structure. A data acquisition system correlates the data from the detectors with the instantaneous beam position and allows elemental maps or compositional information to be generated.

This information can be derived in three different ways. The proton beam may just pass straight through the sample, losing energy as it collides with electrons. This energy loss can be measured revealing the density of the sample at each point scanned. Thus contour maps of energy loss or, equivalently, density can be produced using this technique of Scanning Transmission Ion Microscopy, or STIM. Alternatively, the beam may collide with nucleii in the sample and be scattered: the rebound energy depending on the mass of the nucleus struck. This is Rutherford Backscattering Spectrometry, or RBS.

RBS, as with STIM, takes account of the energy loss of backscattered protons that occurs as the proton makes its way back out of the sample - the degree of energy loss indicates the depth of the nucleus that the proton struck. Hence, RBS provides a 3-D non-destructive means of mapping elements.

RBS can resolve and analyse the lighter elements in the Periodic Table (below sodium), complementing the third means of analysis - measurement of X-rays emitted as the protons collide with electrons: Proton-Induced X-Ray Emission (PIXE). Experimental work here is largely concerned with PIXE analysis or, more specifically, microPIXE since a small (micron/sub-micron) beam size is employed; some simultaneous RBS data are also included.

PIXE involves only collision with electrons in the inner core of the atom - so, like RBS, is not influenced by the chemical state of the sample (chemical effects

generally influencing only the outer electron shells). Thus, PIXE analysis itself is quantitatively accurate providing that the structure of the sample is well-defined since measurements are adversely affected by uncertainty about sample matrix composition, thickness and homogeneity (Grime *et al.*, 1991a; Jaksic *et al.*, 1991). Such information about sample structure is not required for simultaneous PIXE and RBS analysis, even for thick inhomogeneous samples, because this combination is able to confirm that the sample is uniform at the point where the spectrum is taken (Grime *et al.*, 1991a).

PIXE is inherently more sensitive than EPMA because of the much lower background of incidental X-rays produced by secondary electron bremsstrahlung, since protons are weightier particles that are less prone to deflection than electrons during interaction with the target. Thus, detection limits are at least an order of magnitude lower than EPMA, routinely analysing the concentration of elements to ppm levels in many types of sample: detection limits quoted by Vuorinen *et al.*(1990) for archaeological bone include 0.4 ppm strontium, 0.2 ppm manganese, 0.2 ppm iron, 0.3 ppm zinc, 0.5 ppm copper and 0.4 ppm lead. Although the lower detection limits are advantageous, absorption of the soft X-rays characteristic of lighter elements effectively precludes the application of PIXE to elements lighter than silicon (Anderson *et al.*, 1989): however, this has little bearing on the suite of elements typically of interest in archaeological bone and in uptake simulation studies described here.

Biological samples are ideal materials to analyse using PIXE, having the advantage over geological, electronic and metallurgical samples in that they are largely composed of elements with low atomic number (C, H, N and O), so the amount of secondary bremsstrahlung is small and there is no obscuring or masking of X-rays from trace elements caused by low-energy tails from high-energy X-rays. Moreover, because of its small beam size (1 micron or less) PIXE causes little damage to the material as a whole, although in the actual area of analysis loss of material by sample heating or sputtering may occur, together with possible shrinkage or distortion. Rapid scanning of the beam minimises damage.

PIXE has therefore proved a valuable technique in biological applications. Many studies have been carried out on hard tissue ranging from mineralised structures

in plants to animal skeletal material (reviewed by Watt *et al.*, 1991), in order to investigate biomineralisation processes, for example (Rokita, 1991; Cichocki *et al.*, 1990).

Proton microbeam applications in archaeology have been reviewed by Demortier (1987) and include analysis of historical documents, clays and sherds. More recently, PIXE and RBS analyses have been used to characterise the usewear (and hence function) of prehistoric flints by identifying the matter which was worked with them (Christensen *et al.*, 1992).

Proton microbeam studies on archaeological bone are few. An unpublished study (Grime, pers.comm.) examined the diagenetic alteration of bone, focusing on the lead content in early Romano-British skeletons: lead levels were concentrated at the matrix surface, thereby indicating contamination from the surrounding soil. Similarly, work on fluorine profiles revealed fluorine diffusion into bone and teeth (Coote and Holdaway, 1982). One of the most comprehensive studies on archaeological bone to-date is that of Vuorinen *et al.*(1990) who examined a range of major and minor elements in infant bones using *quantitative* PIXE (and PIGE or gamma-ray emission) and attempted to discriminate those of biogenic and diagenetic origin.

It is therefore apparent that relatively little work has been carried out on archaeological bone despite the tremendous potential of PIXE: this may reflect its relative lack of availability and its cost compared to the electron microprobe.

In this study, examples of archaeological bone material from a variety of burial environments have been analysed qualitatively by PIXE, in the form of mapped areas of cortex, and in some cases quantitatively with simultaneous RBS analysis, in order to explore patterns of diagenetic alteration and provide a comparative study with EPMA. These data are predominantly classified as fieldwork and described in Chapter 9.

In addition, PIXE analysis is carried out on examples of bone experimentally exposed to strontium and uranium for direct comparison with corresponding EPMA data. The spatial resolution of the SPM is further exploited in a detailed investigation of the experimentally-induced micro-distribution of uranium near the

bone-solution interface.

It was anticipated that this work would provide a pertinent exploratory investigation into the applications of the SPM in this research field where its tremendous potential has hitherto been unexploited.

4.4.1.4 X-Ray Diffraction (XRD).

X-ray diffraction analysis has been carried out on:

(1) modern bone samples immersed in solutions of different chemical composition under variable conditions, in order to monitor the effects of these variables and of elemental uptake on bone crystallinity, and

(2) archaeological bone examples from a range of burial environments to identify diagenetic contamination, as Kyle (1986) had done by demonstrating calcite and quartz minerals in fossil bone, and to monitor crystallinity, correlating this to the physical and chemical parameters of the burial matrix.

These objectives are discussed in further detail in section 4.2.5. The technique of XRD is detailed by Hardy and Tucker (1988), Klug and Alexander (1974), and Potts (1987). Crystallography itself is comprehensively described by Klug and Alexander (1962).

The phenomenon of X-ray diffraction by crystals results from a scattering process in which X-rays, produced when high energy electrons bombard atoms in the target sample, are scattered by the electrons of these atoms without change in wavelength. The resulting diffraction pattern of a crystal, comprising both the positions (maxima or peaks) and intensities of the diffraction effects, is a fundamental physical property of the substance, and thus provides a means of identification of the crystal structure. Diffraction maxima yield information about the size, shape and orientation of the basic crystal unit (or unit cell) of the 3-dimensional structure.

The diffraction maxima are located at positions that define the "axial ratios" or positioning of the crystal planes (faces) relative to one another. The perpendicular distance between successive planes in the space lattice of a crystal (each plane describing the loci of the atomic or molecular units of the crystal pattern) is the

interplanar distance or *d spacing*. This distance is measured indirectly by monitoring the *2 θ* position of the beam i.e. the angle of deviation of the diffracted beam (the angle between the diffracted beam and the undeviated incident beam).

The diffraction maxima or peaks in the XRD profile become sharper and their resolution increases with increasing crystal size (Posner, 1969). Thus, the crystallinity of a sample can be monitored by measuring the dimensions of these peaks.

With regard to the bone material used in experimental work, it was appreciated that the broad, ill-defined peaks that typify modern bone, and are indicative of extremely small (0.01 microns, or less) crystal size, would afford difficulty in the assessment of true positions of backgrounds and peak maxima; at the same time, the use of ovine bone material (from abattoir origin) would negate variability in crystallinity caused by individual age (Bonar *et al.*, 1983) and taxon dependancy (Legros *et al.*, 1977). Therefore, any observed changes in crystallinity could confidently be attributed to the immersion treatment.

4.4.1.5 X-Ray Fluorescence (XRF).

X-ray fluorescence analysis (XRF) has been employed to measure the total elemental content of (1) bone subjected to immersion treatment and (2) archaeological bone examples and, where possible, associated soil samples.

Comprehensive descriptions of this technique are found in Hendry (1975) and Potts (1987). XRF operates on a similar principle to XRD: X-rays are fired at a sample and interaction of this primary radiation with atoms in the sample causes ionisation of discrete orbital electrons. During the subsequent electronic rearrangement by which the atom then de-excites back to the ground state, fluorescence X-rays of energy characteristic of that element are emitted, and the intensity of emission is measured with a wavelength dispersive X-ray spectrometer. In this way, a wide range of elements (majors, minors and trace) can be detected in a variety of materials.

XRF analysis is commonly used in mineralogical studies for the analysis of soils. This is illustrated by information provided by the International Atomic Energy Au-

thority (IAEA) on soil reference standards†: XRF provides the third most common technique, behind neutron activation (NAA) and atomic absorption (AAS), contributing a large percentage of the data that constitute the quoted reference values. For example, reference values for elements of interest to the archaeologist such as calcium, strontium, uranium, and zinc consist respectively of 27%, 35%, 7% and 20%, contribution from XRF analyses. Thus, XRF is an established and widely used technique in geological studies.

With regard to the analysis of bone, XRF is less typically used. While IAEA literature indicates XRF as one of five techniques (the predominant techniques being AAS and NAA) that contribute to the reference data for bone, with XRF accounting for 8% and 20% of the reference values for calcium and strontium respectively, it must be emphasised that the range of bone reference material available on the market is minimal. This fact provides a major problem for all inorganic analyses of bone, whether modern or archaeological in nature. In an attempt to overcome this drawback, a range of reference/standard materials have been used in this study, consisting of H5 animal bone (IAEA), rock phosphate, synthetic hydroxyapatite, a number of soil standards (for minor and trace elements) and IAEA-312 soil (containing radionuclides). At the same time, it was appreciated that such a compensatory measure would introduce complications caused by variable matrix interference effects.

Nevertheless, XRF offers a number of advantages over the popular alternative techniques (AAS and NAA). XRF precision is good for major, minor and trace element analysis. Sensitivity and detection limits are competitive: for example, detection limts for calcium, strontium and uranium are typically 12 ppm, 3 ppm and 6 ppm, respectively. Sample preparation is relatively simple, and the method is non-destructive. In contrast to spectrophotometric methods, the sample is not required in solution, thereby avoiding potential problems created by incomplete dissolution of the sample (Winter and Marlow, 1991).

Total elemental analyses of bone experimentally exposed to strontium and uranium solutions, and archaeological samples together with associated soils (where possi-

† AQCS, IAEA, P.O. Box 100, A-1400 Vienna, Austria

ble) have been measured using X-ray fluorescence to supplement microanalytical data.

Archaeological bone is analysed by XRF to investigate the sensitivity of this technique in the study of diagenetic contamination. An earlier study had concluded that XRF provided a pertinent contribution to this field when contamination of bone was relatively high (El-Kammar *et al.*, 1989). In addition, soil samples collected in and around the vicinity of some of this material have been analysed in an attempt to identify elemental profiles in the immediate burial environment of bone *in situ* that are indicative of bone-soil interaction and thus diagenetic activity.

4.4.1.6 Carbon-Hydrogen-Nitrogen Analysis (CHN).

A number of representative bone samples have also been subjected to elemental organic analysis to monitor the decay and subsequent removal of the organic component of bone under variable conditions of immersion. By correlating consequent strontium and uranium concentrations with organic content, deductions could be made about the comparative role of this fraction in elemental uptake.

In their study of the effects of bone size and temperature on bone diagenesis, Von Endt and Ortner (1984) monitored the rate and nature of bone disintegration using a modification of the micro-Kjeldahl method. This consisted of a colorimetric determination of nitrogen levels in immersing solutions that had contained bone, where elevated nitrogen levels in solution were interpreted as increased protein degradation. Hare (1980) monitored protein degradation in bone and the effects of water on this process by measurement of the amino acids themselves in immersing solutions.

A more direct approach has been adopted here. The organic content of the bone samples, rather than the immersing solutions, are monitored by carbon-hydrogen-nitrogen (CHN) analysis. This is a routine method of measuring the organic content of solid material and requires little sample preparation.

The CHN analyser system combines combustion methods, gas-chromatographic separation and thermal conductivity measurements and is described briefly as follows. A few milligrams of powdered sample are combusted in a carrier gas (helium)

in the presence of tin which, as it melts, incorporates all organic and inorganic residues and promotes the oxidation of all the carbon present. This "flash combustion" process is followed by catalytic oxidation, generating all the components of the gas mixture which are simultaneously injected into a gas chromatographic column where they are chromatographically separated. Catharometers, possessing differential adsorption capabilities, measure the H_2O, CO_2 and N_2 in the gaseous mixture.

Using this procedure, whole and hydrazine-treated bone samples, exposed to solutions of variable pH (pH 4-10) for variable periods of time (1-12 weeks), have been analysed for their remaining organic content.

Table 4.2 briefly summarises the analytical techniques employed to analyse "experimental" bone and archaeological bone (and associated soils):

Table 4.2: A summary of analytical instrumentation employed to analyse bone and soil material.

Sample Category	Instrumentation						
	Autoradiography	FTA	EPMA	SPM	XRD	XRF	CHN
"Experimental" bone	x	x	x	x	x	x	x
Archaeological bone		x	x	x	x	x	
Soil/sediment					x	x	

4.4.2 The Characterisation of Solutions.

The analysis of solutions emanating from immersion, percolation and chemical separation studies is carried out using liquid scintillation counting and a range of spectrophotometric methods. The elements of interest in these studies are calcium and phosphorus, measured in order to monitor their loss from bone samples by

chemical breakdown (in the case of the chemical separation study), decay or heterionic exchange (in uptake simulation studies); and strontium and uranium, to measure remaining levels after exposure to bone samples and thereby deduce the extent of their respective uptake into bone. In addition, spectrophotometric methods have been used to characterise exchangeable cations - in the form of calcium, sodium, potassium and magnesium - in percolation experiments.

Table 4.3 summarises the analytical techniques used to describe the elemental composition of solutions in experimental studies.

Table 4.3: A summary of the instrumentation employed in the analysis of solutions from uptake simulation studies.

Method	Ca	P	Sr	U	Application
LSC				x	Immersion studies
AAS	x				Immersion and percolation studies Also exchangeable cations (Na, K, Mg)
AES			x		Immersion studies
ICP-AES	x	x	x	x	Chemical separation study

4.4.2.1 Spectrophotometric Methods.

Atomic absorption (AAS) and **emission (AES) spectroscopy** are employed to measure the relatively high levels of calcium and strontium, respectively, in pre- and post-immersing solutions and percolation solutions. These techniques are described by Brown (1980) and Beaty (1978), while David (1962) discusses their application in the determination of strontium in biological materials.

Strontium levels in the chemical separation study were undoubtedly too low for conventional AES detection and so the more sensitive technique of ICP-AES is used here: this had the additional advantage in that phosphorus as well as calcium could be more readily analysed, as too could relatively low uranium levels for the uranium chemical separation study.

AAS, AES and ICP-AES operate on similar principles i.e. those of a conventional spectroscopic technique consisting of the following stages:

1. Sample introduction (nebulization): the sample is introduced into the instrument as a fine aerosol of droplets produced from the bulk liquid by a process called nebulization

2. Sample excitation: the aerosol sample is fed into the flame or 'torch': in the case of AAS and AES, this flame can be air, acetylene or nitrous oxide based (or a combination of these), while in ICP-AES, the flame is caused by the flow of plasma argon through an induction coil producing ohmic heating ie. an interaction (or inductive coupling) of an oscillating magnetic field with flowing gas. The basis for all emission spectrometry (hence, AES and ICP-AES) is that atoms or ions in an energised state (as they pass through the flame) spontaneously revert to a lower energy state and in doing so emit a photon of energy, which is characteristic of the element(s) in the sample and usually proportional to their concentration. Any element that can be excited to emit radiation at a particular wavelength will also absorb radiation at that wavelength. So, absorption spectrometry selects the wavelength characteristic of an element and measures this absorption, which is dependent on the concentration of the element in the sample.

3. Analysis and quantification: the light emitted or absorbed is converted to an electrical signal that can be measured quantitatively. A spectrometer (polychromator) with diffraction grating resolves the light into its component radiation and then a photomultiplier measures the light intensity at the specific wavelength for each element line.

In comparison to AAS, ICP-AES allows a **wider range of elements** to be determined, though detection limits for many elements are comparable to AAS. The best advantage over AAS is its **wide dynamic range**, so that less time is required for multiple dilutions which are minimised or eliminated. ICP-AES is generally **less interference prone** and multi-element measurement allows corrections such as internal standardisation and spectral corrections to be applied. AAS is better for single element determination.

So, the advantages of ICP-AES analysis can be summarised as: (1) a dynamic range typically extending over 5 orders of magnitude, (2) low detection limits, for most elements falling within the 1-100 μg/l range, (3) good precision and accuracy, (4) a wide concentration range of measurement - ultratrace levels to major components, (5) when used in conjunction with a suitable spectrometer, the simultaneous determination of a large number of elements can be accomplished, rapidly and with small sample sizes (0.5 ml for a complete multi-element analysis).

Therefore, ICP-AES provides an ideal method for the determination of calcium, phosphorus, strontium **and** uranium in extractions from the Chemical Separation study, where the respective concentrations of these elements were anticipated to be relatively small and highly variable. Use of this method is limited, however, to the separation study for reasons of cost and availability.

AAS and AES are used routinely in archaeological science for both soil and bone analysis (e.g. work by Lambert *et al.*, 1982,1983), the latter assisted by improvements in bone dissolution methods (Szpunar *et al.*, 1978). ICP-AES analysis has also been applied to a wide range of archaeological materials through its capacity to measure a large proportion of elements typically of interest to the archaeologist. Indeed, ICP-AES can measure more elements than comparable techniques, more rapidly and more economically and this fact has been exploited. Archaeological materials that have been analysed using ICP-AES include flints (Thompson *et al.*, 1987); pottery and clays (Storey *et al.*, 1988); and, most importantly here, bone (Klepinger *et al.*, 1986; Francalacci, 1989; Ezzo, 1992). These studies on bone have exploited the multi-element capabilites of ICP-AES to illustrate the unpredictability of diagenesis, the different diagenetic behaviour of elements and their reliability as palaeodietary indicators. In addition to archaeological applications, ICP-AES has been used in forensic science to assess the pertinence of trace element ratios for the purpose of reassembling scattered and mixed human bones (Fulton *et al.*, 1986).

Spectrophotometry methods are generally not appropriate for the measurement of uranium because of their low sensitivity and high detection limits. For this reason the majority of the immersing and percolating solutions containing relatively

high concentrations of uranium have been analysed by liquid scintillation counting methods.

4.4.2.2 Liquid Scintillation Counting (LSC).

The radioactive decay chain of uranium includes daughter isotopes that emit gamma-rays of characteristic energy. In gamma spectrometry, the gamma spectra from natural (i.e. unirradiated) samples are measured in order to determine the bulk uranium content of the sample. Gamma spectrometry is described in more detail in Ivanovich *et al.*(1982), and includes liquid scintillation methods that provide a simple and rapid measurement of uranium in solution.

The liquid scintillation counter consists of a multiplier with a photosensitive cathode that registers light flashes emitted when heavy ionizing particles e.g. gamma-rays and protons, strike a thin screen of suitable luminescent material. A photomultiplier delivers large pulses of current of short duration, one per scintillation, which are then registered electronically (Curran, 1953). The scintillator is able to discriminate particle type simultaneously with energy measurement (Neiler and Bell, 1965).

The main deficiency of this technique is the limit of detection, restricting its application to the measurement of uranium in immersing solutions where uranium concentrations were high at the outset of the experiment.

4.5 Summary.

In summary, this chapter has described experimental methodologies adopted in the present study, and endeavoured to justify these approaches together with the variety of analytical instrumentation employed.

The more practical aspects of methods, materials and instrumentation are detailed in Chapter 5.

Chapter V

Experimental Procedure: Materials and Methods.

5.1 Introduction.

A detailed practical account is presented here to define experimental procedure. The chapter is divided into four main sections to represent the main categories of experimental *design*, (a) immersion, (b) chemical separation, (c) percolation (cation exchange), and the analytical techniques employed to investigate trace element uptake and interaction with bone.

The first section is the largest and describes a progressive series of **immersion** experiments, represented as Series I, II and III. These experiments share a similar basic methodology whereby bone samples are **immersed** in strontium/uranium solutions, and bone and/or solution subsequently analysed. Conditions of immersion and methods of analysis are modified over time. For this reason, all immersion experiments are included in one section, with progressive modifications and improvements in experimental design and technique described throughout.

The second section describes the **chemical separation** procedure carried out on a limited number of bone samples from earlier immersion experiments in an attempt to identify the actual mode of interaction of trace elements with bone.

The third section describes experiments that comprise a different fundamental approach whereby solutions are **percolated** through bone samples in an arrangement adapted from cation exchange experiments used routinely on soil. Both the cation exchange capacity and identity of exchangeable ions are measured for a range of appropriate samples.

Finally, **analytical procedure** is detailed for the range of instrumentation employed in the analysis of bone and solution, constituting the fourth section. The analytical techniques, their respective sample preparation and procedure, are also applicable to the analysis of both bone and soil samples collected during fieldwork.

Laboratory-based uptake simulation studies, incorporating original experimental design, and fieldwork, where more conventional strategies are tested, are generally discussed separately. Hence, this chapter is concerned predominantly with methods and materials for simulation studies, while both fieldwork methodology and results are discussed largely in Chapter 9.

5.1.1 A Definition of Experimental Studies: Series I, II, III.

Table 5.1 describes the major grouping and nominal classification of the experimental studies conducted to simulate and subsequently characterise the uptake of trace elements into bone. The two main experimental methodologies are immersion and percolation, while material from the former is further subjected to chemical separation procedures in order to determine the respective participation of the organic and inorganic components in elemental uptake.

The following section describes preparation procedures for bone samples and strontium/uranium solutions and details the conditions of the exposure period. In doing so, it focuses on immersion studies since these form the large majority of the experimental work carried out for this thesis. However, much of the preparation work also applies to percolation studies which are subsequently discussed.

5.2 Uptake Simulation: Immersion Studies.

5.2.1 Bone Material

This thesis is concerned with the diagenetic alteration of the chemical content of bone during burial, and its implications for archaeological studies based on the chemical analysis of predominantly **human** bone. However, the availability of modern human bone material (or rather material that has not already been exposed to soil contamination) for laboratory simulation work is inevitably very limited. For this reason, modern sheep bone was used: the distal limbs of sheep (Figure 3.1a), both proximal phalanges and metatarsals, were collected from Sunderland abattoir (Shields Rd., Sunderland SR6 8JL).

The skin, flesh and hoof were removed using scissors and scalpel. Mealworm beetles

Table 5.1: Classification of experimental work.

Experimental description		Element(s) under investigation	Analytical techniques	Variables under investigation
Immersion	Series I	strontium-90 uranium (di-acetate)	autoradiography	size of bone temperature time pH
	Series II	strontium (chloride)	EPMA XRF XRD	whole v. ashed bone time crystallinity
	Series III	strontium (nitrate) uranium (di-nitrate)	EPMA XRF XRD PIXE/RBS FTA	organic:inorganic ratio time crystallinity pH [Sr], [U] in solution
Chemical separation		as for Im. Series II/III	ICP-AES	organic:inorganic ratio
Percolation		exchangeable cations	AAS/AES	organic:inorganic ratio pH CEC

where EPMA = electron probe microanalysis; XRF = X-ray fluorescence; XRD = X-ray diffraction; PIXE/RBS = proton probe microanalysis; AAS = atomic absorption spectroscopy; LSC = liquid scintillation counting; ICP-AES = inductively-coupled plasma atomic emission spectroscopy.

and their larvae (c/o Biological Sciences Dept., Durham) provided a further means of stripping soft tissue from the bones. Scavenging periods ranged from 1-2 weeks. However, this latter method was not found to be wholly successful, since significant quantities of soft tissue still remained attached to the bones after larval action. Removal by dissection was found to be more effective and more convenient.

N.B. A variety of procedures have been used in other studies to remove the soft tissue associated with bone (e.g. Fazekas and Kosa, 1978). These include the use of organic detergents and maceration procedures which are generally more effective than the methods used in this study but remove both the cortical and medullary soft tissue as well as that associated with the periosteum. These procedures also run the risk of softening and gelatinising the remaining bone and altering its matrical structure. Therefore, the removal of soft tissue using minimum interference was employed, thus opting for a low intervention strategy.

Metapodial bone was sliced transversely (see figure 5.1(b)) using a junior hacksaw. Along the length of the shaft, 8mm slices were produced for Series I and II experiments, while 4mm slices were prepared for Series III experiments, in order to reduce the quantity of bone material that had to be laboriously prepared. Bone material was then subjected to a 'degreasing' procedure, that would reduce the degree of hydrophobicity caused by fats repelling water, and thereby facilitate the access of immersing/percolating solutions to the bone matrix. The marrow was removed from the medullary cavity of each slice and the bone then defatted or degreased in distilled water at 70°C for approximately 2 hours. Bone samples were then dried in an oven at 105°C and weighed.

Both whole/unsliced bone (proximal phalanges) and bone slices (all from the shaft region of metapodials) were used in Series I experiments to investigate any differential tracer uptake into these respective samples.

In experimental Series II, only **slices** of bone were used (8mm in length) so that the cross-cortical distribution of strontium could be examined after immersion. Similarly, in Series III, exploring both strontium and uranium distribution, slices of bone were used, together with **powdered** bone for subsequent *quantitative* analysis. Powdered bone has a number of advantages over bone slices in that it can be conveniently weighed out and is easier to control quantitatively than sliced material. However, as outlined in Chapter 4, the use of powdered material forfeits the possibility of examining cross-cortical distribution profiles of elements taken up into the bone matrix.

Figure 5.1a: Diagram to illustrate the anatomy of the ovine limb.

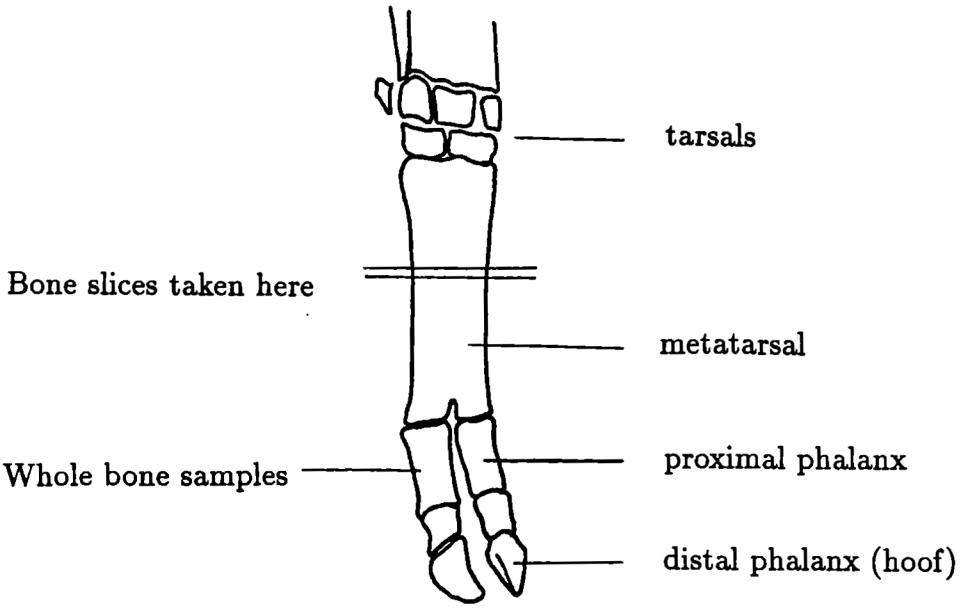

Figure 5.1b: A bone slice illustrating the periosteal (p), medullary (transverse section, or m) and endosteal (e) cortical surfaces.

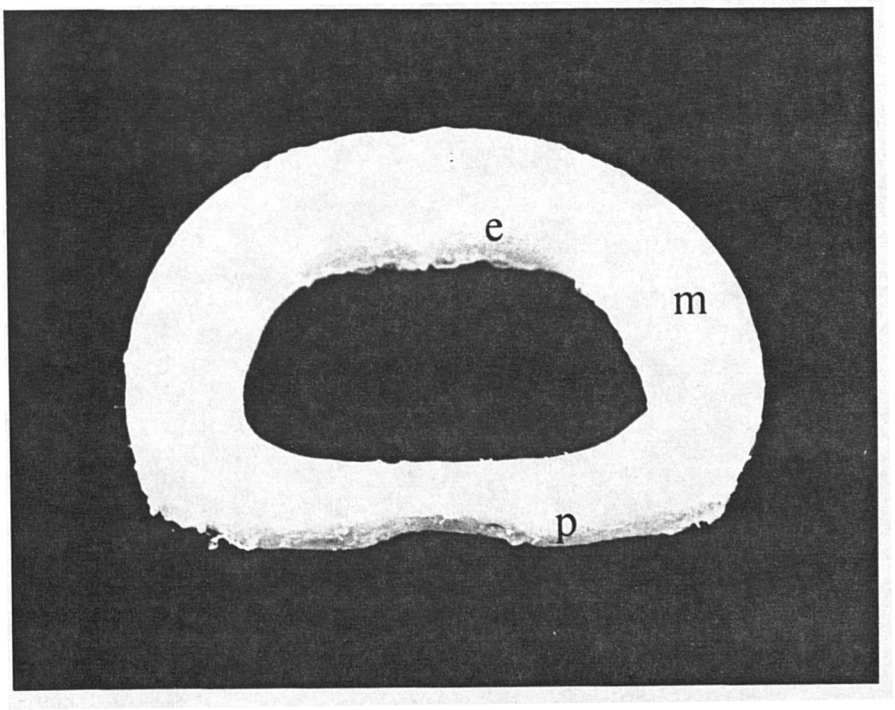

5.2.1.1 Bone slices: technical drawbacks.

The use of sliced bone introduces a number of potential undesirable variables - individual sample variations in weight, depth and, more importantly, the surface area of bone in direct contact with the immersing solution i.e. no two sliced samples are the same.

One of the main problems with using slices of bone is that they present four different surfaces to the immersing solution: the periosteal and endosteal surfaces, and the two transverse sectional areas made on slicing the original bone shaft (refer to figure 5.1(b)). In the burial environment, a relatively intact long bone will only be in *direct* contact with the burial matrix at its periosteal surfaces and possibly its endosteal, should soil have occupied the medullary cavity. Cortical cracks and longitudinal sections will permit soil/groundwater entry directly into the medullary cortex, but generally these types of damaged bone should not be used for chemical analysis.

Two options were available: (a) to use thicker bone sections and to take a middle piece for subsequent analysis, (b) to coat the transverse sections of smaller slices of bone with a non-absorbent, impermeable coating to prevent elemental entry directly into the mid-cortex.

The last option was put into practise, thereby reducing the amount of bone material and preparation time required. Tests were carried out on the suitability of cellulose acetate (nail varnish) to determine its absorbent, adherent and waterproof qualities at the desired pH and temperature regimes of immersion.

An 'osmotic chamber' was designed (figure 5.3a/b), consisting of a perspex box divided into two separate compartments via a perspex sheet with a 1" diameter hole in its middle. A semi-permeable membrane, through which both strontium and uranium ions were able to pass, was positioned over this hole and secured in place with bath sealant, as was the perspex partition. The semi-permeable membrane was coated thoroughly with 2 layers of cellulose acetate. Strontium (4M) or uranium (2000 ppm) solution was placed in one compartment of the chamber, with an equal volume of purified water in the other. At approximately 4-day intervals, 10ml samples were taken from both compartments for 3 weeks. These

samples were analysed by AAS (Sr) or LSC (U); no detectable levels of strontium or uranium had crossed the varnished membrane, suggesting that nail varnish is an effective barrier to strontium and uranium ions.

So, the main objective in coating the transverse sections of each bone sample was to limit the bone surface available for diffusion, adsorption, reaction and exchange to only the cortical (endosteal and periosteal) surfaces. It was anticipated that this arrangement would more closely simulate the predicament of, say, an intact long bone, whose exposed surfaces largely consist of its periosteal cortex and medullary cavity.

Therefore, in Series III experiments, the transverse sections of all bone slices were coated with two layers of cellulose acetate. This was the main refinement in experimental procedure here. The other major difference in design was introduced in the second series of experiments and investigated more thoroughly in the third: this was the alteration of the **organic/inorganic** composition of bone.

5.2.1.2 Alteration of the organic:inorganic ratio of bone.

The partial/complete removal of the organic component of bone, so as to leave an intact inorganic matrix, was achieved in one of two ways: (1) ashing - the heating of bone at sufficiently high temperatures to 'burn off' the organics, (2) hydrazine treatment - the chemical removal of organic material by peptide cleavage. These are reviewed in Chapter 4, subsection 4.2.2.1.

Initial exploratory investigations were carried out to investigate the effect and efficiency of both these procedures. Results of these preliminary investigations into ashing and hydrazine treatment are included in this chapter since, as a consequence, they defined the optimum desired conditions for treatment of bone in subsequent immersion and percolation experiments.

(i) Ashing.

4-5 g bone samples were dried in an oven at 105°C for 2 hours and weighed. They were then ashed in a muffle furnace for 16 hours in a range of temperatures: 500°C, 600°C, 800°C and 1000°C. After cooling to room temperature in a desiccator, each sample was reweighed and the % loss-on-ignition (LOI) calculated (Appendix Ia).

Figure 5.3a/b. Apparatus designed to investigate the suitability of cellulose acetate as a barrier material to trace element penetration.

(a)

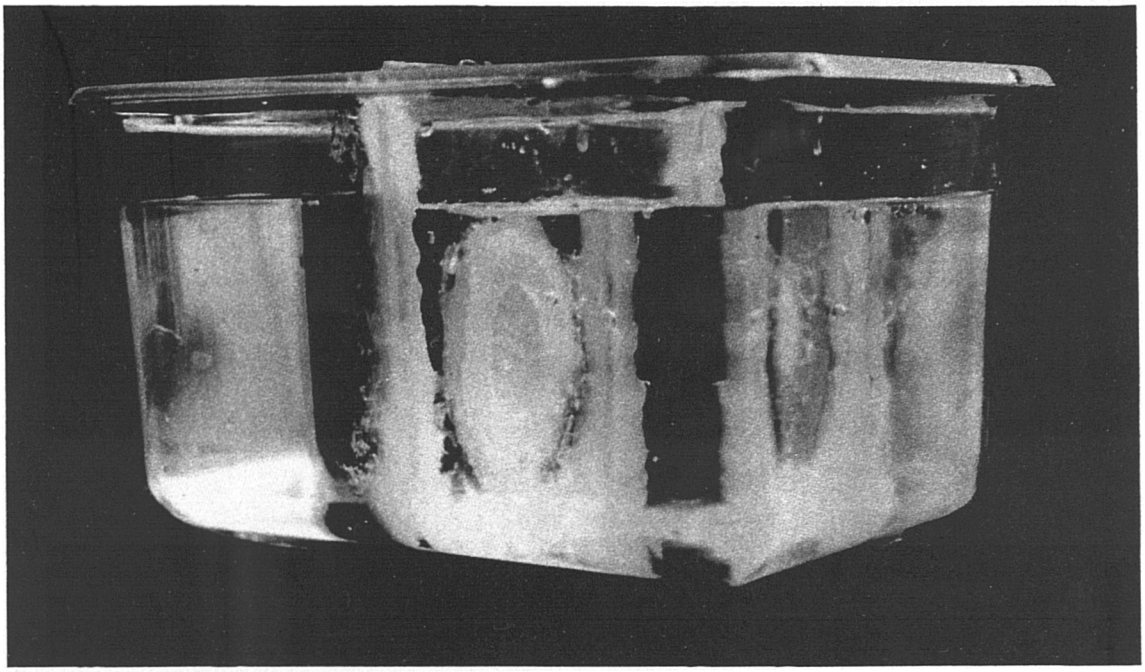

Lateral View - showing middle partition in osmotic chamber.

(b)

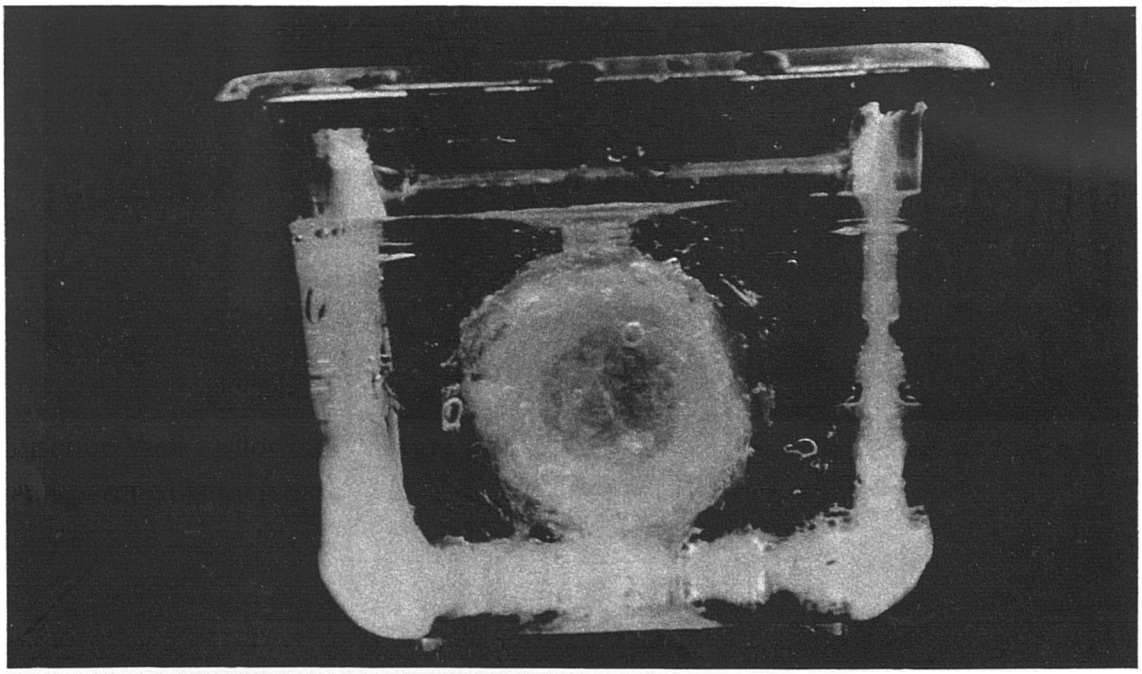

Anterior View - showing aperture in partition covered by cellulose acetate-coated semi-permeable membrane.

In addition to % LOI analysis to assess remaining organic material, the effect of ashing on the inorganic matrix was explored. Both XRF and XRD analyses were carried out on a range of samples to investigate the effect, if any, on the inorganic chemistry and crystallinity, respectively. Whole (untreated) bone samples were also examined as controls.

XRF data for bone ashed at 500°C, 800°C and 1000°C is shown in Appendix Ia. A decline in sodium, potassium and zinc was observed as the ashing temperature increased, while manganese, copper and titanium levels increased.

XRD profiles for these samples are found in Figure 5.4. As the ashing temperature increased, the crystallinity of bone was seen to increase and approach a profile characteristic of highly crystalline synthetic hydroxyapatite. So, heating bone at increasingly high temperatures effected processes of recrystallisation that altered the relatively acrystalline state of biological apatite. The implications of this structural alteration in the subsequent interaction with, and potential uptake of, trace elements in solution was of obvious concern.

- So, bone was ashed at **500°C**, a temperature that removed the organic fraction (without causing the bone to disintegrate) and had minimal effect on both the chemistry and crystallinity of the inorganic matrix.

(ii) Hydrazine-treatment.

Deproteination using hydrazine was investigated using the following procedure (adapted from Termine *et al*, 1973): bone slices were placed in 99% hydrazine at 60 °C for variable periods of time, ranging from 4 to 144 hours. At the end of each respective period, the bone was placed in a solution of 50 % hydrazine/50 % ethanol for 30 minutes, then two 30 minute steps in 100 % ethanol. Samples were washed in acetone, vacuum-dried for 7-10 hours, and then reweighed.

Again % LOI, together with weight loss, following hydrazine treatment was carried out in order to assess the % remaining organic tissue. The disadvantage with % LOI measurements is that they include weight changes caused by loss of water molecules during heating. So, carbon-hydrogen-nitrogen (CHN) analysis was also

Figure 5.4. XRD profiles of bone against temperature of ashing.

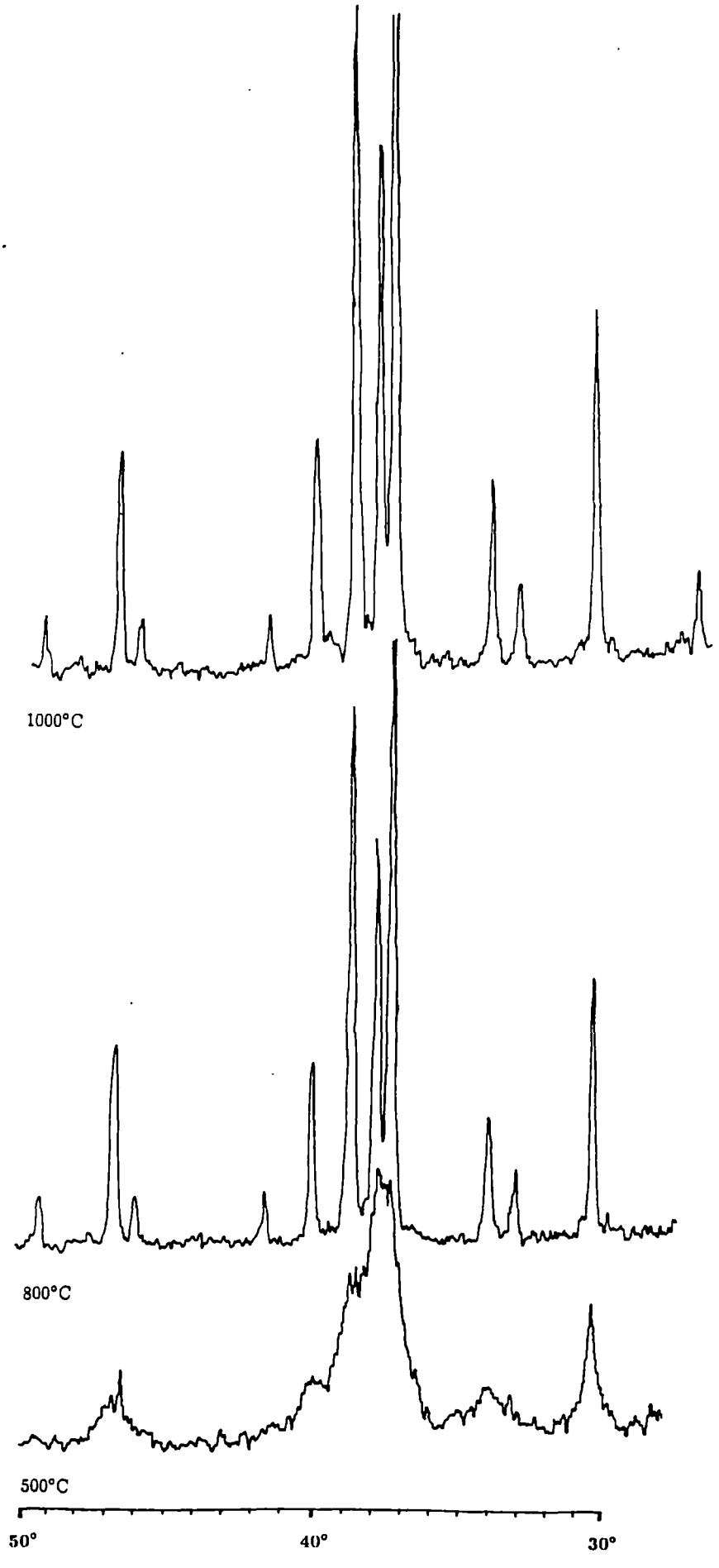

carried out since this omits water loss considerations and is therefore the more reliable indicator of the bone's remaining organic content.

LOI and CHN data for hydrazine experiments are shown in table 5.2.

XRD and XRF analyses of hydrazine-treated bone material were not carried out at this stage because I was satisfied with earlier findings in the original reference (Termine *et al.*, 1973) and similar subsequent studies (Walters *et al.*, 1990) that hydrazine had no significant effect on either the crystallinity or the chemistry of bone.

After hydrazine treatment, the bone was inevitably more brittle and more liable to break into smaller pieces. This was an undesirable effect for probe analysis where intact bone was required.

- Thus, a compromise was necessary: only 10 % of the organic material (LOI = 28 %) was removed for samples subsequently analysed by SEM/probe, while 85 % (LOI = 5 %) was removed for those analysed by XRD/XRF, requiring material in powdered form only.

5.2.2 Immersing Solutions.

5.2.2.1 "Groundwater".

In experiments constituting Immersion Series I, an artificial groundwater was made up based on the commonest constituents of groundwater (Freeze and Cherry 1979) and according to the recipe used by A.Rae (1986) The ingredients are found in table 5.3.

In accordance with Rae's study, 3ml stock solution was required per 500ml distilled water (purified water was used in this study). 500ml Kilner jars were used as immersion vessels to provide an enclosed, sealable environment.

In practise, the ingredients in Table 5.3 did not entirely enter into solution and a precipitate was formed at the bottom of each immersion vessel. In all subsequent experiments, a simulated groundwater was not used. Rather, purified water (resistivity 16-18 megohm-cm at 25°C) was used as the bulk volume of the immersing

Table 5.2: Investigation into the rate and efficiency of hydrazine action on the organic content of ovine bone.

(a) Loss on ignition data.

Treatment (hrs)	δ weight (%)	% Loss on ignition
0	N/A	35.76
2	-8.57	31.00
5.5	-8.65	30.00
9	-8.69	29.00
17	-8.76	28.37
24	-8.95	19.00
48	-9.90	15.70
72	-10.9	5.16
144	-11.49	04.87

(b) CHN Analysis.

Sample	% C	% H	% N	Total % CHN
Control (untreated)	20.49	3.28	3.56	27.33
Hydrazine-treated , 70 °C, 4 hrs	13.41	2.50	5.49	21.40
Hydrazine-treated , 70 °C, 24 hrs	5.29	1.15	1.28	7.72
Hydrazine-treated , 70 °C, 72 hrs	1.43	0.58	0.18	2.19
Hydrazine-treated , 70 °C, 144 hrs	1.38	0.54	0.17	2.09
Ashed , 500 °C, 16hrs	0.94	0.26	0	1.20

Table 5.3 Artificial groundwater recipe.

(Taken from Freeze and Cherry, 1979)

Salt	Mass in stock solution (g)	Mass per 500 ml sample (g)	Concentration per sample (ppm)
NaCl	3	1.8×10^{-2}	36
$CaCO_3$	0.79	0.474×10^{-2}	9.5
$Fe(NO_3)_3$	0.12	0.072×10^{-2}	1.44
$KHCO_3$	0.36	0.216×10^{-2}	4.32
$MgSO_4.7H_2O$	1.47	0.882×10^{-2}	17.65
$NaHCO_3$	4.26	2.556×10^{-2}	51.12

would avoid any interference/complications that might occur in the chemistry of ion exchange/interactions and electrolyte balance, thereby simplifying the whole uptake simulation process and subsequent interpretation of data (see Chapter 4, subsection 4.2.2.2).

5.2.2.2 Strontium and Uranium: Source.

The respective sources of strontium and uranium for each series of experiments were as follows:

(i) Series I: Autoradiography.

Series I experiments employed strontium and uranium tracers that could subsequently be detected by autoradiographic methods:

1. Strontium-90 (Amersham International Plc., Aylesbury, Bucks.) This radiotracer was purchased in the form of strontium nitrate in 1M nitric acid, with an activity of 5mCi per 1ml (185Bq).

2. Uranium (AnalaR, BDH Chemicals). This element was purchased in the form of uranyl di-acetate (50g), containing uranium of natural composition i.e. predominantly consisting of depleted U-238. The U-235 content was 0.2-0.4 %, thus giving a radioactivity of 8900 Bq/g.

Note: A brief experiment was conducted whereby increasing dilutions of uranium solution were measured using a liquid scintillation counter. This uranium salt was found to be sufficiently radioactive to be detected in reasonable quantities by autoradiography; for this reason, and because of its relative safety and cost compared to any uranium radioisotope, uranyl di-acetate was used for this study.

Initial doses of strontium and uranium were estimated at approximately 1 million counts per bone sample, an activity that would be detected by subsequent autoradiography (Pers.comm. J.Gatehouse, Biol.Sci., Durham). Dose calculations are shown in full in Appendix Ic:

1 μ l of the strontium source was micropipetted and diluted 10x's. 1 μ l of this "stock" solution was then added to each 500ml Kilner jar.

Similarly, from values obtained in the liquid scintillation investigation of uranium di-acetate activity, approximately 1g was estimated to give 1 million counts; hence, 1g uranyl di-acetate was added to each 500ml Kilner jar.

(ii) Immersion Series II.

In Series II experiments, the uptake of strontium over time was examined. Strontium-90 was replaced by non-radioactive strontium chloride (BDH Chemicals), and the method of autoradiography by electron probe micro-analysis or EPMA. A stock solution was made up in the ratio of 1:1 strontium chloride by weight i.e. a near-saturated solution. This constituted a 55.58 % strontium solution.

(iii) Immersion Series III.

In the third of the immersion series, the highly concentrated strontium solution (4M) was dramatically reduced, since it was difficult to relate strontium behaviour under such concentrated conditions with 'real' levels present in groundwater (in ppm range). This study employed a much smaller, but still exaggerated, strontium concentration of 139,000 ppm (1M), to ensure that clear patterns in strontium behaviour would be detected. On repeating this series of experiments, the concentration was still further reduced to 100 ppm, with a minimum of 5 ppm. Moreover, non-radioactive strontium nitrate solution was used instead of strontium chloride, since the chloride anion itself is able to interact with the bone matrix, and in doing so can potentially influence the behaviour of the strontium cation. In contrast, the nitrate ion is comparatively inert, and less able to interact with the bone matrix because of its large molecular size (Lambert *et al.*, 1985).

Similarly, uranyl di-nitrate solution was used as the uranium source. Uranium concentrations were also modified: in Series I, a uranium solution representing 1 million counts per sample was used - the equivalent of a 1120 ppm uranium solution. In Series III, a range of uranium concentrations was used: 2240 ppm, 1000 ppm, 100 ppm and 10 ppm. On subsequent detection by the chosen techniques, 1000 ppm was found to be the optimum concentration, and was consequently used for the majority of experiments.

5.2.2.3 pH of solution.

In addition to on-going refinements in strontium/uranium concentrations throughout the experimental series, methods of adjusting the **pH** of the immersing solution were also improved.

(i) Series I.

In Series I, the autoradiographic study, the pH was adjusted to pH 4, 7 or 9 simply by the addition of dilute potassium hydroxide or nitric acid, in accordance with Rae's preliminary uptake studies (1987).

(ii) Series II.

In Series II, the prime concern was to examine strontium uptake over **time**. Hence, pH was not a variable in these experiments, and all solutions were adjusted to a pre-immersion value of pH 7, again simply by the addition of dilute potassium hydroxide.

However, measurement of solution pH after the immersion period revealed that the initial pH value adjusted by the addition of acid/alkali, was not maintained throughout the period at the desired value.

(iii) Series III and Percolation study.

Since previous attempts to set and maintain immersion conditions at a particular pH by acid/alkali addition were evidently ineffectual, **buffers** were introduced into the immersion system in Series III and in percolation (cation exchange) studies.

This study required environmental pH regimes of pH 4, 6, 7, 8 and 10. Unbuffered solutions containing bone, with or without strontium or uranium, maintain a fairly stable pH around 4 (Rae, 1987; preliminary work here), so a buffer was not strictly necessary for this pH value. The pH range 6-10 was too broad for one buffer type to operate effectively, an arrangement that would have been desirable in reducing the number of variables in the system. Instead, HEPES (*N* -2-Hydroxyethylpiperazine-*N* '-2-ethanesulphonic acid) was selected for pH's 6, 7 and 8, and CHES (2-(Cyclohexylamino) ethanesulphonic acid) for pH 10 (refer to Chapter 4, subsection 4.2.2.2). Their respective pKa values are 6.8 and 9.0, although these values are temperature variable. It was assumed that these buffers would not have differential effects on bone, or vice-versa. Certainly the literature states that HEPES does not complex with calcium and the majority of cations (Good *et al.*, 1972), and buffers were required that would not themselves react with strontium or uranium, and thus interfere with any bone-solution interaction.

Stock buffer solutions for each pH were made up at 0.4 M buffer strength, with the appropriate quantity of alkali (NaOH) added, as calculated from the Henderson-Hasselbach equation. Strontium and uranium solutions that were twice the desired concentration were made up and 10 ml of each pipetted into 25 ml Sterilin tubes, together with 10 ml of the appropriate buffer solution. Final solutions made up are shown in table 5.4.

Table 5.4: Buffer solutions required for desired pH range

pH of Solution	Concentration of Acid Buffer	Concentration of Alkali
4	0.2 M HEPES	-
6	0.2 M HEPES	0.025 M NaOH
7	0.2 M HEPES	0.117 M NaOH
8	0.2 M HEPES	0.187 M NaOH
10	0.2 M HEPES	0.2 M NaOH
10	0.2 M CHES	0.1818 M NaOH

5.2.3 Immersion Period: Temperature and Duration.

5.2.3.1 Vessels.

In Series I, kilner jars (500ml capacity) were used as immersion vessels, providing enclosed sealable environments. In subsequent studies, screw-capped Sterilin tubes (20ml capacity) were used, because these were a more convenient size and at the same time reduced the quantities of strontium/uranium solutions required. Furthermore, the possibility of adsorption/exchange processes with the surface of the glass vessels was removed from the immersion system.

The sterilin tubes containing bone and solution were tightly screw-capped and the lids sealed using bath sealant, in an attempt to reduce evaporation of the solutions at elevated immersion temperatures.

5.2.3.2 Temperature of immersion.

The effect of **environmental temperature** on elemental uptake was investigated in Series I. Here, samples were left on the laboratory bench at 20-25°C or placed in an oven at 60°C. Having established the expected trend of increasing temperature

effecting an increase in the rate of reaction (uptake), as shown in Chapter 6 section 6.1, 70 °C was chosen as an appropriate temperature for the timescale of the experiment in all subsequent studies.

5.2.3.3 Duration of immersion.

With regard to the **timescale**, samples remained immersed for a period ranging from 1 to 12 weeks. During this time, samples exposed to 60/70 °C were systematically re-positioned within the oven, in order to compensate for small temperature gradients existing in this equipment (since the oven was not fan-assisted). Furthermore, the pH of samples representing each 'condition' was monitored throughout the immersion period, to check that each respective pH was maintained for the duration.

Gamma-irradiation was used to **sterilise** the sealed Kilner jars and their contents in an attempt to reduce the action of any microorganisms in the system and thus endeavour to keep the system as clean and simple as possible. Such treatment was not necessary for samples kept at 60/70 °C, since such temperatures are not conducive to microbial activity.

Cobalt-60 provided the gamma source (c/o Chemistry Dept., Durham); there was no risk of this gamma action affecting tracer activity within the jars since cobalt-60 operates at a lower threshold and would therefore cause no further reactions in the vessel (pers.comm. R.Wiltshire, Harwell). The standard sterilisation dose for equipment is typically 2.5 megarads or 25 kilograys at a rate of 0.1-1 megarads per hour (Freshney 1987). These values are dependent on the distance of the sample from the centre of the source-casing, there being an inverse-square law relationship between this distance and the rate of dosage received. For example, at 8cm distance from the source centre, the rate of dosage is 2.216 mrad/24h; at 10cm, 1.68 mrad/24h; and at 12cm, 1.15 mrad/24h.

Therefore, the jars were placed approximately 12cm from the source and were given a dose of 2.5 megarads. Thus, the duration of gamma-irradiation was 2.5/1.15 x 24h = 52h i.e. 2 days and 4 hours.

5.2.4 Post-Immersion Procedure.

5.2.4.1 Immersing solutions.

After the predetermined immersion period, the pH of the immersing solutions was measured, and the majority were retained for analysis by spectrophotometry or liquid scintillation counting for measurement of strontium and uranium, respectively.

5.2.4.2 Bone samples.

In the case of powdered bone samples, solutions were decanted after centrifugation, to ensure that none of the bone material was lost. All bone samples were washed thoroughly in order to remove superficial surface adherents and excess strontium/uranium material: each was ultrasonically washed in approximately 20 ml purified water for 30 minutes. This was repeated three times, each in fresh purified water, and each subsequently centrifuged to avoid material loss. It was assumed that all, or at least most, of the remaining surface adherents would be removed after this 90 minute ultrasonic wash.

After the final wash, each bone sample was collected, powdered samples under filtration using a Buchner funnel, and dried thoroughly. Bone material from Series I immersions was weighed and any change in weight after immersion noted.

Samples were prepared for subsequent quantitative and/or qualitative analyses to assess the extent and nature of elemental uptake. In addition, material from control (buffered water) immersions was analysed for its CHN content, in order to get an indication of the relative/preferential organic decay over the pH range.

Finally, a number of samples from Series II and III were retained for chemical separation procedures in order to assess the relative contribution of the organic and inorganic components in elemental uptake mechanisms.

5.3 Chemical Separation of Organic and Inorganic Components.

A selection of whole bone samples from the immersion experiments were retained for subsequent chemical separation procedures (see Chapter 4, section 4.2.3).

Each bone slice, weighing approximately 0.70g, was crushed into small pieces. The pieces were divided into two and each half weighed accurately. One half was placed in a sealed Sterilin tube containing 5ml 95 % hydrazine and placed in an oven at 70 °C for deproteination. The other was placed in 5ml dilute (3-5%) nitric acid for demineralisation. After 72 hours, each solution was filtered and the filtrate retained for analysis.

A requirement for analysis by inductively-coupled plasma atomic emission spectroscopy (ICP-AES) is that samples are acidic in nature - usually about 5% nitric acid. So, no further preparation was required for the 'inorganic' fractions. 'Organic' fractions, on the other hand, consisted predominantly of hydrazine which is both caustic and basic: these samples were transferred to glass vials and then evaporated to a residue on a hotplate at 120 °C (the boiling point of hydrazine is 119 °C). 5ml 5% nitric acid was added to each. Care was taken to ensure that all the residue dissolved in nitric acid before the samples were transferred back to Sterilin tubes. (N.B. Samples were transferred to glass vials for this evaporation procedure because Sterilin tubes melt around 100 °C).

Standards consisted of H5 bovine bone (IAEA H5) treated in a similar way to the experimental samples. Assuming that the chemical separation procedure was effective, 0.7 g H5 bone in 5ml nitric acid would contain 7.116 ppm Sr, 15085.496 ppm Ca, and 7258.116 ppm P before dilution. In addition, a range of strontium and uranium standard solutions were made up in 5% nitric acid to represent 1 to 100ppm concentrations.

Samples were diluted as necessary to fit the calibration range of the instrument. All analytical work was carried out in the Department of Mineralogy at the Natural History Museum, London.

5.4 Cation Exchange Systems: Percolation Experiments.

5.4.1 Introduction.

The second experimental strategy that was adopted to investigate elemental uptake processes in the laboratory involved the percolation of solutions through columns of

powdered sample material and the subsequent collection of the leachates (Chapter 4, section 4.2.4).

Percolation experiments consisted of examining general cation exchange properties of a range of bone fractions: this comprised the measurement of the total Cation Exchange Capacity (CEC) and a number of exchangeable bases.

5.4.2 Sample Material.

The range of samples shown in Table 5.5 were prepared as powders. The exception was collagen, which exists as a fibrous material. These samples represented materials possessing a range of organic:inorganic ratios.

Table 5.5: Range of Samples for Cation Exchange Experiments.

Description of sample	Percentage organic content
Collagen	100
Whole, untreated bone	30
Hydrazine-treated bone (17hrs treatment)	25
Hydrazine-treated bone (72hrs treatment)	5
Ashed bone	0
Calcium phosphate standard	0
Rock phosphate	0

5.4.3 Total CEC and Exchangeable Bases.

A small wad of sterile cotton wool was placed in the bottom of a leaching tube (bore diameter= 15mm), and a measured amount of oven-dried sample placed on top (this amount was dependent on availability and typically ranged 0.5 - 1 g

material). The sample was then compacted with a second wad of cotton wool to form a sample plug through which the solution would be leached.

100ml 1M ammonium acetate solution, buffered to pH 7, was leached through each sample column and the leachate collected. The rate of filtration of ammonium acetate was variable, being rapid (1-2 hrs) for collagen and whole bone, while slow (2-3 days) for hydrazined samples and phosphate standards. If the leachate took less than 2 hours to drain through the sample column, then it was put through the sample again - up to 3 times.

Each leachate was made up to 100ml with distilled water as required.

5.4.3.1 Exchangeable Ca, Na, K and Mg.

Values for exchangeable cations were then determined for each leachate by atomic absorption spectrometry. Having obtained the concentrations of respective cations in ppm, the milliequivalent per gramme of sample was calculated using the following procedure (taken from the Soil Analysis Handbook, produced by the Geography Department at Durham University):

STAGE 1: Conversion of ppm of cation into mmoles (+) per litre -

$$\text{N ppm} = \frac{N}{EW} \text{ mmol (+) } l^{-1}$$

where EW = equivalent weight of element being determined (EW Ca = 20; EW Mg = 12; EW K = 39)

STAGE 2: Amount of element present in cmol (=) kg^{-1} sample, or meq/100g -

$$\frac{N}{EW} \text{ x dilution factor x } \frac{100}{W}$$

where N = ppm of element, W= weight of sample (0.5 - 1 g), dilution factor variable.

STAGE 3: Correction for the sample:leachate(extract) ratio -

$$\text{ppm from AAS x } \frac{vol.leachate}{weightofsample}$$

5.4.3.2 Total CEC.

The total CEC of each sample was then determined (refer to Chapter 4, section 4.2.4). Excess ammonium acetate was washed out of each column with 20ml ethanol, and the 'washed' samples leached with 100ml 1M sodium chloride. The leachate was again made up to 100ml with distilled water if required. The total CEC was obtained using the Markham distillation apparatus:

A 10ml aliquot of leachate was distilled with 5ml 40 % sodium hydroxide into 10ml boric acid and mixed indicator. 30ml of the distillate was collected and titrated with 0.05M HCl acid until the colour changed from blue to red. Total CEC was then calculated as follows:

Total CEC meq/100g sample = ml titre x dil.factor x 0.02 x 100/w

where 0.02 = milliequivalent of 0.02 M HCl/l, and w = weight of sample, and dilution factor = original volume solution/10 ml aliquot.

5.5 Analysis: Preparation, Operation and Procedure.

This section describes the respective preparation stages for bone samples and solutions, prior to their analysis using one or more of the following techniques: (1) for bone - autoradiography, fission track analysis, EPMA, proton microprobe, XRD, and XRF; and (2) for solutions - AAS/AES, ICP-AES and LSC methods. Furthermore, a specification of the instrumentation, together with operating conditions and analytical procedures, are included in this section. Detailed accounts of the theory and principles of these analytical techniques can be found in Chapter 4, section 4.4.

5.5.1 Analysis of Bone.

5.5.1.1 Autoradiography.

Autoradiographs were produced for bone exposed to Sr-90 and uranium solutions at variable temperature and pH (Immersion Series I).

Each bone sample was sectioned using a low-speed rotating diamond-blade saw. Bone slices were cut as thin as possible (approx. 0.75mm); in general, midshaft slices were taken from whole metatarsal bone samples, while slices 1-2 cm from either end of the bone sections were used. Bone slices were simply taped to the reactive film (a medium-grain photographic emulsion (Fuji)), and trials carried out varying the duration of exposure: 24 hours proved a satisfactory exposure time for 'strontium bone samples', while 2.5 days for 'uranium bone samples'. After this period, the film was developed and the traces examined using image analysis on a Microscale TC (DigiHurst Ltd.).

One sample was subjected to a "leaching simulation" procedure: it was placed in mildly acidic (very dilute nitric acid) for 3 weeks to determine whether any radioelement associated with the bone would subsequently be washed out or leached. In this way, the permanence of any strontium and/or uranium association with bone might be assessed.

5.5.1.2 Fission Track Analysis.

Fission track analysis was carried out to measure uranium distribution in whole bone samples immersed in approximately 2500 ppm uranium for up to 20 weeks, and in a number of archaeological bone samples later described in Chapter 9.

Small pieces of bone (1-2 g) in transverse section were taped to CA80-15, a solid-state nuclear track detector (SSNTD), and irradiated for 8 hours at 2 x $10^{12} n.cm^2$: this dose was sufficient to detect uranium presence in the 1-100 ppm range (C.T.Williams, pers. comm.).

Samples were subsequently etched in 6M NaOH at 70°C for variable periods of time, ranging from 3 to 10 minutes according to the extent of fission tracks present. After etching, samples were placed in dilute HCl and rinsed.

Fission tracks recorded on the plastic's surface were examined under the light microscope. Micrographs were produced to illustrate the *relative* abundance and distribution across samples representing both exhumed bone and ovine samples experimentally exposed to uranium in the laboratory. Quantitative (densitometric) analysis, as described for autoradiographs, was **not** employed here.

5.5.1.3 Electron probe microanalysis (EPMA).

EPMA was one of two techniques that were used to plot the cross-cortical distribution of elements in both exhumed and experimental bone samples, the other being scanning proton microprobe analysis (SPM) (refer to Chapter 4, subsection 4.4.1.2/3). The preparation procedures for each technique are similar.

(i) Preparation of sample for microanalysis.

Both techniques require that a beam of high-energy electrons/protons be fired into the bone sample. Since bone is a porous, non-conducting material, a charge can build up in the tissue reaching potentially the value of the accelerator voltage - 3 MeV in the case of the SPM. This charge causes an undesirable level of bremsstrahlung which may totally camouflage any 'real' deflected radiation produced by elements in the sample. To reduce this charge effect, the bone samples were resin-embedded, surface-polished and *carbon-coated.* Resin-embedding ensures that a total surface is available for complete carbon-coating, as well as making the porous, brittle bone easier to manipulate: this is particularly important for SPM preparation where thin sections are required.

The clear embedding resin was an air-inhibited, polyester-based resin (EM306Pa from Trylon Ltd), activated at around 0.25% . A liquid catalyst, or hardener (methyl ethyl ketone peroxide solution in plasticiser) was added to the resin at 2 % by weight. The setting time depended on both the temperature of the resin (which is best stored below 20 °C) and on that of the vacuum impregnation. At 20 °C, the gel time was 60-70 minutes.

The clarity of qualitative map data together with the accuracy of quantitative elemental concentrations extracted from X-ray spectra required a high degree of surface finish. Silicon carbide wet-grinding paper of decreasing coarseness provided the lapping surface, mounted on a Struer DAP polishing machine at 250 rpm. Finally, the samples were polished using diamond paste (1 micron grain size) on a short-nap cloth, lubricated with an oil-based suspension.

In this form, after carbon-coating, the samples were ready for electron microprobe analysis (see Figure 5.5).

Figure 5.5: The polished surface of resin-embedded bone samples prepared for microprobe analysis.

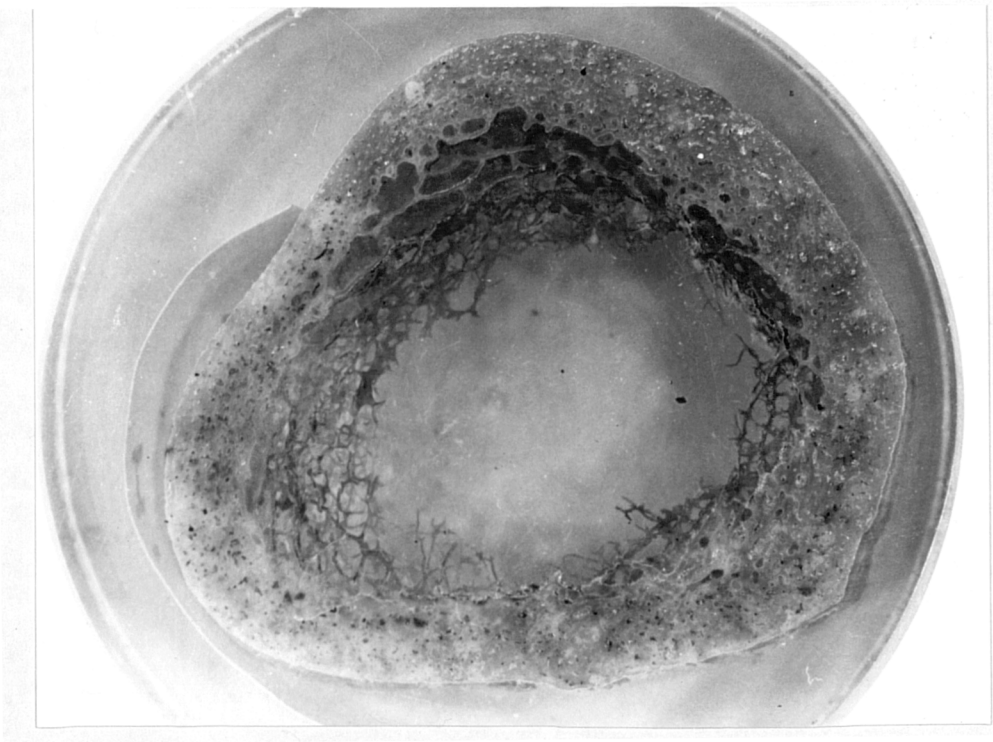

(ii) Instrumentation.

The electron microprobe facility in the Department of Metallurgy, Newcastle University, was used for the majority of analyses in these studies. It comprises a JEOL JSM-35 scanning microscope, equipped with a LINK QX2000 energy-dispersive system. Both quantitative and qualitative data were collected using this instrument.

(iii) Analytical procedure.

Cross-cortical linescans at low magnification (x30) were produced in order to get a general description of strontium/uranium distribution and hence mobility patterns across the width of the bone; areas of particular interest were mapped under higher magnification.

Each linescan was the product of an electron beam effectively analysing a 7 micron diameter spot for 2 seconds approximately every 15 microns along a linear route. Respective cross-cortical distributions of calcium, phosphorus and strontium or uranium were plotted on the same graph for each sample: the horizontal scale (x-axis) was dependent on the magnification employed, while the vertical scale (y-axis) represented the signal strength or the intensity of X-rays generated for each respective element. Since inter-element signal strengths were highly variable, their assignment to the same graph necessitated a different vertical scale for each element, so that elemental content and distribution were *relative*: direct quantitative inter-element comparisons could **not** be made from such graphs. However, since both the scale and resolution of the signal strength were consistent for each element, direct intra-element comparisons could be made across samples.

This fact enabled the linescans of one particular element across a number of samples to be plotted together, with minor adjustment for any small differences in total yield or the position of the cortical edge. In this way, any trends in elemental distribution against pH and the bone's organic content could be seen more clearly.

Signal strength does not directly correspond to elemental concentration *per se* unless correlated with a standard. Quantitative 'spot' analyses were carried out on some samples, to give an indication of the approximate levels of elements throughout the bone samples; care was taken to work only on areas of high mineral content (as assessed by P values), whilst identifying features such as porosities.

Qualitative compositional maps of areas mapped and/or profiled by SEM were obtained from backscattered-electron images (B.E.I). These areas were predominantly located in peripheral cortical regions in order to clarify any trends in strontium/uranium mobility and diffusion. The images were referred to in conjunction with respective X-ray maps of individual elements, thereby facilitating the identification of the exact nature of the elements' association (pore-filling, apatite incorporation etc).

It was anticipated that such a protocol would provide locational, qualitative illustrations of strontium and uranium behaviour under variable conditions.

5.5.1.4 Scanning proton microprobe analysis (PIXE and RBS).

(i) Sample preparation.

Sample preparation was similar to that described for EPMA. In contrast to EPMA, however, SPM analysis required samples in *thin-section* in order to further reduce background radiation (refer to Chapter 4, subsection 4.4.1.3). In general, the thicker the target sample the less accurate the qualitative and particularly quantitative analysis.

In the present study, bone sections were 100 microns thick, thereby constituting a thick target inhomogeneous sample. Samples prepared as described for EPMA were mounted on slides (polished side down) using superglue, and then polished down to 100 microns, measured using a micrometer. Both 'sides' of the sample were polished to a 1 micron finish. The edges of the resin were trimmed, and the thin section carefully peeled away from the slide using tweezers. Each was mounted onto an SPM sample holder, after carbon-coating one surface.

(ii) Instrumentation.

The majority of analyses were carried out on predominantly archaeological material using the Oxford SPM facility at Oxford University (see Figure 5.6). This comprises a National Electrostatics 1.7 MeV pelletron tandem accelerator with a General Ionex off-axis duoplasmatron ion source and two separate beam lines (for details see Grime *et al.*, 1991a). All data were collected using a 3 MeV proton energy with a 100 pA proton current at 1 micron spatial resolution (spot size). Scan times averaged about 15 minutes. A pepperpot filter was used to filter the calcium signal down to 0.1 %, so that it would not obscure the other elements present. PIXE maps were generated and collected on-line using a CAMAC ADC and VME system incorporating a colour display and 68020 microprocessor (Grime *et al.*, 1991). Both PIXE and RBS data were collected.

In addition, a detailed study of bone exposed to uranium solutions was carried out in order to further explore the microdistribution of uranium in bone and thus identify characteristics of interaction. The Proton Microprobe facility at Surrey University (Department of Electrical and Electronic Engineering) was used here. This instrument does not incorporate an automatic scanning facility. Therefore,

Figure 5.6: The Scanning Proton Microprobe Facility at Oxford University.

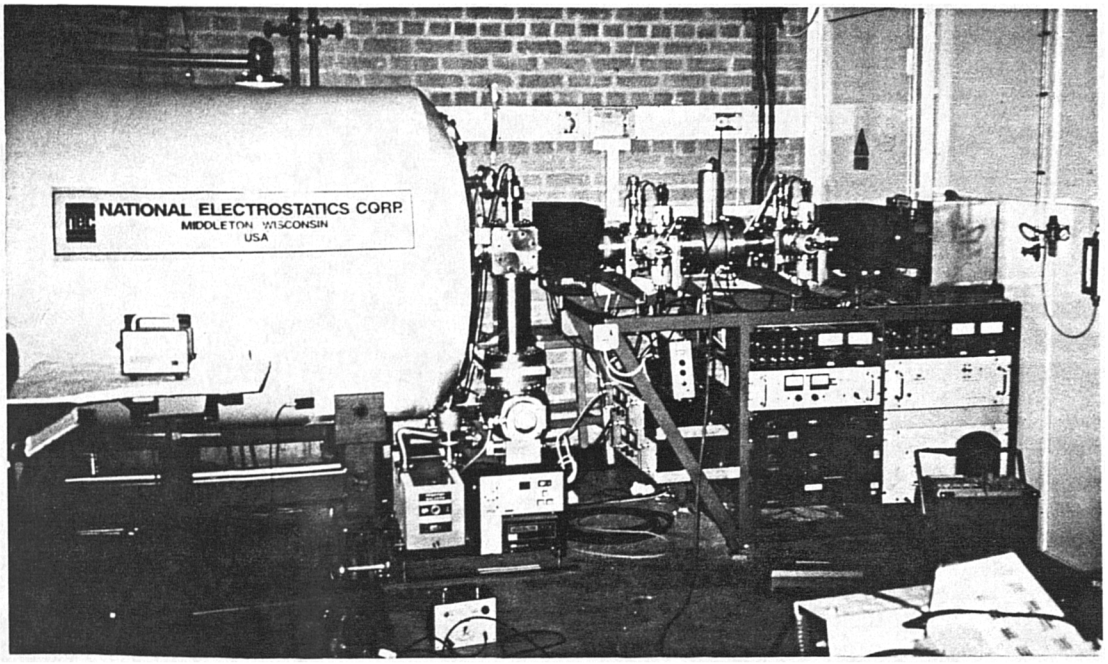

(a) The ion chamber where protons are produced and fired into the accelerator.

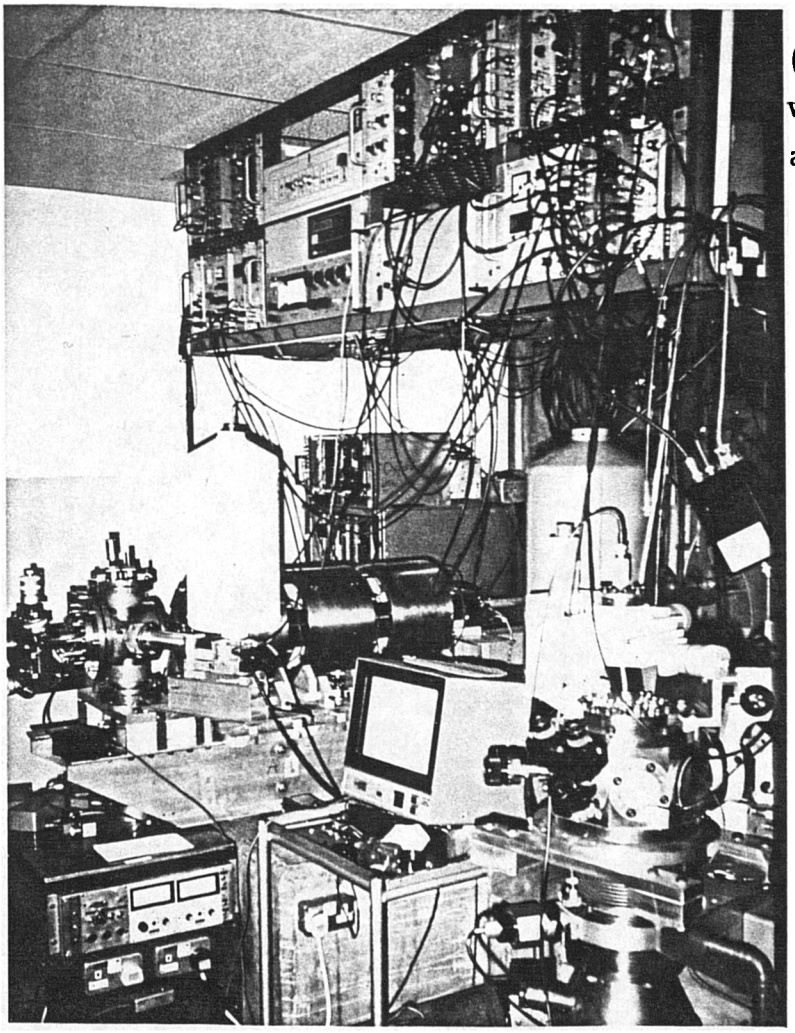

(b) The target chambers with viewing apparatus.

analytical procedure was rather crude and time-consuming in comparison to the instrument at Oxford: by varying the beam steering voltage, the samples were scanned in a *stepwise* fashion in 3 micron intervals. The methodology is described in more detail in Chapter 7 (Section 7.6), where it clarifies the data illustrated.

5.5.1.5 X-ray fluorescence (XRF).

A small number of samples were briefly analysed using energy-dispersive XRF at Oxford. These samples were analysed as whole sections of bone, to give a rough indication of strontium concentrations.

However, the majority of samples in this category were prepared for wavelength-dispersive XRF as ashed, pelletised samples (refer to Chapter 4, subsection 4.4.1.5). The instrument used was a Philips PW1400 Wavelength Dispersive X-Ray Spectrometer, equipped with a rhodium X-ray tube at 80kV and 35mA operating conditions. Peaks for calcium, phosphorus and strontium (K-alpha lines) and uranium (L-alpha line) were corrected against background. Reference materials consisted of a range of standard soils from British Geological Standards for a variety of trace elements, together with H5 animal bone (IAEA) and SARM-32 rock phosphate (S.A Bureau of Standards) for calcium phosphate matrix standards.

Note: For analytical techniques requiring the preparation of powdered bone, the bone was ashed prior to grinding: attempts were made to grind whole (unashed) material in a motorised agate mill, designed to crush the hardest of geological specimens, but these were ineffective. Bone in its natural entirety is extraordinarily resilient and, despite the defatting procedure, was found to be too greasy to grind into a powder.

5.5.1.6 X-ray diffraction (XRD).

Bone samples were analysed using XRD in order to identify their mineral component and to investigate any crystallinity changes (refer to Chapter 4, subsection 4.4.1.4).

Bone material was ground into a homogeneous powder and mounted evenly on a glass slide using acetone/methylated spirit as a distributing medium. Diffraction

patterns were recorded on a Phillips' diffractometer monochromatised to cobalt K-alpha radiation. Overall mineral diffraction profiles between 3 and 65 °2 θ were carried out on continuous scan mode at a rate of 1 °2 θ per minute, at time constant 4 seconds.

The equation $\underline{B}$ = B - b where $\underline{B}$ is the peak breadth intrinsic to the sample, and b is the instrumental breadth, was used to correct for the effect of instrumental factors (Klug and Alexander, 1962). The instrumental breadth was determined using 3 highly crystalline reference standards (silicon powder, synthetic, silicon prepared c/o Geological Sciences Department in Durham, JCPDS corundum,syn.) and was measured at 2.3 mm. Three measurements were subsequently recorded to describe the crystallinity of each sample: D, B/H and I (refer to Chapter 4, section 4.2.5 for details).

5.5.1.7 CHN analysis.

A Carbo Erba Strumentazione Elemental Analyser (c/o Chemistry Department, Durham University) was used to measure the CHN content of a number of bone samples subjected to the immersion procedure. Samples were powdered and 2-3 milligrams introduced into the analyser (See Chapter 4, subsection 4.4.1.6). A measurement period of approximately 7 minutes was required for each CHN determination to allow sufficient time to completely elute H_2O.

5.5.2 Analysis of Solutions.

5.5.2.1 Spectrophotometry (AAS/AES).

Atomic absorption (AAS) and atomic emission (AES) spectrophotometry were carried out on solutions from both immersion and percolation experiments (see Chapter 4, subsection 4.4.2.1).

Solutions were analysed using a Perkin Elmer Model 5000 Spectrophotometer, with a flame comprising an acetylene/nitrous oxide mixture. Calcium levels were measured by atomic absorption spectrophotometry (AAS) using a Ca-Mg hollow cathode lamp with a quartz window. Since no strontium lamp was available, flame

emission spectrophotometry (AES) was used to measure strontium levels: this type of spectrophotometry is less sensitive than AAS but since strontium levels in these experiments were sufficiently high (greater than 10-20ppm) this posed no problem.

Calcium measurement, in particular, is subject to ionisation interferences. Ionisation interferences occur when the flame temperature has sufficient energy to cause the removal of an electron from the atom creating a free ion. As electronic rearrangements reduce the number of ground state atoms, absorption is reduced. Calcium sensitivity is reduced in the presence of elements that give rise to stable oxysalts: these include Al, Be, P, Si, Ti, V, Zn. Strontium measurement is affected slightly by HCl, H_2SO_4, HNO_3 which decrease the absorption of strontium.

The addition of an excess of easily ionized element to both standards and samples controls this interference. Therefore, since solutions here were both pH-variable and predicted to contain significant phosphorus concentrations, lanthanum chloride was added to the samples. Lanthanum chloride controls the effects of Si, Al, phosphates, sulphates, etc. and makes absorption independent of pH (Coult, pers.comm.). 4ml of each sample was transferred to a vial and 0.3ml 10% w/v lanthanum chloride added to each. Calcium and strontium concentrations were then determined using AAS and AES, respectively.

5.5.2.2 ICP-AES.

ICP-AES was carried out on solutions collected from the Chemical Separation study. As described in section 5.3, solutions were prepared in 5 % nitric acid and analysed using the ICP-AES facility in the Department of Mineralogy at the Natural History Museum (an ARL 3410 ICP with Minitorch).

5.5.2.3 Liquid scintillation counting (LSC).

Solutions collected from uranium immersion experiments were analysed for their uranium content using the scintillation counter facility in the Department of Biological Sciences, Durham University. Samples were transferred to vials and scintillation fluid, containing 32^P, was added volume for volume. Each sample was counted for a period of 20 minutes, and counts subsequently converted to ppm

values using a range of standard solutions representing 1-2000 ppm uranium (see Appendix IIIb).

5.6 Summary.

The data collected from each of these analyses are described in the next four chapters. The first, Chapter 6, describes strontium uptake studies, and Chapter 7, those of uranium: each explores temporal and spatial patterns of uptake, and the effects of pH and the organic:inorganic integrity on uptake processes.

Chapter 8 investigates more general aspects of diagenetic alteration. These include monitoring (1) the loss of the organic component and (2) crystallinity changes of the inorganic component, induced by the immersion procedure mimicking the effects of groundwater; furthermore, an investigation of the cation exchange properties of bone fractions and related minerals using a percolation system. Thus, Chapter 8 is concerned with examples of typical diagenetic processes (organic decay, crystallographic changes and ion exchange) that may be related, but are not specific, to the observed uptake of strontium and/or uranium.

Finally, Chapter 9 deals with fieldwork studies to provide archaeological examples of the diagenetic alteration of a variety of major, minor and trace elements, including strontium and uranium, with which to compare experimental observations.

Part III

Results

Chapter VI

Strontium Uptake Studies.

This chapter is divided into 5 main sections, which are summarised in Table VI. The first describes data obtained from a preliminary uptake study set up to establish the probability of inducing strontium-bone interaction under the experimental conditions defined. This study constitutes Immersion Series I, and employed autoradiography as the main method of analysis. Subsequent sections are divided according to the major variable under investigation: these consist of (1) the pattern of uptake over time, (2) the effect of pH, and (3) the organic/inorganic content of the bone. These sections encompass a variety of data from both Immersion Series II and III, and the respective data from each are clearly delineated. In addition, experiments investigating the roles of organic and inorganic components in strontium uptake using chemical separation procedures are included in this chapter.

6.1 Preliminary Investigation: Series I.

Preliminary investigations into strontium uptake and interaction with bone were carried out using the radioisotope strontium-90 as a tracer for **autoradiographic techniques**. All bone samples exposed to strontium-90 were found to possess considerable radioactivity, registering up to 500 cps on the Geiger counter. In contrast, groundwater readings were negligible. This indicated that most of the strontium tracer had been taken up into the bone tissue. The beta-emitting activity of this radioelement produced traces on X-ray film, and after initial exploratory trials, the duration of exposure to this film was found to be optimum at 24 hours.

6.1.1 Autoradiographs.

Observations were made directly from the autoradiographs and patterns more clearly demonstrated with the aid of line-profiles obtained using image analysis equipment (refer to sub-section 4.4.1.1). These were produced by taking a line

Table VI : Classification and Experimental Details of Strontium Uptake Studies.

Description of experiment	Parameters under investigation	Description of immersing solution	Post-immersion analysis			
			Solution		Bone	
			Chemical changes	Physical changes	Chemical changes	Physical changes
Series I						
Preliminary experiment (Section 6.1)	Bone size Temperature (20°C, 60°C) (pH) Leaching	Strontium-90 1 million cts Acid/alkali addition (10 weeks immersion)	AAS (Na, Ca, K, Mg)	pH	Autoradiography	
Series II						
Uptake against Time (Section 6.2)	Time (1, 6, 10 weeks) Whole v. ashed bone	Strontium chloride 555800 ppm (4M) pH 7 (unbuffered) 60°C	AAS (Ca) AES (Sr)	pH	XRF EPMA (qual/quant) PIXE	% weight change
Series III						
Uptake against Time cont. (Section 6.2)	Time (1, 2, 5, 12 weeks)	Strontium nitrate 100 ppm pH 7 (z.buffering) 70°C	AES (Sr)		EPMA (qual.) PIXE	
Uptake against pH (Section 6.3)	pH (4,6,7,8,10) Time (2, 12 weeks) [Strontium]	Strontium nitrate (a) 1 Molar (2 weeks immersion) (b) 500 ppm (2 weeks immersion) (c) 100 ppm (2, 12 weeks immersion) (d) 5 ppm (2 weeks immersion) 70°C, z.buffering	AAS (Ca) AES (Sr)		XRF EPMA (qual/quant) ICP-AES (Ch.Sep.) (Section 6.5)	XRD (see Ch.8)
Uptake against Organic:Inorganic Ratio (Section 6.4)	Org:inorg. ratio (whole, hydrazined, ashed) pH Time (2, 12 weeks) [Strontium]	Strontium nitrate (a) 1 Molar (2 weeks immersion) (b) 100 ppm (12 weeks immersion) 70°C, z.buffering			XRF EPMA (qual)	XRD (see Ch.8)

across the autoradiographic trace (fig. 6.1a) and plotting its cross-cortical density as a measure of the relative absorbance of visible light, in arbitrary units, absorbance being linearly proportional to the density of the trace; thus, peaks correspond to areas of high density/increased absorbance of the tracer, and troughs to low density/decreased absorbance (fig.6.1b).

Line profiles were plotted to compare the uptake of strontium in whole and sliced bone, under different pH and temperature regimes. One of the major problems with this technique was the lack of discrimination between the actual depth of penetration into the bone and the spread/blurring of the trace caused by high densities of tracer, perhaps by surface adsorption to the sample. Variations in sample thickness would further complicate this phenomenon and this variable was carefully controlled throughout by slicing the bone to consistent depths (approximately 2mm).

6.1.1.1 Effects of bone size and temperature.

In Figure 6.2, a more pronounced strontium uptake was observed in sliced bone immersed at 20°C and pH 4, with clear peaks corresponding to the outer cortical surfaces. The broad width of the surface peaks implied either extensive penetration of the tracer into the bone cortex, or simply its presence at the cortical surface in large quantities. There were very small peaks at the base of each major peak which probably corresponded to the endosteal surfaces of the cortex. In contrast, whole bone immersed in a similar environmental regime demonstrated clear peaks at both periosteal and endosteal surfaces. This was perhaps rather surprising since one might have expected greater strontium association with the endosteal surfaces of the sliced bone whose medullary cavity was more accessible to the immersing solution. However, the peaks of this whole bone sample were considerably smaller than the periosteal peaks of the sliced bone sample.

Bone immersed in pH 4 solution at 60°C (fig 6.3) revealed large peaks for both whole bone and sliced bone samples. The higher temperature provoked more extensive uptake in whole bone, although endosteal peaks were either lost or masked by the larger periosteal peaks. The height of the peaks in sliced bone was comparable to those formed at lower immersion temperatures (note the vertical scale is smaller in this figure), but the peaks were broader at 60°C; since exposure times to

Figure 6.1 (a) T.S. ovine metatarsal showing position of line scan taken for autoradiographs, and (b) a typical line profile.

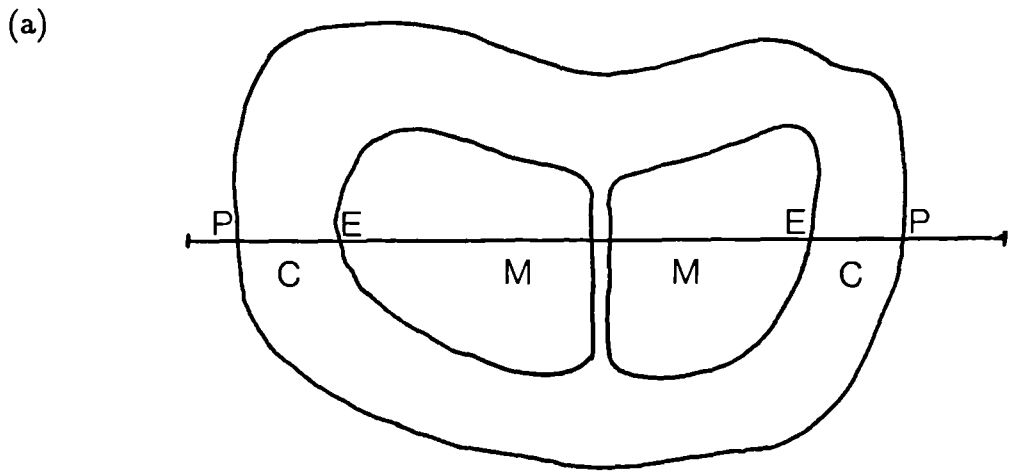

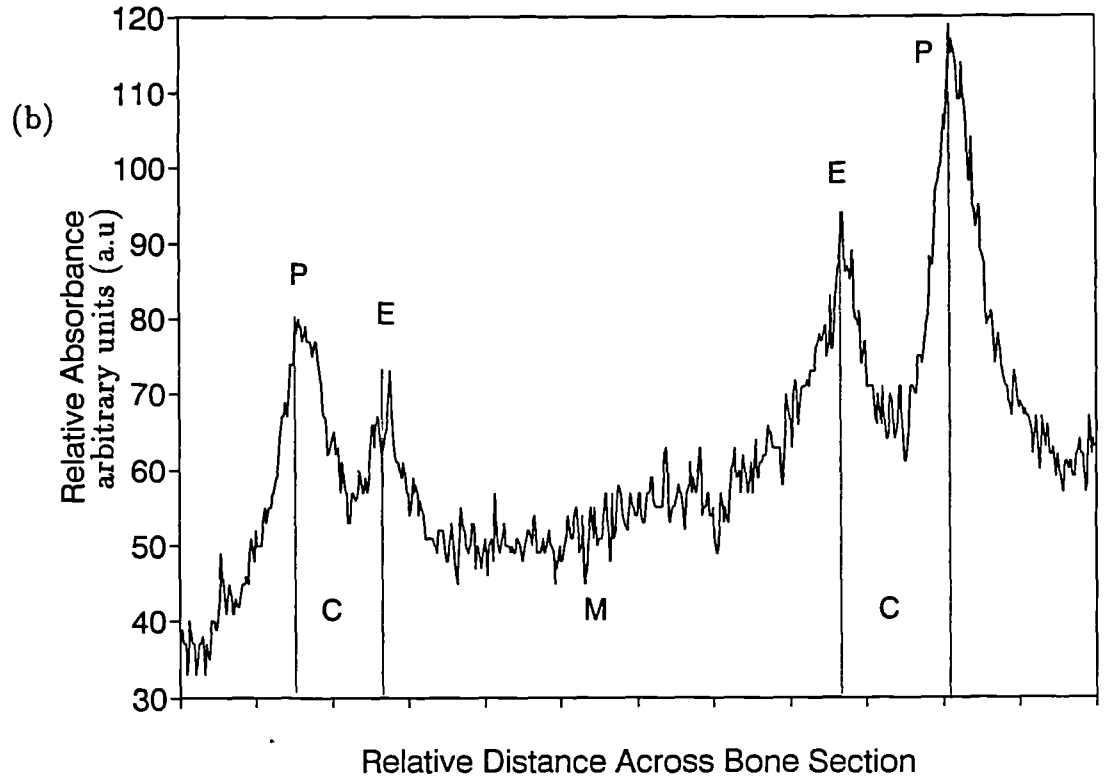

KEY

P = Periosteal cortical edge
E = Endosteal cortical edge
C = Bone cortex
M = Medullary cavity

the X-ray film were kept constant, this last observation would indicate relatively more tracer associated with sliced bone immersed at 60°C.

A direct comparison of uptake at different temperatures is illustrated in figs. 6.4 and 6.5 for whole and sliced bone, respectively, at pH 4 immersion. These figures corroborate the last observation in stating that the temperature of immersion had a profound effect on whole bone samples with increased peak height (allowing for differences in baseline level), but less of an effect on sliced bone samples where only a slight increase in peak width was observed.

The expected trend of greater strontium association with sliced bone compared to whole bone was maintained for samples immersed at pH 7 and 9 in both temperature regimes (figs. 6.6, 6.7, 6.8, 6.9). In contrast to fig 6.2, figs 6.7 and 6.8 showed clear peaks at periosteal **and** endosteal surfaces for sliced bone, as opposed to whole bone, reflecting the relative ease of access of the immersing solution to the inner cortical areas via the exposed medullary cavity.

In a similar way to bone at pH 4, immersion at higher temperatures for pH 7 and 9 generally had more of an effect on uptake into whole bone with peaks increasing in height (figs. 6.10, 6.12). In fact, sliced bone samples at pH 7 and pH 9 possessed relatively more strontium-90 at lower temperature than higher: this was certainly the case at pH 7 (fig. 6.11). Temperature appeared to have the least effect on bone immersed at pH 9 (figs 6.12, 6.13).

6.1.1.2 The effect of pH.

Figs 6.14-6.17 examine the trends in strontium uptake with pH for both whole and sliced bone. For whole bone samples, strontium uptake was more pronounced at pH 7 in both temperature regimes (20°C, fig. 6.14, 60°C, fig. 6.15) with very little difference observed between samples at pH 4 and 9. Bone at pH 4 (fig 6.14) showed clear peaks at periosteal and endosteal surfaces, and at 60°C (fig 6.15) revealed larger peaks than pH 9, despite its lower baseline level.

However, a different pattern emerged for sliced bone samples. The relative absorbance of tracer was clearly lower at pH 7 than pH 4 and 9 at 20°C (fig 6.16), where peaks for pH 4 and 9 samples were similar, while at 60°C (fig 6.17) there was no significant difference across pH.

Figure 6.2: A comparison of strontium uptake into whole and sliced bone samples immersed in pH 4 solution at 20 °C .

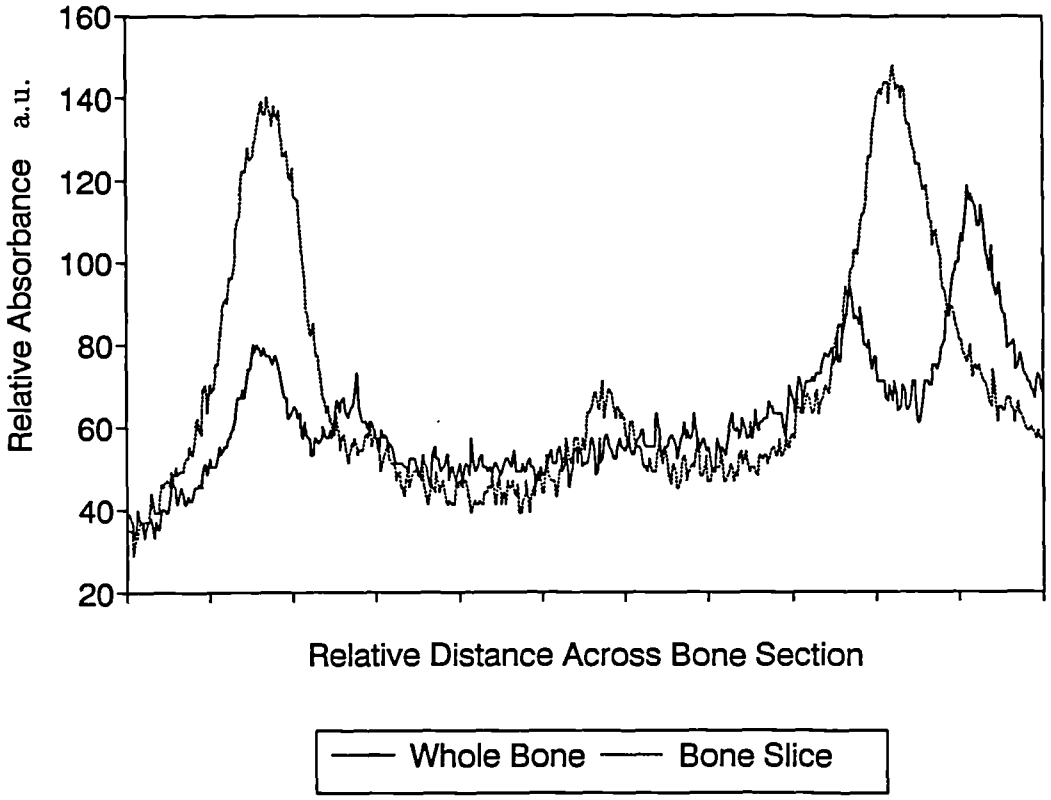

Figure 6.3: A comparison of strontium uptake into whole and sliced bone samples immersed in pH 4 solution at 60 °C .

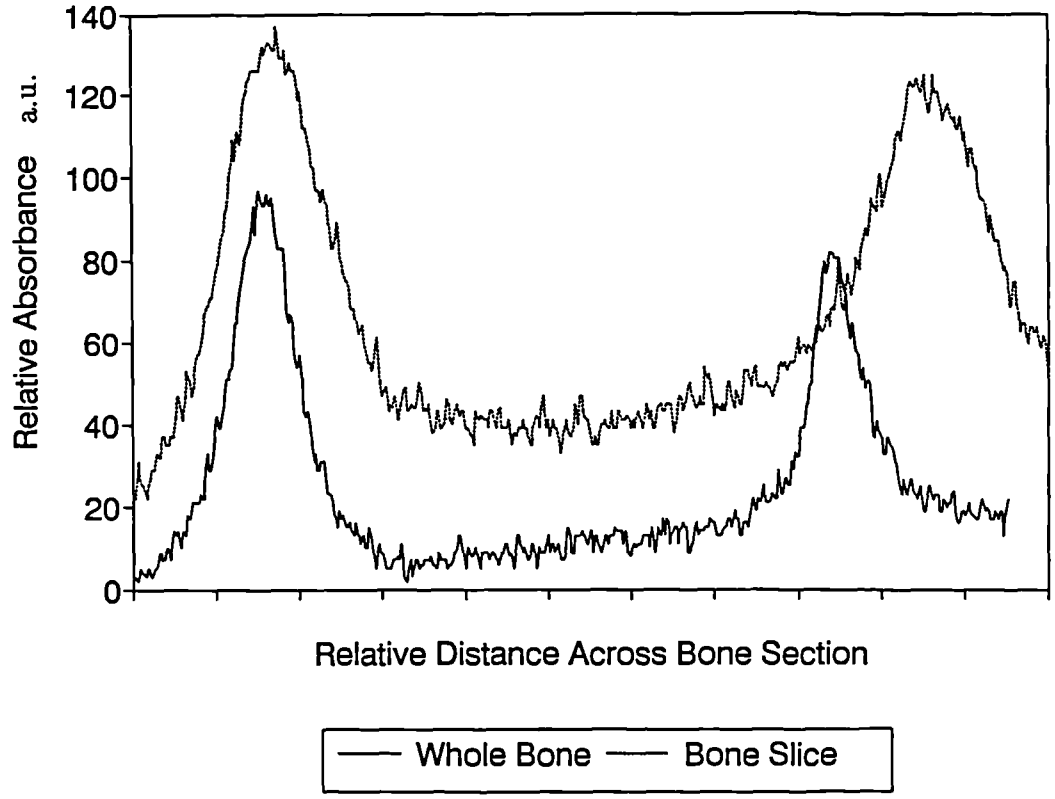

Figure 6.4: A comparison of strontium uptake into whole bone samples immersed in pH 4 solution at 20 °C and 60 °C.

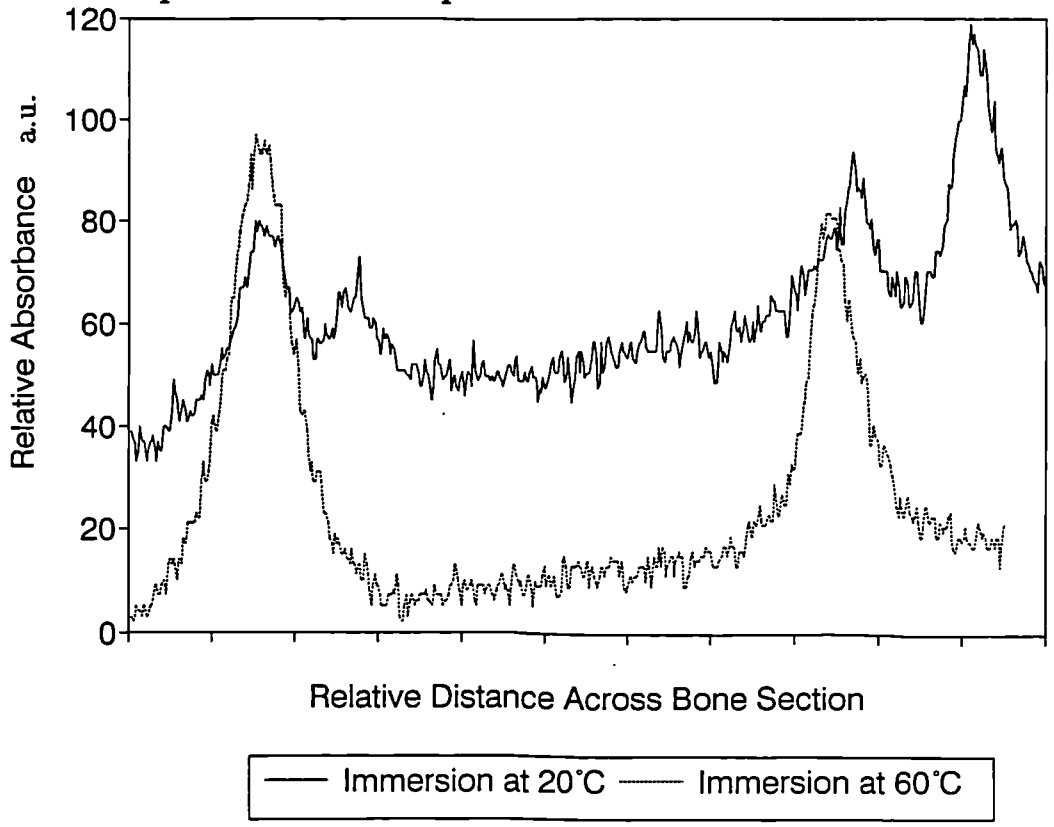

Figure 6.5: A comparison of strontium uptake into sliced bone samples immersed in pH 4 solution at 20 °C and 60 °C .

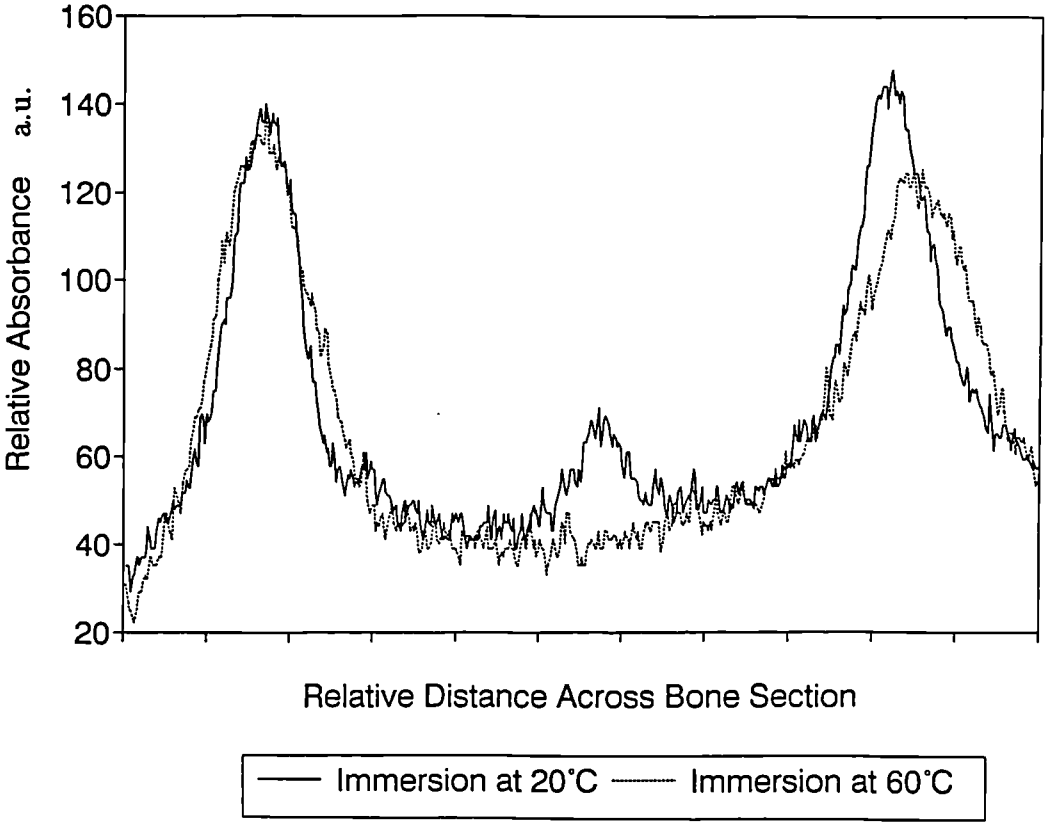

Figure 6.6: A comparison of strontium uptake into whole and sliced bone samples immersed in pH 7 solution at 20 °C .

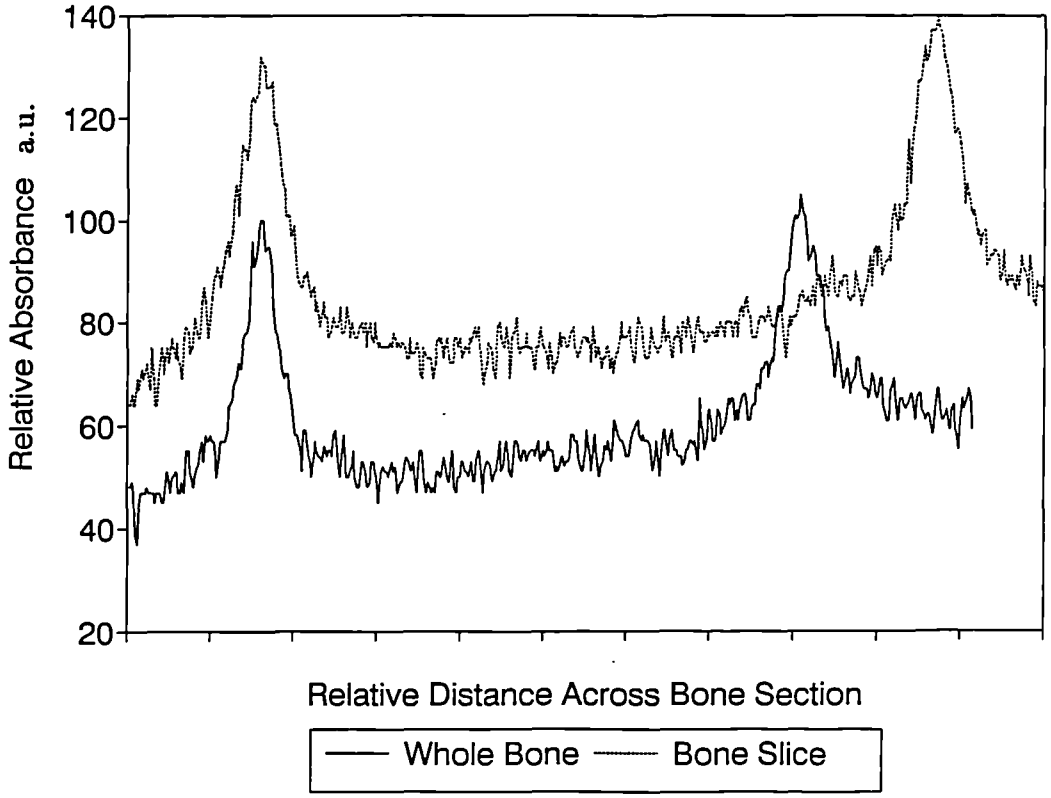

Figure 6.7: A comparison of strontium uptake into whole and sliced bone samples immersed in pH 7 solution at 60 °C .

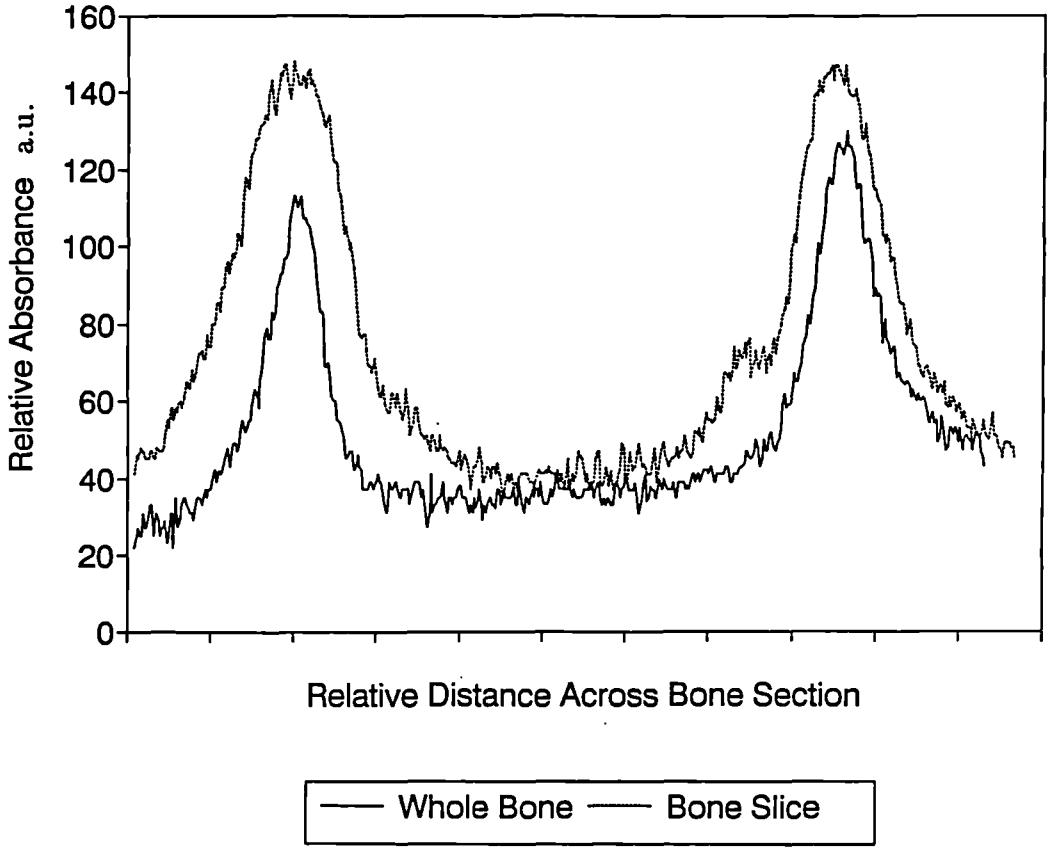

Figure 6.8: A comparison of strontium uptake into whole and sliced bone samples immersed in pH 9 solution at 20 °C .

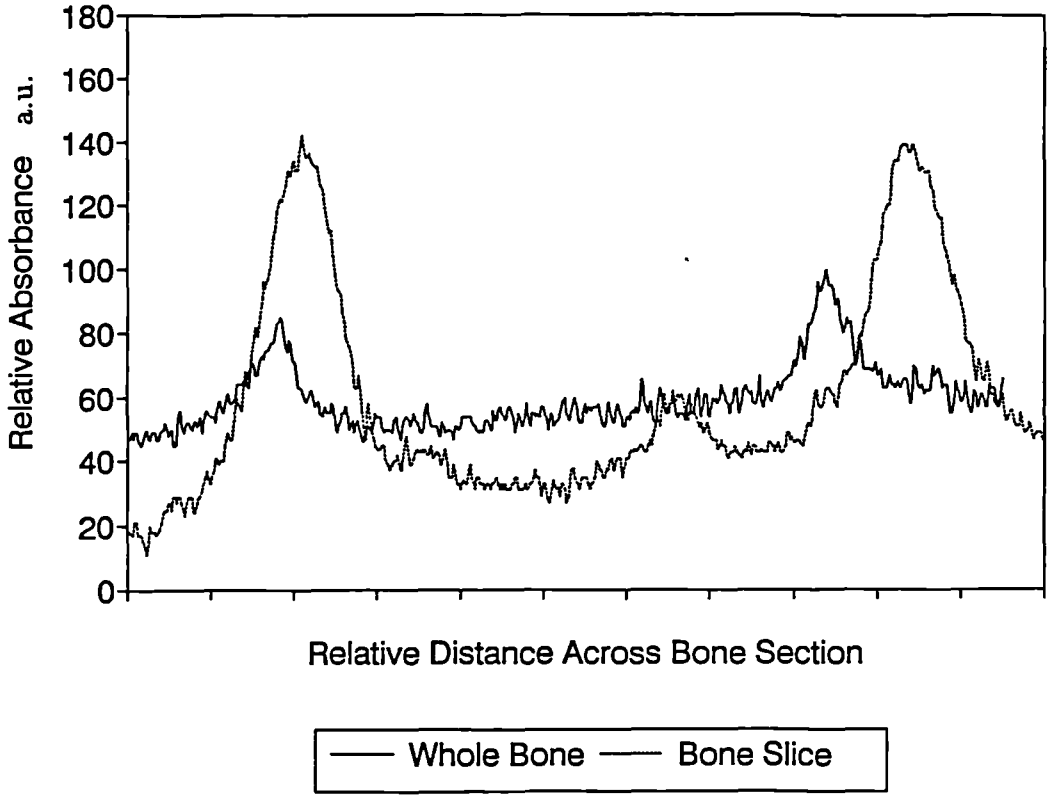

Figure 6.9: A comparison of strontium uptake into whole and sliced bone samples immersed in pH 9 solution at 60 °C .

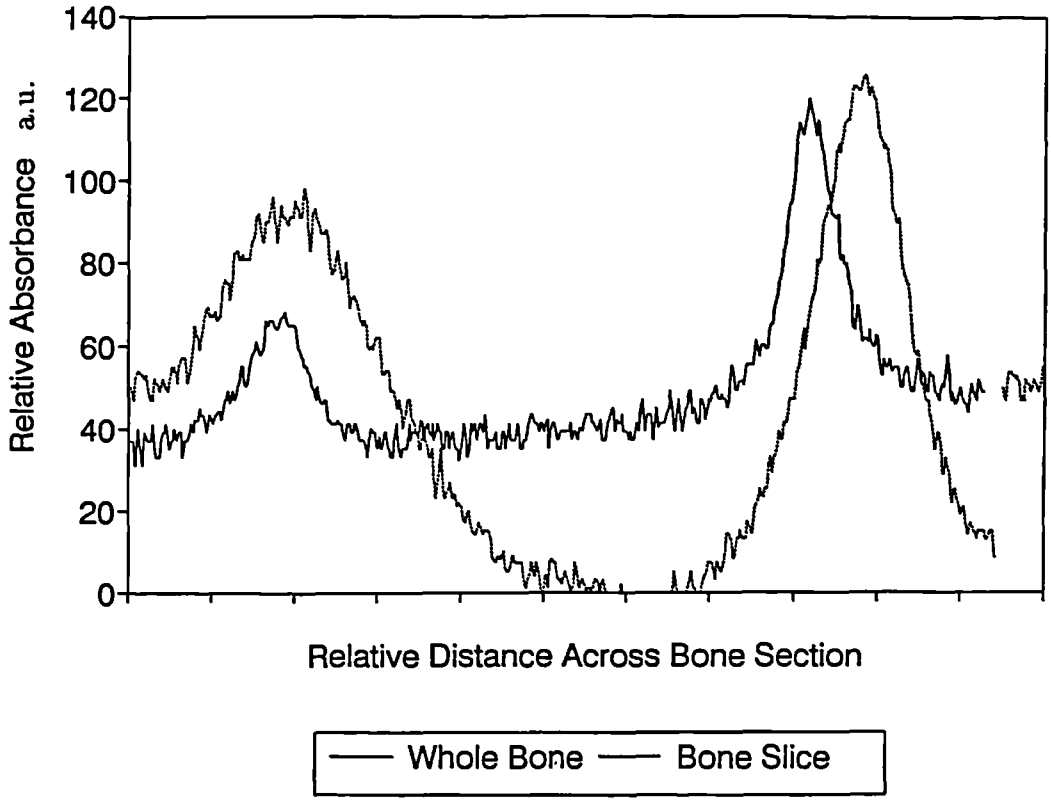

Figure 6.10: A comparison of strontium uptake into whole bone samples immersed in pH 7 solution at 20 °C and 60 °C.

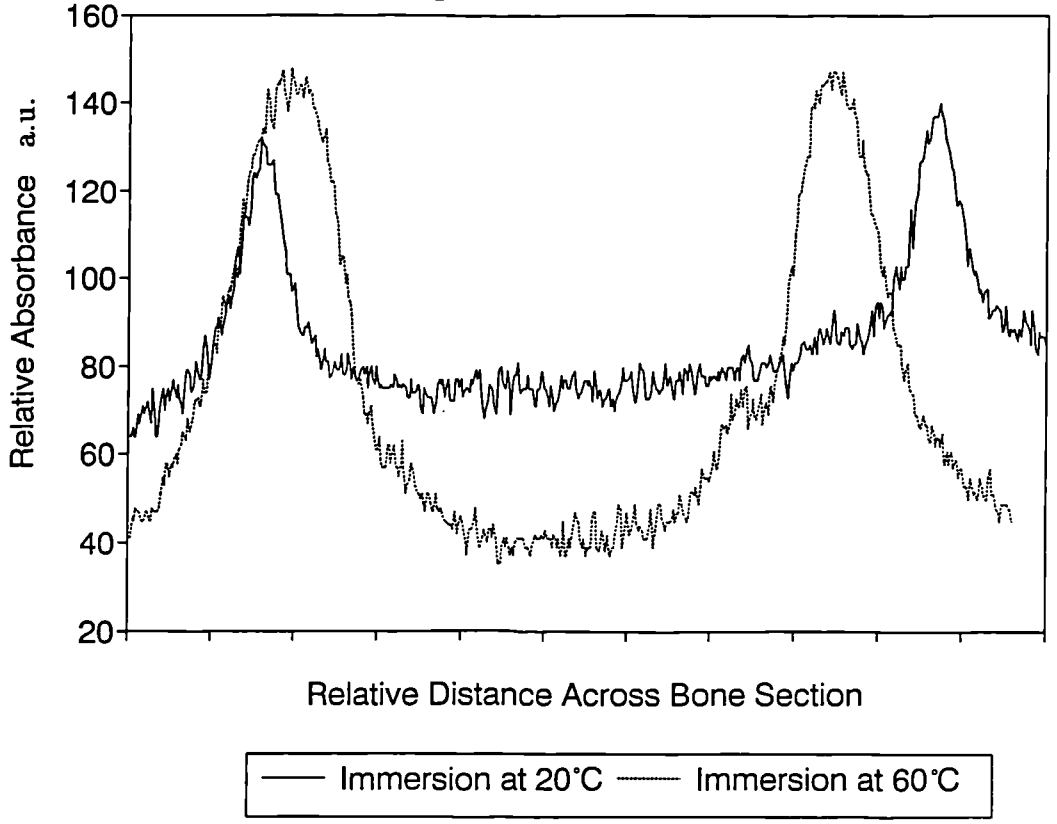

Figure 6.11: A comparison of strontium uptake into sliced bone samples immersed in pH 7 solution at 20 °C and 60 °C.

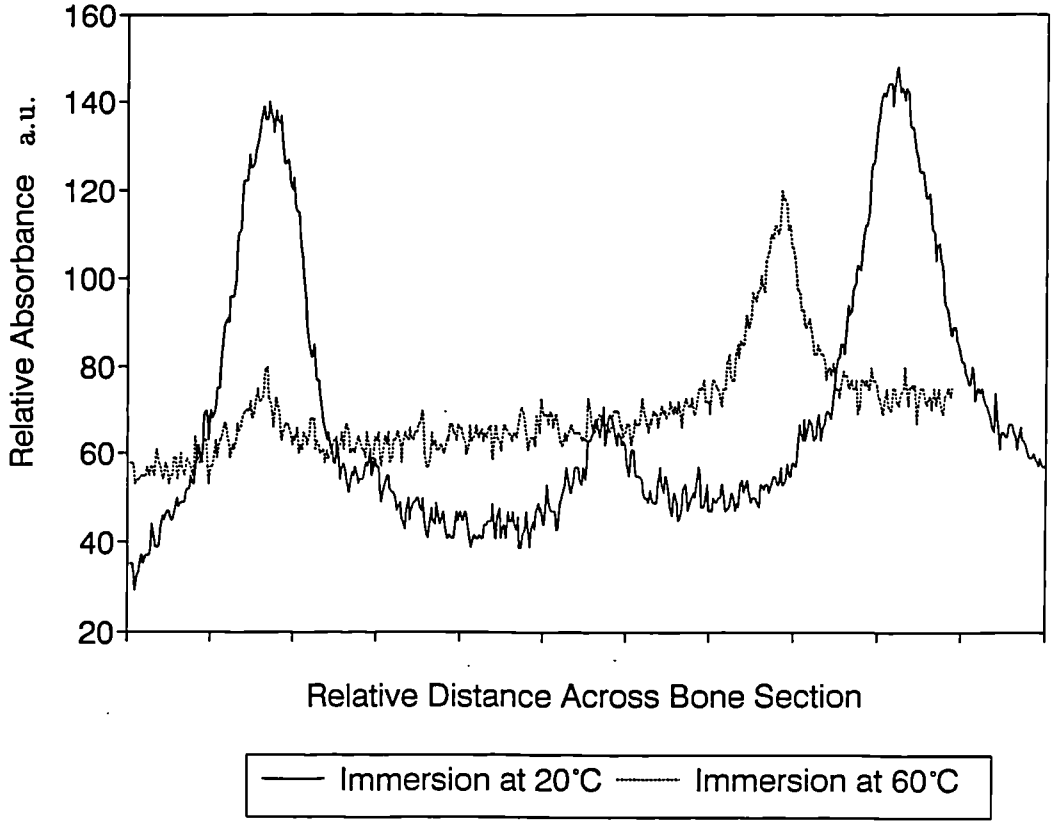

Figure 6.12: A comparison of strontium uptake into whole bone samples immersed in pH 9 solution at 20 °C and 60 °C.

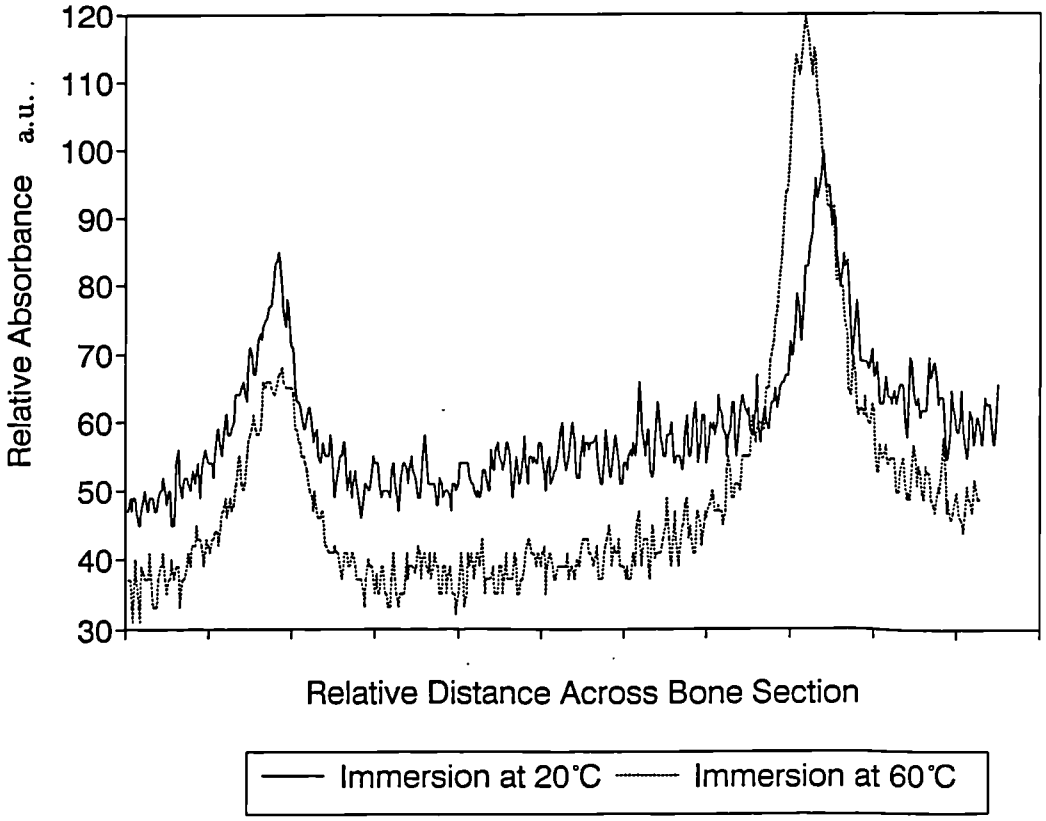

Figure 6.13: A comparison of strontium uptake into sliced bone samples immersed in pH 9 solution at 20 °C and 60 °C.

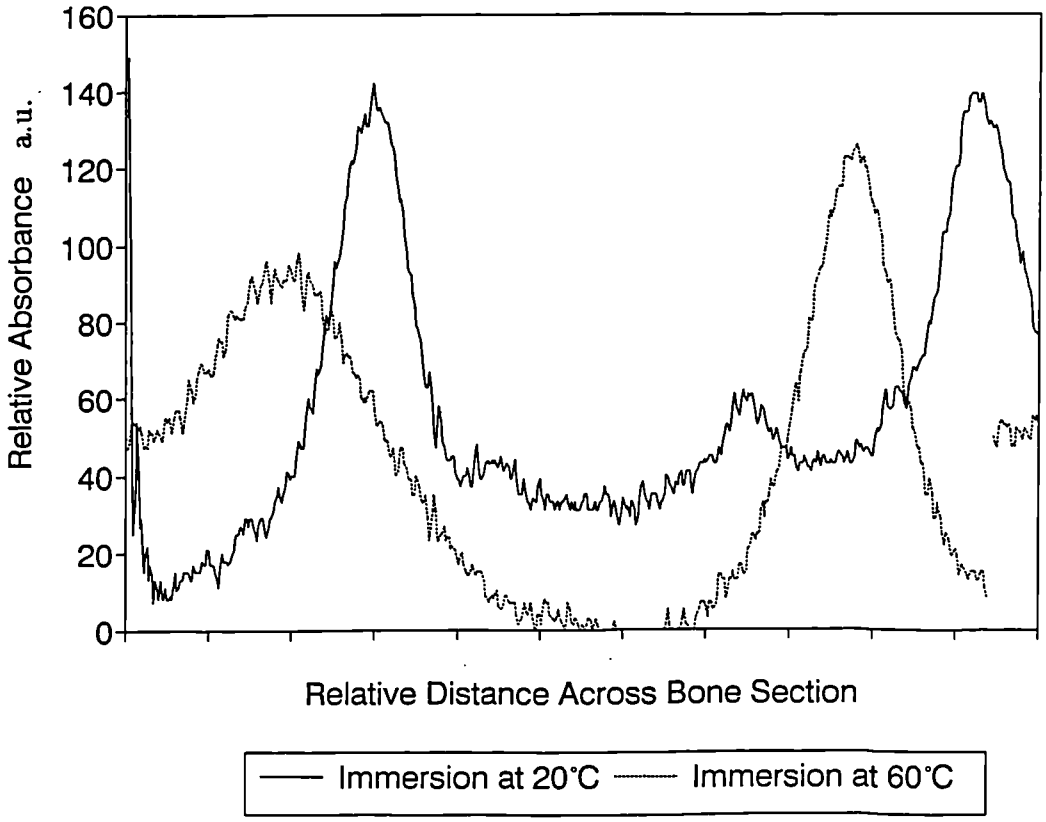

Figure 6.14: The effect of pH on strontium uptake into whole bone samples immersed at 20 °C .

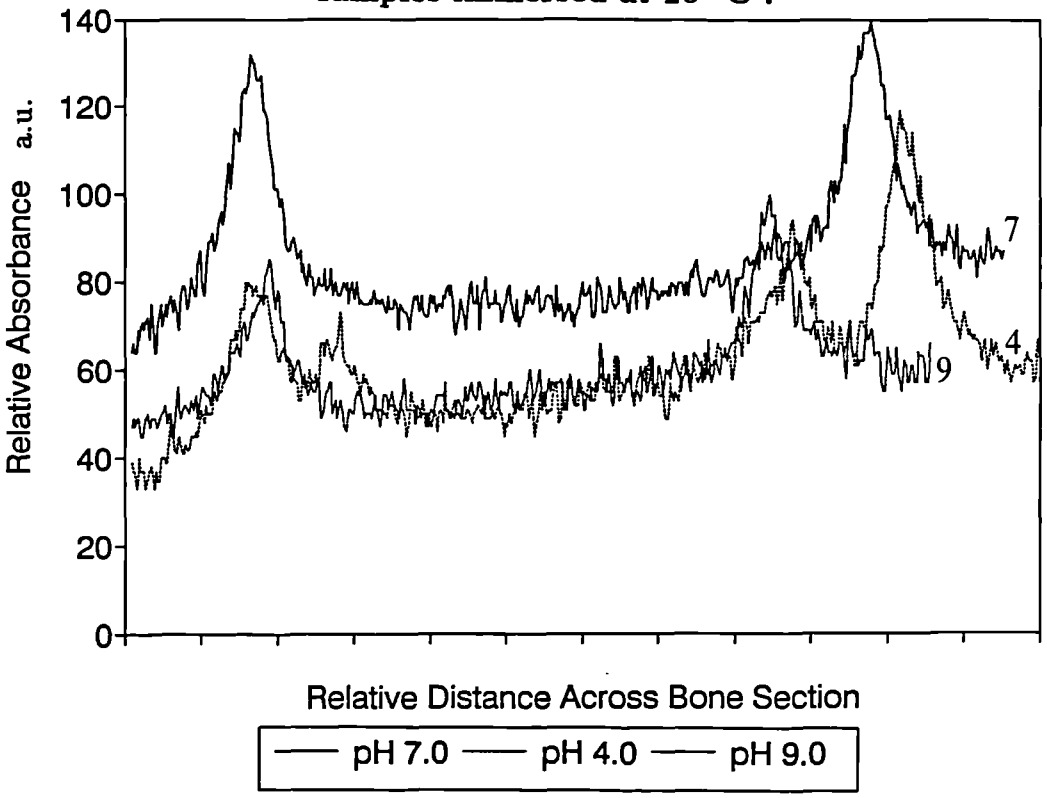

Figure 6.15: The effect of pH on strontium uptake into whole bone samples immersed at 60 °C .

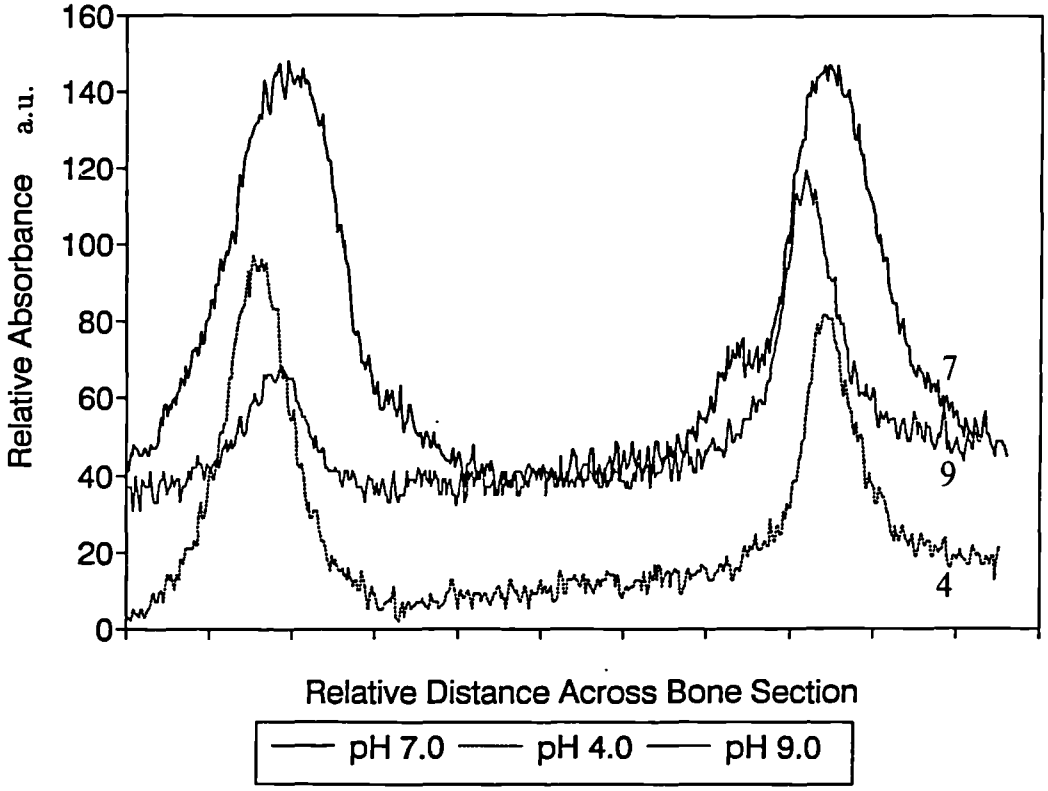

Figure 6.16: The effect of pH on strontium uptake into sliced bone samples immersed at 20 °C .

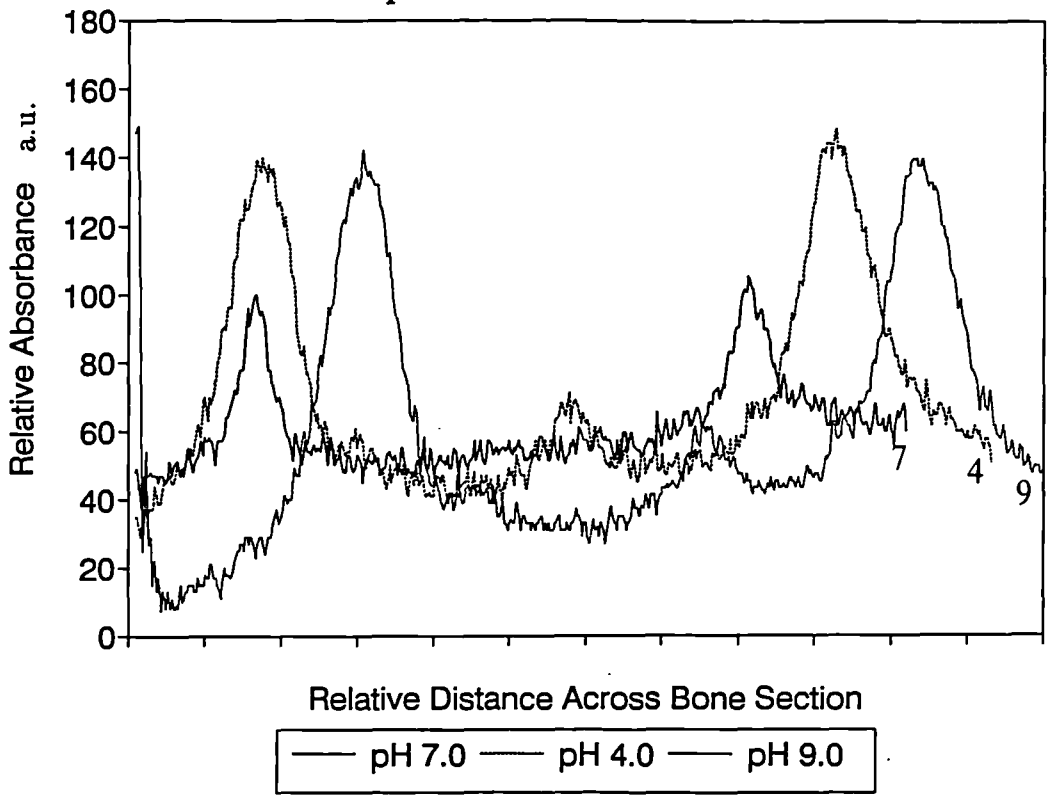

Figure 6.17: The effect of pH on strontium uptake into silced bone samples immersed at 60 °C .

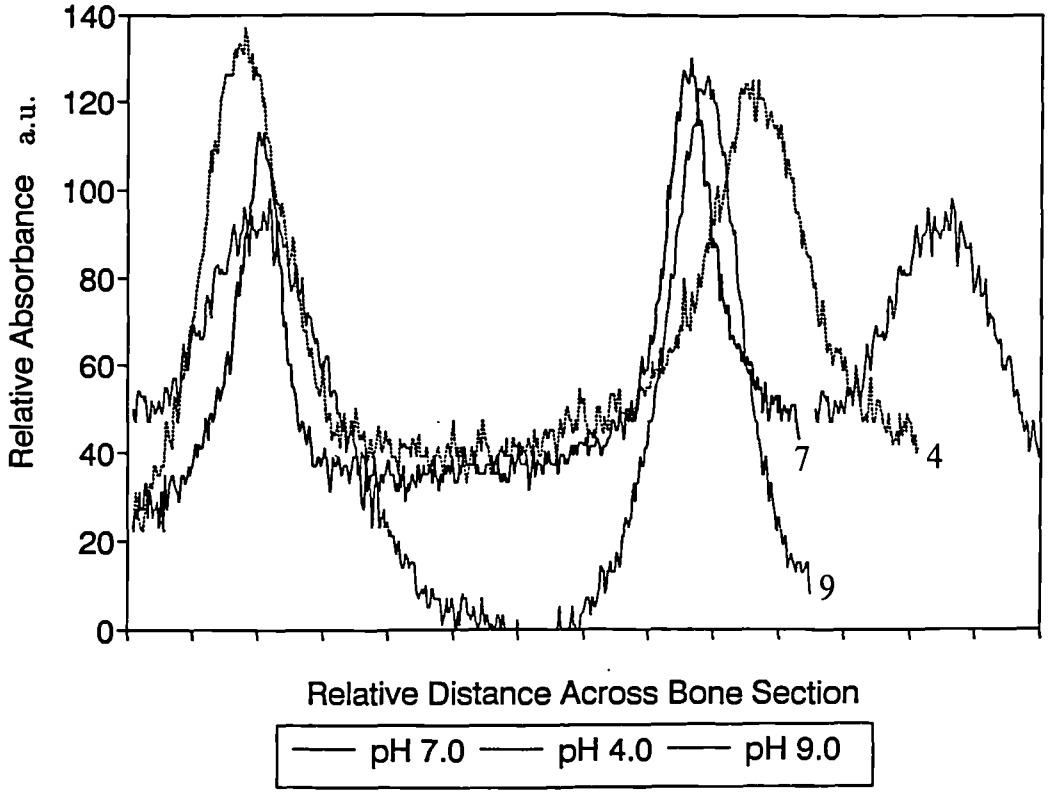

Therefore, no comprehensive pattern with uptake across pH was observed using this autoradiographic technique. Measurement of the area under each peak may have produced a more thorough study of any trends but subsequent analysis of the immersing solutions found that the desired pH values, initially adjusted by acid/alkali addition, were not maintained throughout the immersion period. Since the immersing solutions were ineffectively buffered, a pertinent study of uptake against pH could not justifiably be made here.

6.1.1.3 Leaching experiment.

This autoradiographic technique was able to demonstrate the permanence of strontium interaction with bone: figure 6.18 shows that strontium persisted in the bone even after three weeks immersion in mildly acidic solution (pH 6.0- 6.5). There was no indication of any leaching of the radiotracer, which would have produced a reduction in the size (width and/or height) of the peaks (note: the profiles, or *positioning* of the peaks, before and after leaching were different because they represented different bone samples that were, nevertheless, subject to the same immersion treatment). The fact that neither the height nor the width of these peaks were observed to alter suggested a strong interaction of radiotracer and bone, rather than simple pore-filling and excess adherence to the surface.

The affinity of strontium-90 for bone is demonstrated in fig. 6.19 as a pseudo 3-D image. Here, measurement of density was converted to altitude - the lighter-shaded areas at the peaks corresponding to high density (high absorbance), while the darker-shaded areas at the base of the peaks (the 'valleys') to low density (low absorbance).

6.1.2 Immersing Solution.

The simulated groundwater solutions remaining after the immersion period were also examined.

6.1.2.1 pH measurements.

After the immersion period, pH values tended to approach an acidic-neutral pH range - between 5.5 and 7.0 (table 6.1). These values were dependent on the

Figure 6.18: A comparison of strontium profiles in bone before and after experimental leaching attempts.

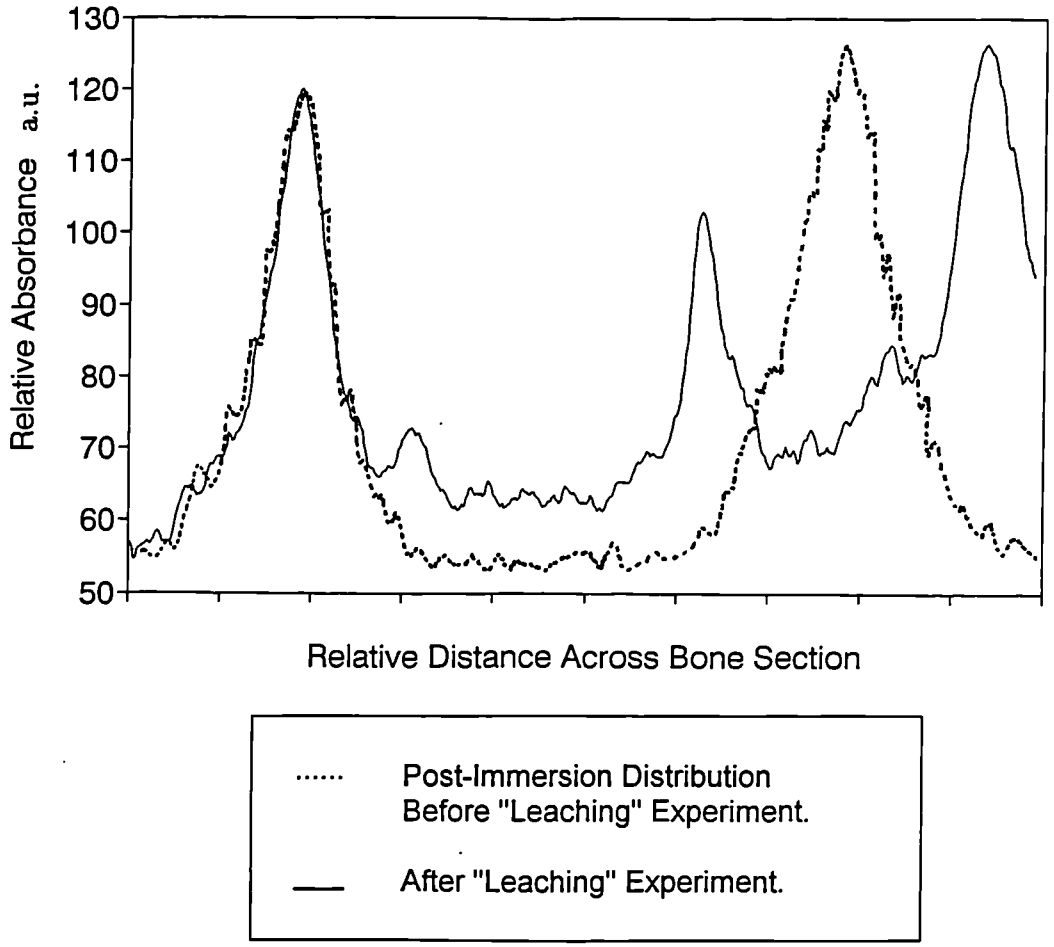

presence of dissolved ion complexes formed in solution e.g. phosphate ions, and also on decaying organic matter; indeed, all the solutions were very oily due to degreasing of the bone and organic decay.

The effect of temperature on these values was marked: for each respective pH regime, those samples at 60°C had a significantly lower pH than those at 20°C. For example, the pH values of whole and sliced bone immersed at 20°C were 6.4 and 6.3 respectively, while those at 60 °C were both pH 5.7. (These pH values were

Figure 6.19.: Pseudo 3-D representation of autoradiograph demonstrating the uptake of strontium-90 into bone slice.

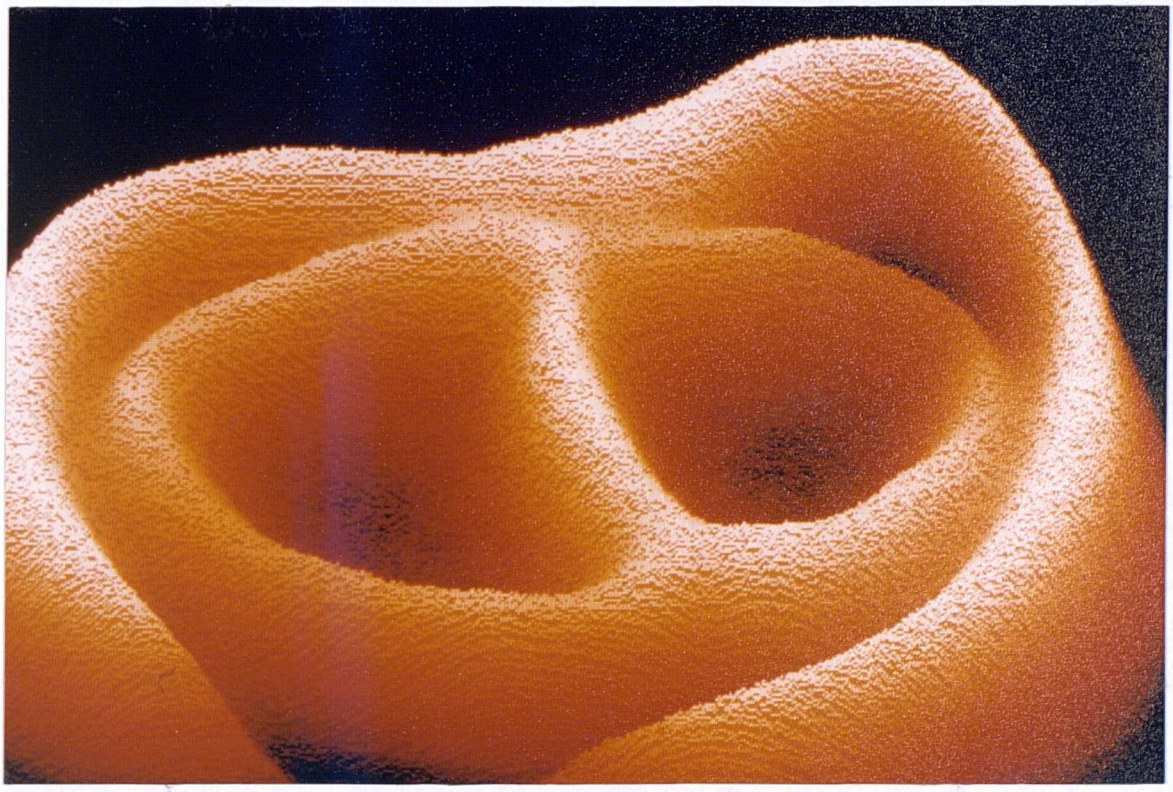

temperature compensated). This observation was predictable since it undoubtedly reflected the increased rate of organic breakdown, and thus formation of organic acids at higher temperatures. There generally appeared to be little difference in pH values (+/- 0.1 pH in most cases) between whole and sliced bone kept in similar environments: for example, post-immersion pH values for whole and sliced bone at 20 °C were 6.8 and 6.9 respectively. The exception was the sliced bone sample immersed at pH 9, 60°C whose pH was significantly lower (pH 5.2) than its whole bone counterpart (pH 6.1). One might have predicted lower pH values in sliced bone samples whose organic matrix was more vulnerable to "attack".

Rae, in her study (1987), suggested that bone is self-buffering and able to control its environment to a certain extent. In this study, it was evident that the final pH values tended to be lower in samples that were initially at pH 4 and 9, rather than pH 7. Samples immersed at pH 7 appeared to remain fairly stable (final values ranging between 6.6 and 6.9) while comparatively large changes were seen with pH 4 and 9 samples (where final values ranged between 5.7 and 6.4 for "pH 4 immersions", 5.2 and 6.4 for "pH 9 immersions"). This suggested an over-compensatory measure by bone's self-buffering mechanisms under more extreme pH regimes. Subsequent studies were able to control for this phenomenon using appropriate buffers.

Table 6.1: Recorded pH changes in immersing solutions after 10 weeks.

Bone description	Immersion Temperature (°C)	Initial pH	Final pH
whole	20	4.0	6.4
slice	20	4.0	6.3
whole	20	7.0	6.8
slice	20	7.0	6.9
whole	20	9.0	6.3
slice	20	9.0	6.4
whole	60	4.0	5.7
slice	60	4.0	5.7
whole	60	7.0	6.6
slice	60	7.0	6.6
whole	60	9.0	6.1
slice	60	9.0	5.2

6.1.2.2 Chemical analysis.

Chemical analysis of the simulated groundwater solutions was also carried out. Atomic absorption/emission spectroscopy was able to detect a limited number of elements (shown in table 6.2). Post-immersion values of Na, Ca, K and Mg were higher than their pre-immersion groundwater state. This may reflect the loss of these elements from the bone during its diagenetic alteration. However, due to the radioactivity and thus contaminative potential of the bone material, it was not possible to confirm this with post-immersion chemical analysis of the bone.

However, these solution measurements appeared to be unreliable: values obtained by AAS for pre-immersion groundwater did not correspond well to the theoretical concentrations of the original groundwater recipe. All measured values were much lower. This might indicate an incomplete dissolution of the ingredients.

Unfortunately, strontium concentrations were too small to be detected by atomic emission spectroscopy.

Table 6.2: A.A.S. analysis of immersing solutions after 10 weeks (ppm).

Sample description	Na	Ca	K	Mg
Pre-immersion groundwater (theoretical)	36.00	9.50	4.32	17.65
Pre-immersion groundwater (measured)	36.80	2.77	1.88	1.97
Whole bone, 20°C, pH 4	66.20	25.61	16.42	11.22
Sliced bone, 20°C, pH 4	45.90	13.56	13.96	4.32
Whole bone, 20°C, pH 7	61.00	4.66	10.06	3.51
Whole bone, 20°C, pH 9	65.90	9.26	15.41	6.91
Sliced bone, 60°C, pH 4	69.30	2.65	15.10	9.44
Sliced bone, 60°C, pH 7	51.7	0.82	11.77	2.43
Sliced bone, 60°C, pH 9	71.40	9.62	14.06	13.58

6.1.3 Summary.

To summarize, this preliminary study using autoradiography demonstrated that strontium uptake was generally more pronounced

(1) in sliced/sectioned bone than in whole bone for corresponding environmental regimes, and

(2) at higher temperatures of immersion.

Moreover, this study demonstrated both the **readiness** and **permanence** of strontium uptake into bone. The radiotracer appeared to be associated with the inner cortex as well as the outer cortex, predominantly in sliced bone, due to the increased accessibility of immersing solution into the medullary cavity. The effect of pH on strontium uptake was less clear and required further investigation using more appropriate controls on the environment of immersion, and using analytical techniques that allowed more detailed study of the mechanisms of strontium interaction with bone.

The following **EPMA** studies would fulfil both of these requirements in the experimental Series II and III. In addition to the study of **pH** effect, the **temporal pattern** of strontium uptake was explored in more detail, by immersing bone slices in variable concentrations of strontium chloride and later nitrate solution for variable periods of time. The respective roles of the **organic and inorganic components** of bone in the uptake mechanism were also explored in Series III. These are discussed in turn in the following sections.

6.2 Uptake Over Time: Series II and III.

Studies investigating the temporal pattern of uptake (included in both Series II and III) are discussed in this section. In these and in subsequent studies, the term "whole" bone applies to uncompromised material, in contrast to ashed and hydrazine-treated material whose organic matrix is compromised, and all samples are either sliced or powdered.

- **Immersion Series II.**

Here an unbuffered, saturated strontium solution was used, whose pre-immersion pH was set at pH 7, with an immersion temperature of 60°C. Whole and ashed (sliced) bone samples, together with immersing solutions were analysed after 1, 6 and 10 weeks. Four samples represented each duration of immersion.

6.2.1 Series II: Analysis of Solutions.

6.2.1.1 pH changes in solution.

The pH values of the immersing solution were noted before and after immersion. These are found in table 6.3, together with the calculated percentage weight changes of bone (discussed in the next section). pH values were measured using Whatman indicator paper and a Philips' portable pH meter (these two methods of measurement concurred). By week 1, the pH had dropped from pH 7 to pH 4-5; by week 10, the pH had stabilised to pH 4 for all samples. pH equilibrium was reached more quickly in ashed bone samples; this phenomenon is contrary to the expectation that the decay of organic tissue in whole bone samples would effect a more rapid reduction in pH than those of ashed bone. The latter evidently acted more effectively as a proton donor (or an acid). Certainly it is clear that this reduction in pH was not solely due to the release of organic acids themselves during organic decay but rather the self-buffering action of the bone matrix played an important part.

6.2.1.2 Chemical analysis of immersing solution.

Post-immersion calcium and strontium levels in the remaining immersing solutions were analysed by AAS and AES, respectively, in order to explore the rate of loss of calcium ions from the bone matrix and establish any correlation with the rate of uptake of strontium into the bone. These data are shown in table 6.4, three samples representing each duration for both whole and ashed material. An increased release of calcium into solution was observed over time for **whole** bone samples. This pattern of release was partly explained by the leaching of calcium as a result of immersion in an increasingly acidic solution over time, and was further reinforced in the presence of strontium. Strontium levels in solution were found to decline

Table 6.3: Table showing percentage weight change of bone and final pH value of immersing solutions after 1, 6 and 10 week immersions.

Immersion period	Bone description	% weight change for each sample	Av. % wt. change	Final pH
1 week	Whole bone	6.81		5.0
		6.66		5.0
		4.99		5.1
		7.22	6.42	5.2
1 week	Ashed bone	38.99		4.4
		35.59		4.5
		32.73		4.3
		42.46	37.46	4.5
6 weeks	Whole bone	5.99		4.9
		6.02		4.8
		3.77		4.5
		9.86	7.51	4.8
6 weeks	Ashed bone	48.11		4.0
		38.59		4.0
		42.68		4.1
		42.30	42.93	4.0
10 weeks	Whole bone	8.58		4.0
		5.66		4.1
		6.43		4.0
		7.06	6.93	4.1
10 weeks	Ashed bone	35.87		4.0
		30.20		4.0
		29.86		3.9
		32.96	32.23	4.0

over time, so that after 10 weeks immersion up to 72 % of available strontium in the original solution had been taken up into *whole* bone i.e. (555800 - 152000) / 555800. Since calcium levels released into solution in the presence of strontium were much higher than those released in its absence (controls) over a similar period, this indicated heterionic exchange of these elements in the inorganic bone matrix. (Strontium levels in control immersions were not measurable since the original strontium concentration in bone was relatively low - approximately 130 ppm).

In contrast, no clear temporal patterns of calcium release and strontium uptake were observed in solutions in which **ashed** bone samples had been immersed. This might reflect the relative importance of surface adsorption phenomena rather than heterionic exchange for the uptake mechanism of strontium into ashed material. Certainly strontium had been taken up into *ashed* bone in some fashion since up to 78 %, or (555800 - 124000) / 555800, of the available strontium in the original immersing solution had been removed from solution.

Table 6.4: Calcium and strontium concentrations in post-immersion solutions.

Bone description	[Calcium] (ppm)			[Strontium] ppm		
	1 week	6 weeks	10 weeks	1 week	6 weeks	10 weeks
*Control** whole bone	57	83	126	b.d.l	b.d.l	b.d.l
Whole bone	1207	1330	2940	188000	164000	152000
	1290	1500	3070	186900	176000	160000
	1100	1420	2790	199000	182000	157000
Ashed bone	2100	3620	2200	160000	124000	140000
	1890	1840	1700	172000	130000	132000
	1750	1960	1966	156000	149000	145000

* where control = immersion in pure water, no strontium.

'b.d.l'= levels below detection limit

6.2.2 Series II: Analysis of Bone.

6.2.2.1 Weight changes of bone.

Percentage weight change (table 6.3) did not follow an increasing trend with time: the greatest changes were seen at week 6 for both ashed and whole bone. This might imply that maximum 'uptake' or strontium saturation had been reached by around week 6, and that after this time strontium may have moved back into the immersing solution, perhaps the decreasing pH favouring this movement. However, any change in weight could not be attributed solely to strontium movement into and out of the bone; other constituents of the bone -its organic and inorganic components- would also be leached out of the bone, thereby affecting its weight. Indeed, the environment became increasingly acidic with time, inevitably enhancing bone decay processes. Moreover, subsequent ashing of post-immersion bone samples found a percentage loss-on-ignition of 31 % for bone immersed for 1 week while only a 24 % loss for 10 week immersions, indicating loss of organic tissue during immersion. Thus, the measurement of weight changes in bone after immersion was not a useful indication of the degree of elemental uptake: for this reason its measurement was omitted in subsequent studies.

6.2.2.2 Chemical changes in bone.

(i) Whole bone analysis: XRF.

The percentage weight change of ashed bone samples was much greater than that of whole bone, demonstrating the former's sponge-like property in "soaking up" strontium, largely via adsorption to its increased surface area. This was verified by analysis of a limited number of representative samples of post-immersion bone using *energy-dispersive XRF* (see Chapter 5, sub-section 5.5.1.5). Data can be found in Table 6.5. 2-3 sq.mm areas of bone (1 sample representing each condition) were scanned for 1 minute, concentrating on the yield at 14.1 kV, the position of the strontium k-alpha line. A graph of strontium count against immersion period (6.5a) gave an indication of trends in strontium concentration over time, although it was appreciated that the marker count could not be directly related to concentration, since factors such as matrix composition must be taken into account. Nevertheless, the strontium count increased with duration of immersion

Table 6.5: Energy-dispersive XRF data for strontium immersions over time, plotted in 6.5a.

Bone description	Immersion time (weeks)	Total Strontium Count in 60 secs.
Whole bone-control	N/A	109
Ashed bone-control	N/A	116
Whole bone	1	5102
	6	7200
	10	7914
Ashed bone	1	9699
	6	11108
	10	11198

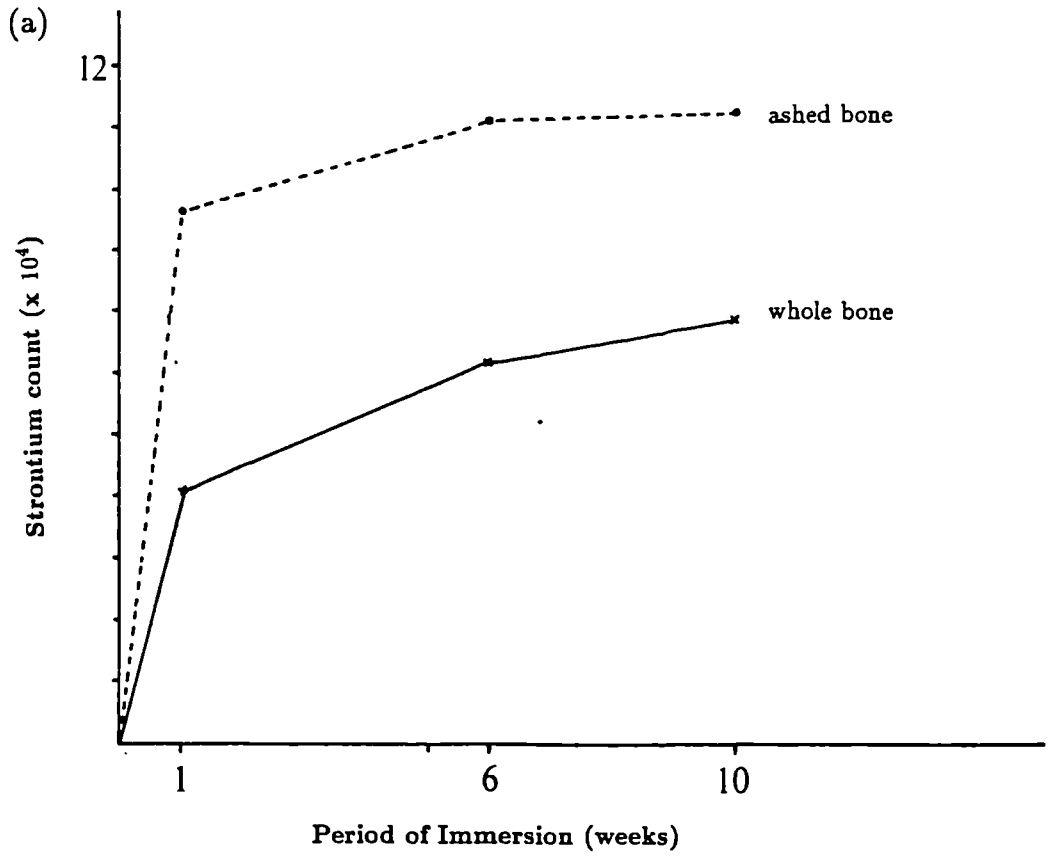

in whole bone, whilst being even higher in ashed samples, again illustrating the latter's absorbent properties. In both cases, the uptake was a two-stage process: an initial rapid uptake in the first two weeks (by extrapolation) as illustrated by the steep gradient in this period, and a second slower, more progressive uptake, until, presumably, an equilibrium between bone and solution was set up. The first stage was more rapid in ashed bone while the second less rapid compared to whole/unashed bone.

Wavelength-dispersive XRF (analytical details are found in Chapter 5, sub-section 5.5.1.5) was also carried out on the post-immersion bone samples. These data are shown in table 6.6, and in Appendix IIb, together with values for reference apatite material (certified values are found in Appendix IIa). Patterns of elemental content in bone correlated with those measured in solution. Strontium/calcium ratios were found to increase in whole bone over time, while those in ashed bone showed no clear trend. Calcium/phosphate ratios for both whole and ashed samples also showed no definite pattern over time, reflecting differential rates of loss from the bone matrix.

Table 6.6: Wavelength-dispersive XRF analysis for strontium immersions over time.

Bone description	Immersion (weeks)	% CaO	% P_2O_5	% Sr	Ca/P	Sr/Ca
Whole bone	1	50.24	38.71	7.82	1.30	0.218
	6	52.02	34.97	9.03	1.49	0.243
	6	49.57	40.08	8.64	1.24	0.244
	10	49.73	24.81	10.01	2.00	0.282
Ashed bone	1	36.94	24.28	12.25	1.52	0.464
	6	36.47	21.70	14.35	1.68	0.551
	6	46.43	27.68	11.18	1.68	0.337
	10	35.35	23.36	13.64	1.51	0.540
H5 IAEA std	N/A	40.36	24.98	0.013	1.62	0.0003
SARM 32 std	N/A	55.20	37.53	0.46	1.47	0.008

(ii) Micro-analysis of bone: EPMA.

EPMA was carried out to look in more detail at the cross-cortical distribution patterns and micro-locational details of the elements of interest in whole and ashed samples representing each duration of immersion. Both qualitative (line-profiles) and quantitative (probe analyses) data were collected (analytical details are described in Chapter 5, sub-section 5.5.1.3). The respective cross-cortical distributions of calcium, phosphorus, strontium and chloride were plotted and each line fitted to a single scan chart to represent samples at a particular magnification (reflected in the x-axis scale).

The vertical scale of these line-profiles represented the signal strength (X-ray intensity) for each respective element. Elemental concentrations were correlated to signal strength by quantitative analysis at 3 single points along this same line. N.B. Only calcium, phosphorus, strontium and chlorine concentrations were mapped because (1) these were the elements of interest, and (2) only these elements were quantifiably detectable, in addition to trace amounts of magnesium, aluminium and sulphur. All other elements were either below the detection limit at the scale set or at levels that were dismissed since % weight errors were too high to be acceptable.

To clarify any trends/patterns in uptake for each variable, the linescans for each element across a number of samples were plotted together; minor adjustments were made for any small differences in total yield and the position of the cortical edge, so that any trends in elemental distribution against pH and the bone's organic content could be seen more clearly.

(a) Qualitative analysis.

Qualitative analyses consist of cross-cortical linescans and backscattered electron images (B.E.I.) (refer to Chapter 5, sub-section 5.5.1.3). Qualitative compositional maps were obtained from B.E.I.'s, where lighter areas represent areas of higher mean atomic number: one example of ashed and whole bone was recorded in this way, and these are shown in Figures 6.20(a) and (b). The whole bone example (6.20(a)) represents a sample immersed in strontium solution for 6 weeks, and the lighter areas illustrate the location of strontium infiltration. This area of bone is

Figure 6.20: Backscattered electron images of (a) whole and (b) ashed bone examples. Mag. x40 and x60, respectively.

a

b

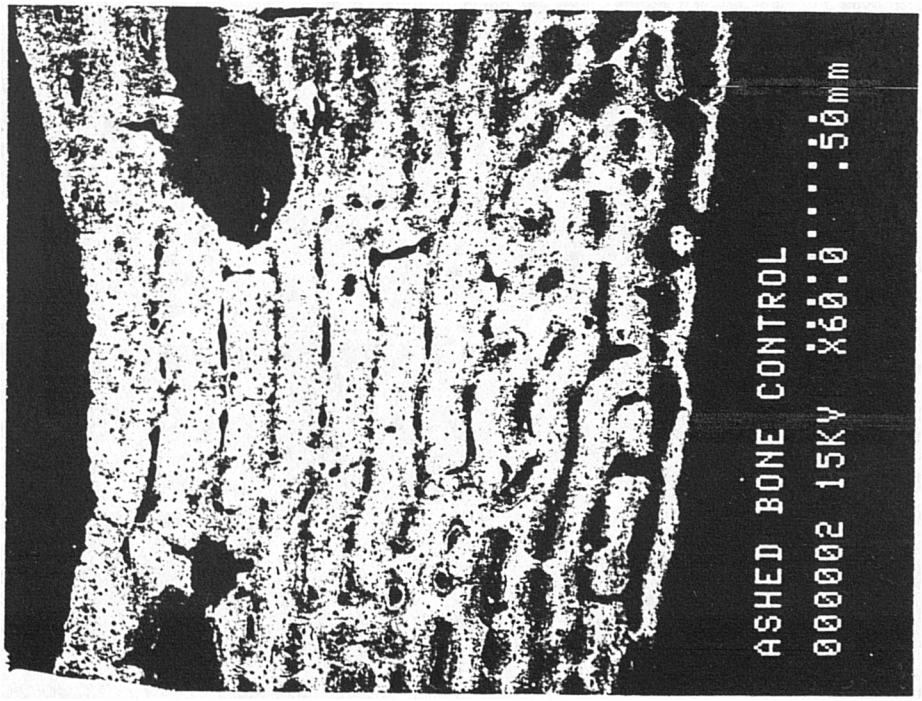

represented as an elemental map in figure 6.21, plotting the respective distributions of calcium, phosphorus and strontium.

Figure 6.21: Elemental maps of the cortical area illustrated in figure 6.20(a) representing whole bone immersed in 4 M strontium solution for 6 weeks.

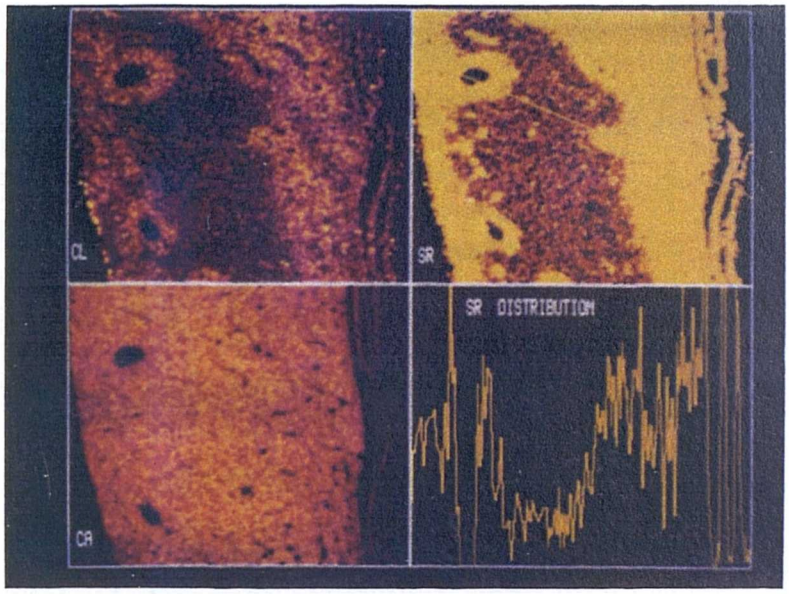

The ashed bone example in figure 6.20(b) represented control bone that had not been exposed to either immersion treatment or strontium. Natural distribution levels of strontium were not convincingly detectable above background "noise", and cross-cortical profiles of calcium and phosphorus distribution were very erratic, reflecting its porous nature: the position of pores was indicated by sudden simultaneous declines in elemental levels. These were not to be confused with interference effects caused by surface debris where virtually total blocking of readings occurred over relatively larger areas than the pore features.

Whole ovine bone controls showed a more homogeneous distribution of calcium and phosphorus across the bone cortex, maintaining a Ca:P ratio of approximately 3:2, as predicted by the formula of hydroxyapatite , $Ca_3(HPO_4)_2$. Natural strontium levels were again too low to be detected.

(1) Whole/untreated bone immersions.

Measurable levels of strontium were detected after one week of immersion: strontium had entered both whole and ashed bone across its whole cortical width. Figure 6.22 demonstrates a typical diffusion pattern in whole bone, with emphasis of strontium in the inner cortical region. Near the outer cortex, there was a clear example of strontium occupying a pore/void in the bone matrix.

After 1 week immersion, the preferential uptake of strontium was evident in peripheral cortices: this was demonstrated by the clear differentiation of strontium and chlorine (chloride) profiles in these areas where strontium levels were elevated in comparison. This indicated an *active* uptake mechanism for strontium rather than simple adsorption of the strontium chloride salt. This phenomenon was increasingly evident after 6 and 10 weeks immersion.

Bone immersed for 6 weeks (Figure 6.23) revealed a 'U'-shaped strontium profile typical of diffusion, with strontium concentrated predominantly in peripheral cortices. There was also evidence of strontium adsorption at the endosteal *surface*, possibly associated with remnant endosteal organic tissue. Strontium uptake and distribution was clearly more extensive after 6 weeks immersion.

After 10 weeks immersion, the rate of strontium uptake as a whole had declined, with only relatively small increases in strontium concentration observed despite the immersion period being twice as long (Figure 6.24). Strontium levels were highest in the periosteal cortex.

These figures are summarised in one plot (Figure 6.25) to show more clearly the cross-cortical distribution patterns of strontium over time. These data are discussed in more detail in the next section in conjunction with corresponding quantitative analyses.

Figure 6.22: Cross-cortical distribution profiles in whole bone after 1 week immersion. Microscope operated at Mag. x45.

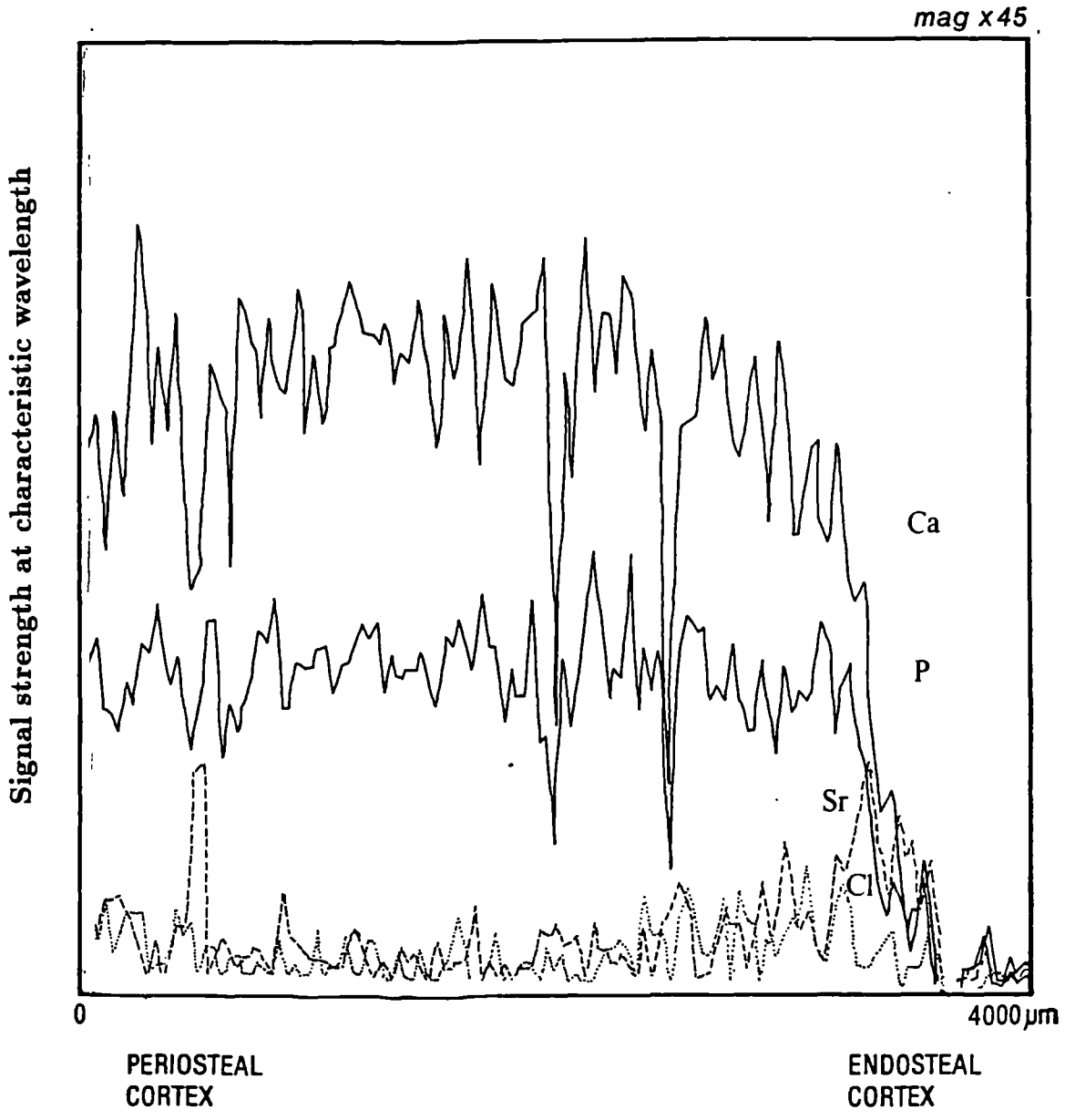

Figure 6.23: Cross-cortical distribution profiles in whole bone after 6 weeks immersion. Microscope operated at Mag. x60.

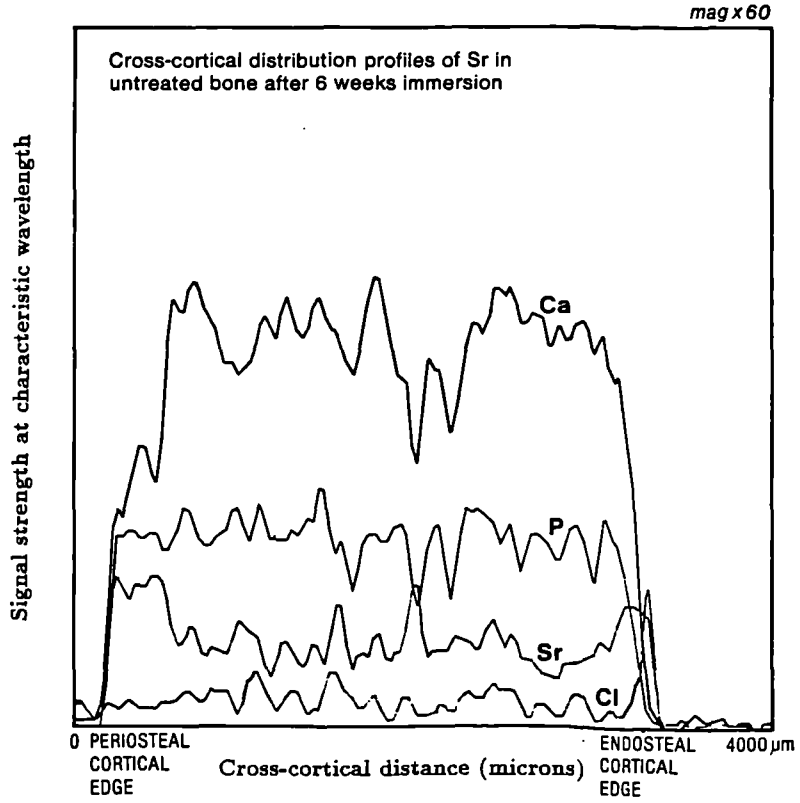

Figure 6.24: Cross-cortical distribution profiles in whole bone after 10 weeks immersion. Microscope operated at Mag. x60.

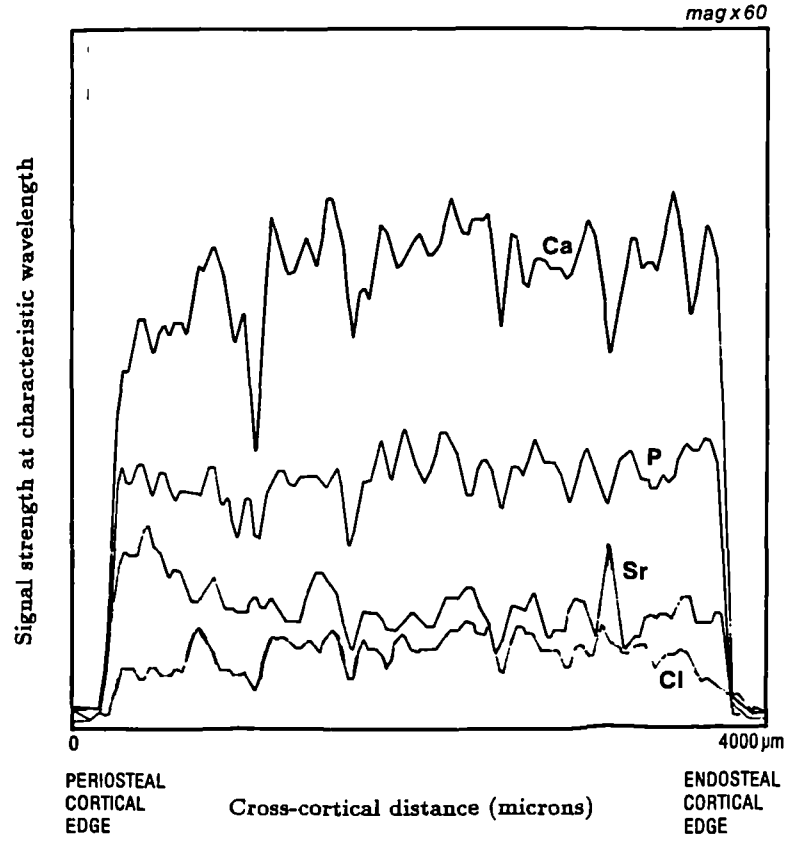

Figure 6.25: A comparison of cross-cortical distribution profiles of strontium in whole bone against time. Microscope operated at Mag. x60.

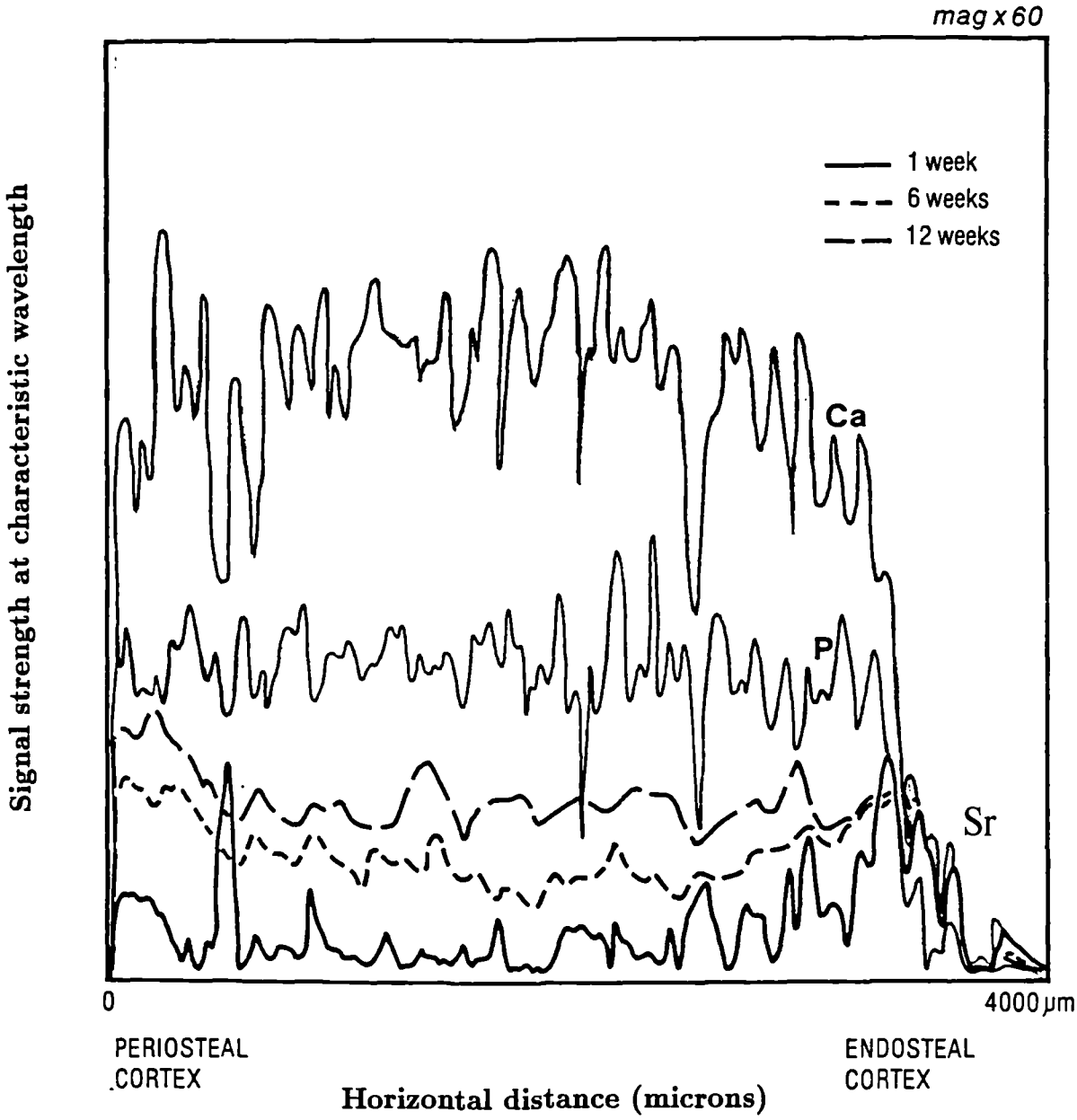

(2) **Ashed bone immersions.**

Ashed bone was immersed for up to 6 weeks. After 1 week immersion, a relatively even distribution of strontium was observed across the whole cortex, due to the larger surface area of bone available for surface adsorption and/or heterionic exchange (Figures 6.26 and 6.27). The 6 week sample clearly illustrated mid-cortical pore-filling. Both examples demonstrated a significant uptake of chloride ions as well as strontium, particularly at the cortical surfaces where chloride levels actually appeared to be greater than strontium, perhaps reflecting preferential *adsorption* mechanisms for chlorine (chloride ions) over strontium at cortical surfaces.

(b) **Quantitative analysis.** (see Chapter 5, section 5.5.1.3 for analytical details).

The elemental yield, measured as % oxide values, was found to be very variable (see Table 6.6a). In theory, the actual volume of material measured depended on the material's density, which determined the beam's depth of penetration. So, in this case, considering the same area of bone in its (1) ashed and (2) whole form: the total yield of (1) should have been relatively larger compared to that of (2) since its density was less; thus beam penetration would be greater and relatively more of the inorganic matrix measured. This trend did not appear to apply in this study (Table 6.6a). Variability in total % oxide yield may have been due to:

(a) the porosity of the bone, so that measurements taken may have been a combination of bone and resin substance,

(b) areas consisting of elements that were present other than as oxides, e.g. organic material, or as elements not analysable, e.g. water, carbonates: the electron microprobe would therefore not recognise these, and so the total % oxide was seen to be relatively lower.

For this last reason in particular, *elemental ratios* along any one line were calculated, rather than individual % values (Table 6.6b). Quantitative analyses were carried out in **three** positions (representing the outer, mid and inner cortical regions) along **two** cross-cortical lines for each sample. Graphs were plotted to determine trends in average Sr:Ca ratios (see figure 6.28) over time in each cortical region. In addition, the maximum strontium concentration in each sample was

Figure 6.26: Cross-cortical distribution profiles in ashed bone after 1 week immersion. Microscope operated at Mag. x45.

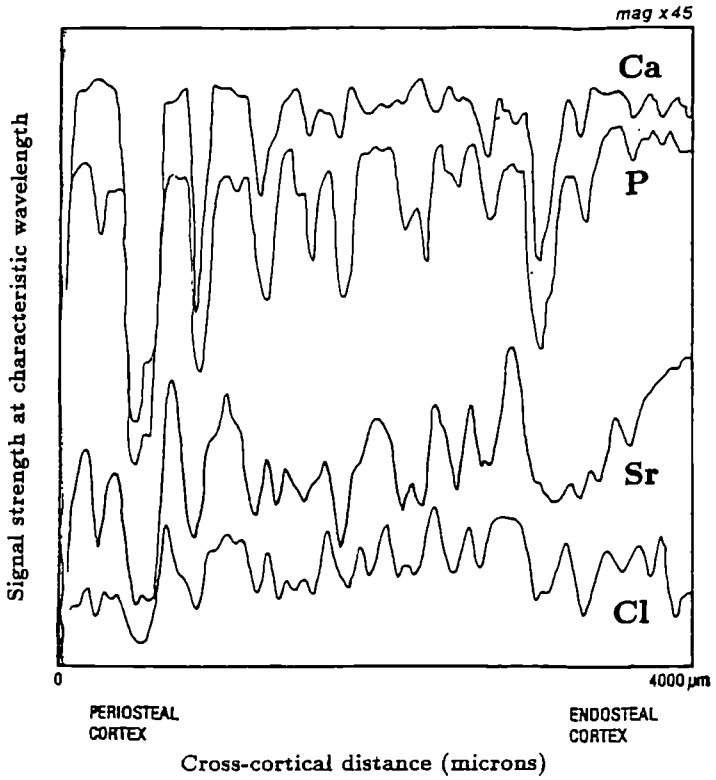

Figure 6.27: Cross-cortical distribution profiles in ashed bone after 6 weeks immersion. Microscope operated at Mag. x45.

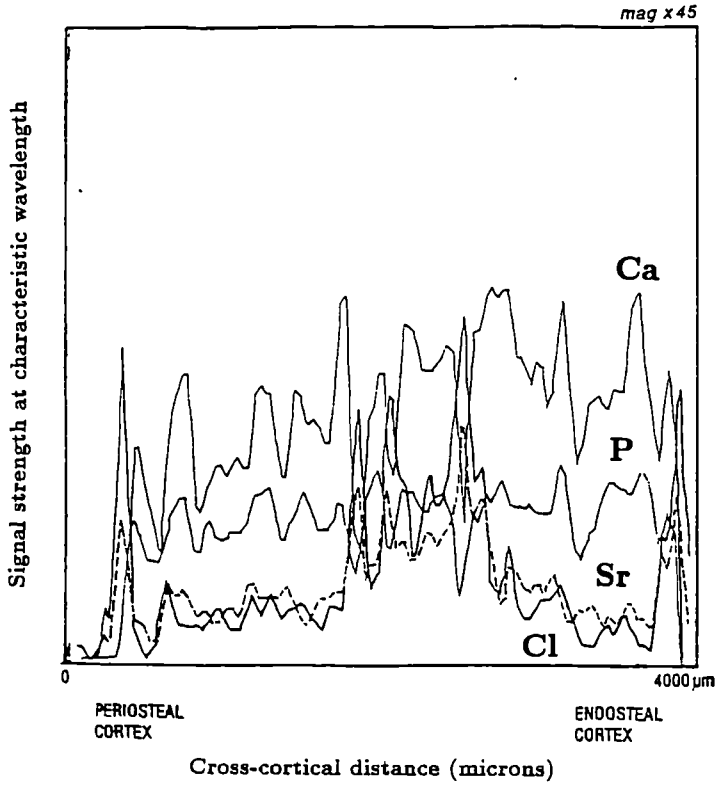

Table 6.6a: Quantitative analyses of cortical regions of bone samples (different sections of the same bone) immersed in saturated strontium solution for variable duration.

Bone	Immersion (weeks)	Location	% CaO	% P_2O_5	% SrO	% Cl
Whole	0	P	30.20± 0.2	21.74± 0.2	(0.34)	0.19± 0.1
		M	29.26± 0.3	20.82± 0.2	(0.33)	0.21± 0.1
		E	28.24± 0.2	19.18± 0.2	(0.32)	0.16± 0.1
Whole	1	P	27.06± 0.2	19.24± 0.2	4.01± 0.2	2.25± 0.8
		M	30.04± 0.2	20.53± 0.2	0.90± 0.1	0.61± 0.1
		E	23.86± 0.2	18.08± 0.2	6.55± 0.2	1.70± 0.1
Whole	6	P (1)	31.36± 0.3	23.44± 0.2	6.36± 0.2	0.71± 0.1
		M (1)	39.25± 0.3	26.72± 0.2		0.58± 0.1
		E (1)	26.33± 0.2	21.05± 0.2	14.88± 0.3	1.44± 0.1
		P (2)	28.16± 0.3	24.72± 0.2	16.25± 0.3	1.10± 0.1
		M (2)	26.42± 0.2	20.29± 0.2	9.32± 0.3	0.71± 0.1
		E (2)	20.28± 0.2	20.58± 0.2	16.53± 0.3	0.85± 0.2
Whole	10	P (1)	29.52± 0.3	24.49± 0.2	12.73± 0.3	1.27± 0.1
		M (1)	36.32± 0.3	26.69± 0.3	9.31± 0.3	3.34± 0.1
		E (1)	36.77± 0.3	27.56± 0.3	7.81± 0.3	0.80± 0.1
		P (2)	30.17± 0.2	21.42± 0.2	6.60± 0.3	1.94± 0.1
		M (2)	31.78± 0.3	23.03± 0.2	8.77± 0.3	2.11± 0.1
		E (2)	30.65± 0.3	22.59± 0.23	5.51± 0.2	0.81± 0.1
Ashed	0	P	31.63± 0.3	21.96± 0.2	(0.36)	0.26± 0.1
		M	42.27± 0.3	28.35± 0.2	(0.40)	
		E	33.91± 0.3	22.69± 0.2	(0.37)	
Ashed	1	P	15.24± 0.2	12.43± 0.1	5.36± 0.2	0.83± 0.1
		M	12.08± 0.1	12.89± 0.1	4.34± 0.2	1.14± 0.1
		E	16.23± 0.2	12.56± 0.1	3.60± 0.2	0.90± 0.1
Ashed	6	P (1)	22.96± 0.2	20.49± 0.2	8.73± 0.3	3.79± 0.1
		M (1)	22.40± 0.2	18.24± 0.2	15.06± 0.3	8.49± 0.2
		E (1)	16.52± 0.2	16.92± 0.2	5.99± 0.2	2.02± 0.1
		P (2)	21.91± 0.2	19.05± 0.2	5.43± 0.2	1.60± 0.1
		M (2)	31.31± 0.3	24.25± 0.2	7.47± 0.3	3.18± 0.1
		E (2)	6.06 ± 0.1	8.98± 0.2	2.99± 0.2	0.76± 0.1

where 0 = control (no immersion), and P = periosteal cortex, M = mid-cortex, E = endosteal cortex. (1) & (2) represent different lines of quantitative analysis where more than 1 profile line was analysed for each sample.

Values in brackets are unacceptably low (below acceptable detection limits)

Table 6.6b: Elemental ratios in cortical regions of bone as in table 6.6a

Bone	Immersion (weeks)	Location	Ca:P	Sr:Ca	Sr:Cl
Whole	1	P	1.41	0.15	1.79
		M	1.46	0.03	1.48
		E	1.32	0.27	3.86
Whole	6	P (1)	1.34	0.20	8.95
		M (1)	1.47	-	-
		E (1)	1.25	0.57	10.32
	6	P (2)	1.14	0.58	14.77
		M (2)	1.30	0.35	13.19
		E (2)	0.98	0.81	19.45
	10	P (1)	1.21	0.43	9.99
		M (1)	1.36	0.26	2.79
		E (1)	1.33	0.21	9.77
	10	P (2)	1.41	0.22	3.40
		M (2)	1.38	0.28	4.15
		E (2)	1.36	0.18	6.82
Ashed	1	P	1.23	0.35	6.45
		M	0.94	0.36	3.81
		E	1.29	0.22	4.01
Ashed	6	P (1)	1.12	0.38	2.31
		M (1)	1.23	0.67	1.78
		E (1)	0.98	0.36	2.96
	6	P (2)	1.15	0.25	3.40
		M (2)	1.29	0.24	2.35
		E (2)	0.68	0.49	3.94

where 0 = control (no immersion) and P = periosteal cortex, M = mid-cortex, E = endosteal cortex, and (1) & (2) represent different lines (profiles) of quantitative analysis where more than 1 profile line was analysed for each sample.

estimated by extrapolation of measured levels located at specific points along a line scan to correspond to the highest point(s) located in the profile: this would provide a comparison against quantitative trends revealed by whole bone analysis (section 6.2.2.2). Table 6.7 summarises the general trend observed in quantitative analyses by showing the cortical position and estimated values of maximum strontium as taken from the respective line-profiles. % oxide values in this table were only approximate.

Table 6.7: Estimated maximum strontium concentration and its cortical location in each sample.

Bone	Immersion (weeks)	Line	Max. Sr % oxide	Std max. yield	Cortical location
Whole	1	2	6 - 9	15	Inner cortical edge
		1			Inner cortical edge
Whole	6	1	23	36	Inner-mid cortex
		2	20	30	Mid-cortex
Whole	10	1	16	21	Outer cortex
		2	15	24	Mid-outer cortex/pore
Ashed	1	1	6 - 7	19	Mid-outer cortex
	6	1	26	47	Mid-outer cortex
	6	2	15	33	Mid-cortical pore

Quantitative data revealed a number of trends which largely confirmed qualitative patterns represented in the line-profiles. The highest strontium concentrations found in whole bone were located in the inner cortical/endosteal region after a short period of exposure to saturated solution. This reflected the less dense, more cancellous bone tissue found in this area surrounding the medullary cavity. With time, strontium maximum tended to shift towards the mid-outer cortex. After 10 weeks immersion, periosteal bone contained the highest strontium concentration which followed a gradient down to the endosteal bone: a typical 'U'-shaped profile was not observed in the 10 week sample.

Figure 6.28: Sr:Ca ratio plotted for each cortical region against period of immersion.

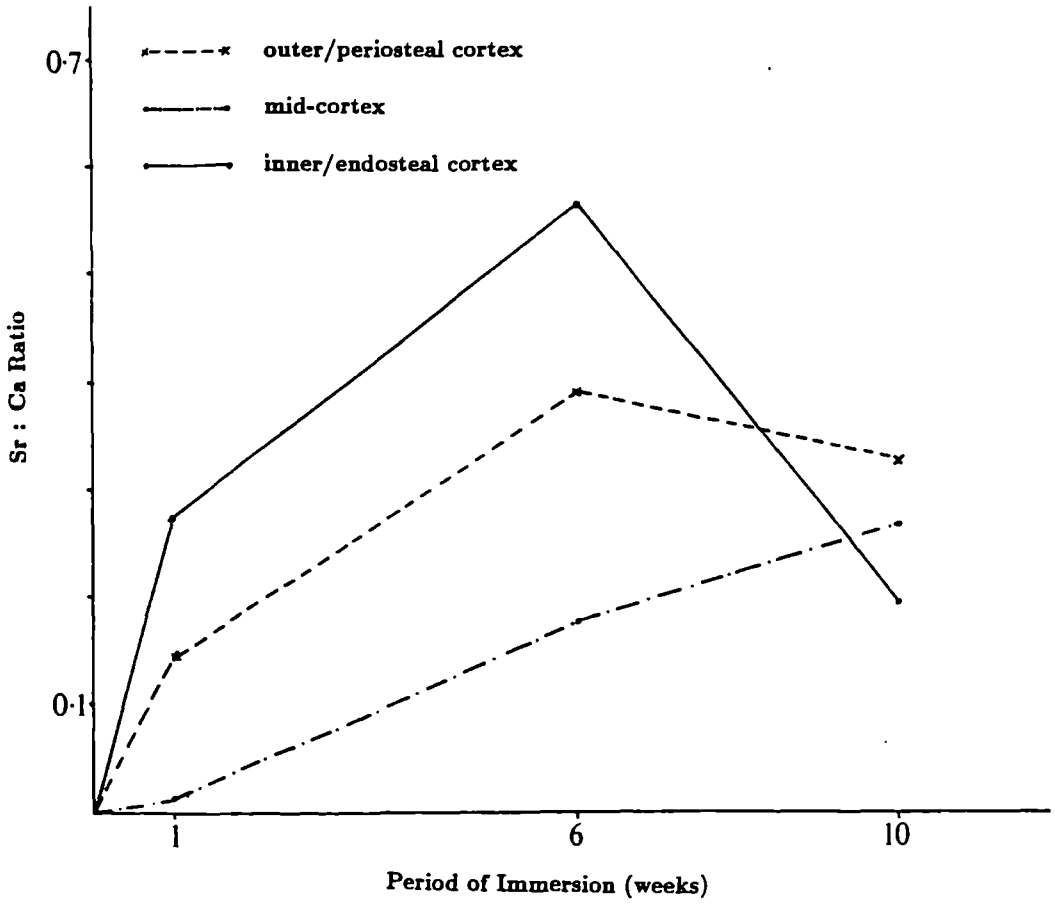

This overall pattern was not observed for ashed bone samples where highest strontium concentrations tended to occur in the more dense periosteal tissue and in mid-outer cortical pores. Some pore-filling was observed in whole bone but predominantly in samples immersed for 10 weeks.

Quantitative analyses found that levels of Sr in whole bone did not appear to increase between weeks 6 and 10, but rather redistributed themselves across the cortex. For example, table 6.7 shows a decrease in the estimated maximum strontium concentration between 6 and 10 weeks immersion. This may have represented

a redistribution phenomenon; at the same time, it demonstrates that the pattern did not simply reflect a saturation effect otherwise the maximum strontium level would have reached a peak and remained there.

Average Sr:Ca ratios for each whole bone sample are shown plotted in Figure 6.28. A general increase with time was observed in outer and mid-cortical regions, while a quite different pattern was evident for the inner cortical region: after 6 weeks immersion, a decline in ratio value had occurred so that at 10 weeks, it was below the value observed after 1 week immersion. A small decline in Sr:Ca ratio had also occurred in the outer cortex between 6 and 10 weeks, while a steady increase in the mid-cortical region.

These cross-cortical patterns based on quantitative analyses corresponded with qualitative line-profiles in identifying a "redistribution" phenomenon. Both recognised that initially, a rapid strontium uptake occurred in the endosteal cortex and at a slower rate the periosteal cortex, so that up to around 6 weeks immersion a 'U'-shaped cross-cortical profile existed. After this time, the profile altered as strontium was redistributed across the cortex so that highest levels were located in the periosteal region. However, whereas quantitative data indicated a dramatic decrease in levels in the endosteal region, with some decline in the periosteal, qualitative line-profiles indicated a halt in uptake and a decline in the rate of uptake in these respective cortical regions. Both registered a steady uptake in the mid-cortical region.

Sr:Cl ratios followed a similar cross-cortical pattern over time. This suggests that strontium was not entering the bone simply by diffusion in its chloride form: had this been the case, the ratio would have remained at 0.5558, the elemental ratio of the original strontium chloride salt. Rather, strontium was being preferentially taken up / adsorbed and possibly incorporated into the bone structure. Sr:Cl values were highest after 6 weeks immersion. After this time, a decline was observed indicating either a subsequent loss in the bone's strontium content or an uptake of chlorine itself into the bone around this time. Quantitative data (table 6.6) confirmed the latter, and the heterionic exchange of hydroxyl ions in the mineral lattice for chloride ions is well-documented (Kibby and Hall, 1972; McLean and Urist, 1955).

(iii) Further micro-analysis of bone: PIXE analysis.

Figures 6.29(a) and (b) show the energy spectrum and elemental maps, respectively, of a bone sample that had been immersed for 10 weeks, obtained using the proton microprobe. Elemental maps were generated for each element by selecting all X-rays whose energies lie between the limits corresponding to the characteristic energy of that element. The location of each X-ray was used to build an array of pixels with the value in each cell equal to the number of counts received from that point: the darker the point, the higher the number of X-ray counts. In the 2.5 sq.mm area scanned, a high strontium concentration was observed (note: these mapped areas only provide an indication of relative concentration for each element i.e. they are qualitative; absolute or true values of different elements cannot be compared).

With this in consideration, a number of observations were made. Firstly, the PIXE spectrum indicated an extensive strontium content in the sample, indicated by the large peak at around 14 keV (Figure 6.29(a)). Indeed, strontium was observed in high concentrations throughout much of the cross-cortical area of the bone, largely in the mid-cortex, but relatively depleted towards the endosteal cortical region. This distribution probably reflected strontium entry directly into the mid-cortex of the bone slice which presented a large surface area for diffusion/ionic interaction. Thus, a typical cross-cortical diffusion gradient was not observed because there was no simple diffusion surface: the immersing solution could access the bone from every surface. The larger pores visible in the matrix were empty i.e. strontium had not "passively" filled these voids in their entirety, although it may have filled smaller pores in the same way that elements such as iron and manganese are known to behave in the burial environment.

This PIXE analysis highlighted the problems posed by using bone *slices*, with strontium able to enter the bone more readily than would otherwise be expected in the burial predicament. Series III introduced the coating of transverse sections of bone slices with cellulose acetate to reduce this phenomenon.

Figure 6.29: (a) PIXE spectrum and (b) digimap of whole bone immersed in 4M strontium solution for 10 weeks.

a

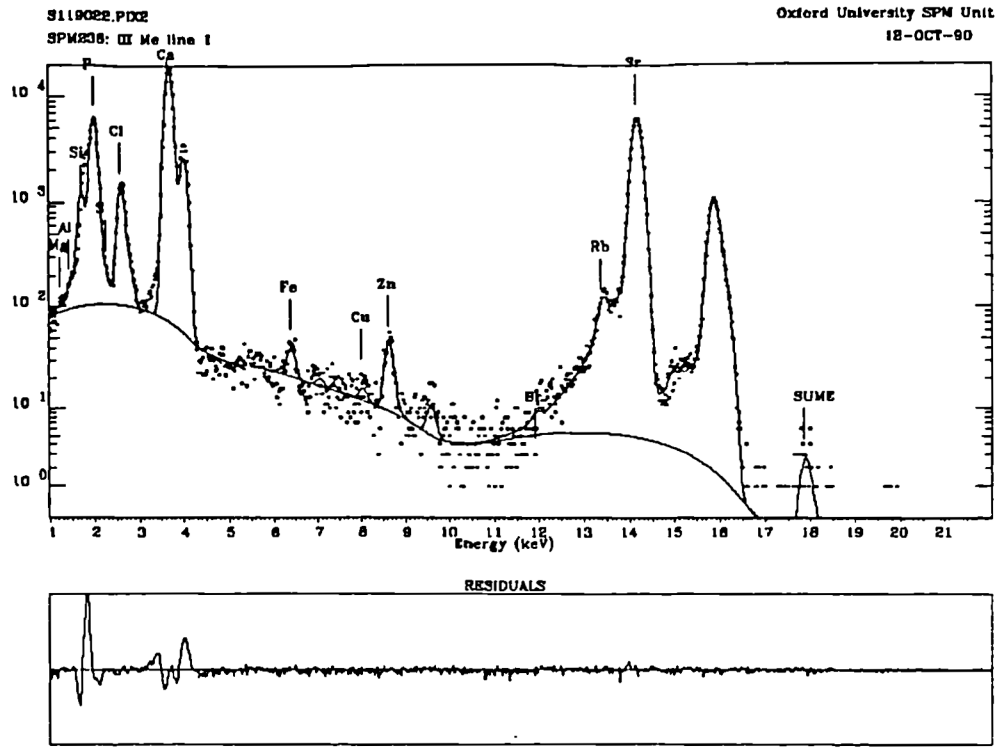

b

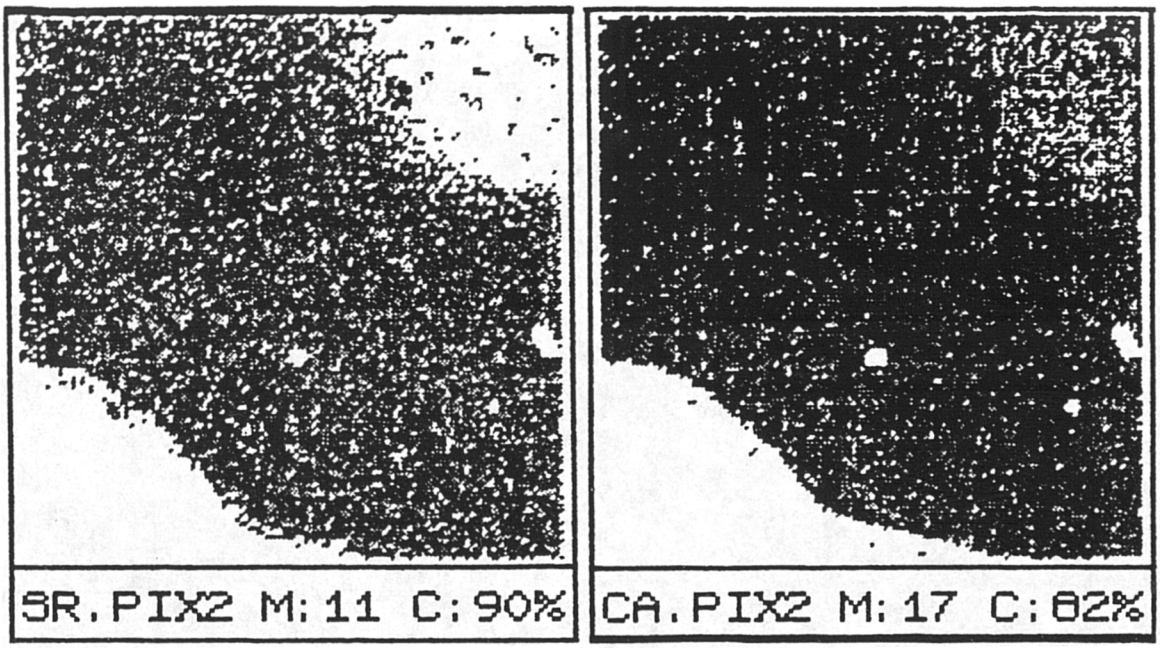

- **Immersion Series III.**

6.2.3 Series III: Analysis of Solutions.

With the introduction of effective buffering of solutions during the immersion period, there was no longer any need to measure the pH of post-immersion solutions since pH values were maintained at their originally defined values throughout.

This buffering system itself, however, posed problems for subsequent chemical analysis of solutions using spectrophotometric methods. Neutral to alkaline solutions contained sufficient sodium (from sodium hydroxide addition: Chapter 5, sub-section 5.2.2.3) to obscure the presence of strontium and particularly calcium measured by flame emission/absorption, since sodium emits a bright orange (high absorption, high emission) flame.

While absolute values for the limited strontium measurements taken were not wholly reliable for this reason, a general pattern over time did emerge: solutions containing whole bone at pH 7 possessed declining strontium levels with time, as shown in table 6.8. The data here would suggest a 76 % uptake of the available strontium in solution after 12 weeks, but this is likely to be an over estimation since real strontium levels remaining in solution were masked to some extent by sodium ("blank" buffered solutions measured 9 ppm, yet this solution was calibrated as zero strontium).

Table 6.8: Strontium levels measured in immersing solutions containing whole bone at pH 7 for variable duration.

Period of immersion (weeks)	Strontium concentration (ppm)
Control "blank"	9
1	90
2	65
5	50
12	25

6.2.4 Series III: Analysis of Bone.

For this series, only qualitative data from EPMA and PIXE analysis were collected to compare the temporal patterns of strontium uptake in 100 ppm solutions with those obtained from immersion in saturated solutions.

6.2.4.1 Micro-analysis of bone: EPMA.

Figure 6.30 shows the distribution of strontium in the periosteal cortex (magnification x1000) of whole bone after 1, 2, 5 and 12 weeks immersion in a 100 ppm strontium nitrate solution buffered at pH 7. After 1 week, strontium was observed across the whole cortical width with a slight elevation at the immediate edge of the cortex. During the time span of the experiments, strontium levels in the cortex increased but this increase did not continue at the rate initially set in the first few weeks of immersion. The difference in strontium content between 1 and 2 weeks, for example, was similar to that observed between 5 and 12 weeks. Moreover, at 12 weeks the strontium elevation observed earlier at the cortical edge was beginning to level out.

Therefore, a similar temporal pattern of strontium uptake was observed in 100 ppm strontium immersions (Series III) and in saturated solutions (Series II).

Figure 6.31 plots the calcium/strontium ratio at the periosteal cortex at 1, 5 and 12 weeks immersion. This ratio was observed to decline and to some extent level out over time, illustrating either (1) simple leaching of calcium into solution over time with simultaneous strontium uptake, or (2) a more intimate relationship between the two processes as strontium actively exchanged with calcium in the inorganic lattice.

6.2.4.2 Micro-analysis of bone: PIXE data.

PIXE analysis was carried out on bone immersed in 100 ppm strontium nitrate solution for only 1 week. Figures 6.32(a) and (b) show mapped areas of the periosteal cortical edge at different magnifications. The first maps a 2500 square micron area and shows that after 1 week, strontium had penetrated the cortical tissue up to 250 microns. At higher magnification, the diffusion profile of strontium from the

Figure 6.30: Strontium distribution over time in the periosteal cortex of whole bone at pH 7. Microscope operated at Mag. x1000.

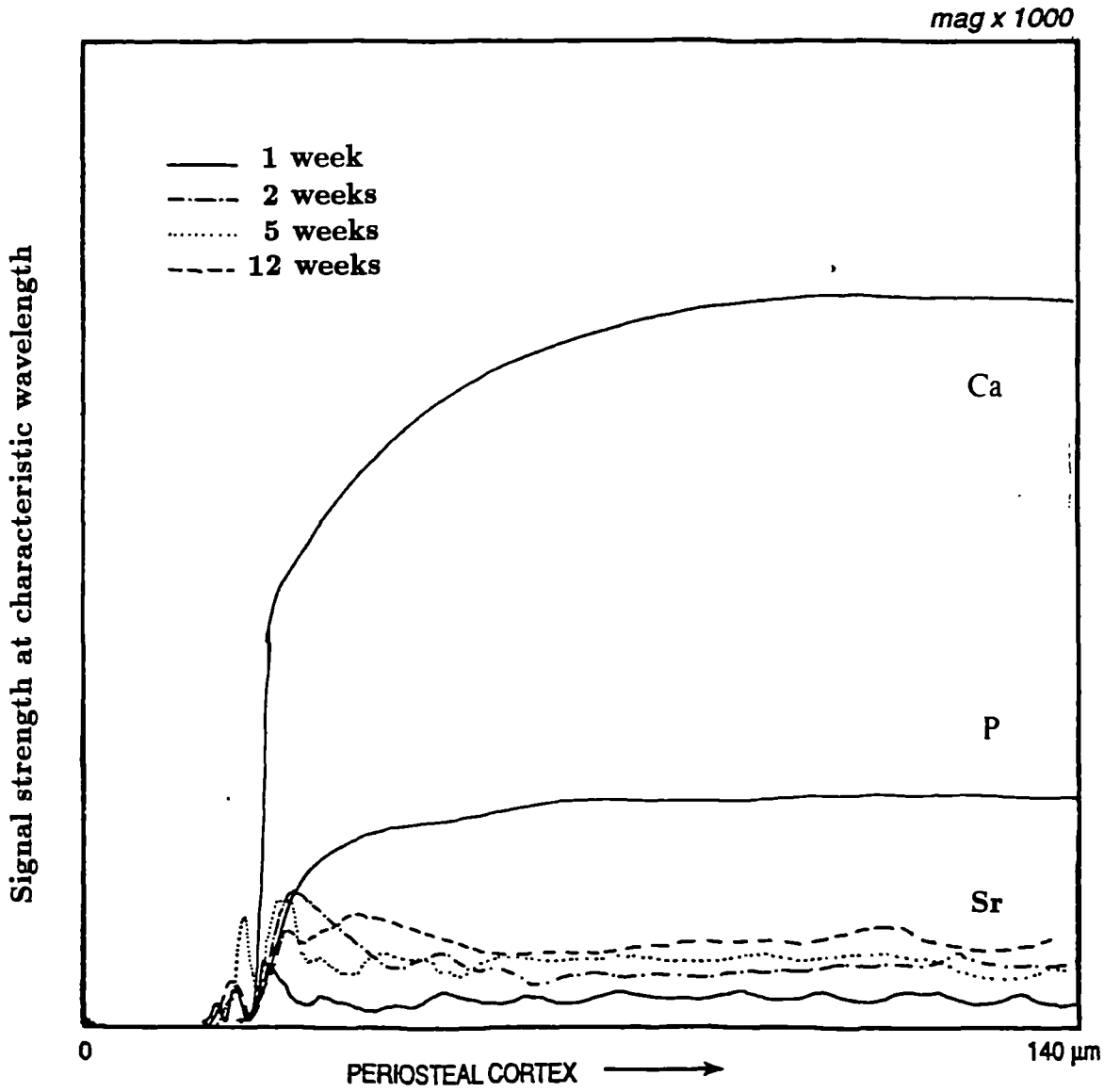

Figure 6.31: Calcium/strontium ratios over time in the periosteal cortex of whole bone at pH 7. Microscope operated at Mag. x1000.

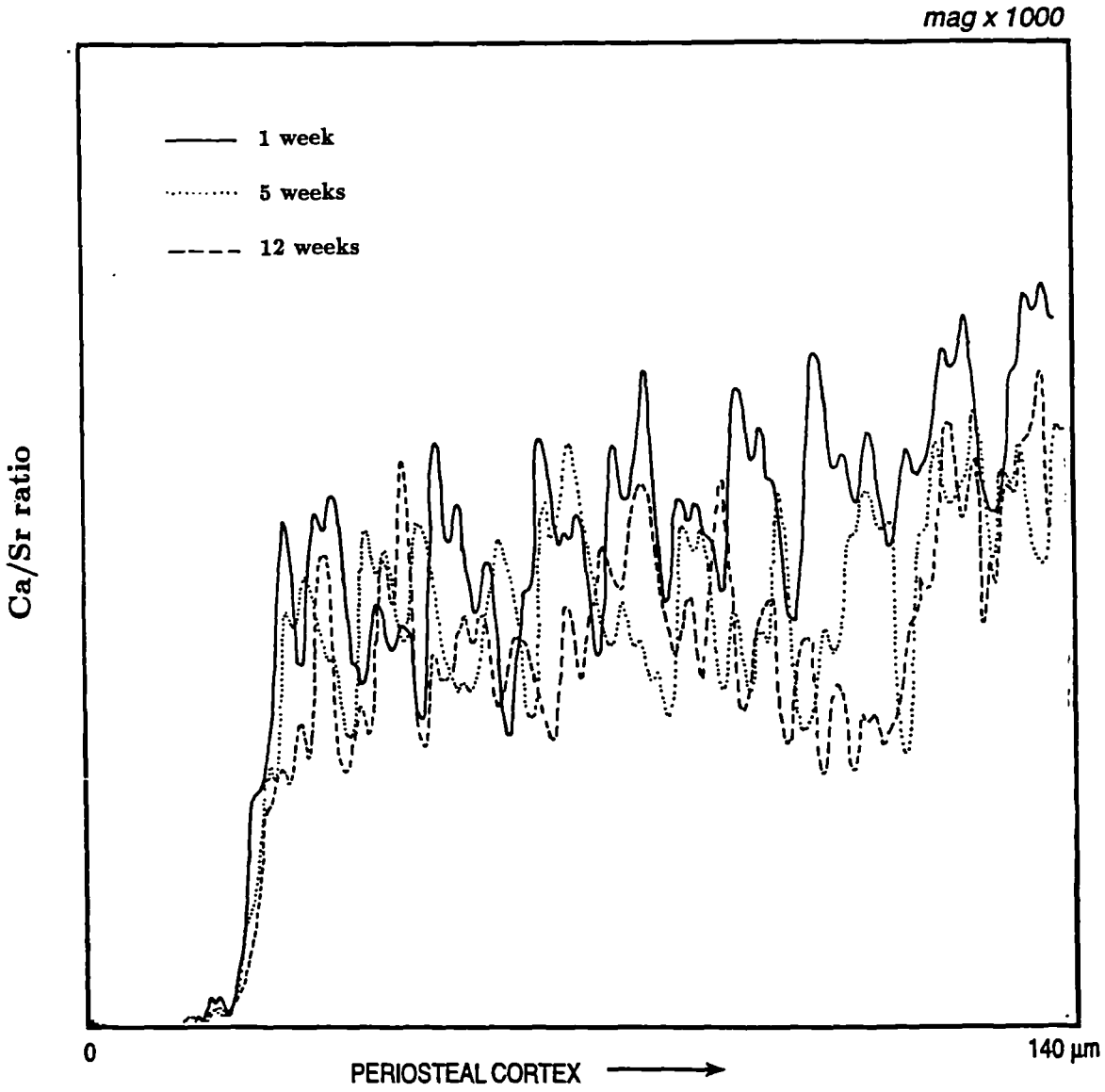

Horizontal distance of scan (microns)

Figure 6.32: PIXE maps representing (a) 2500 sq.microns and (b) 250 sq.microns, of the periosteal cortical region of bone immersed in 100 ppm strontium solution for 1 week.

a

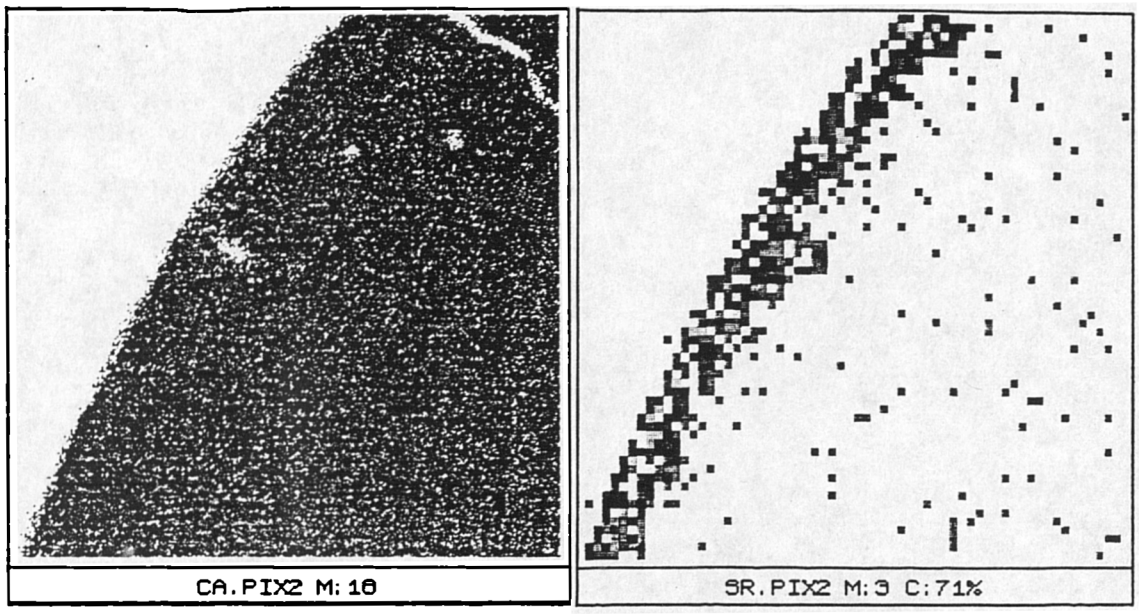

b

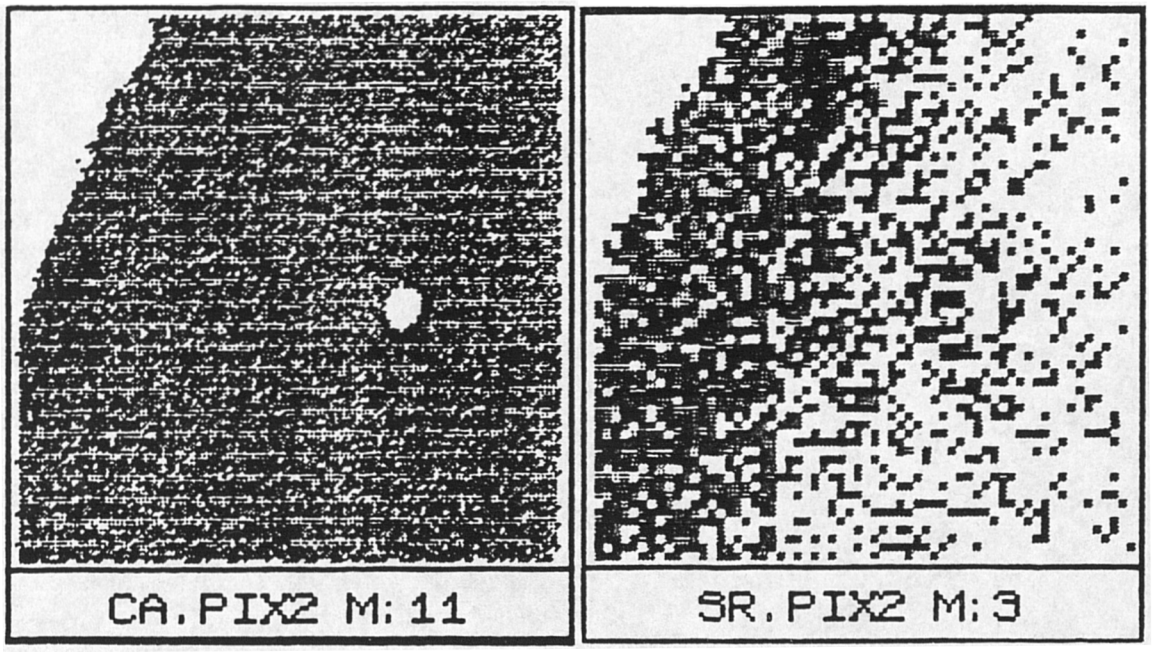

cortical edge could be seen more clearly and confirmed this depth of penetration. Moreover, strontium was found to be slightly concentrated around a pore structure in the cortex though it was not observed to fill this structure.

These PIXE data confirmed (a) the 100 ppm strontium solution as the more appropriate concentration to use, and (b) the effective barrier imposed on the transverse sections of experimental bone slices by cellulose acetate, by revealing distribution profiles of strontium more typically found for many trace elements in exhumed bone than those illustrated in the earlier experimental series (figure 6.29b).

With this in consideration, the effect of pH on strontium uptake into bone was explored in the experimental series III.

6.2.5 Summary.

These studies have demonstrated the tremendous potential of strontium uptake into bone, with up to 78 % of the strontium available in a saturated solution apparently being taken up into bone. Strontium was readily taken up into both whole and ashed bone material, and much of the data suggested that the predominant mechanism of uptake for each was heterionic exchange with calcium and surface adsorption, respectively.

The pattern of uptake over time was similar in solutions of widely ranging strontium concentration. Uptake was initially rapid and typically followed a classic 'U'-shaped cross-cortical profile with elevated levels at the cortical edges i.e. around the diffusion interfaces. With time, both quantitative and qualitative data suggested that the rate of uptake declined and at the same time the cross-cortical distribution of strontium shifted, or redistributed to form a relatively level profile. This was not simply a saturation effect as demonstrated by the similarity in temporal trends in bone immersed in 100 ppm solutions with that immersed in saturated solutions.

6.3 The Effect of pH on Uptake: Series III.

This section solely comprises the Immersion Series III experiments. Here, the immersion procedure had been sufficiently refined to include effective buffering of immersing solutions and the coating of transverse sections with cellulose acetate. The variables in experimental procedure here included the strontium concentration of the immersing solution (ranging from 5ppm to 139,000ppm (1M) solution), the duration of immersion and, naturally, the parameter under investigation - pH.

6.3.1 Analysis of Solutions.

Problems were encountered with the measurement of strontium and calcium in post-immersion solutions by spectrophotometric methods for the reasons outlined earlier: the interference of sodium in the alkali component of the buffer mix. Thus any measurements taken were interpreted tentatively.

Strontium and calcium levels in immersing solutions were measured after 2 weeks immersion of whole bone in 1M strontium solution, buffered at pH 4, 7 and 10, and compared to those obtained in control buffered solutions of pure water. These are shown in table 6.9, and can be found in Appendix IIc (control immersions) and Appendix IId (strontium immersions).

In all cases, the concentration of calcium released into solution was found to increase with increasing acidity, as the inorganic matrix of the bone was dissolved. Calcium released into solution was higher in the presence of strontium, confirming earlier observations (sub-section 6.2.1.2) and indicating potential heterionic exchange of the two elements.

Strontium measurements indicated an increased uptake into bone in more alkaline conditions, since the remaining strontium in solution was lowest for this pH. However, taking the original concentration into account (1M or approximately 139,000 ppm), all measured strontium levels after immersion were very low in comparison. Certainly the masking effect of sodium in pH 7 and more thoroughly in pH 10 solutions would result in lower readings for both strontium and calcium. However, in an attempt to circumvent such interference problems, strontium/calcium ratios in solution were examined and found to be lowest in the more acidic immersions,

perhaps indicating a relative uptake (removal from solution) and loss (addition in solution) of strontium and calcium, respectively. This might suggest that acidic conditions promote the heterionic exchange of calcium and strontium in bone.

Table 6.9: Calcium and strontium concentrations in immersing solutions containing whole bone for 2 weeks at variable pH.

Immersing solution	pH of immersion	[Calcium] ppm	[Strontium] ppm	Sr/Ca ratio
Buffered pure water	4	60	9	0.15
	7	6	5	0.83
	10	0	0	0
1M Strontium	4	189	639	3.38
	4	166	600	3.61
	7	37	602	16.27
	7	44	550	12.50
	10	2	230	115.00
	10	2	185	92.50

6.3.2 Analysis of Bone.

6.3.2.1 Whole bone analysis: XRF.

Table 6.10 shows the strontium/calcium ratios measured in whole bone samples immersed for 2 weeks in molar strontium solutions (refer to Appendix IId).

All strontium/calcium ratios were very similar, but maximum and minimum values were observed at pH 7 and pH 4, respectively. Thus, on the basis of quantitative data for whole bone samples using XRF analysis, strontium uptake was apparently favoured under neutral-alkaline conditions.

Table 6.10: Strontium/calcium ratios for whole bone immersed in molar strontium solution for 2 weeks at variable pH.

pH of immersion	% CaO	% P_2O_5	Sr (ppm)	Sr/Ca Ratio
4	48.98	43.97	13301	0.038
4	51.17	42.36	15158	0.041
6	49.22	31.02	16002	0.046
7	50.58	42.70	17849	0.049
7	52.61	42.76	21252	0.057
8	51.53	34.96	17539	0.048
10	50.03	43.03	17430	0.049
10	52.83	40.02	17647	0.047
SARM-32 std	55.13	37.63	4687	0.009

6.3.2.2 Micro-analysis of bone: EPMA.

(a) **Qualitative analysis.**

Strontium was found to penetrate the whole cortical width after 2 weeks immersion whether present in solution in high concentrations (1 Molar, for example), or in solutions as weak as 5ppm (figure 6.33). Cross-cortical distribution profiles predictably revealed that the extent of uptake increased with the concentration of the immersing solution. Moreover, a 'U'-shaped distribution profile (i.e. more pronounced at the cortical edges) became increasingly evident as the strontium concentration in immersing solutions increased for corresponding periods of exposure. A similar pattern in the distribution of calcium, and to some extent phosphorus, was observed at the cortical edges: the degree of strontium uptake in these regions appeared to be related to the degree of calcium decline.

This comparison of uptake in bone immersed in varying concentrations of strontium solution was useful in that it reinforced the patterns of uptake observed over time as a *temporal* phenomenon rather than one of strontium saturation, since the cross-

Figure 6.33: The cross-cortical distribution profiles of strontium against its concentration in the immersing solution. Microscope operated at mag. x45.

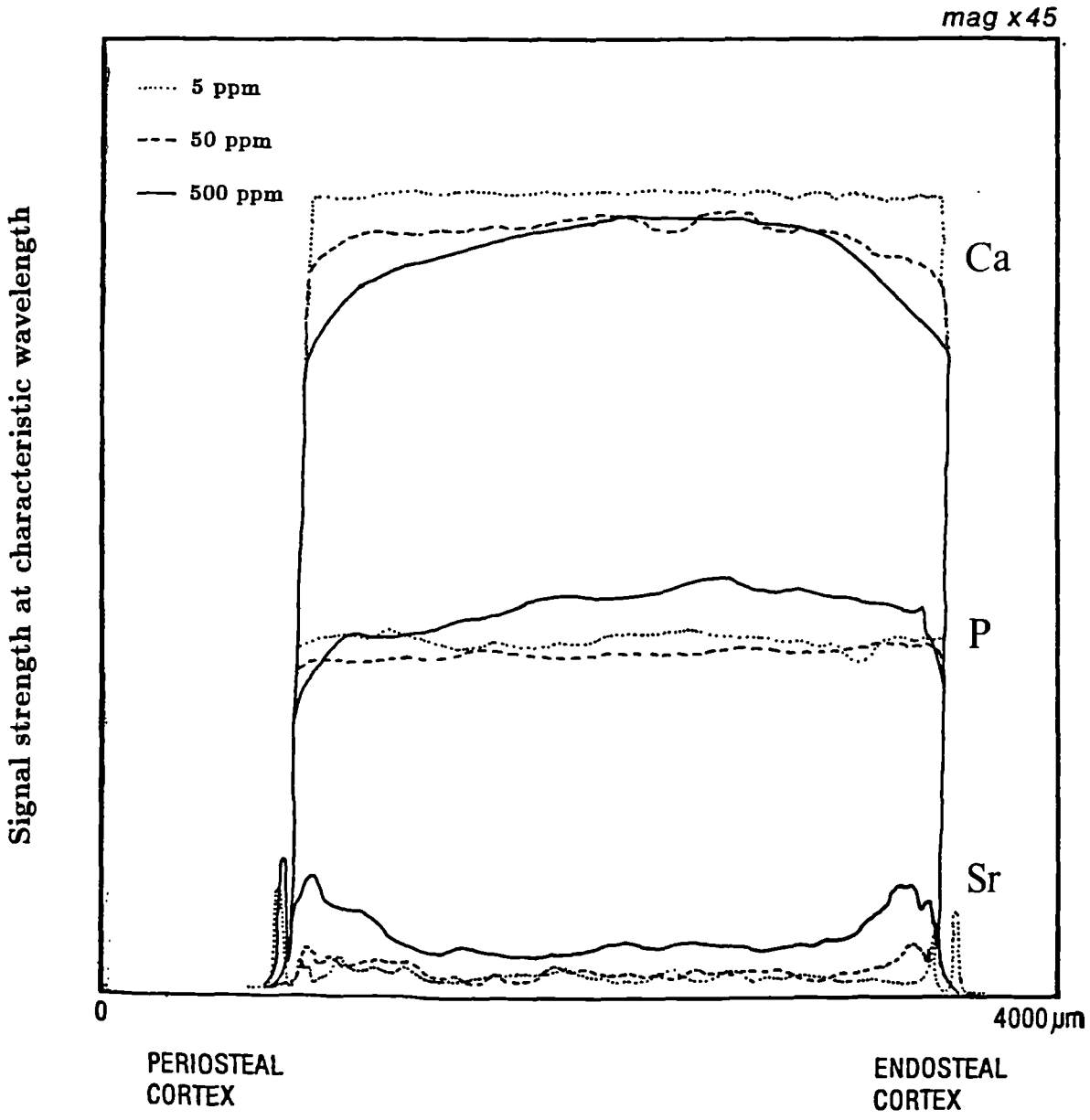

cortical distribution pattern against concentration was different to that against time (refer to sub-section 6.2.2.2).

Experiments examining the relationship of uptake with pH (Series III) used two concentrations of strontium in the immersing solution: 1 molar and 100 ppm. A distinction was made for each when discussing the respective data.

(1) Bone immersed in 1M strontium solution for 2 weeks.

The effect of pH on strontium uptake was examined initially by immersing whole bone in a molar solution of strontium nitrate for a two week period. Solutions were adjusted to pH 4, 6, 7 ,8 or 10. Subsequent analysis found strontium distributed across the full cortical width for all pH regimes. Examination of this full width at low magnification, however, was not able to distinguish any clear differences in uptake patterns across pH (figure 6.34). This was undoubtedly due to the high strontium concentration of the immersing solution. Such availability of strontium enabled a rapid uptake into the bone so that any patterns in strontium behaviour against pH were not evident at the full cross-cortical level. All three pH conditions revealed bone with a fairly even distribution of strontium across the whole cortical width, with elevations at the cortical edges. This classic 'U'-shaped distribution is illustrated in figure 6.35 for bone immersed at pH4.

At higher magnification (x1000) of the periosteal cortex, trends in uptake against pH began to emerge (figure 6.36). Uptake appeared to be promoted under conditions of acidity: strontium levels were highest in bone immersed at pH 4 and at pH 6. The lowest concentrations of strontium were found in pH 8 and pH 10. Thus, strontium concentration correlated with the pH of immersion: in descending order of concentration - pH4, pH6, pH7, pH10 and pH8, thereby following a general trend of uptake increasing with acidity. Strontium peaks were observed in areas just exterior to the cortical surface in bone immersed in pH 4, 6 and 8 solutions: this probably represented surface adsorption of strontium , perhaps to remnant soft tissue adhering to the surface. However, one might have expected this soft tissue to have decayed under more acidic conditions.

This region of bone immersed at pH 4 is shown in figure 6.37(b) as an electron micrograph. There were no obvious signs of remnant organic tissue at the surface.

Figure 6.34: Cross-cortical distribution profiles of strontium in whole bone against pH of immersion. Microscope operated at Mag. x45.

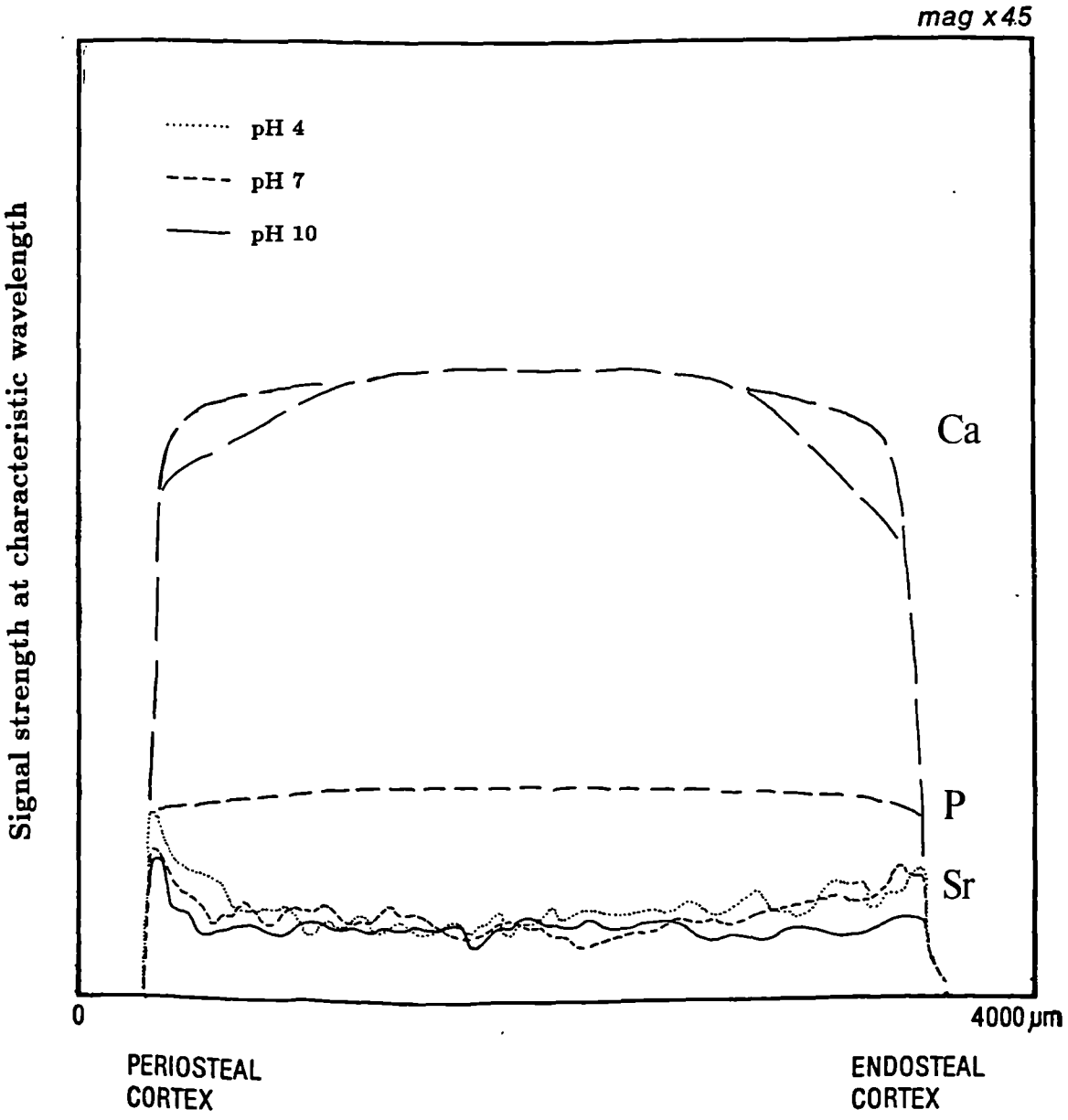

Figure 6.35: Cross-cortical distribution profiles of strontium, calcium and phosphorus in whole bone immersed at pH 4. Microscope operated at mag.x45.

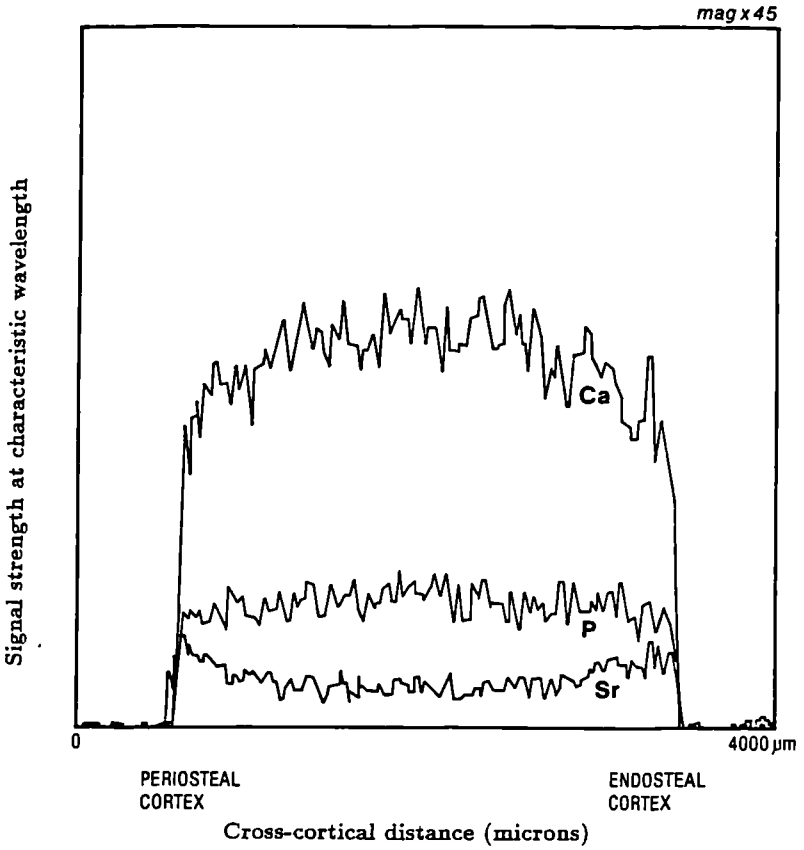

It is possible that the strontium peaks observed near the sample surface in figure 6.36 may have been excess strontium filling the gap at the bone-resin interface as the bone was found to invariably shrink in the resin. On more thorough examination of this region in pH 4 bone, the line profile at x250 magnification (figure 6.38) showed calcium levels declining in the outer cortical region in correspondence to a similar rate of increase in strontium levels. It could be argued that this observation simply reflected changes in the relative proportional signal of each element, as opposed to any heterionic exchange. However, phosphorus (phosphate) levels remained fairly constant across the cortex, apparently unaffected by the increasing strontium signal, thereby propounding the existence of an inverse correlation between strontium and calcium.

Figure 6.36: Strontium distribution profiles in the periosteal cortex of whole bone against pH of immersion. Microscope operated at mag. x1000.

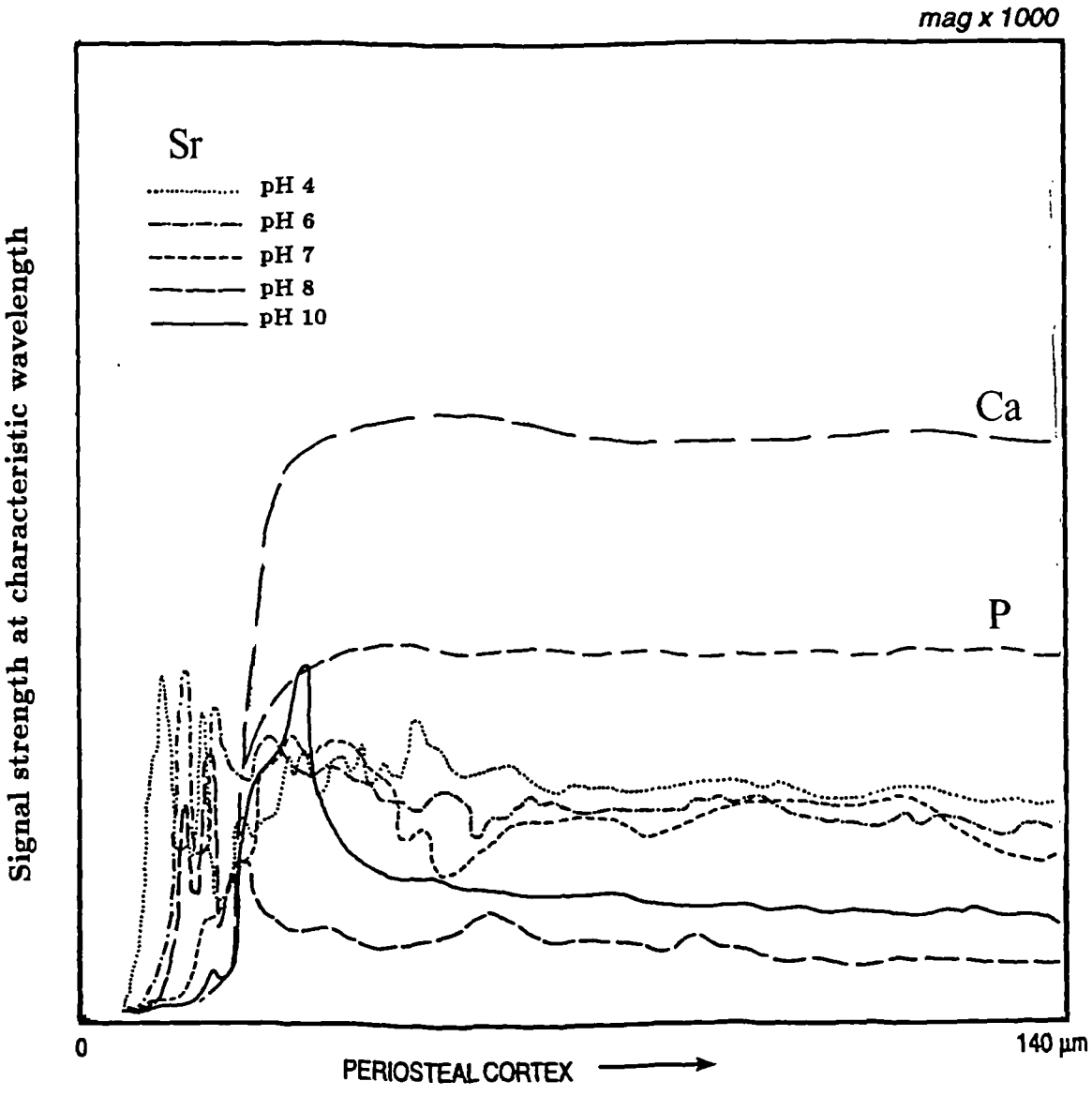

Horizontal distance of scan (microns)

Figure 6.37: Electron micrographs of bone immersed in strontium solution at pH 4 showing (a) the location of line-profiles across the full cortical-width, and (b) a magnified area of the periosteal cortical edge shown as a line-profile in figure 6.38.

(a)

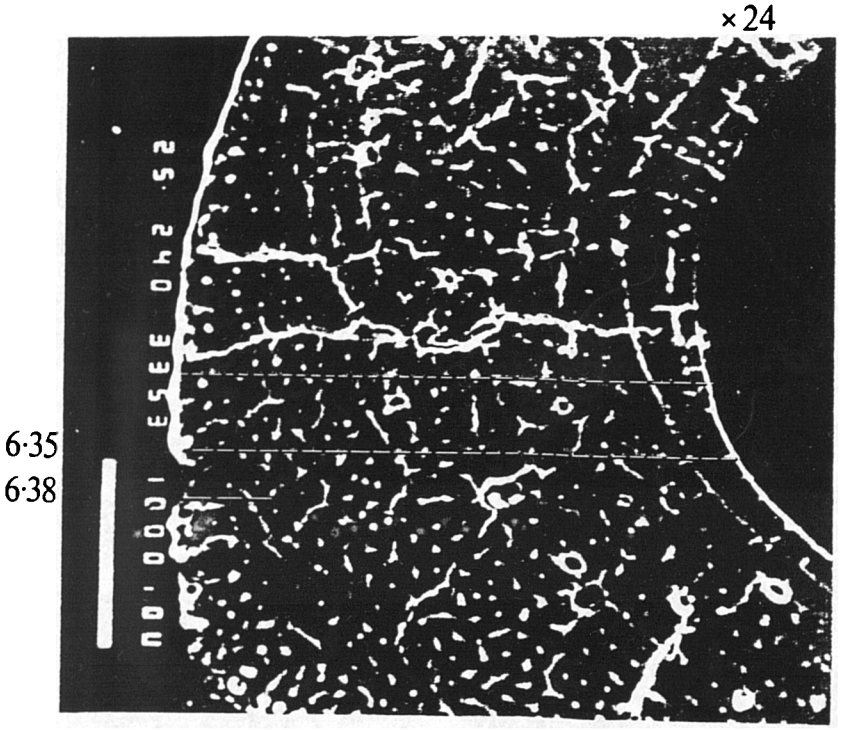

(b)

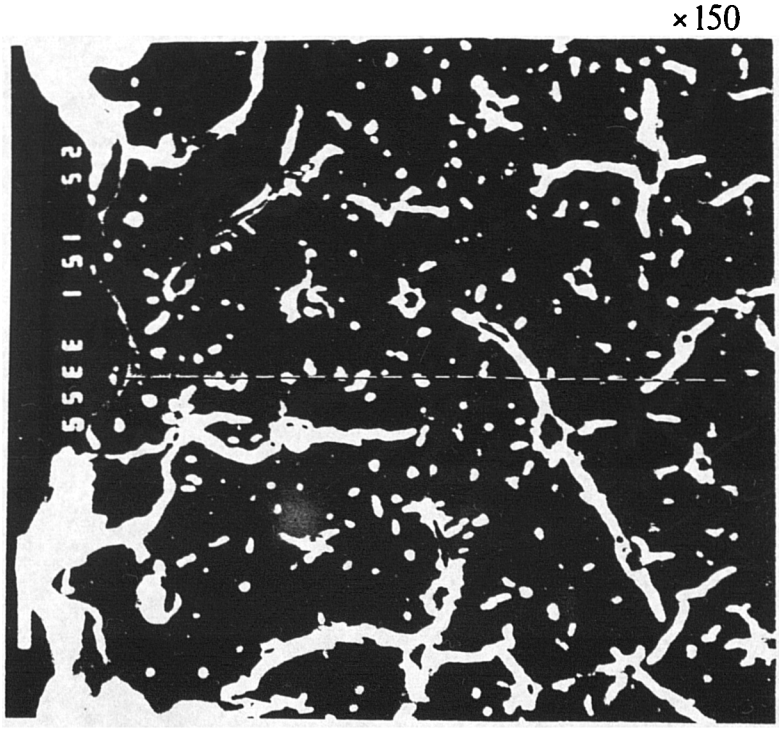

Figure 6.38: Strontium distribution in the periosteal cortex of bone immersed at pH 4. Microscope operated at mag. x250.

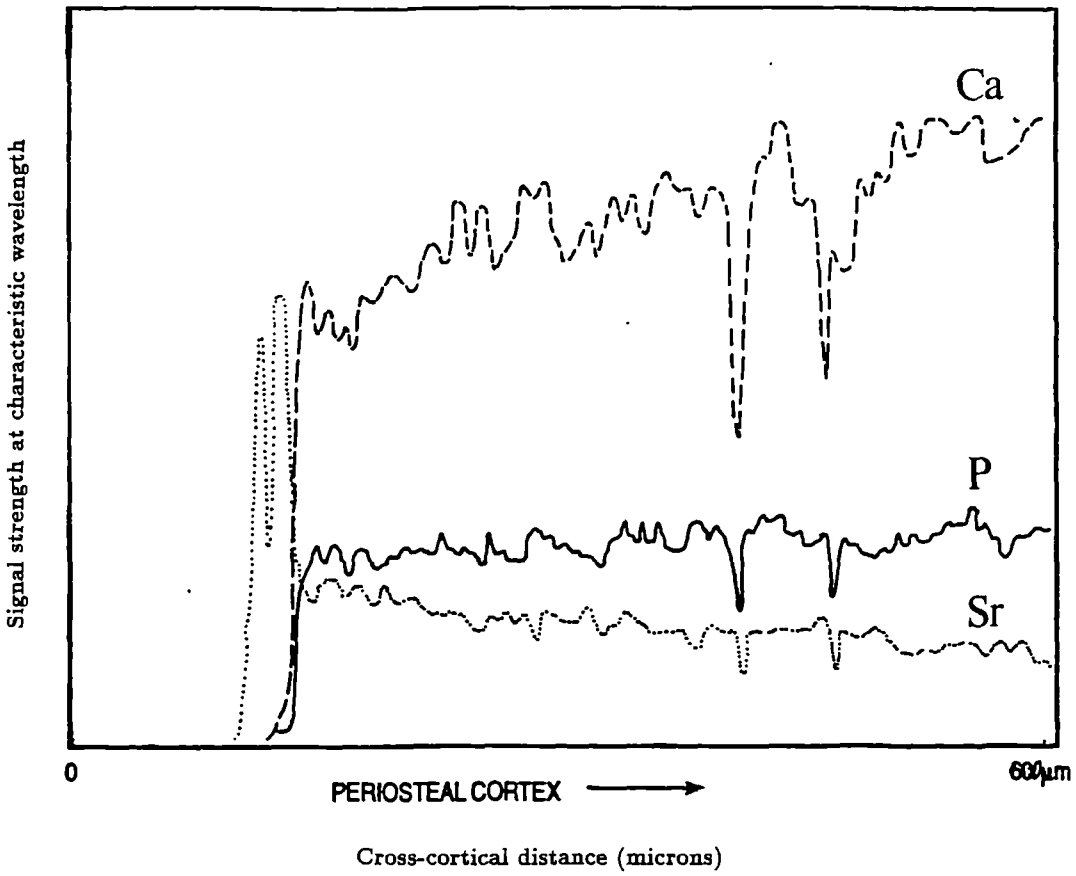

The electron micrograph shown in figure 6.37(a) shows the locations of the cross-cortical line-profiles shown in figure 6.34 and the magnified area of the cortical edge in figure 6.38 in whole bone immersed at pH 4.

In addition to indications of direct interaction with the inorganic matrix, strontium was also found to fill natural pores/voids in the cortical microstructure: figure 6.39 shows three osteonal systems in the mid-cortical tissue of whole bone immersed at pH 4, with strontium occupying the Haversian canal microstructures.

(2) Bone immersed in 100 ppm strontium solution for 12 weeks.

On examination of whole bone samples (one sample representing each pH) im-

Figure 6.39: EPMA digimap of mid-cortical region of whole bone immersed at pH 4 showing strontium pore-filling. Microscope operated at mag. x750.

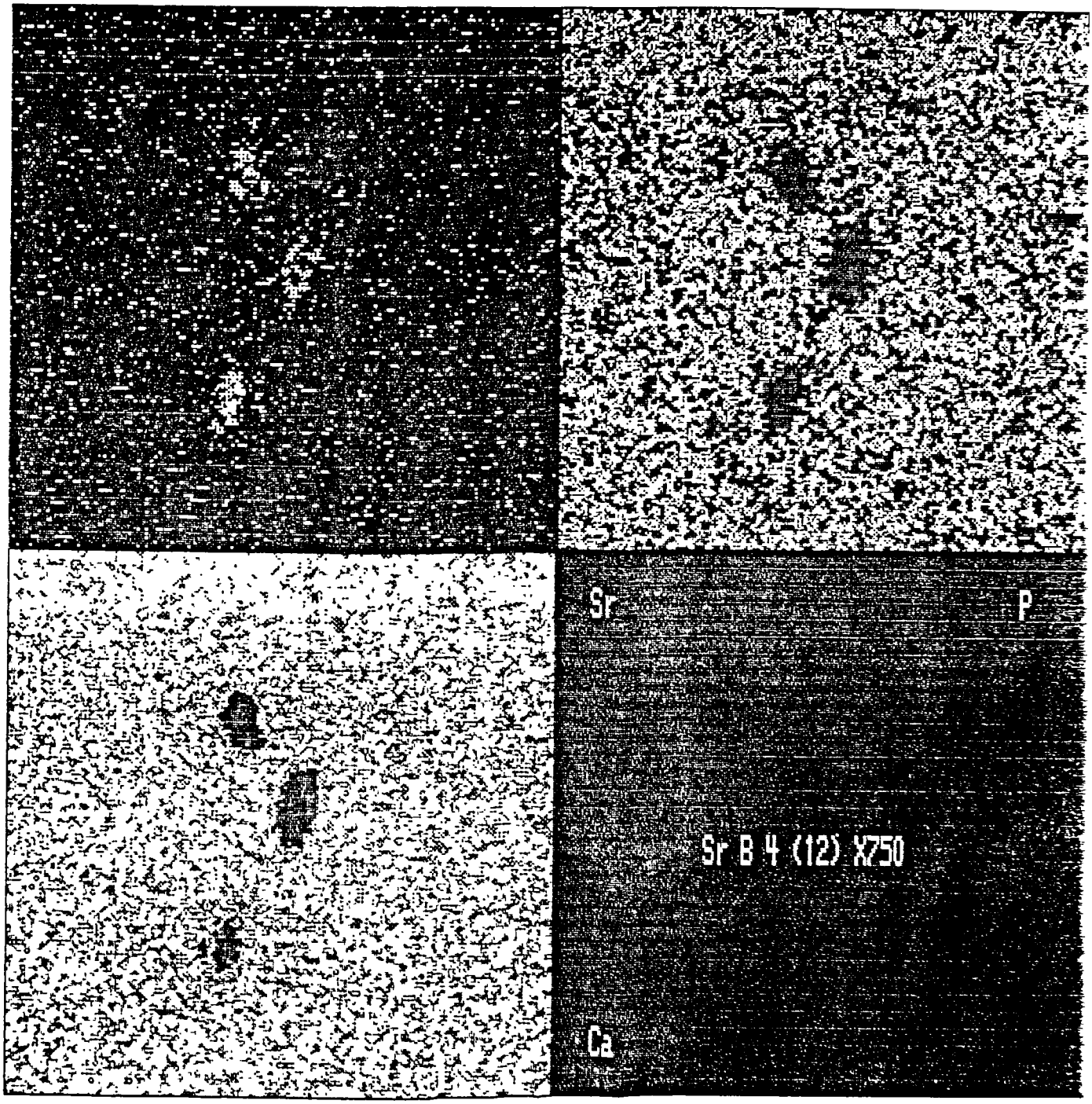

mersed in less concentrated strontium nitrate solutions (100 ppm) for 12 weeks, a similar pattern of uptake across pH was observed. Figure 6.40 shows the periosteal cortical region of whole bone.

NOTE: The y-axis scale for each respective element was maintained so that strontium distributions could be directly compared across bone samples immersed in different concentrations of strontium solution. Strontium levels here were lower than those immersed in molar solutions, and patterns in uptake were consequently less easily distinguishable. Figure 6.40a shows profiles traced directly from original datasheets, but in order to clarify any uptake patterns, these images were processed more extensively than earlier line-profiles had required in order to smooth out the profiles (as shown in figure 6.40b). Processing simply consisted of taking average values of the peaks at each point. As a consequence, some of the detail in distribution was lost.

With this procedure, the processed image was able to confirm earlier observations in more concentrated strontium immersions: again, strontium uptake was more pronounced at pH 4 and declined with increasing alkalinity.

(b) **Quantitative analysis.**

Quantitative analysis using EPMA was carried out on bone immersed in molar strontium solutions for 2 weeks.

Calcium-phosphorus-strontium ratios were examined more closely by quantitative analysis of the inner, mid and outer cortices of samples representing each pH. Three different areas were analysed in each cortical region: all quantitative values are shown in table 6.11 and their averages plotted in figures 6.41(a) and (b).

Calcium:phosphate ratios were highest in the mid-cortex for all samples. This suggested that calcium was less prone to dissolution or, indeed, strontium 'attack' in the medullary cortex, therefore remaining relatively uncompromised. The range of calcium:phosphate ratio values was greatest for endosteal bone, demonstrating the differential decay of this trabecular tissue with pH of immersion. In contrast, the dense cortical tissue of periosteal bone was less vulnerable to the actions of the immersing solution.

Figure 6.40: Distribution profiles of strontium in the periosteal cortex of whole bone against pH of immersion. (a) original images, (b) processed images.

(a)

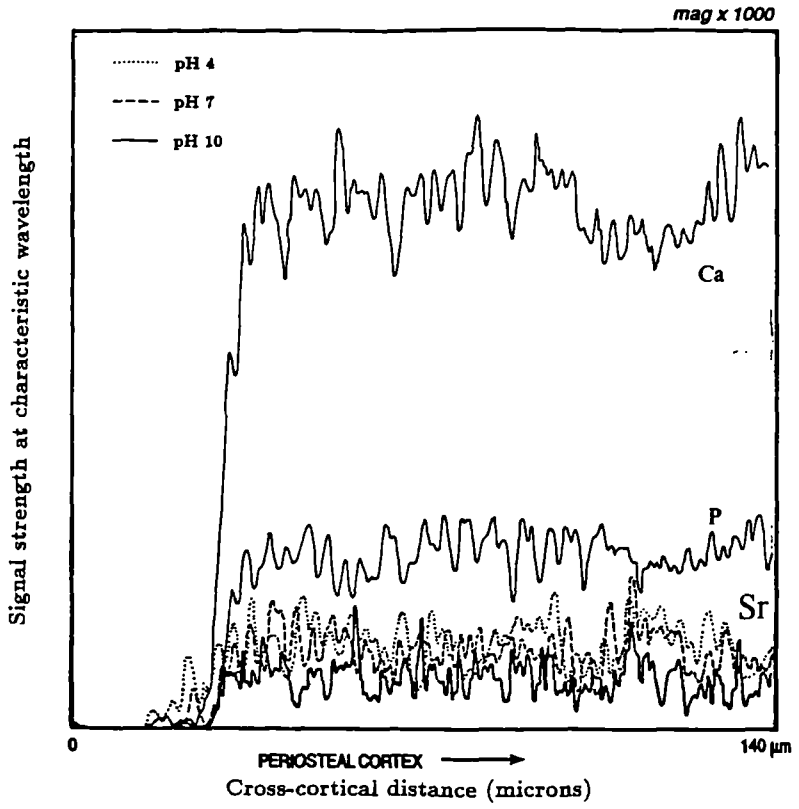

(b)

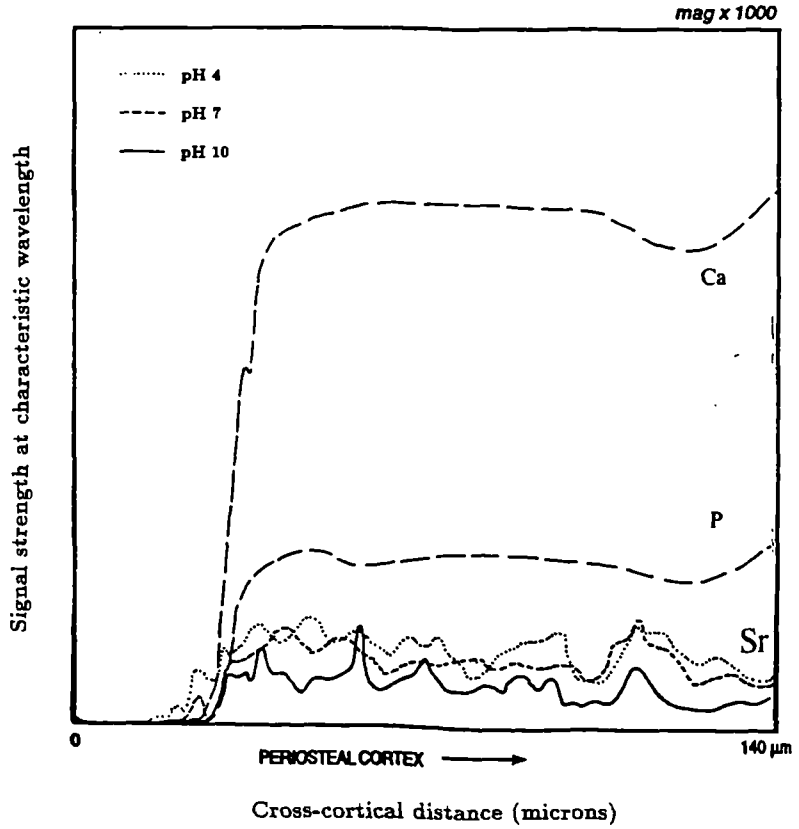

Table 6.11: Quantitative analysis of the major cortical regions of whole bone samples immersed in molar strontium solutions of varying pH for 2 weeks.

pH of immersion	Cortical region	% Ca	% P	% Sr	Ca/P	Sr/Ca
pH 4	P	17.5	9.4	10.0	1.86	0.571
		8.8	4.0	5.3	2.20	0.602
		17.8	9.9	10.3	1.80	0.579
	M	31.2	12.7	5.6	2.46	0.179
		31.0	12.8	6.2	2.42	0.200
		27.8	11.7	5.6	2.38	0.201
	E	16.2	11.8	19.2	1.37	1.185
		21.7	12.4	15.2	1.75	0.701
		19.8	11.6	15.0	1.71	0.758
pH 7	P	27.7	13.9	14.4	1.99	0.520
		26.9	12.5	11.8	2.15	0.439
		32.0	14.4	9.8	2.22	0.306
	M	31.3	13.5	5.8	2.32	0.185
		32.1	13.6	6.2	2.36	0.193
		30.4	12.8	6.8	2.38	0.224
	E	26.8	12.7	11.6	2.11	0.433
		29.2	13.9	11.4	2.10	0.390
		28.9	13.4	9.3	2.16	0.322
pH 10	P	31.8	13.8	10.8	2.30	0.340
		31.5	14.1	12.1	2.09	0.384
		29.9	14.0	12.8	2.14	0.428
	M	39.8	15.9	4.4	2.50	0.111
		40.2	15.9	4.7	2.53	0.117
		37.1	13.2	3.6	2.81	0.097
	E	37.4	15.3	9.0	2.44	0.241
		32.6	14.5	10.8	2.25	0.331
		33.3	14.6	8.9	2.28	0.267

where P = periosteal cortex, M = mid-cortex, E = endosteal cortex.

Values were measured as % oxides and subsequently corrected for % element for elemental ratio calculations.

Figure 6.41 (a) Calcium:phosphate ratios and (b) strontium:calcium ratios, measured by EPMA, in the major cortical regions of bone immersed in molar strontium solutions of varying pH for 2 weeks.

(a) Calcium:phosphate ratios.

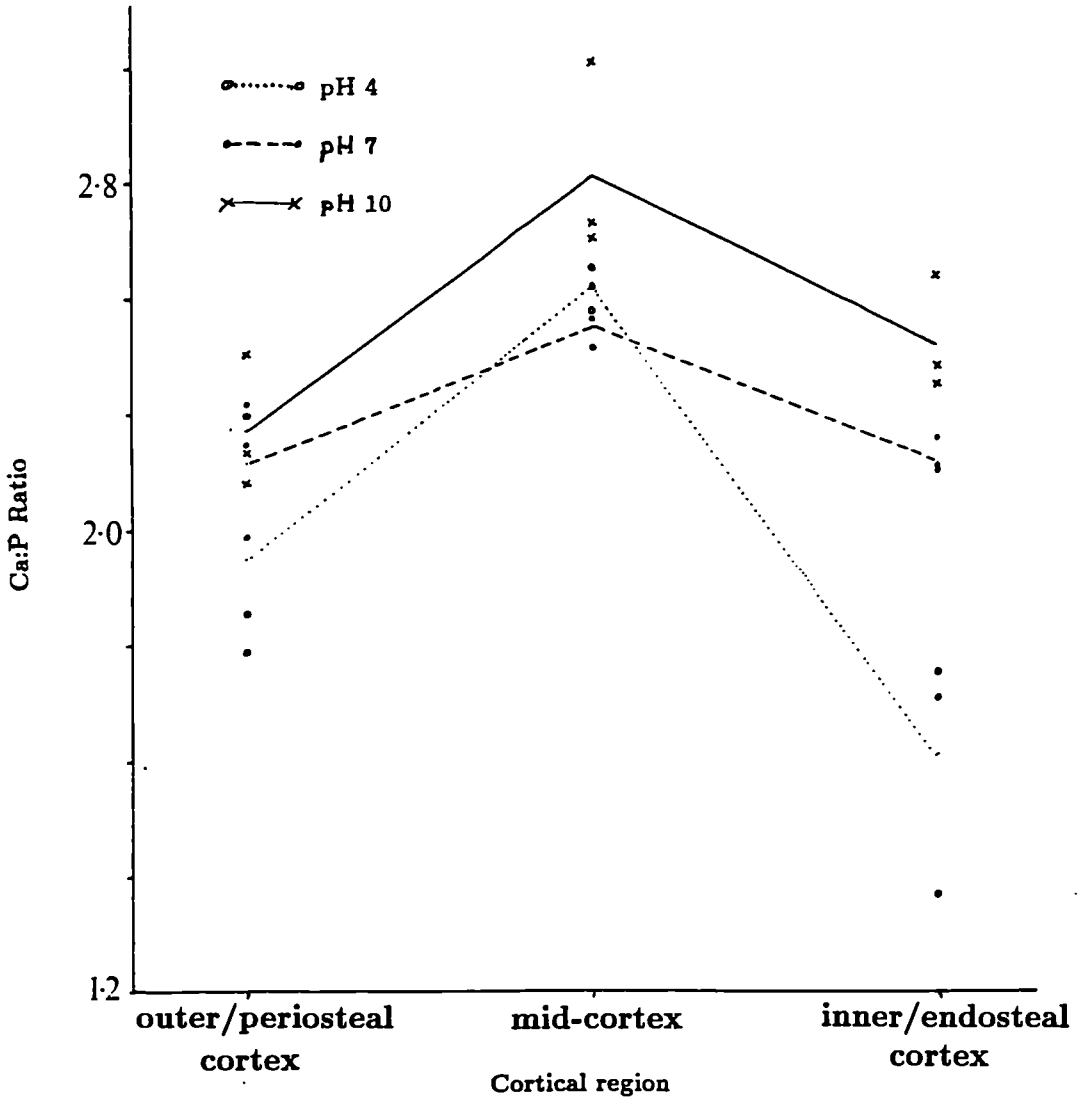

Figure 6.41 cont.

(b) Strontium:calcium ratios.

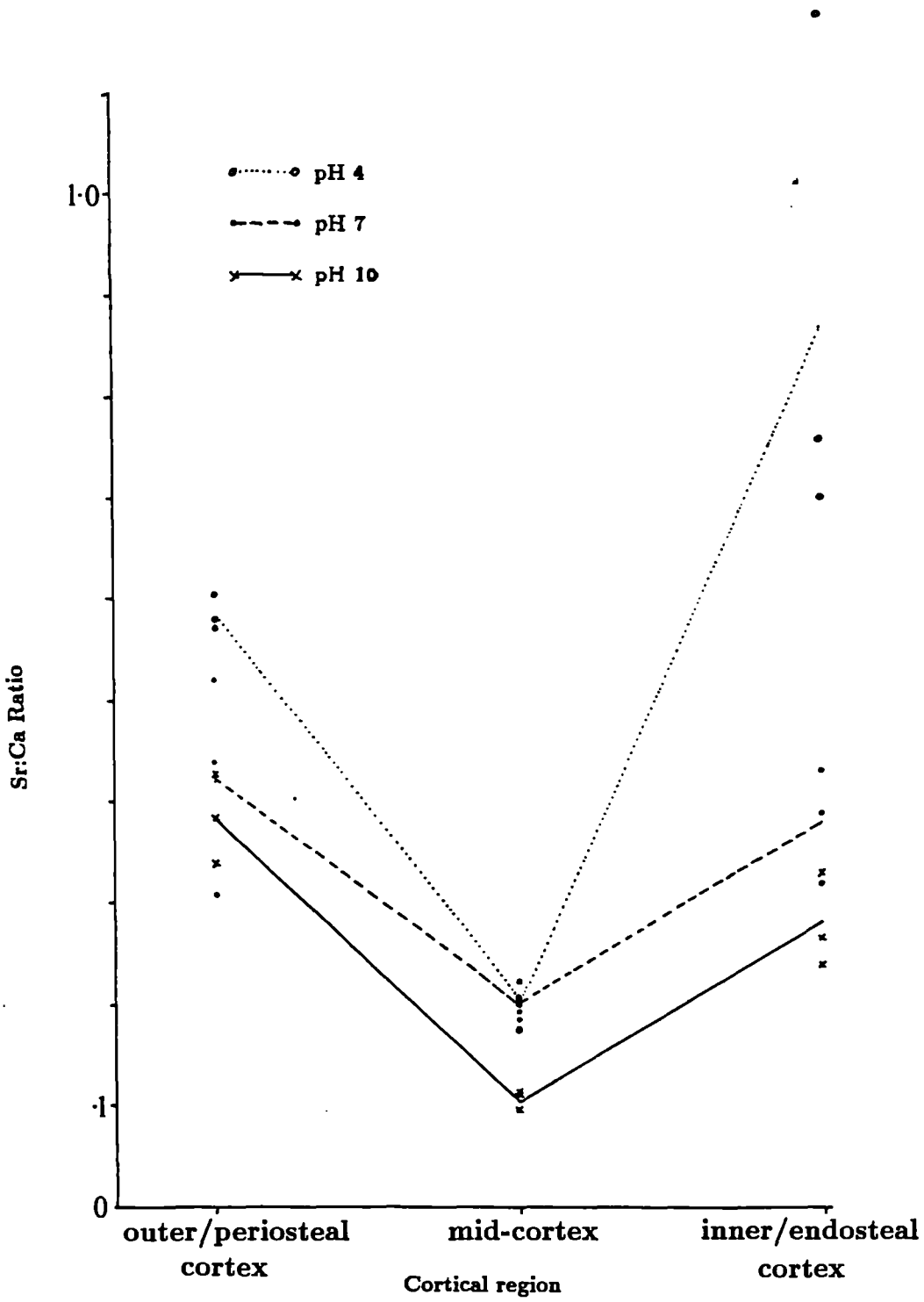

Strontium:calcium ratios followed a 'U'-shaped profile and were generally the mirror image of their respective calcium:phosphate profiles. Bone immersed in pH 4 solutions possessed the highest strontium:calcium ratios and the lowest calcium:phosphate ratios. Conversely, bone immersed at pH 10 possessed the opposite pattern in ratio values. These observations reflected the variable stability of the hydroxyapatite matrix under changing pH conditions.

Strontium:phosphate ratios followed the opposite pattern to calcium:phosphate ratios i.e. highest in the outer cortex, lowest in the mid-cortex for pH 7 and pH 10, whilst being higher in the inner cortex for pH 4. Clearly, bone was behaving differently in more acidic conditions compared to neutral-alkaline conditions.

Since strontium:calcium ratios are used to derive palaeodietary information, this ratio was examined more closely. Strontium:calcium levels followed the same trend as strontium:phosphate. Since dietary analysis examines the strontium:calcium value representative of whole bone rather than regional values, average values were noted for each pH, and ratios were found to increase with the acidity of immersion:

pH of immersion	Average Sr:Ca
4	0.5529
7	0.3347
10	0.2603

A similar methodological procedure of quantitative analysis was carried out for cross-comparison on whole bone immersed in a 500 ppm strontium solution at pH 7. Table 6.12 shows the data for each major cortical region as before.

Again, a 'U'-shaped profile was apparent, with slightly higher values in the periosteal cortex. Thus, a similar cross-cortical pattern of calcium, phosphorus and strontium distribution was observed in bone immersed in variable concentrations of strontium solution.

Table 6.12: Quantitative analysis of the major cortical regions of whole bone immersed in 500 ppm strontium solution at pH 7 for 2 weeks.

Cortical region	% Ca	% P	% Sr	Ca/P	Sr/Ca
Periosteal cortex	31.5	13.1	5.7	2.40	0.181
	32.6	12.4	5.2	2.63	0.160
	27.5	10.9	5.0	2.52	0.182
Medullary cortex	37.2	14.2	1.6	2.62	0.043
	30.1	10.7	1.2	2.81	0.040
	33.6	11.9	1.0	2.82	0.030
Endosteal cortex	30.5	13.1	5.1	2.33	0.167
	31.8	12.9	4.8	2.47	0.151
	28.4	10.9	5.0	2.61	0.176

Values were measured as % oxides and subsequently corrected for % elements

6.3.3 Summary.

Quantitative and qualitative data examining the pattern of strontium uptake against pH of immersion were not always in agreement. Quantitative analysis of post-immersion solutions was hindered to variable degrees by chemical interferences in buffered solutions. This may account for any discrepancies in uptake patterns revealed on the basis of solution analysis compared to data collected from bone analyses using different analytical techniques, although strontium:calcium ratio values in solution did generally concur with micro-analyses of the bone.

Quantitative XRF analysis of bone was not in agreement with EPMA data. The former indicated an increased strontium uptake under more alkaline conditions, while the latter suggested that uptake was promoted in more acidic conditions. Clearly, analyses based on the total elemental content of the bone as a whole

differed from those that examined locational/cross-cortical distributions in more specific areas of bone.

However, both quantitative and qualitative data obtained by EPMA for bone immersed in strontium solutions of varying concentration and pH confirmed that strontium levels were highest in bone at pH 4, and showed a decrease with increasing alkalinity. It was clear that the degree of strontium uptake into bone was closely correlated with the relative stability of the hydroxyapatite matrix, thereby implicating strontium interaction with the inorganic component as the mechanism of uptake of this element into bone.

The next section explored this implication in more detail.

6.4 Uptake against Organic:Inorganic Ratio: Series III.

Quantitative analysis of bone using XRF and qualitative analysis using EPMA were both carried out to investigate any trends in strontium uptake with the bone's organic/inorganic content.

Quantitative analysis of immersing solutions by spectrophotometric means was not carried out here because of the obvious interference complications encountered with solutions similarly buffered in this experimental series.

6.4.1 Analysis of Bone.

6.4.1.1 Total elemental analysis: XRF.

Table 6.13 shows the strontium/calcium ratios measured in whole, hydrazine-treated and ashed bone samples immersed in molar solutions of strontium for two weeks at variable pH (up to 3 samples representing each condition). The log values of these ratios are also tabulated and are shown plotted in figure 6.42. The respective % oxide and ppm values for calcium, phosphorus and strontium are included in Appendix IIc for control immersions and Appendix IId for strontium immersions.

Table 6.13: Strontium/calcium ratios for bone samples of varying organic content immersed at different pH, measured by XRF analysis.

Immersion	Bone description	pH of immersion	Sr/Ca ratio (x 10^{-4}	log (Sr/Ca)
Buffered pure water	Whole	4	5.81	0.764
		7	6.56	0.817
		10	6.94	0.841
	Hydrazined	4	5.08	0.706
		7	5.64	0.751
		10	5.90	0.771
	Ashed	4	2.49	0.396
		7	3.39	0.530
		10	3.77	0.576
1 molar strontium	Whole	4	270	2.431
		4	300	2.477
		6	330	2.519
		7	350	2.544
		7	400	2.602
		8	340	2.531
		10	350	2.544
		10	330	2.519
	Hydrazined	4	280	2.447
		4	260	2.415
		4	250	2.398
		7	300	2.477
		7	320	2.505
		10	400	2.602
		10	340	2.531
	Ashed	4	380	2.580
		4	370	2.568
		4	390	2.591
		7	390	2.591
		7	450	2.653
		7	460	2.663
		10	440	2.643
		10	480	2.681
		10	450	2.653
Reference apatite SARM-32	Ashed powder	N/A	82	1.914

Figure 6.42: Log value of the strontium/calcium ratios, measured by XRF, for bone of varying organic content immersed in either control or strontium solutions at variable pH.

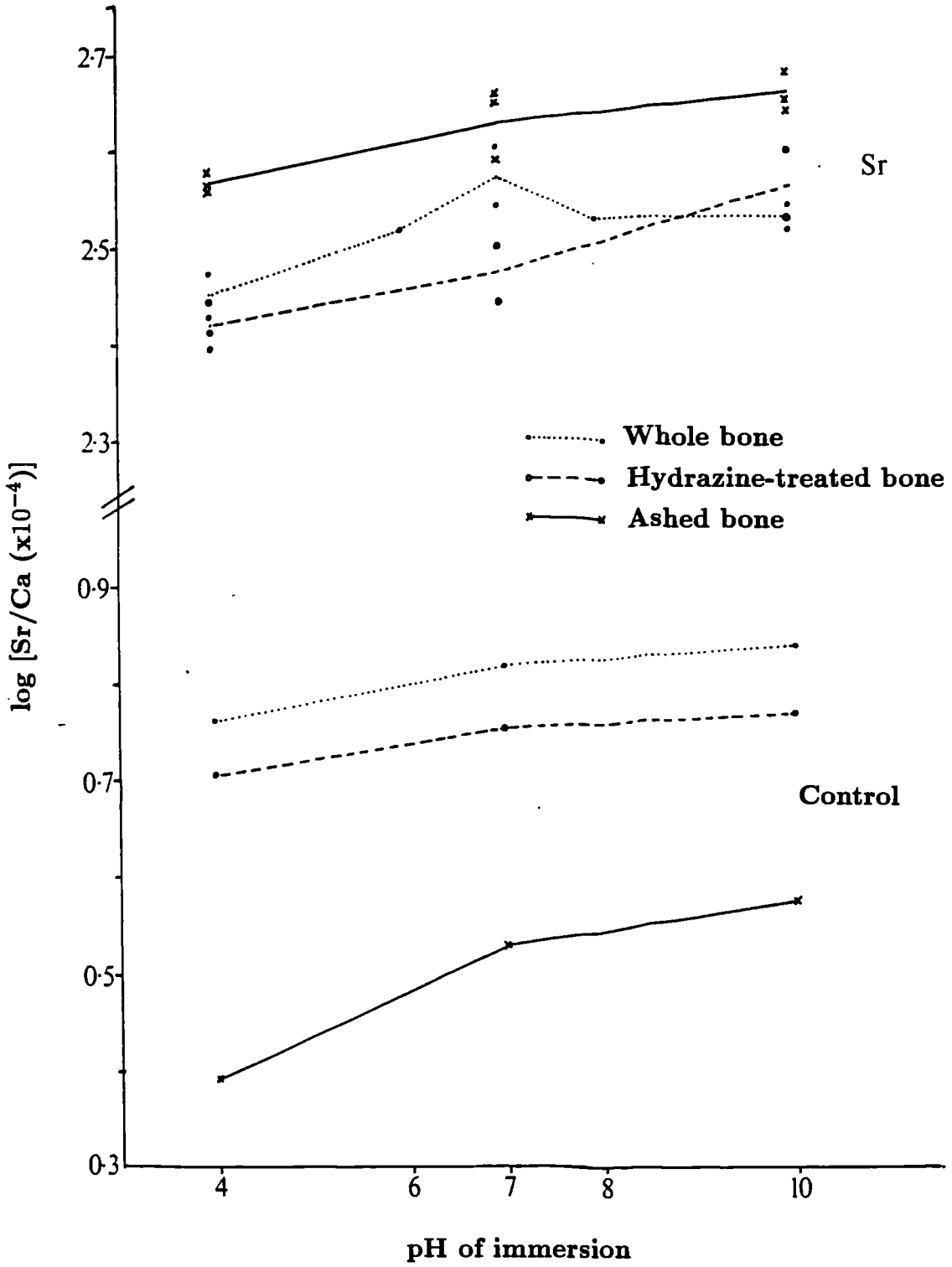

These values show that

(i) strontium/calcium ratios in all bone samples immersed in buffered water declined with the acidity of solution: this would suggest that the rate of loss of natural strontium in bone was greater than that of calcium. It might also suggest that intrinsic strontium (approximately 130 ppm in this ovine material) was preferentially leached from the bone.

(ii) ratios were lowest in ashed bone samples immersed in buffered water, due to the increased accessibility of the immersing solution through its porous structure and thus a heightened potential for elemental leaching from the exposed inorganic matrix.

(iii) strontium/calcium ratios were obviously much higher (two orders of magnitude) in bone immersed in strontium solutions compared to that in buffered water, indicating strontium uptake into the samples.

(iv) the pattern of strontium/calcium ratio against pH was similar for control and strontium immersions i.e. the ratio was observed to increase with increasing alkalinity.

(v) uptake was higher in ashed samples for all three pH regimes. At pH 4 and 7, the lowest ratios were those of hydrazine-treated bone, while at pH 10 values declined with increasing organic content. This might suggest that the relative role of inorganic and organic components in the mechanism of strontium uptake into bone is dependent on the environmental pH of reaction.

This possibility was explored in more detail by investigating elemental distributions in bone of varying organic content, exposed to strontium solutions, using micro-analysis (EPMA).

6.4.1.2 Micro-analysis of bone: EPMA.

Only qualitative analysis was carried out here in order to determine the relative roles of the organic and inorganic components, and thus establish a feasible mechanism for strontium-bone interaction. The effect of pH on the relative contribution of these components was explored.

The examination of cross-cortical distributions of strontium across the whole cortical width revealed no pattern of uptake against organic content for either samples immersed in molar or 100 ppm strontium solutions under any of the pH regimes. Figure 6.43 demonstrates this fact.

The following data presented refer to samples immersed for 12 weeks in 100 ppm strontium solutions.

Figure 6.44 demonstrates that under higher magnification of bone material immersed at pH 7 the calcium/strontium ratio was lower in ashed and hydrazine-treated bone samples than in whole bone. This reinforces the probability of strontium interaction with the inorganic matrix, incorporation effecting a lower calcium/strontium ratio. Strontium levels in hydrazine-treated bone at this pH were marginally higher than those in ashed bone, suggesting that any trends in strontium uptake were not solely attributable to the organic/inorganic ratio. The reason for the the large peak observed at the cortical edge of ashed bone is unclear.

Strontium uptake against pH was examined for hydrazine-treated and ashed bone respectively. Whereas whole bone samples examined in a similar way in the previous section (see figures 6.40 and 6.41(b)) revealed an increasing uptake with acidity, both hydrazine-treated and ashed bone demonstrated higher strontium levels in more alkaline conditions, as shown in figures 6.45 and 6.46, respectively.

Obversely, figures 6.47-49 examine the uptake of strontium into these bone samples under each pH regime. At pH 7 and 10, uptake was most pronounced in ashed bone material. At pH 4 this trend was not apparent and all bone samples appeared to possess similar strontium distribution profiles.

6.4.2 Summary.

The data presented here have reiterated the predominance of strontium interaction with the **inorganic** component of bone. The correlation of strontium and calcium data in both qualitative and quantitative form have confirmed the existence of heterionic exchange of the two elements as the main mechanism of strontium uptake into bone.

Figure 6.43: Cross-cortical distribution of strontium in bone of varying organic/inorganic ratio immersed in 1M strontium solution at pH 7. Microscope operated at mag. x45.

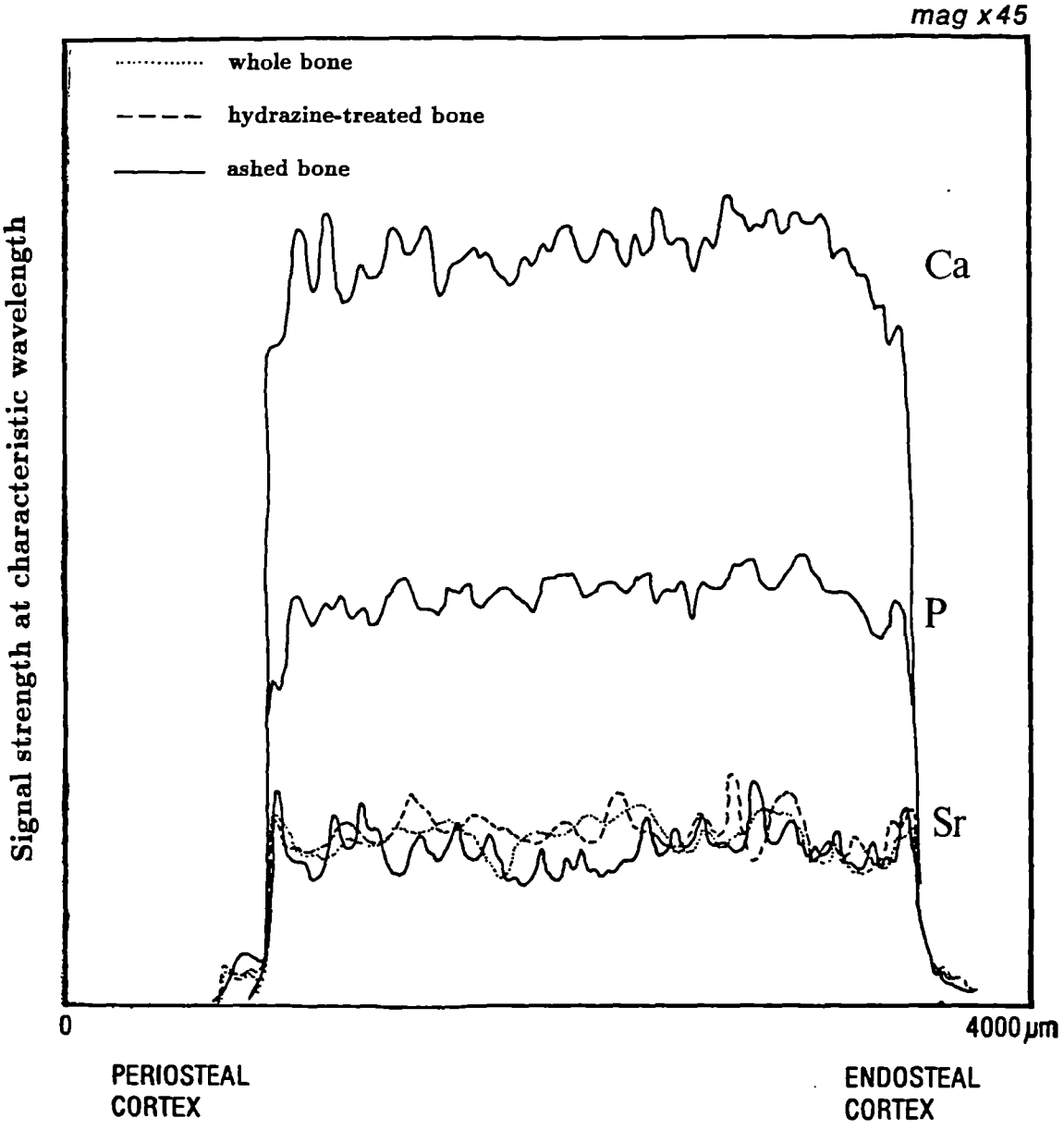

Figure 6.44: Calcium/Strontium Ratios in the Periosteal Cortex of Bone with Varying Organic:Inorganic Content Immersed at pH 7. Microscope operated at mag. x1000.

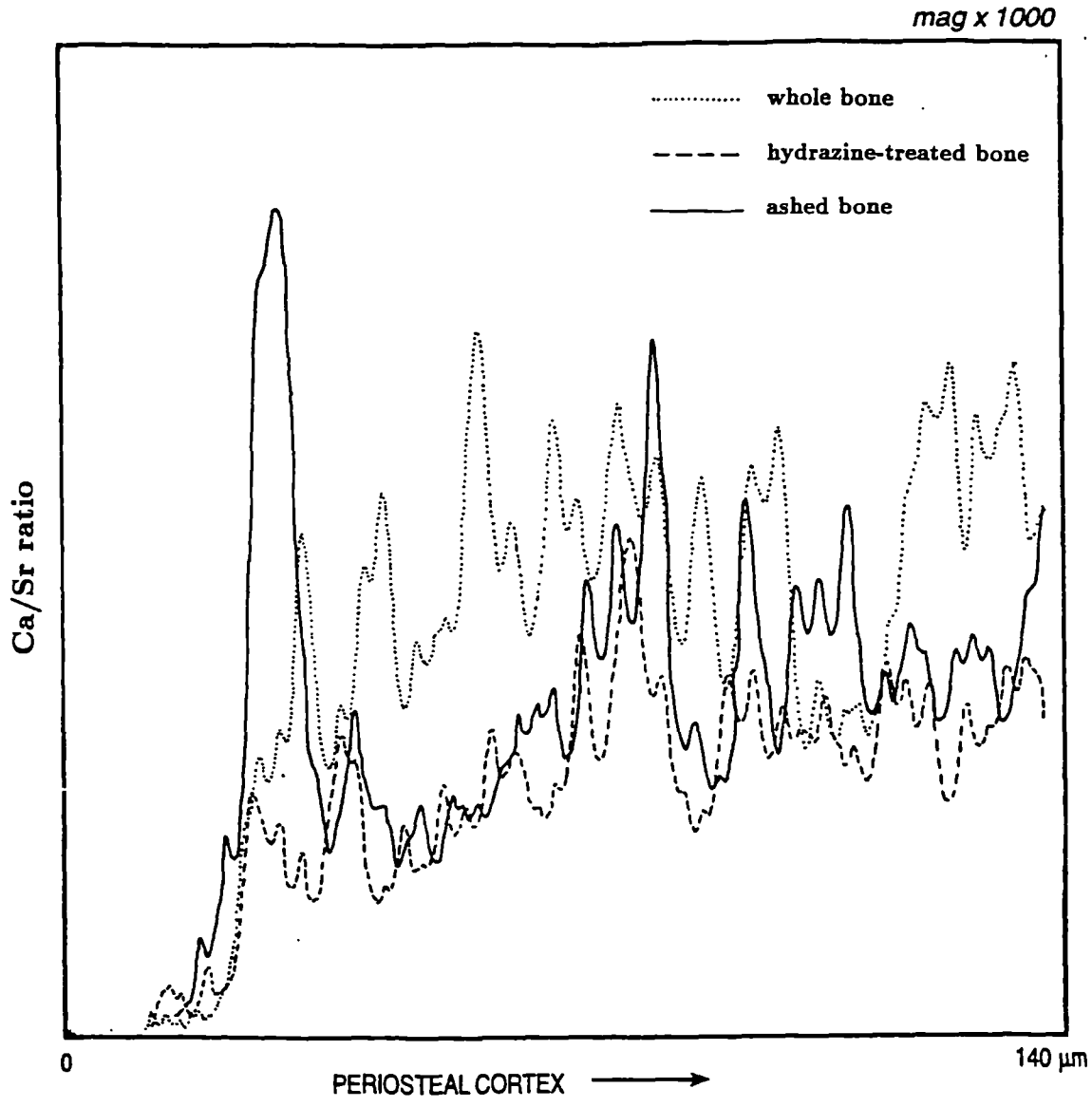

Figure 6.45: Strontium distributions in the periosteal cortex of hydrazine-treated bone immersed at variable pH. Microscope operated at mag. x1000.

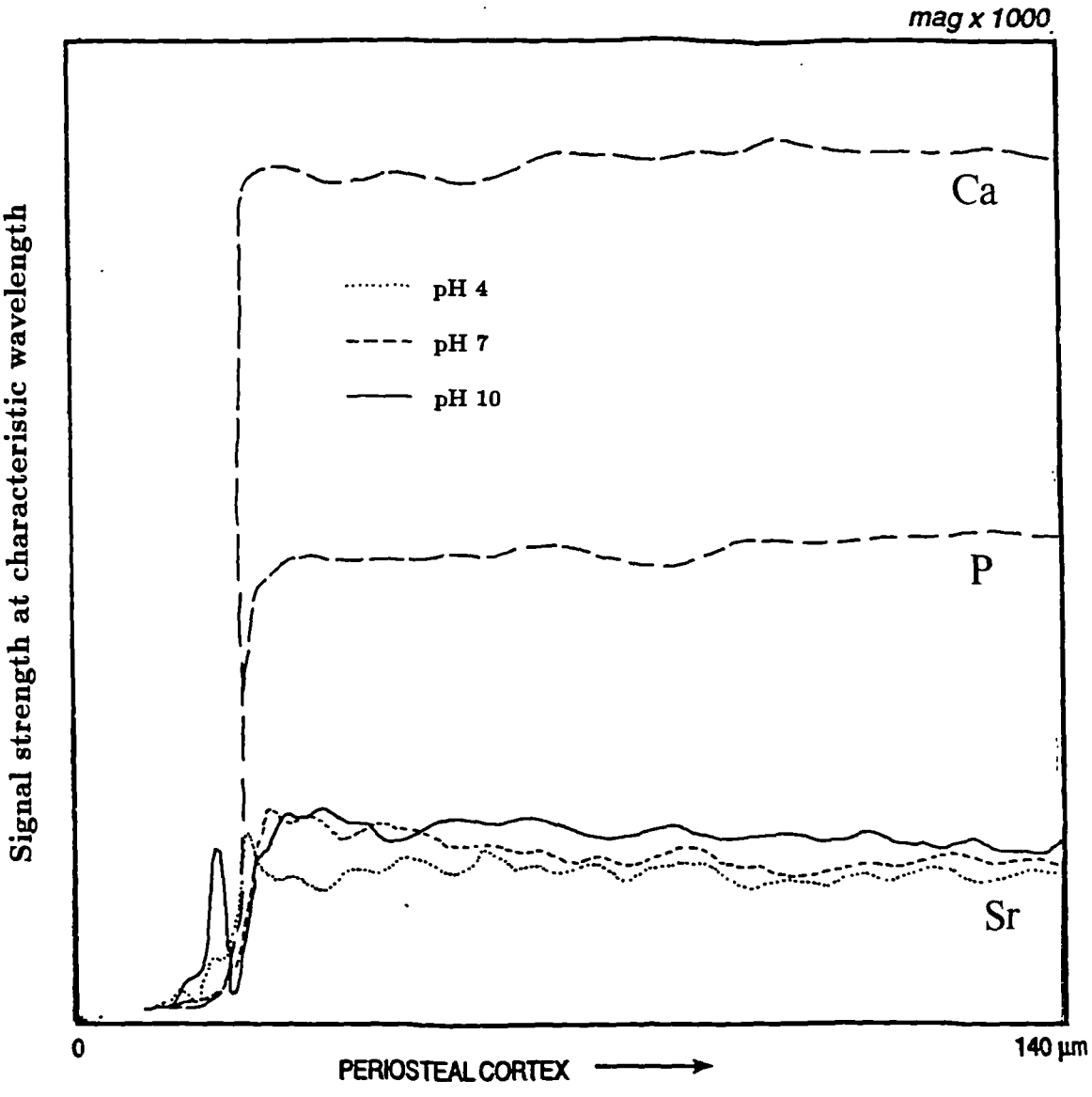

Figure 6.46: Strontium distributions in the periosteal cortex of ashed bone immersed at variable pH. Microscope operated at mag. x1000.

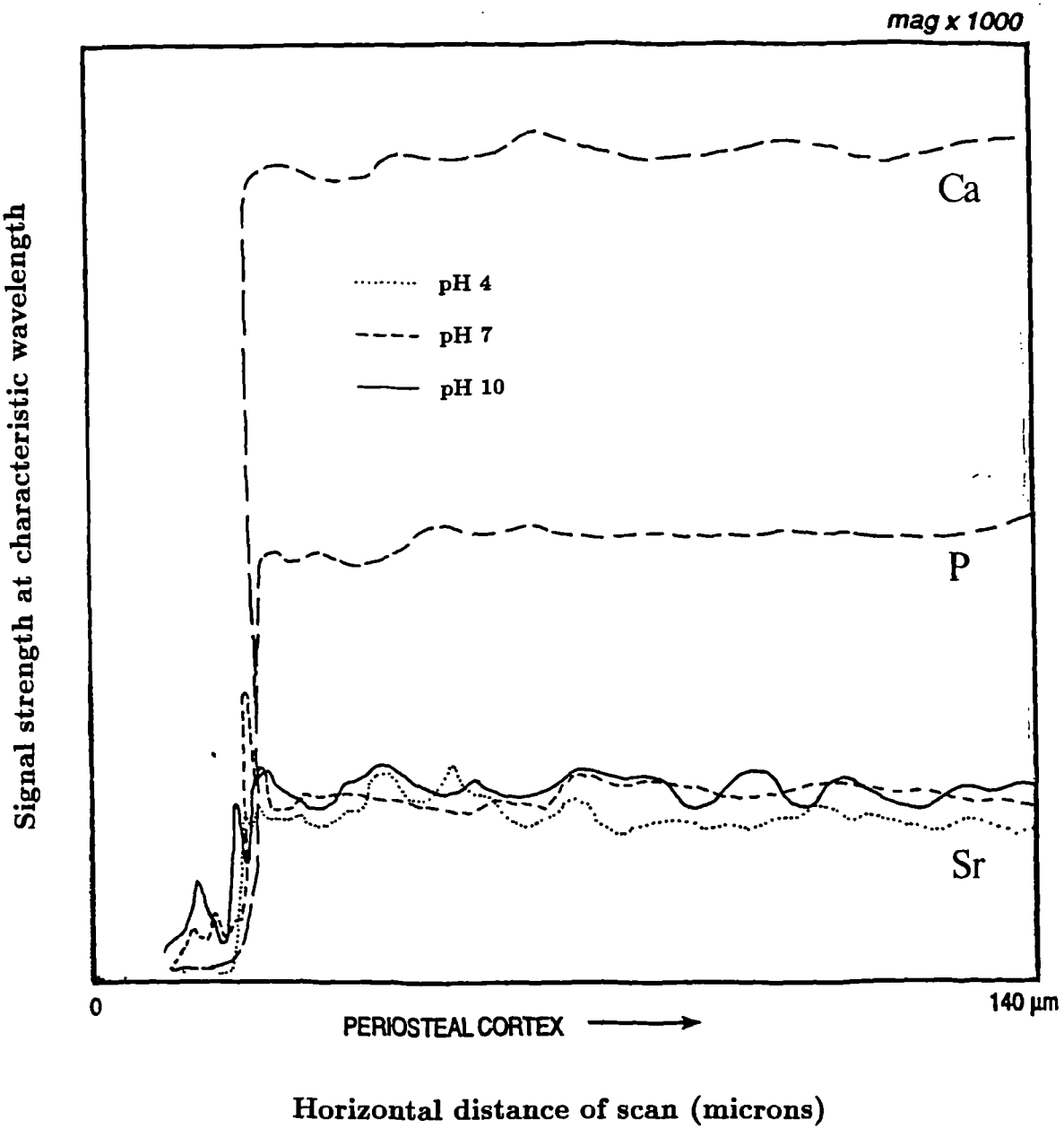

Figure 6.47: Strontium distributions in the periosteal cortex of bone of varying organic/inorganic content immersed at pH 4. Microscope operated at mag. x1000.

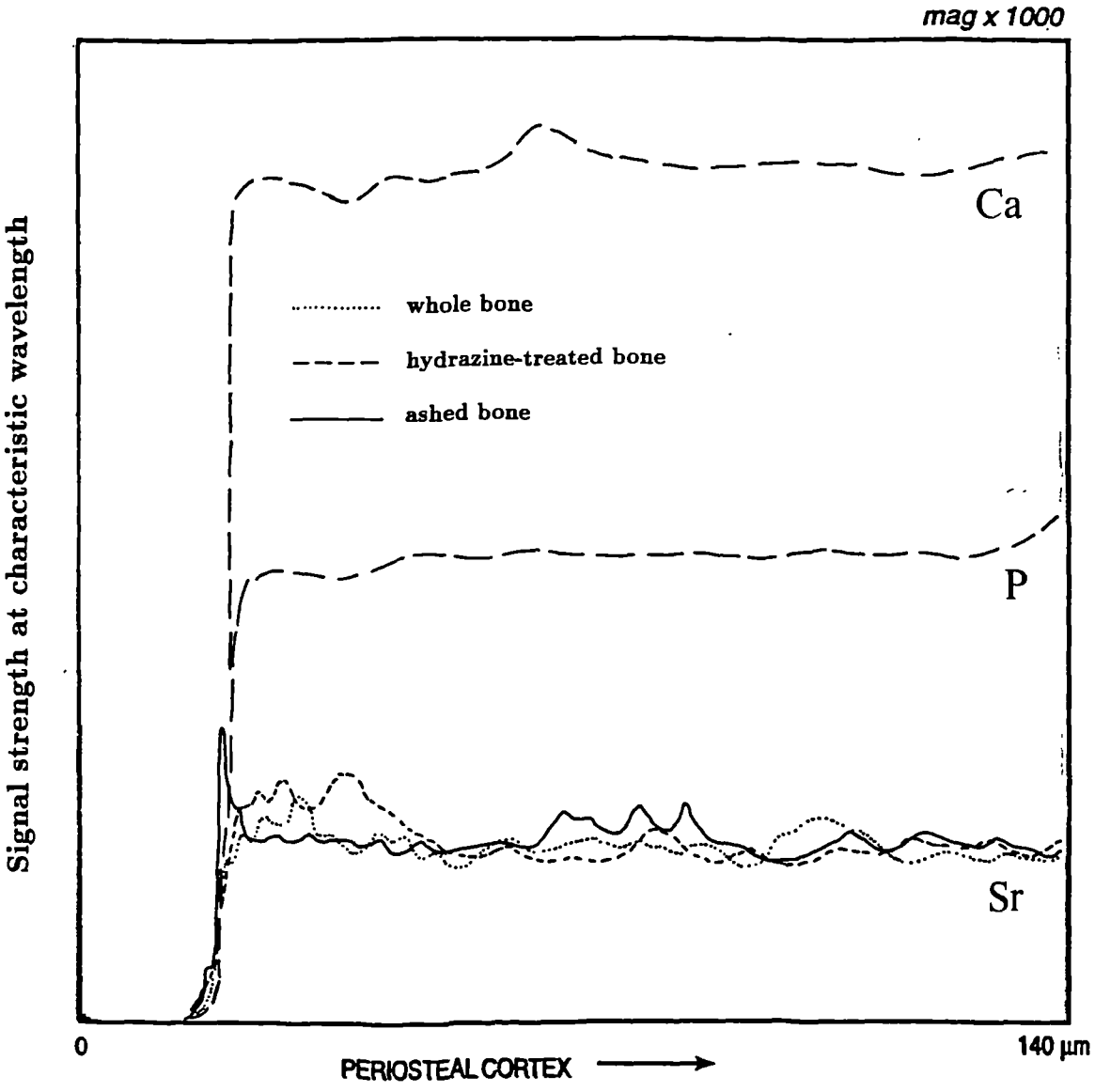

Horizontal distance of scan (microns)

Figure 6.48: Strontium distributions in the periosteal cortex of bone of varying organic/inorganic content immersed at pH 7. Microscope operated at mag. x1000.

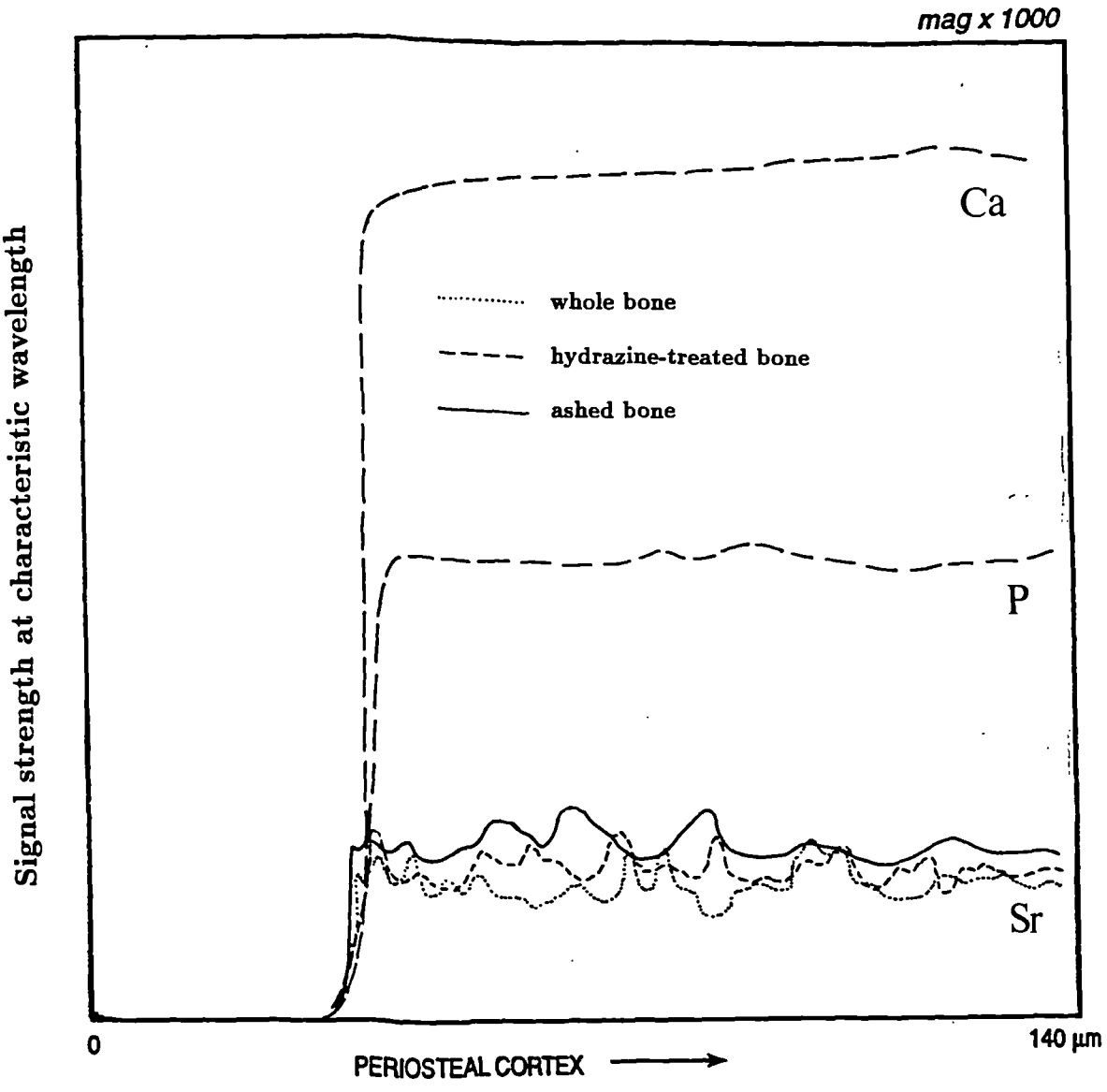

Figure 6.49: Strontium distributions in the periosteal cortex of bone of varying organic/inorganic content immersed at pH 10. Microscope operated at mag. x1000.

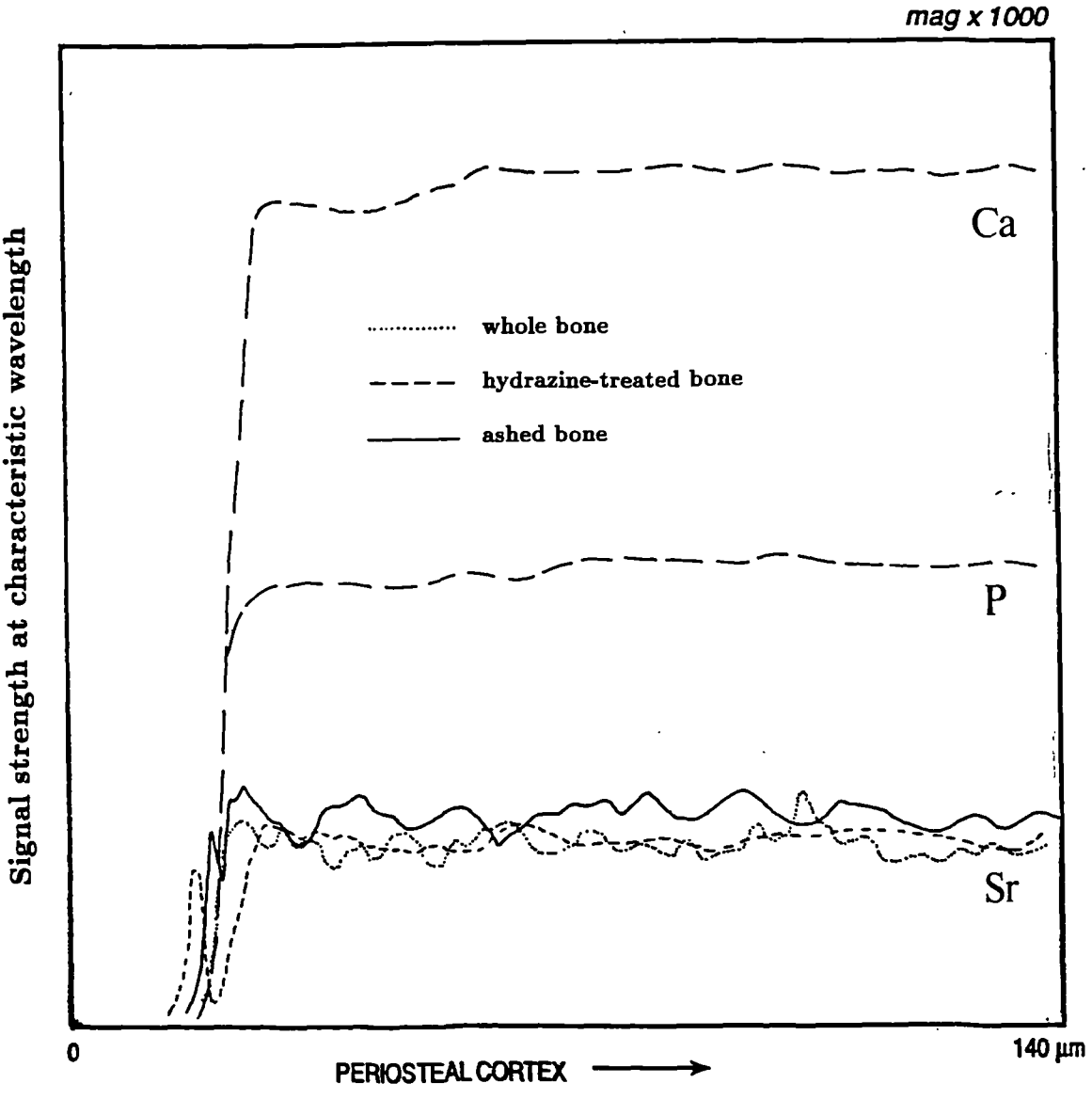

However, the data did not present clearly defined patterns in strontium uptake with organic/inorganic content of the bone, nor were any differential trends with pH consistent. Nevertheless, this study has demonstrated effectively a *contrast* in strontium uptake behaviour for bone samples with different organic/inorganic ratios under variable pH of immersion. Quantitative XRF and qualitative EPMA have shown that both ashed and hydrazine-treated bone indicated more extensive strontium association with alkalinity; however, while XRF analysis found a more pronounced uptake in neutral-alkaline conditions for whole bone, EPMA clearly demonstrated enhanced uptake at acidic pH in this material. The reason for such a discrepancy is unclear.

Generally, contrasting data may reflect different mechanisms of uptake related to the organic and inorganic matrices. Certainly quantitative data have indicated the possibility of some strontium interaction with the organic component at neutral-acidic pH. Moreover, alkaline conditions might be expected to promote strontium interaction with the inorganic matrix because of the attraction of this cation to the more negatively-charged surfaces that would exist in these conditions.

Studies attempting to separate the organic and inorganic fractions of bone by chemical means after its exposure to strontium solution would perhaps throw some light on the possible mechanisms of strontium interaction.

6.5 Chemical Separation of Organic and Inorganic Components.

The separation of organic and inorganic components of whole bone immersed in pH 4, 7 or 10 solutions (two examples of each) from Series III immersions was carried out in order to identify the relative contribution of each fraction to the uptake and subsequent incorporation/adsorption of this element. Organic and inorganic extractions were analysed using ICP-AES: calibration procedures determined detection limits (in ppm in solution) as approximately 0.2 ppm Ca, 5 ppm P, and 0.005 ppm Sr. Inorganic extractions were diluted one hundred-fold for the measurement of calcium and phosphorus, and in some cases for strontium. All concentrations were corrected for dilution, small variations in the mass of the bone

Table 6.14: ICP-AES data for organic and inorganic extractions of whole bone immersed in strontium solution.

Sample description	Experiment #	Extraction	Ca (ppm)	P (ppm)	Sr (ppm)
Blank nitric acid	N/A	Inorganic	NF	NF	0.130
Blank nitric acid	N/A	Organic	NF	NF	0.060
H5 animal bone	N/A	Inorganic	44268	18522	17.430
	N/A	Organic	NF	<=13.92	0.084
Ovine bone control	N/A	Inorganic	52643	24207	20.590
	N/A	Organic	<=0.56	NF	0.056
pH 4 immersion	1	Inorganic	22227	10823	711.250
		Organic	NF	NF	0.156
pH 7 immersion	1	Inorganic	21710	10990	1295.790
		Organic	NF	NF	0.137
pH 10 immersion	1	Inorganic	20379	9975	1065.43
		Organic	NF	NF	0.181
pH 4 immersion	2	Inorganic	60148	27652	328.680
		Organic	NF	NF	0.100
pH 7 immersion	2	Inorganic	3939	1788	209.070
		Organic	NF	NF	0.120
pH 10 immersion	2	Inorganic	10782	4749	376.34
		Organic	NF	NF	0.178

experiment # 1 = 1M Sr immersions ; # 2 = 100 ppm Sr immersions.

'N/A' = not applicable. 'NF'= 'not found' i.e. below quoted detection limit.

'<=' refers to figures at limit of detection.

All values are corrected for variable original bone mass and each standardised to 1 gramme bone matrix.

sample and instrumental drift. Final concentrations are shown in ppm standardised for 1g bone material in table 6.14. 'NF' refers to elements 'not found' i.e. either present in quantities below the quoted detection limit or totally absent from the solution.

Bone samples immersed in molar (139,000 ppm) and 100 ppm strontium solutions from Immersion Series III were included in this study: extraction solutions from these two sources were not directly (quantitatively) comparable, but *trends* observed for each experiment were compared.

Table 6.14 shows that the blank solutions were devoid of Ca and P, as expected, but did contain traces of strontium. Since ultrapure water and nitric acid were used, impurities should have been minimal and the source of this strontium is unclear.

Despite this small contamination, theoretical and actual measurements for the H5 animal bone standard were in good agreement. Assuming complete extraction of the inorganic component, the expected values for Ca, P and Sr in 1 gramme of bone are shown in table 6.15 together with actual measurements and the percentage error:

Table 6.15: Theoretical and actual measurements of inorganic extractions of H5 animal bone.

Element	Theoretical ppm	Actual ppm	% Error
Ca	42400.01	44267.69	+4.4 %
P	20400.00	18522.16	-9.2 %
Sr	16.86	17.43	+3.4 %

The success of the inorganic and organic extractions was confirmed by the fact that Ca and P levels were only observed in the former, while they were predominantly absent in organic extractions. However, there was a considerable variation in the

ppm yields of these elements for inorganic extractions: Ca yields, for example, ranged between 4000 ppm and 60,000 ppm (Table 6.14). Since the Ca:P ratio for each sample remained relatively constant, this variation suggested a loss of bone material during the extraction procedure. To compensate for this problem, elemental ratios were calculated and are shown in table 6.16.

Examining absolute values of strontium (table 6.14), it was found that very little strontium was detected in any of the organic extractions. Under conditions of high concentration (Series II), strontium uptake appeared to be greatest in bone immersed at pH 7, and least in bone at pH 4. Conversely, in the more dilute strontium immersing solution (Series III), uptake was greatest at pH 10 and least at pH 7. So, there was no clearly defined trend for absolute values, largely explained by the aforementioned variations in yield.

Examining the Sr:Ca ratio data in table 6.16, strontium uptake was highest in pH 7 immersions for both experiments, followed by pH 10 immersions and least in those at pH 4. Organic strontium levels were corrected against background and compared to the corresponding inorganic levels. (Background levels were insignificant against inorganic values to 2 decimal places, so corrections were not made for the latter.) Organic:inorganic strontium ratios are shown in table 6.17. Under conditions of high concentration (1M Sr), relatively little of the organic component contributed to strontium uptake at pH 7 compared to pH 4 and pH 10 immersions. However, in Series III experiments where 100 ppm strontium solution was used, there appeared to be an increase in the significance of the organic component with increasing alkalinity.

6.5.1 Summary.

Strontium was found predominantly in inorganic extractions for all samples, indicating the interaction of this element with the hydroxyapatite matrix. Moreover, neutral pH conditions appeared to promote this interaction since strontium/calcium ratios were highest in pH 7 extractions.

Certainly, in agreement with EPMA data, the relative contribution of organic and inorganic components in strontium uptake appeared to alter with the ambient pH.

Table 6.16: Strontium:calcium ratios in inorganic extractions of bone from Immersion Series II and III at variable pH.

Sample description	pH	Ca:P	Sr:Ca ($\times 10^{-4}$)
H5 animal control	N/A	2.4	3.94
Ovine control	N/A	2.2	3.91
Immersion Series II	4	2.1	320
	7	2.0	597
	10	2.0	523
Immersion Series III	4	2.2	54.6
	7	2.2	530
	10	2.3	349

Table 6.17: Organic:inorganic strontium ratios for bone samples immersed under variable pH conditions.

Sample description	Organic:Inorganic strontium (x 10^{-5})
H5 animal bone	138.0
Ovine bone	*
1M Sr, pH 4	13.5
1M Sr, pH 7	5.9
1M Sr, pH 10	11.4
100ppm Sr, pH 4	12.1
100ppm Sr, pH 7	28.7
100ppm Sr, pH 10	31.4

(* blank [Sr] higher than organic extraction)

where organic [Sr] = measured [Sr] - blank [Sr] (0.06)

Data for Series II and III were conflicting with regard to the effect of pH on the mechanism of strontium interaction: data from Series III indicated that the role of the organic matrix became more significant with alkalinity. Series II data found that strontium-organic interaction was relatively low at neutral pH compared to the more extreme ends of the pH scale. This might be explained by the degree of organic stability under different pH regimes. Certainly protein hydrolysis would be enhanced at extreme pH's and this breakdown process might offer compatible surfaces for strontium interaction. Possible mechanisms of strontium interaction with bone are discussed in more detail in Chapter 10.

Chapter VII

Uranium Uptake Studies.

This chapter is divided into 6 main sections, which are summarised in Table VII. The first comprises autoradiographic experiments - Immersion Series I. Subsequent sections are divided, as in Chapter 6, according to the main variable under investigation: (1) the pattern of uptake over time, (2) the effect of pH, and (3) the role of organic and inorganic components in the uptake mechanism. Furthermore, proton microprobe analysis was carried out to examine patterns in uranium uptake under higher magnification and thus explore uranium-bone interaction in more detail than conventional micro-analytical techniques (EPMA) would allow. These sections describe data from Immersion Series III.

7.1 Preliminary Investigation: Series I.

Experimental details regarding autoradiography are described in Chapter 5, subsection 5.5.1.1. Despite the low activity levels observed - a depleted uranium salt was employed rather than a radiotracer - several pH-related uptake trends were observed.

7.1.1 Autoradiographs.

1. Effect of pH on uranium uptake.

Uranium uptake was more pronounced in neutral conditions, where peaks of relative absorbance were much larger than those of pH 4 and pH 9 samples (figure 7.1). These latter two samples showed relatively little difference in uranium absorbance: the background levels of each were slightly different, and taking these into account, the peaks in the alkaline (pH 9) conditions were marginally larger than those in acidic (pH 4) conditions. However, as outlined for strontium autoradiographic results, any apparent trends in uptake against pH were viewed tentatively because of the ineffective buffering of the solutions.

Table VII : Classification and Experimental Details of Uranium Uptake Studies.

Description of experiment	Parameters under investigation	Description of immersing solution	Post-immersion analysis			
			Solution		Bone	
			Chemical changes	Physical changes	Chemical changes	Physical changes
Series I						
Preliminary experiment (Section 7.1)	Bone size Temperature (20°C, 60°C) (pH)	Uranyl di-acetate 1120 ppm (1 million cts equiv.) Acid/alkali addition (10 weeks immersion)	AAS (Na, Ca, K, Mg)	pH	Autoradiography	
Series III						
Uptake against Time (Section 7.3)	Time (1, 5, 12 weeks) (pH)	Uranyl di-nitrate 1000 ppm pH 7 (z.buffering) 70°C			EPMA (qual)	
Uptake against pH (Section 7.4)	pH (4,6,7,8,10) Time (2, 12 weeks) [Uranium]	Uranyl di-nitrate (a) 2240 ppm (2 weeks immersion) (b) 1000 ppm (12 weeks immersion) 70°C, (z.buffering)	AAS (Ca) LSC (U)		EPMA (qual) XRF (for 2240 ppm) PIXE/RBS (Section 7.6) ICP-AES (Ch.Sep) (Section 7.7)	XRD (see Ch.8)
Uptake against Organic:Inorganic Ratio (Section 7.5)	Org:inorg. ratio (whole, hydrazined, ashed) pH	Uranyl di-nitrate 2240 ppm (2 weeks immersion) 70°C, (z.buffering)	AAS (Ca) LSC (U)		EPMA (qual) PIXE/RBS (Section 7.6)	XRD (see Ch.8)

Figure 7.1: A comparison of uranium uptake into sliced bone immersed in solutions of varying pH at 60 °C.

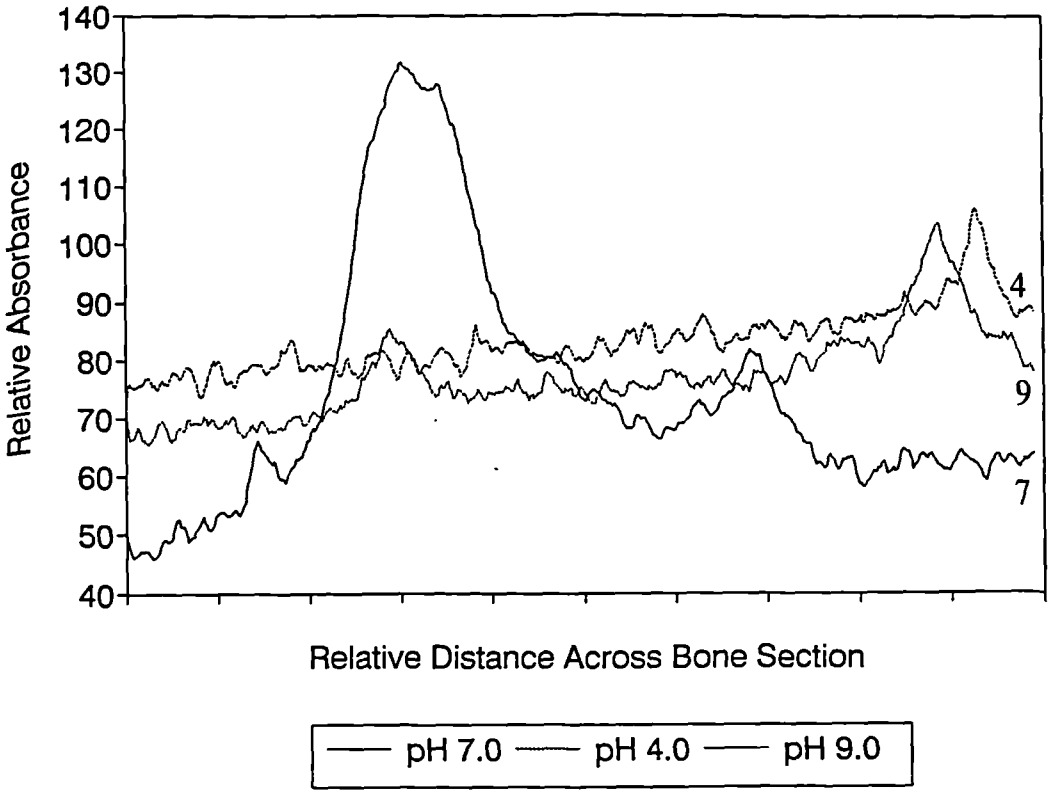

Figure 7.2 shows a photograph of a pseudo 3-D image of an autoradiograph trace, obtained using an image analyser (in much the same way as the strontium example shown in figure 6.18), indicating the distribution of uranium salt across a bone slice (immersing conditions for this particular sample were pH 7, 60°C). Areas of uranium enrichment were observed lining the outer and inner cortical surfaces (coloured red). The "bean-shaped" features at the top left- and right-hand "corners" of the bone reflected the uneven surface of the bone slice, these areas being slightly thicker in section than the rest of the bone. The majority of uranium was represented by the green-yellow areas (representing the peaks or areas of highest absorbance), which generally corresponded to areas near the endosteal bone surface, and perhaps just exterior to the cortical tissue itself. Such a distribution might suggest an association with remnant organic material lining the

inner cortical surface. This distribution pattern was not observed in bone samples immersed in either pH 4 or pH 9 solutions, and this might, perhaps, be explained by the breakdown of organic material by acidic and basic hydrolysis, respectively, although this is only speculation.

Figure 7.2 Pseudo-3D image analysis of autoradiograph demonstrating uranium uptake into bone.

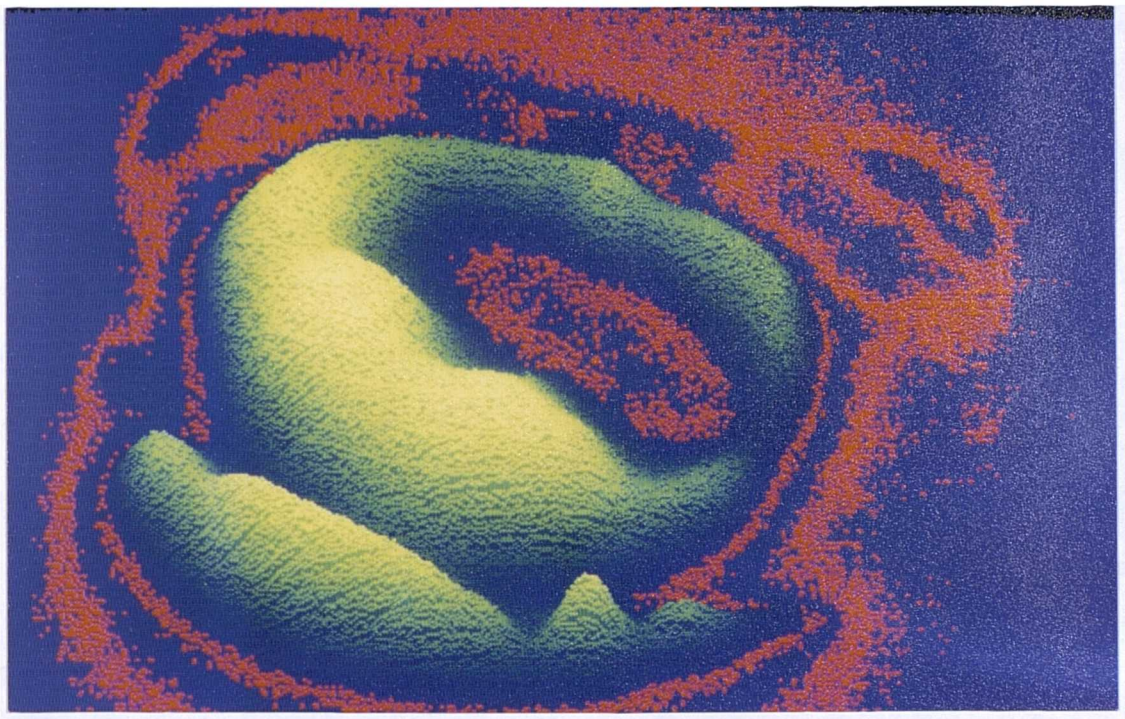

2. The effects of temperature.

The autoradiographic traces for bone immersed at 20°C were too faint for image analysis because the density of the traces was very low. The samples represented in figure 7.1 were those immersed at 60°C, so the trend of increasing uptake under higher temperatures was again observed here.

7.1.2 Immersing Solution.

1. pH measurements.

As in the strontium study, the simulated groundwater solutions remaining after the immersion period were examined. Table 7.1 shows the post-immersion pH values. Post-immersion pH values of uranium - containing solutions were generally lower than corresponding samples containing strontium suggesting the formation of an acidic uranyl complex. This suggestion was further reinforced by comparing samples (bone slices) immersed at pH 7 and exposed to variable uranium quantities, where the higher the uranium concentration the lower the final pH.

Table 7.1: pH changes of immersing solutions after 10 weeks

Bone description	Immersion temperature (°C)	Initial pH	Final pH
slice	20	4.0	6.0
slice	20	7.0	6.6
slice	20	9.0	6.1
slice	60	4.0	5.3
slice	60	7.0	6.4
slice	60	9.0	5.1
slice ($\frac{1}{2}$ uranium)	60	7.0	6.7
slice (no uranium)	60	7.0	6.9

2. Chemical analysis.

Anticipated levels of uranium in solution were well below the detection limits obtainable by AAS. Table 7.2 shows that, as in the case of the strontium immersion study, sodium, calcium, potassium and magnesium were the only detectable elements using this technique. Their concentrations were higher in solution after immersion than before, suggesting the leaching of these elements from the bone

during its immersion. As before, values for each respective element were generally higher in samples immersed in the higher temperature solutions.

Table 7.2: A.A.S. analysis of immersing solutions after 10 weeks (ppm).

Sample description	Na	Ca	K	Mg
Pre-immersion groundwater (theoretical)	36.00	9.50	4.32	17.65
Pre-immersion groundwater (measured)	36.80	2.77	1.88	1.97
Sliced bone, 20°C, pH 4	43.56	11.12	10.75	3.68
Sliced bone, 20°C, pH 7	40.77	4.90	8.97	3.12
Sliced bone, 20°C, pH 9	42.51	9.02	10.06	3.59
Sliced bone, 60°C, pH 4	70.32	12.61	10.93	4.77
Sliced bone, 60°C, pH 7	42.39	5.22	9.27	3.94
Sliced bone, 60°C, pH 9	69.71	13.87	8.97	5.01

All values are ppm.

7.1.3 Summary.

To summarise, this initial study was able to demonstrate uranium uptake into bone, which was evidently more pronounced under neutral pH conditions and higher temperatures of immersion. There was also an indication of uranium interaction with both inorganic and organic bone fractions.

7.2 Preliminary Microprobe Analyses.

Improvements in solution management during the immersion period, to counteract pH changes, were made in subsequent studies, together with detailed analysis using more sensitive and specific techniques. The role of the organic and inorganic

components in uranium uptake into bone, together with the effect of pH on such interactions were further investigated using EPMA and SPM analysis.

Sections 7.2-7.4 describe Immersion Series III experiments consisting predominantly of EPMA studies on whole bone. Basic experimental variables included the uranium concentration of the immersing solution, ranging from 1000 ppm to 2240 ppm. All solutions were buffered effectively using zwitterionic buffers, so that measurement of post-immersion pH was not applicable. Nor were the weight changes of bone samples monitored since such measurements were found to be of little use in corresponding strontium uptake studies described in the preceding chapter.

The basic distribution pattern of uranium contrasted with that of strontium as determined from microprobe studies and experiments varying the location of cellulose acetate coating.

Figures 7.3 (a) and (b) show EPMA line-profiles of uranium distribution at the periosteal cortical edge of whole bone samples and illustrate the effect of cellulose acetate coating. Figure 7.3 (a) compares the uranium distribution in the periosteal cortex of bone whose *transverse sections* were coated (dashed line) with bone whose *periosteal and endosteal surfaces* were coated (whole line): on the latter, the coating had successfully prevented uranium accumulation/interaction at the surface while apparently permitting uranium uptake into the bulk of the cortical tissue exposed in transverse section. However, on more thorough examination using the proton microprobe it transpired that uranium was only present in measurable quantities in the peripheral cortices. Figures 7.4 (a) and (b) show a PIXE map and line-profile, respectively, of the full cross-cortical width of whole bone immersed in 2240 ppm uranium solution at pH 7: uranium was observed at the periosteal and predominantly the endosteal surfaces, penetrating the cortical tissue up to 150 microns. Figure 7.4 (c) represents the PIXE spectrum for this mapped area of bone showing a large peak for uranium at around 13.5 keV. Figure 7.5 (a) illustrates an area of periosteal cortex under higher magnification of bone immersed in 1000 ppm uranium at pH 7. Here, despite a 12 week immersion period, uranium had only penetrated the cortical tissue up to 30 microns. Quantitative analysis of uranium levels in this cortical area was carried out using simultaneous PIXE and

RBS methods: their respective spectra are shown in figures 7.5 (b) and (c), along with the combined quantitative data. Calculated concentrations were based on the quoted target composition and thickness, and measured uranium at 5.5 % by weight. Since the natural level of uranium in this ovine bone material was only a few ppm, these data suggested that uranium uptake and association with only very localised areas of cortex was nevertheless substantial.

Thus, under the experimental conditions set in these laboratory-based uptake studies, uranium did not diffuse across the whole cortical width but rather interacted extensively at the cortical edges and in the peripheral cortices.

The series of experiments described in the following sections focused on these periosteal and endosteal cortical areas in order to explore temporal patterns of uptake, the effect of pH and the relative contribution of the organic and inorganic components of bone. These are discussed in turn.

EPMA studies were followed by SPM analysis which examined patterns of uptake in more detail.

7.3 Uptake over Time: Series III.

The data presented in this section examining the temporal patterns of uranium uptake consist of qualitative EPMA data in the form of line-profiles and digimaps. Quantitative measurements of bone and immersing solutions were not taken.

7.3.1 Micro-analysis of Bone: EPMA.

Whole bone was immersed in 1000 ppm uranium nitrate solutions at pH 7 for periods of 1, 5 and 12 weeks. Figure 7.6 shows the cross-cortical distribution profiles of uranium after each duration. Both the concentration level and pattern of distribution were similar across the cortices of all samples. However, at the cortical surfaces uranium was found to increase with duration of exposure: both the height and the breadth of the peaks generally increased with time as uranium was adsorbed and/or incorporated in these areas. This pattern was demonstrated more clearly at higher magnification of the periosteal edge (figure 7.7). The uranium profile in bone immersed for 12 weeks at pH 10 instead of pH 7 was also included

Figure 7.3 (a) and (b): The distribution of uranium in the periosteal cortex of bone with variable cellulose acetate coating measured by EPMA. Microscope operated at mag. x1000.

(a)

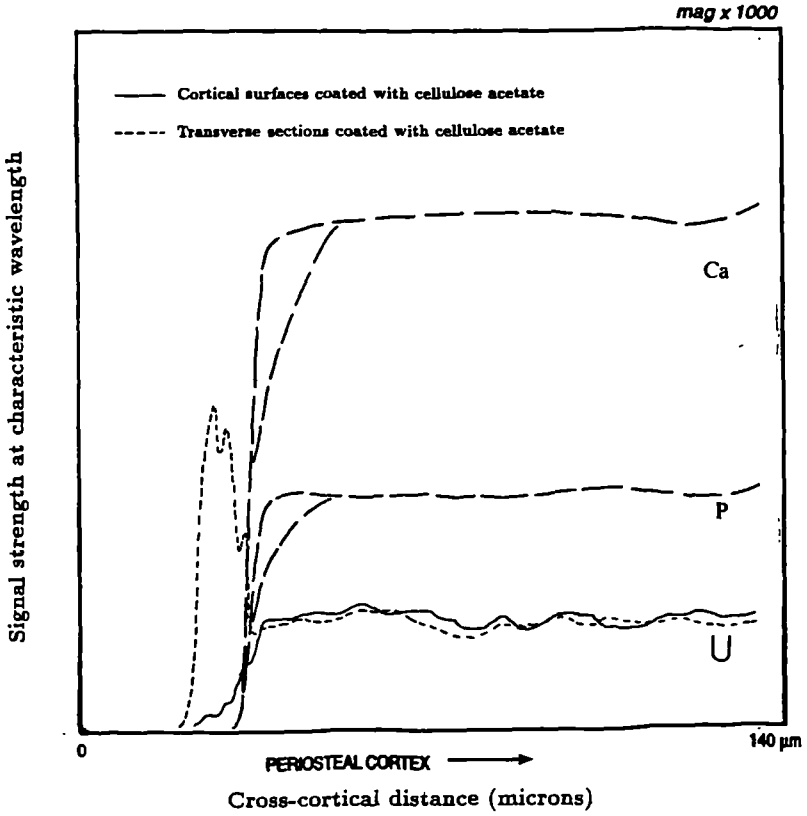

Cross-cortical distance (microns)

(b)

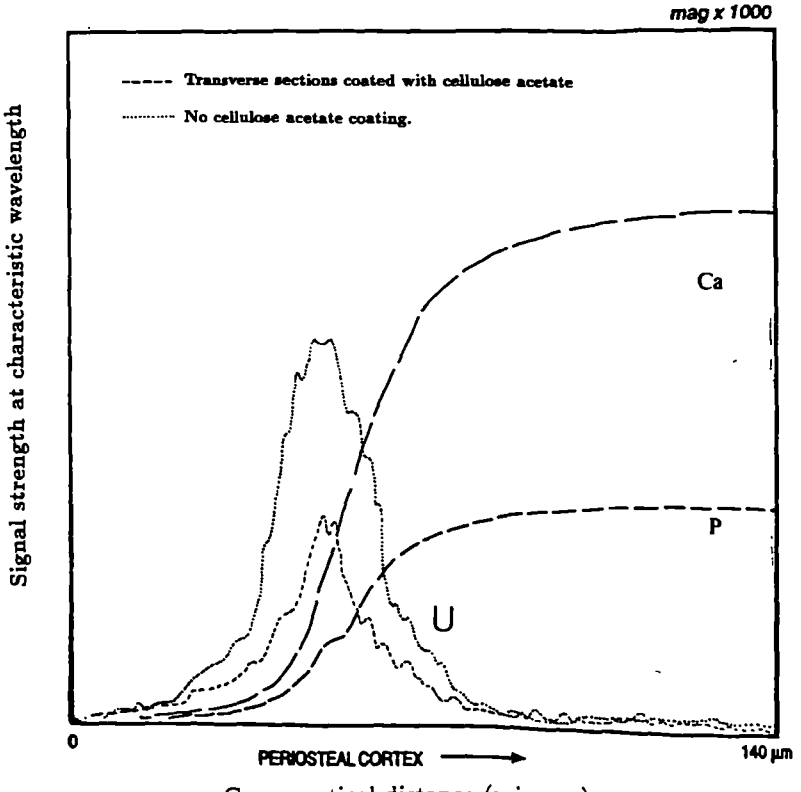

Cross-cortical distance (microns)

Figure 7.4: (a) PIXE digimap and (b) corresponding line-profile of the cross-cortical width of whole bone to illustrate the distribution pattern of uranium uptake. (c) the PIXE spectrum of this cortical area.

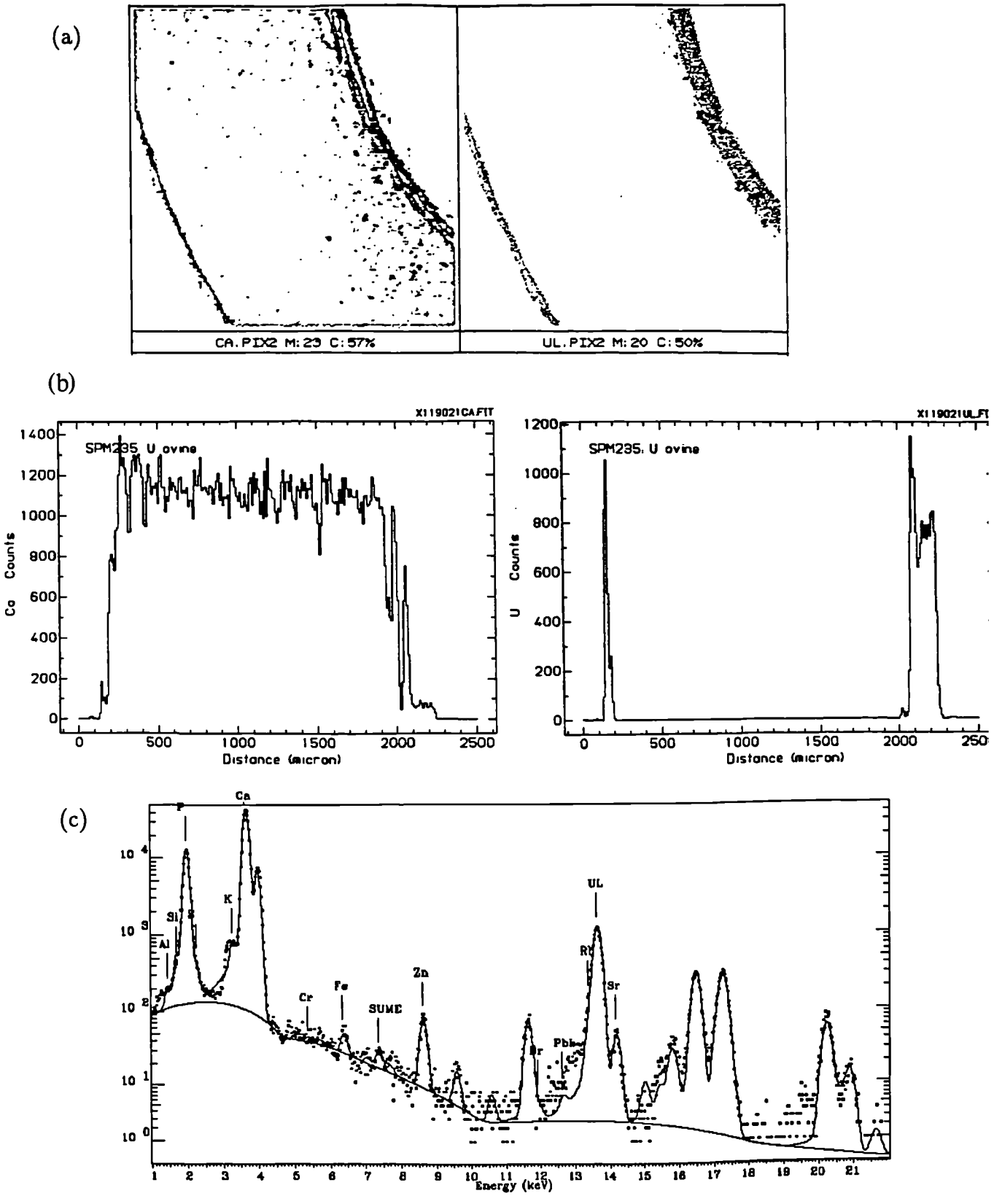

Figure 7.5: (a) PIXE digimap of a 75 sq.micron area of periosteal cortex of bone immersed in 1000 ppm uranium solution. (b) PIXE and (c) RBS spectra of this cortical area with corresponding quantitative data.

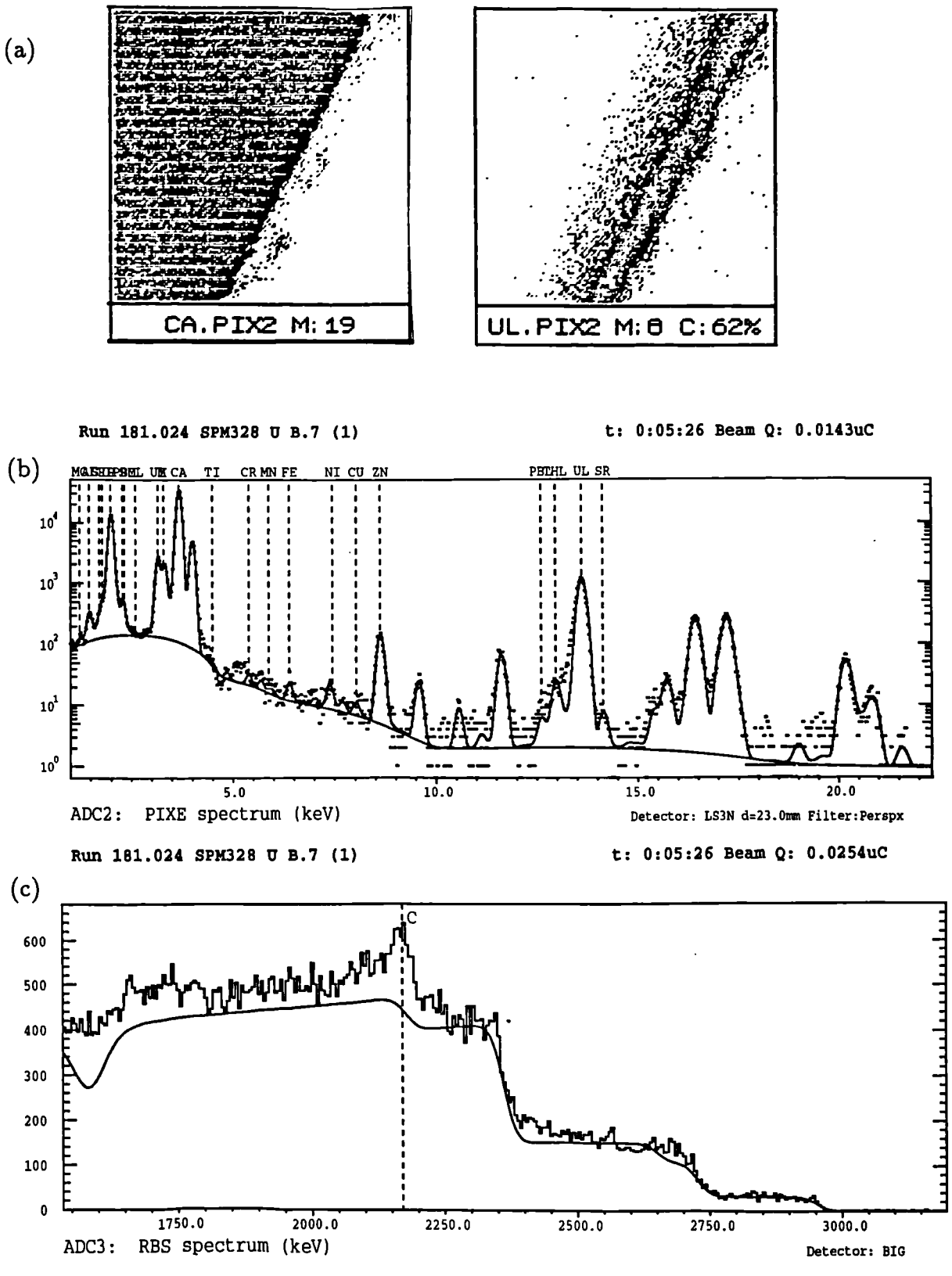

in figure 7.6 for comparison, and the peaks for this sample were found to be much higher than the corresponding sample at pH 7: the effects of pH on uptake and its implications were discussed in more detail in the next section.

Since the uranium in these samples was not removed by thorough ultrasonic cleaning, effective bonding/interaction of this element with the bone surface had clearly occurred, either by its incorporation into the peripheral matrix by some exchange mechanism(s), or by surface adsorption processes.

The **calcium/uranium ratios** in the periosteal cortex were also plotted for samples representing each immersion period (figure 7.8, a smoothed image to clarify temporal distribution trends). The calcium/uranium ratio was found to be similar in bone immersed for 1 and 5 weeks, but was clearly lower in 12 week samples for at least 120 microns into the cortex. This would suggest that only after at least 5 weeks exposure to uranium solution under these experimental conditions did uranium-calcium exchange begin to occur in outer cortical regions, and that before this time the mechanism of uptake was largely adsorption-based. Figure 7.9 represents a digimap of a still further magnified area (5000x) of the periosteal edge, the horizontal width of cortex mapped being approximately 60 microns. Lighter areas represent higher elemental concentration. Thus, uranium was concentrated predominantly in the outer 20-30 microns of the matrix, diffusing at least 60 microns where it was thinly and homogeneously dispersed in the cortical tissue. Corresponding calcium and phosphorus concentrations were observed to decline at the cortical edge where uranium levels were highest: however, this did not necessarily indicate a direct exchange mechanism for uranium with either/both of these elements since respective distribution patterns may simply have reflected the relative proportion of the X-ray signal contributed by each element. Thus, the molecular relationship of these three elements could not be interpreted with any definition.

7.3.2 Summary.

Uranium uptake into bone was only observed in the outer cortical regions of the bone matrix. Under the physical and chemical parameters of the experimental arrangement, together with the time limits imposed, uranium was not taken up across the whole cortical width of the bone but instead was found to penetrate

Figure 7.6: The cross-cortical distribution profiles of uranium in samples immersed in uranyl di-nitrate solutions at pH 7 and 10 for variable duration, measured by EPMA. Microscope operated at mag.x45.

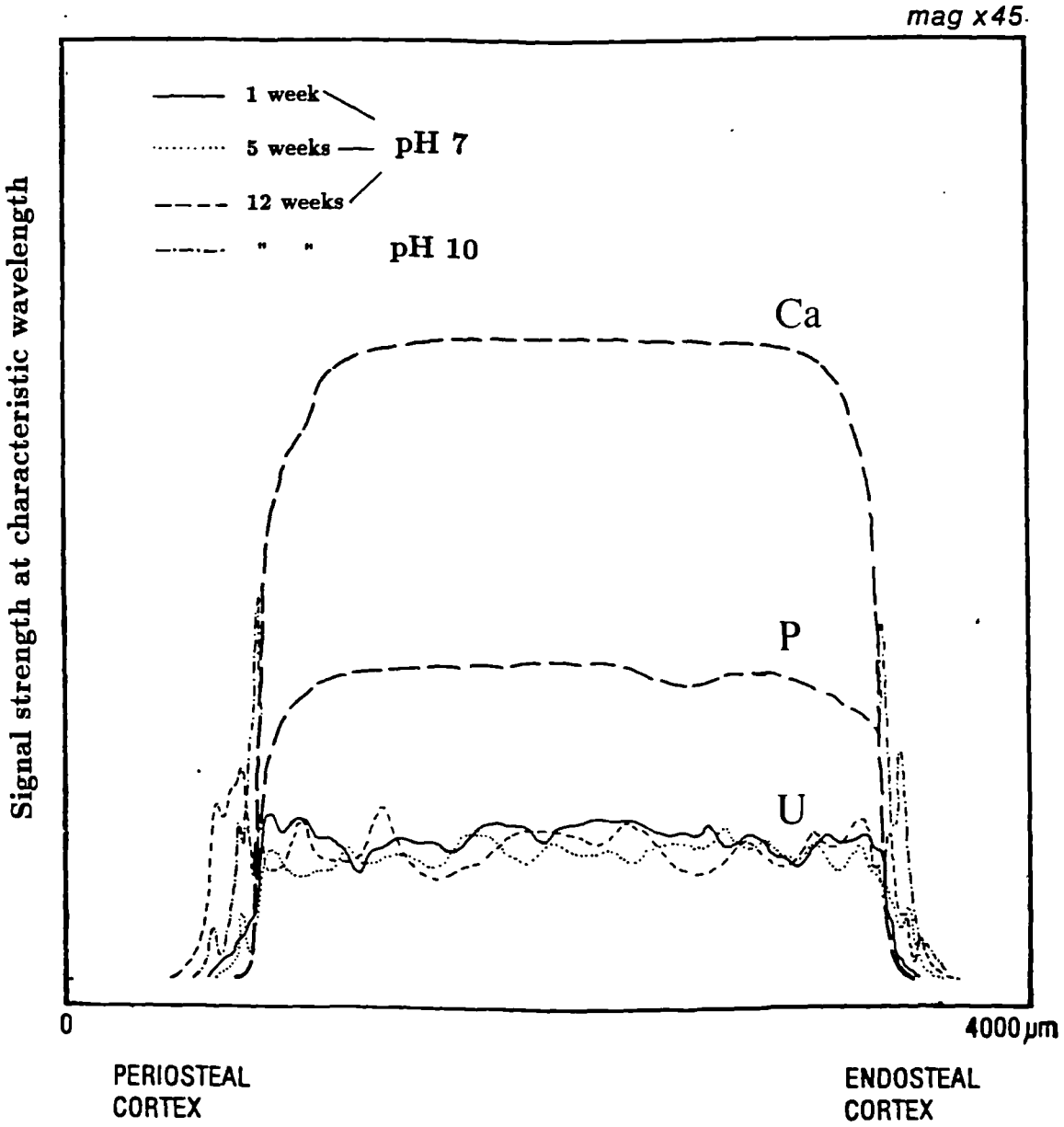

Figure 7.7: Distribution profiles of uranium in the periosteal cortex of samples immersed in uranyl di-nitrate solutions at pH 7 for variable duration. Microscope operated at mag. x1000.

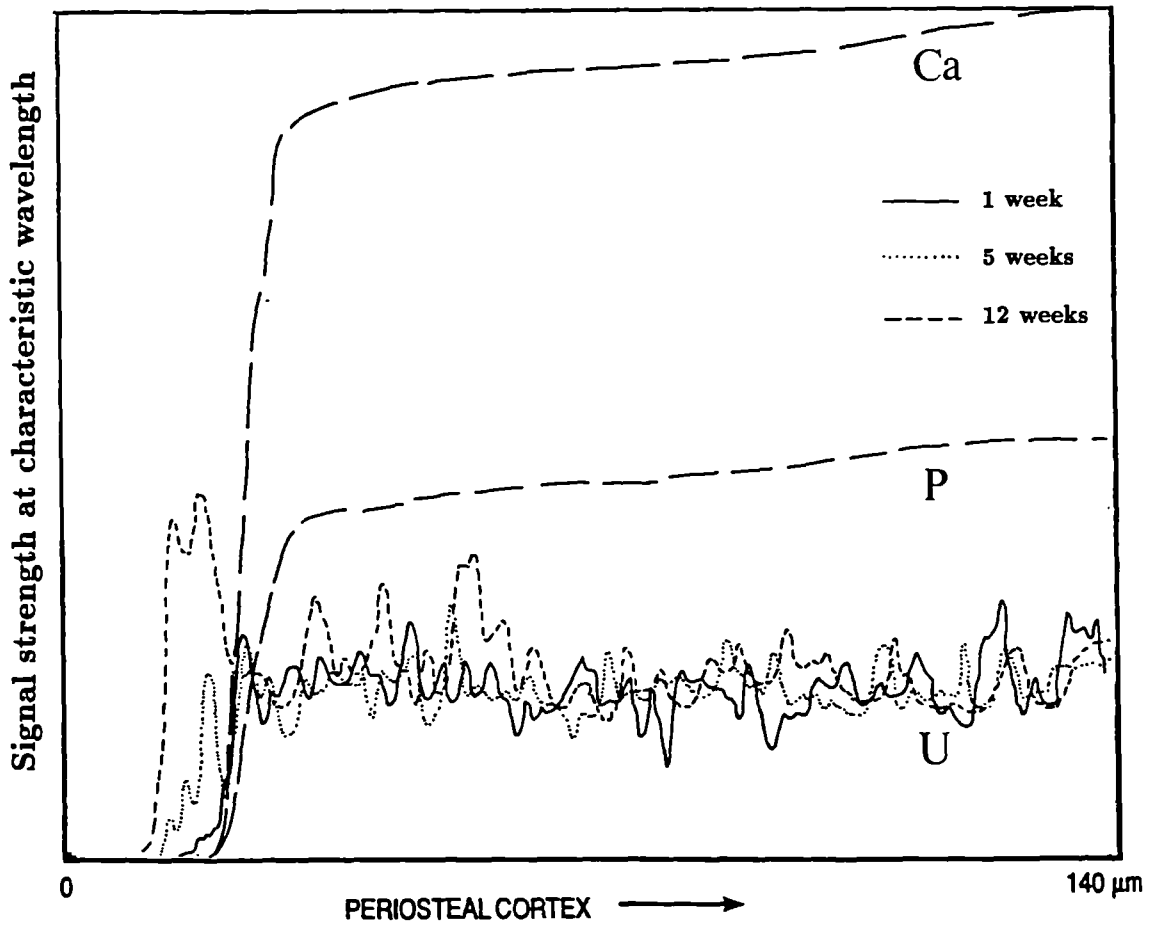

Figure 7.8: Calcium/uranium ratios in periosteal cortex of bone illustrated in Figure 7.7.

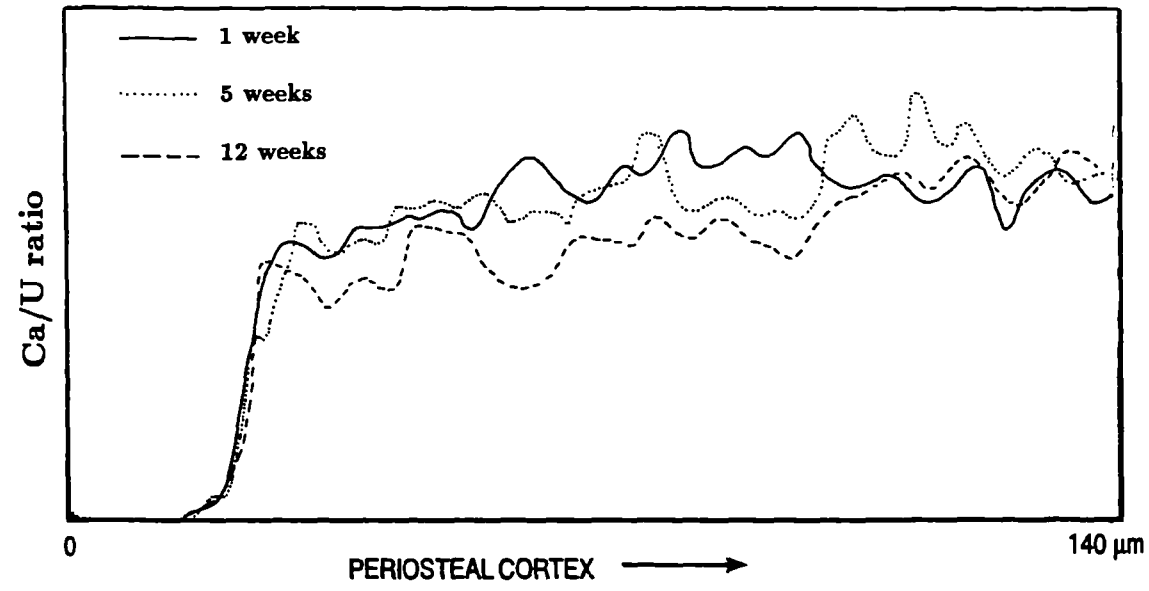

Figure 7.9: Digimaps detailing calcium, phosphorus and uranium distributions in a magnified area of the periosteal cortex, approximately 60 sq.microns.(Microscope operated at mag. x5000).

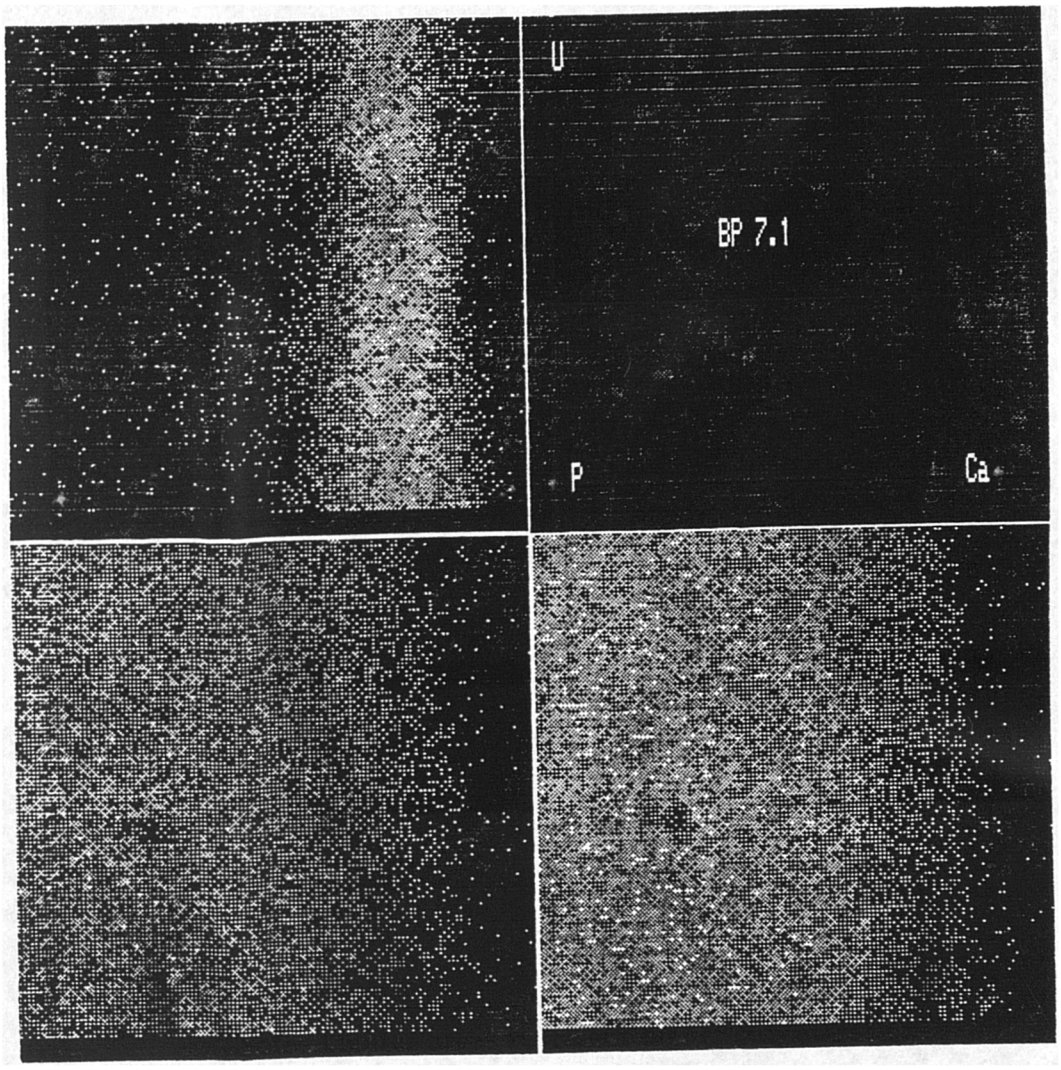

Note: Lighter areas represent higher concentration.

the tissue at least 120 microns after 12 weeks immersion. It seemed plausible that surface adsorption processes were in operation early on in the immersion period and continued with time, whereupon the comparatively slow mechanism of uranium-calcium exchange became apparent after some time (5-12 weeks), as demonstrated by declining calcium/uranium ratios in the outer cortex.

7.4 The Effect of pH on Uptake: Series III.

7.4.1 Analysis of Solutions.

Measurements of calcium and uranium in the remaining immersing solutions were made using AAS and LSC methods, respectively (see Appendix IIIa, and Appendix IIc for control immersions). In the former, problems with sodium interference from the buffering agent, as encountered in corresponding solutions from strontium immersion studies, undoubtedly reduced calcium levels measured in pH 7 and 10 solutions. Data for calcium are nonetheless shown in table 7.3, together with uranium measurements obtained by LSC. Counts per minute (cpm), averaged over a counting period of 10 minutes, were converted to parts per million (ppm) by reading values from a graph plotting cpm against known uranium concentrations in a set of standard solutions ranging from 22.4 to 2240 ppm. The background reading was subtracted for each and a "B" in the table denoted where immersing solutions possessed uranium counts at or below this value. Data for uranium standards and background level used for ppm conversions can be found in Appendix IIIb.

Calcium values were dramatically higher in pH 4 solutions as a result of both the lack of sodium interference and the increased loss of calcium from the bone under acidic conditions. Moreover, values were generally higher in uranium immersions compared to pure water immersions suggesting that calcium loss from the bone was enhanced in the presence of uranium.

Uranium values in control immersions, measured as 20-30 ppm, were probably below the detection limit for uranium, which is typically 2 or 3 times the background level (Williams, pers.comm.). These values were only marginally lower than uranium immersing solutions at pH 4. Uranium levels in pH 7 and pH 10 immersions were similar and more than twice as high as those at pH 4. This suggested that

Table 7.3: Calcium and uranium concentrations in immersing solutions originally containing 2240ppm uranium at pH 7 after the immersion of whole bone for 2 weeks.

Immersing solution	pH of immersion	[Calcium] ppm	[Uranium] ppm
Buffered pure water	4	60	29.5
	7	6	19.9
	10	0	19.1
2240 ppm uranium solution	4	142	B
	4	168	47.9
	7	13	131.8
	7	11	104.7
	10	1	109.7
	10	0	128.8

bone immersed at pH 4 had taken up more uranium than samples immersed in neutral/alkaline conditions. In fact, most of the uranium had been removed from pH 4 solutions.

7.4.2 Analysis of Bone.

7.4.2.1 Total elemental analysis: XRF.

Quantitative analysis of whole bone samples immersed in 2240 ppm uranium solution at variable pH was carried out using XRF; 1 to 2 samples were measured for each pH. Values for calcium, phosphorus and uranium, together with the uranium/calcium ratio are shown in table 7.4, and can be found in Appendix IIIa.

Data in table 7.4 indicated a relatively small uranium uptake at pH 4 with an average uranium/calcium ratio of 2.1 x 10^{-4}. The highest ratio was found in bone immersed at pH 6, with a value of 166 x 10^{-4}. However it must be noted that

Table 7.4: Quantitative analysis of whole bone samples immersed in 2240 ppm uranium solution for 2 weeks at variable pH.

pH of immersion	% CaO	% P_2O_5	U (ppm)	U/Ca ratio (x 10^{-4})
pH 4 control	49.83	43.07	2.86	0.057
pH 7 control	48.80	43.53	2.25	0.046
pH 10 control	50.00	43.72	0	-
pH 4	50.64	43.08	93.51	1.85
pH 4	51.36	42.81	117.01	2.28
pH 6	49.60	43.22	8253.73	166
pH 7	50.56	43.69	7479.96	147
pH 7	50.86	40.81	6262.07	123
pH 8	51.17	40.85	4173.45	82
pH 10	50.97	41.40	2772.88	54
pH 10	52.14	41.84	7328.88	141
SARM-32 std	*55.20	**37.53	-	-
IAEA-312 std	-	-	***15	-

Certified values: *54.44 **39.96 ***16.5

values within a pH regime were highly variable, and the highest *averaged* ratio, albeit calculated from only 2 values, was found at pH 7, with an approximately 40 % decline in this maximum at pH 10. Thus, XRF analysis of the bone indicated highest uranium uptake at pH 6-7.

7.4.2.2 Micro-analysis of bone: EPMA.

EPMA data in this section were collected from whole bone samples immersed either in 2240 ppm or 1000 ppm uranium solutions for 2 and 12 weeks respectively. As with the strontium studies, the pH of the immersing solution was maintained at pH 4, 7 or 10. The line-profile data for each concentration and duration of immersion are summarised in figures 7.10 (2240 ppm) and 7.11 (1000 ppm). Figures represent areas of the periosteal cortex/edge magnified 5000 and 1000 times respectively i.e.

in order to identify and establish any trends in uptake with pH, a small area focusing on the cortical edge was examined. In this way, uranium was observed both at the surface of the bone **and** penetrating into the peripheral cortical tissue.

However, at **pH 4** no clear profile of uranium distribution was observed above background in any part of the cortical width, even when viewed at higher magnification (5000x upwards) for either 1000 ppm or 2240 ppm uranium immersions.

In contrast, at **pH 7** uranium levels were elevated at the cortical edges (both periosteal and endosteal) in much the same way as illustrated in the previous section examining uptake against time which employed bone immersed at pH 7. At higher magnification (5000x) of the periosteal region of bone immersed in 2240 ppm solutions (figure 7.10), uranium was observed to peak just at the periosteal surface i.e. before the sudden rise in Ca and P levels marking the edge of the inorganic phase. This pattern of distribution suggested a surface adsorption process in operation. The uranium profile gradually declined as it entered the bone, moving at least 10 microns into the cortex.

Figure 7.12 shows a mapped region of the endosteal cortex of this whole bone sample magnified 200 times, illustrating the association of uranium with the cortical edge, its lining of the cancellous bone and a general peppering, with some pore-filling, of uranium throughout this cortical region: the lighter areas denote higher elemental concentration.

Thus, uranium uptake into endosteal bone evidently included its lining the endosteal cortical edge, association with the trabecular bone in this region, and filling its cavities and trabeculae.

Figure 7.11 illustrates the uranium distribution in the periosteal cortex of bone immersed in 1000 ppm solutions for 12 weeks. The vertical scale for uranium on this plot was magnified slightly in an attempt to enhance any differences in uranium location and abundance with pH. In this way, it became evident that despite uranium levels in the bulk of the cortical width being almost indistinguishable from the background, levels were higher in samples immersed at pH 7 and 10 (moreso in the former) than those immersed at pH 4. At the cortical surface,

Figure 7.10: Uranium distribution profiles at the periosteal cortical edge of whole bone immersed in 2240 ppm uranium solution at variable pH for 2 weeks. Microscope operated at mag. x5000.

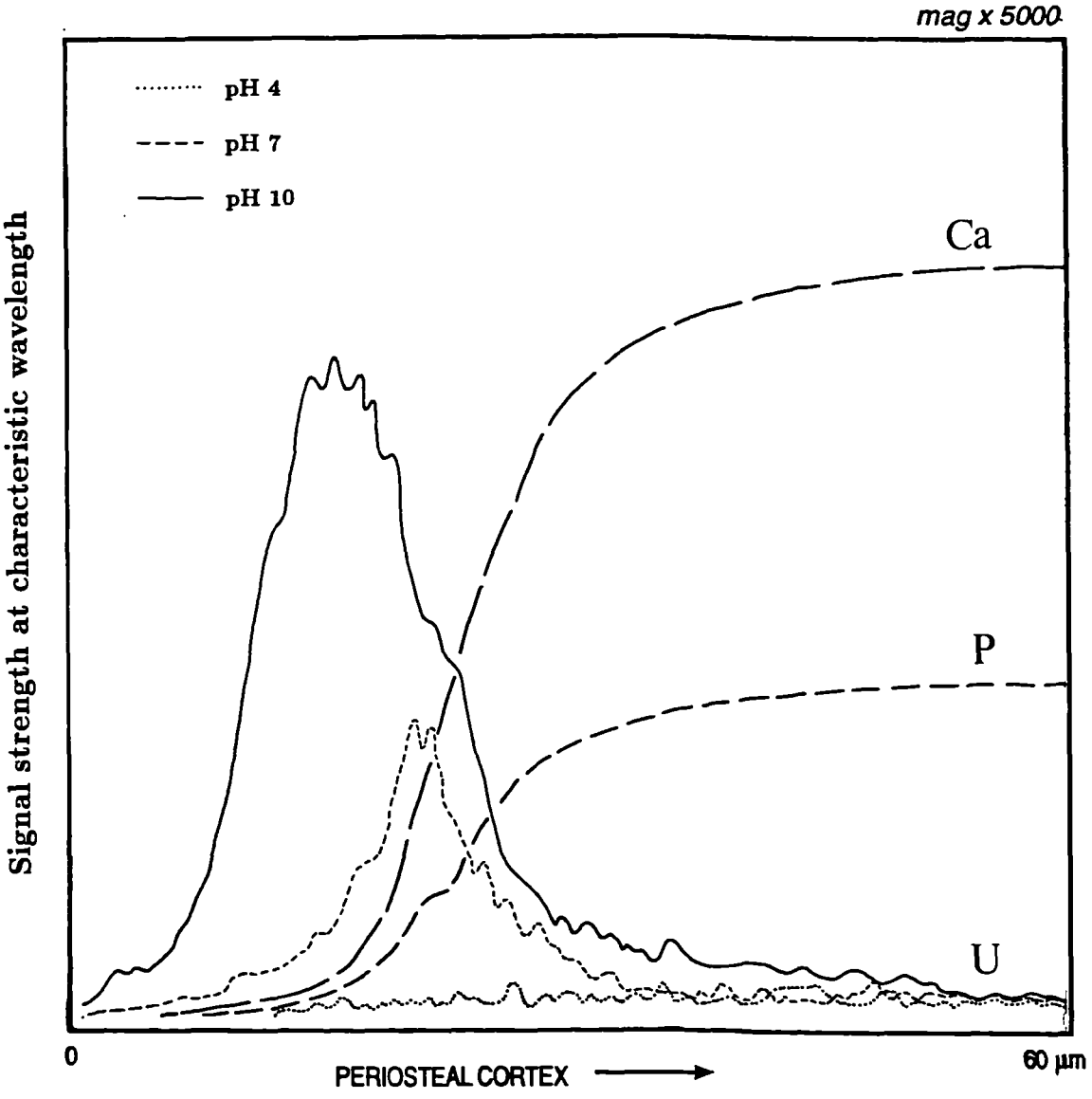

Figure 7.11: Uranium distribution profiles in the periosteal cortex of whole bone immersed in 1000 ppm uranium solution at variable pH for 12 weeks. Microscope operated at mag. x1000.

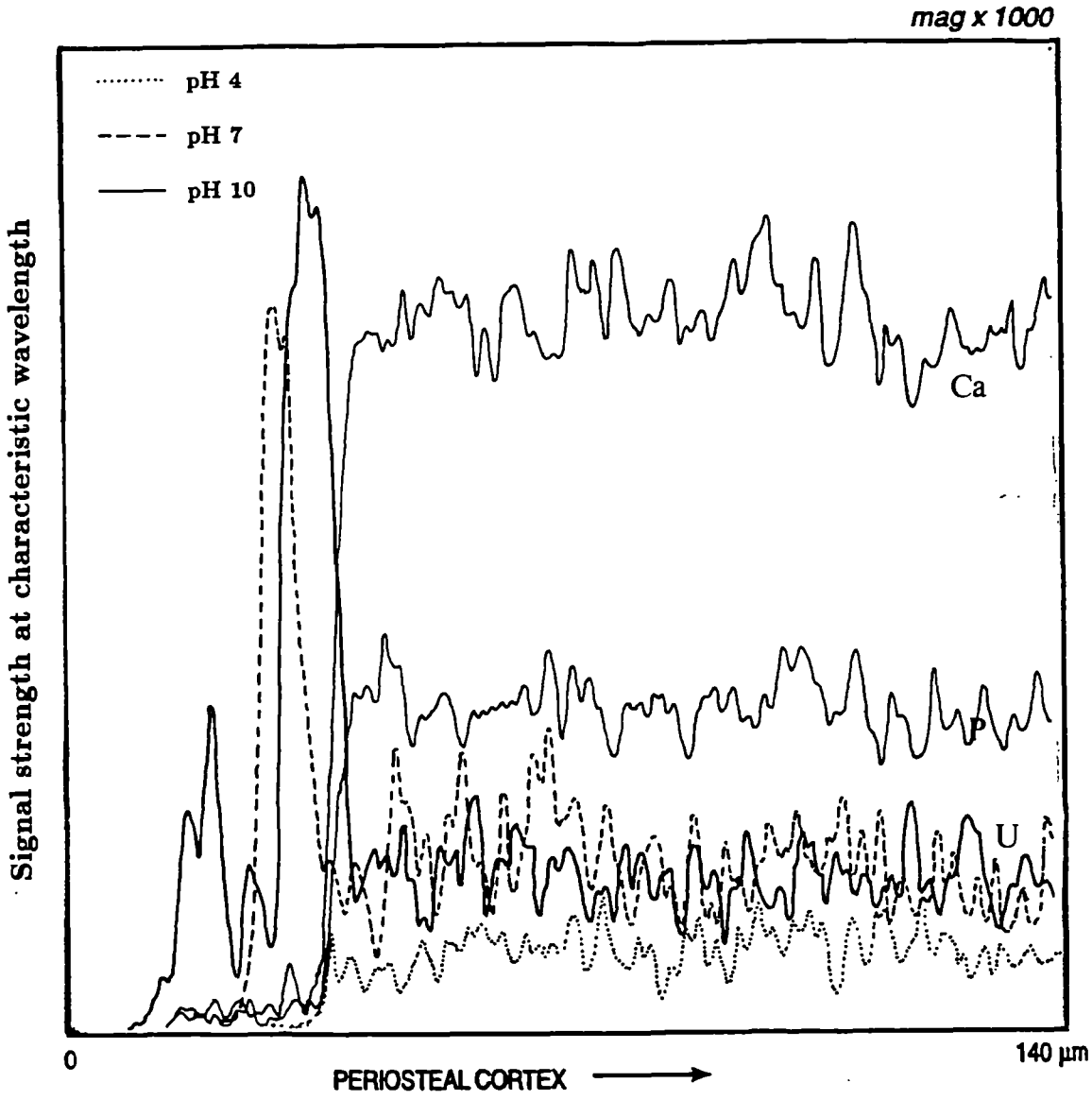

Cross-cortical distance (microns)

the uranium peak increased with the alkalinity of the immersion, confirming the pattern in figure 7.10.

So, bone immersed at **pH 10** showed similar uranium profiles to pH 7 samples with slight elevations in the peripheral cortical tissue peaking at the cortical surfaces. The level of uranium at these surfaces was considerably higher in pH 10 samples, while within the bone tissue itself higher at pH 7 (figure 7.11). Indeed, magnification (5000x) of the periosteal edge (figure 7.10) confirmed this general pattern: while more uranium was detected in pH 10 bone, *proportionately* less of it was actually associated with, or had penetrated into the cortex; rather, it was largely adhering to the surface.

A mapped area of the periosteal/medullary cortex magnified 750 times (figure 7.13) (again, lighter areas denoting higher elemental distribution) shows uranium predominantly lining the periosteal surface, with small traces throughout the cortex (these may simply be background). There was no indication of pore-filling. The majority of the uranium detected in this region was located external to the bone in an area that was clearly not part of the inorganic matrix since calcium and phosphorus were absent. It is possible that this area relatively rich in uranium may have represented remnant organic tissue (part of the periosteum).

The relative contributions of the organic and inorganic components to the uptake of uranium into bone had yet to be established. Certainly there were indications of uranium interaction with organic tissue at pH 10. Moreover, calcium/uranium ratios in the periosteal cortex, plotted in figure 7.14, were found to be variable with pH of immersion: ratios were lowest in bone immersed at pH 4, and highest in pH 7 samples. This, together with the cross-cortical uranium distributions plotted, indicated calcium-uranium exchange at least in neutral pH conditions.

7.4.3 Summary.

Quantitative analyses of bone and solution, together with qualitative cross-cortical profile analysis were not in agreement. Measurements of post-immersion solutions indicated an enhanced uranium uptake under more acidic conditions. Conversely, both total elemental and profile analyses of the bone revealed relatively low uranium levels in pH 4 immersions, with discrepancies arising as to whether neutral

Figure 7.12: Elemental maps of calcium, phosphorus and uranium distribution in the inner cortical region of whole bone immersed in 2240 ppm uranium solution at pH 7 for 2 weeks. Mag x200.

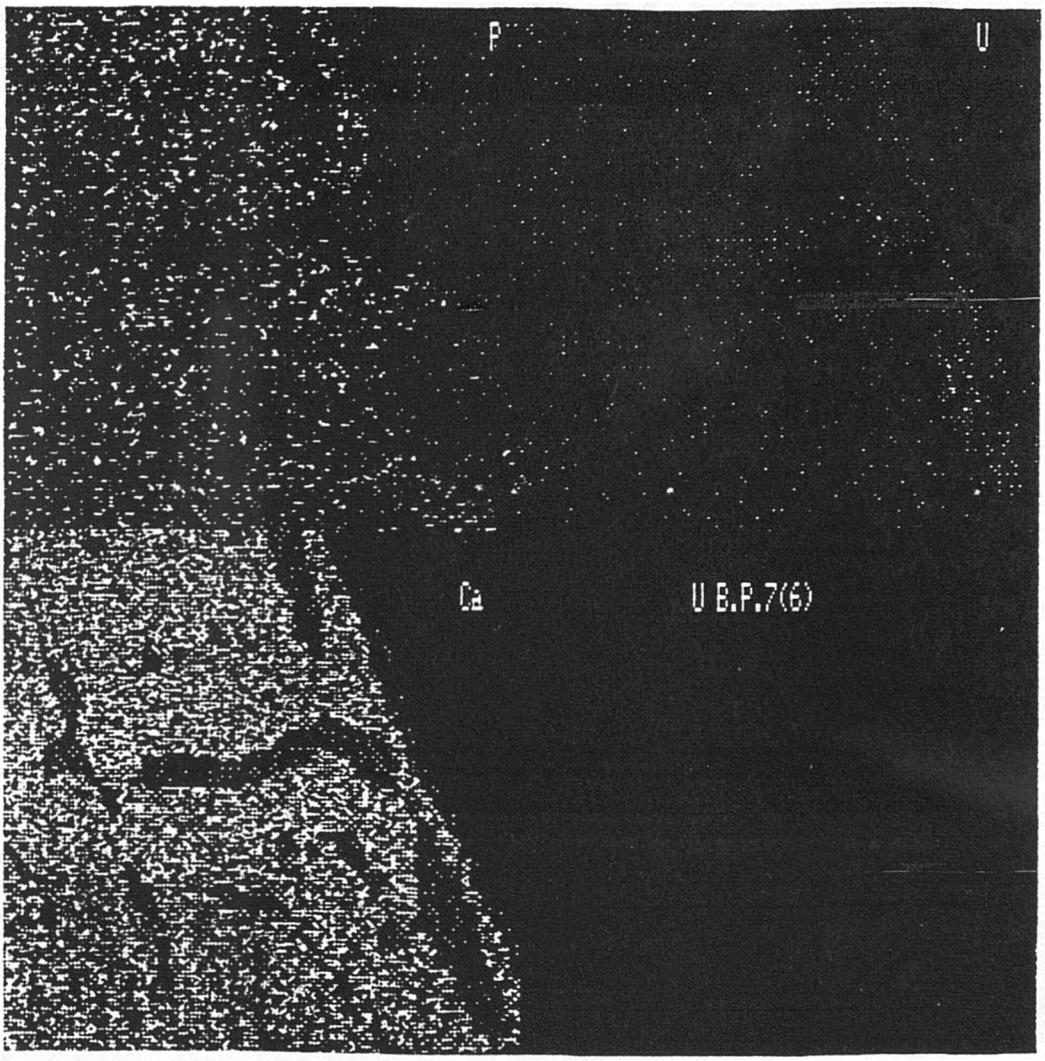

Figure 7.13: Elemental maps of calcium, phosphorus and uranium distribution in the outer cortical region of whole bone immersed in 1000 ppm uranium solution at pH 10 for 12 weeks. Mag x750.

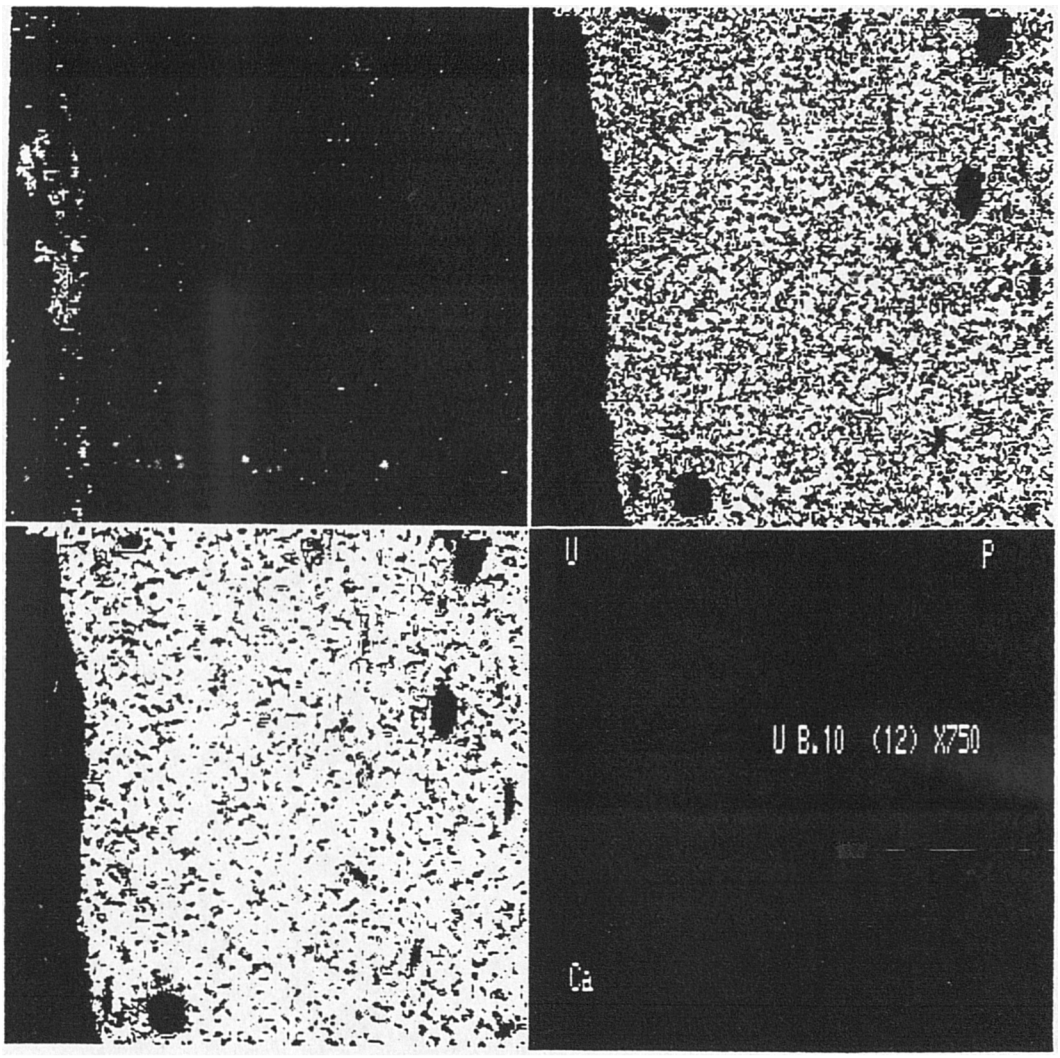

Figure 7.14: Calcium/uranium ratios in the periosteal cortex of whole bone immersed in 1000 ppm uranium solution for 12 weeks. Mag x1000.

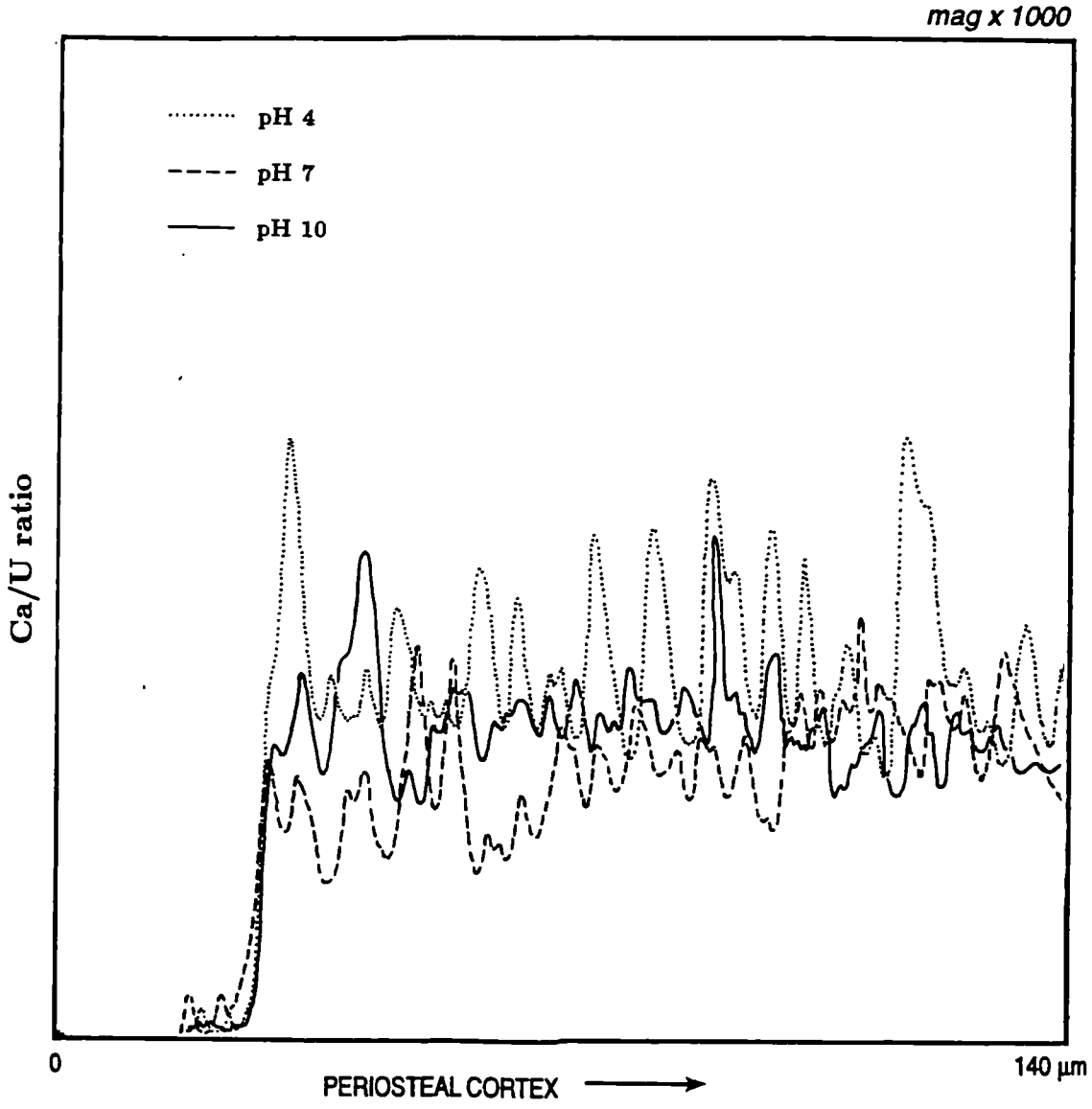

or alkaline conditions favoured uptake.

Comparison of uranium *distribution profiles* in whole bone immersed at variable pH found that little, if any, uranium was associated with bone at pH 4. While pH 10 bone revealed higher uranium levels than pH 7 at the immediate cortical surfaces, proportionately more uranium was located within the bone matrix at pH 7. This would suggest the predominance of surface adsorption processes at pH 10, possibly involving both organic and inorganic matrices, while at pH 7, ionic exchange mechanisms of interaction, as supported by calcium-uranium ratios across pH.

7.5 Uptake against Organic:Inorganic Ratio: Series III.

As in the earlier strontium study, the respective roles of the organic and inorganic components of bone in the uranium uptake mechanism were explored by comparing uranium distribution profiles in bone with varying organic:inorganic content. The effect of the pH of immersion on respective distribution patterns was also investigated.

7.5.1 Analysis of Solutions.

Table 7.5 shows calcium and uranium levels measured by AAS and LSC, respectively, in solutions buffered to either pH 4, 7 or 10, in which bone of variable organic content was immersed for 2 weeks. The original uranium concentration was 2240 ppm. As before, "B" denoted a uranium value at or below background readings. Values for whole bone immersions are shown again for direct comparison with hydrazine-treated and ashed samples (Appendix IIIa).

As in the corresponding strontium study, calcium levels were highest in immersing solutions that had contained ashed bone, followed by those containing hydrazine-treated bone because of the increased vulnerability of their exposed inorganic matrices. Calcium levels were observed to decline with the alkalinity of solution in all cases.

Uranium concentrations were highest in solutions containing whole bone across the pH range indicating that whole bone had taken up less uranium in all pH

Table 7.5: Calcium and uranium concentrations in immersing solutions containing bone of variable organic content at variable pH for 2 weeks.

Bone description	pH of immersion	[Calcium] ppm	[Uranium] ppm
Whole bone	4	142	B
	4	168	48
	7	13	132
	7	11	105
	10	1	110
	10	0	129
Hydrazine-treated	4	146	B
	4	131	B
	4	115	B
	7	14	38
	7	12	30
	7	15	56
	10	0	B
	10	1	B
	10	0	B
Ashed bone	4	220	19
	4	237	B
	4	245	B
	7	34	B
	7	38	B
	7	34	B
	10	0	20
	10	1	38
	10	0	46

"B" = value at or below background level.

regimes than samples with a lower organic:inorganic ratio. In fact, many of the remaining immersion solutions that had contained ashed and hydrazine-treated bone possessed uranium levels that were below background, suggesting almost complete removal of available uranium in the original solutions: these solutions represented pH 4 immersions (the exception being one of the pH 4 solutions for ashed bone where a 19 ppm uranium value was recorded, highlighting the variability of "within group" measurements). The main difference between solutions that had contained ashed and hydrazine-treated bone samples was that the highest uranium levels were measured in solutions maintained at pH 10 and pH 7, respectively. Thus, uranium was apparently taken up into ashed bone least readily at pH 10. On the other hand, hydrazine-treated bone was least effective in taking up uranium at pH 7. This observation suggested a differential contribution of the organic and inorganic components to uranium uptake according to the pH of the immediate environment.

7.5.2 Analysis of Bone.

7.5.2.1 Total elemental analysis: XRF.

Table 7.6 shows the averaged uranium/calcium ratios measured in whole, hydrazined and ashed bone samples immersed in 2240 ppm uranium solutions for 2 weeks at variable pH. The respective % oxide values for calcium, phosphorus and uranium are included in Appendix IIIa for uranium-exposed bone and in Appendix IIc for control immersions in buffered water.

Uranium/calcium data for control (pure water) immersions are included in table 7.6 for comparatory purposes, but it was noted that uranium concentrations here were below the minimum acceptable detection limit for the sensitivity of the XRF technique (approximately 6 ppm).

Uranium concentrations and uranium/calcium ratios were lower in whole bone than in ashed and hydrazine-treated samples; levels in the latter were marginally higher for all pH immersions. All ppm values for uranium, particularly for hydrazine-treated bone were very high (see Appendix IIIa).

The pattern of uranium/calcium ratio across pH was different according to the

Table 7.6: Average Uranium/calcium ratios for bone samples of varying organic content immersed at variable pH, measured by XRF analysis.

Immersing medium	Bone description	pH of immersion	U/Ca ratio (x 10^{-4})
Buffered pure water	Whole	4	0.080
		7	0.065
		10	-
	Hydrazined	4	0.042
		7	-
		10	0.014
	Ashed	4	0.064
		7	0.181
		10	0.003
2240 ppm uranium soln.	Whole	4	2.9
		6	232.0
		7	189.7
		8	114.2
		10	115.4
	Hydrazined	4	334.5
		7	293.7
		10	314.9
	Ashed	4	299.0
		7	282.5
		10	251.3

Missing values: uranium levels not measurable.
Oxide values (%CaO) corrected for *elemental* ratios (U/Ca)

bone condition. In whole bone immersions, the lowest ratios were seen at pH 4, followed by pH 10, with highest values at pH's 6 and 7. This suggested an enhanced uranium uptake around neutral pH conditions.

However, a very different pattern was revealed for ashed and hydrazine-treated bone samples. Both absolute uranium values and uranium/calcium ratios were highest in pH 4 immersions, indicating that acidic conditions might promote uranium uptake into bone with a lower organic:inorganic content.

The relative effect of neutral and alkaline conditions on uranium uptake was apparently different in ashed and hydrazine-treated samples. Uranium/calcium ratios in the former were higher at pH 7, while in the latter, pH 10.

Clearly, the pH of the surrounding medium was able to influence the interactive potential and thus the relative contribution of the organic and inorganic components in uranium uptake into bone.

7.5.2.2 Micro-analysis of bone: EPMA.

(a) pH 4 immersions.

At pH 4, little uranium was found in both ashed and hydrazine-treated bone in much the same way as for whole bone. However, interesting variations in uranium distribution and behaviour were observed in pH 7 and 10 immersions.

(b) pH 7 immersions.

At pH 7, **ashed bone** possessed a higher uranium content in terms of both cortical surface adsorption and penetration into the cortex than either whole or hydrazine-treated samples. This is illustrated in figure 7.15 in the periosteal region of bone samples immersed in 2240 ppm solutions for 2 weeks. The pattern of distribution indicated the occurrence of surface adsorption phenomena arising from the increased porosity and nature of ashed bone, offering a far greater surface area for interaction with the immersing solution. However, a digimap of an Haversian system in the mid-cortex of this ashed bone sample (mag x650) showed a relatively homogeneous distribution of uranium throughout the matrix, with no apparent concentration in and around lacunae and canals (figure 7.16) (lighter areas indicating higher concentrations). This observation may either indicate that

Figure 7.15: Uranium distribution profiles in the periosteal cortex of bone with variable organic content immersed in 2240 ppm uranium solution at pH 7 for 2 weeks. Microscope operated at mag x5000.

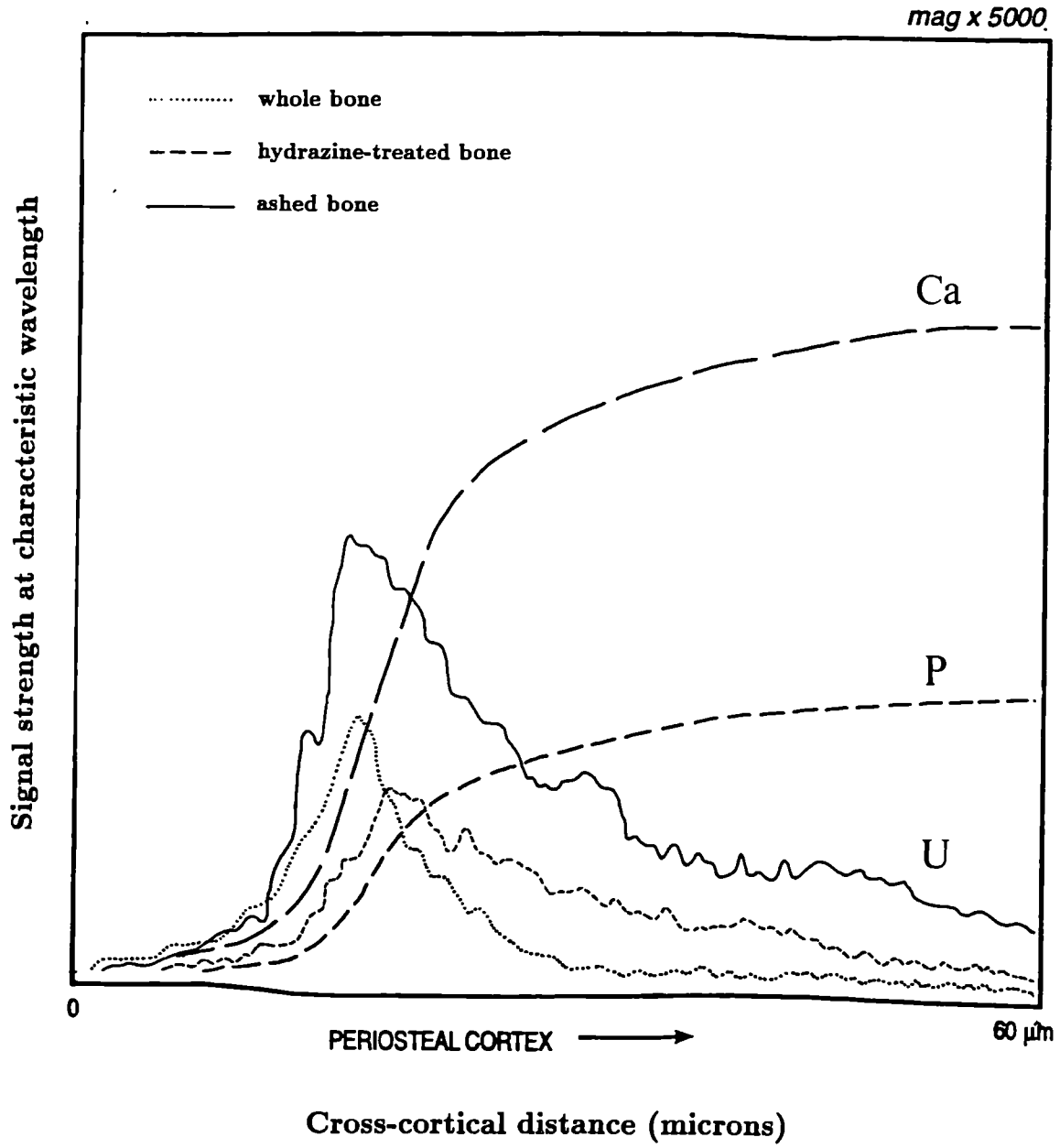

the uranium levels in the sample were simply below the detection limit of the instrument (approximately 500 ppm), or suggest that, since there was no indication of "passive" pore-filling, extensive surface adsorption mechanisms and/or actual incorporation into the inorganic lattice had occurred.

The uranium profile in the periosteal region of **whole bone** indicated both cortical surface adherence and some penetration into the cortical tissue itself (figure 7.15). In contrast, **hydrazine-treated bone** showed little periosteal association but rather more extensive cortical penetration, intermediate to that of ashed and whole bone. Therefore, the extent (in terms of distance and quantity) of uranium diffusion into the cortical tissue appeared to correlate with the porosity and cortical surface area properties of the bone sample, increasing with progressive removal of the organic fraction. The pattern of uranium distribution observed at the periosteal surface was less clear: uranium adsorption was observed in both ashed and whole bone but not hydrazine-treated bone. This might suggest that uranium was adsorbed most effectively by the inorganic matrix (hence the peak in ashed bone), but this would not explain the lack of adsorption in hydrazine-treated material whose inorganic matrix was more exposed than that of whole bone, thus offering a larger surface area for interaction.

Figure 7.17 shows the calcium/uranium ratio distributions in the periosteal region for each bone sample, this time immersed in 1000 ppm uranium solutions for 12 weeks (both original and processed images are shown). The ratio in whole bone was generally higher in this region except at the cortical edge. Here ashed bone possessed the highest ratio, despite the high uranium observed at the edge: this would suggest the predominance of adsorption processes in operation, rather than calcium-uranium heterionic exchange, since a corresponding reduction in calcium levels would be expected in the case of the latter. The calcium/uranium ratio in hydrazine-treated bone was found to be highest in the peripheral cortex, again where its uranium levels were most elevated.

(c) pH 10 immersions.

At pH 10, a very different pattern of uptake was observed, as illustrated in figure 7.18. **Ashed bone** was the least effective in interacting with uranium, particularly at the periosteal surface. **Whole bone** appeared to possess most uranium at

Figure 7.16: Elemental maps of calcium, phosphorus and uranium distribution in an osteonal microstructure located in the mid-cortical region of ashed bone immersed at pH 7. Mag.x650

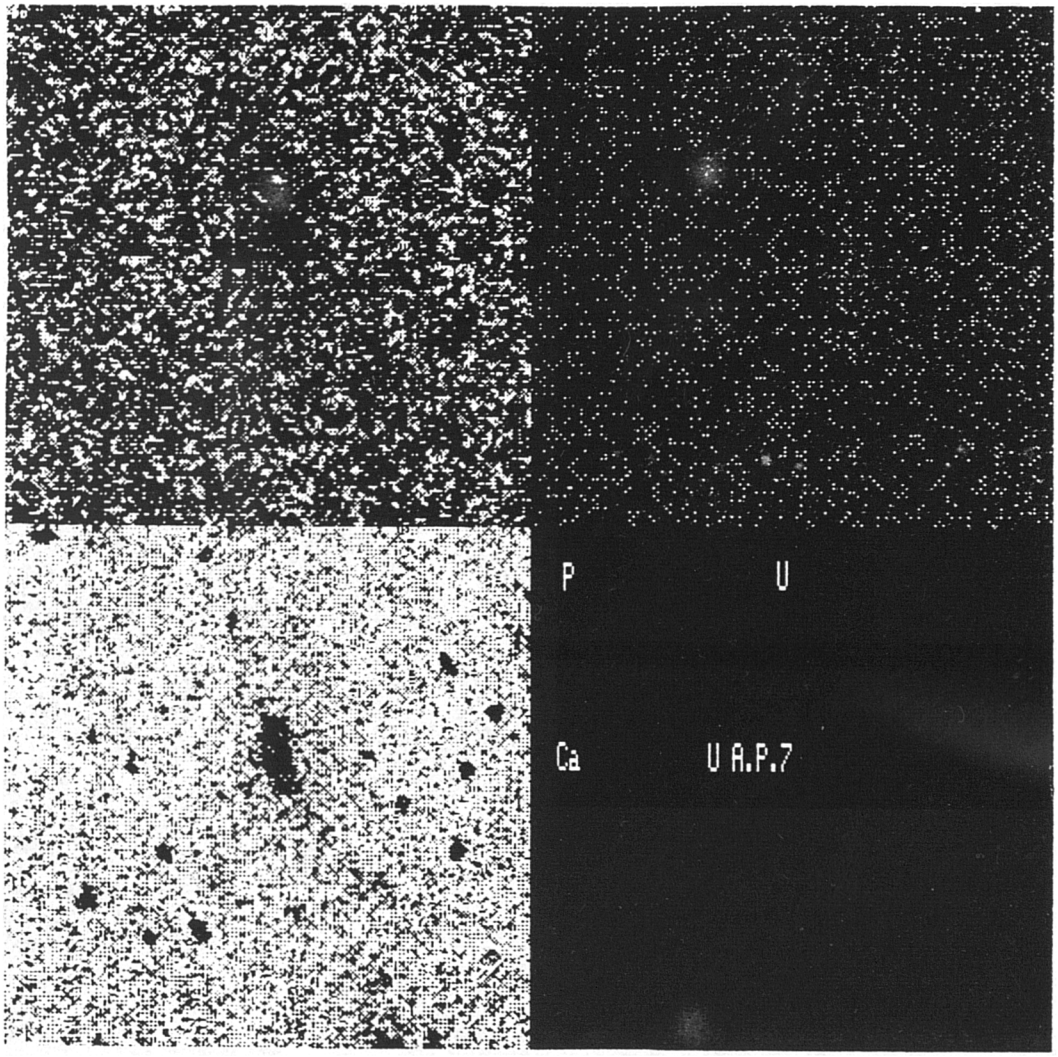

Figure 7.17: Calcium/uranium ratios in the periosteal cortex of bone with variable organic content immersed in 1000 ppm uranium solution for 12 weeks. Microscope operated at mag. x1000.

(a) original image

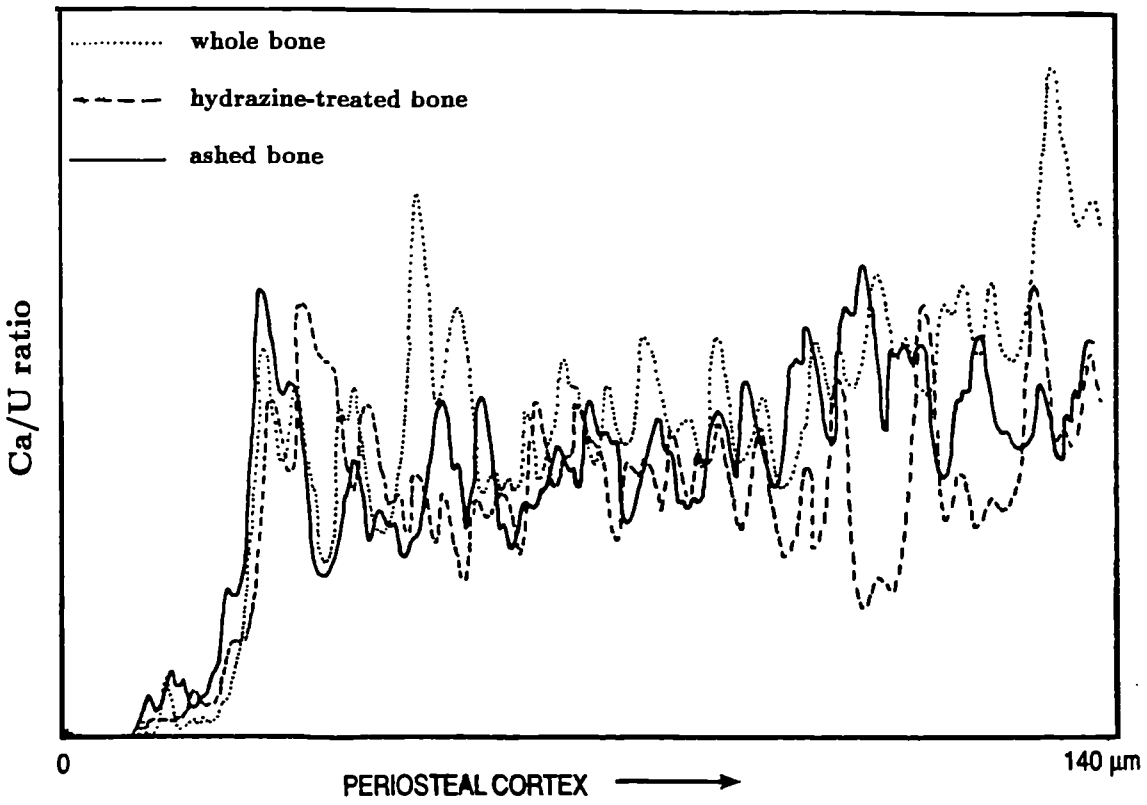

(b) processed ('smoothed') image

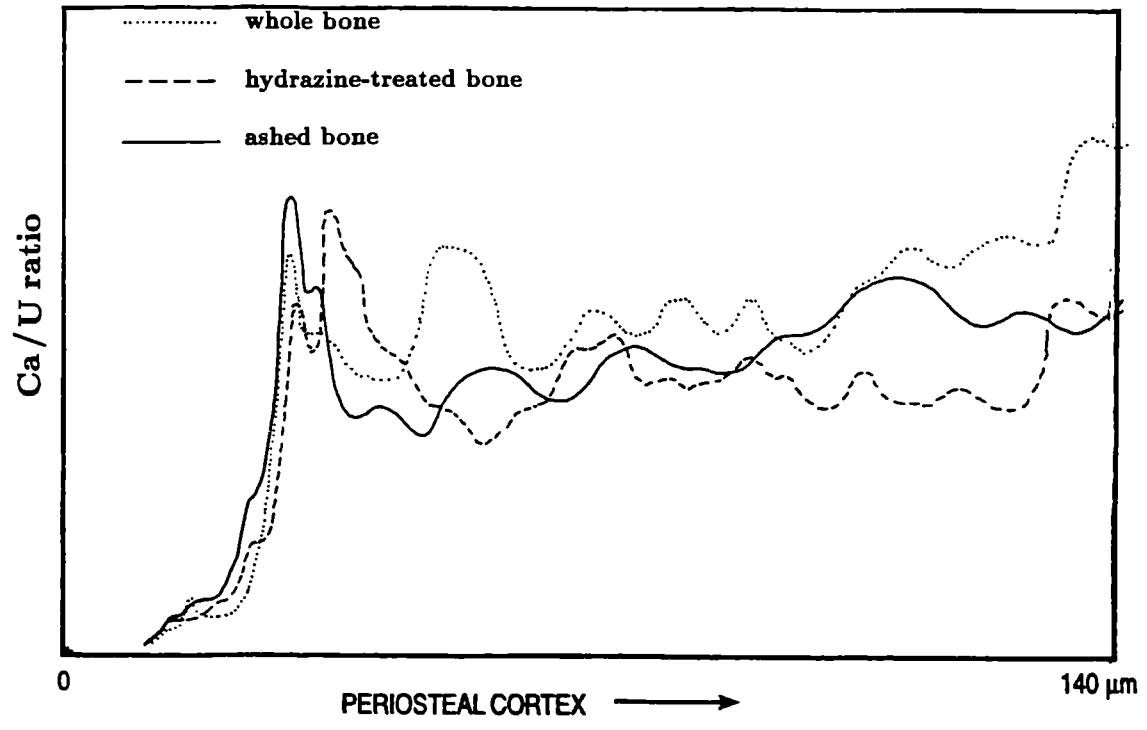

the immediate surface, suggesting a role for the organic fraction in uranium-bone interaction under more alkaline conditions. A similar intracortical distribution was observed for whole and hydrazine-treated bone.

7.5.3 Summary.

The data presented in this section do not arrive at any one clearly-defined trend in uranium uptake against organic content. The major discrepancy lies with the degree of uranium uptake in acidic conditions: quantitative analysis of immersing solutions found that uptake was apparently enhanced at pH 4, and XRF analysis of the bone confirmed this for ashed and hydrazine-treated samples but not for whole bone whose uranium concentration was lowest at pH 4. In contrast, EPMA data clearly demonstrated little if any uranium uptake at pH 4.

All analytical approaches did agree on the relative uptake patterns observed at neutral and alkaline pH for ashed and hydrazine-treated bone: data seemed to indicate that uranium more readily interacted with the inorganic matrix at neutral pH, while in more alkaline conditions was more likely to interact with the organic component.

Certainly, discrepancies in uranium distribution at the cortical surface and across the cortex, both within and between samples in their respective pH environments leads to the conclusion that the relative contribution of the organic and inorganic components in the uranium uptake process changes according to the pH of the environment.

Analytical approaches thusfar on bone material immersed in uranium solutions encountered a major problem which limited the amount of useful qualitative and quantitative data that could be collected: uranium uptake was observed predominantly and, in some cases, exclusively at the cortical edges of bone, penetrating the cortical tissue only a small distance. Hence, the analytical techniques that tackled the strontium-exposed samples with relative ease were less appropriate for objectively examining localised uranium distribution. A more detailed study of the cortical edges of respective samples was required using a more sensitive technique with the facility to examine much smaller areas of tissue, both quantitatively

Figure 7.18 Uranium distribution profiles in the periosteal cortex of bone with variable organic content immersed in 2240 ppm uranium solution at pH 10 for 2 weeks. Microscope operated at mag x5000.

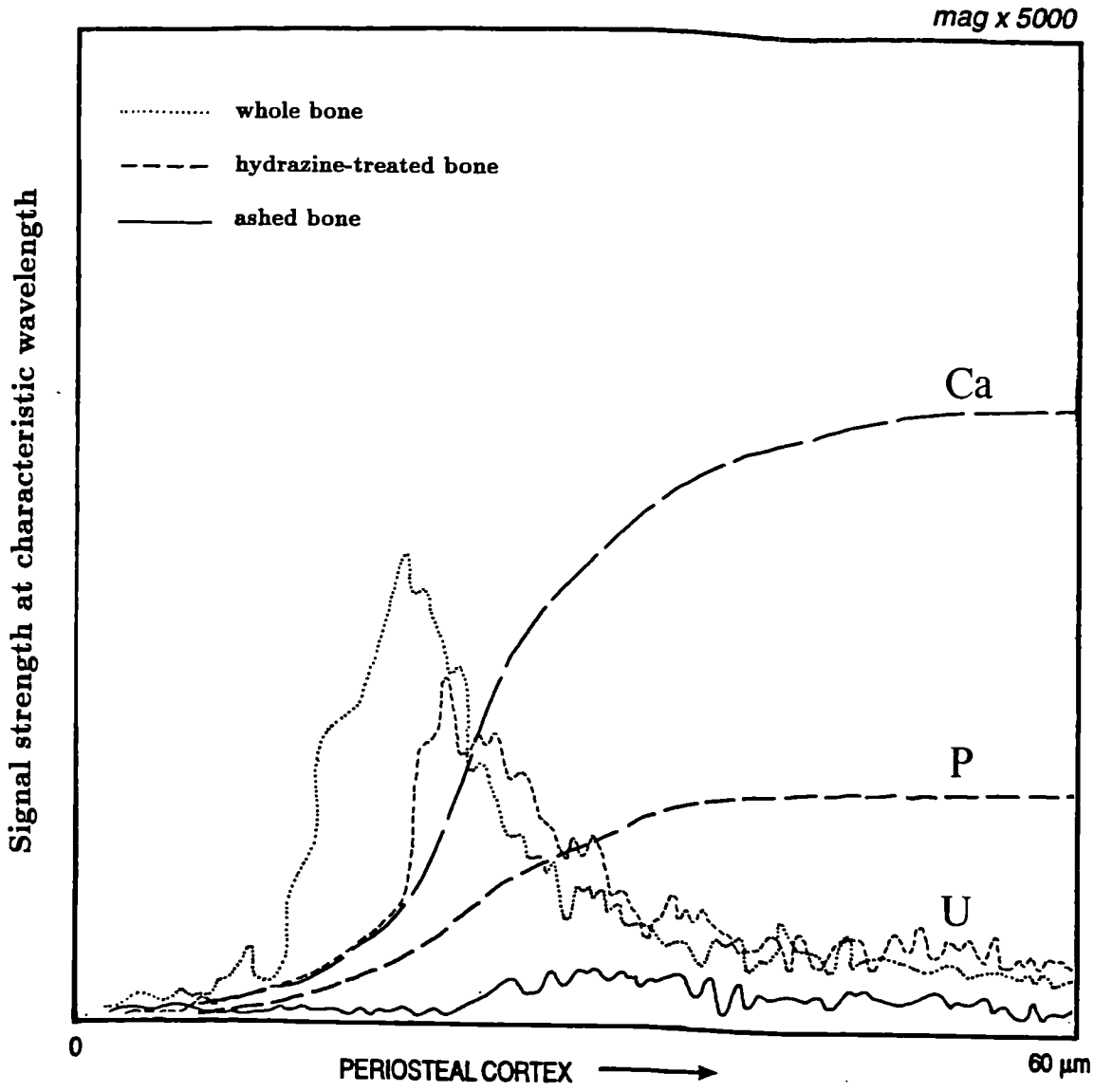

and qualitatively. For this reason, detailed proton microprobe analysis of uranium-exposed bone was carried out and the results are described in the following section.

7.6 Proton Microprobe Analysis: Series III.

Since detailed analysis using the proton microprobe was used only on a selection of samples from Series III uranium immersions and did not apply on such a wide scale as techniques common to both strontium and uranium uptake studies (such as EPMA), it seemed more appropriate and more convenient to include the methodology here.

7.6.1 Methodology.

One example of whole, hydrazine-treated and ashed bone each immersed in pH 4, 7 or 10 uranium (2240 ppm) solutions from Series III (thus a total of 9 samples) were further examined using simultaneous PIXE and RBS analysis. The aim of this investigation was to accurately measure the respective depth of uranium penetration into the cortical tissue of each sample. A proton microbeam with beam energy 2MeV and a diameter approximately 12 microns was used to scan the samples. Normal incidence and a backscattering angle of 165°was set for the RBS analysis geometry, with simultaneous PIXE. By varying the beam steering voltage, the samples were scanned in a stepwise fashion using 3 micron intervals.

All PIXE spectra were normalised to the same charge. Uranium X-ray signals $L_{\alpha 1}$ (13.6keV), $L_{\beta 2}$ (16.4keV) and $L_{\beta 1}$ (17.16keV) were located at channel numbers 314, 374 and 390, respectively. In addition, K_{α} (3.7keV) calcium signals were located at channel 105 and K_{β} (4.0keV) at channel 111.

With regard to the RBS spectra, U, Ca, P, O and C surface signals were located at channel numbers 422, 389, 378, 335 and 308, respectively. It was anticipated that while Ca and P signals would provide information concerning the inorganic matrix, O and C signals would give some indication of the organic material present.

The presence of uranium signals in RBS spectra was consistent with those in corresponding PIXE spectra. Figures 7.19 and 7.20 are examples of typical RBS and PIXE spectra for samples with and without uranium content, respectively.

Figure 7.19 a,b: Typical (a) RBS and (b) PIXE spectra of control bone sample (no uranium).

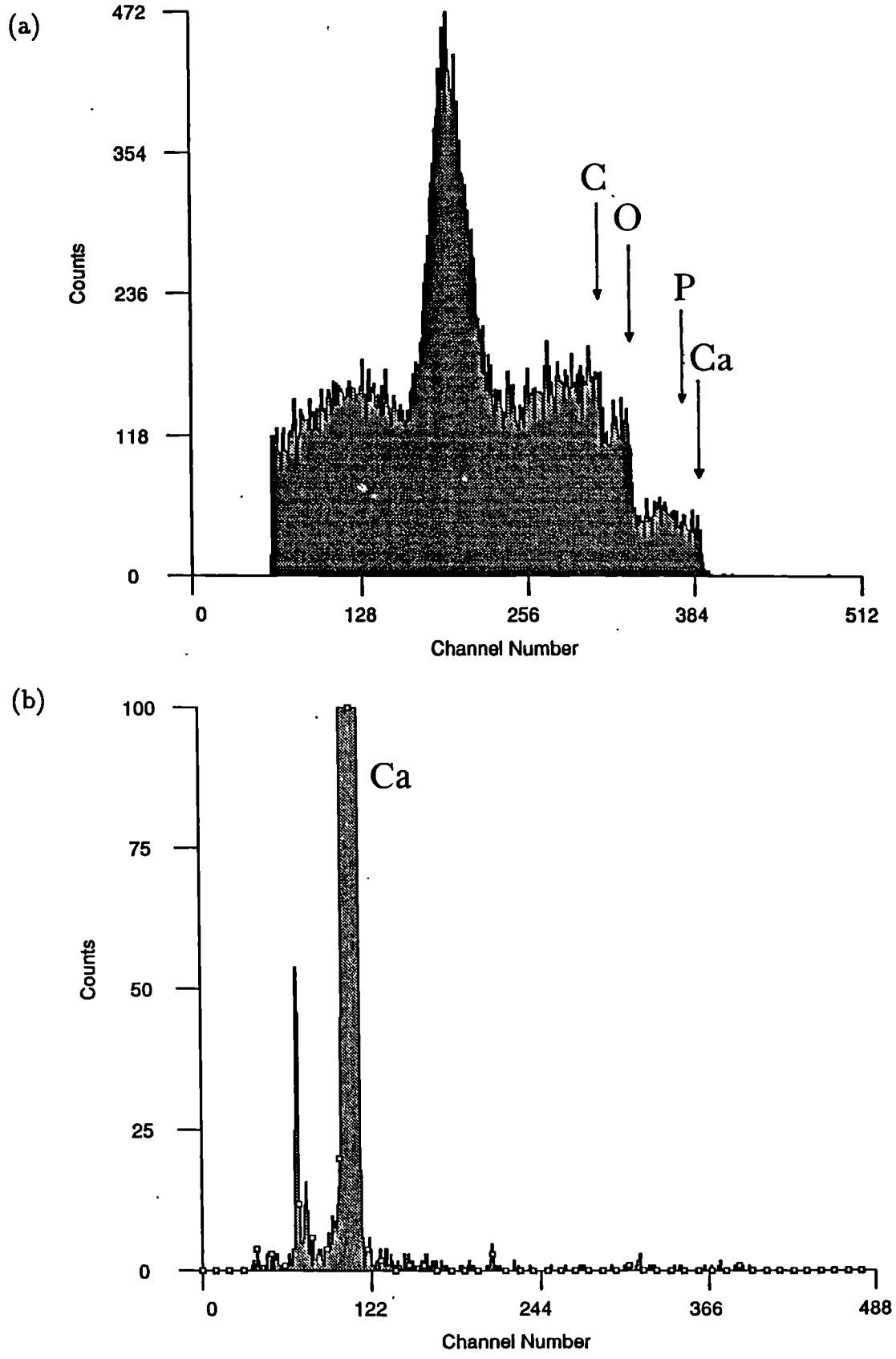

Figure 7.20 a,b: Typical (a) RBS and (b) PIXE spectra of bone sample containing uranium.

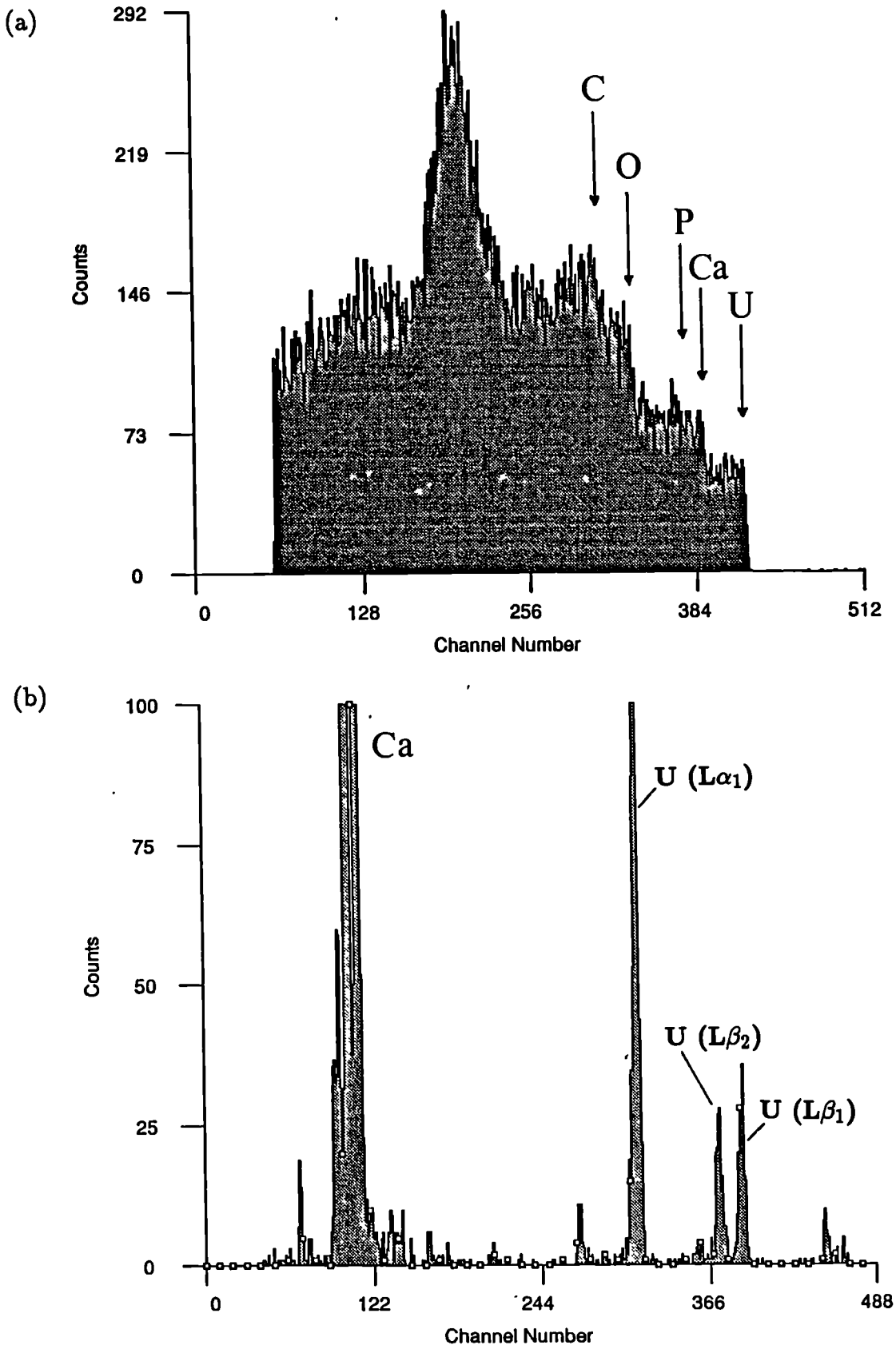

From the PIXE spectra, the counts within the regions 'channel no.s 370-401' and 'channel no.s 304-320' were integrated where the uranium X-rays were found. These two regions were chosen to exclude Sr, Y and Zr K-lines, which were observed in some samples. During measurement, the beam began scanning at a position near the interface between the bone and resin where minimum acceptable calcium counts were obtained. The beam was moved at incremental distances of 3 microns towards the bone material itself. Calcium profiles were plotted with reference to the beam position, determined from electronic scan values and the total calcium counts within the region (channels 89-124). The edge of the bone was determined from an abrupt change in the calcium signal, and if this could not be clarified the sample was subsequently examined using high power light microscopy to view the beam trace (only slightly visible).

In order to eliminate any inconsistencies in percentage yield, the U to Ca ratio distribution was plotted for each sample, thus normalising uranium distribution to the calcium signal. In this way, 'real' trends in uranium distribution across samples could be observed, irrespective of how much of the beam fell on the resin.

Reliable quantitative measurement of uranium levels was obtained by integrating PIXE and RBS data: respective data are found in Appendix IIIc(i). By comparing uranium and calcium signal heights, the percentage U/Ca atomic ratio could be deduced. Quantification using RBS data was to a certain extent limited because there were only 10 channels between the calcium and phosphorus signals in the RBS spectra and with high concentrations of uranium the background effect on the calcium signals was very high.

The percentage U/Ca atomic ratio was also obtained from the PIXE spectra. Again there were limitations here because uranium is a good absorber of the calcium X-rays and hence the calcium signal would drop as the uranium concentration increased. PIXE and RBS systems were correlated to define the scale factor or absorption correction:

$$S = R_{RBS}/R_{PIXE}$$

where R_{RBS} and R_{PIXE} are the U/Ca atomic % obtained from RBS and PIXE, respectively.

Figure 7.21: Graph of scale factor against RBS U/Ca atomic ratio data.

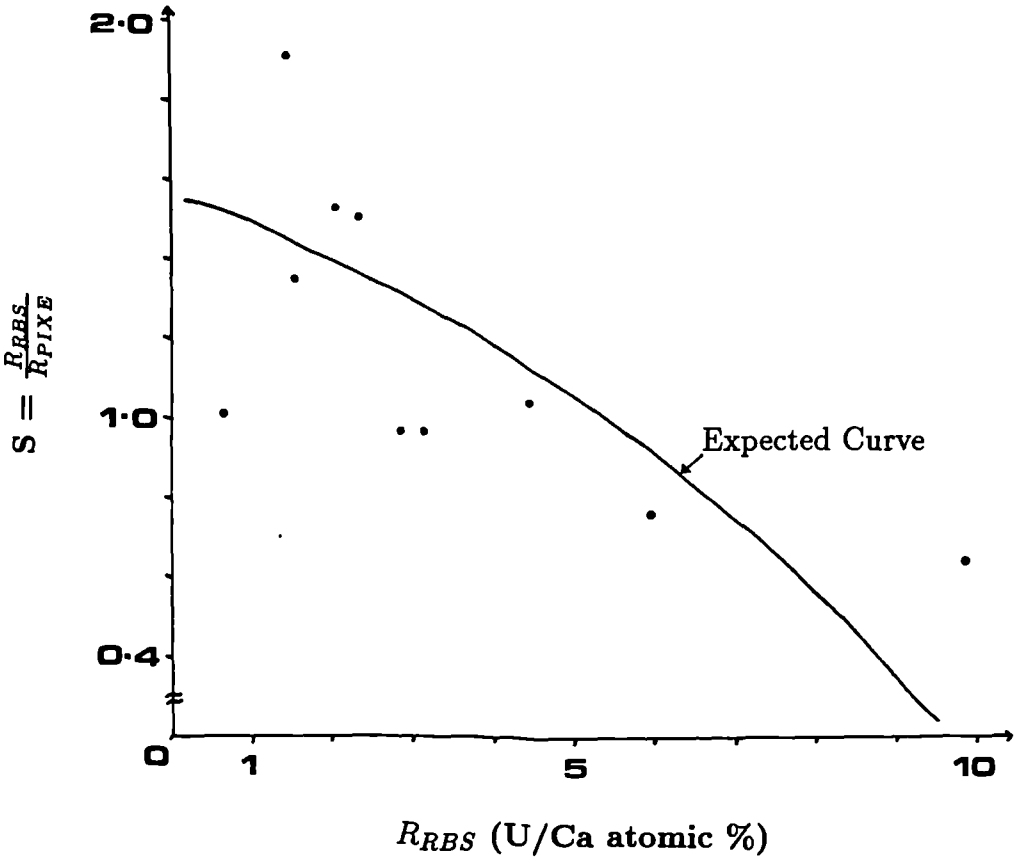

S versus R_{RBS} plot (figure 7.21) is shown for selected spectra. The expected curve demonstrates that as the uranium atomic % increased, the absorption correction would vanish. However, from the S versus R_{RBS} plot it can be seen that for some experimental data with similar U atomic %, the variation of S was as high as a factor of 1.9. Such variation was probably due to the variability of the sample material: whilst the proton microbeam for RBS looks at the surface of the sample, it penetrates relatively deep into the sample for PIXE analysis, thereby increasing the potential for absorption phenomena. Thus, the inhomogeneity of bone and differences in the organic content probably caused these variations in absorption. Spectra 8f (figure 7.22) for example, representing a scan of whole bone immersed

at pH 10, had an R_{RBS} = 1.01 atomic % and S = 0.24 (see table 7.7), which was not in accordance with the expected value. In fact, comparing the whole bone sample in figure 7.22 with an ashed example (fig 7.23), far less carbon was observed in the former (noting the difference in the y-axis scale), demonstrating a clear difference in the material matrix and thus an expected difference in the value for S. The ashed sample in figure 7.23 showed a large non-Rutherford carbon signal (located between channels 128 and 256) at a depth such that the beam energy was approximately 1.6 MeV: this signal probably represented a resonance factor, and was observed in the majority of RBS spectra (Figures 7.19a, 7.20a, 7.22a, 7.24). Moreover, the variability of matrix *within* samples is illustrated in figure 7.24 which shows two RBS spectra for consecutive scans i.e. adjacent areas of cortex in a hydrazine-treated bone example: the peak(s) in the channel no. 128-256 region are very different.

Despite the variability in relative sensitivity of Ca/U X-rays, as shown by the range of S values in table 7.7, an average scale factor value of 1 was used for the plots shown in subsequent figures for ease of comparison.

7.6.2 Results.

Quantitative PIXE data are found in Appendix IIIc, and are plotted in subsequent figures here.

In accordance with EPMA data, no uranium was found in either whole, hydrazined or ashed bone samples immersed in pH 4 solutions: uranium peaks/signals were absent in both PIXE and RBS spectra (figure 7.19).

In contrast, consecutive scans of all bone types immersed in neutral and alkaline pH solutions revealed the presence of uranium at the cortical edge and in the immediate outer cortex. Figure 7.25 shows consecutive PIXE spectra (incremental distance 9 microns) taken for ashed bone immersed at pH 10. Spectra (a) represented an area at the bone-resin interface i.e. adjacent to the edge of the bone sample: only a slight calcium peak was present but a set of uranium peaks were clearly visible. This represented either simple surface adsorption or uranium infilling of the gap between the bone and resin. Spectra (b) showed a clearer calcium signal,

Table 7.7: Selected RBS spectra for cross-checking U/Ca atomic % with those of PIXE.

RBS file	H_U	H_{Ca}	R_{RBS} (%)	R_{PIXE} (%)	Scale factor S
thick 2bf.dat	52.00	25.00	9.90	15.57	0.64
2bk.dat	19.60	15.50	6.03	7.90	0.76
2bn.dat	4.75	31.15	0.73	0.70	1.04
2mf.dat	7.45	23.45	1.52	0.80	1.90
3m.dat	33.75	54.85	2.89	3.00	0.96
7g.dat	24.25	25.75	4.49	3.72	1.21
7k.dat	15.70	23.40	3.20	3.33	0.96
8f.dat	4.80	22.60	1.01	4.15	0.24
9h.dat	7.95	17.75	2.14	1.41	1.52
9k.dat	6.35	18.85	1.61	1.20	1.34
9e.dat	7.65	14.95	2.44	1.63	1.50

where H_U = average height of the 20 channels (401-420) representing U

H_{Ca}= average height of the 10 channels (379-388) representing Ca

and sample 2 = hydrazine-treated bone immersed at pH 7, sample 3 = ashed bone at pH 7, sample 7 = hydrazine-treated bone at pH 10, sample 8 = whole bone at pH 10, sample 9 = ashed bone at pH 10.

Finally, R_{RBS} and R_{PIXE} can be defined in more detail as follows:

$$R_{RBS} = \frac{20^2}{92^2} \times \frac{H_U}{H_{Ca}} \times \frac{8.41}{8.331}$$

and,

$$R_{PIXE} = \frac{U(L\alpha_1 + L\beta_1 + L\beta_2)}{Ca(K\alpha + K\beta)} = \frac{\int_{370}^{401} + \int_{304}^{320}}{\int_{89}^{124}}$$

Figure 7.22a: RBS spectra for whole bone immersed in uranium solution at pH 10.

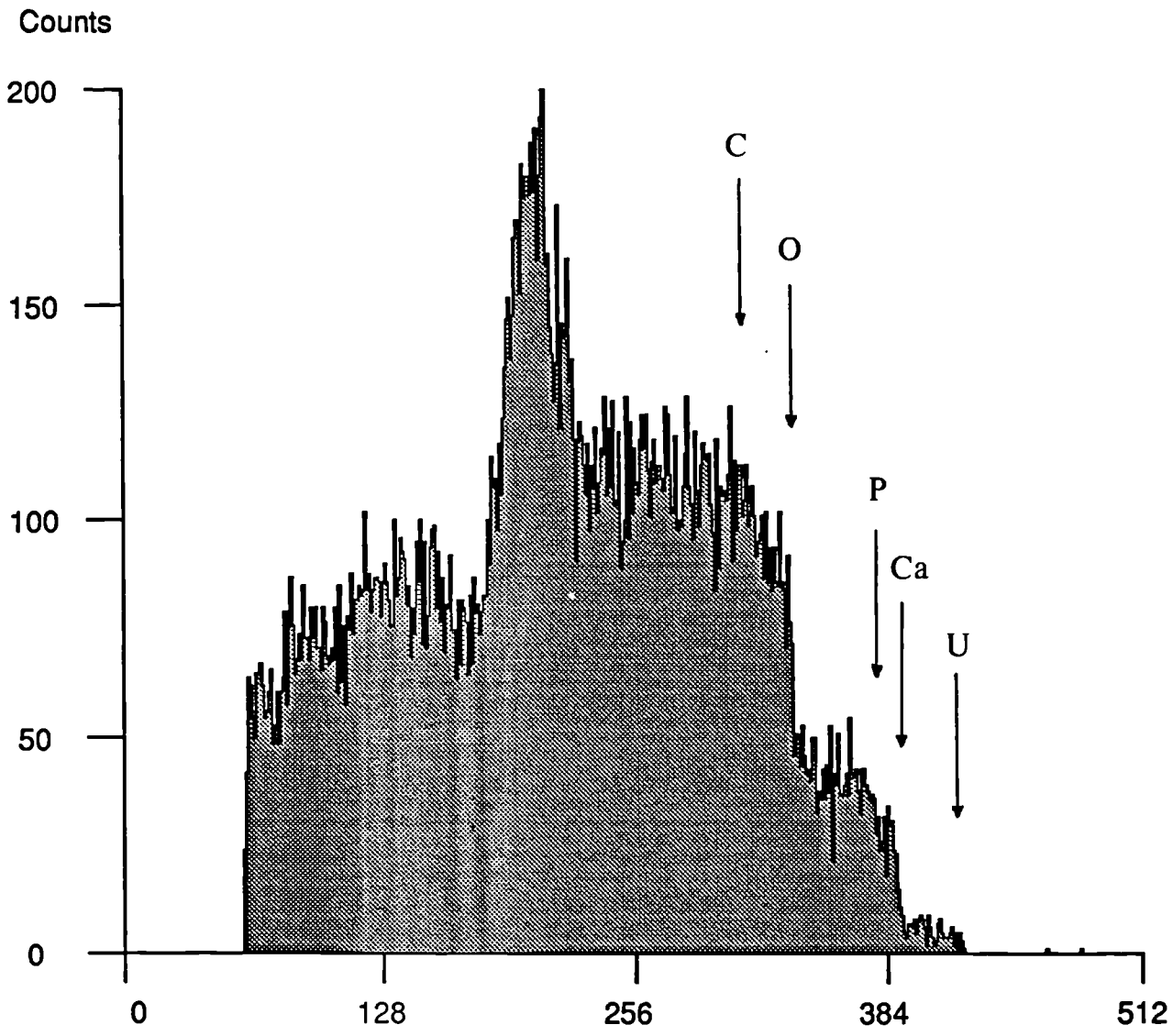

Channel Number	1	2	3	4	5	6	7	8	9	10	11	12	13	14	15	16	17	18	19	20
0	0	0	0	0	0	0	0	0	0	0	0	0	0	0	0	0	0	0	0	0
20	0	0	0	0	0	0	0	0	0	0	0	0	0	0	0	0	0	0	0	0
40	0	0	0	0	0	0	0	0	0	0	0	0	0	0	0	0	0	0	0	24
60	42	64	62	55	50	65	65	67	62	55	56	61	66	49	53	61	49	61	64	79
80	58	79	87	76	65	68	74	68	85	73	73	68	80	73	80	71	71	66	80	77
100	69	67	71	68	80	61	85	63	76	58	78	75	88	74	82	82	85	83	84	102
120	84	88	79	84	87	87	86	78	86	90	86	82	76	76	100	83	87	96	93	91
140	81	85	69	80	74	95	86	100	72	95	71	78	94	98	99	80	93	77	87	70
160	81	80	92	75	75	64	82	67	82	80	77	65	83	67	87	79	81	74	79	83
180	83	100	90	115	108	110	98	118	106	124	136	147	152	138	148	166	170	170	153	183
200	175	180	180	176	188	177	191	161	180	194	201	160	162	145	139	128	137	173	122	146
220	143	144	161	133	138	119	91	119	123	120	113	106	118	98	113	108	122	102	109	117
240	116	129	106	122	108	128	104	105	121	89	95	100	129	96	123	102	117	109	106	119
260	125	117	125	112	101	114	119	109	113	113	110	107	127	125	111	102	103	120	98	100
280	99	108	116	129	108	104	96	121	107	99	113	118	115	115	116	104	97	84	119	89
300	108	106	107	105	111	127	91	114	98	113	113	101	105	113	99	102	108	101	92	95
320	97	101	87	102	86	94	84	94	86	85	102	86	84	71	92	77	72	46	51	50
340	44	53	46	42	43	40	50	50	33	38	36	43	36	44	38	53	22	42	39	51
360	37	37	39	42	37	55	42	41	43	38	33	43	43	39	38	36	37	36	28	32
380	24	26	32	18	34	30	31	24	23	15	11	9	5	4	7	7	6	8	5	8
400	9	8	6	2	9	6	4	2	3	7	8	5	4	4	4	5	6	2	5	1
420	5	3	1	0	0	0	0	0	0	0	0	0	0	0	0	0	0	0	0	0
440	0	0	0	0	0	0	0	0	0	0	0	0	0	0	0	0	0	0	0	0
460	0	0	0	0	1	0	0	0	0	0	0	0	0	0	0	0	0	0	0	0
480	0	1	0	0	0	0	0	0	0	0	0	0	0	0	0	0	0	0	0	0
500	0	0	0	0	0	0	0	0	0	0	0	0								

Figure 7.22b: PIXE spectra for whole bone immersed in uranium solution at pH 10.

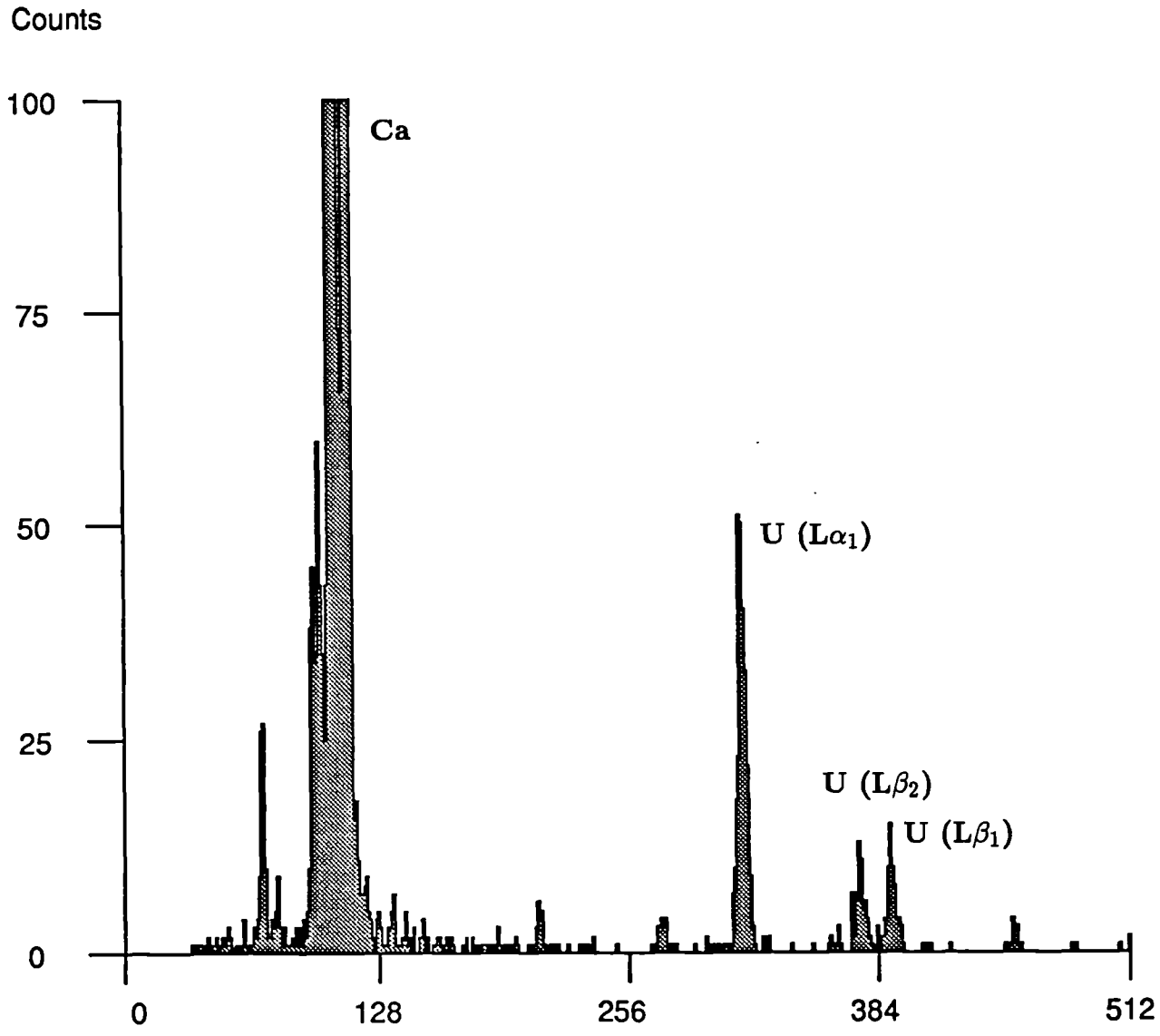

Channel Number	1	2	3	4	5	6	7	8	9	10	11	12	13	14	15	16	17	18	19	20
0	0	0	0	0	0	0	0	0	0	0	0	0	0	0	0	0	0	0	0	0
20	0	0	0	0	0	0	0	0	0	0	0	0	0	1	1	0	1	1	1	0
40	1	2	0	1	1	2	0	1	2	1	2	3	2	0	0	1	1	0	1	4
60	1	0	1	1	3	2	4	9	26	27	10	2	2	4	3	5	9	3	1	3
80	1	1	1	2	1	3	1	3	1	4	2	5	10	38	45	34	35	60	43	35
100	25	43	149	705	1996	2569	1430	391	73	66	289	585	638	302	113	16	18	11	7	7
120	8	9	5	4	2	0	4	5	3	1	1	1	3	3	5	7	1	1	1	2
140	2	5	1	2	0	3	0	0	2	2	4	0	2	0	0	1	1	2	2	1
160	0	1	2	0	2	1	0	0	0	0	1	0	2	0	0	2	1	0	1	0
180	1	1	1	0	1	0	1	0	3	1	0	1	0	1	0	1	0	2	1	0
200	0	0	0	0	1	0	1	1	3	6	4	5	1	0	0	1	0	1	0	1
220	0	0	0	0	1	0	0	0	0	0	1	1	0	1	1	0	0	2	0	0
240	0	0	0	0	0	0	0	0	0	1	0	0	0	0	0	0	0	0	0	0
260	0	0	0	0	0	0	0	0	1	0	0	3	3	4	3	4	1	0	1	0	1
280	0	0	0	0	0	0	0	0	0	1	0	0	0	0	0	2	1	0	1	0
300	0	1	0	0	1	1	1	0	1	7	10	18	23	51	50	40	33	22	9	3
320	1	0	0	0	2	0	0	2	0	0	0	0	0	0	0	0	0	0	0	1
340	0	0	0	0	0	0	0	0	0	0	1	0	0	0	0	0	0	0	1	2
360	1	1	1	3	1	0	0	0	0	0	7	2	7	6	13	11	5	6	4	2
380	1	0	0	3	0	2	2	4	4	10	15	10	8	4	4	3	1	0	0	0
400	0	0	0	0	0	0	1	0	1	0	1	0	0	0	0	0	0	0	0	0
420	1	0	0	0	0	0	0	0	0	0	0	0	0	0	0	0	0	0	0	0
440	0	0	0	0	0	0	0	0	1	1	1	1	4	3	3	1	1	0	0	0
460	0	0	0	0	0	0	0	0	0	0	0	0	0	0	0	0	0	0	0	0
480	0	0	1	0	1	0	0	0	0	0	0	0	0	0	0	0	0	0	0	0
500	0	0	0	0	0	0	1	0	0	0	0	2								

Figure 7.23a: Typical RBS spectra for ashed bone immersed in uranium solution at neutral-alkaline pH.

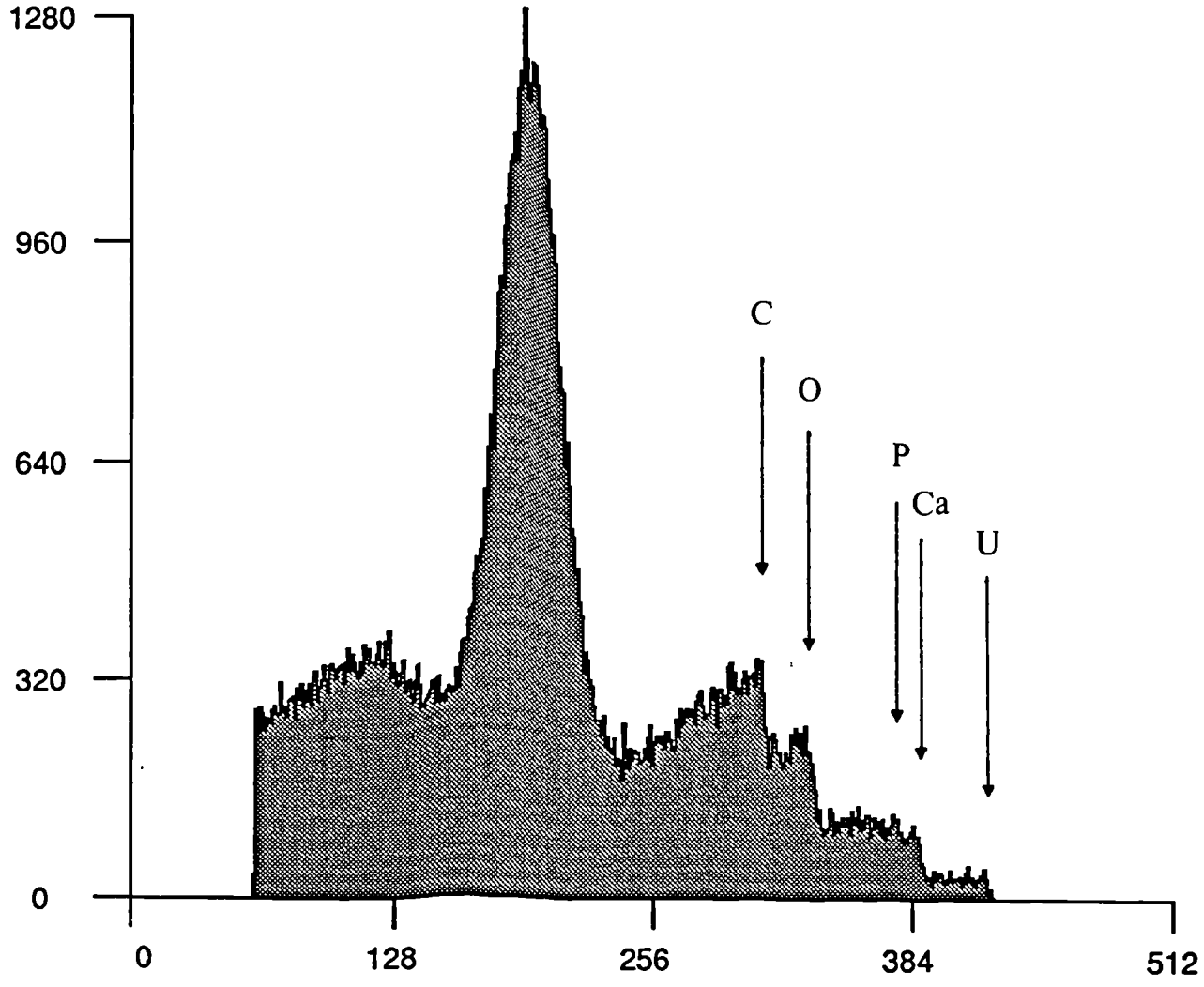

Channel Number	1	2	3	4	5	6	7	8	9	10	11	12	13	14	15	16	17	18	19	20
0	0	0	0	0	0	0	0	0	0	0	0	0	0	0	0	0	0	0	0	0
20	0	0	0	0	0	0	0	0	0	0	0	0	0	0	0	0	0	0	0	0
40	0	0	0	0	0	0	0	0	0	0	0	0	0	0	0	0	0	0	0	38
60	276	246	279	271	249	267	263	257	277	283	273	273	319	282	277	268	293	295	297	267
80	309	296	316	283	306	292	317	284	323	332	289	311	320	343	320	303	343	345	335	325
100	338	341	344	318	348	368	337	359	349	334	324	348	334	372	351	365	344	344	343	357
120	373	348	338	374	369	389	322	343	330	311	309	327	346	299	314	317	291	282	314	333
140	303	273	273	281	285	292	303	293	273	308	272	279	272	287	292	284	288	285	316	289
160	336	355	357	357	387	399	403	449	472	465	482	499	567	563	628	673	628	737	766	852
180	875	863	949	982	1028	1048	1059	1092	1049	1158	1186	1166	1281	1204	1143	1171	1203	1200	1171	1139
200	1110	1129	1113	1040	999	948	963	924	810	773	741	734	631	665	599	539	528	473	480	429
220	411	328	358	345	316	308	277	256	257	257	237	264	220	232	217	211	231	191	200	198
240	171	250	212	187	215	199	213	210	209	194	199	215	200	230	247	193	226	232	226	234
260	232	217	240	239	227	214	216	258	234	273	250	267	271	264	271	267	251	282	292	297
280	276	259	267	267	295	305	290	248	301	300	277	292	279	333	339	301	324	295	305	294
300	315	326	296	321	318	325	308	346	331	342	295	244	233	189	208	235	227	211	209	196
320	188	210	201	197	237	224	244	221	240	211	235	248	214	209	196	178	158	117	131	104
340	96	101	104	130	125	96	112	99	109	118	109	106	119	94	129	118	111	134	102	116
360	103	123	122	92	103	118	105	114	96	117	91	103	95	107	122	117	117	94	97	85
380	90	85	93	98	108	93	92	82	55	49	37	32	34	23	42	30	35	39	36	25
400	26	31	44	28	31	31	32	35	22	29	40	48	32	33	22	29	32	36	33	46
420	31	13	15	3	0	0	0	0	0	0	0	0	0	0	0	0	0	0	2	0
440	0	0	0	0	0	0	0	0	0	0	0	2	0	0	0	1	1	0	1	0
460	0	1	0	0	0	0	0	0	1	0	0	0	0	0	2	0	0	0	0	1
480	0	2	0	0	1	0	0	0	1	1	0	1	1	1	0	0	2	0	2	0
500	1	2	0	0	0	0	1	0	0	1	1	1								

Figure 7.23b: Typical PIXE spectra for ashed bone immersed in uranium solution at neutral-alkaline pH.

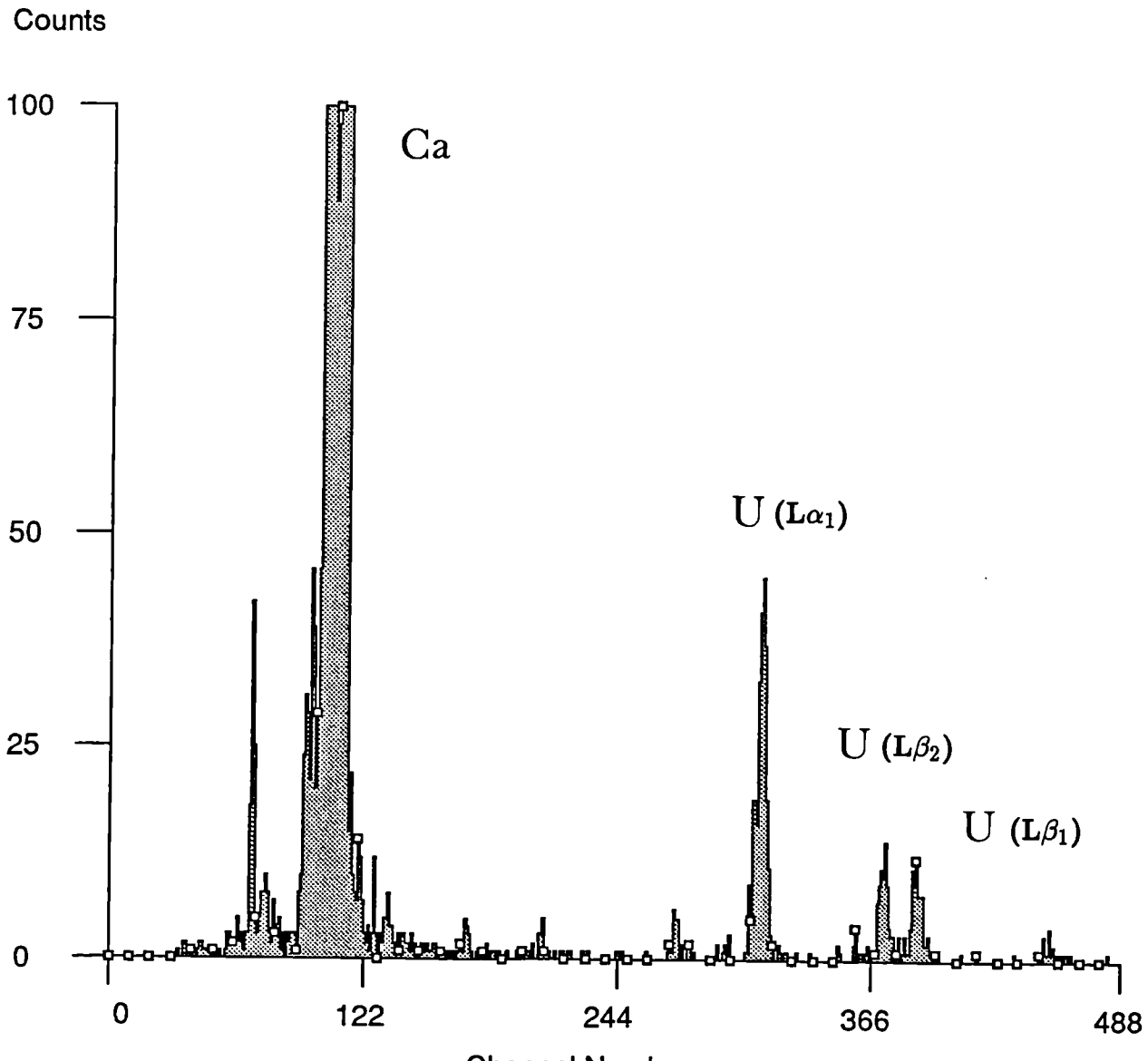

Channel Number	1	2	3	4	5	6	7	8	9	10	11	12	13	14	15	16	17	18	19	20
0	0	0	0	0	0	0	0	0	0	0	0	0	0	0	0	0	0	0	0	0
20	0	0	0	0	0	0	0	0	0	0	0	0	0	1	0	0	2	2	0	0
40	1	0	0	1	2	1	1	1	1	0	1	1	0	1	0	0	1	3	3	2
60	2	2	5	2	3	1	3	18	42	25	5	3	5	8	8	10	8	3	2	7
80	3	4	5	1	3	0	3	2	3	3	1	8	10	24	31	29	21	46	39	20
100	29	46	192	1019	2749	3514	1924	443	89	98	387	849	822	401	124	15	22	10	8	7
120	14	12	7	3	2	4	1	3	12	3	0	3	2	5	8	4	4	2	1	3
140	1	3	3	2	2	1	3	1	2	0	1	2	2	1	2	1	2	2	0	1
160	1	1	1	0	1	0	1	0	1	1	2	1	5	4	3	1	0	0	1	0
180	1	0	2	0	1	1	1	0	1	0	0	0	1	0	0	0	0	1	1	0
200	1	1	1	0	2	0	0	3	3	5	1	1	1	0	0	1	0	0	1	1
220	0	0	1	0	0	0	0	0	1	0	0	1	0	0	0	0	0	0	0	1
240	0	0	0	0	0	1	0	1	0	0	0	0	0	0	0	0	0	0	0	1
260	0	0	0	0	0	0	0	0	0	1	2	1	4	5	5	0	2	0	0	2
280	2	0	1	0	0	0	0	0	0	0	0	0	0	2	0	0	1	2	0	3
300	0	0	0	0	0	0	0	1	1	9	5	19	16	33	41	45	37	19	11	3
320	2	0	0	2	1	0	1	1	0	0	0	0	1	0	0	0	0	0	1	0
340	0	0	0	0	0	0	0	0	0	0	0	0	2	1	0	0	0	0	0	2
360	4	0	1	1	0	1	2	0	1	1	1	7	9	11	10	14	9	4	3	0
380	1	3	0	1	3	1	1	4	11	9	12	8	8	6	2	2	3	1	1	0
400	1	0	0	0	0	0	0	0	0	0	0	0	1	0	0	0	0	1	0	0
420	1	0	0	0	0	0	0	0	0	0	0	0	0	0	0	0	0	0	1	0
440	0	0	0	0	0	0	0	0	0	0	1	0	3	1	1	4	1	2	0	1
460	0	1	0	1	1	0	1	0	0	0	0	0	0	0	0	0	0	0	0	0
480	0	0	0	0	1	0	0	0	0	0	0	0	0	0	0	0	0	0	0	0
500	2	1	0	0	1	0	3	1	1	1	2	2								

Figure 7.24: Two consecutive RBS spectra taken from adjacent areas of cortex highlighting the apparent *within sample* variation in matrix composition.

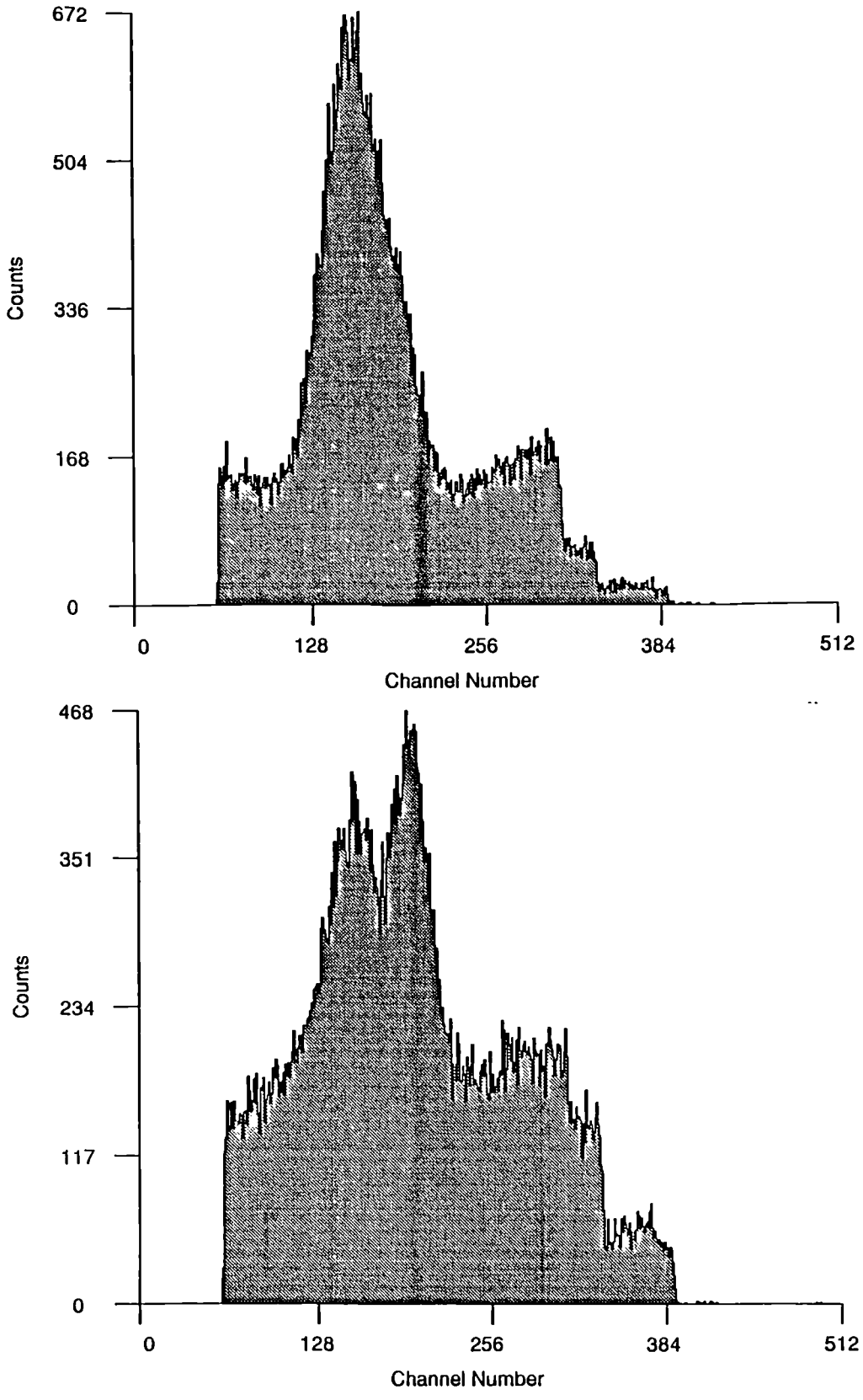

representing the edge of the bone, while at (c) a maximum calcium signal was observed as the whole scan area fell onto the bone cortex.

Maximum uranium peaks were seen in spectra (b) and (c) where the cortical tissue was at its most dense. Spectra (d) and (e) show a progressive decline in the size of the uranium peaks as the scan moved down the diffusion profile of uranium.

The following parameters were defined to reflect/describe the shape of the uranium profile at the cortical edge:

i. M, the maximum U / Ca atomic %

ii. V, the U /Ca atomic % value at the "estimated cortical edge"

iii. D, the distance from the "edge" to the V/2 position.

iv. W, the whole diffusion distance into the cortical tissue.

Consecutive spectra were brought together in one plot for each respective sample and illustrated in figures 7.26-7.31. The parameters M, V, D and W were labelled in figure 7.26 for the whole bone sample at pH 7, and values tabulated for each sample in table 7.8.

Figures 7.26 (a) and (b) show the calcium and uranium distribution profiles and the U/Ca ratio, respectively, for whole bone immersed at pH 7. Below position 4.5, calcium counts were very low as the beam was only partially on the edge of the sample. Position 4.5, the 'half height' of the steep calcium gradient was taken as the estimated cortical edge. From the uranium profile and the U/Ca ratio plot, most of the uranium was found to be distributed at the cortical surface, with a diffused profile extending up to about 18 (6 divisions) microns (W) into the cortex. The M, V and D values were 2.2 atomic % (or 22000 ppm), 1.9 atomic % (or 19000 ppm) and 3 microns, respectively.

Figures 7.27 (a) and (b) represent traces for hydrazine-treated bone at pH 7. In figure 7.27, the cortical edge was estimated at position 1. Calcium signals were seen to dramatically drop as the beam moved into the cortical tissue, between positions 12 and 15: this was probably due to the beam falling onto a pore. The U/Ca ratio at the apparent edge of this pore was very high. Uranium diffusion

Figure 7.25: Consecutive PIXE spectra at cortical edge of ashed bone showing uranium uptake profile; incremental distance between each point approximately 9 microns.

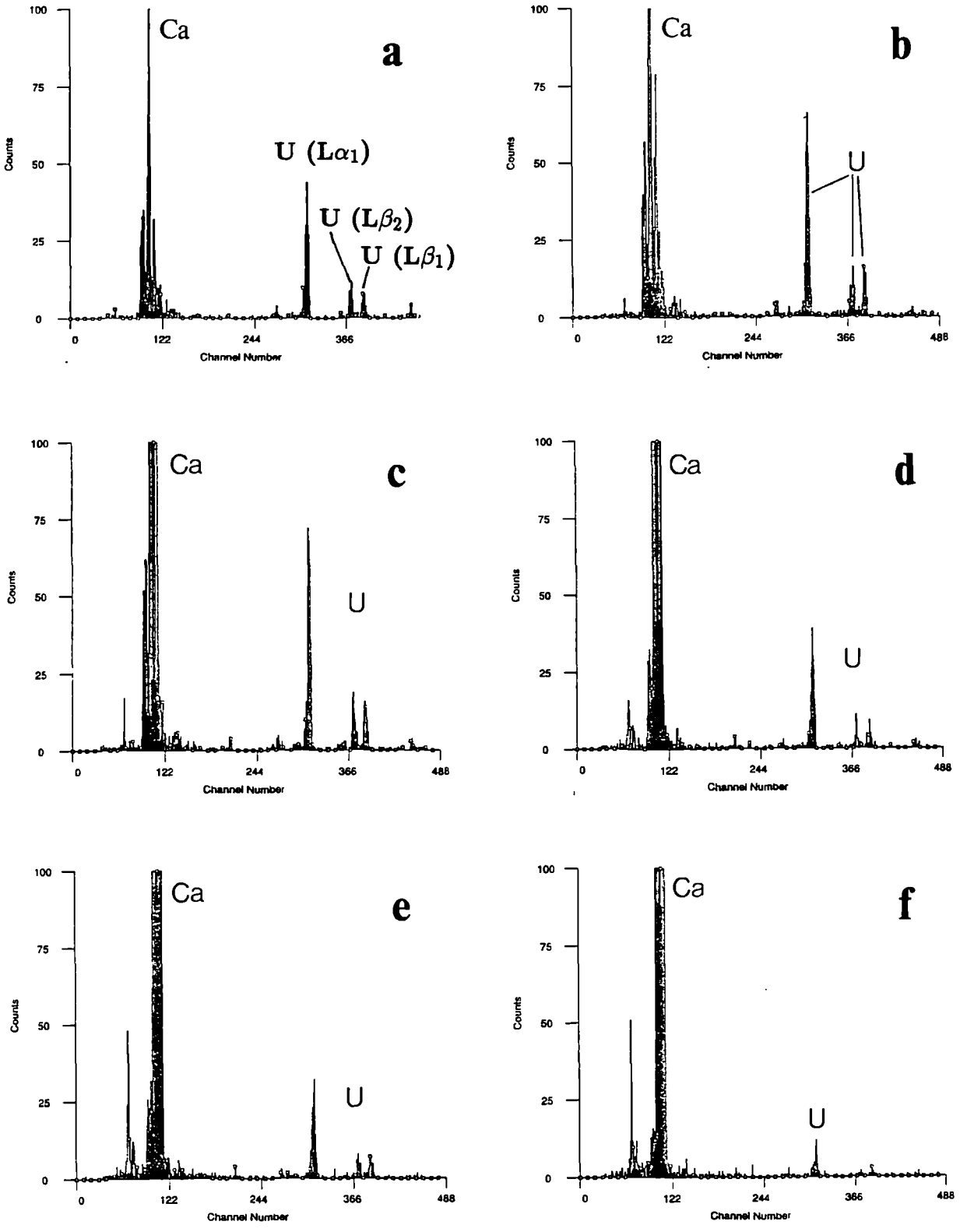

extended about 75 microns into the cortex (W), the M, V and D values being 35%, 13.5% and 51 microns, respectively.

Table 7.8: Summary of the uranium diffusion lengths (D and W) and U / Ca atomic % (M and V) of the samples.

Bone description	pH of immersion	M	V	D	W
Whole					
Hydrazined	4	N/A	N/A	N/A	N/A
Ashed					
Whole		2.2	1.9	3.0	20.0
Hydrazined	7	35.0	13.5	51	75.0
Ashed		30.0	15.0	9.0	95.0
Whole		12.0	6.8	7.0	36.0
Hydrazined	10	39.0	5.8	54.0	156.0
Ashed		2.1	1.8	120.0	240.0

M = maximum U/Ca atomic %

V = U/Ca atomic % at edge

D = distance from edge to V/2 position (microns)

W = total diffusion distance into the cortex (microns)

Ashed bone immersed at pH 7 is represented in Figures 7.28 (a) and (b). The estimated cortical edge was at position 3. From the U/Ca ratio plot, again much of the uranium was located at the surface, diffusing into the cortex to a depth of about 90 (30 divisions) microns. M, V and D values were 30 atomic %, 15 atomic % and 9 microns, respectively. The reason for the decline in calcium counts moving

Figure 7.26 : (a) Calcium and uranium profiles and (b) uranium/calcium ratios at the cortical edge of whole bone immersed for 2 weeks in 2240 ppm uranium solution at pH 7.

(a)

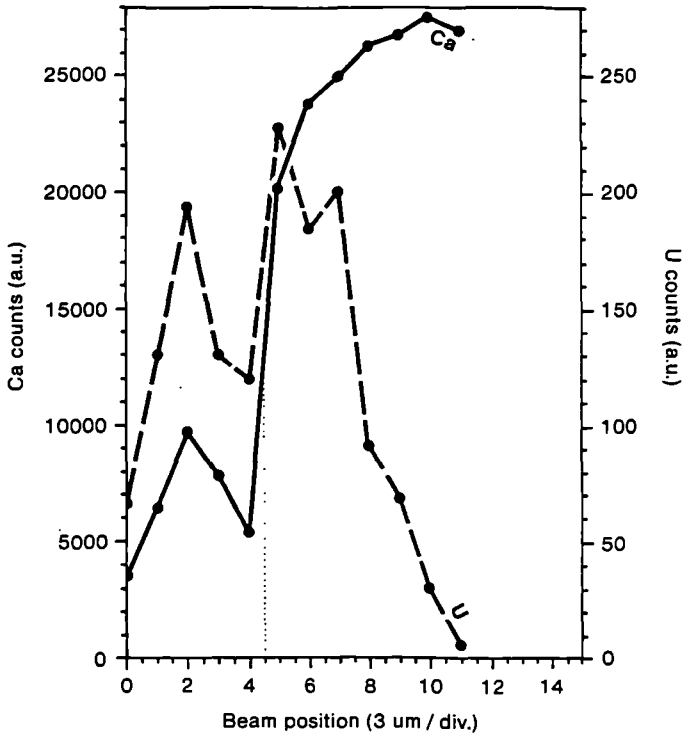

(b)

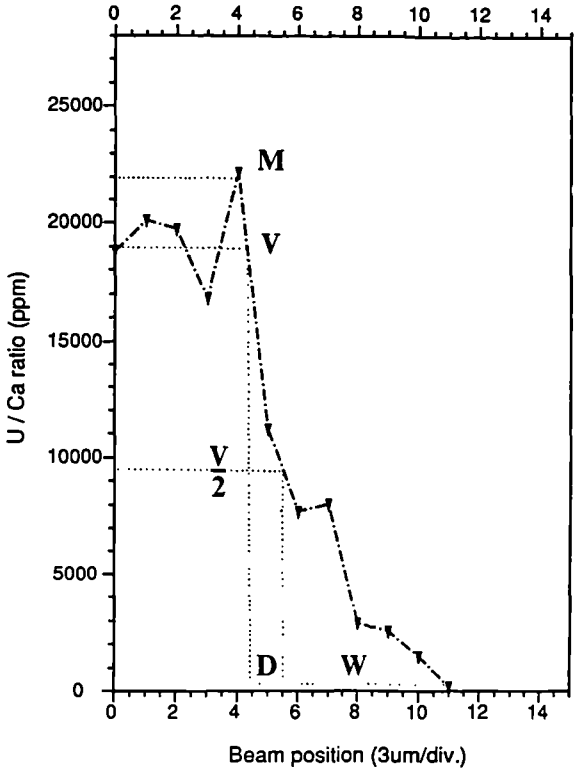

Figure 7.27 : (a) Calcium and uranium profiles and (b) uranium/calcium ratios at the cortical edge of hydrazine-treated bone immersed for 2 weeks in 2240 ppm uranium solution at pH 7.

(a)

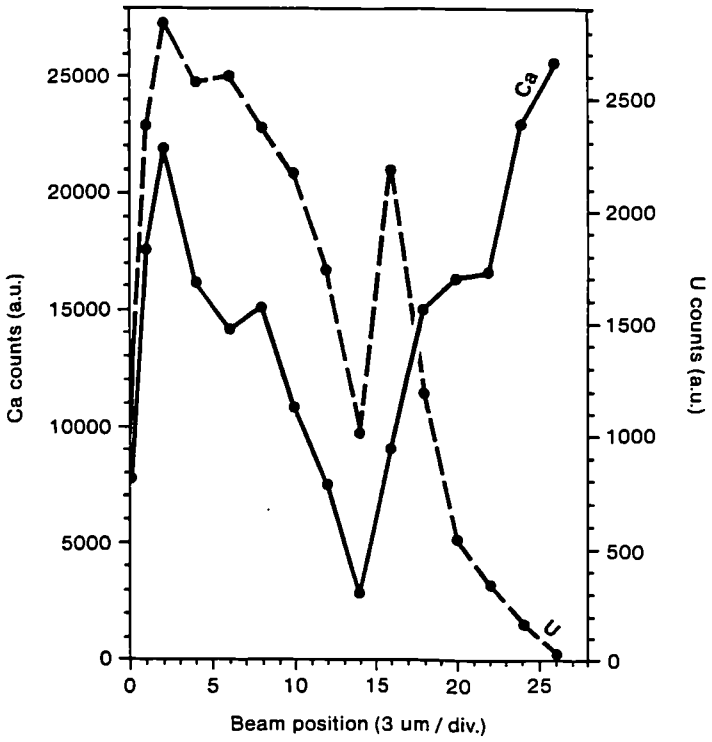

(b)

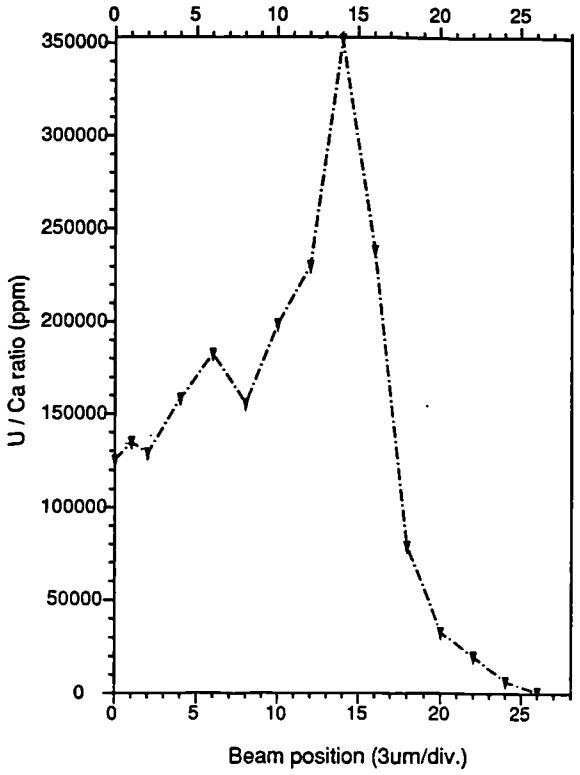

into the cortex was not clear, but it casts some doubt on the uranium/calcium ratio profile plotted in figure 7.28(b).

In comparison, bone immersed at pH 10 revealed the following values. Whole bone is represented in figures 7.29 (a) and (b). The cortical edge was estimated at position 3, the uranium profile extending up to at least 36 (12 divisions) microns. Respective M, V and D values were 12 atomic %, 6.8 atomic % and 7 microns.

Figures 7.30 (a) and (b) represent hydrazine-treated bone at pH 10. Position 4 was chosen as the cortical edge. A long diffusion profile extending at least 156 microns (52 divisions) was observed, with values for M at 39 atomic %, for V at 58 atomic % and D at 54 microns.

Finally, ashed bone immersed at pH 10 is represented by figures 7.31 (a) and (b). Position 2 approximates to the cortical edge. Uranium diffusion into the bone was even deeper here, extending to at least 240 microns (80 divisions). M, V and D values were 2.1 atomic %, 1.8 atomic % and 114 microns (38 divisions).

These profiles for bone immersed at pH 7 and at pH 10 are summarized in figures 7.32 and 7.33.

7.6.3 Summary.

A comparison of PIXE and RBS quantitative data demonstrated both between and within sample variability in the material matrix. This was caused by the inhomogeneity of bone, which was probably enhanced by alterations of the organic:inorganic content.

Data here concurred with earlier EPMA studies by finding uranium absent in all bone immersed in pH 4 solutions. In contrast, uranium was found in whole, ashed and hydrazine-treated bone immersed at both pH 7 and pH 10, exclusively in the peripheral cortices. Moreover, there was evidence of pore-filling, surface adsorption and possible organic complexing mechanisms of interaction as illustrated by uranium distribution profiles. Uranium was found to penetrate the cortex of ashed bone most extensively at both pH's, reflecting the high porosity/surface area of this material and illustrating the predominance of uranium interaction at bone surfaces.

Figure 7.28 : (a) Calcium and uranium profiles and (b) uranium/calcium ratios at the cortical edge of ashed bone immersed for 2 weeks in 2240 ppm uranium solution at pH 7.

(a)

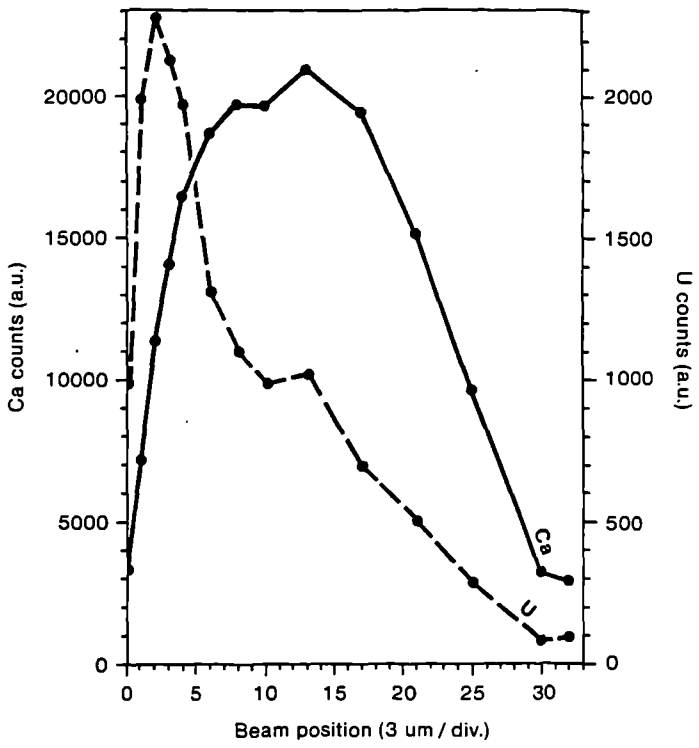

(b)

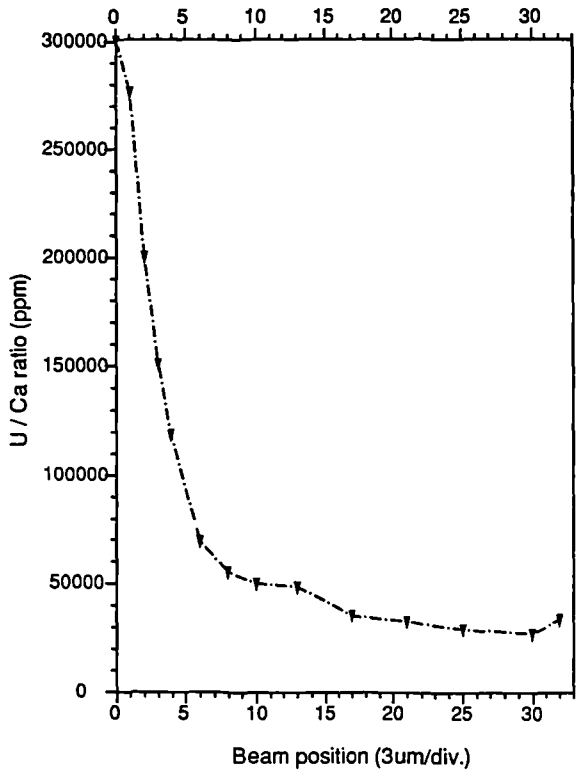

Figure 7.29 : (a) Calcium and uranium profiles and (b) uranium/calcium ratios at the cortical edge of whole bone immersed for 2 weeks in 2240 ppm uranium solution at pH 10.

(a)

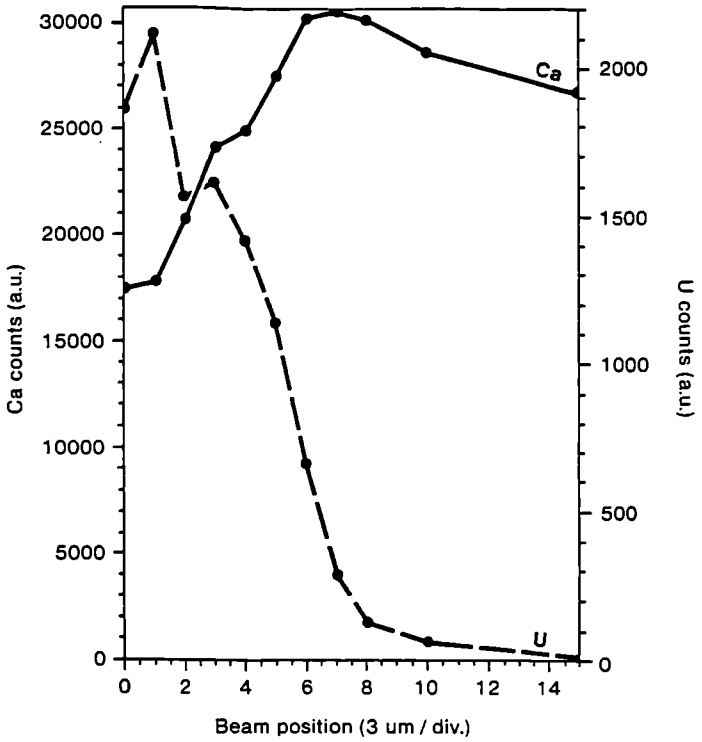

(b)

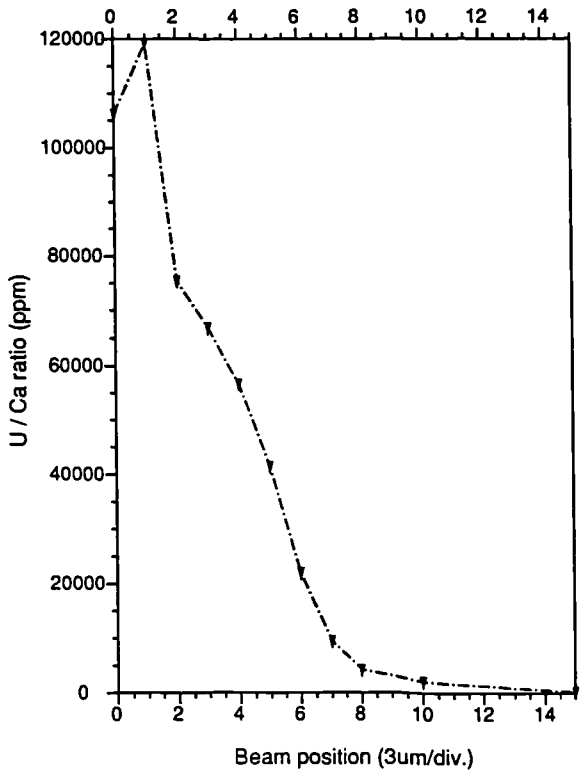

Figure 7.30 : (a) Calcium and uranium profiles and (b) uranium/calcium ratios at the cortical edge of hydrazine-treated bone immersed for 2 weeks in 2240 ppm uranium solution at pH 10.

(a)

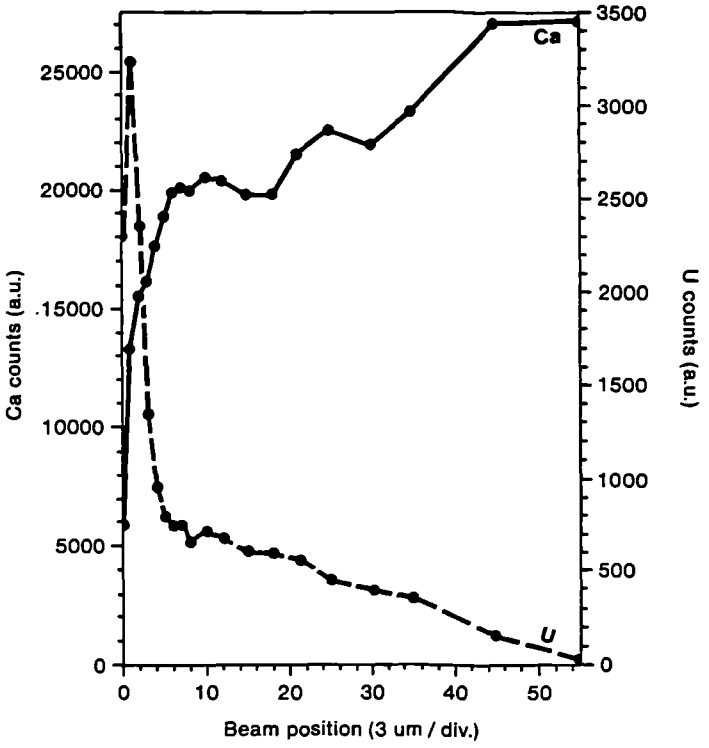

(b)

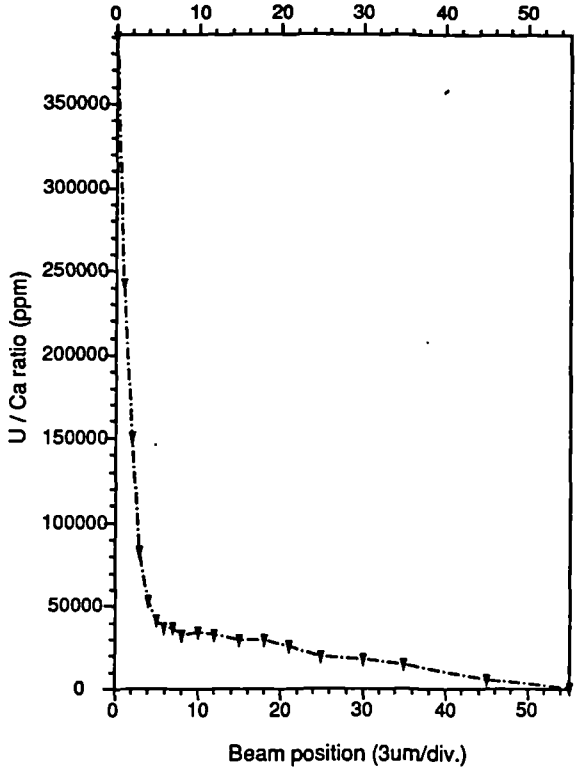

Figure 7.31 : (a) Calcium and uranium profiles and (b) uranium/calcium ratios at the cortical edge of ashed bone immersed for 2 weeks in 2240 ppm uranium solution at pH 10.

(a)

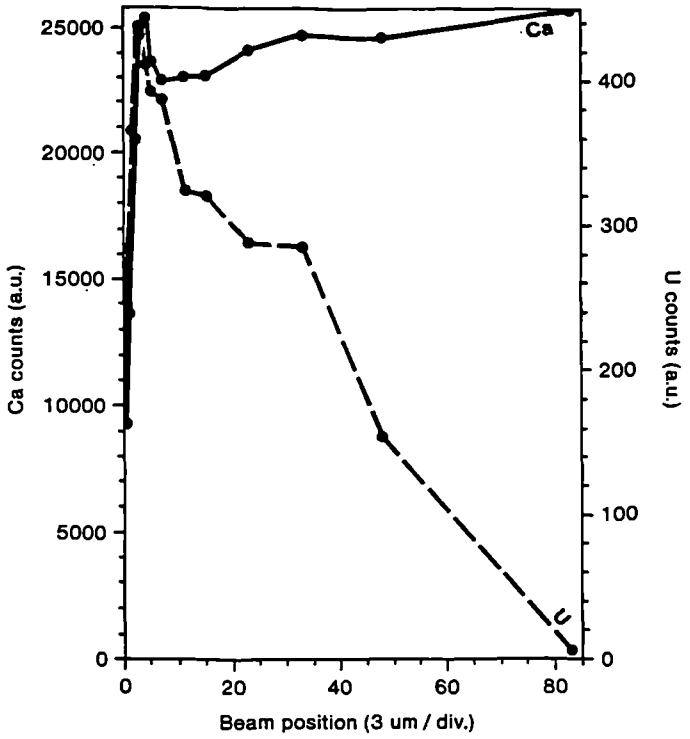

(b)

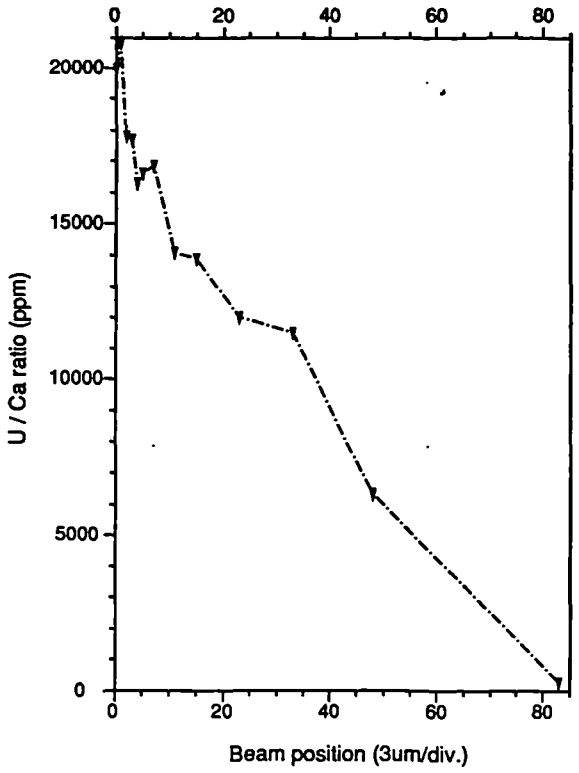

Figure7.32: Summary of uranium distribution profiles in bone with variable organic:inorganic ratio immersed at pH 7.

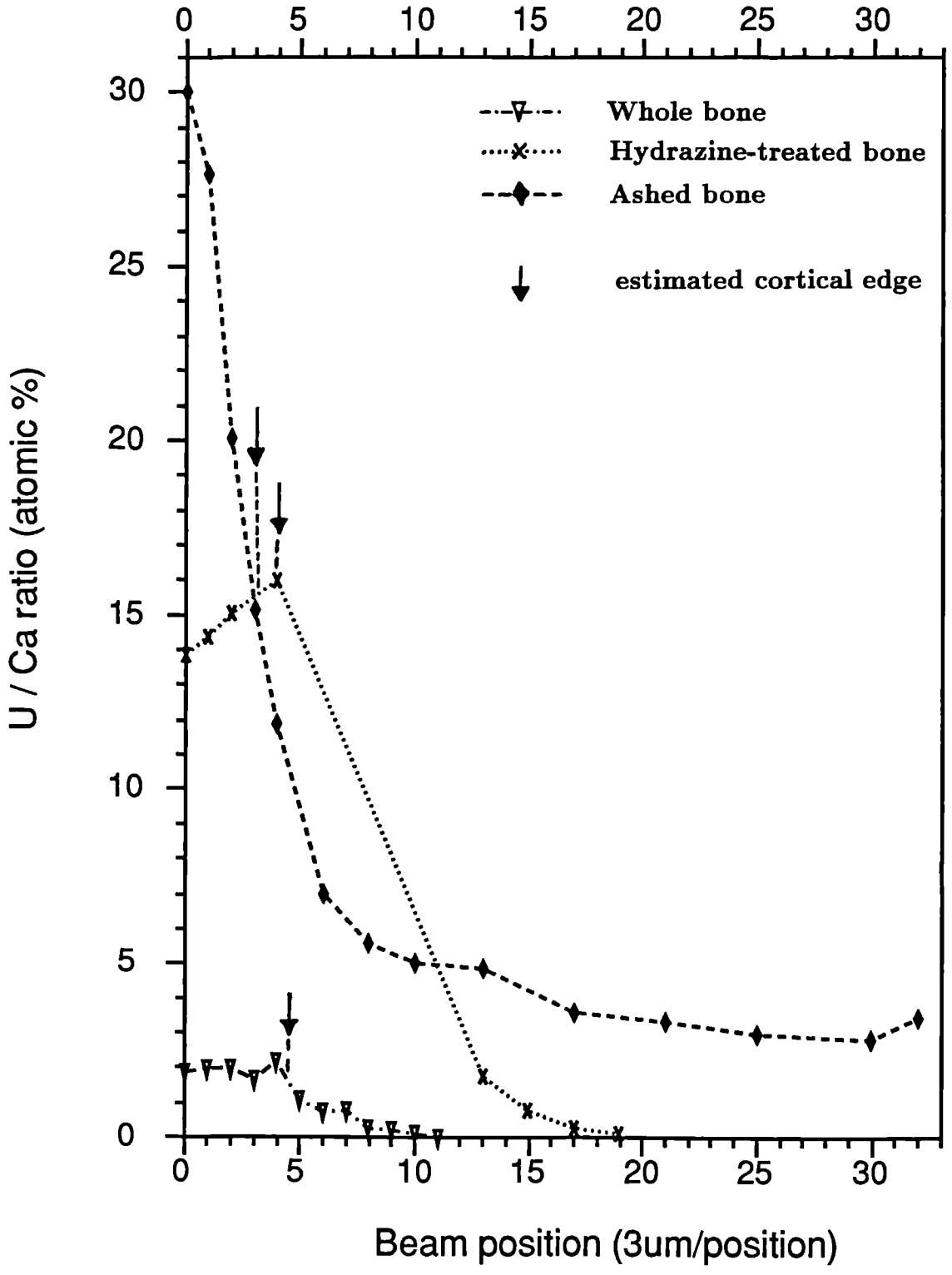

Figure7.33: Summary of uranium distribution profiles in bone with variable organic:inorganic ratio immersed at pH 10.

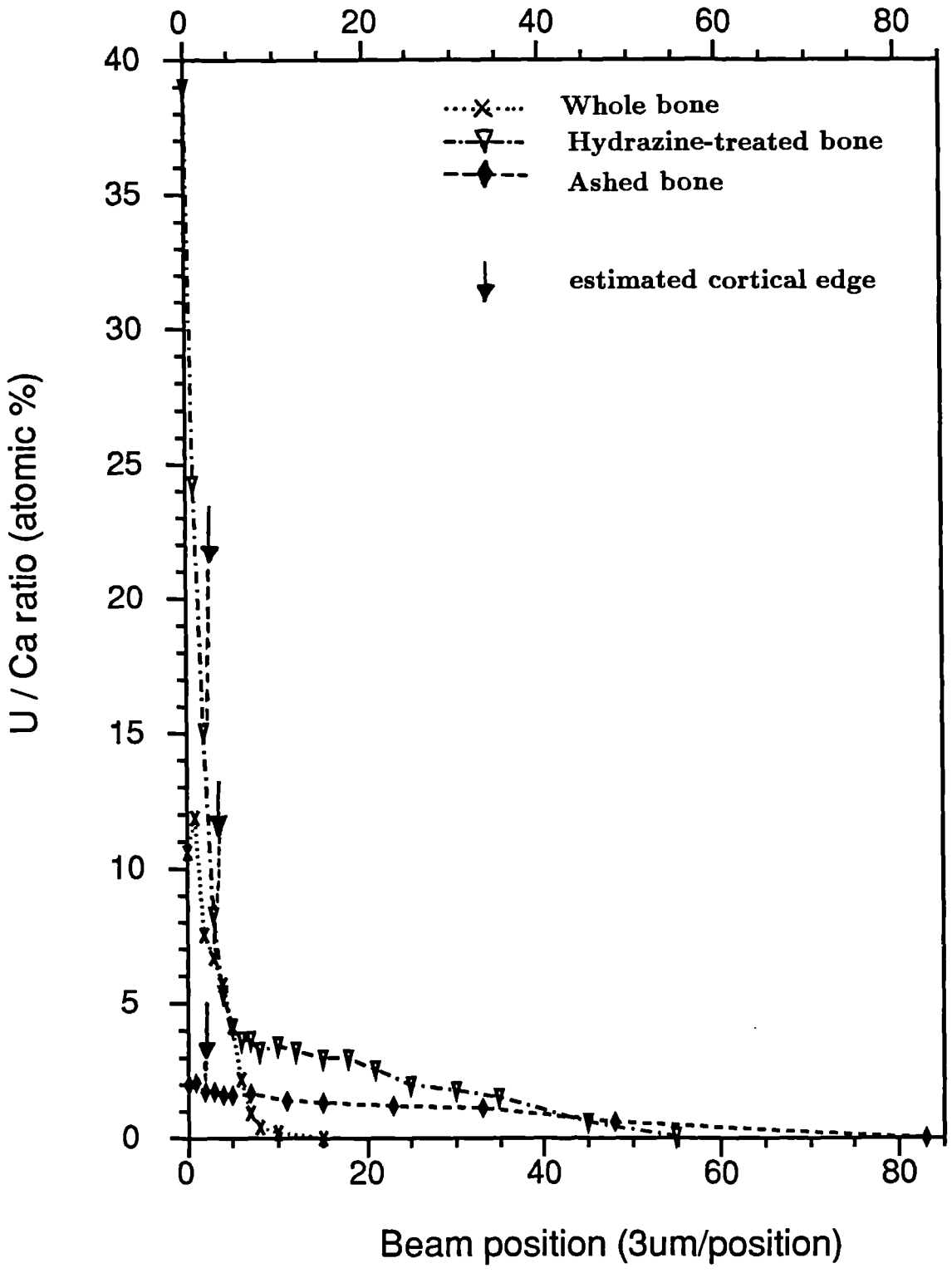

The pattern of uranium distribution, as indicated by a number of parameters describing the diffusion profile at bone surfaces, was not clear, and depended to a certain extent on the parameter selected.

The contribution of organic and inorganic components of bone in the mechanism of uranium uptake under conditions of variable pH were further explored using chemical separation procedures followed by analysis of the respective extractions for their uranium concentration.

7.7 Chemical Separation of Organic and Inorganic Components.

The separation of organic and inorganic components of a representative batch of bone samples that had been immersed in uranium solution was carried out in order to identify the relative contribution of each fraction to the uptake and subsequent incorporation/adsorption of this element. As in the corresponding strontium study, organic and inorganic extractions were analysed using ICP-AES, calibration procedures determining detection limits (ppm in solution) of approximately 0.2 ppm calcium, 5 ppm phosphorus and 0.3 ppm uranium. As before, all concentrations were corrected for any dilution, small variations in the mass of the bone sample and instrumental drift. Final concentrations are shown in ppm standardised for 1g bone material in table 7.9, with 'NF' denoting values either below the quoted detection limit or simply undetected. Control samples and standards were identical to those quoted in the corresponding strontium study but are included again for reference.

Note: Chemical separation procedures were carried out on bone samples immersed in 2240 ppm uranium (Series II) and 1000 ppm (Series III) at variable pH. Data from these extractions were therefore not directly (quantitatively) cross-comparable but rather *trends* for each experiment were compared.

Uranium values in organic and inorganic extractions are shown in table 7.9. No uranium was detected in blank solutions, nor in H5 and ovine samples. Many of the uranium levels detected in the experimental samples were at or below the quoted detection limit. However, a number of observations were made.

Table 7.9: ICP-AES data for organic and inorganic extractions of whole bone immersed in uranium solutions at variable pH.

Sample description	pH of immersion	Extraction	Ca (ppm)	P (ppm)	U (ppm)
Blank nitric acid	N/A	Inorganic	NF	NF	NF
Blank nitric acid	N/A	Organic	NF	NF	NF
H5 animal bone	N/A	Inorganic	44268	18522	NF
	N/A	Organic	NF	<=13.92	NF
Ovine bone control	N/A	Inorganic	52643	24207	NF
	N/A	Organic	<=0.56	NF	NF
Immersion Series II	4	Inorganic	22342	10593	5.01
	4	Organic	NF	NF	NF
	7	Inorganic	22250	10749	241.08
	7	Organic	NF	NF	<=1.19
	10	Inorganic	22358	10416	209.84
	10	Organic	NF	NF	NF
Immersion Series III	4	Inorganic	17014	7678	NF
	4	Organic	16.89	NF	1.97
	7	Inorganic	15051	6715	(0.074)
	7	Organic	NF	NF	3.26
	10	Inorganic	2675	1010	(0.137)
	10	Organic	NF	NF	<=0.86

'NF'= 'not found' i.e. below quoted detection limit.

'<=' refers to figures at limit of detection.

All values were corrected for variable original bone mass and each standardised to 1 gramme bone matrix.

In Immersion Series II, where the uranium concentration of the immersing solution was 2240 ppm, inorganic extractions contained far more uranium than organic ones where levels were negligible. A small quantity of uranium (1.19 ppm) was detected in the organic extraction of the pH 7 immersion but this value was very close to the quoted detection limit, and again at this pH uranium levels were much higher in the inorganic extraction.

In Immersion Series III, where the uranium concentration was 1000 ppm, quite different patterns were observed. Here, organic extractions contained relatively more uranium, again highest in pH 7 immersions.

Examining elemental ratios to compensate for variable yield (table 7.10), U:Ca ratios for Series II were highest in the pH 7 sample and lowest in that of pH 4. U:Ca ratios could not be calculated for Series III samples where uranium levels were nil or unacceptably low.

Table 7.10: Uranium:calcium data for inorganic extractions of bone immersed in uranium solutions at variable pH.

Sample description	pH	Ca:P	U:Ca ($\times 10^{-4}$)
H5 animal control	N/A	2.4	-
Ovine control	N/A	2.2	-
Immersion Series II	4	2.1	2.2
	7	2.1	108
	10	2.1	93.9
Immersion Series III	4	2.1	NF
	7	2.2	NF
	10	2.6	NF

'NF'= 'not found' i.e. below quoted detection limit.

7.7.1 Summary.

Calcium and phosphorus yields in organic and inorganic extractions would suggest that the chemical separation procedures were successful, since neither of these two elements were detected in the hydrazine-treated samples.

Data from this chemical separation study were inconsistent across the two Immersion Series. Bone immersed in 2240 ppm uranium solutions revealed uranium association with only the inorganic fractions, with little if any uranium in organic extractions. Conversely, material from Immersion Series III possessed uranium in the organic fractions, with only negligible uranium in inorganic extractions. Small sample sizes - 2 samples representing each pH of immersion - did not assist in the interpretation of these data.

However, all extractions did demonstrate higher uranium and uranium/calcium values in bone immersed at pH 7, suggesting that uranium uptake into either bone fraction was enhanced in neutral pH conditions. Bone at pH 10 generally possessed slightly less uranium than pH 7 samples, with significantly lower content in pH 4 samples, except in the organic extraction of bone from Series III.

7.8 Further Investigation: Fission Track Analysis.

Discrepancies in data across the three Immersion Series, further highlighted in the chemical separation study, might indicate the importance of **uranium availability** in the immersing solution in determining both the degree and mode of uranium interaction with bone. Cross-cortical distribution profiles in bone immersed in varying uranium concentrations demonstrated the respective extent of uptake over a relatively short period of exposure. Thus, both the **concentration** of uranium in solution and the **time-scale** of the experiment were **limiting factors** in determining the amount of information that could be gained from such simulation studies.

With this fact in mind, a few whole bone samples were immersed in more concentrated uranium solutions (5000 ppm) for approximately 20 weeks at 70°C. These

samples were subjected to Fission Track Analysis to determine the degree and location of uranium uptake under these still further exaggerated conditions.

- **Fission Track Analysis.**

Irradiation and etching conditions were as described in Chapter 5, section 5.4. Light micrographs of the fission tracks are shown in figures 7.34-36. Quantitative analysis using densitometry methods as for autoradiographs was **not** carried out here.

Figure 7.34 shows the cross-cortical distribution of uranium across the full width of bone. Uranium was present throughout the whole bone largely filling pores and voids in the cortical tissue, predominantly in the inner cortical areas. A dark "band" of uranium was observed lining the periosteal surface (magnified in figure 7.35) and to a lesser extent the endosteal edge: figures 7.36a/b show extensive uranium distribution in the endosteal cortex together with a layer of what appears to be remnant organic tissue silhouetted by uranium.

These fission track plots therefore demonstrate the potential of uranium to interact extensively with bone

(1) permeating its full cortical width largely by filling natural pores/voids, particularly in trabecular bone, and

(2) lining cortical edges, predominantly periosteal surfaces, with evidence of association with remnant organic tissue at endosteal surfaces.

The microdistribution of uranium and its implications with regard to the mechanism(s) of uranium interaction with bone are discussed in more detail in Chapter 10.

Figure 7.34: Micrograph showing the cross-cortical distribution of uranium in whole bone immersed in 5000 ppm uranium solution for 20 weeks (p = periosteal surface, e = endosteal surface). Mag. x64.

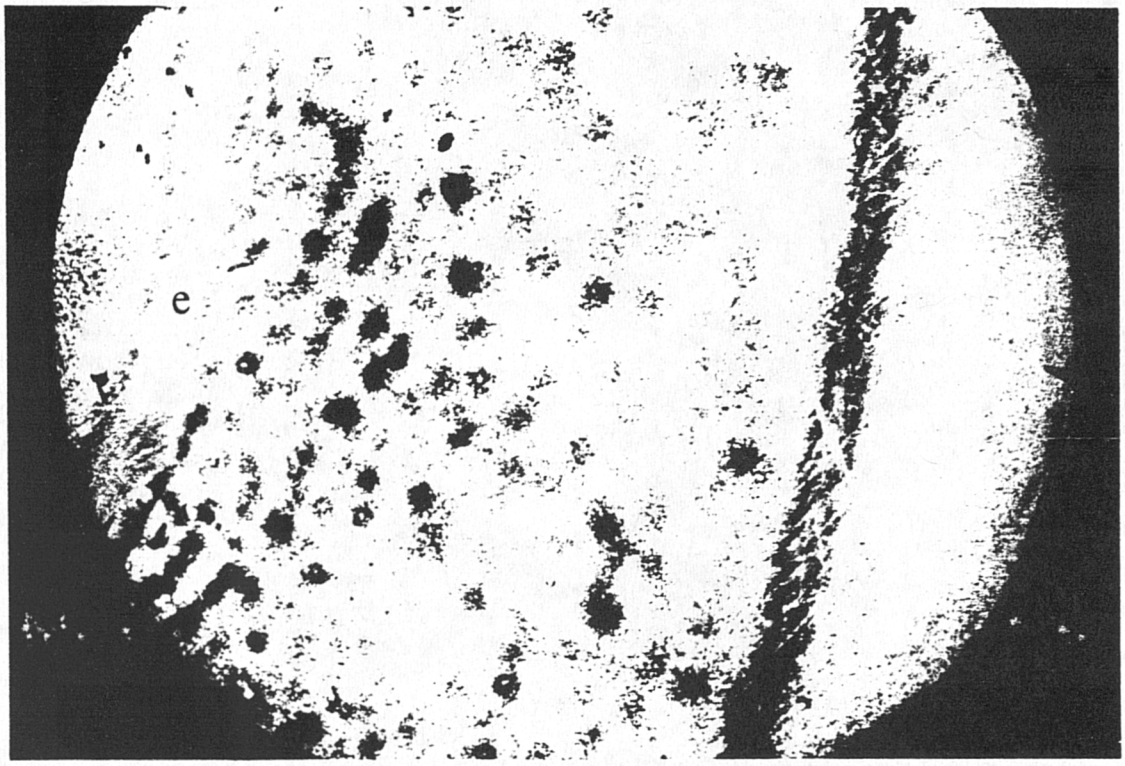

Figure 7.35: Uranium distribution in the periosteal cortex of bone sample in Figure 7.34 (ce = cortical edge). Mag.x64.

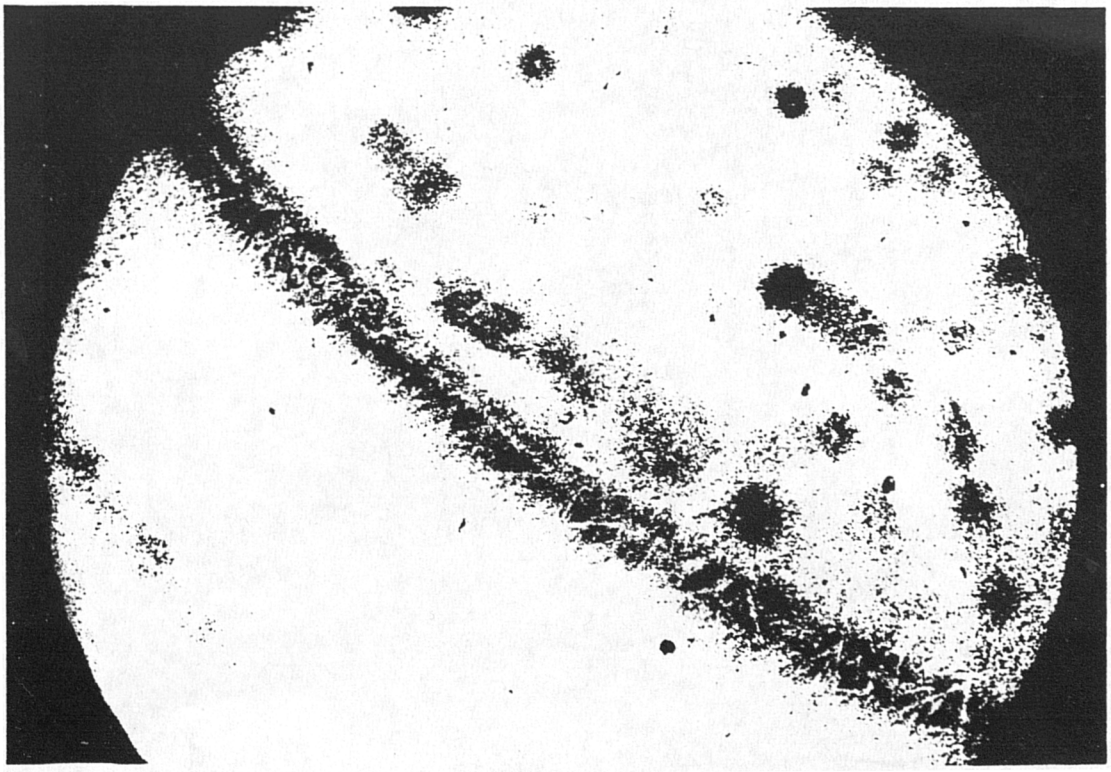

Figure 7.36 a/b: Uranium distribution in the endosteal cortex of bone immersed in 5000 ppm uranium solution for 20 weeks, with evidence of uranium interaction with remnant organic tissue (o). Mag.x64.

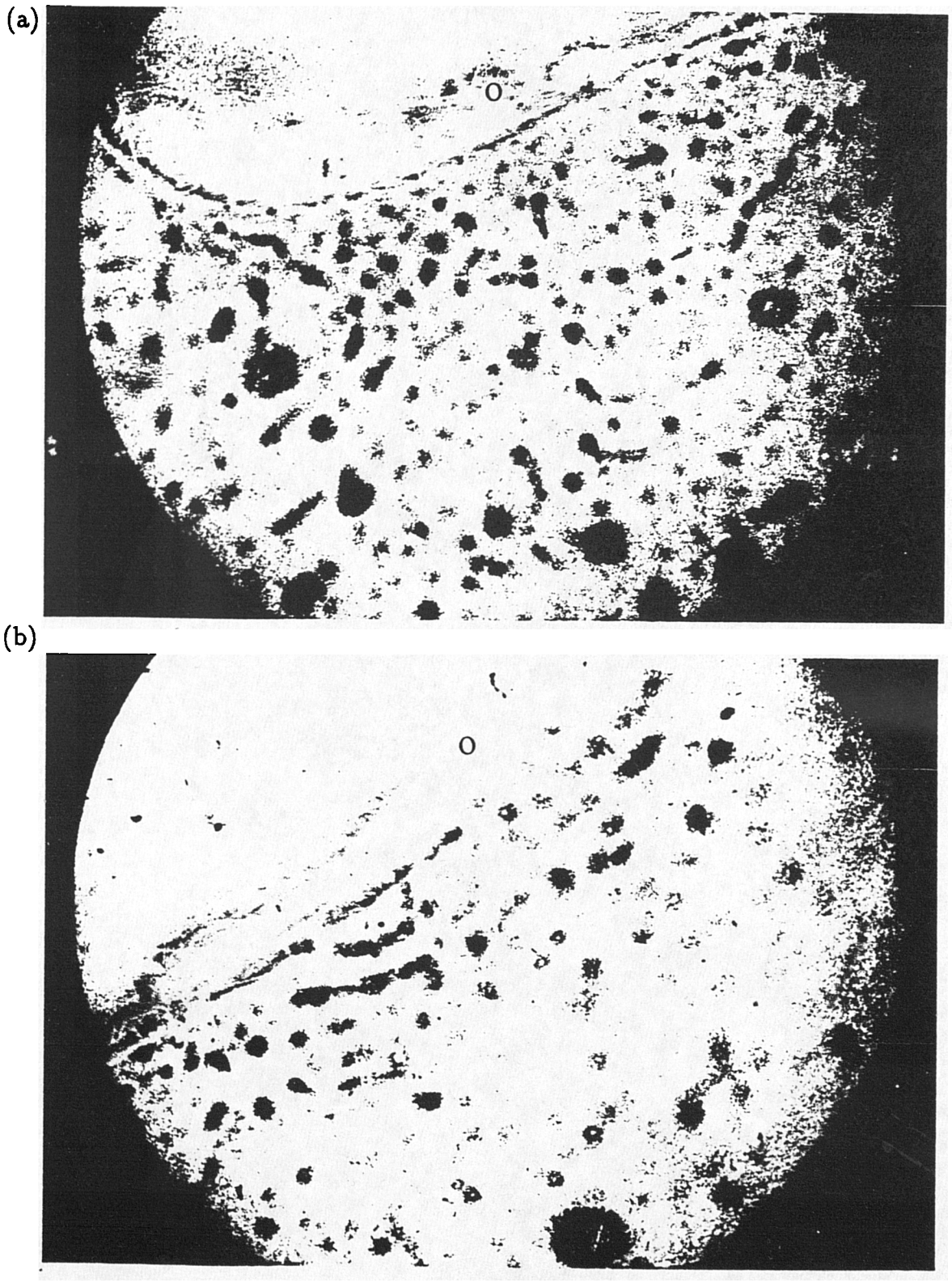

Chapter VIII

Complementary Studies of Diagenetic Alteration.

This chapter complements elemental uptake studies by exploring more general aspects of diagenetic alteration. The data provide a further means of elucidating the possible mechanisms of uptake phenomena (such as those described for strontium and uranium in Chapters 6 and 7, respectively). Thus, studies here have predominantly focused on different aspects of the effects of immersion on the character and integrity of bone itself, examining the specific and combined effects of the following:- organic content, pH of immersion and strontium/uranium exposure. The effects of these variables on the **crystallinity** of the inorganic bone matrix were examined using XRD analysis, while the **total organic content** of immersed bone was explored using CHN analysis.

In addition, potential ion exchange mechanisms were explored by measuring **cation exchange properties** of bone fractions and related material collected from percolation experiments. It was anticipated that these would provide some indication as to the possible roles of organic and inorganic components in elemental uptake.

Therefore, experimental work presented here has examined three processes typically observed in the diagenetic alteration of bone: (1) crystallinity changes in the inorganic matrix, (2) the decay of the organic component, and (3) ion exchange phenomena.

8.1 Crystallinity Studies: XRD Analysis.

8.1.1 Introduction.

The aim of this investigation was two-fold:

1. to illustrate the potential effects of (a) organic content, (b) pH of immersion, (c) strontium/uranium immersion on the crystallinity of hydroxyapatite, using 002, 112/211 and 310 hkl peaks as indicators.

2. to detect the presence of any non-apatite peaks which may represent either the original salt of strontium or uranium, or intermediates formed in reaction with hydroxyapatite.

Hydrazine-treated bone and ashed bone were predominantly used in order to facilitate the preparation of fine, homogeneous powders essential for comparative XRD studies. Only a relatively small number of whole bone samples were analysed, because in general it was not possible to obtain an even-grained homogeneous sample.

Hence, the following samples were examined:

- controls for whole, ashed and hydrazine-treated bone (no immersion)
- ashed and hydrazine-treated samples immersed in buffered solutions at 70°C,
- ashed and hydrazine-treated bone exposed to buffered strontium/uranium solutions at 70°C.

Crystallinity was described in one of two ways: (1) visual, qualitative examination of the XRD spectra, and (2) quantitative measurement of specific peaks in the spectra. Where changes and trends in crystallinity were not apparent **visibly** , measurements of crystallinity were made to provide a **quantitative** indication of the more subtle trends.

Quantitative measurement of crystallinity was carried out on the peaks 002, 112/211 and 310 using 3 different indices of crystallinity: these are reviewed in Chapter 4. Values can be found in Appendix IVa. Figure 8.1 summarises the measurements taken for each peak:

(1) D, the reciprocal of the corrected peak breadth

(2) $\frac{B}{H}$, the breadth:height ratio

(3) I, the peak intensity (effectively the area under the peak i.e.. B x H)

Figure 8.1: Example diffraction profile of hydroxyapatite showing measurements of crystallinity.

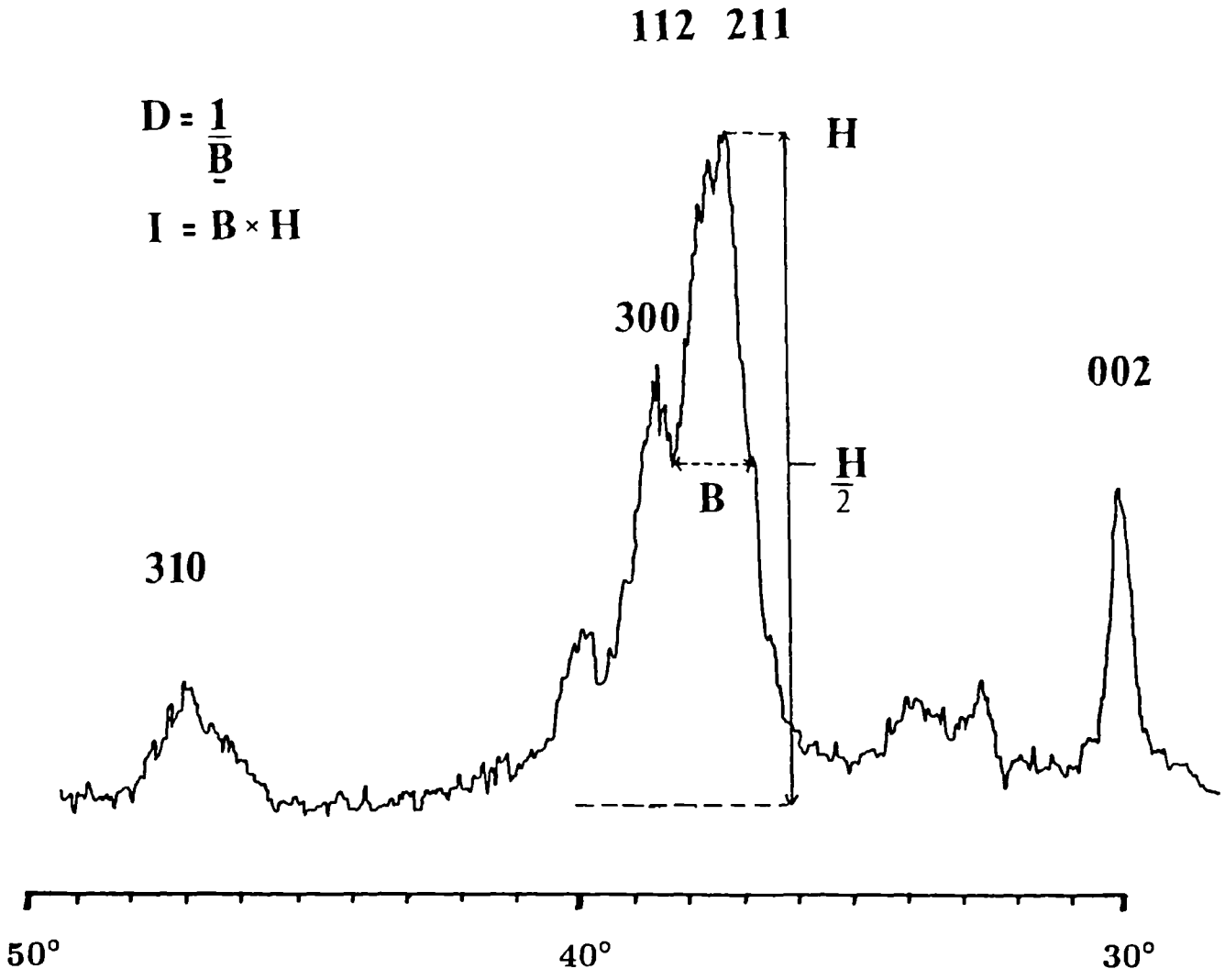

8.1.2 Results.

1. Organic content.

Figure 8.2 shows the XRD profiles of four bone samples whose organic content ranged from the full complement (whole bone), through two stages of progressive hydrazine treatment to bone material ashed at 500°C (refer to Appendix Ib for CHN values). A hydroxyapatite standard was also included for reference to demonstrate the position of the major apatite mineral peaks. It was found that as the organic fraction of the bone decreased, the peaks generally became more clearly defined or resolved i.e. crystallinity *apparently* increased. This trend was particularly apparent with peak hkl=002, and with the gradual separation of peak 300 from peak 112.

Note: Care was taken when making comparisons of whole and hydrazine-treated bone with ashed bone because of the effect of the heating process itself on crystallinity, as demonstrated in Chapter 5.

2. pH of immersion.

Figures 8.3, 8.4 and 8.5 show the XRD profiles of whole, hydrazine-treated and ashed bone, respectively. All samples were immersed in buffered purified water for 12 weeks. In all cases, immersion *per se* effected an increase in crystallinity, if only small. This was demonstrated most clearly as before by the gradual separation of peak 300 from peak 112. In all cases, bone immersed at pH 4 possessed the most crystalline structure, while samples immersed in neutral-alkaline conditions were less easy to distinguish. Whole bone immersions revealed a relatively lower crystallinity in bone immersed at pH 7, suggesting the material was more stable or less subject to crystallinity changes in neutral conditions. This may reflect the relative stability of the organic matrix at this pH: at pH's 4 and 10 this matrix is vulnerable to "attack" by acidic and basic hydrolysis, respectively. However, bone is more stable in alkaline than in acidic conditions, and indeed ashed and hydrazine-treated samples were evidently least affected by immersion at pH 10.

Figure 8.2: X-ray diffraction profiles for bone with variable organic content.

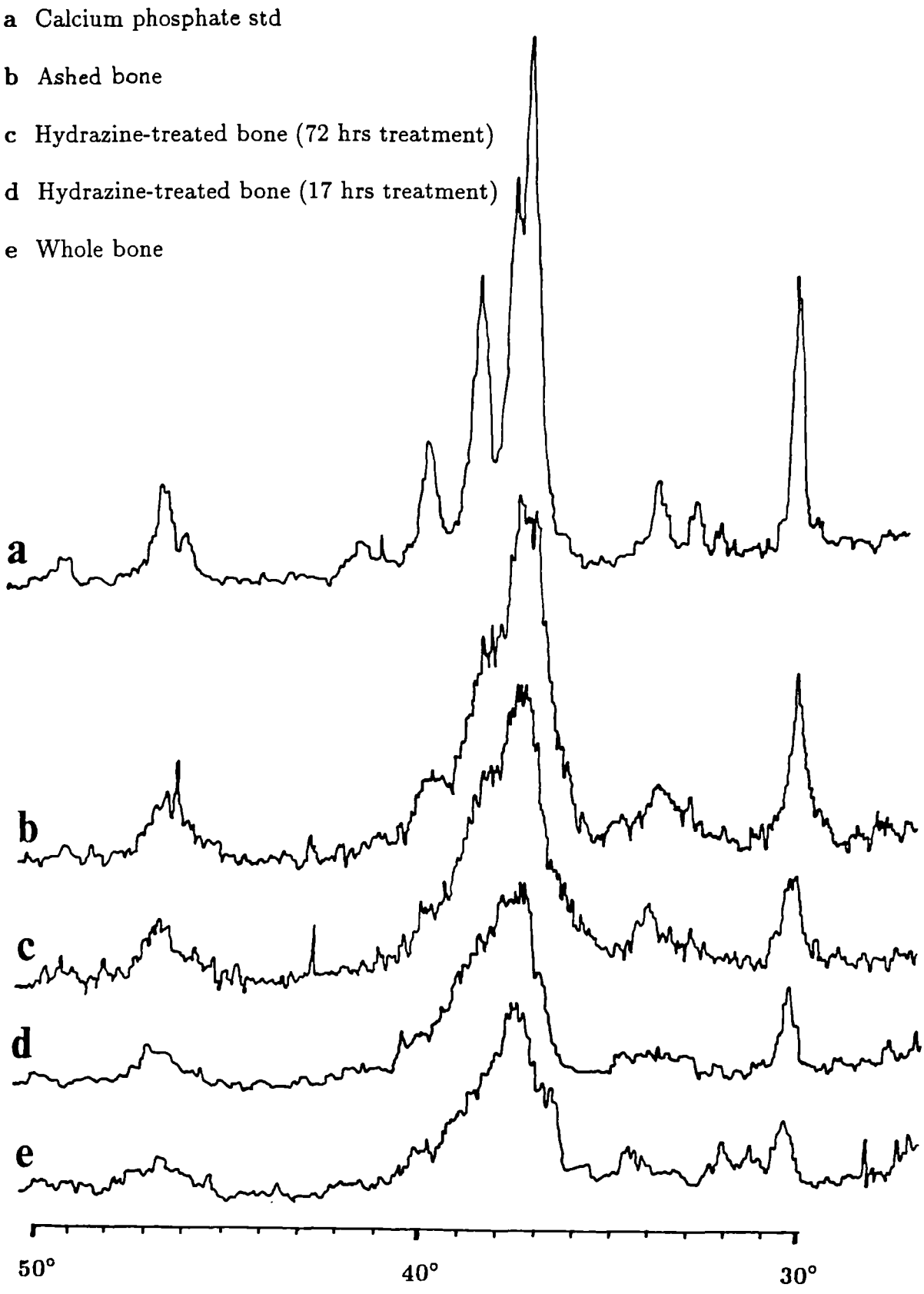

Figure 8.3: X-ray diffraction profiles of whole bone immersed in solutions of varying pH.

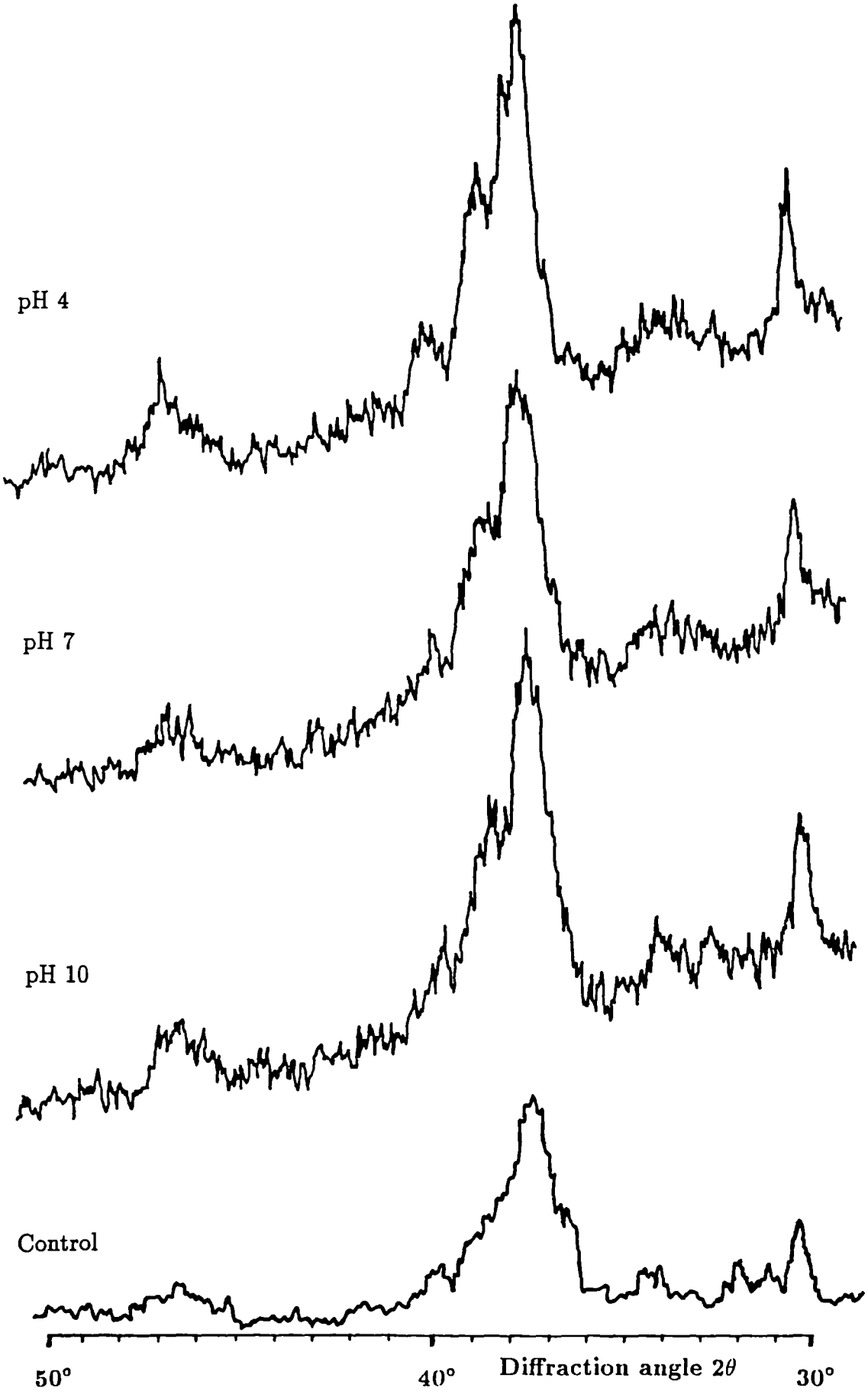

Figure 8.4: X-ray diffraction profiles of hydrazine-treated bone immersed in solutions of varying pH.

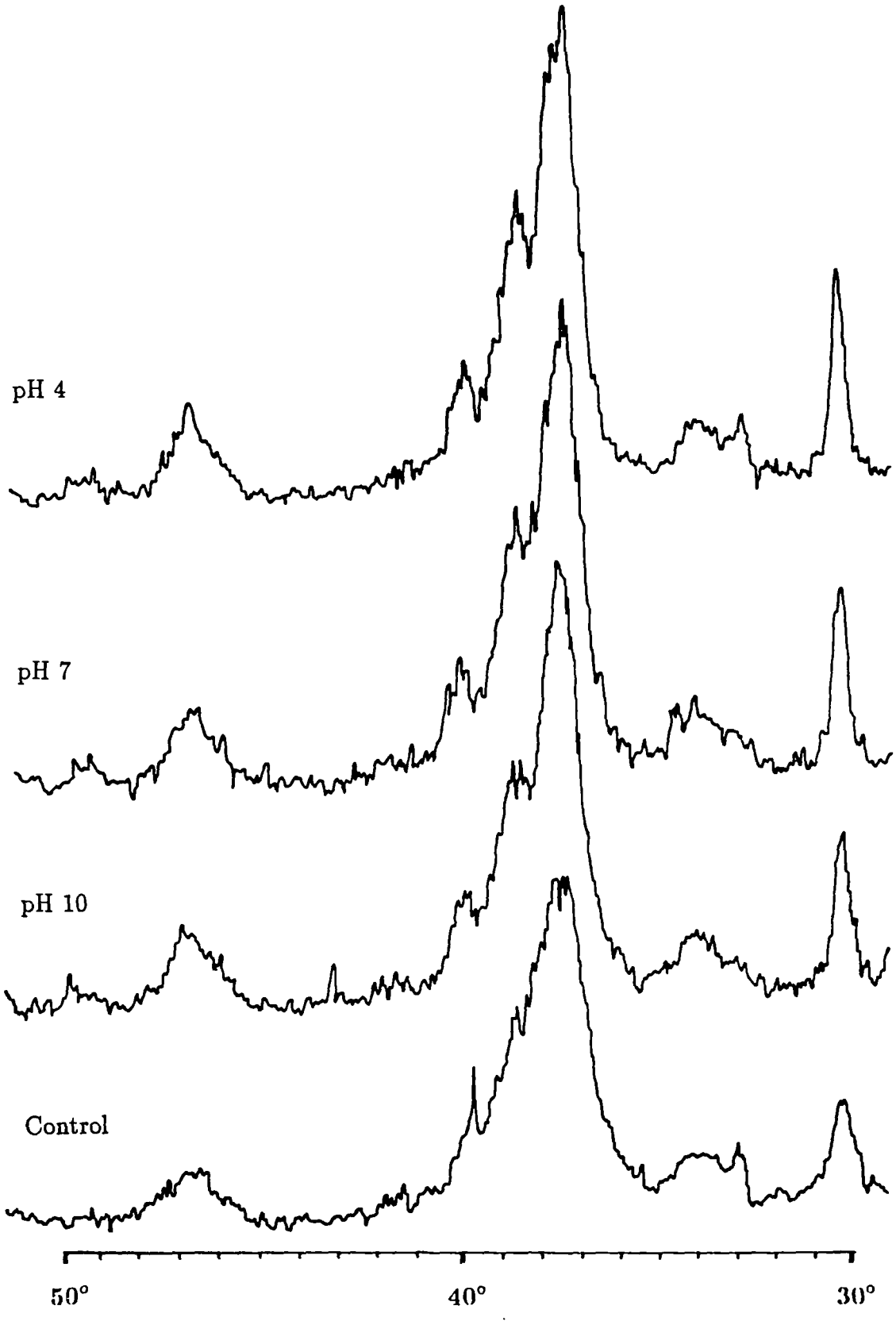

Figure 8.5: X-ray diffraction profiles of ashed bone immersed in solutions of varying pH.

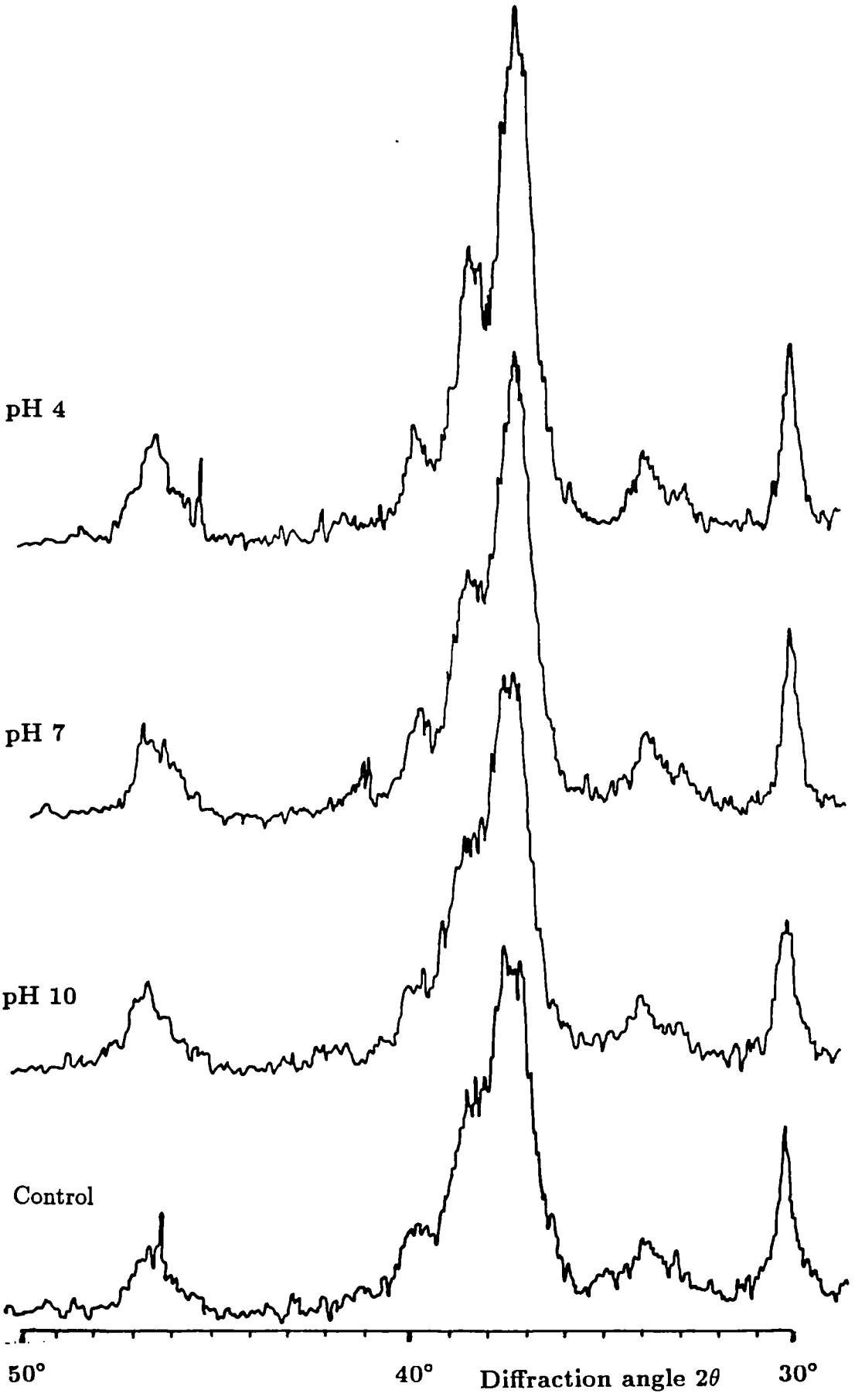

3. Strontium/uranium immersion.

The exposure of bone mineral to salt solutions with different chemistries necessitated examination of both the crystallinity and identity of peaks.

(a) Identification of peaks.

Recorded peaks were identified on the basis of the 2-θ positions of their maxima. These values were then converted to d-spacing, measured in Angstroms, using appropriate tables where d had been calculated using Braggs' equation. Mineral phases were identified by comparison with standard patterns compiled by JCPDS, a minimum of 3 peaks usually being sufficient for positive identification.

The majority of peaks identified were characteristic of hydroxyapatite, as determined by reference to the hydroxyapatite standard (BDH Chemicals) - a highly crystalline, stoichiometric synthetic hydroxyapatite.

The diffraction profiles of all samples from Immersion Series III (immersed in either 100 ppm strontium or 1000 ppm uranium solutions) consisted *only* of peaks intrinsic to hydroxyapatite. There were no **detectable** peaks representing either of the original salts in solution i.e. strontium nitrate or uranyl di-nitrate.

However, a number of peaks extrinsic to hydroxyapatite were seen in bone samples from Series II immersed in 4 M strontium solution: the strontium salt used in this study was strontium chloride hexahydrate. The large peaks observed at around 15°2θ and 26°2θ for all ashed bone samples exposed to this solution were characteristic of the main peaks of strontium chloride hexahydrate ($SrCl_2.6H_2O$) and probably represented strontium salt predominantly *adsorbed* to the exposed surfaces of this bone, or *crystallised* in cracks and/or pore spaces. The number of peaks extrinsic to hydroxyapatite increased with duration of immersion (see figure 8.6). Many peaks correlated with strontium chloride di-hydrate ($SrCl_2.2H_2O$), though there were also peaks common with strontium chlorate, strontium carbonate, various forms of strontium hydrogen phosphate, and β strontium-calcium phosphate; these were largely present in ashed bone immersed for 10 weeks. While the number of peaks extrinsic to hydroxyapatite increased with time in ashed samples, the relative intensity of peaks representing strontium chloride hexahydrate

(particularly its two major peaks- 100 and 110 hkl, marked 'a' and 'b' on the figure) was maximum at 6 weeks immersion. Measurements of relative intensity of these two main peaks in bone immersed for variable duration are shown in table 8.1. This confirmed earlier EPMA studies on immersion in strontium saturated solutions.

Table 8.1: Relative Intensities of 100 and 110 hkl Peaks of Strontium Chloride Hexahydrate in Ashed Bone Samples Immersed for Variable Duration

Sample	Relative Intensity %	
	100 hkl (15°2θ)	110 hkl (26°2θ)
$SrCl_2.6H_2O$	100.0	87.0
1 week	86.1	95.4
6 weeks	100.0	86.0
10 weeks	57.0	39.8

There was little indication of peaks extrinsic to hydroxyapatite in samples immersed as whole bone, except for the presence of a few peaks representing $SrCl_2.2H_2O$ in bone immersed for 10 weeks. It must be noted that samples immersed as whole bone in this study were ashed prior to XRD analysis to facilitate the powdering of this material. For this reason, crystallinity measurements of these samples were not useful because any changes caused by strontium would inevitably be masked by the heating process.

Figure 8.6: X-ray diffraction profiles of ashed bone immersed for variable duration in saturated strontium solution.

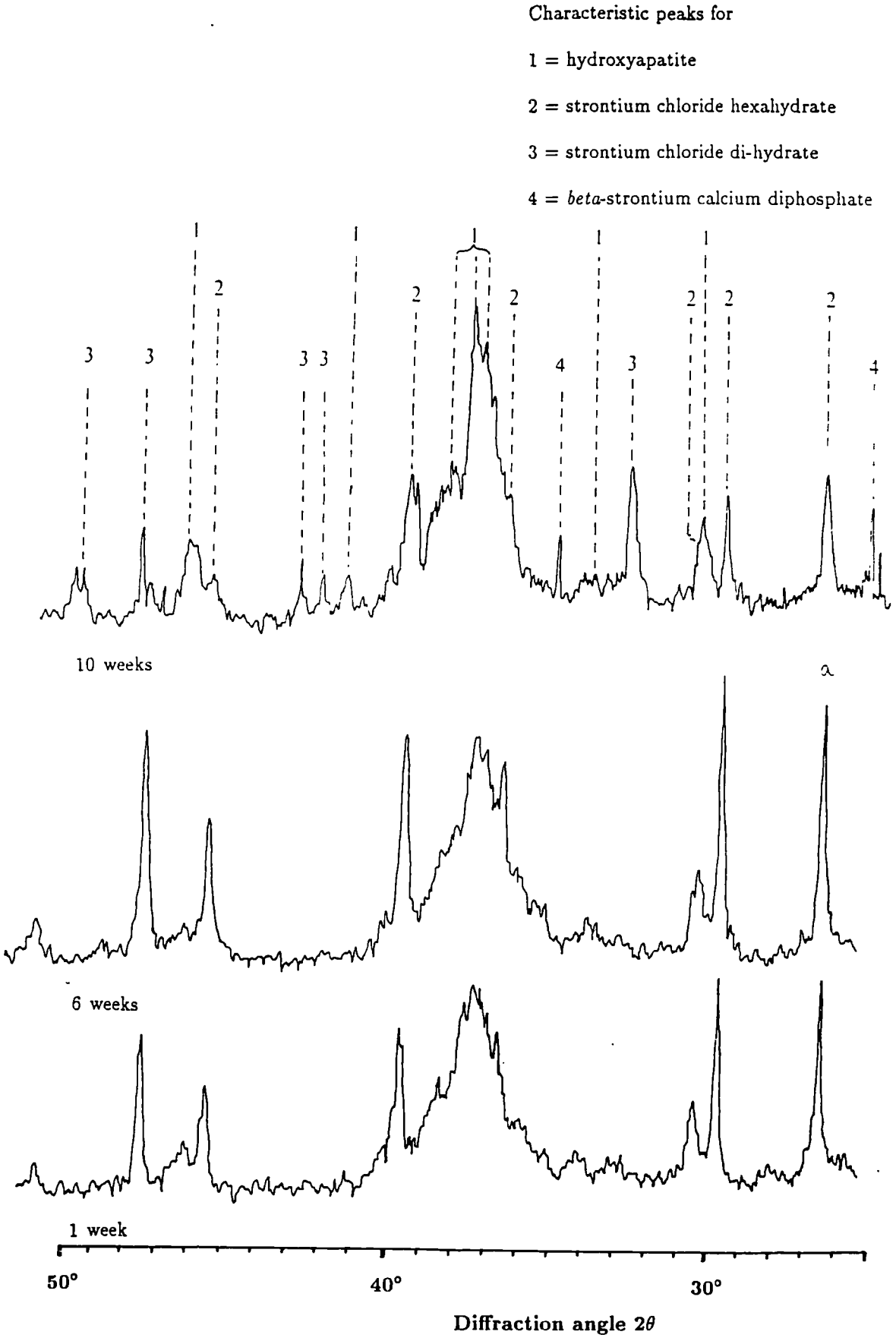

(b) Crystallinity measurements.

(i) *Immersion Series II.*

Crystallinity measurements were taken for ashed samples (see table 8.2) from Immersion Series II, an examination of strontium uptake over time. D, breadth/height and intensity values for corresponding peaks were compared across samples and are shown plotted in figures 8.7i, ii and iii.

Table 8.2: Crystallinity Measurements of Ashed Bone Immersed in Saturated Strontium Solution for Variable Duration.

hkl peak	Crystallinity	1 week	6 weeks	10 weeks
002	D	.3704	.3704	.3704
	$\frac{B}{H}$	.1038	.1000	.1038
112/211	D	.1031	.1299	.1493
	$\frac{B}{H}$	.1492	.1132	.0720
310	D	.2703	.5882	.3700
	$\frac{B}{H}$	.2846	.1700	.1080

The graphs show the following trends with increasing duration of immersion:

(1) a general increase in D for peaks 112/211 and 310 (although a slight drop after 6 weeks for 310), and a relative constancy for 002;

(2) a reduction in breadth/height ratio;

(3) a general increase in the intensity of peaks 112/211 and 310, while an apparent constancy in peak 002 over time.

In fact, none of the crystallinity measurements for peak 002 significantly altered over time. This was a clear isolated peak, relatively easy to measure, thereby providing a potentially reliable indication of crystallinity. Its apparently unchanging

Figure 8.7 Graphs to show changes in (i) D, (ii) breadth/height ratio and (iii) intensity for ashed bone against period of immersion.

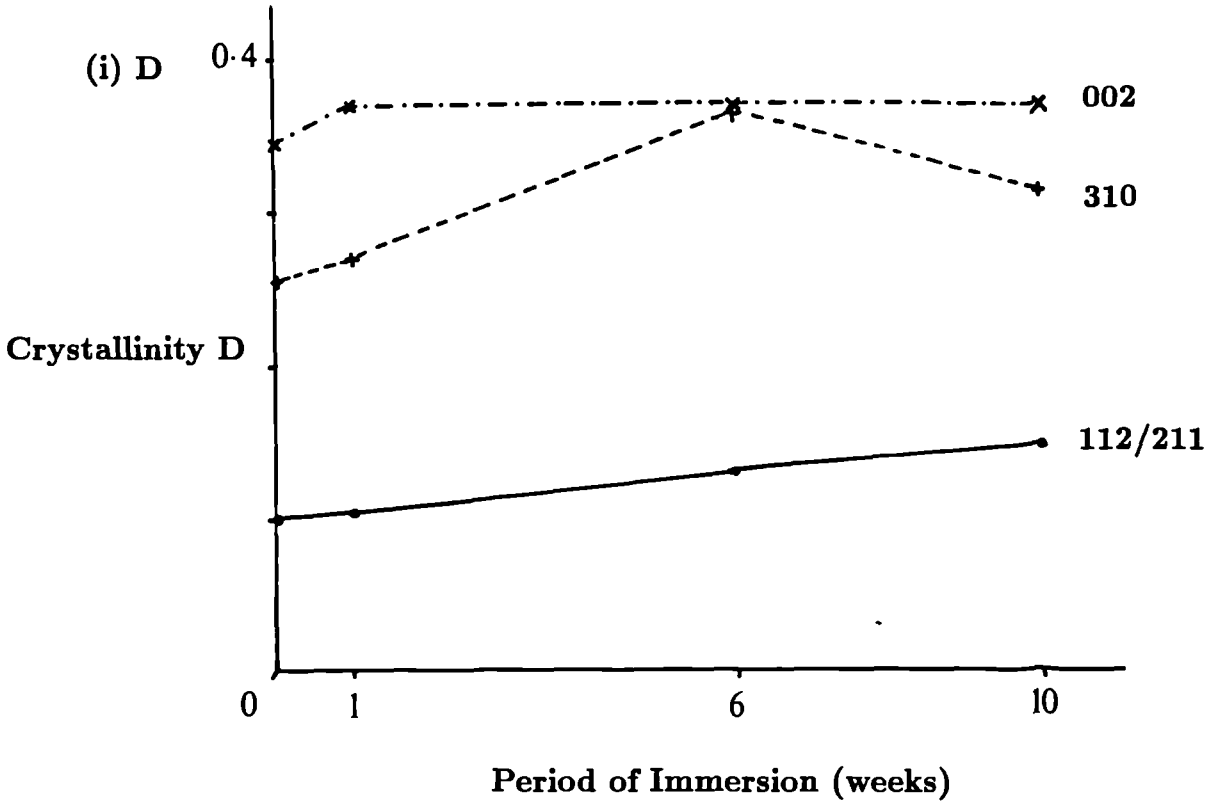

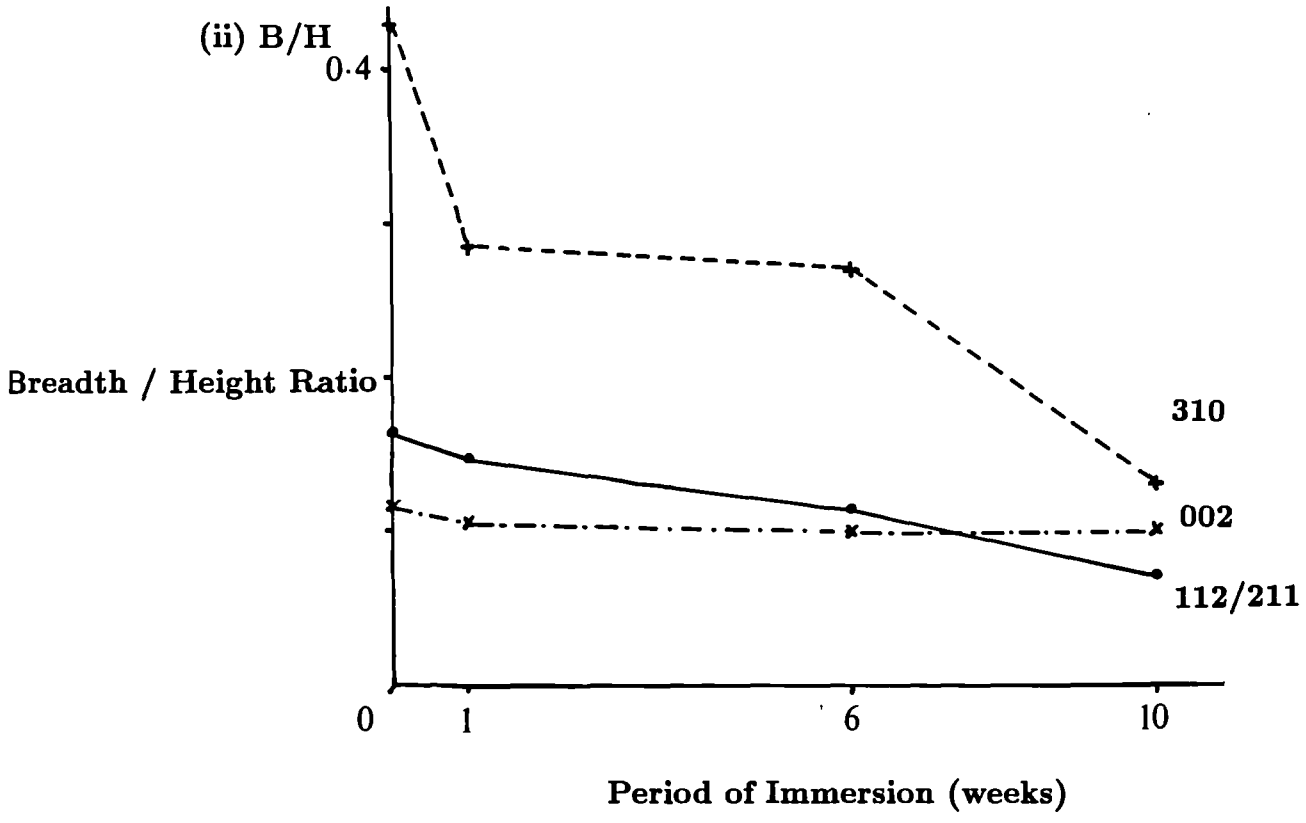

(iii) I

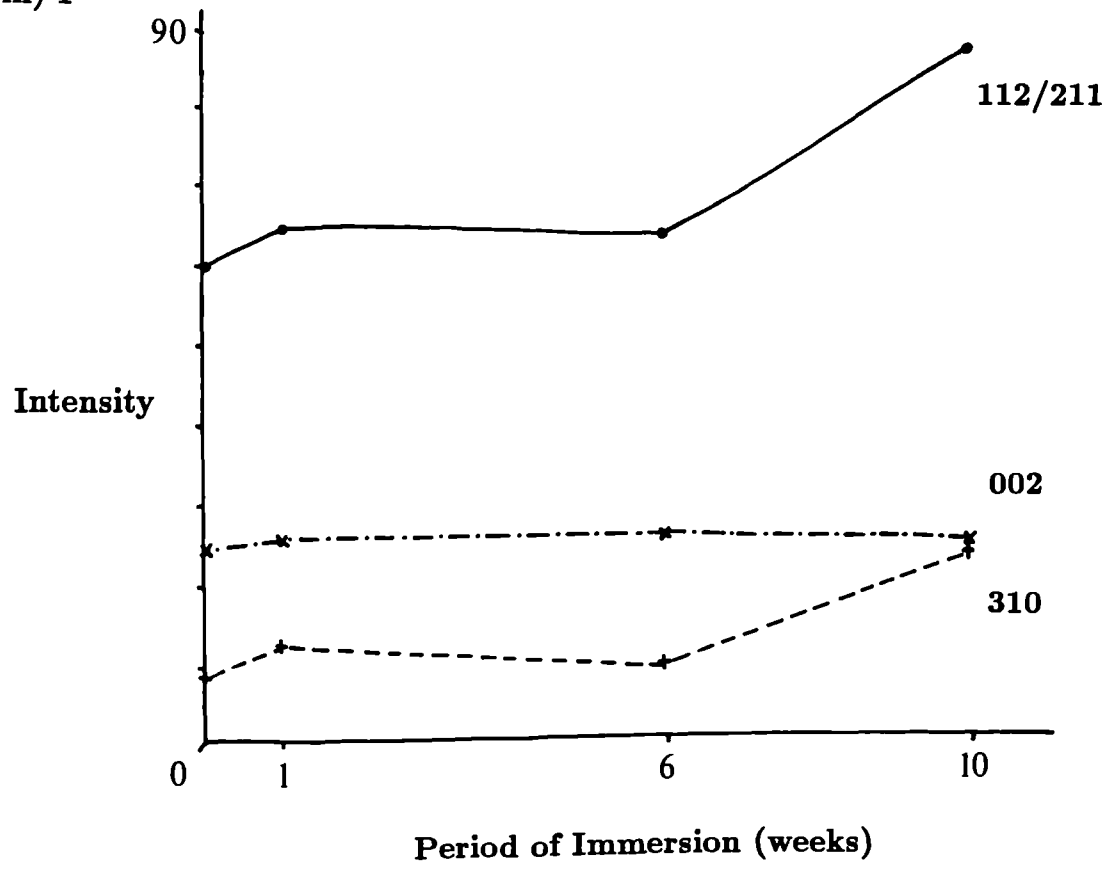

crystallinity over time suggested that immersion in strontium solution did not affect the axial (directional) reflection denoted by this peak. Alternatively, it may be that interference caused by the 200hkl peak of $SrCl_2.6H_2O$ in this 2θ region was responsible, although it seems unlikely since this peak is of relatively low intensity ($\approx$5%) in the aforesaid compound.

Peak 310, on the other hand, was rather difficult to measure because of its small and, in some cases, relatively undefined character: this may account for fluctuating trends over time. Peak 112/211, the largest and most clearly defined peak for hydroxyapatite, was consequently regarded as the most reliable index for crystallinity measurement. Results for this peak suggest that the immersion procedure carried out in this study effected an increase in bone crystallinity. However, the *relative* importance of immersion *per se* and the presence of strontium considered as separate entities was as yet unclear.

(ii) *Immersion Series III.*

Only ashed and hydrazine-treated bone material was used in subsequent immersion studies (Series III) because of the problems of whole bone preparation outlined earlier. Again, differences in crystallinity were observed for bone immersed in 1000 ppm uranium or 100 ppm strontium at variable pH, as demonstrated in figures 8.8 and 8.9 representing hydrazine-treated material. These show similar patterns in crystallinity for hydrazine-treated bone in strontium (8.8) and uranium (8.9) solutions as those found in earlier pH experiments in control buffered solutions: bone immersed at pH 4 possessed slightly greater crystallinity, with pH 10 having the least effect. No other differences were apparent and no visible distinction between strontium and uranium immersions could be made.

Therefore, a statistical analysis of crystallinity measurements was carried out on bone from Immersion Series III to determine

(a) any significant differences in crystallinity and, as a consequence,

(b) identify patterns and trends.

In this way, it was anticipated that both the individual and combined effects of the organic/inorganic status of the bone, pH of immersion and strontium/uranium in solution could be determined.

8.1.3 Statistical Analysis of Crystallinity.

The experimental design of these immersion studies was constructed to examine the possible effects of bone condition, treatment and pH i.e.. a number of independent variables, on a measurement of crystallinity, the dependent variable, which was measured in three different ways: M1- the D index, M2- the breadth/height ratio, and M3- the peak intensity.

These measurements were all dependent variables, but independent of one another. Thus, M1, M2 and M3 could not be pooled as one measurement. Conversely, the corresponding values for both measurement type and peak could be grouped together e.g. M1 for all peaks.

Figure 8.8: XRD profiles of hydrazine-treated bone immersed in strontium solution of variable pH.

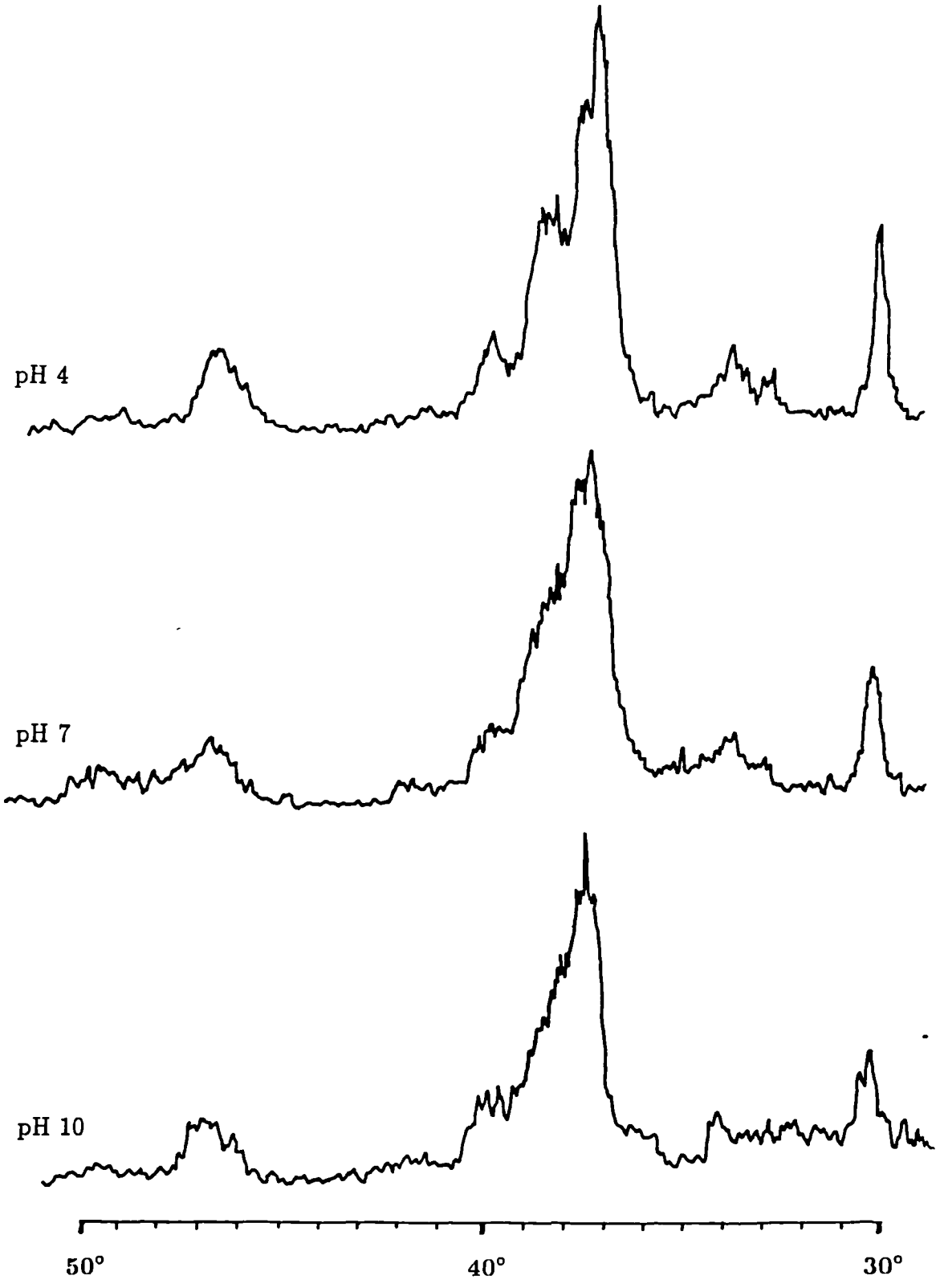

Figure 8.9: XRD profiles of hydrazine-treated bone immersed in uranium solution of variable pH.

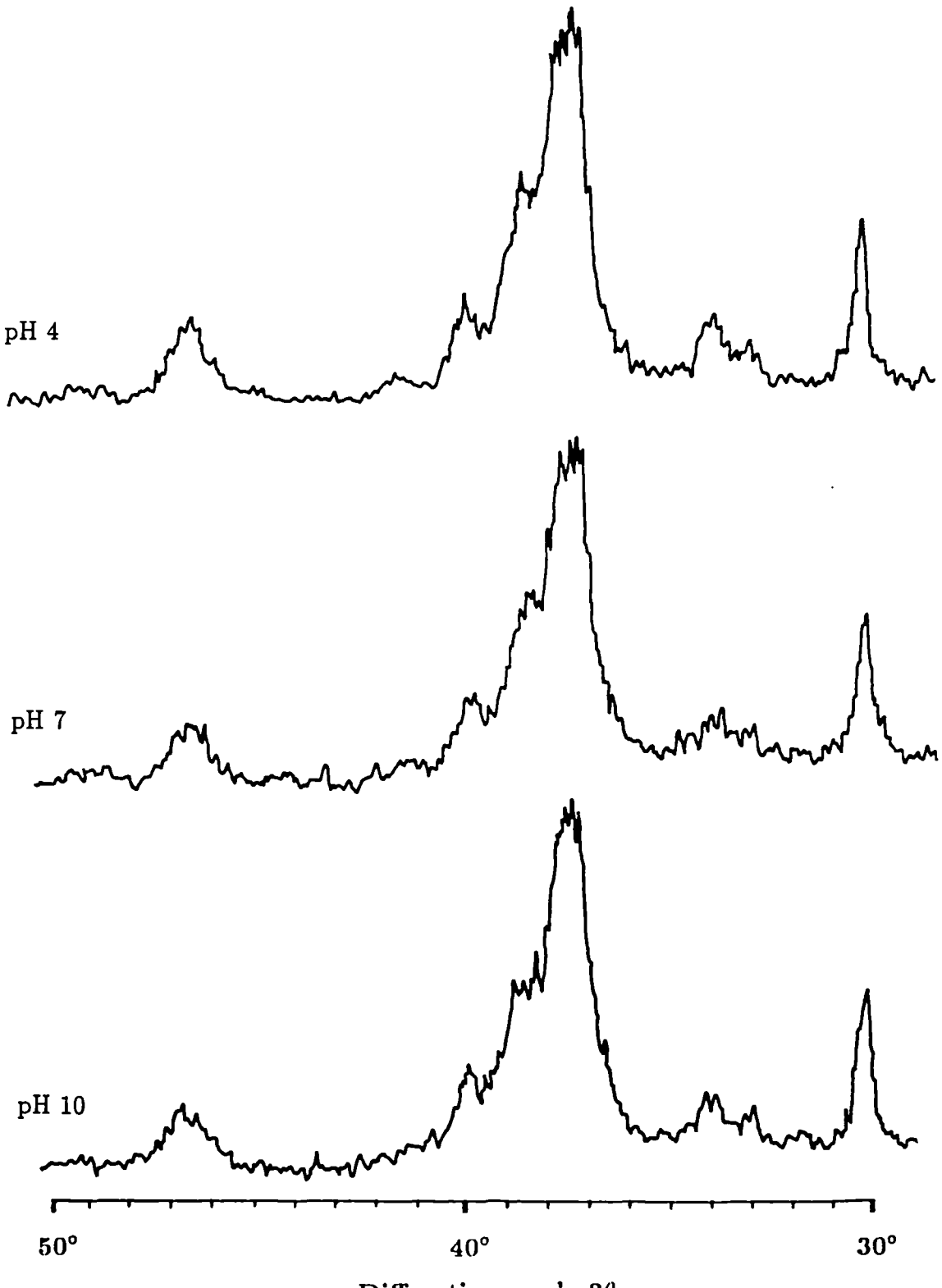

An appropriate statistical method for the analysis of such data is **three-way ANOVA.** This enables three factors or independent variables to be used in one design, analysing several dependent variables in one ANOVA procedure.

ANOVA assumes normality of distribution, that the groups have equal variances and that the groups are uncorrelated i.e.. that adjacent groups are no more closely related than non-adjacent groups. ANOVA uses the fact that the variability of measurements making up different samples from the same population may be determined from: (a) the variability of all individual measures making up all the samples (total), (b) the variability between the sample means (between), (c) the variability of the individual measures within the various samples (within). After taking account of the appropriate degrees of freedom, each of these measures of variability should be under the same null hypothesis; in this case, that there is no difference between the means of the measurement variables for the groups.

Hypothesis tests are based on the ratios of the mean squares of each source of variation to the mean square for the residual: this is the variance ratio or **F value** . The mean squares are calculated by dividing the sum of squares (measures of variability) for within-groups and between-groups by their degrees of freedom. The between-group degrees of freedom are k-1, where k is the number of groups, while the within-group degrees of freedom are N-k, where N is the number of cases in the entire sample.

F is calculated as the ratio of the between-group sum of squares to the within-group sum of squares. Large values of F indicate that there is more variability between the 'treatment' means than expected from the residual variance i.e.. the experimental error or variance found within the samples once the possible effect of the 'treatments' has been subtracted from the total variance. The observed significance level is obtained by comparing the calculated F value to the F distribution with k-1 and N-k degrees of freedom. The observed significance level is the probability of obtaining an F statistic at least as large as the one calculated when all population means are equal (the reference F value). If this probability is small enough, the hypothesis that all means are equal i.e.. that there is no significant difference in means, is rejected.

N.B. A significant F statistic indicates only that the population means are probably unequal: it does not pinpoint where the differences are.

This experiment produced a three-way **factorial design** : there were 3x2x3=18 combinations of independent variables (pH, condition and treatment, respectively) for each measurement type for each peak. A *factorial design* is a design in which all main effects and all orders of interactions are included.

This experimental design opted for three different measurements (M1, M2, M3) on three different peaks or reflections (002, 112/211, 310) for one sample representing each combination of immersion variables, rather than one measurement on replicated samples. The design incorporated a number of variables, and as this number increased the number of cases in each cell (each combination of variables) rapidly diminished, making statistically meaningful comparisons difficult. For this reason, the main problem encountered with this design was the fact that "unique" sums-of-squares were produced due to the assumption that the redundant effects (those largely caused by missing cells) were actually null.

Three-way ANOVA tests are found in Appendix IVb, together with preliminary histogram frequency plots for each measurement index for control and immersed bone to demonstrate normality of distribution for each bone type (Appendix IVa.i) (hence the two groupings of frequency distribution representing hydrazine-treated and ashed bone).

The ANOVA data illustrate the aforementioned problem in experimental design. The sum of squares for each combination of independent variables was extremely small because there was an insufficient sample number for each category to get a within-group variation with which to compare the between-group variation i.e. there were too many empty cells in the 2x3x3 matrix.

Therefore, a one-way ANOVA test was carried out (see Appendix IVc). This test is not as powerful as three-way ANOVA, but was deemed more appropriate for a small sample population. It examines the effect(s) of one independent variable at a time rather than the effects of a combination of variables.

In order to prevent a further reduction in sample number, respective measurement indexes for each peak were pooled together. Despite this pooling, the sum

of squares were still very low, so that the F ratio values were low and F probablilities consequently high (table 8.3). This would suggest insignificant differences across samples i.e. none of the independent variables had significant effect on bone crystallinity. However, this is unlikely, as earlier XRD profiles have shown. An alternative explanation concerns the pooling procedure itself. Pooling the respective measurements for each peak assumed that any effects an independent variable may have had on crystallinity, were similar for all three peaks. Figures 8.7i, ii and iii have shown that was not necessarily the case.

With these limitations in mind, data from both ANOVA tests (a summary of one-way ANOVA data is shown in table 8.3) showed that any differences were more identifiable using (i.e. had more of an effect on) the breadth/height ratio as an index of crystallinity: its F probability values were lower i.e. any differences were less likely to be due to chance. The organic content of the bone apparently had least effect on crystallinity than exposure to Sr/U, which in turn had less of an effect than the pH of immersion i.e. pH effects on crystallinity were the most evident. But all were statistically insignificant because of an insufficient sample size, and probably because of inappropriate pooling of the peaks/reflections.

Table 8.3: One-way ANOVA Data Examining the Individual Effects of Three Independent Variables.

Independent variable	Dependent variable	F ratio	F probability
Condition of bone	D	0.0612	0.9407
	B/H	0.0742	0.9286
	I	0.0363	0.9644
pH of immersion	D	0.0856	0.7708
	B/H	0.1705	0.6810
	I	0.0006	0.9812
Sr / U exposure	D	0.1557	0.8561
	B/H	0.2123	0.8093
	I	0.1159	0.8907

8.1.4 Summary of XRD Data.

Diffraction profiles indicated improvements in crystallinity of the hydroxyapatite component of all bone immersed in buffered solutions i.e. the immersion process itself apparently effected an increase in crystallinity. Bone immersed in pH 4 solutions possessed the sharpest and most clearly resolved maxima reflecting the enhanced leaching effects of acidic solutions, and probably the degree of organic decay at this pH. Indeed, diffraction profiles were more clearly defined in samples with decreasing organic content: this may have represented improved crystallinity or simply improved resolution as the organic "noise" was reduced.

The effects of strontium and uranium on bone crystallinity were not clear. There was little indication of either's incorporation into the inorganic matrix, as determined by characterisation of peaks that might represent modified apatites or intermediates in their formation and by the hydroxyapatite reflections themselves. Only after 6 weeks immersion in 4M strontium solution were peaks extrinsic to those of hydroxyapatite observed in ashed bone, indicating surface adsorption of this strontium salt.

Statistical analysis of the data was carried out to identify any significant effects of bone condition, pH and strontium/uranium on bone crystallinity. ANOVA tests found no significant differences across the sample population that could reliably be assigned to real rather than chance phenomena. Since diffraction profiles were *visibly* variable, it may have been that statistical tests were limited by the small sample size and the fact that peaks or reflections were pooled for each respective crystallinity index: a parallel study found that peaks were not affected to the same degree.

A fundamental problem encountered in this study was the interpretation of diffraction profiles in terms of crystallinity and/or resolution, and how to separate the two. The former was a property of the inorganic component while the later predominantly the organic fraction.

The organic content of immersed bone samples was explored in more detail using CHN analysis in order to monitor the extent and/or rate of its decay under variable immersing conditions. It was anticipated that such a study would further clarify

XRD data, and provide additional information with regard to the role of the organic matrix in strontium/uranium uptake.

8.2 Monitoring the Organic Content of Immersed Bone: CHN.

CHN measurements were made on a limited number of samples representing bone that had previously been immersed in buffered solutions of varying pH. Bone samples were immersed in three forms: (a) as powdered whole bone , (b) as sliced whole bone and (c) hydrazine-treated bone.

% C, H, N and total % CHN values can be found in the Appendix IVd. Figure 8.10 plots total %CHN against period of immersion and pH, respectively. Values are summarised as follows:

Whole *sliced* bone possessed a much higher CHN content than either powdered or hydrazine-treated samples, because it was less accessible to the action of the ambient solution and offered a relatively small surface area for any leaching processes. Hydrazine-treated bone naturally possessed the lowest CHN content because a large proportion of its organic component had been removed at the outset.

All samples demonstrated the same trend in CHN content with pH. The organic matrix was found to be more stable at neutral pH and in more alkaline conditions compared to acidic pH. Indeed, for powdered samples, organic decay at pH 4 was very rapid and apparently complete (or at least reached an equilibrium) after only two weeks: little change was observed between two and twelve weeks. Bone at pH 10, in contrast, demonstrated a steeper gradient over time, indicating that organic removal in these conditions was a rather more slow and continuous process, and even moreso at pH 7.

This study demonstrates the differential loss of organic material in various forms of bone and finds that it is pH-dependent. It is probable that the data highlight the relative stability of the organic matrix in neutral and more alkaline conditions. Organic material is broken down in both alkaline and acidic conditions by amide hydrolysis. However, more energy is required to hydrolyse peptide bonds in alkaline conditions so that organic material is generally quite stable up to about pH 8.5, but will be broken down at pH 6 and below (March, 1977).

Figure 8.10: Total % CHN Values for Whole and Hydrazine-Treated Bone Samples Immersed in Solutions of Variable pH for Variable Duration.

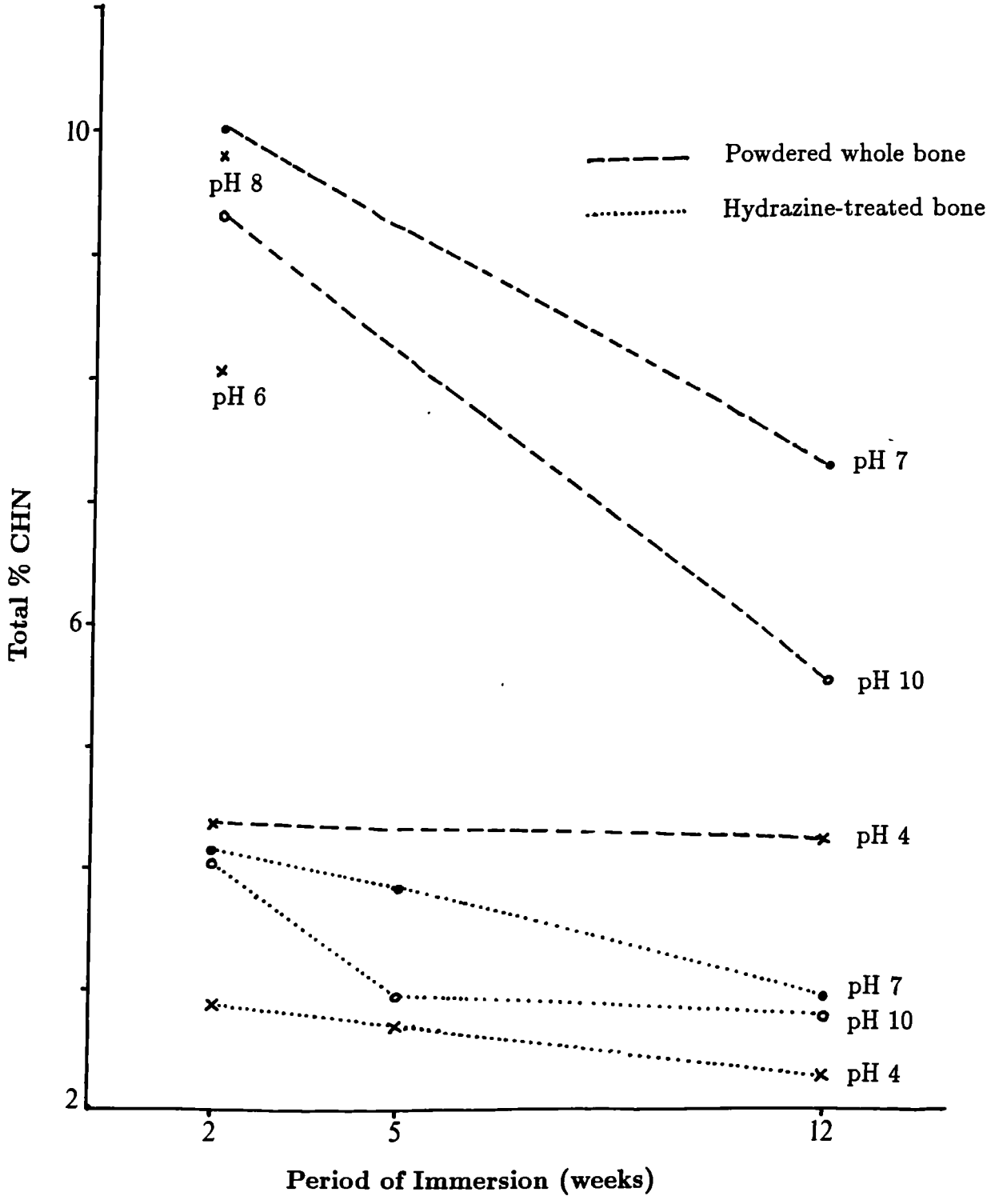

Figure 8.10:

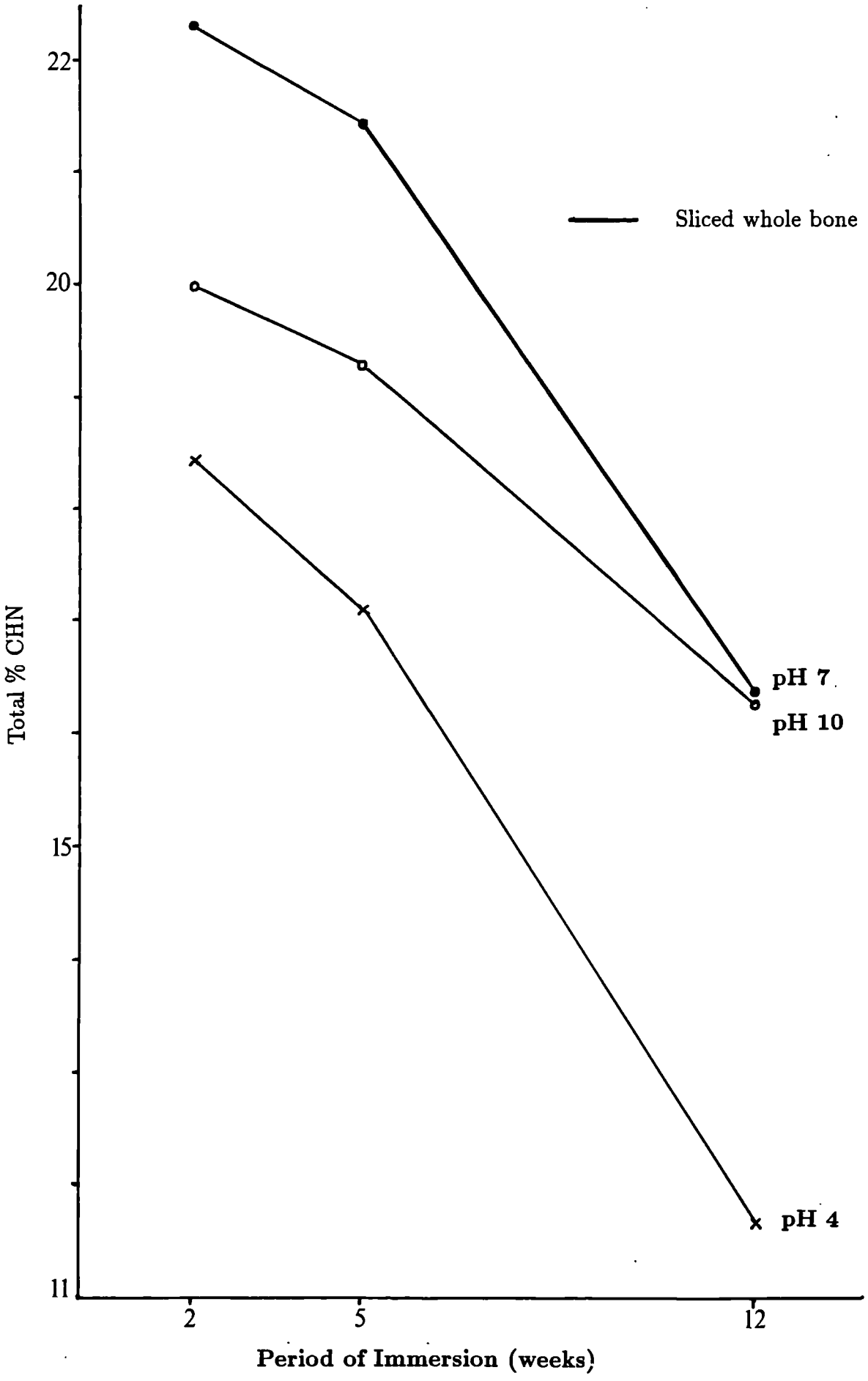
22
20
15
11
Total % CHN
Sliced whole bone
pH 7
pH 10
pH 4
2
5
12
Period of Immersion (weeks)

The mechanisms of organic breakdown at different pH, together wth their implications for elemental uptake into bone are discussed in more detail in Chapter 10.

8.3 Cation Exchange Properties of Bone Fractions.

The respective Cation Exchange Capacities of the organic and inorganic fractions of bone were investigated in order to determine the *potential* of each to remove cations from solutions to which they were exposed. In this way, it was anticipated that plausible mechanisms for strontium/uranium uptake would form that, in addition to crystallinity and CHN studies, would clarify the interpretation of uptake simulation experiments.

Both **total** Cation Exchange Capacity and a number of **specific cation** exchange capacities were investigated for a range of bone fractions: collagen, whole bone, hydrazine-treated bone (to varying degrees), and ashed bone. Rock phosphate and synthetic hydroxyapatite material was included to represent more crystalline forms of apatite. Three samples representing each were analysed to obtain average values.

8.3.1 Total Cation Exchange Capacity.

Cation exchange capacities (CEC) were measured in neutral pH conditions because CEC can vary considerably with pH. Values were calculated using the equation described in Chapter 5, section 5.4, and are shown in Table 8.4 as averaged values: the full dataset can be found in Appendix IVe.

Table 8.4 shows that whole bone possessed the highest CEC, with values in the range 66.29 - 68.57 milliequivalents per 100 g bone. This would suggest that uncompromised bone material, with the intimate association of organic and inorganic matrices intact, provided the most effective medium for cationic exchange. Indeed, it is this structural organisation that endows bone with many of its unique physical and chemical properties.

Moreover, the data here would suggest that the role of the inorganic matrix in

Table 8.4: Total Cation Exchange Capacities of bone fractions containing variable organic content.

Sample description	% Organic content	Av.total CEC (meq/100g *bone**)
Collagen	100	43.07
Whole	37	67.05
Hydrazine (4 hrs)	30	33.77
Hydrazine (17 hrs)	25	32.60
Hydrazine (72 hrs)	5	32.80
Ashed	0	28.00
Hydroxyapatite std	0	15.60
Rock Phosphate	0	5.13

* milliequivalent per 100g bone is the same as cmol (+) kg^{-1}

cation exchange processes may be secondary to that of the organic matrix, since the CEC of collagen was found to be at least 27 % greater than hydrazine-treated samples and about 54 % greater than ashed material. Indeed, a comparison of hydrazine-treated samples alone indicated a higher CEC in samples treated for 4 hours, with a 25 % organic content, than in those treated for 17 hours or more. The only discrepancy with this pattern of CEC increasing with organic content was between samples treated for 17 and 72 hours with hydrazine: despite the significant difference in organic content, an associated trend in CEC values was not found, and the CEC was actually marginally smaller in samples treated for 17 hours.

Hydrazine-treated bone was apparently more effective in exchanging with cations in the surrounding/percolating medium than ashed bone, geological apatite (rock phosphate) and synthetic apatite. CEC values in descending order were for hydrazined bone, ashed bone, synthetic hydroxyapatite and rock phosphate. This trend may have been a function of their respective crystallinites, since CEC val-

ues were inversely proportional to crystallinity: the more crystalline a sample, the lower its CEC.

8.3.2 Exchangeable Cations.

The relationship between CEC and the inorganic matrix was further investigated by measuring **exchangeable calcium** for each sample. In addition, exchangeable sodium, magnesium and potassium were measured because analysis of immersing solutions in Series I and II studies had indicated the release of these elements from bone during immersion.

Calculated values for these exchangeable cations are found in Table 8.5, and the data used in the intermediate stages of calculation are found in Appendix IVf. The calculation procedure is described in Section 5.4, and was dependent on the following variables: mass of sample in column, volume of extract collected and the atomic mass of the cation in question. (In the majority of cases, 1g sample was used and 100ml of ammonium acetate passed through the column.)

Whole bone possessed the highest exchangeable calcium values and this, as expected, was largely a function of the inorganic matrix since hydrazine-treated and ashed bone samples possessed only slightly lower values. Collagen, on the other hand, gave a value of 3.1 cmol (+)/kg. Indeed, exchangeable cation values for collagen were predictably low, as were those for synthetic hydroxyapatite reflecting the stable nature of this stoichiometric highly crystalline material. Phosphate rock demonstrated relatively low exchangeable capability except for calcium, and certainly geological apatite naturally exists in a variety of forms.

Sodium, magnesium and potassium values were generally higher in hydrazine-treated and ashed bone samples. This probably reflects the less stable nature of the biologic apatite matrix compared to the more crystalline and energetically stable apatite forms of synthetic hydroxyapatite and rock phosphate.

Table 8.5: Exchangeable calcium, sodium, magnesium and potassium in bone fractions and reference materials.

Sample description	Calcium	Sodium	Magnesium	Potassium
Whole bone	65.3	8.7	11.0	0.8
Collagen	3.1	1.7	0.6	0.3
Hydrazine (17 hrs)	63.7	19.4	24.2	1.1
Hydrazine (72 hrs)	57.9	13.2	19.4	0.8
Ashed bone	56.4	5.3	13.7	0.5
Phosphate rock	54.2	0.1	8.0	0.2
Synthetic HA	13.9	0.1	4.3	0.2

All values in cmol (+) per kg sample i.e. meq per 100g.

8.3.3 Summary.

The cation exchange capacities of a range of bone fractions and reference materials appeared to be dependent on a number of factors:

(i) the organic content of the sample, which was more effective in cationic exchange than inorganic components.

This is probably due to anionic carbonyl groups on the amino acids in protein components (collagen, glycoproteins etc.) attracting the cationic ammonium ions as they percolate through the sample. So, the process observed in this study is not necessarily one of cation exchange, but rather a sequestering process.

(ii) the crystallinity of the sample.

The less crystalline a sample, the more readily it renders its calcium ions for exchange, reflecting the relative instability or reactivity of apatite matrices more

closely resembling their biologic form. Synthetic hydroxyapatite (stoichiometric and perfectly crystalline) and rock phosphate (apatite in its crystalline geologic form) possess stable structures so that exchange of their more tightly bound calcium ions is less energetically favourable.

The exchangeable cation study largely confirmed these observations, demonstrating that the "CEC property" of collagen is really a misnomer: the mechanism of ammonium ion uptake is not cation exchange but a sequestering or complexing process. In addition, cation exchange values are related to the crystallinity and matrix stability of samples, and these values highlight the importance of cation exchange capacity/exchangeable cation studies as opposed to those that simply measure total elemental content.

The implications of these findings to the mechanisms of elemental uptake in the burial environment are explored in the Discussion (Chapter 10), in conjunction with observations based on uptake-simulation studies (Chapters 6 and 7) and fieldwork (Chapter 9). Fieldwork was carried out to test laboratory-based findings on the trends in elemental uptake and on the general behaviour of bone in solution, so that subsequently models of elemental uptake could be drawn up.

Chapter IX

Field Studies.

9.1 Objectives.

Archaeological bone material was excavated from a range of burial environments and examined for the following reasons:

4. to investigate further the diagenetic alteration of buried bone and its relationship/dependence on the conditions of burial. Associated soils and sediments were examined where available.

5. to examine the patterns of contamination by trace elements, in particular strontium and uranium, and compare this with laboratory-based simulation studies.

Thus, the aims of this section were to explore *actual* diagenetic alteration in a range of exhumed bone material excavated from a variety of burial environments.

The archaeological material used in this study included fragments of unprovenanced bone from a number of sites of "special interest", which were kindly donated to me for research purposes. However, the majority of bone material was obtained from three sites in the U.K. I was present at each of these excavations and was able to take *in situ* soil measurements and samples, noting the contexts and corresponding skeletal finds for each.

Several conventional methods of analysis were used, together with the predominant technique here - scanning proton microprobe analysis, incorporating PIXE and RBS measurements. So far as I am aware, this analytical technique has not been used for such investigations before, and its applicability to such purpose is discussed.

In addition, the suitability of soil analyses similar to those adopted by Lambert *et al.*(1983,1985) (described in Chapter 3) as a means of identifying diagenetic processes by *in situ* elemental gradient profiles was investigated.

Patterns of diagenetic alteration observed in archaeological specimens were correlated with measured burial parameters and compared with observations made by experimental uptake studies where possible.

The following experimental strategy was adopted for these terrestrial excavations.

9.2 Experimental Strategies.

9.2.1 On-Site Procedures.

A general description of the site's soil type(s) was made according to knowledge of the local geology and characterisation of the subsoil/bedrock material using a number of criteria: these included soil colour (using the Munsell colour chart) and soil texture. Soil pH and Eh values were measured, both in and around grave contexts, using a hand-held Philips' PW9424 pH meter with attaching combination pH electrode and platinum redox electrode, as shown in Figures 9.1(a) and (b). pH and Eh measurements were automatically temperature-compensated via a temperature probe attachment.

pH was measured in two different ways, either (1) by placing the electrode *in situ* , buried in relatively undisturbed soil and taking a reading after approximately 30 minutes (allowing time for the reading to settle), or (2) by placing a soil sample in a beaker and making up a soil paste with distilled water, leaving for 1 hour to settle and then taking a measurement. However, it must be noted that the measurement of pH depended very much on the soil:water ratio used in the determination, as well as the amount of soluble ions present. In each case, sufficient water was added to make a thin paste. pH measurements were found to be very similar and comparable for both these methods, and any changes in pH value across a site and even within grave contexts were noted.

The redox potential, or Eh, is a particularly difficult parameter to measure. The insertion of the platinum electrode into the soil, however carefully, will disturb the soil and automatically alter its redox conditions. Similarly, Eh will tend to increase (i.e. become more oxidising) with transportation and handling/sampling.

Figure 9.1(a),(b) *In situ* **measurement of the pH, Eh and temperature of the burial matrix.**

(a)

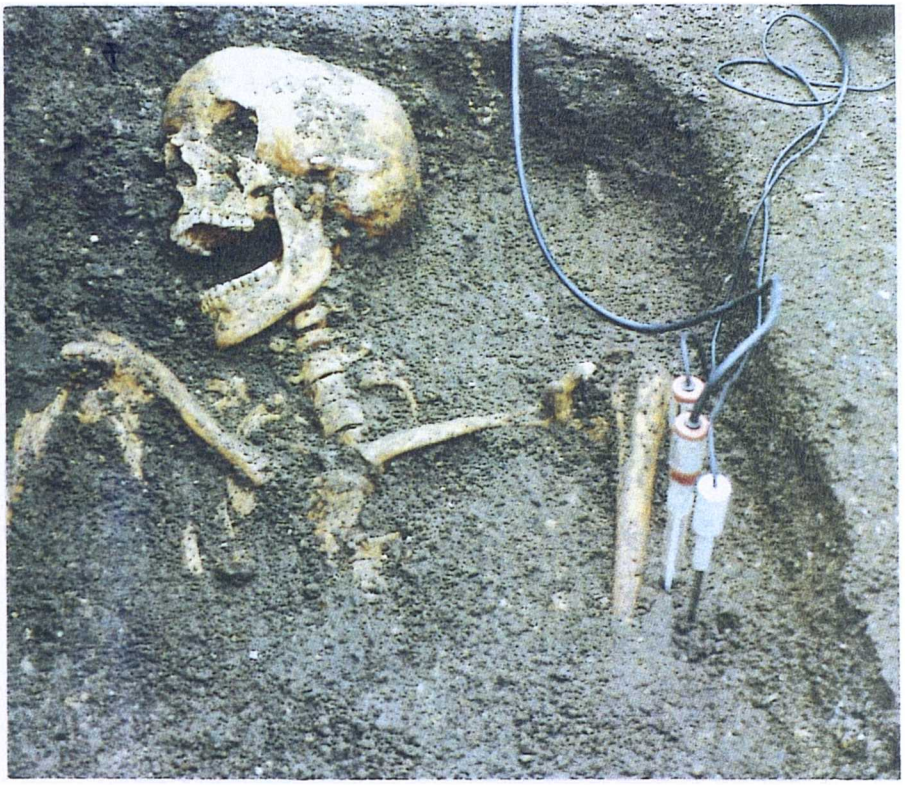

(b)

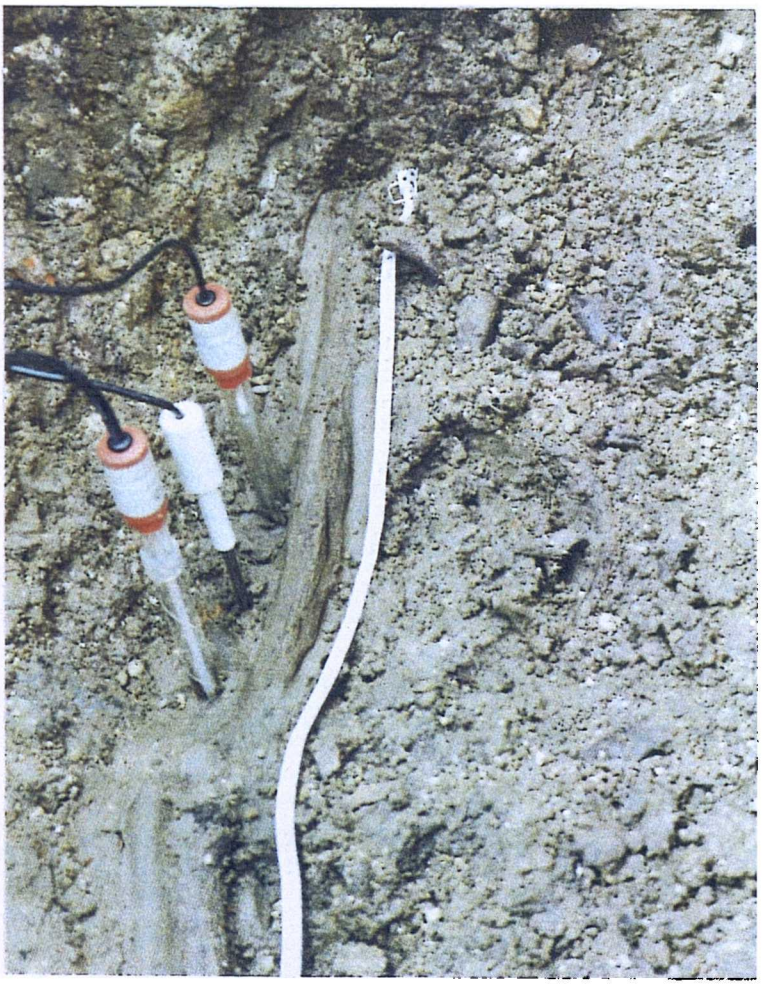

Therefore, Eh was measured *in situ* in a similar way to pH, but allowing up to 2 hours for equilibration and thus a stable reading.

Soil samples were collected for subsequent laboratory analysis. 20-50 g soil was removed from localised areas of grave contexts in a systematic manner: from immediately adjacent to and lining whole tibia/femurs lying *in situ*, and then taken at increasing distances away from the bone, at incremental distances of 5 cm, up to 25 cm away (see Figure 9.2). Soil samples were also taken more generally from around the site.

9.2.2 Laboratory-Based Procedures.

Representative soil samples were prepared for elemental analysis by XRF. 5 g soil was dried in an oven at 105 °C for 2 hours and then ground with a mortar and pestle into a fine homogeneous powder. Each was then made into a pellet using a hand press.

The long bones corresponding to the soil samples collected were selected and their general state of preservation noted. Slices of bone were cut transversely along the mid-shaft region, ultrasonically washed to remove extraneous material, such as the soil observed in the cancellous and medullary areas in Figure 9.3, and then each prepared in 1 of 5 ways:

1. as a thin section for light microscopy, to examine the general state of structural preservation at the microscopic level.
2. as a powder for XRD and/or XRF analysis.
3. as a section for EPMA.
4. as a thin section for subsequent PIXE analysis.
5. as a section for fission track analysis.

Figure 9.4 illustrates a typical example of a resin-embedded slice of archaeological bone in transverse section, prepared for EPMA.

A similar range of preparation methods was carried out on bone excavated elsewhere, at sites of "special interest". However, analysis was not as extensive in

Figure 9.2 An illustration of the sampling strategy for soils within and around the location of graves.

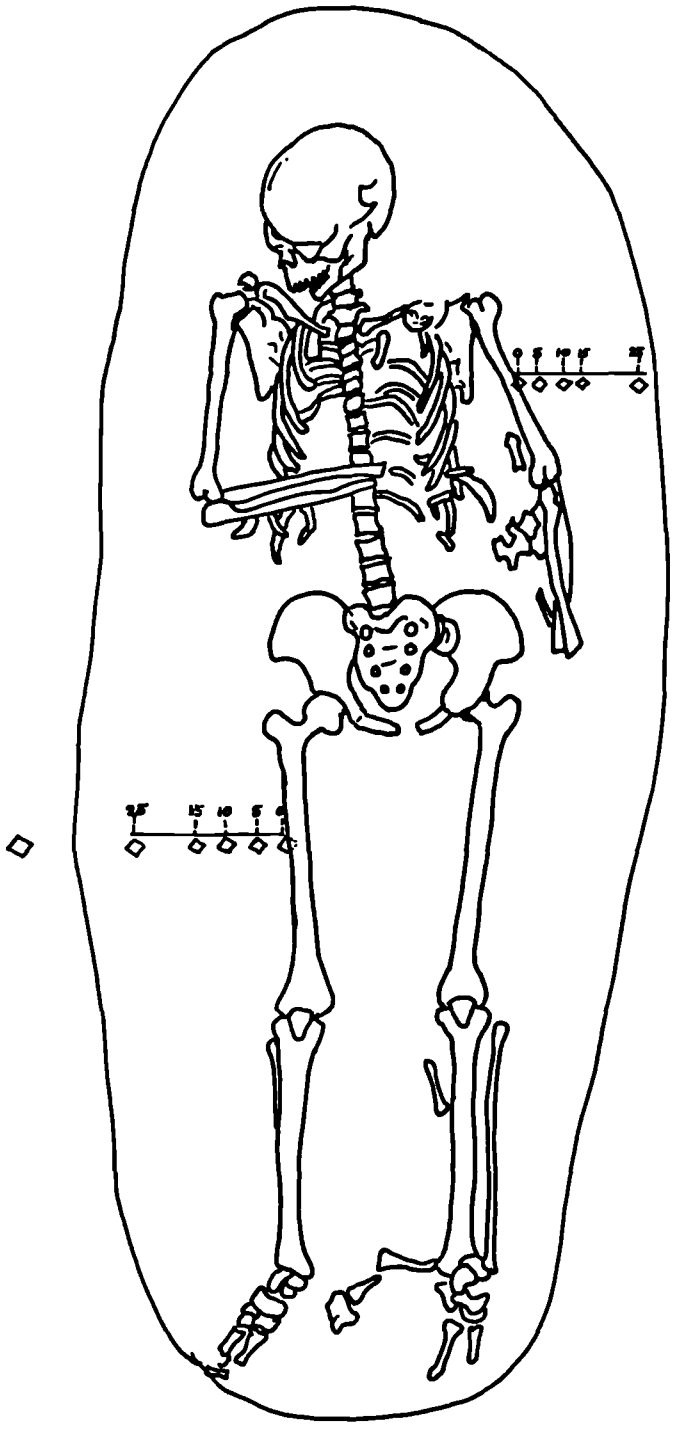

Figure 9.3: A typical example of a long bone specimen excavated from the British mainland sites.

Figure 9.4: Resin-embedded archaeological bone specimen in transverse section (after polishing).

these cases because of the limited availability of the material. Where possible, any accompanying sedimentary material was collected for subsequent characterisation using XRD.

With regard to microprobe techniques, the polished surface of resin-embedded samples was coated with a thick layer of evaporated carbon, as described in Chapter 5, to avoid sample charging problems. For PIXE analysis, the samples were analysed using a beam of 3MeV protons focused to a diameter of 1 micron at a beam current of 100-150 pA. The induced x-rays were detected using an 80 sq.mm Si-Li detector. A pepperpot filter was used to filter the calcium signal down to 0.1 %, so that it would not obscure the other elements present in trace amounts. In some cases, simultaneous detection of backscattered protons (RBS) was used to give information on the major element stoichiometry of the sample and also on the depth uniformity when point analyses were required.

The data collected were in the form of two-dimensional elemental maps, one-dimensional elemental line profiles or point analyses. The point analyses were processed using PIXAN (Clayton, 1986) as implemented in the Oxford data reduction program SPEX, which allows the use of information from the RBS spectrum to be use for thick target matrix correction (Jaksic *et al.*, 1991).

9.3 Description of Archaeological Bone Material.

The following samples were chosen to represent a wide range of burial conditions:

1. Human femur material from three archaeological sites in the U.K.:

(a) A mediaeval Franciscan friary site in **Hartlepool, Cleveland**, described by Daniels (1986). This site was dated around 1240 A.D. It was located on a calcareous magnesian limestone bedrock (with dolomite and anhydrite influences), with a loamy/sandy alkaline soil whose pH was measured at pH 7.1-7.7, and Eh 334-370 mV. The Munsell soil colour registered as 7.5 YR 3/2 (yellowy-red).

(b) A mediaeval priory (St.Gregory's) in **Canterbury, Kent**, dated over the period 12th - 16th centuries. This site was located in a loamy-clay soil with a neutral (6.95-7.15) pH and a measured Eh 313-323 mV i.e. oxidising, on a brick-earth bedrock. The Munsell colour description was 2.5 Y 3/2 i.e. a reddish yellow.

Chalks, flints and oyster-shells were abundant in the soil. Some graves were lined with limestone.

(c) A Saxon settlement in **Watchfield, Oxfordshire**. Here, the ferruginous (iron pan) soil, deep red in colour, was slightly acidic to neutral pH (6.6- 7.02) and oxidising (250-330 mV). The latter was confirmed with a positive iron test indicating the presence of Fe 3+.

2. Human clavicle (unprovenanced) from the **"Mary Rose" wreck**. The "Mary Rose" was the flagship of Henry VIII and, whilst in action against the French off Portsmouth, capsized and sank with the loss of most of her crew. Her remains were salvaged in 1982. Conditions of burial were probably anoxic, and XRD analysis of the sediment associated with the bone material revealed peaks characteristic of illite, quartz, mica, kaolinite and montmorillionite or clay, i.e. largely argillaceous/detrital sedimentary rock containing colloidal material (see Figure 9.5a).

3. Human femur material from an Arabian shipwreck, located at a depth of 54m off the north-west side of Saint Marguerite Island off the Mediterranean coast of France. The bone material has been described in detail by Arnaud *et al.*(1978) and radiocarbon dated at 560 A.D. The sedimentary milieu, again anoxic, was prevalently alkaline, as determined by the mineral composition of "slime" associated with the bone (Arnaud *et al.*, 1978). XRD analysis of the sediment by Arnaud identified a sandy silt deposit containing quartz and calcite.

4. Fragments of unprovenanced bone, probably human fibula, from **Pompeii**, dated 55 A.D. XRD analysis of the sediment in and around the bone material identified peaks characteristic of calcite and phosphate (see Figure 9.5b).

5. Recent mammalian (bovid) metapodial bone from **Olduvai, Africa**, whose geology has been described by Williams and Marlow (1987). It reflects an alkaline and oxidising environment, that was once lacustrine. The two/three year-old bone sample used in this study was found on the surface, partly exposed to the aerial environment (labelled 'T') and partly buried in the soil ('B'): a clear definition was made between these two areas.

The geophysical features of each respective burial environment are summarised in table 9.1.

Table 9.1 . A summary of the geophysical description of burial sites.

Location of site	Soil description	pH	Eh (mV)
Hartlepool, Cleveland	Loamy/sandy	Alkaline (7.1-7.7)	Oxidising (334-370)
Canterbury, Kent	Loamy-clay	Neutral (6.9-7.2)	Oxidising (313-323)
Watchfield, Oxford.	Iron pan / clay	Acidic (6.6-7.0)	Oxidising (250-330)
English Channel	Detrital sediment and clay	N/K	Reducing
Meditteranean Sea	Detrital sediment and sand	Alkaline	Reducing
Pompeii, Italy	Calcite and phosphate	N/K	N/K
Olduvai, Africa	Claystone/sandstone	Alkaline	Oxidising

Figure 9.5a/b. XRD Profiles of Sediment Associated with (a) "Mary Rose" and (b) Pompeii bone material.

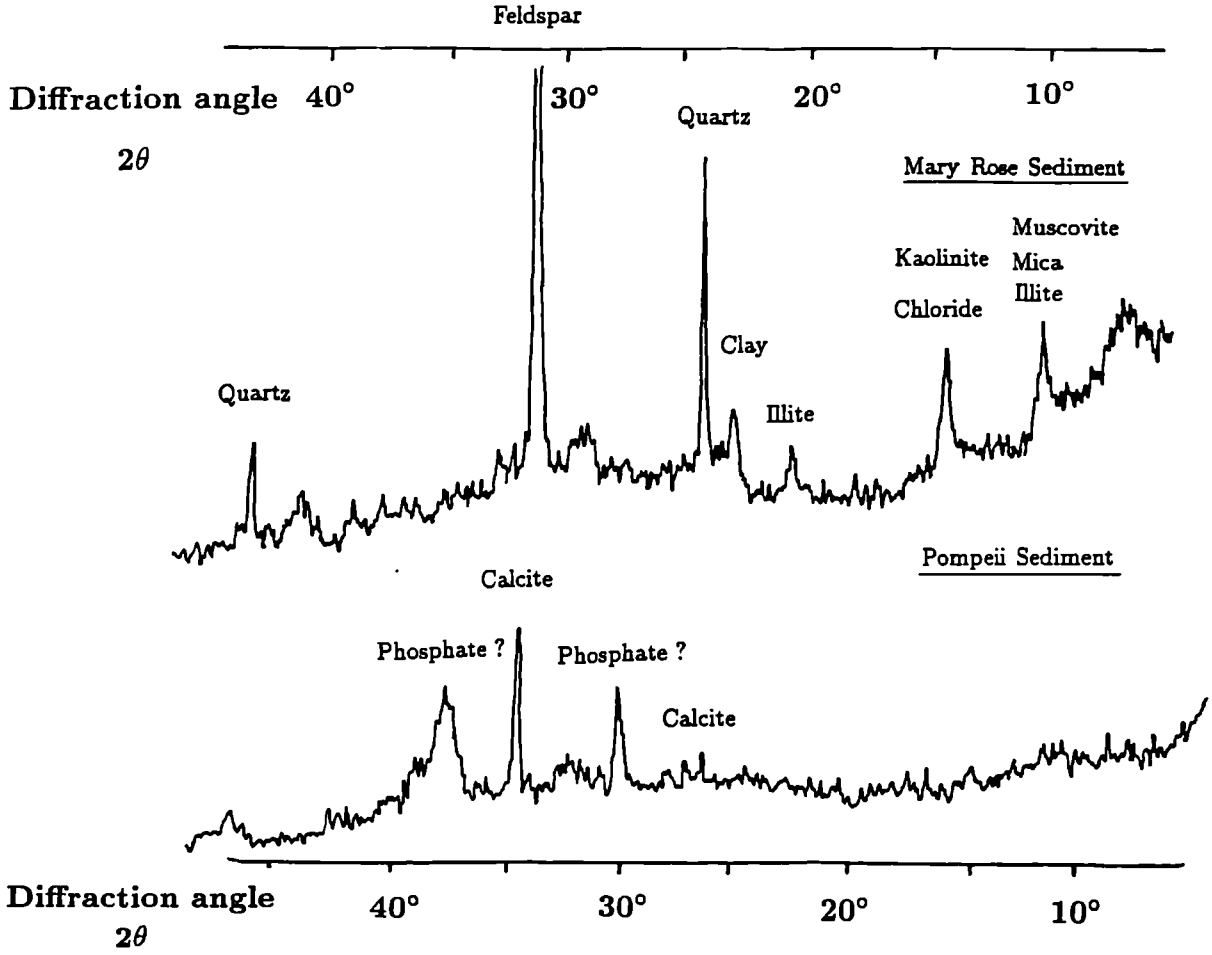

9.4 Results.

9.4.1 Structural Preservation: Light Microscopy.

The general condition of all skeletal material used in this study and excavated from the British mainland sites was good. Figures 9.6 and 9.7 show examples of material excavated in Hartlepool and illustrate the general trend of predominantly whole and relatively undisturbed skeletons exhumed from the British mainland sites. (Figure 9.7 is particularly interesting in that it features the joint burial of mother and foetus/newborn baby, whose delicate bones are positioned under the adult's right arm).

Preservation of the bone's structural and material components was examined using light microscopy under (1) normal reflected and (2) polarised light. The latter provides information on the *submicroscopic* arrangement or molecular structure of inhomogeneous tissue elements that possess anisotropic properties (Everson Pearse, 1972). Anisotropy means 'preferred direction of symmetry': a medium displays anisotropy when it is characterized by an asymmetrical and oriented spatial arrangement of bodies. So, the anisotropic (A) bands of striated muscle fibres in collagen will form **birefringent** patterns in plane polarised light by rotating the plane of polarization. Birefringence itself is defined as the possession of different refractive indices with respect to light polarised in different directions. Thus, micro-examination of thin-sections of bone in polarised light reveals the location of preserved collagen, as shown by a bright image against a dark background. As the fibril arrangement of collagen is broken down by postmortem decay processes, its anisotropic/birefringent properties are lost.

The majority of the specimens examined by light microscopy in this study demonstrated clearly identifiable osteonal/Haversian microstructures under reflected light. Birefringence patterns under polarised light revealed considerable preservation of the organic component (collagen at least) of the bone matrix. Figures 9.8 (a) and (b) show the degree of osteonal structural preservation in bone excavated from the "Mary Rose" under (a) reflected light and (b) polarised light. The latter shows clear birefringence of the collagen substance. Figures 9.9 (a) and (b) similarly reveal good preservation of the microstructure and collagen component in bone excavated from Hartlepool. Canterbury material, however, was not preserved to

the same degree (figures 9.10 (a) and (b)): its osteonal structures were less easily discernible and pore-filling was evident. Collagen preservation was apparent only in the medullary cortical areas, rather than the peripheral cortices (on the right of the figure).

In contrast, the pattern of preservation in Watchfield material, whose burial environment was acidic in comparison, was very different. Here, preservation of the microstructure was poor, the cortical tissue being rather "pulpy". This is illustrated in Figure 9.11(a). Under polarised light, birefringent patterns were only observed at the immediate cortical edge of the bone, approximately 150 microns into the cortex (Figure 9.11(b)).

"Banding" patterns were observed in the sea-water burial example from the Mediterranean in the outer cortical region of the bone. These were referred to in the original Arnaud reference. Figures 9.12(a) and (b) show these bordering zones, present in both outer and inner cortices, in reflected and polarised light, respectively. The preservation of typical inorganic and organic components was only observed in the mid-cortical regions. Figures 9.13(a) and (b) show the interface between apparently altered and preserved bone under increasing magnification. On closer examination it can be seen that these zones contained a network of canaliculi-type structures that ressemble those produced by fungi that live in soil-buried bone (Marchiafava *et al.*, 1974). However, these are more likely to have been produced by sea-water amoeboid forms (Ascenzi and Silvestrini, 1984).

The photographs taken under the light microscope were useful in an additional capacity, other than as an indication of the degree of structural preservation. In some cases, the *colour* of the bone sections would provide clues as to the presence of any contaminants. The "Mary Rose" material, for example, contained many areas orangey-red and/or black in colour: this appearance suggested the presence of iron- and manganese-containing minerals, respectively. Figures 9.14 (a) and (b) illustrate the degree of penetration of these coloured minerals, with infiltration of the lacunae and canaliculi microstructures of an Haversian system.

Figure 9.6 and 9.7: Skeletons lying *in situ* at the Hartlepool Friary excavation site.

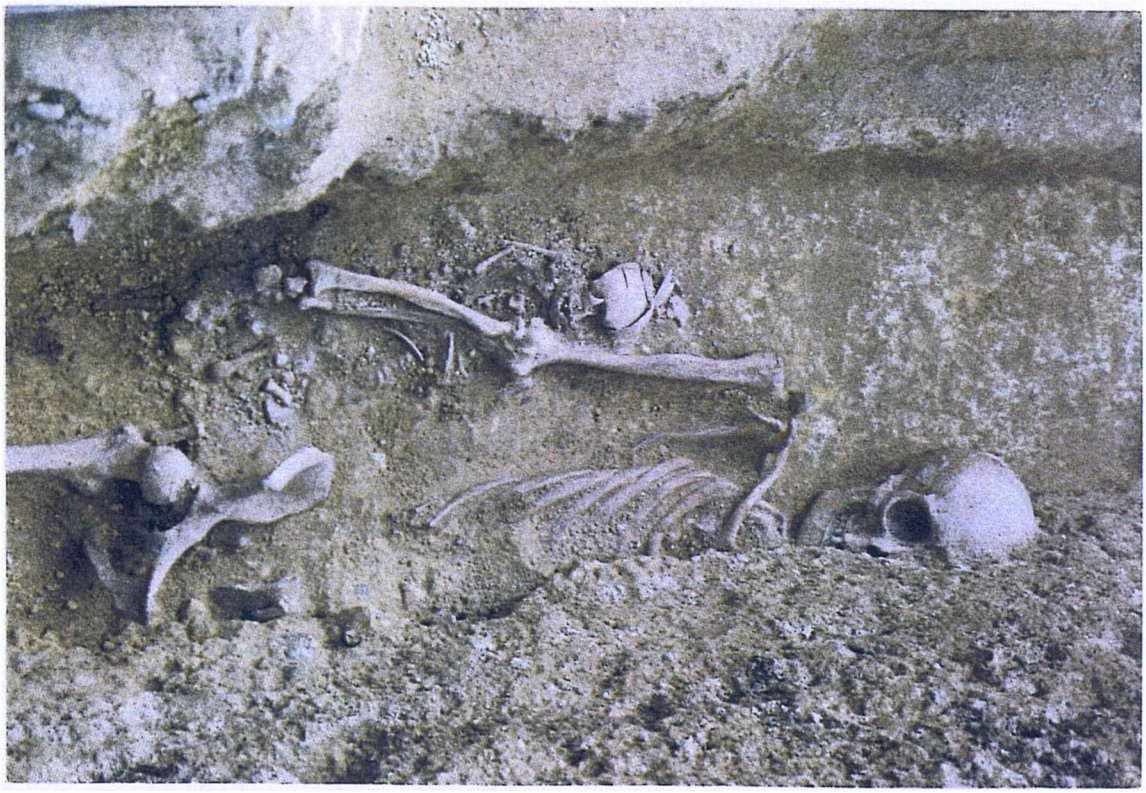

Figure 9.8: Light micrographs of the cortical tissue of bone excavated from the "Mary Rose" site under (a) reflected (mag. x200) and (b) polarised light (mag. x400).

a

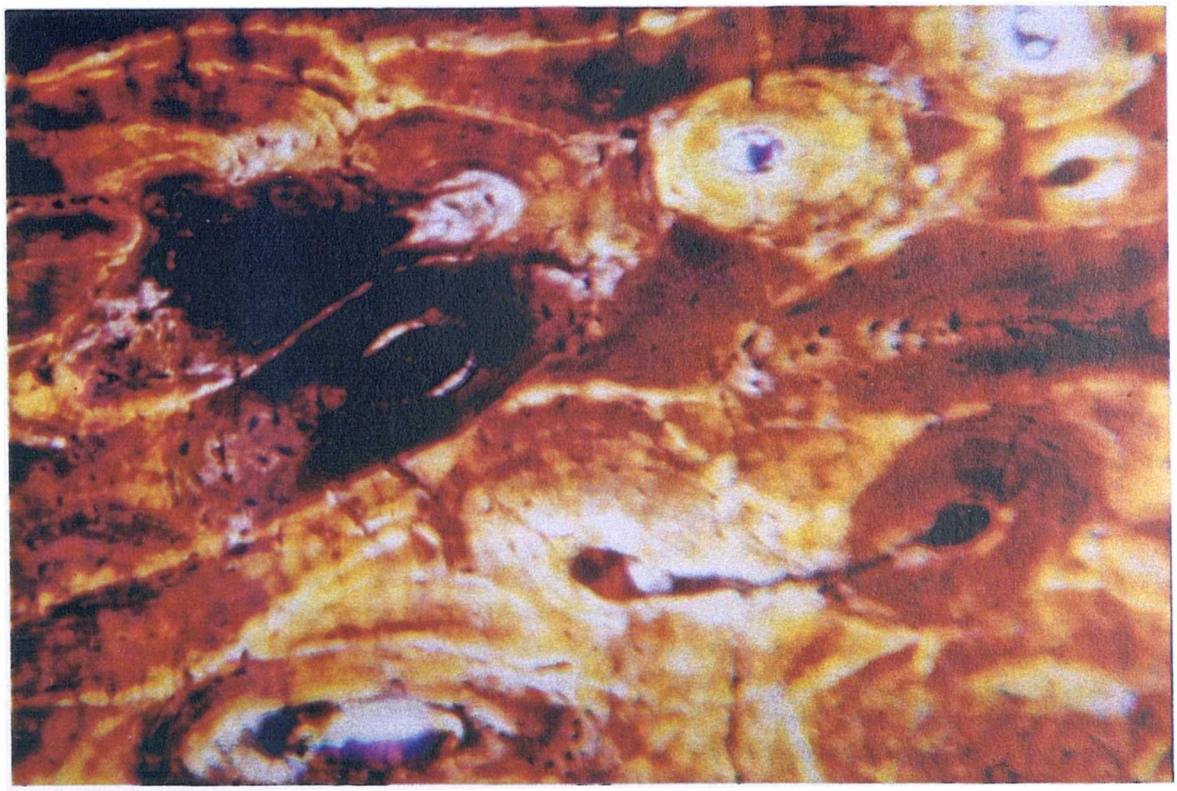

b

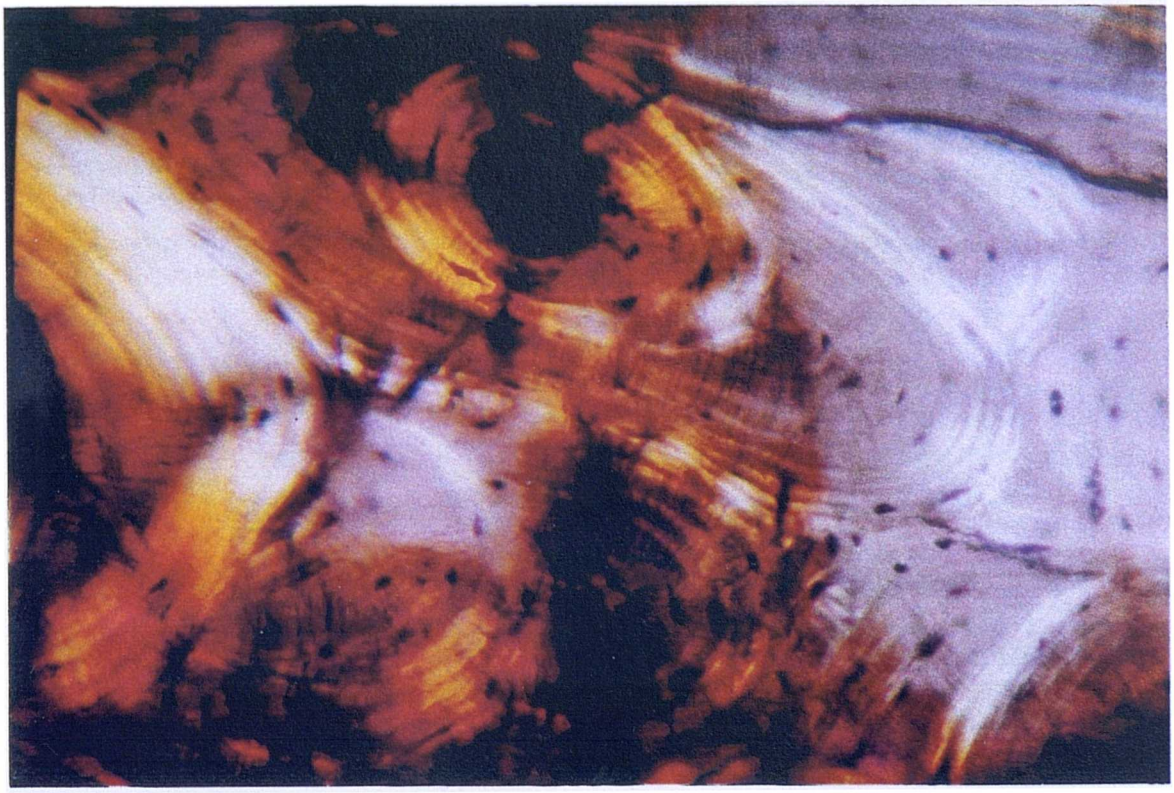

Figure 9.9: Light micrographs of the cortical tissue of bone excavated from Hartlepool, shown under (a) reflected and (b) polarised light. Mag. x400.

a

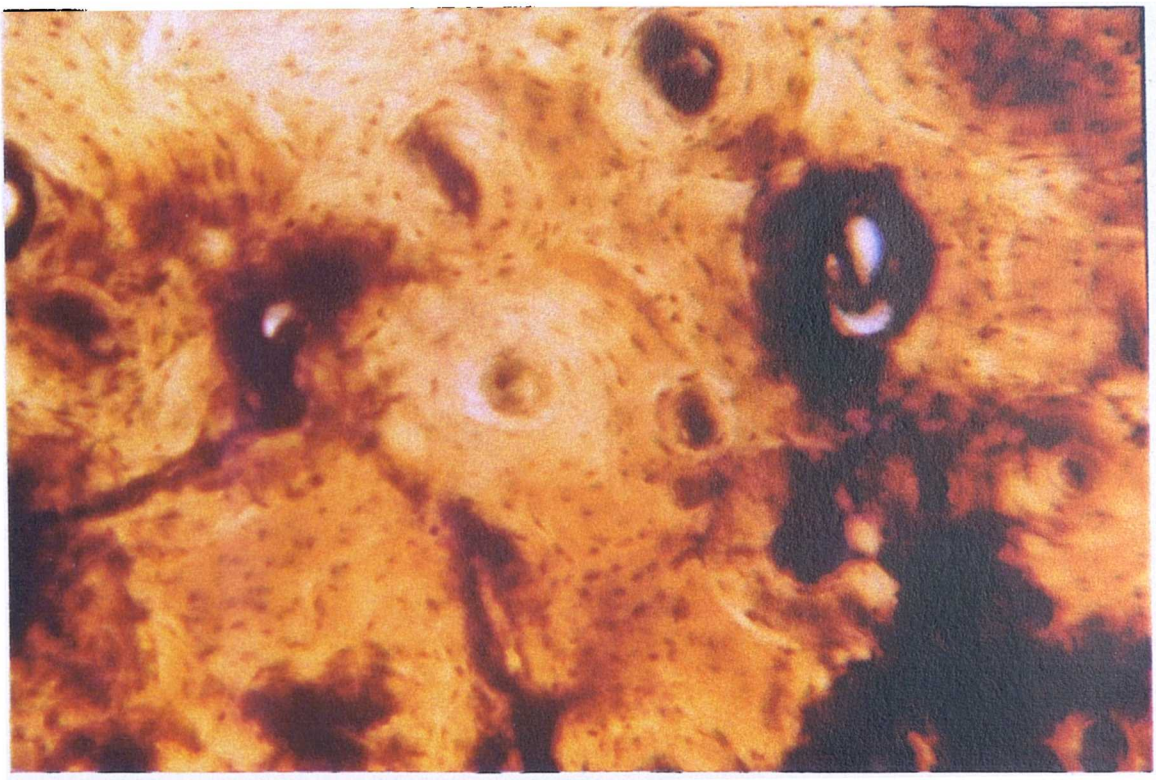

b

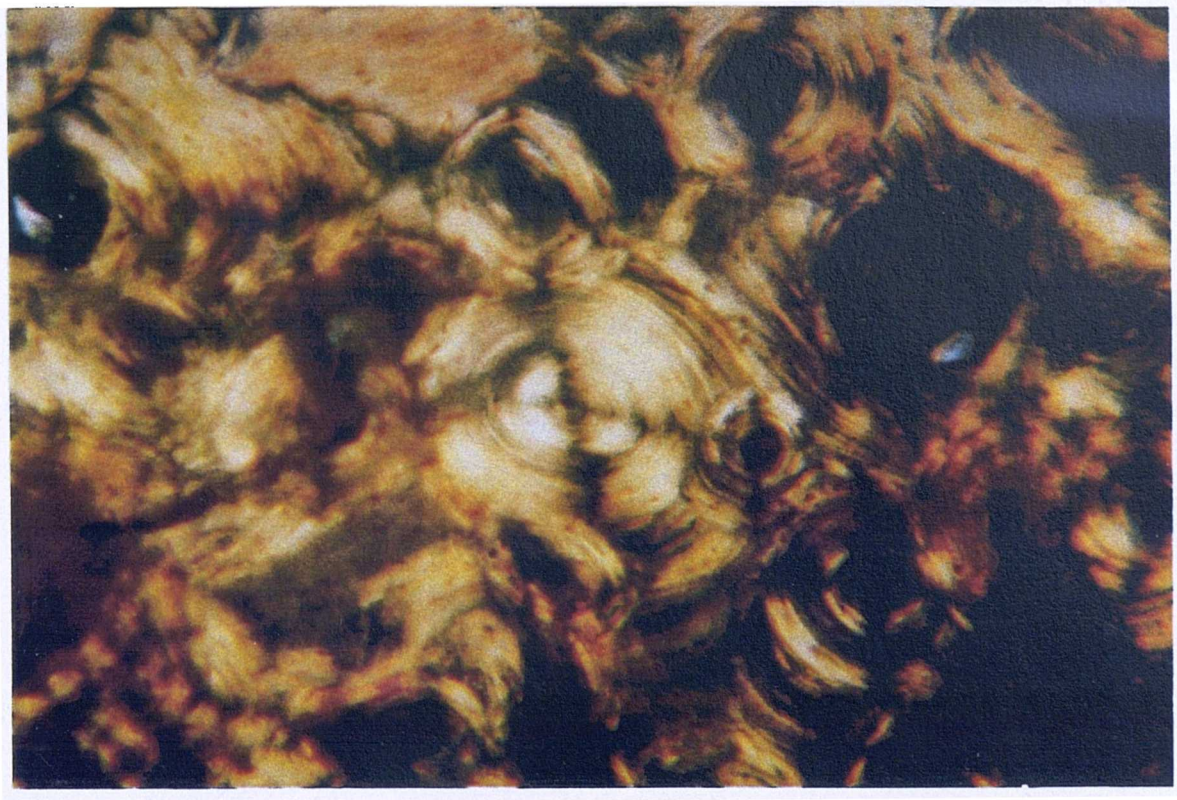

Figure 9.10: Light micrographs of the cortical tissue of bone excavated from Canterbury, shown under (a) reflected and (b) polarised light. Mag. x400.

a

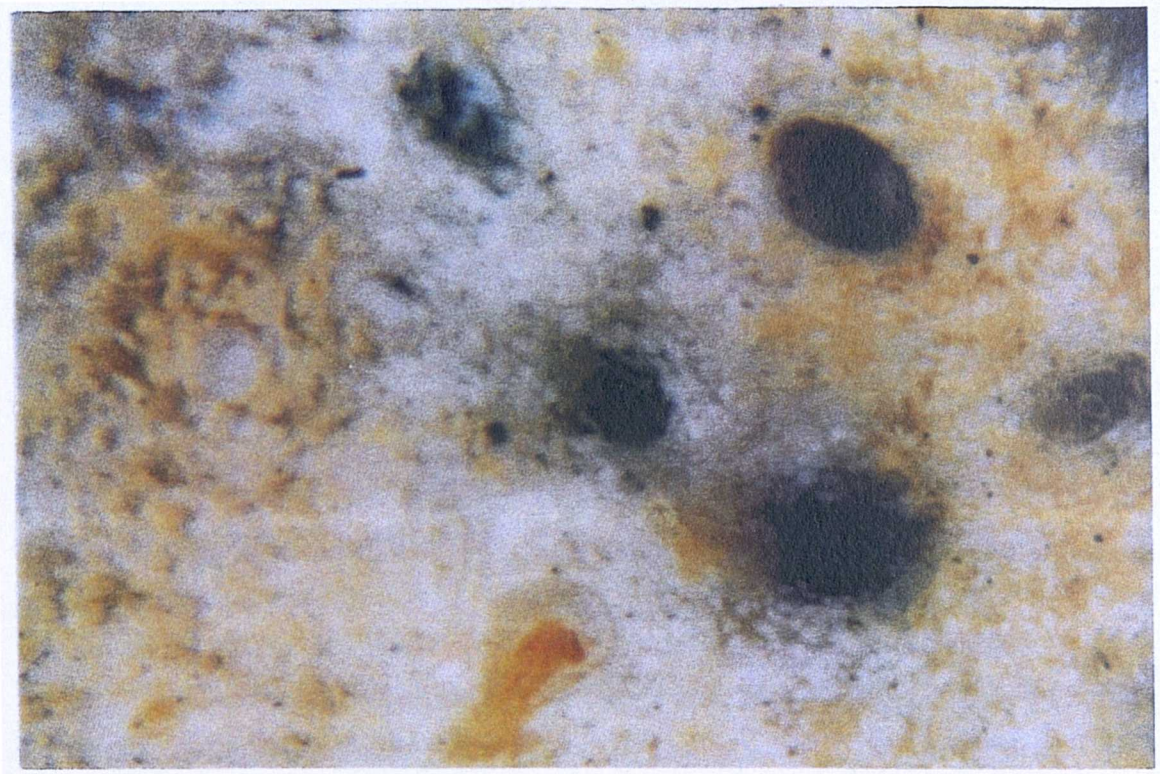

b

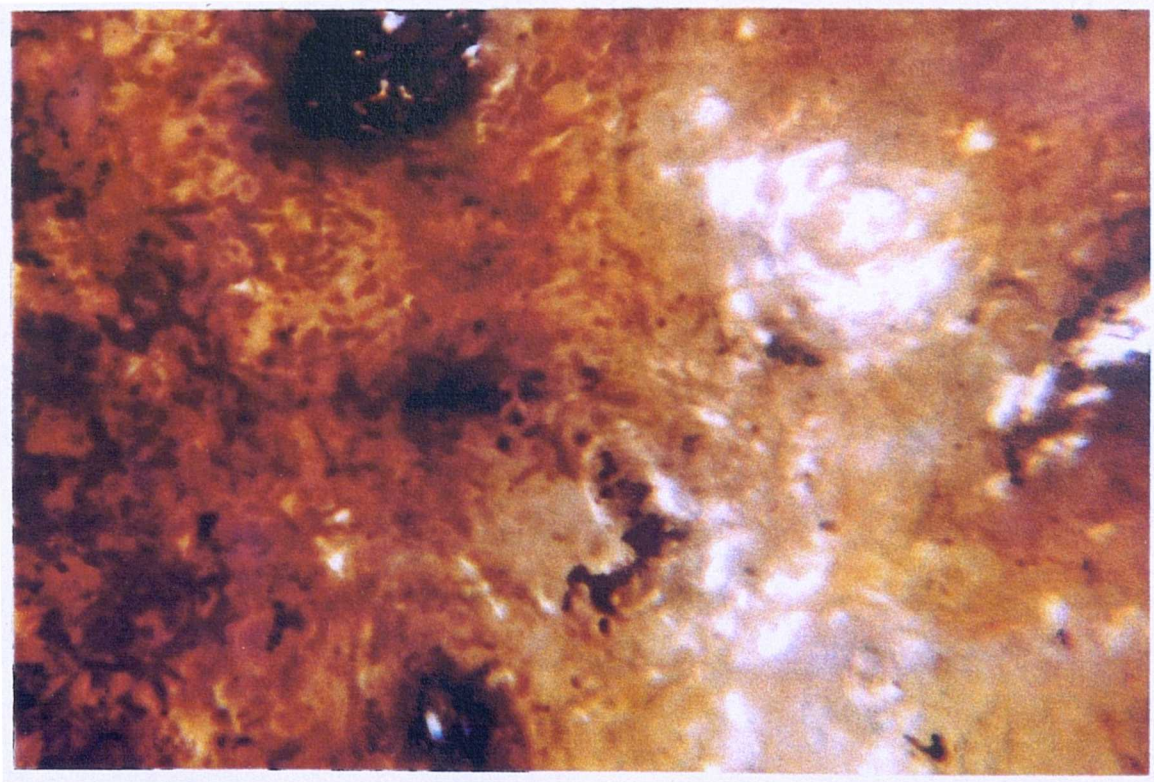

Figure 9.11: Light micrographs of the cortical tissue and outer cortical edge,respectively, of bone excavated from Watchfield, shown under (a) reflected (mag. x200) and (b) polarised light (mag. x220).

a

b

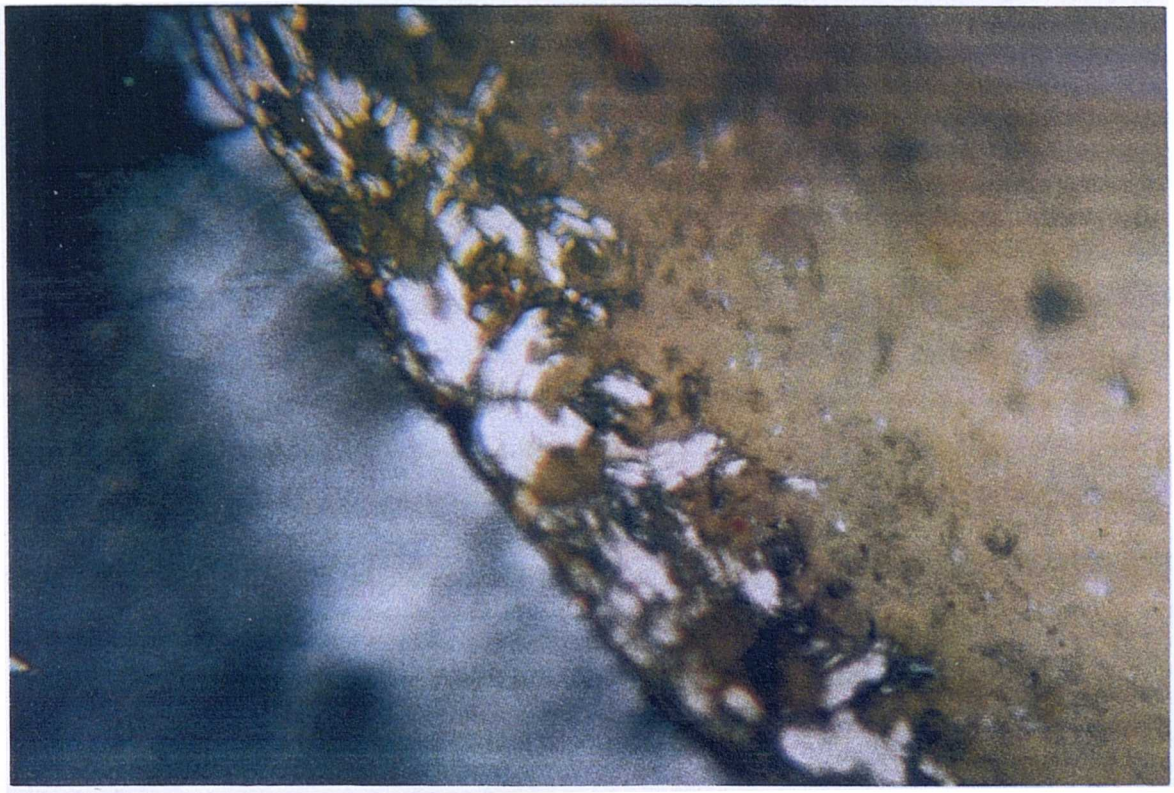

Figure 9.12: Light micrographs of bone from the Mediterranean Sea burial under (a) reflected (mag. x170) and (b) polarised light (mag. x200).

a

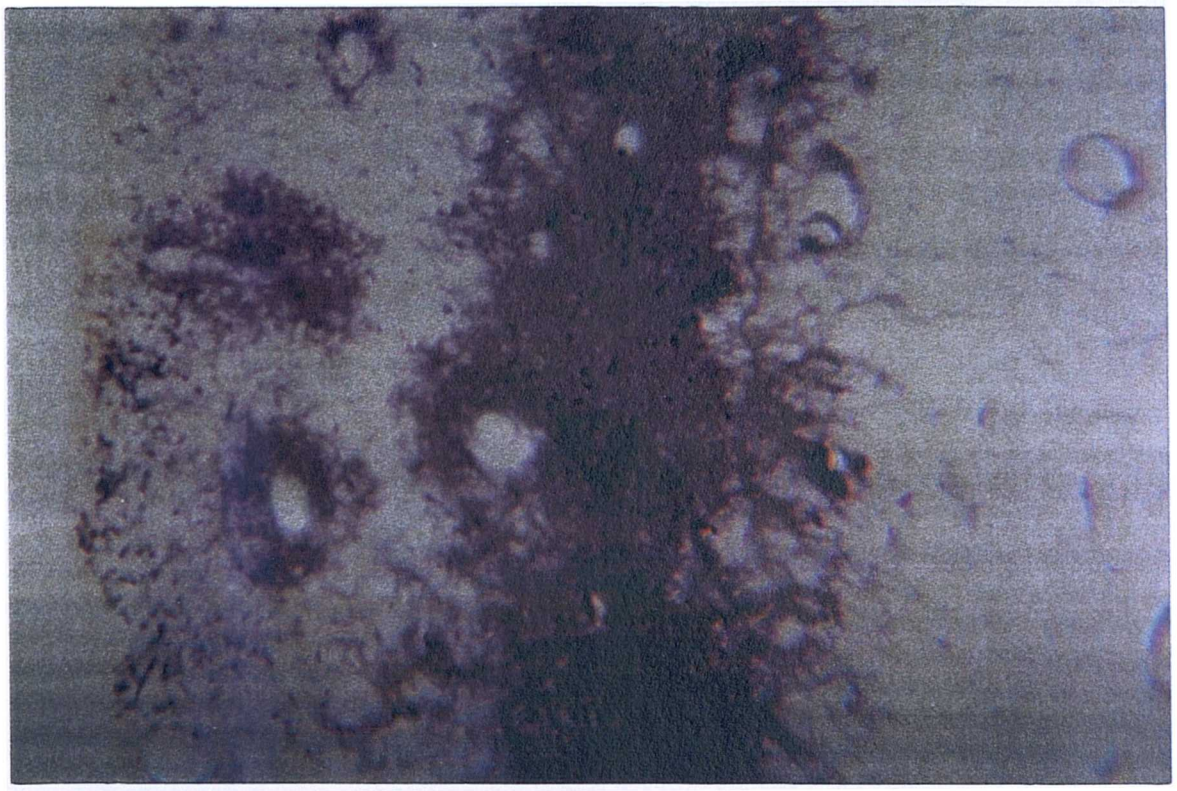

b

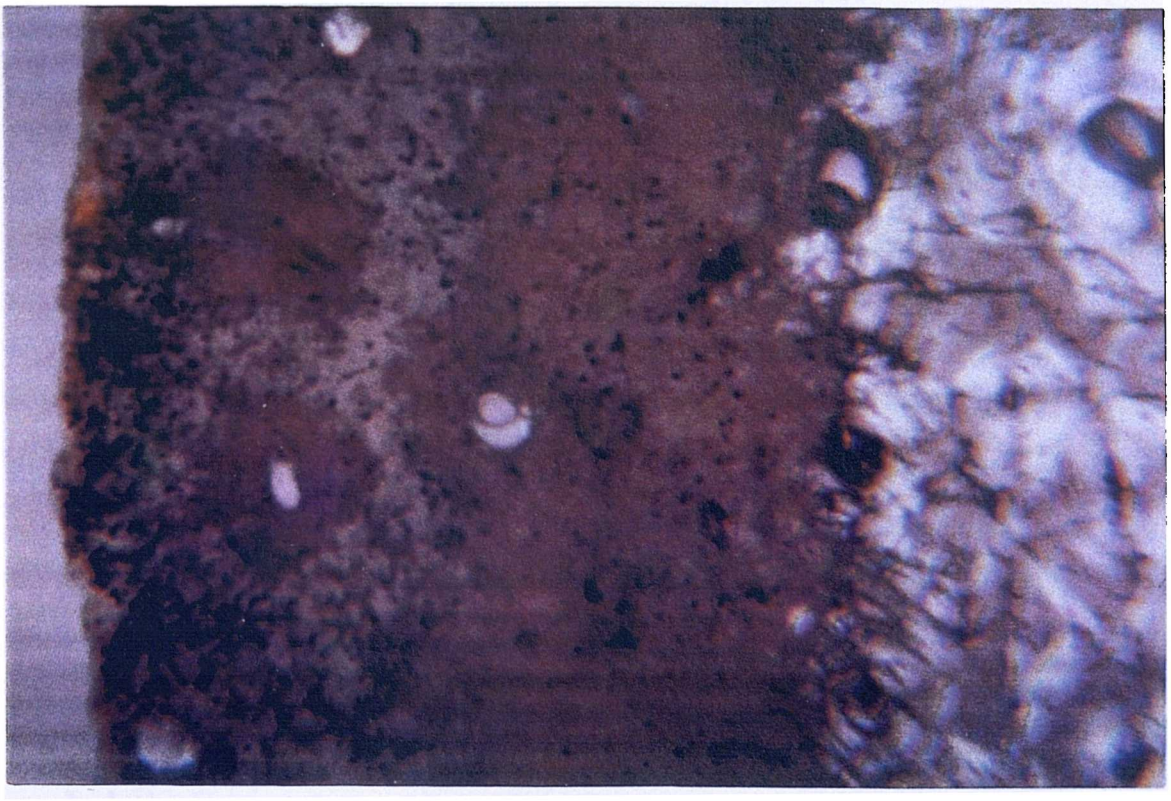

Figure 9.13: Light micrographs of the edge of the bordering zone present in bone from the Mediterranean Sea burial. (a) mag. x400 (b) mag. x2000

a

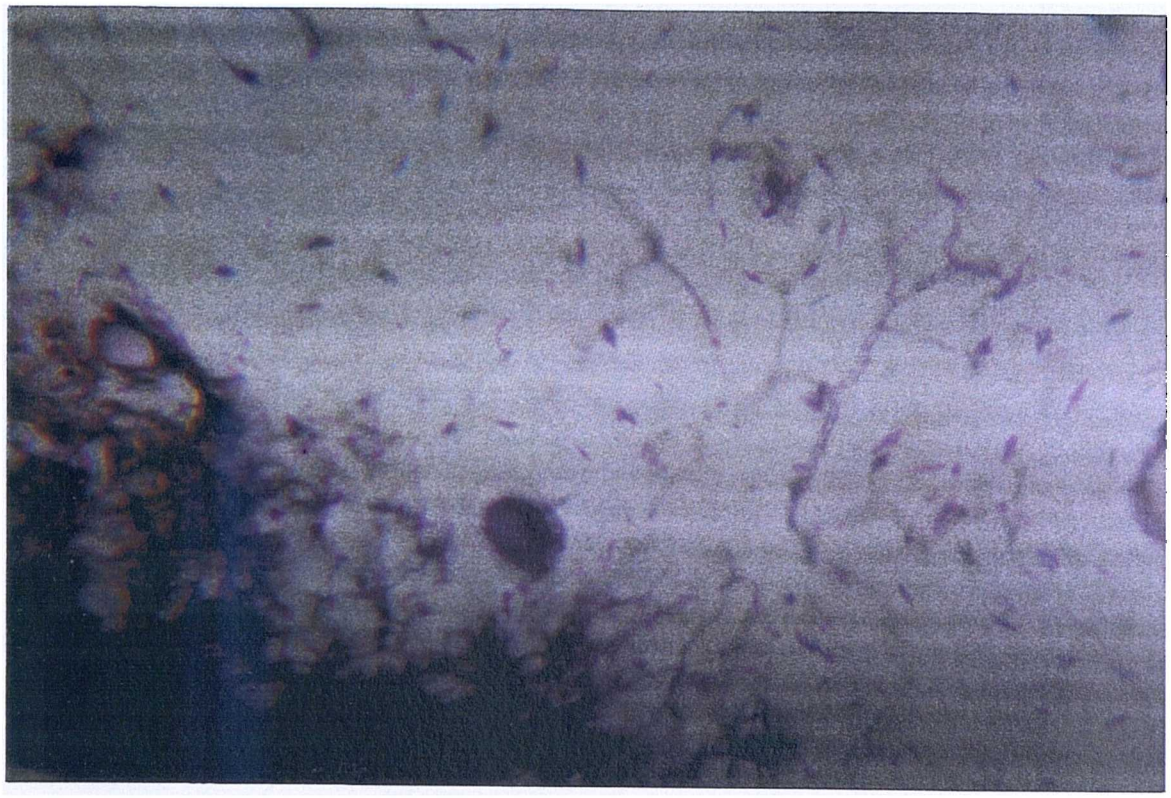

b

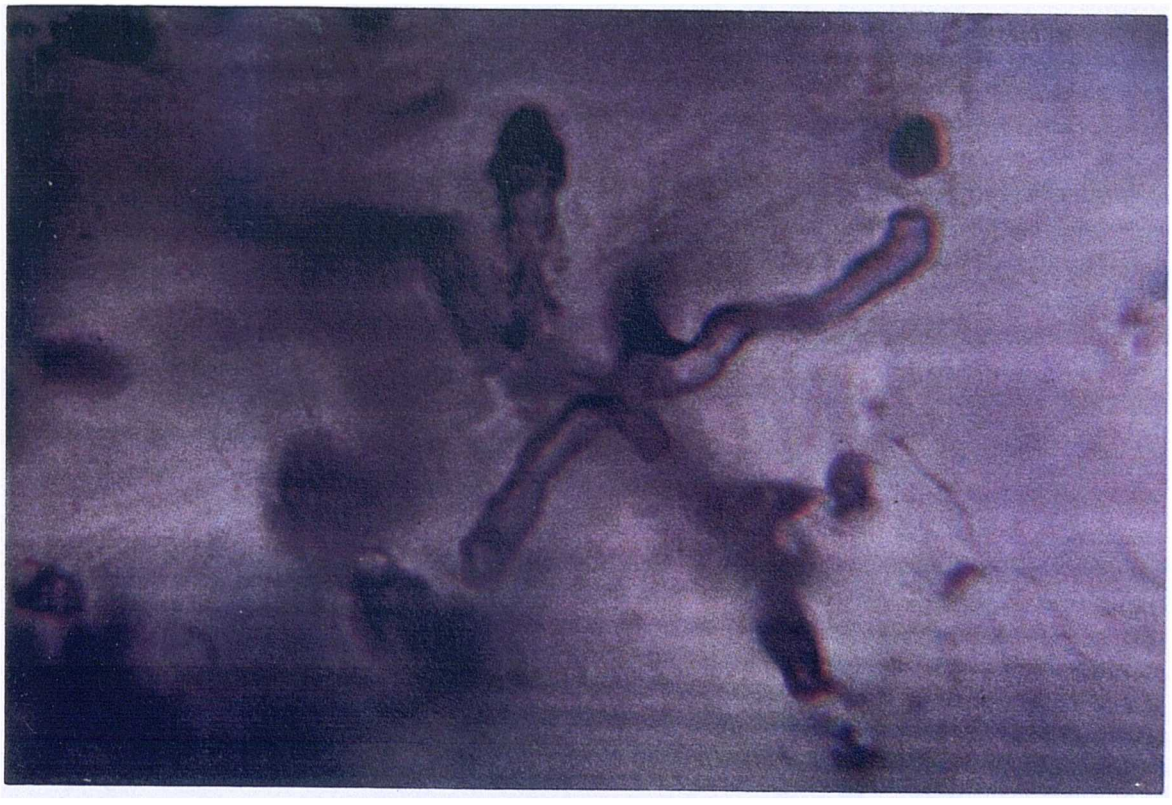

Figure 9.14: Light micrographs of Haversian systems in the cortical tissue of bone excavated from the "Mary Rose". Mag. x1000

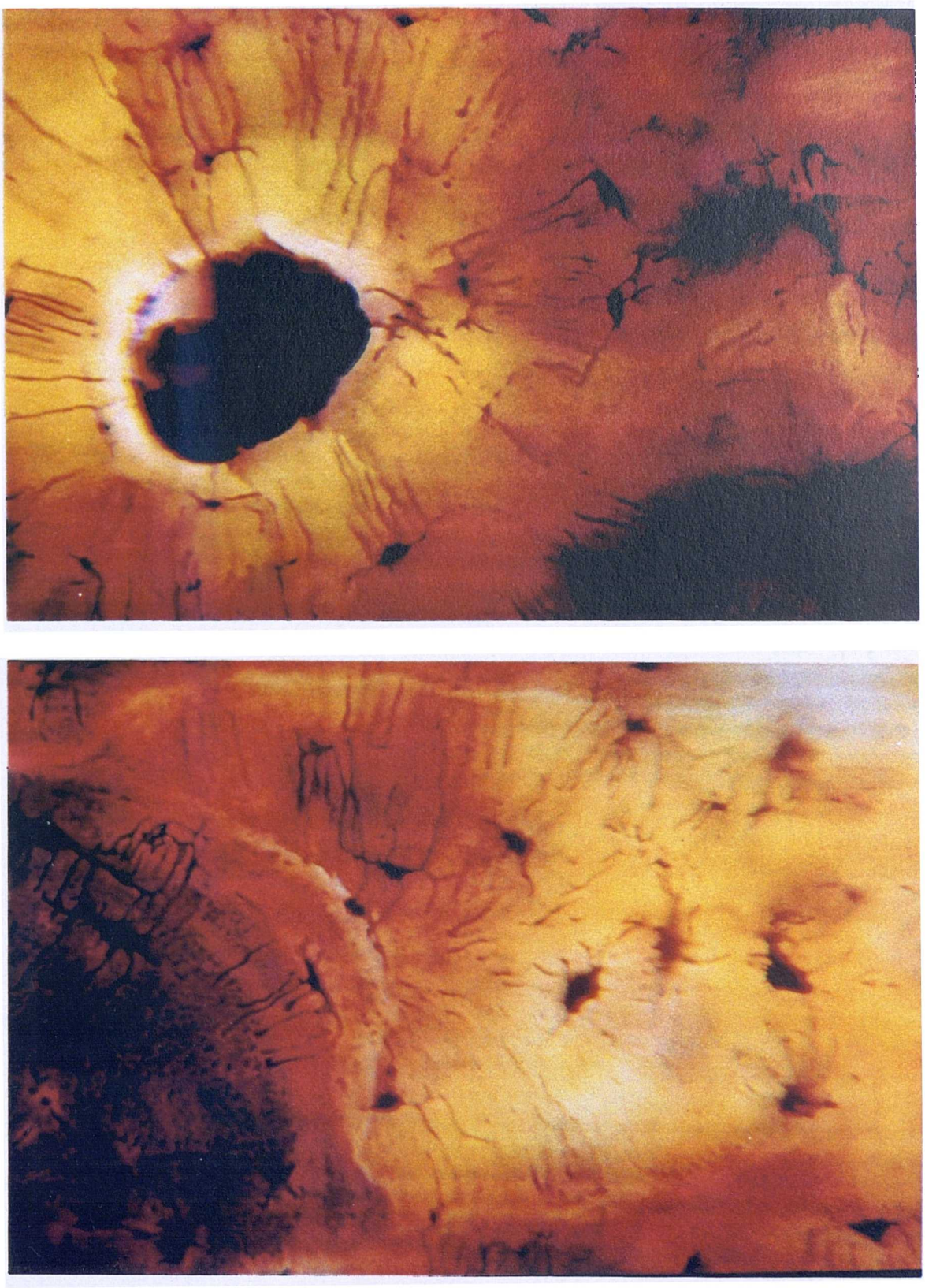

- Summary.

Light microscopy is a useful elementary diagnostic means of determining the degree of structural preservation. Examination of samples in reflected and polarised light respectively illustrated the microstructural organisation (defined largely by the inorganic matrix) and collagen content (representing the organic matrix) in excavated bone. The pattern of preservation of each component was variable across sites indicative of different burial conditions throughout their respective inhumation periods.

Chemical analysis of bone and soil samples, together with a more detailed investigation of the inorganic character of bone using crystallinity studies would further elucidate the relationship between bone and its burial environment.

9.4.2 Bone Crystallinity: XRD Analysis.

Bone material excavated from the British mainland sites was analysed using X-ray diffraction in order to identify any mineral phases that had been introduced diagenetically and to study the respective crystallinities of the bone's own inorganic phase.

In all samples, diffraction profiles consisted exclusively of peaks representing hydroxyapatite; evidence of other mineral phases was not apparent.

XRD analysis of the British mainland bone samples indicated a relatively higher crystallinity in the Watchfield example compared to those of Canterbury and Hartlepool, as shown in Figure 9.15. Peaks 002 and 310 were clearly sharper in Watchfield bone and the separation and sharpening of peak 300 from 112/211 was evident.

So, the crystallinity of these archaeological samples appeared to increase with the acidity of respective burial sites. This confirmed earlier observations on modern bone artificially exposed to solutions of variable pH (Chapter 8: figure 8.3).

XRD profiles of Olduvai 13.3 are shown in Figure 9.16, comparing 'B' and 'T' samples. Peak 002 was clearly sharper in bone exposed to soil, as was peak 202. There

was also slight evidence of a clearer distinction of peak 300 from 112/211. Although less convincing than earlier XRD investigations into crystallinity, it would appear that small changes in crystallinity had occurred over a very short period of time after the initial deposition of this Olduvai sample.

9.4.3 Micro-analysis of Bone I: EPMA.

EPMA was carried out on three of the archaeological bone specimens: examples from Pompeii, the "Mary Rose" and Hartlepool.

Preliminary probe analysis revealed very little apparent extraneous material in the bone sample from Pompeii, with only small traces of aluminium and silicon being detected in the bone matrix. These elements were largely found lining pores and cortical surfaces, as demonstrated in figure 9.17 mapping an Haversian system.

In the "Mary Rose" sample, silicon, iron and sulphur were observed lining pores and cortical surfaces, as shown in map form in figure 9.18.

Quantitative analyses of these samples were not carried out using this technique. However, quantitative cross-cortical probe analysis was carried out on Hartlepool bone, and these data can be found in Appendix Va. Generally, the only elements found in any significant quantities were (Ca and P) sulphur, aluminium and magnesium. Cross-cortical line-profiles of these elements did not reveal any patterns/trends in distribution indicative of diffusion or pore-filling, and mapped areas were not collected for this sample.

Qualitative/digimap analyses obtained using the electron microprobe were compared with corresponding proton microprobe studies described in the following section.

Quantitative analyses using a number of techiques are described in more detail in Section 9.4.6.

Figure 9.15: XRD profiles of bone excavated from British mainland sites.

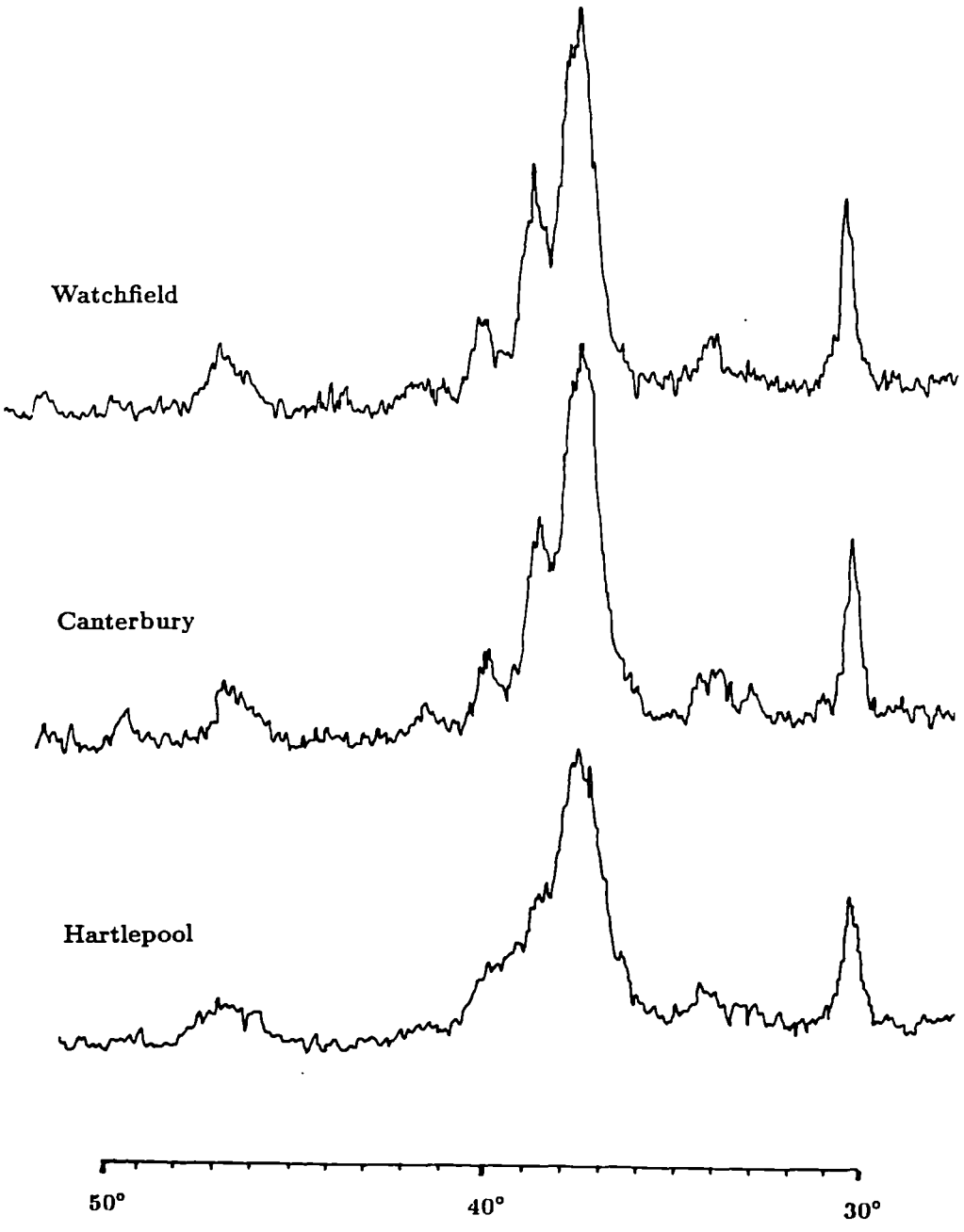

Figure 9.16: XRD profiles of modern mammalian bone found at the surface level at Olduvai, comparing bleached and soil-coloured cortices.

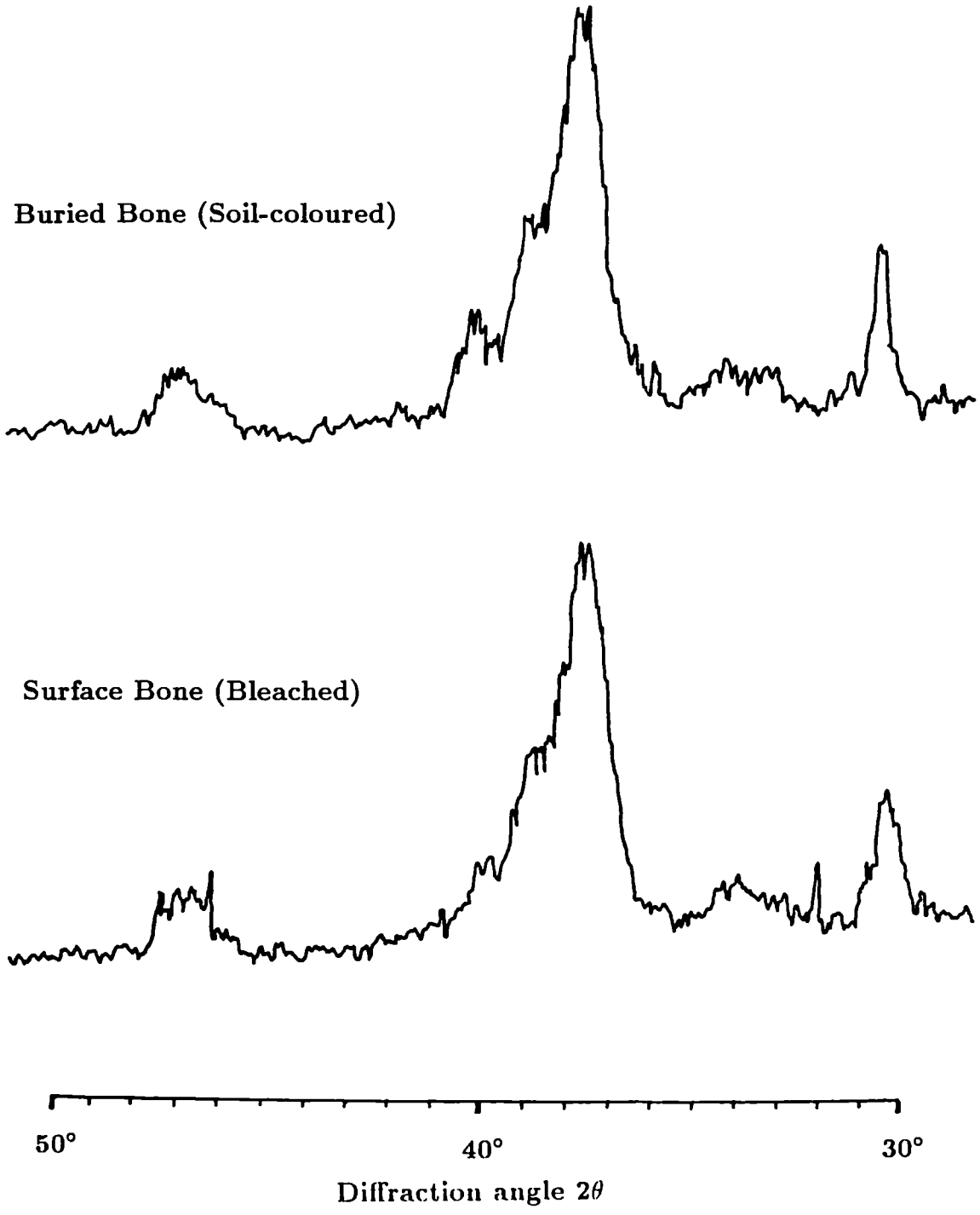

Figure 9.17: EPMA digimap of an Haversian system in the cortex of bone material from Pompeii. Mag. x600.

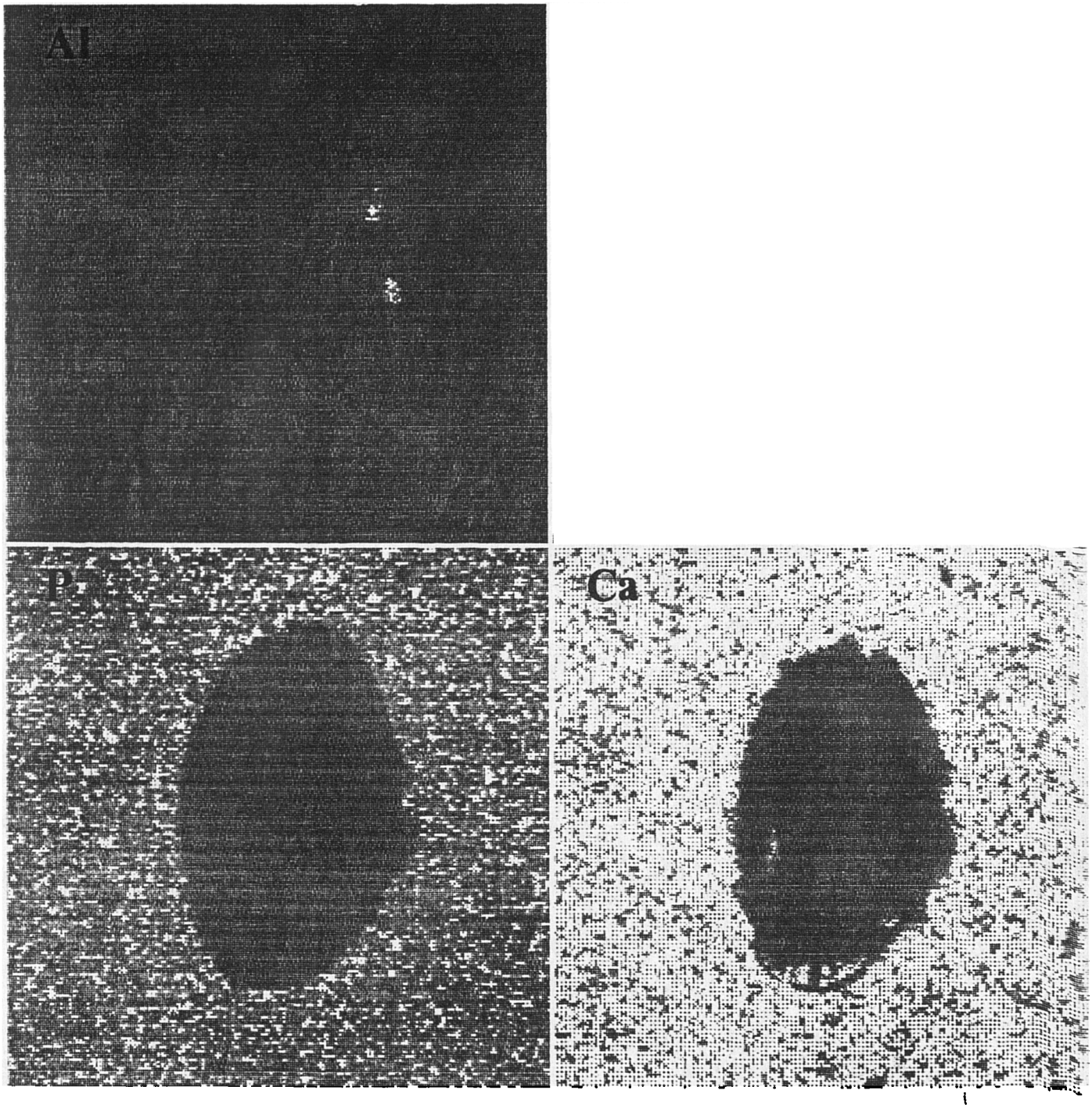

Figure 9.18: EPMA digimap of a pore in the mid-cortical region of bone material from the "Mary Rose".

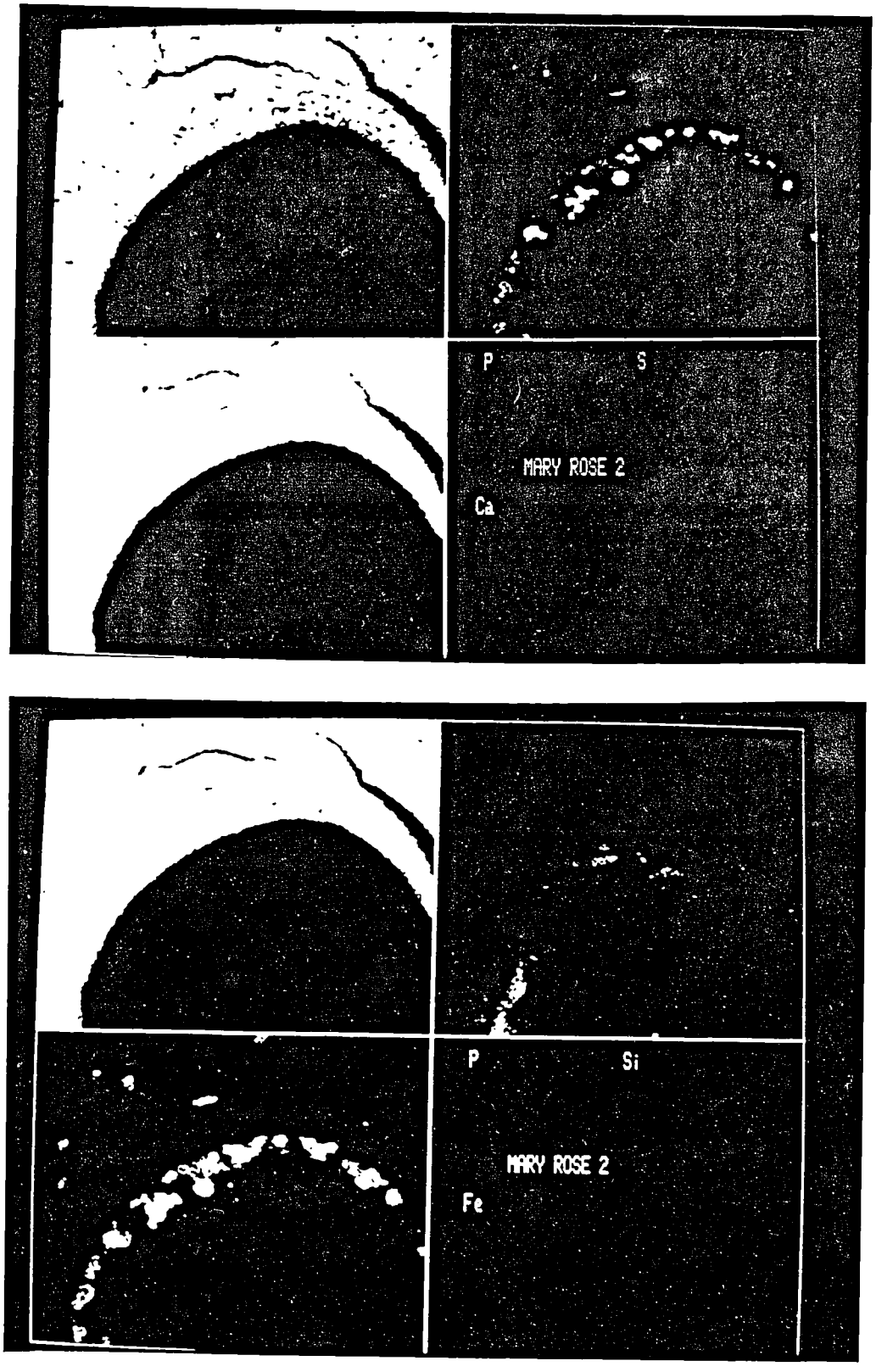

9.4.4 Micro-analysis of Bone II: PIXE.

Figure 9.19 a-d shows PIXE spectra typical of the archaeological bone samples studied here:'a-c' represent each of the British terrestrial sites, and 'd' a seawater burial. These spectra illustrate the wide variety of elements found in bone, a combination of those intrinsic to the bone and those diagenetically introduced and/or altered during its interment.

These elements are discussed in turn after a brief description of the PIXE data from respective sites, each represented by one example (femoral where possible). PIXE data are arranged according to their respective sites, and are presented in the form of line profiles and elemental maps. The latter consist largely of mapped areas of cortex up to 2500 microns square (where maps were all produced under identical operating conditions), located predominantly in periosteal and endosteal regions. The basic structure of the bone is shown outlined in calcium for most cases. Strontium and uranium distributions are also shown for subsequent comparison with experimental uptake studies. PIXE data illustrated in this chapter are, to a large extent, representative of the archaeological samples studied and have been selected on the basis of clarity, interest and aesthetic value. Further PIXE data are included in Appendix Vb.

9.4.4.1 Brief Description of Sites.

1. British terrestrial sites.

Bone material from all three British sites possessed a range of elements (*quantitative* values for Hartlepool material, measured using this technique, can be found in Appendix Vc to give an indication of absolute concentration levels, and are further discussed in Section 9.4.6). Many of these elements had clearly been diagenetically introduced, as determined by elemental gradients typically at cortical edges/surfaces and by the presence of pore-filling minerals.

Hartlepool data are shown in figures 9.20(a) and (b) as digimaps and in 9.21 (a) and (b) as line-profiles in the periosteal cortex: these reveal clear indications of contamination by iron, manganese, zinc and bromine. Other contaminatory elements included copper and nickel (see Appendix Vb). Lead was also detected,

and while a diffusion gradient was not evident in map form, the corresponding line-profile did show slightly elevated levels in the peripheral cortex. Line-profiles for strontium and uranium also indicated slight elevations at the immediate cortical edge, though again this was not clear in map form.

Canterbury data are shown in more detail as a series of maps analysing an area of the periosteal cortex (figure 9.22), the endosteal cortex (figure 9.23) and a magnified cortical edge (figure 9.24). Line-profiles corresponding to the former are shown in figure 9.25(a) and (b). Contaminants clearly illustrated included manganese, iron and zinc. Strontium and uranium distributions are also shown and are referred to later in the text.

Figures 9.26, 9.27, 9.28(a) and (b) represent areas of **Watchfield** bone, specifically periosteal and endosteal cortices and a magnified pore structure in the mid-cortex. These reveal contamination by iron, manganese, bromine, zinc and copper. Lead and nickel were also apparent (see Appendix Vb). While the source of the small uranium content was unclear, strontium was observed in elevated levels at the periosteal edge, shown most clearly as a line-profile (figure 9.29).

2. Other exhumed bone (terrestrial burials).

Data obtained from **Pompeii** material is shown in figure 9.30: the upper maps represent periosteal cortex, while the lower, endosteal cortex. Zinc, iron and also sulphur (for the latter see Appendix Vb) were observed as contaminants.

Figure 9.31 represents the periosteal cortex of **Olduvai** bone: this sample possessed elevated levels of strontium and zinc at the cortical edge, while the uranium pattern was not clearly discernible.

3. Sea-water burials.

Bone excavated from sea-water burial sites differed from the terrestrial sites in two important respects. They generally revealed a wider range of elements, both cations and particularly anions, that were affected by diagenetic processes. Furthermore, changes were observed as *depletions* in concentration as well as elevations at cortical surfaces.

Figures 9.32, 9.33 and 9.34 represent, respectively, areas of periosteal and endosteal cortices and a magnified pore in the mid-cortex of the **"Mary Rose"** clavicle. Elements altered, in whatever manner, by diagenetic processes included iron, lead, manganese, sulphur, rubidium, titanium, copper, chlorine, sodium , bromine and zinc: examples of elements found in depletion and those that were clearly contaminants are found in Figures 9.35 and 9.36, respectively. A similar suite of elements affected by diagenesis were found in the **"Bay of Agay"** sample (figures 9.37(a) and (b)). From these elements the following were found in depleted concentrations at cortical surfaces: calcium, magnesium, sodium, phosphorus and chlorine. These are discussed further in the following section.

9.4.4.2 Diagenetically altered elements.

1. Iron and manganese.

The elements most commonly found as contaminants in exhumed bone, as demonstrated by earlier EPMA studies and confirmed here using PIXE, are **iron** and **manganese** . All samples examined were found to contain these elements, either on cortical surfaces or filling pores within the matrix. For example, figures 9.27, 9.23 and 9.33 clearly illustrate **iron** lining trabecular bone in the endosteal region of Watchfield, Canterbury and "Mary Rose" bones, while Figure 9.20(b) shows elevated iron levels at the periosteal edge of bone from Hartlepool (represented in Figure 9.21(b) as a lineprofile). In addition, this element was observed lining large pores and filling smaller voids, as exemplified in Figures 9.28(b), 9.24, 9.32 in outer/mid cortical bone, and further in Figures 9.29(b) and 9.25(b) as a line profile where iron peaks occur intermittently across the full cortical width corresponding to the location of pores/voids. While the line profile in Figure 9.29(b) demonstrated iron at the surface of the endosteal edge (on the right-hand side of the profile), it also showed iron penetration up to 300 microns in the periosteal cortex (on the left-hand side). Iron penetration into apparently dense cortical tissue was probably due to surface adsorption to phosphate ions in the hydroxyapatite matrix, since the fixation of iron by phosphate is a well-established phenomenon (Eidt, 1977). As a "passive" pore-filler, iron probably existed in an oxide or sulphide form. Certainly in the reducing environment of the "Mary Rose" burial iron

sulphide can exist, and this explains the correlation in distribution patterns of iron and **sulphur** shown in Figure 9.33. The distribution pattern of **manganese** in this sample was also similar. Manganese was found lining cortical surfaces in some samples (e.g. Figure 9.20(b), 9.21(b)), but more commonly was seen filling pores and voids within the cortical tissue (e.g. Figures 9.22, 9.24, 9.25(a), 9.28(b)), probably as various simple and complex oxides. Thus, manganese tended to concentrate within the bone as patterns that correspond to the bone's canal and canaliculi structures that permeate the matrix, providing nutrients to the bone tissue during life. As the organic matrix of the bone decays, these fine structures are accessible to percolating groundwaters and the minerals carried in them. In contrast, iron more typically fills the larger pores in the bone matrix e.g. Haversian canals, and lines its cortical surfaces. The light micrograph shown earlier in Figure 9.14a/b of an Haversian system in the "Mary Rose" specimen probably illustrates the infiltration of an Haversian canal and its surrounding lacunae and canaliculi by predominantly iron and manganese minerals.

Manganese is one of a number of elements that can be introduced into bone as pore-fillers by their association with secondary carbonates e.g. calcite, and quartz (Pate and Hutton, 1987). These are both commonly found in soils and sediments, as XRD has demonstrated. Calcite ($CaCO_3$) precipitates along fractures and voids created by organic decay and it is often contaminated with manganese and other ions from the soil solution (Roeder and Grams, 1987). Similarly. quartz (SiO_2) is commonly contaminated by colloidal or clay-sized material containing aluminium, iron,and manganese (Kyle, 1986).**Silicon** contamination was observed in the marine samples and in Pompeii bone (see appendices). The latter also contained traces of **aluminium** as a pore-filling contaminant. With the exception of these traces of silicon and aluminium, together with iron and zinc (figure 9.30), there appeared to be very little obvious contamination in the Pompeii specimen.

2. Zinc.

In addition to confirming EPMA studies by demonstrating the types of diagenetic alterations that are typical in buried bone, such as iron and manganese infiltration, PIXE was also able to reveal the contamination of elements less acknowledged to be diagenetically altered. **Zinc** was also clearly a contaminant, introduced into the

bone from the surrounding burial matrix, as shown by typical diffusion profiles at the periosteal and endosteal surfaces (Figures 9.20(b), 9.24) and lining pores/voids in the bone matrix (Figure 9.28(b)). The line profiles in Figures 9.21(b), 9.25(b) and 9.29(b), representing all three British mainland sites, clearly demonstrate elevated levels of zinc at the cortical edges of both periosteal and endosteal bone, penetrating at least 500 microns into the bone before levelling out to pre-mortem levels. This observation is of particular importance to the biological anthropologist since the zinc content of bone has been used in the past to assess the relative proportion of meat in ancient diets (Parker and Toots, 1980). This convincing demonstration of postmortem contamination by zinc is contrary to many previous studies that state zinc's insusceptibility to diagenetic influences, e.g. Lambert *et al.*(1982), Gilbert (1985), and demands a re-evaluation of its suitability as a palaeodietary indicator (e.g. Rheingold *et al.*, 1983).

3. Strontium.

As reviewed in Chapter 2, the strontium content of bones can also provide information about the diet of past populations (eg. Gilbert, 1985). The extent to which strontium is subject to diagenetic alteration is a matter of debate, and for a long time it was widely believed to be one of the least affected elements (e.g. Lambert *et al.*, 1982, 1983, 1985). Indeed, in this study, diffusion profiles for strontium were not apparent in many of the samples examined by PIXE. Bone material from Hartlepool and Canterbury showed no apparent contamination in the form of gradient profiles, as indicated in the maps shown in figures 9.20(a) and 9.22/23 and as line-profiles in figures 9.21(a) and 9.25(a). Nor was this element seen associated with pore-filling minerals (e.g. figure 9.28(a)), despite its common association with secondary minerals (Kyle, 1986; Roeder and Grams, 1987). However, strontium contamination was observed in Watchfield bone, where strontium levels were elevated at the periosteal edge, penetrating at least 400 microns into the cortex (Figure 9.29(a)). Though clearly visible in this line profile format, the equivalent mapped area shown in Figure 9.26 was not conclusive, nor were maps representing endosteal cortical tissue in corresponding samples (Figure 9.27).

Elevated strontium levels in the peripheral cortices of bone material from Olduvai (figure 9.31) is clearly indicative of contamination, despite the fact that this bone

was only partially buried, probably for a period of 1 to 2 years. Therefore, the diagenetic alteration of strontium may potentially be very rapid, and appears to be dependent on the depositional environment.

Perhaps rather surprisingly, there was no indication of any diffusion profiles in the sea-water burial sample from the "Mary Rose" (Figure 9.32), despite the fact that strontium concentrations in sea-water are considerably higher than those in average groundwaters (8-13 ppm cf. 0.03-0.07 ppm). This would suggest an apparent lack of contamination of strontium. However, the high density of pixels representing strontium in Figure 9.32, together with subsequent quantitative analysis of the "Mary Rose" bone, revealing a strontium concentration of 1899 ppm (discussed in Section 9.4.6), indicates an enhancement of this element from an external source.

In contrast, strontium profiles indicating contamination were clearly observed in bone from the Mediterranean wreck, as illustrated in Figure 9.37, and more clearly as a line profile in Figure 9.38. The distribution of strontium correlated with the inner and outer bordering zones described by Arnaud *et al.*(1978) where the bone matrix changed colour and increased in fragility. Observations made by Arnaud *et al.*and light microscope work here suggest that these zones were created by the action of micro-organisms. The boring/tunnelling action of these microorganisms inevitably served to increase the porosity of the bone in these zones, thus enabling more extensive percolation of sea-water. In this way, elements present in the sea-water medium were able to penetrate the bone matrix and potentially interact with its increasing surface area.

Figures 9.37/(a) and 9.38 show *contamination* in these zones by **iron**, **copper** and **strontium**; other elements included **bromine**, **lead**, **manganese**, **silicon** and **sulphur** (see Appendix Vb). At the same time, *depletions* in **calcium**, **sodium**, **chlorine**, **phosphorus** and **magnesium** (figures 9.37(a) and 9.39) were observed in these zones.

The depletion of these elements in the bordering zones also reflected the relative ease of access of percolating sea-water, thereby enhancing the potential leaching action of the aqueous medium, in addition to any depositing action.

The distribution of the contaminant elements may also have been a *direct* consequence of microbial metabolic activity, either by

(1) metal-binding mechanisms: metal cations may adsorb to the negatively-charged sites at microbial surfaces (indeed, of the mineral identified in the sediment, illite and chlorite may be considered to induce a cation-rich environment), or metals can be deposited by microbial-induced formation of insoluble metal complexes,

or,

(2) oxidation/reduction mechanisms: metals that can exist in more than one valence state may be deposited by oxidation e.g. iron and manganese, or by reduction e.g. uranium.

4. Uranium.

PIXE data did not reveal much evidence for **uranium** contamination in bone samples analysed here. Furthermore, profiles of uranium distribution in the sea-water examples were not plotted since no uranium was detected from their respective PIXE spectra.

Canterbury and Watchfield bone material contained only traces of uranium with no obvious distribution patterns at the cortical surfaces (Figures 9.22, 9.25(a) and 9.27). At higher magnification of a pore in the mid-cortex of a Watchfield sample, however, there was a small accumulation of uranium (figure 9.28(a)). The distribution profile of an area mapped in the periosteal cortex of bone from Hartlepool revealed slight elevations at the cortical edge (figure 9.20(a)): this was more clearly identified in a line-profile of this area (figure 9.21(a)).

Uranium diffusion profiles were not evident in the Olduvai example (figure 9.31). This is contrary to studies by Williams and Marlow (1987). However, subsequent quantitative analysis of this material by XRF (Section 9.4.6) would reveal relatively high uranium concentrations (up to 22 ppm), suggesting diagenetic alteration had occurred.

Figure 9.19: PIXE Spectra Representing Archaeological Bone Material from (a) Hartlepool, (b) Canterbury, (c) Watchfield, and (d) the "Mary Rose".

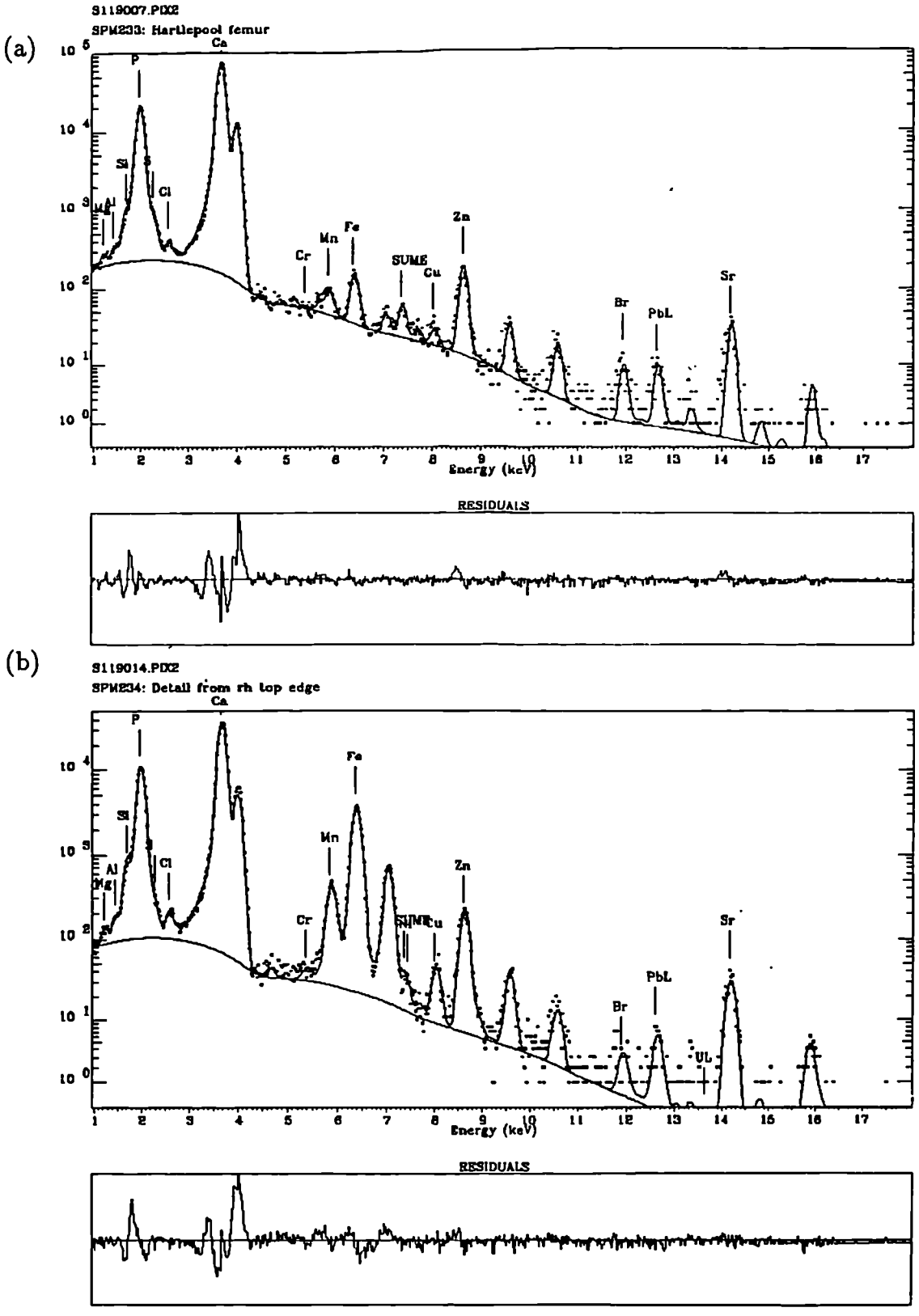

Figure 9.19 cont.

(c)

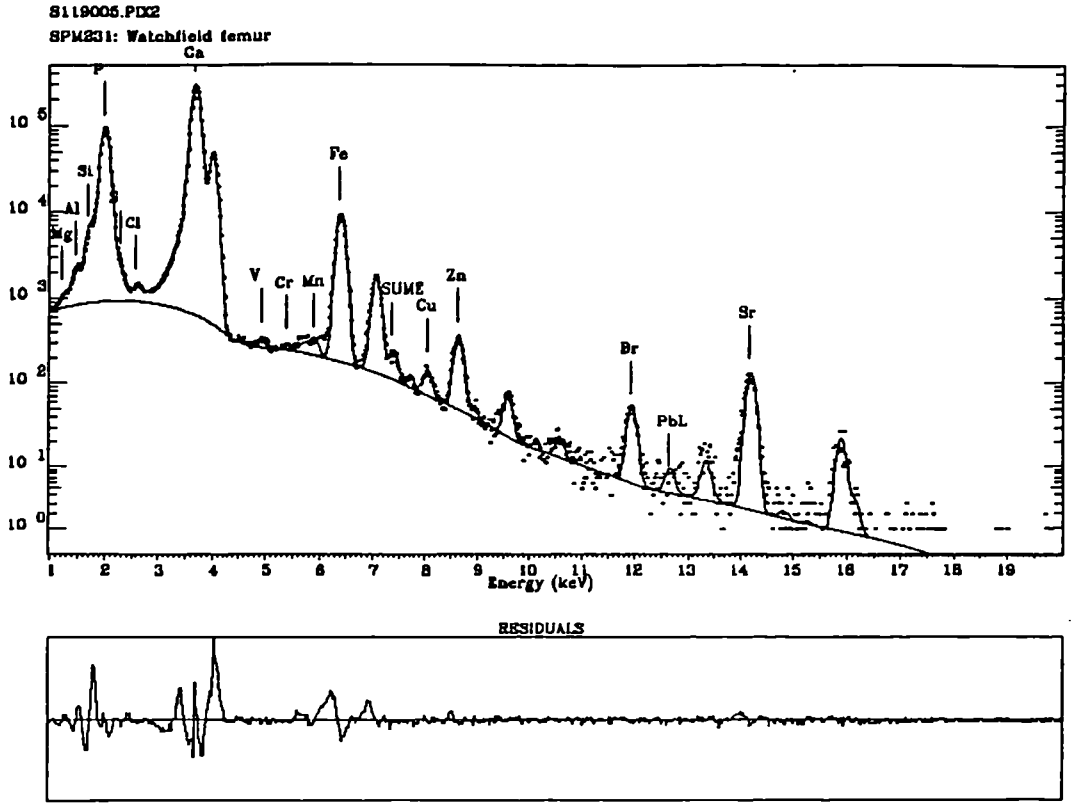

(d)

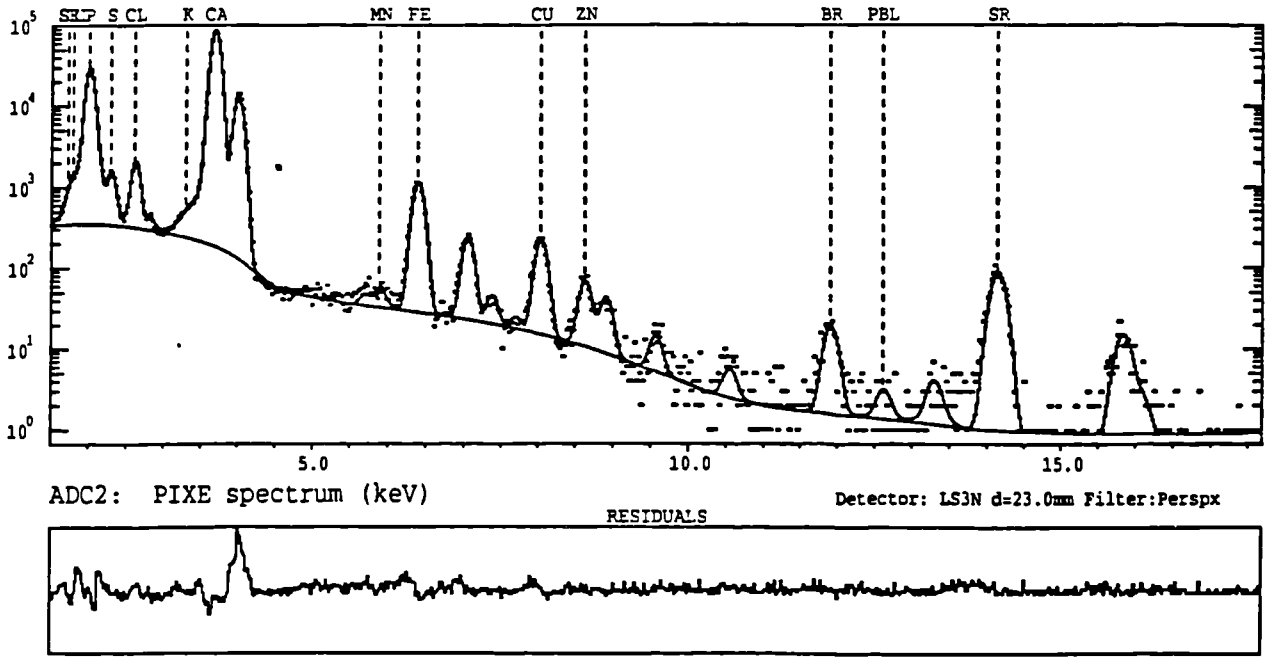

Figure 9.20(a) and (b): PIXE Maps of Elemental Distribution in the Periosteal Cortex of Bone from Hartlepool, Cleveland. (2500 sq.microns).

(a)

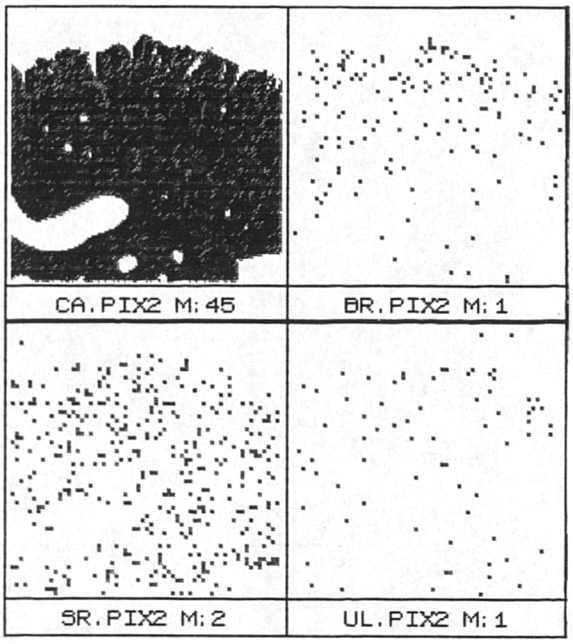

(b)

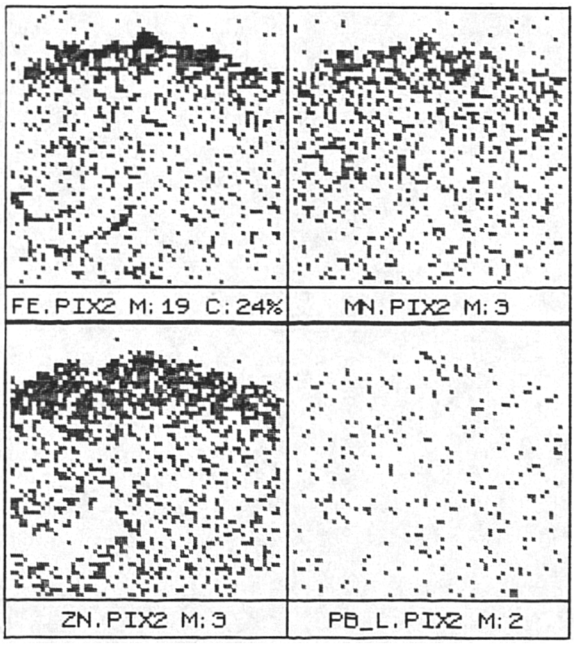

Figure 9.21(a) and (b): PIXE Line-Profiles of Elemental Distribution in the Periosteal Cortex of Bone (mapped in figure 9.20) from Hartlepool, Cleveland. (cortical width = 2500 microns).

(a)

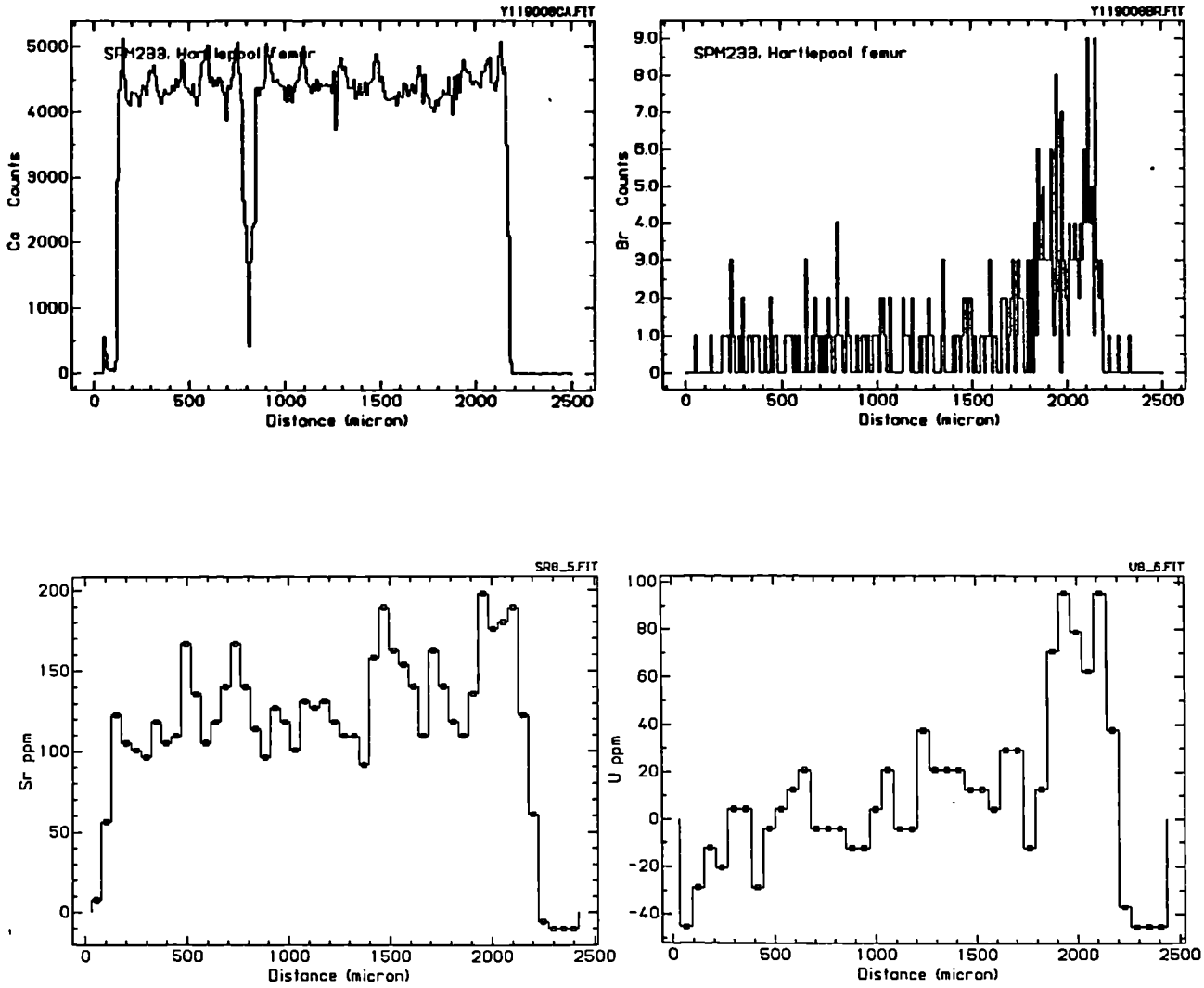

Figure 9.21 cont.

(b)

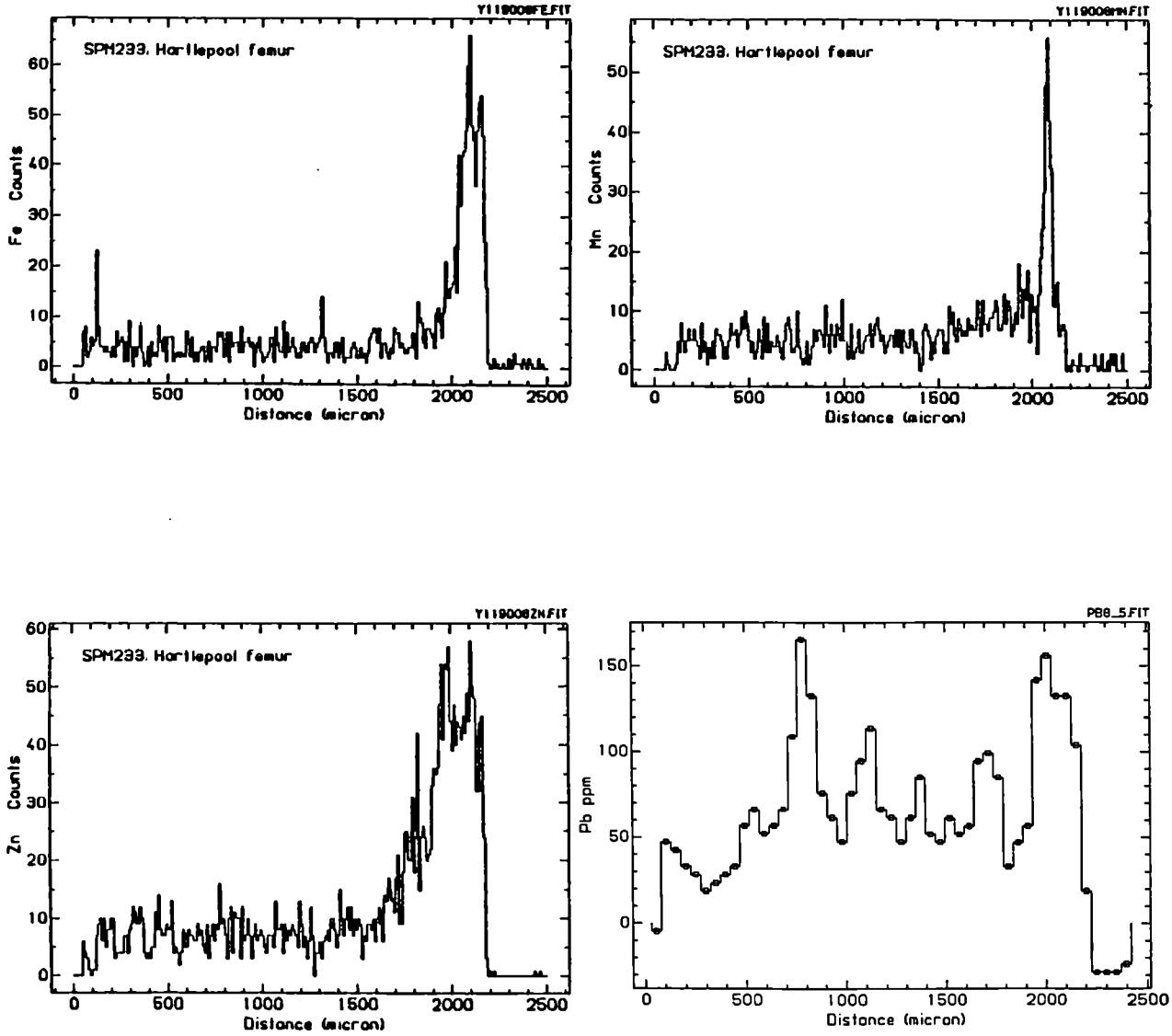

Figure 9.22: PIXE Maps of Elemental Distribution in the Periosteal Cortex of Bone from Canterbury, Kent. (2500 sq.microns).

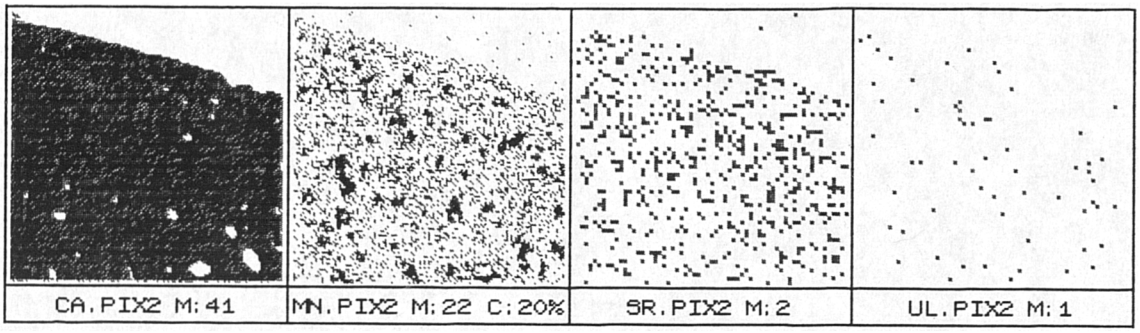

Figure 9.23: PIXE Maps of Elemental Distribution in the Endosteal Cortex of Bone from Canterbury, Kent. (2500 sq.microns).

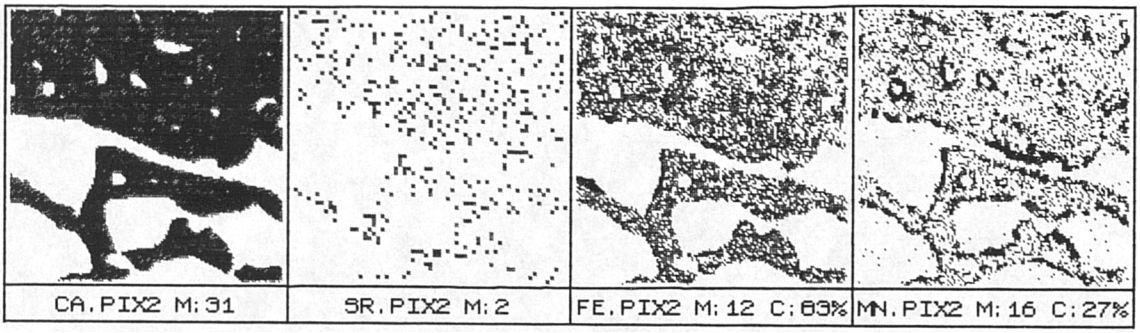

Figure 9.24: PIXE Maps of Elemental Distribution at the Periosteal Edge of Bone from Canterbury, Kent. (300 sq.microns).

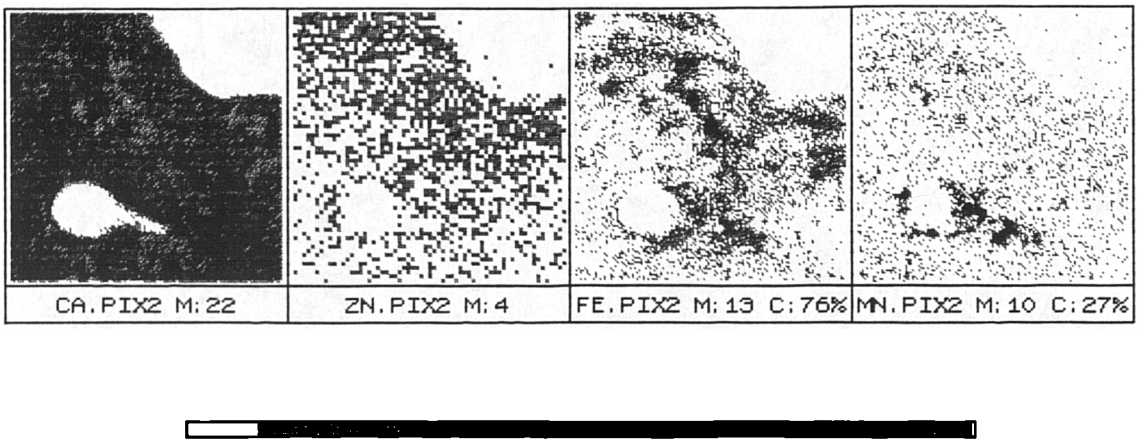

Figure 9.25(a) and (b): PIXE Line-Profiles of Elemental Distribution in the Periosteal Cortex of Bone (mapped in figure 9.22) from Canterbury, Kent. (cortical width = 2500 microns).

(a)

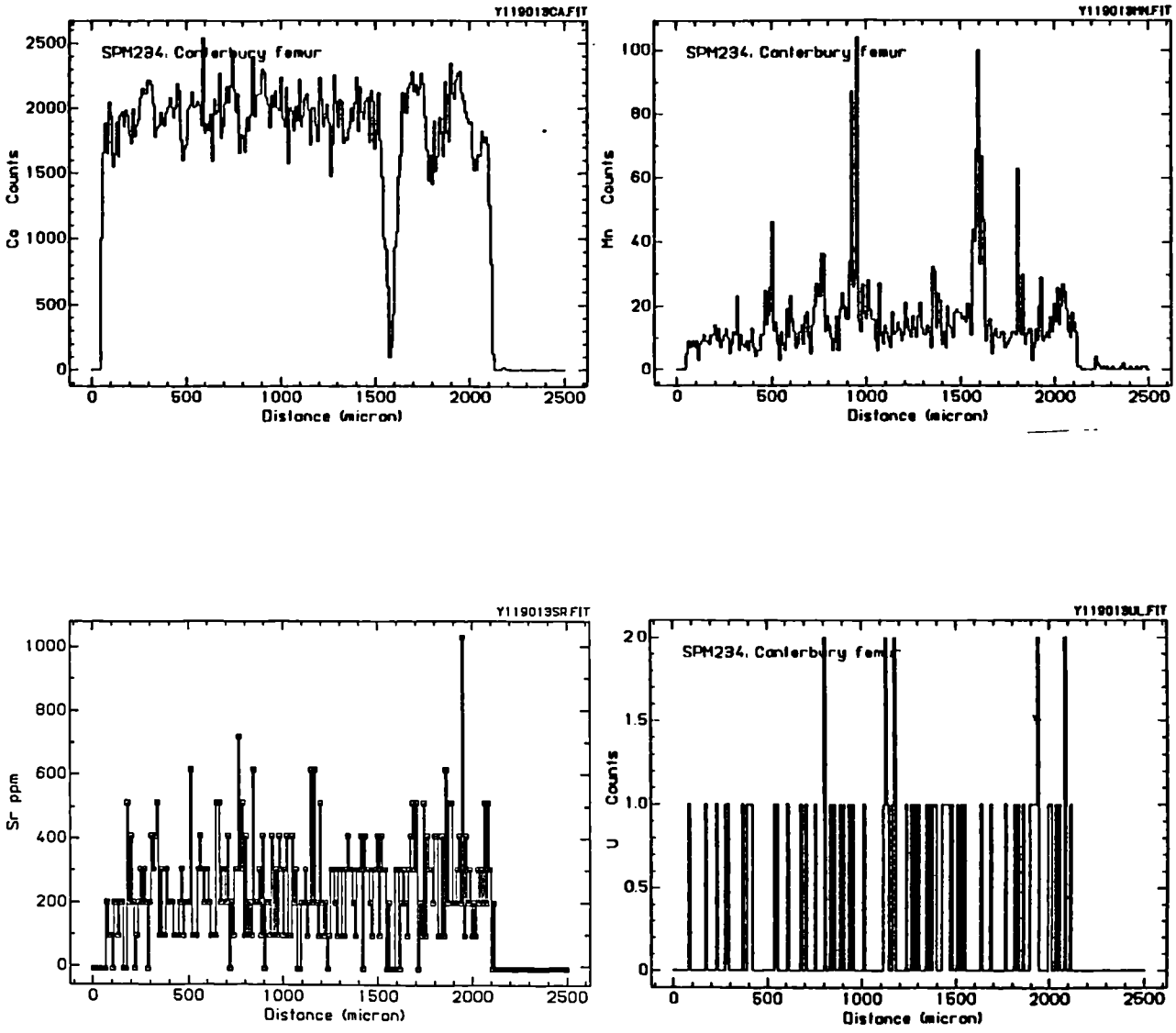

Figure 9.25 cont.

(b)

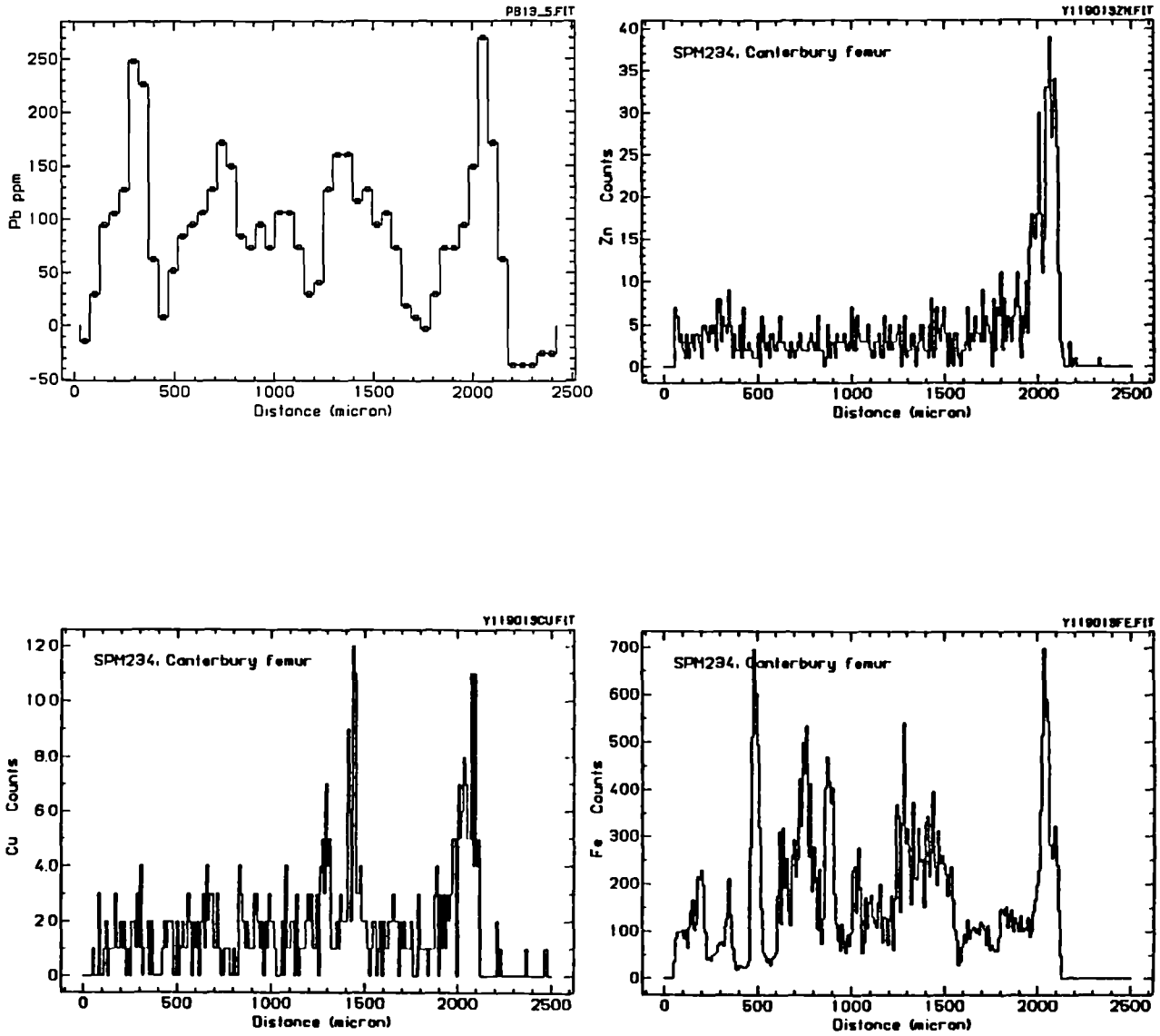

Figure 9.26: PIXE Maps and Corresponding Line-Profiles of Calcium and Strontium Distribution in the Periosteal Cortex of Bone from Watchfield, Oxfordshire. (2500 microns width).

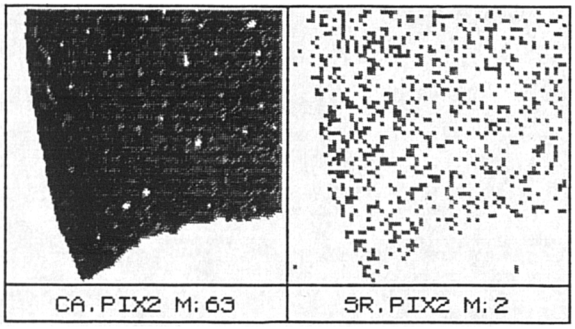

Figure 9.27: PIXE Maps of Elemental Distribution in the Endosteal Cortex of Bone from Watchfield, Oxfordshire. (2500 sq.microns).

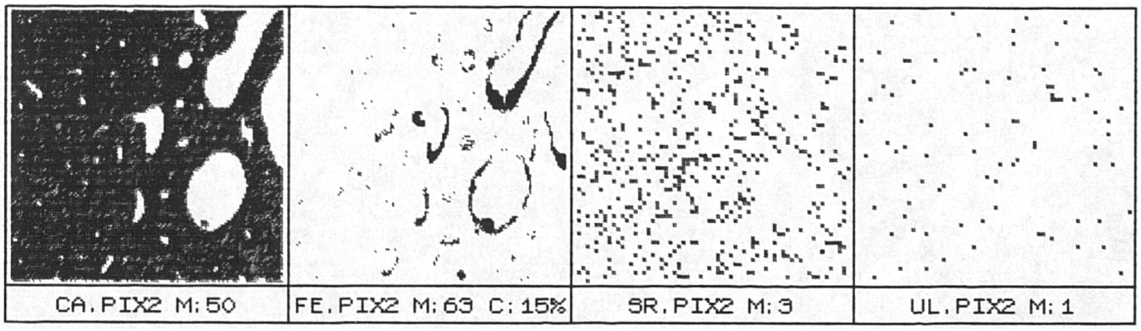

Figure 9.28(a) and (b): PIXE Maps of Elemental Distribution In and Around a Pore in the Mid-Cortical Region of Bone from Watchfield, Oxfordshire. (100 sq.microns)

(a)

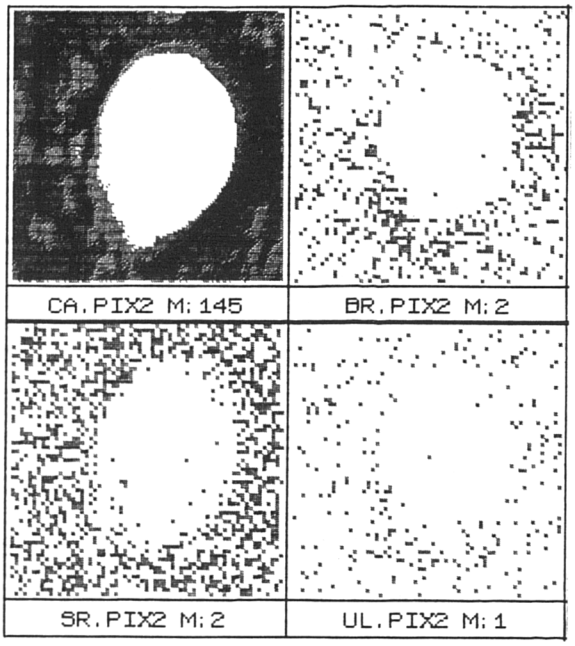

(b)

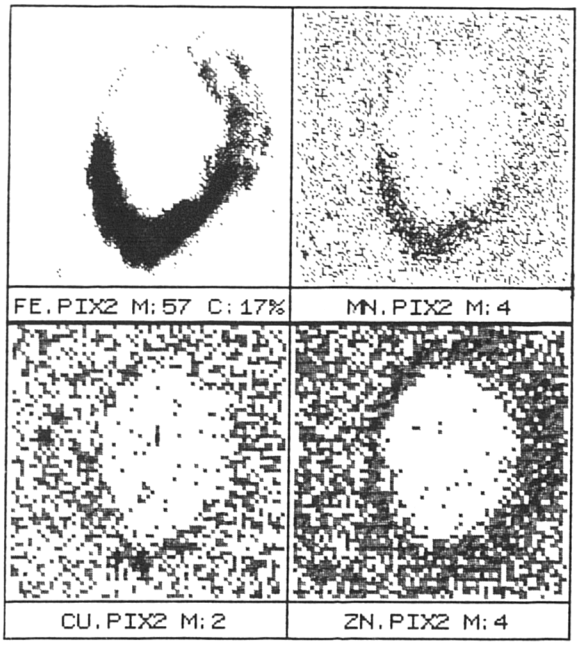

Figure 9.29(a) and (b): PIXE Line-Profiles of Elemental Distribution in the Periosteal Cortex of Bone (mapped in figure 9.26) from Watchfield, Oxfordshire. (cortical width 2500 microns)

(a)

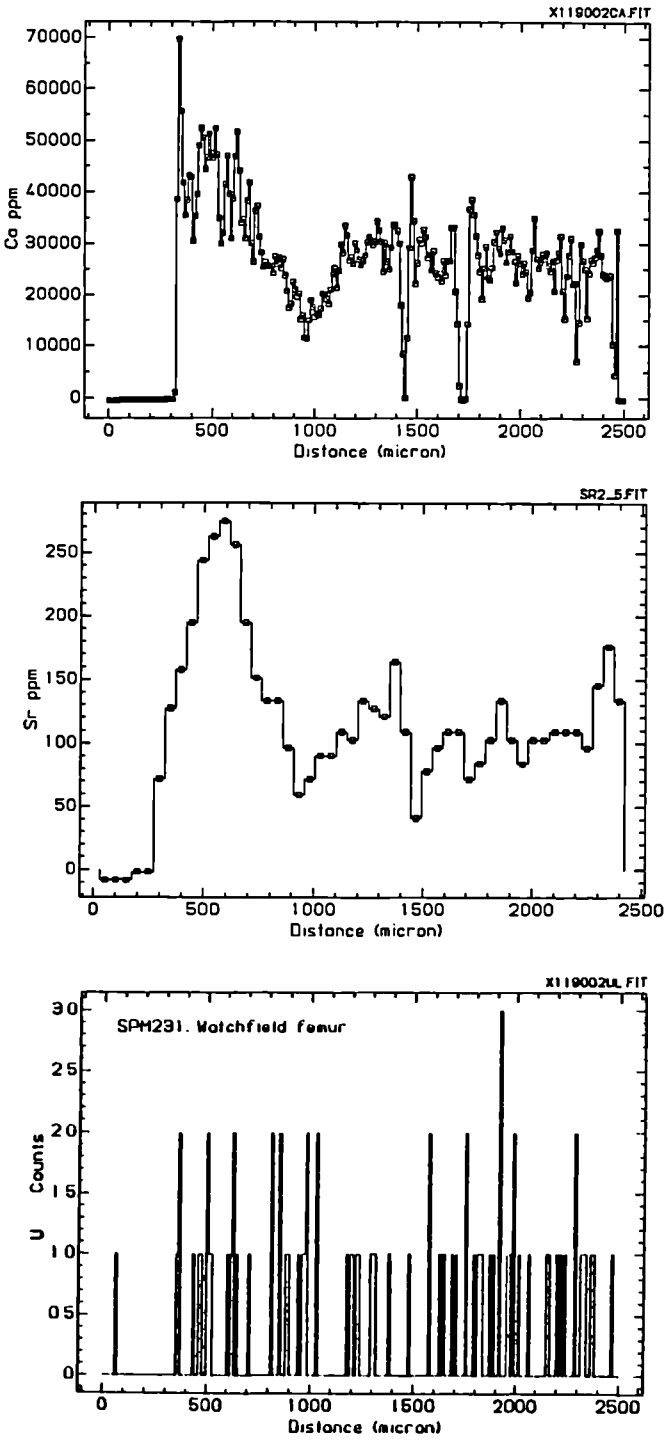

Figure 9.29 cont.

(b)

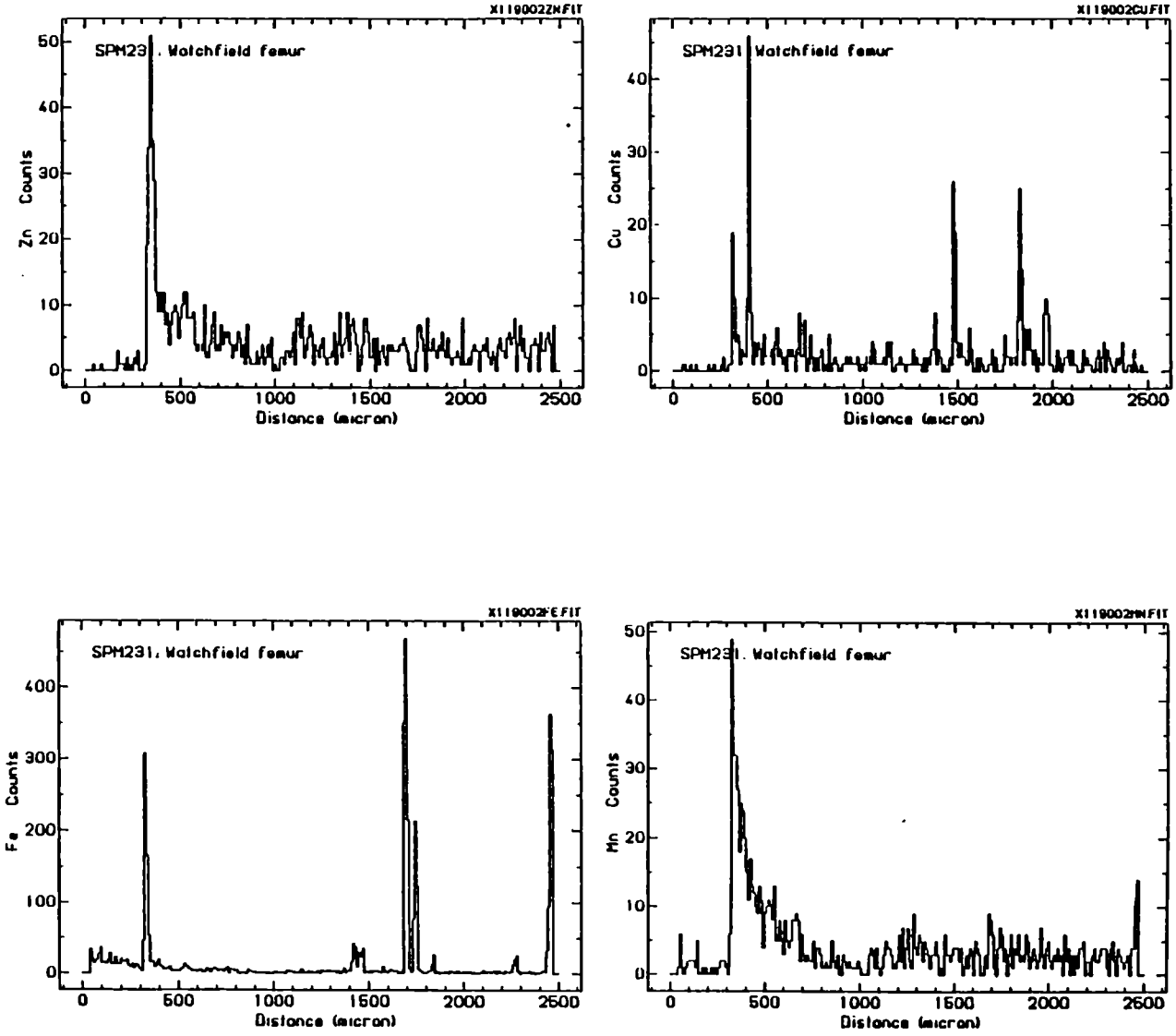

Figure 9.30: PIXE Maps of Elemental Distribution in the Periosteal (Ca, Zn) and Endosteal (Ca, Fe) Cortices of Bone from Pompeii, Italy. (2500 sq.microns)

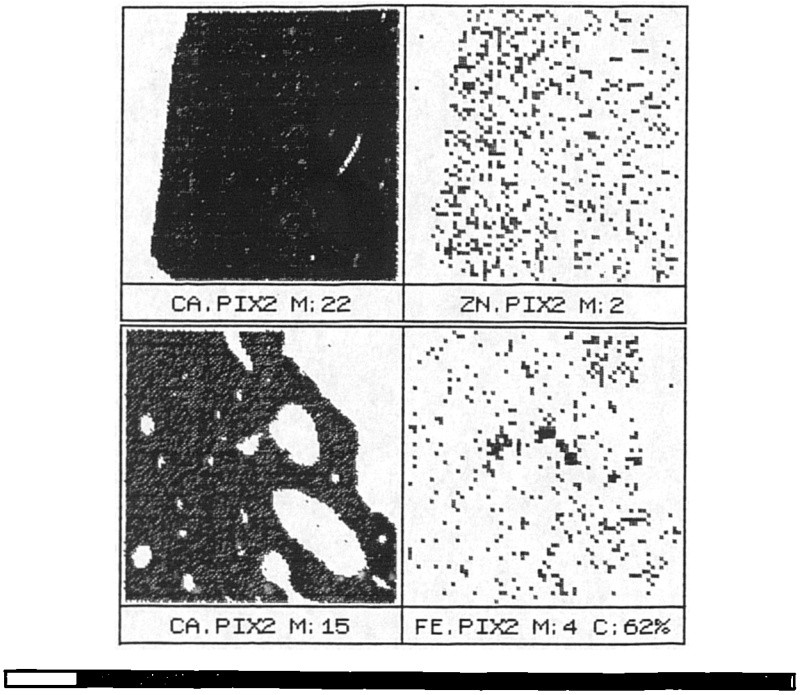

Figure 9.31: PIXE Maps of Elemental Distribution in the Periosteal Cortex of Bone from Olduvai, Africa. (2500 sq.microns)

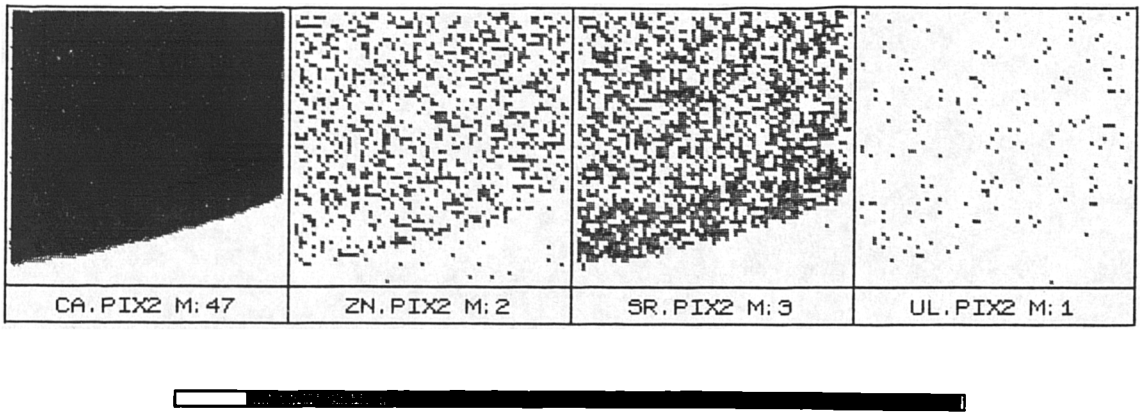

Figure 9.32: PIXE Maps of Elemental Distribution in the Periosteal Cortex of Bone from the "Mary Rose" (2500 sq.microns)

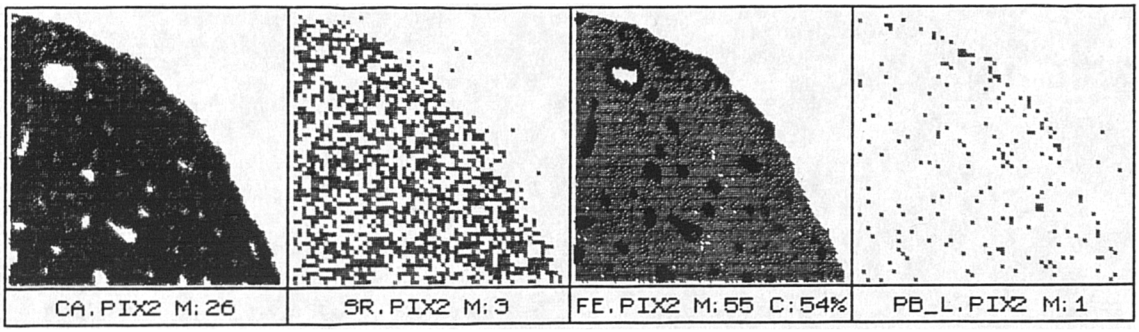

Figure 9.33: PIXE Maps of Elemental Distribution in the Endosteal Cortex of Bone from the "Mary Rose". (2500 sq.microns)

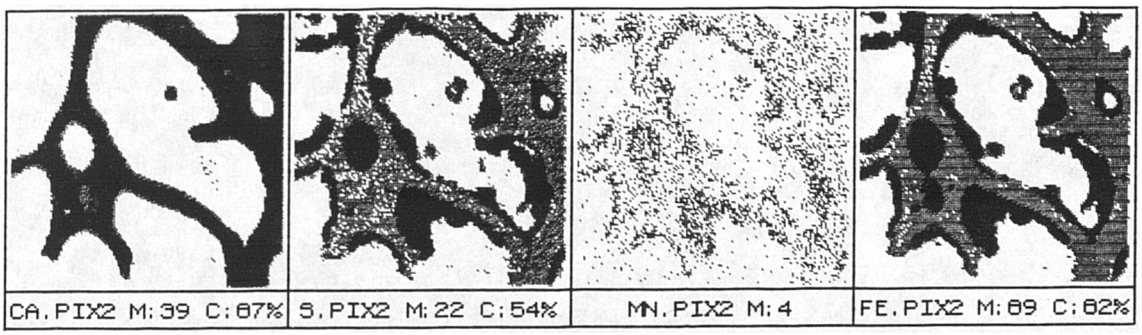

Figure 9.34: PIXE Maps of Elemental Distribution in a Pore Located in the Mid-Cortical Region of Bone from the "Mary Rose". (100 sq.microns)

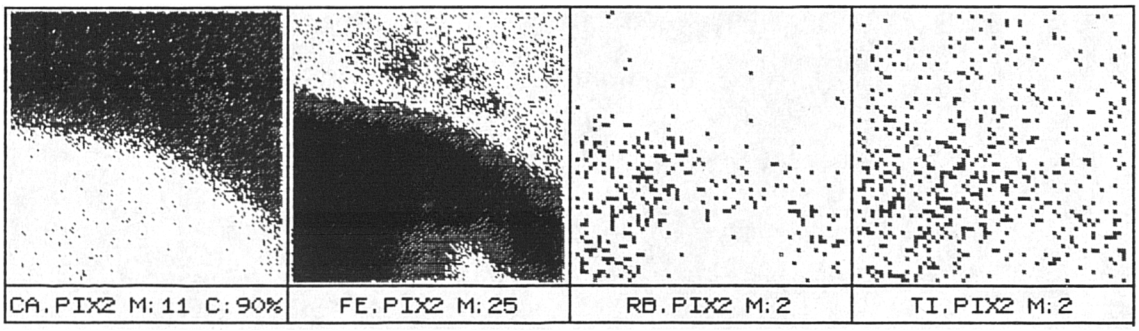

Figure 9.35: PIXE Line-Profiles of Elemental Distribution in the Periosteal Cortex of Bone (mapped in figure 9.32) from the "Mary Rose", Indicating Elemental Depletion. (cortical width 2500 microns)

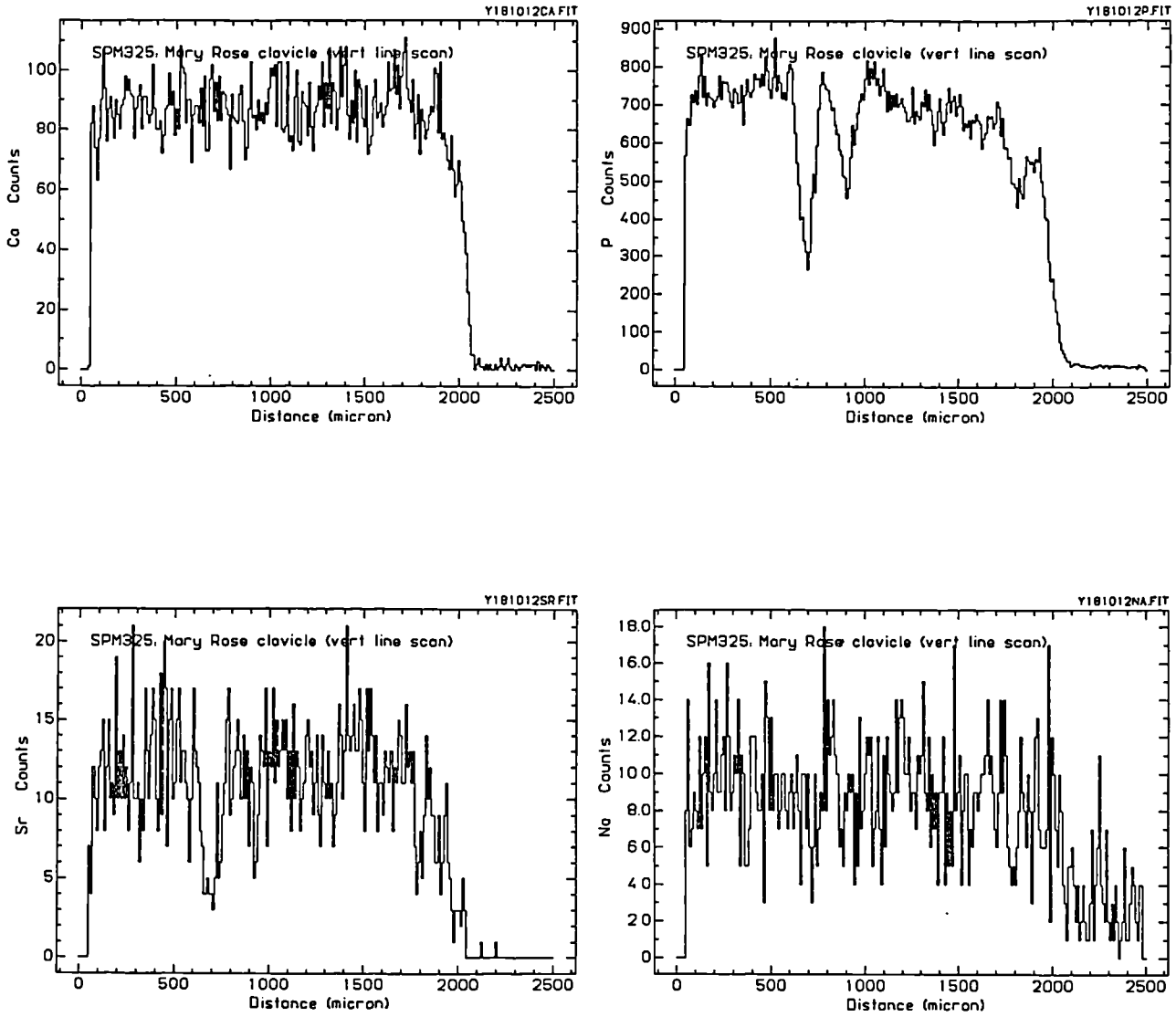

Figure 9.36: PIXE Line-Profiles of Elemental Distribution in the Periosteal Cortex of Bone (mapped in figure 9.32) from the "Mary Rose" Indicating Elemental Contamination. (cortical width 2500 microns)

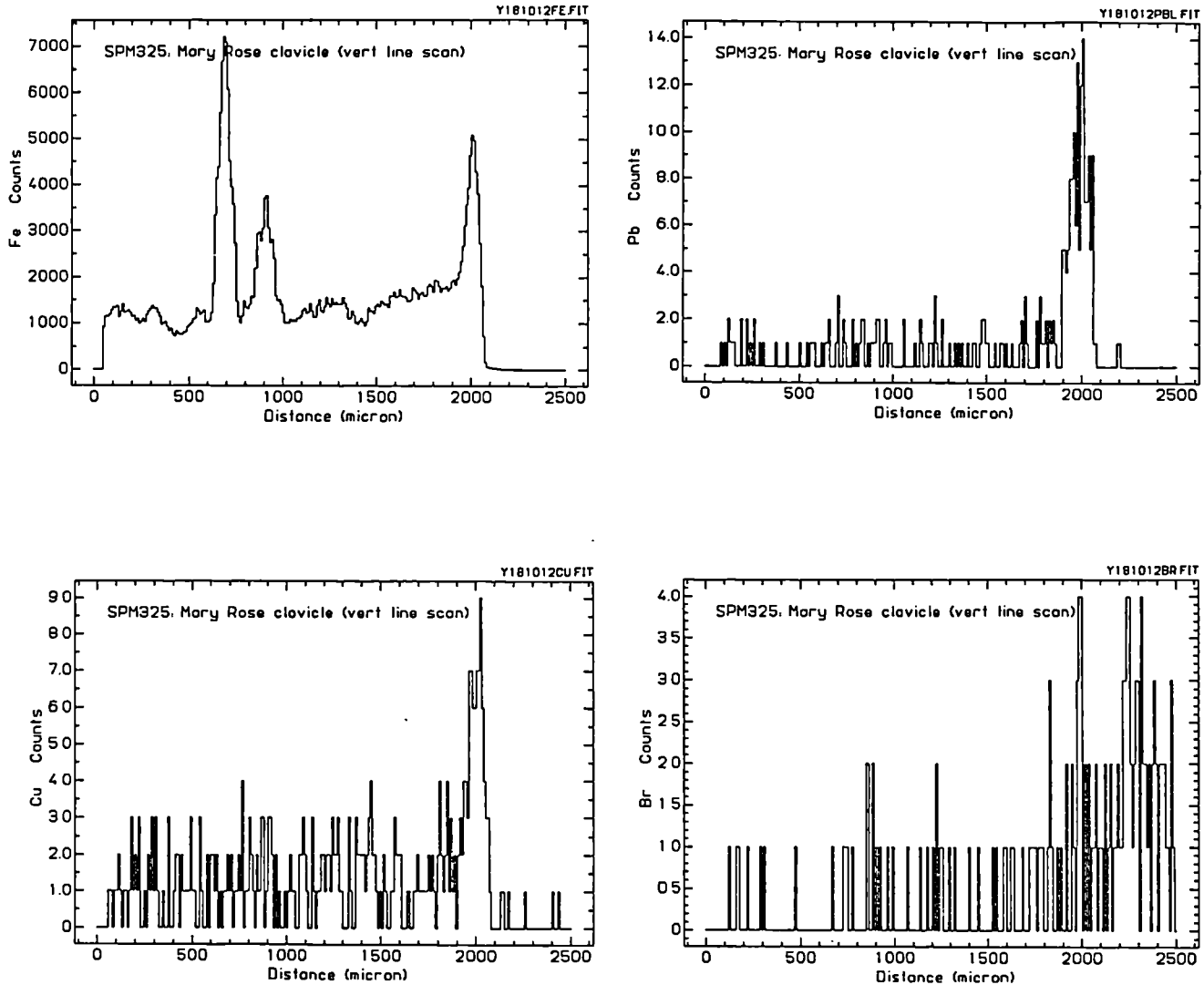

Figure 9.37(a) and (b): PIXE Maps of Elemental Distribution in the Periosteal Cortex of Bone from the Bay of Agay Wreck, Indicating (a) Contamination and (b) Depletion. (2500 sq.microns)

(a)

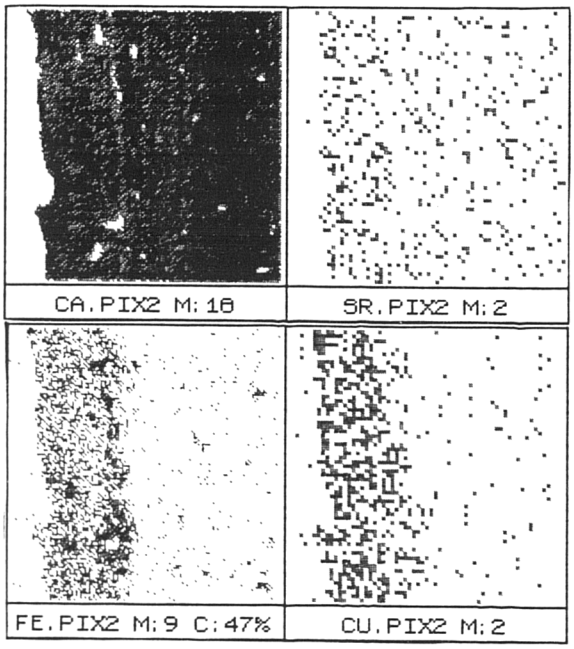

(b)

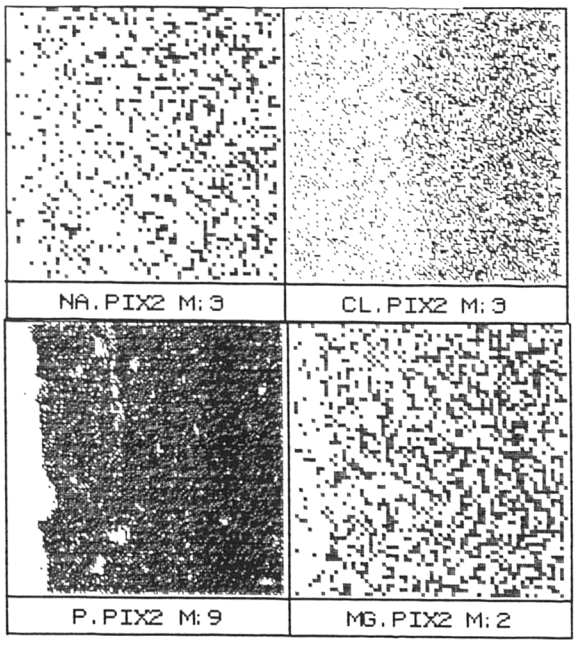

Figure 9.38: PIXE Line-Profiles of Elemental Distribution in the Periosteal Cortex of Bone (mapped in figure 9.37) from the Bay of Agay Wreck Indicating Elemental Contamination. (cortical width 2500 microns)

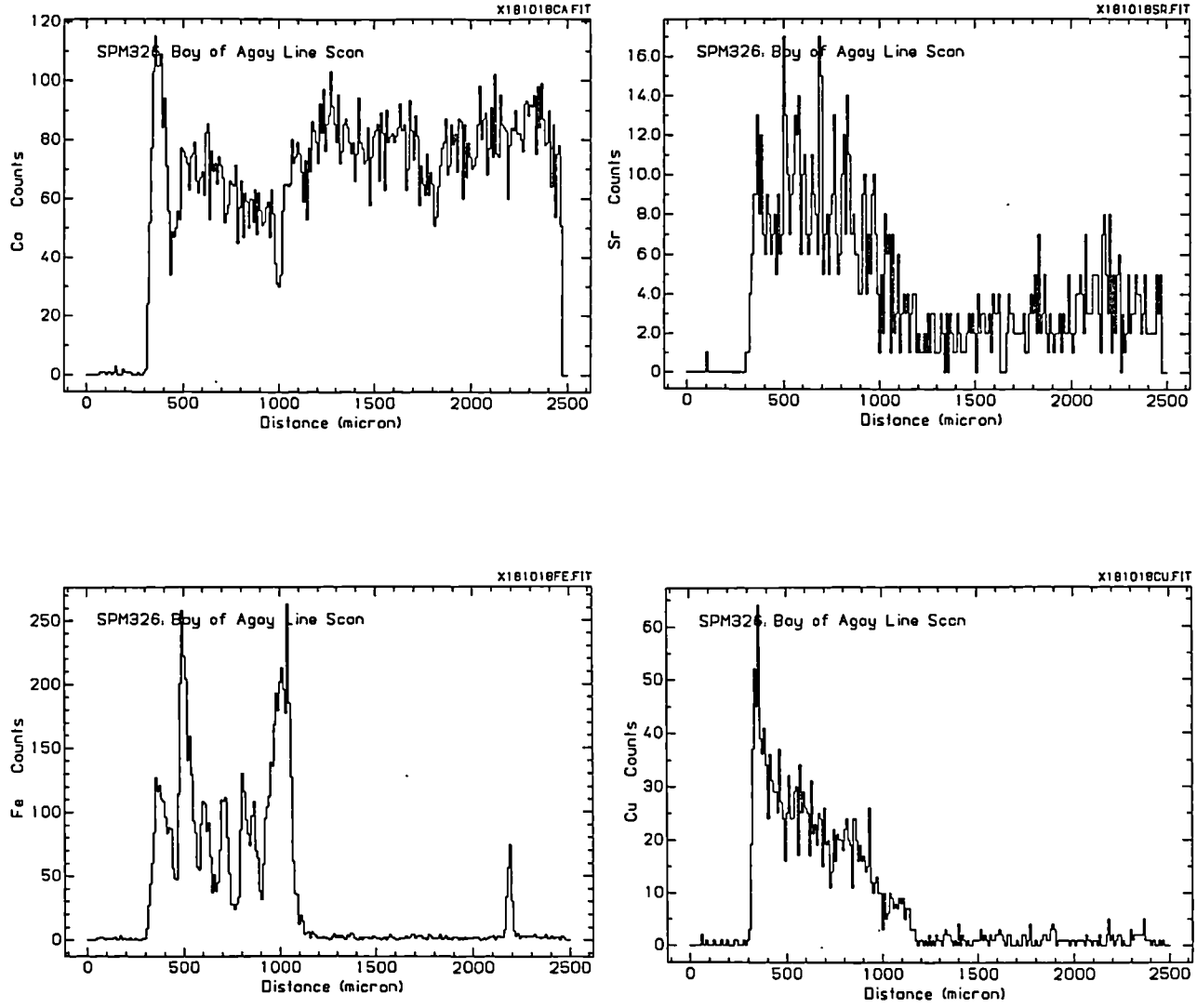

Figure 9.39: PIXE Line-Profiles of Elemental Distribution in the Periosteal Cortex of Bone (mapped in figure 9.37) from the Bay of Agay Wreck Indicating Elemental Depletion. (cortical width 2500 microns)

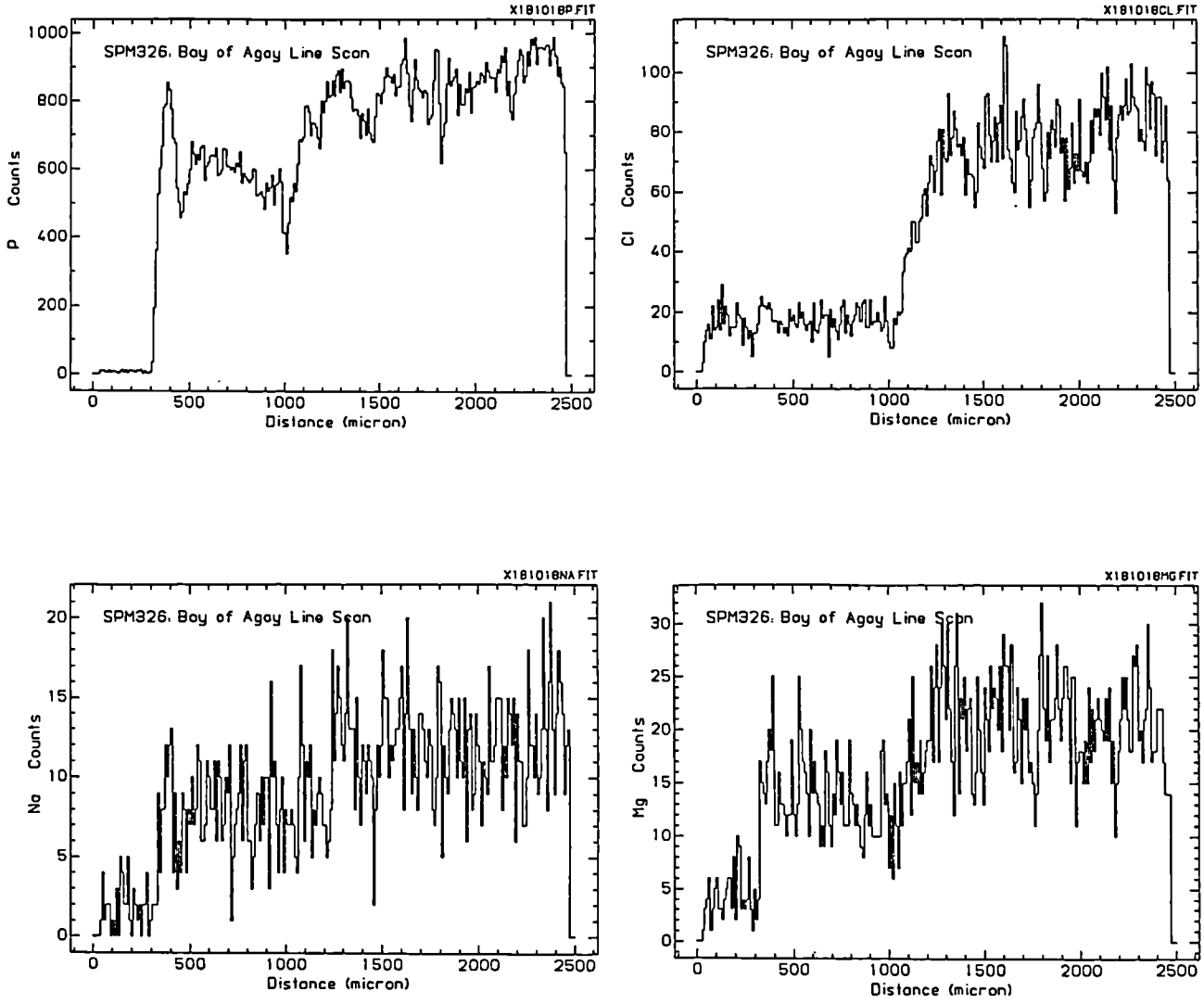

- Summary.

PIXE analysis of a number of bone samples excavated from a variety of geological environments found that bone is subject to contamination from a wide range of trace elements. Moreover, this technique was able to identify elements that were undetected by EPMA. Both *contamination* and *depletion* of elements were observed in sea-water examples.

In some cases, it was apparent that contamination was not necessarily identifiable on the basis of cross-cortical elemental gradient patterns; some elements, such as strontium and uranium in "Mary Rose" and Olduvai samples respectively, were measured in significantly high concentrations despite an apparently homogeneous distribution profile.

Although PIXE is able to detect uranium at lower concentration levels than EPMA, for the majority of samples studied here the levels are still below that of PIXE. Therefore, in order to gain a more complete description of uranium distribution in exhumed bone, the more sensitive technique of fission track analysis was carried out on a range of bone material.

9.4.5 Micro-distribution of Uranium: FTA.

Fission track analysis revealed more extensive uranium uptake into British archaeological bone material than was detected by earlier PIXE analysis, because of its better sensitivity. Uranium was distributed throughout the cortical tissue and lining the cortical surfaces of bone samples from Hartlepool, Canterbury and Watchfield. Figure 9.40 shows a typical fission track pattern, magnified 640x, created by the fission of a uranium particle here located in the mid-cortical tissue of Hartlepool bone.

A comparison of the uranium distribution patterns in bone samples representing each British mainland site was made in order to (1) determine any relationship between uptake and burial environment, and (2) identify types of interaction.

1. Watchfield: Uranium was observed across the whole cortical width of bone, located predominantly in the periosteal (figures 9.41(a) and (b)) and endosteal (figure 9.41(b)) cortices. Magnification of the former (figure 9.41(c)) demonstrates some cortical lining of the periosteal surface, together with pore-filling which was extensive throughout the periosteal and mid-cortical regions.

2. Canterbury: Uranium had again penetrated the full cortical width, but in contrast to Watchfield data, uranium was not concentrated towards the peripheral cortices but was distributed fairly homogeneously throughout the cortical tissue. Figures 9.42(a) and (b) demonstrate this pattern. Relatively little pore-filling was observed in this sample.

3. Hartlepool: Uranium distribution was not as extensive or as dense in material excavated from this site. Uranium was localised predominantly at the cortical edges in both periosteal (figure 9.43(a)) and endosteal (9.43(b)) bone. There was little uranium in the mid-cortex with clear indications of pore-filling (on a smaller scale than Watchfield material, however).

Absolute quantitative uranium values for each example are shown in Table 9.3, and are discussed in detail in Section 9.4.6.

- Summary.

Fission track analysis was able to provide a relatively detailed description of uranium distribution in bone from Watchfield, Canterbury and Hartlepool. There was evidence for pore-filling, surface adsorption and incorporation mechanisms of interaction. The homogeneous distribution of uranium in the cortex of Canterbury bone suggested the latter, while pore-filling and adsorption at the cortical surfaces were more evident in Watchfield and Hartlepool material. This might suggest that uranium-calcium exchange is promoted in neutral pH conditions while pore-filling and adsorption are enhanced in more extreme pH conditions.

Hartlepool bone possessed the lowest uranium content, while a quantitative comparison of the other two samples could not be estimated with confidence.

Quantitative analyses of each bone sample are described in the next section.

Figure 9.40: Fission tracks created by a uranium particle located in mid-cortical bone. Mag. x640.

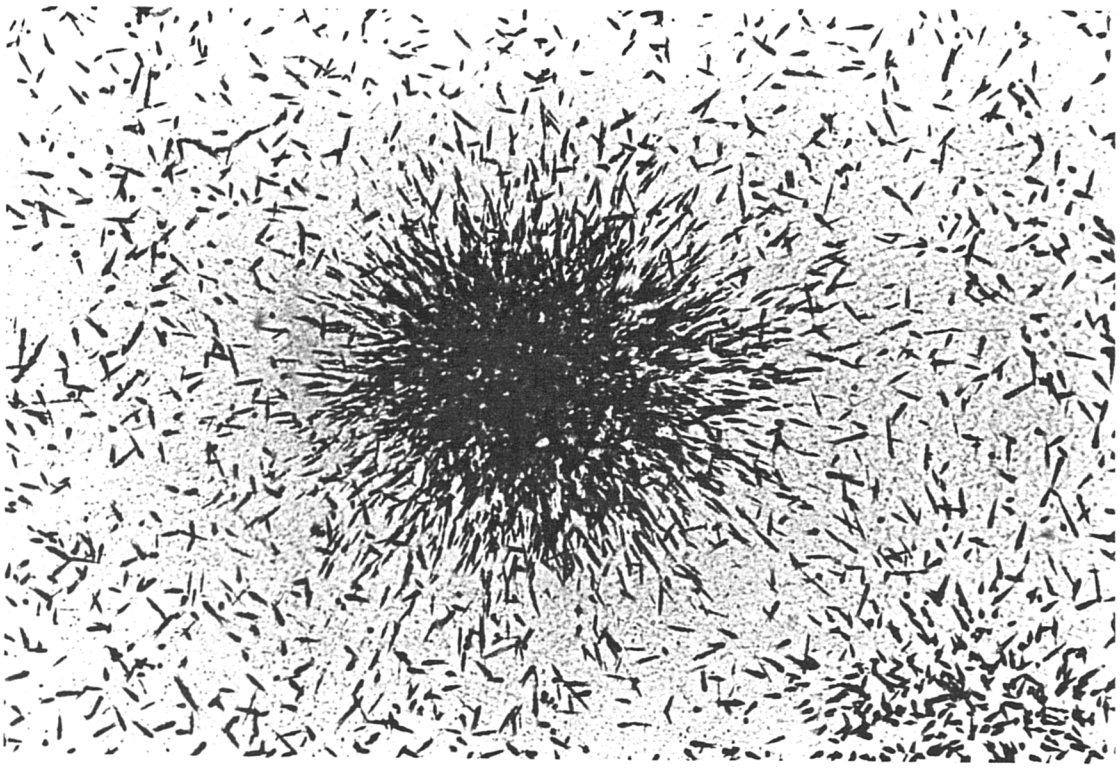

Figure 9.41(a): Fission track distribution in periosteal bone showing uranium pore-filling (p) and lining of the cortical edge (ce). Mag. x64.

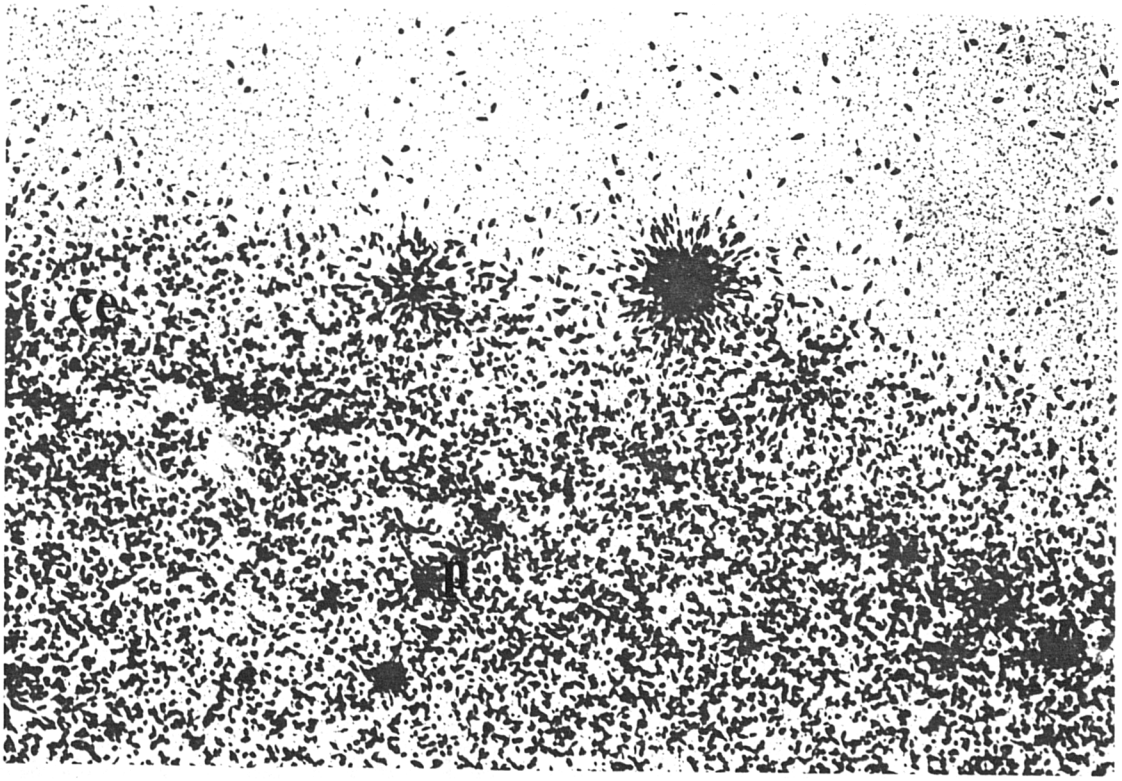

Figure 9.41(b): Fission track distribution in the outer cortex of bone excavated from Watchfield (ce = cortical edge). Mag. x64.

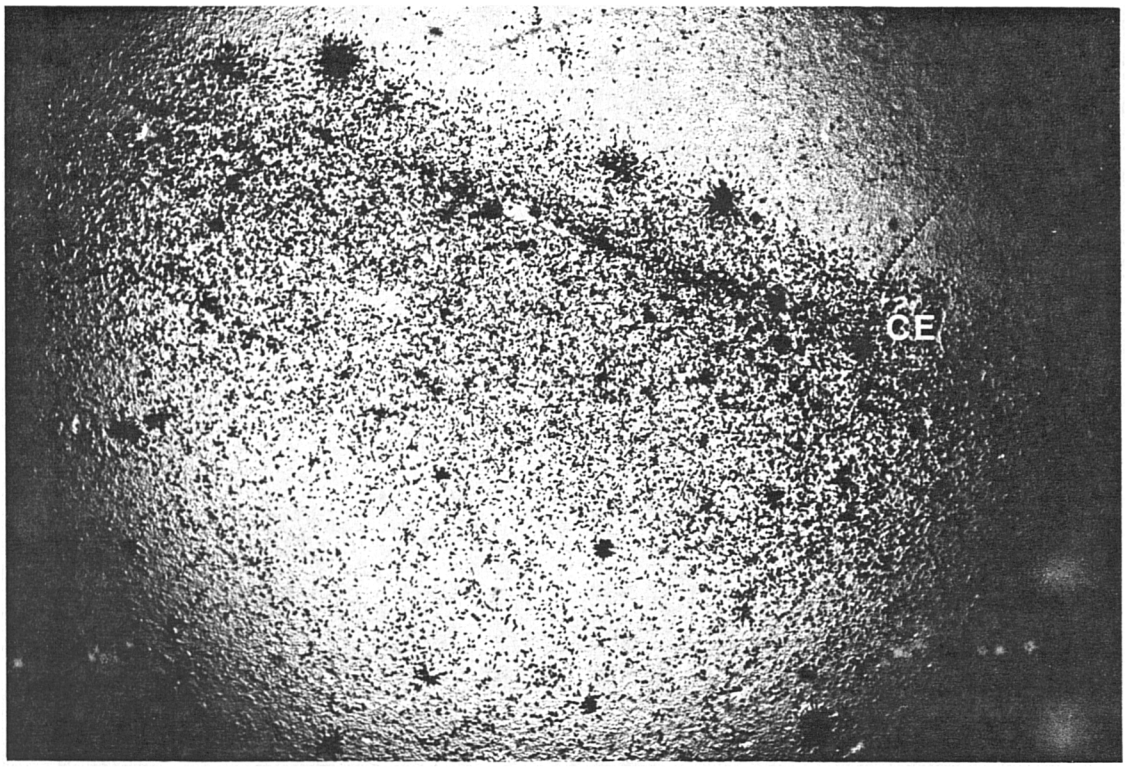

Figure 9.41(c): Fission track distribution in cancellous bone of inner cortex of bone excavated from Watchfield. Mag. x64.

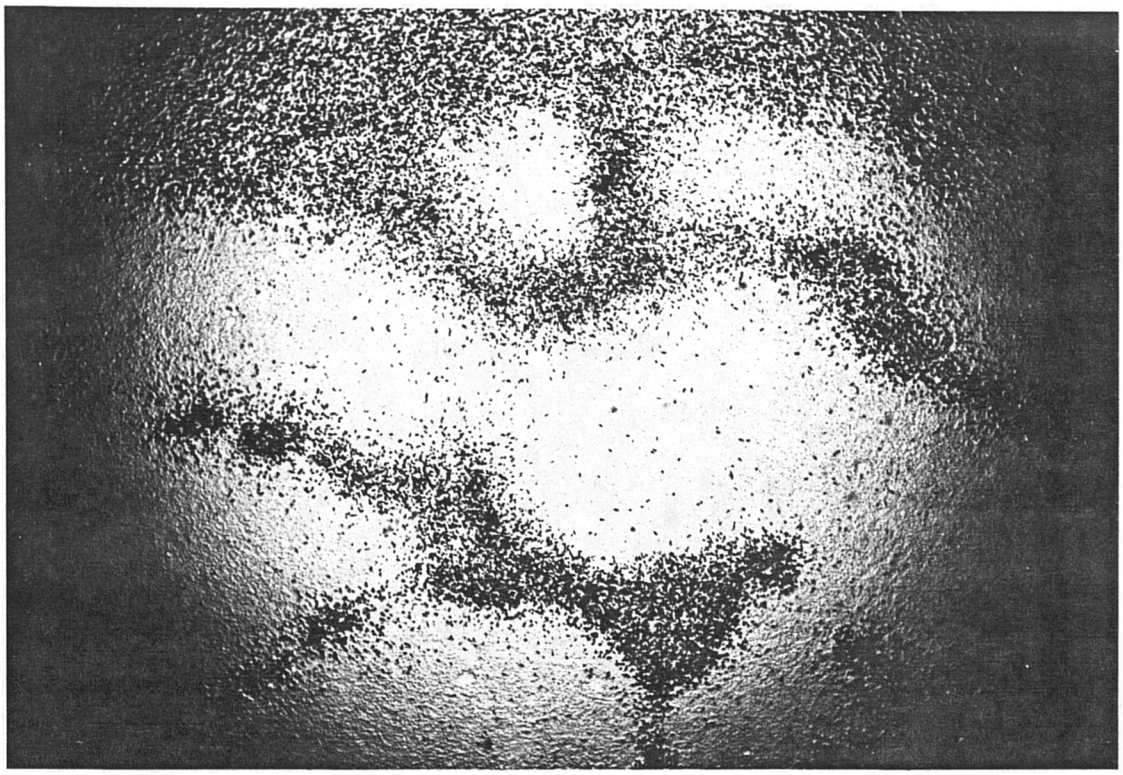

Figure 9.42(a): Fission track distribution in the cortex of bone excavated from Canterbury (p = periosteal cortex, e = endosteal cortex). Mag. x64.

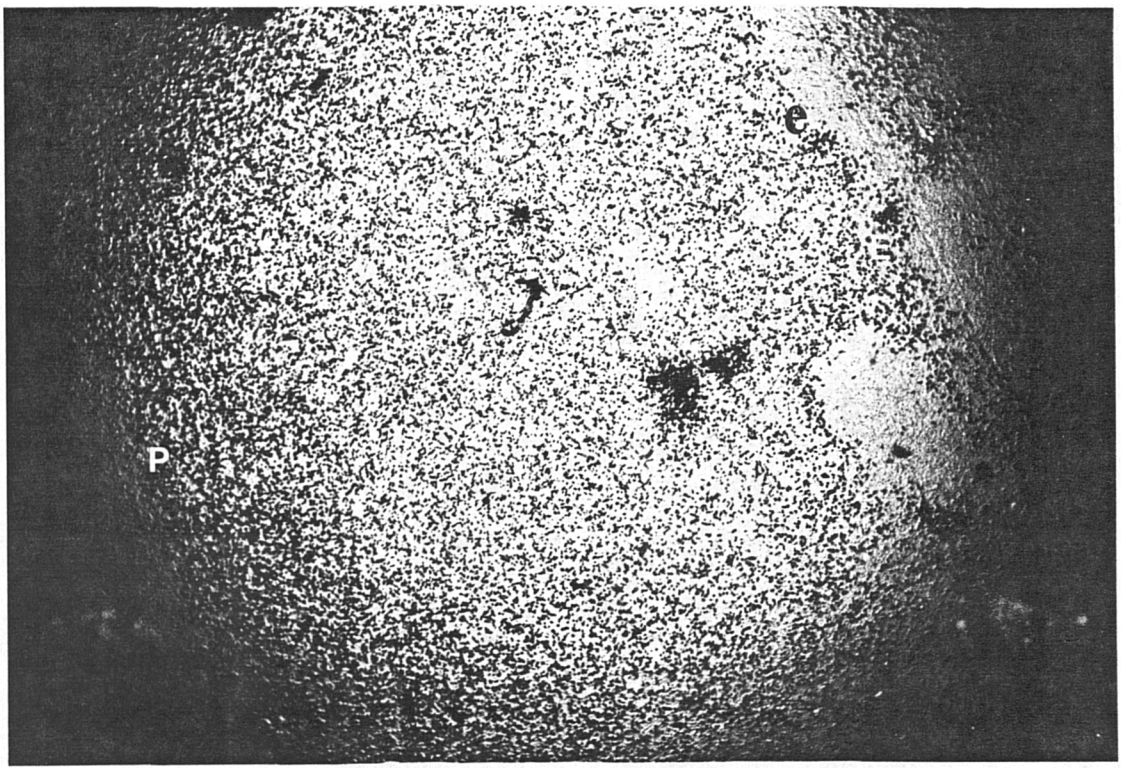

Figure 9.42(b): Fission track distribution in cancellous bone of inner cortex of bone excavated from Canterbury. Mag. x64.

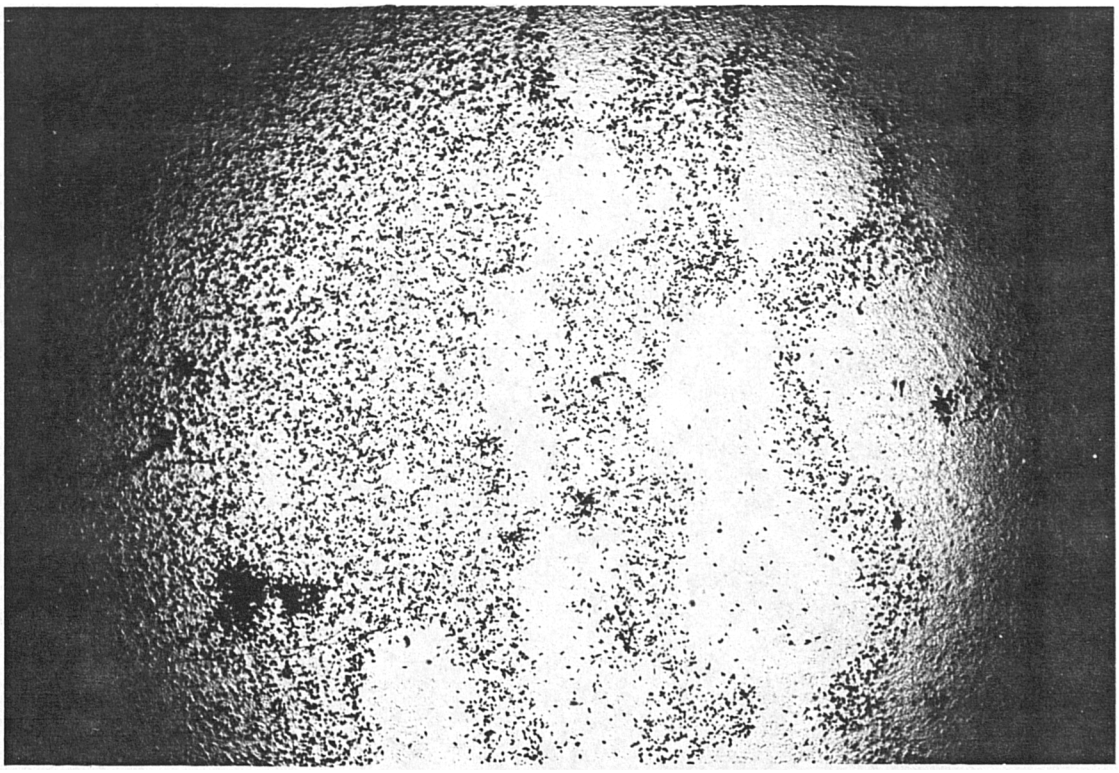

Figure 9.43(a): Fission track distribution in the cortex of bone excavated from Hartlepool. Mag. x64.

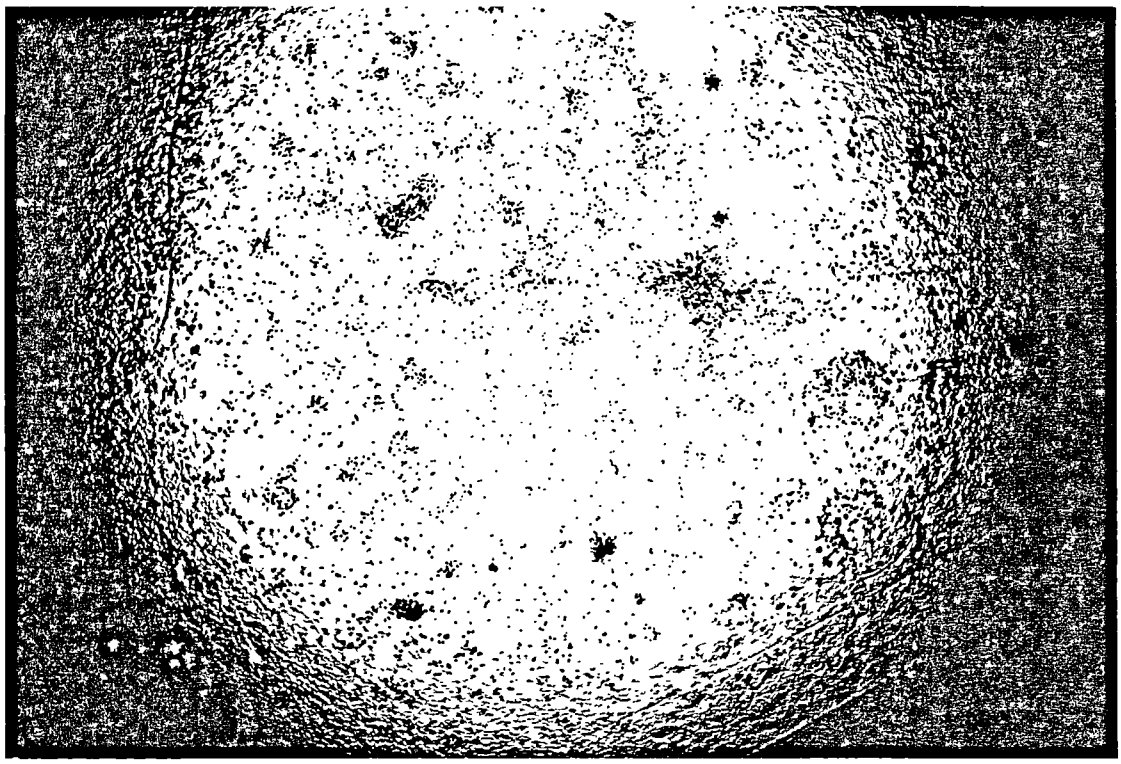

Figure 9.43(b): Fission track distribution in cancellous bone of inner cortex of bone excavated from Hartlepool. Mag. x64.

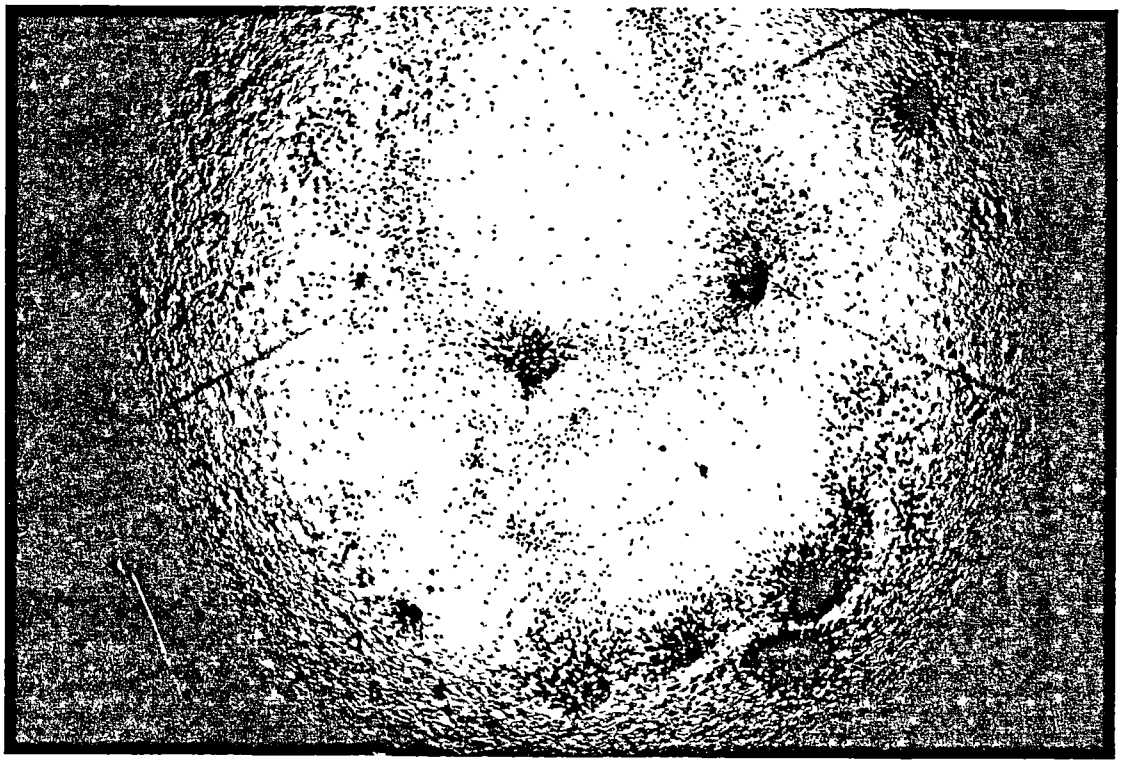

9.4.6 Quantitative Analyses of Excavated Bone.

9.4.6.1 A comparison of quantitative analyses using different techniques.

Two bone samples - from the "Mary Rose" and Hartlepool - were quantitatively analysed using two different techniques: PIXE and XRF. A comparison of these methods, together with average values of cross-cortical electron probe analysis for Hartlepool material, are shown in table 9.2.

Table 9.2 A comparison of quantitative analyses of archaeological bone by different methods.

Sample	Method	Ca	P	Sr	U	Zn	Mn	Fe	Pb	Si	S
Hartlepool	XRF	53.8%	39.0%	239	3	189	100	1200	45	8300	1800
	PIXE	5.8%	3.3%	155	N/K	97	15	N/K	95	N/K	729
	EPMA	34.9%	21.9%		N/K					N/K	
Mary Rose	XRF	50.2%	42.5%	1899	28	N/K	N/K	N/K	N/K	N/K	N/K
	PIXE	20.6%	13.5%	1824	N/K	64	N/K	52800	N/K	1651	23200
*H5 ref.bone	XRF	40.36%	24.98%	129	N/K	120	N/K	200	N/K	N/K	N/K

*Certified values by IAEA reference authority found in Appendix Vg. Values for calcium and phosphorus represent % oxide values (CaO and P_2O_5, respectively). All other values are measured in ppm. XRF = total in homogeneous powdered sample; PIXE = areal scans 2500 sq.microns; EPMA = averaged cross-cortical probe analyses (6 probes, each representing 70 sq.microns)

Generally, PIXE and XRF data were not in agreement. PIXE analysis of Hartlepool bone material was clearly in error as indicated by the extremely low % oxide figures for Ca and P. This sample was much thicker than the "Mary Rose" sample (200 cf. 80 microns) with a higher areal density. Moreover, simultaneous RBS analysis was not carried out for this sample since it was not a possible option at the time of analysis. So, there was no matrix correction factor used here. This would

explain the poor % oxide values for Hartlepool bone; small differences in proton beam and detector set-up, together with slight differences in the thickness of the perspex filters (see Appendices Vc and Vd) were probably not responsible for such dramatic differences in elemental concentrations in "Mary Rose" and Hartlepool PIXE analyses.

9.4.6.2 XRF analysis of excavated bone material.

XRF analysis of the remaining excavated samples were carried out for Ca, P, Sr and U concentrations only. These are shown in table 9.3. A range of samples (4-6 in number) were analysed for Hartlepool, Watchfield and Canterbury sites to give an indication of the *within-site variation* of bone chemistries and to compare those of long bones, consisting predominantly of dense cortical tissue, with rib bones, or cancellous/trabecular bone. Statistical analysis was not carried out on data from these samples for each respective site because of an insufficient sample size (4-6). The full dataset can be found in Appendix Ve.

The Sr/Ca and U/Ca ratios for each of these averaged samples are shown in Table 9.4: these values are probably more indicative of the relative diagenetic activity of strontium and uranium because they account for any slight differences in elemental yield. (The full dataset of these ratios can be found Appendix Ve).

In both tables, the values shown in brackets indicating the range/spread of values where more than one sample represented a particular category (e.g Hartlepool femur material) emphasised the degree of variability in the chemistry of bone samples of the same type (e.g. femur) excavated from a similar geological context. Corresponding values for strontium and in particular uranium showed such a high within-site variability for respective bone types that between-site comparisons could not feasibly be made because of the high degree of overlap of values in these ranges.

Nevertheless, a number of observations were made with extreme caution, using averaged values where possible.

Table 9.3 Averaged quantitative XRF data for strontium and uranium content in excavated bone samples

Bone sample	Number of samples	Ca % oxide	P % oxide	Sr ppm	U ppm
Mary Rose	1	50.24	42.47	1899	28.27
Olduvai 2.1	1	52.21	42.29	3983	22.18
Olduvai 13.3 (whole)	1	50.71	43.08	1575	9.56
Olduvai 13.3 T	1	51.20	43.43	1817	6.77
Olduvai 13.3 B	1	52.35	40.04	1462	17.20
Hartlepool (femurs)	3	53.38 (1.04)	38.37 (1.55)	225 (24)	5.96 (6.91)
Hartlepool (rib)	1	51.89	36.47	247	13.78
Watchfield (femurs)	3	52.43 (3.59)	42.23 (3.17)	461 (168)	5.29 (5.71)
Watchfield (ribs)	2	51.67 (0.75)	42.04 (1.65)	458 (114)	5.60 (7.09)
Canterbury (femurs)	5	52.41 (4.35)	31.10 (1.63)	352 (112)	2.88 (2.59)
Canterbury (rib)	1	47.84	26.49	389	6.26
*SARM-32 apatite std	3	54.91	38.20	4816	N/K
IAEA-312	3	N/K	N/K	N/K	15ppm*

Values in brackets represent the range/spread of values where sample number $>$ 1 within a category. *Certified values can be found in Appendix IIa. **Certified value= 16.5ppm

1. Within-site trends.

(a) Canterbury: comparing rib and femur analyses from the same skeleton, the strontium level in rib bone was 11% higher than that in the femur bone, and the strontium/calcium ratio even greater because of the lower calcium and phosphorus levels obtained in rib bone (Sr/Ca femur = 67.2 (x 10^{-5}) compared to Sr/Ca ratio rib = 81.3 (x 10^{-5}), an increase of 21 % in rib bone). The lower levels of calcium and phosphorus in rib bone compared to all other femur samples suggested a diagenetic loss of these elements from cancellous bone, with a relatively higher uptake of strontium.

Comparing femur samples, a significant degree of elemental variation was observed - strontium levels ranging from 288 to 400 ppm. Indeed, one of the femora possessed

Table 9.4 Average Sr/Ca and U/Ca ratios for exhumed bone material.

Bone sample	Sr/Ca ratio (x 10^{-5})	U/Ca ratio (x 10^{-5})
Mary Rose	378	5.63
Olduvai 2.1	763	4.25
Olduvai 13.3 (whole)	311	1.89
Olduvai 13.3 T	355	1.32
Olduvai 13.3 B	279	3.29
Hartlepool (femurs)	42.2 (4.29)	1.17 (1.29)
Hartlepool (rib)	47.6	2.66
Watchfield (femurs)	87.9 (35.71)	1.01 (1.00)
Watchfield (ribs)	88.6 (23.38)	1.08 (1.37)
Canterbury (femurs)	67.2 (20.72)	0.54 (0.58)
Canterbury (rib)	81.3	1.31

Values in brackets represent the range/spread of values where sample number $>$ 1 within a category.

more strontium than the rib sample, although its Sr/Ca ratio was smaller.

Uranium measurements also indicated a much higher uptake in the rib sample compared to the femur samples, and consequently a higher uranium/calcium ratio.

(b) Watchfield: with regard to pooled rib and femur samples from this site, the strontium level in rib samples was lower but its Sr/Ca ratio higher than femur samples. Similarly, uranium levels and U/Ca ratios were higher in rib samples, indicating an increased uptake of both uranium and strontium into cancellous bone.

Comparing rib and femur analyses for respective skeletons, strontium levels were

higher in ribs for both skeletons by 4.2% (SK#108) and 15% (SK#304). Uranium values were very variable, and variation in all elements was again observed across samples within this site.

(c) Hartlepool: as for the other sites, the strontium and uranium concentrations in rib were higher and the calcium and phosphorus levels lower than in femur samples.

To summarise within-site trends observed in this study:

- strontium- and uranium- calcium ratios were invariably higher in rib samples than in femur bone, while calcium and phosphorus levels were generally lower: this confirms observations made by other workers (e.g. Lambert *et al.*, 1982) and reflects the different nature of the tissue in each, highlighting the importance of the choice of bone for chemical analysis.
- a high within-site variability of elemental concentrations was observed for all samples, particularly for measured uranium levels in Watchfield material.

2. Between-site variation.

Sr/Ca and U/Ca ratios for each sample, categorised for each respective site are shown plotted in Figures 9.44 and 9.45.

When comparing the Sr/Ca ratios for bone excavated from British mainland sites (figure 9.44) a clear correlation was observed between increasing ratio value and increasing acidity of the burial environment; Watchfield sited bone possessing the highest Sr/Ca ratios and Hartlepool the lowest.

The "Mary Rose" sample possessed high levels of strontium (1899 ppm), a Sr/Ca ratio of 378 x 10^{-5} . This undoubtedly reflected the comparatively high levels of strontium typically found in sea-water compared to freshwater.

Olduvai material also contained high levels of strontium, particularly Olduvai 2.1 (3983 ppm Sr, a Sr/Ca ratio of 762.95 x 10^{-5}). Olduvai 13.3 contained less strontium but still high values: contrary to expectations and previous similar studies, less strontium and a lower Sr/Ca ratio was found in bone 'B' than in bone 'T'. Although originally darker in colour due to direct contact with the soil

Figure 9.44: Sr/Ca ratios measured in exhumed bone samples plotted against pH of the respective burial environments.

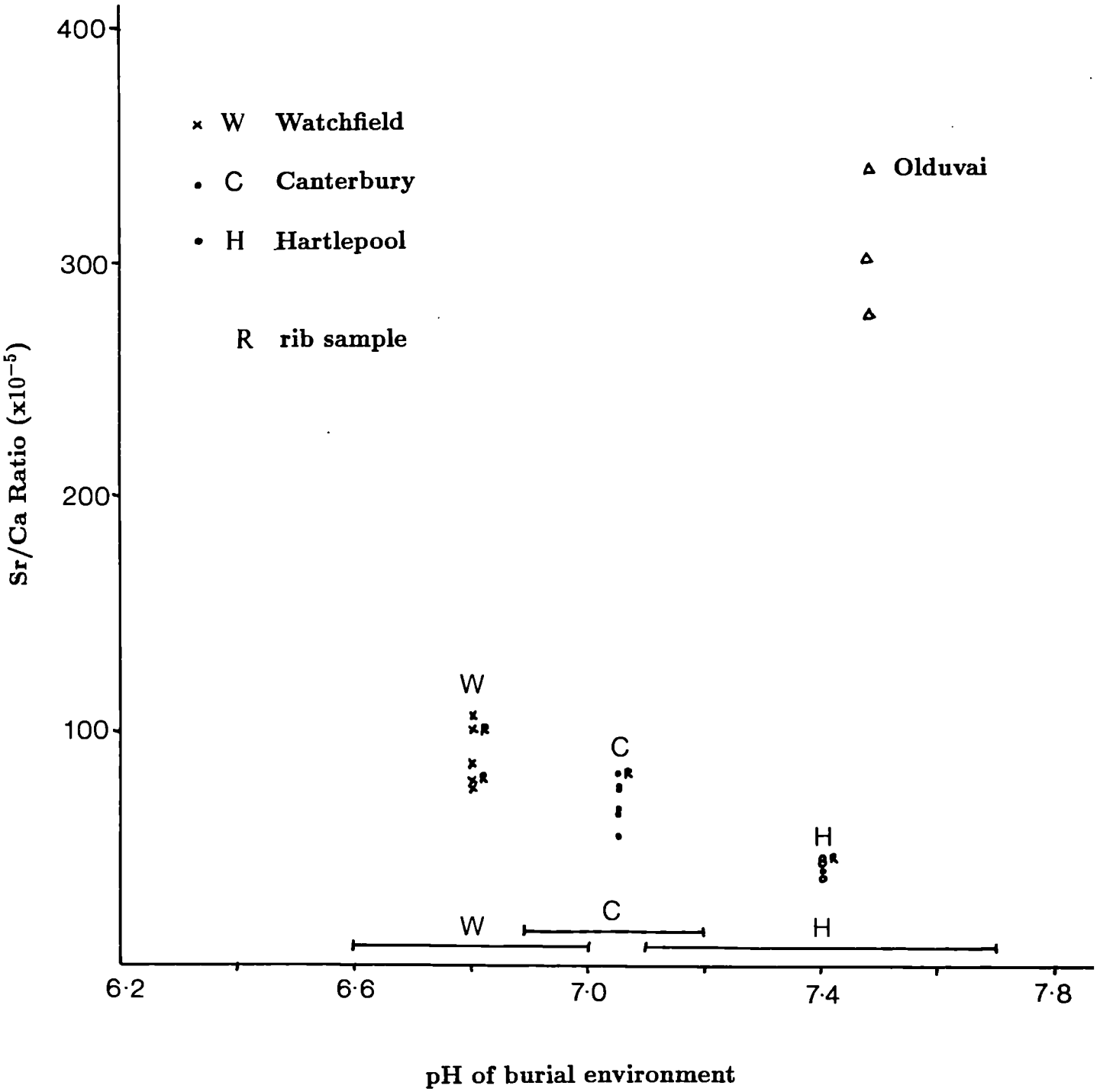

Figure 9.45: U/Ca ratios measured in exhumed bone samples plotted against pH of the respective burial environments.

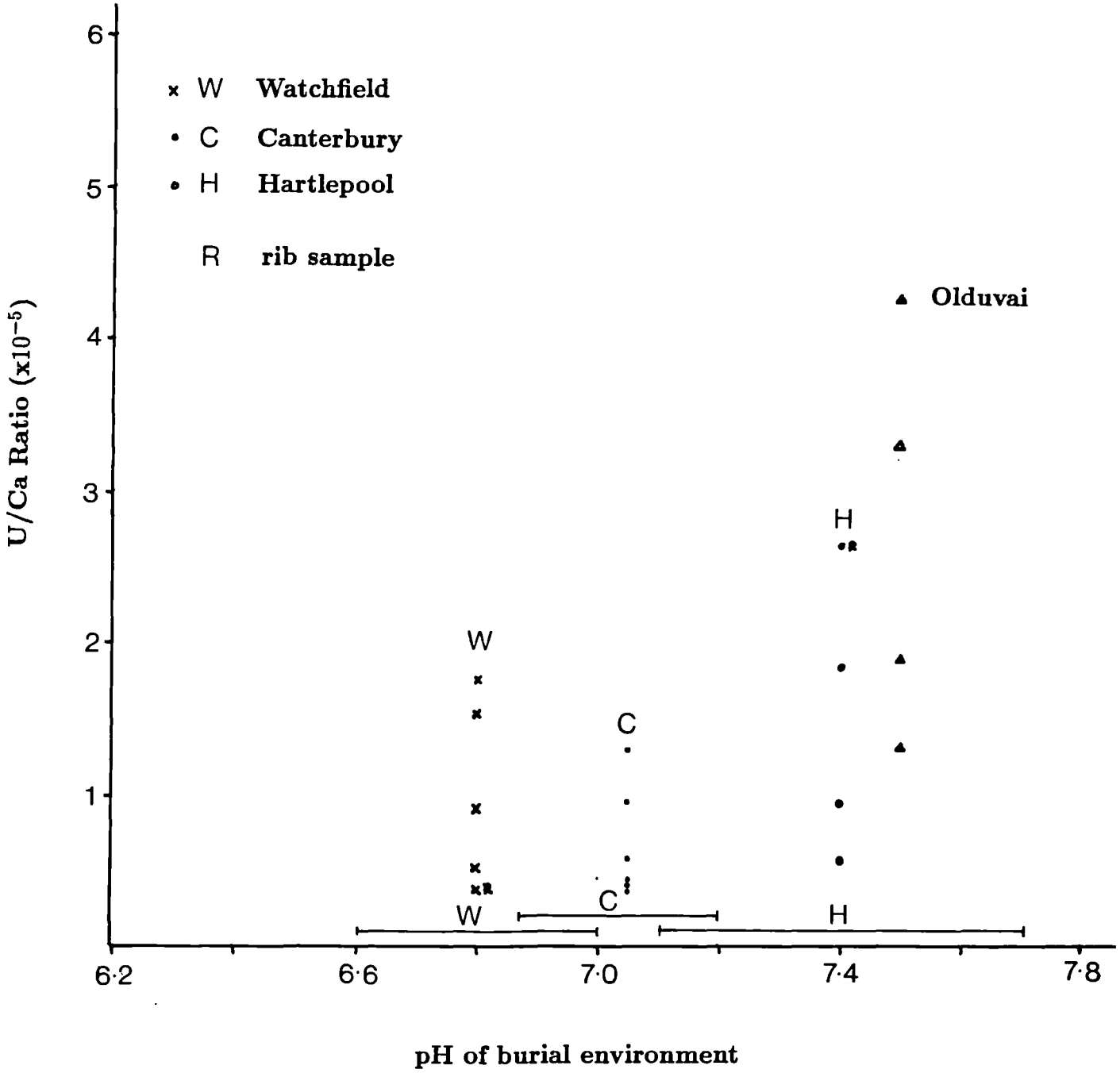

compared to the bleached surface bone 'T', strontium results here might suggest that the bone was not in this position for the whole post-depositional duration.

However, figure 9.45 shows that uranium levels in Olduvai 'T' were lower than in 'B', confirming work by Williams and Marlow (1987), and presumably reflecting exposure to uranium-containing groundwaters. Uranium uptake into bone can be rapid and it may be that this higher uranium in 'B' bone represented uranium taken up rapidly, soon after deposition.

The uranium concentration of "Mary Rose" bone was higher than Olduvai material (28.27 ppm U, or U/Ca ratio 5.63 x 10^{-5}), reflecting the reducing environment of detrital sediments at the sea-bed.

Uranium/calcium ratios plotted for the three British mainland sites showed no clearly defined trend with pH. Canterbury bone samples generally possessed the lowest values with least range, while samples from Watchfield and Hartlepool fell within a much broader range. The highest uranium/calcium ratio was measured in a rib bone from Hartlepool (2.66 x 10^{-5}).

9.4.6.3 Summary.

Quantitative data from XRF and PIXE analyses were not in agreement largely because RBS was not carried out simultaneously with the latter to enable matrix correction procedures. In any case, a comparison of data obtained solely by XRF analysis found a high within-sample variability. This made significant between-site comparisons difficult; nevertheless, trends in average values within and between sites showed that in the large majority of cases elemental contamination was higher in rib samples than in femora, while calcium and phosphorus levels were lower. This represents the relatively porous nature of the cancellous/trabecular rib bone which is more accessible to percolating groundwaters than the predominantly dense cortical tissue of femoral bone.

Strontium/calcium ratios in British archaeological bone showed a clear correlation with the pH of the burial environment: higher ratios were associated with more acid soils. However, no clear patterns emerged for uranium/calcium ratios.

The relationship between bone chemistry and the physical and chemical description

of respective burial environments was explored in more detail in the next section by studying elemental distribution profiles in soil associated with burials.

9.4.7 Analysis of Soils.

A range of soils from the three British terrestrial sites, collected in the systematic manner described in Section 9.2, were analysed for their major, minor and trace element content by XRF analysis. The full dataset can be found in Appendices Vf and Vg. Any trends in elemental distribution around bone *in situ* were described; plots for calcium, strontium, iron and manganese distributions were drawn up.

Many elements appeared to show no trends in distribution against distance from bone: these included aluminium, silicon, magnesium, potassium, barium and, perhaps surprisingly, phosphorus (Appendix Vf). These elements possessed either a relatively stable distribution or demonstrated an inconsistent pattern (increasing and/or decreasing in concentration away from the bone). Sodium, potassium, silicon and barium levels *generally* demonstrated decreasing values with distance from bone. One might, perhaps, have expected a correlation between Si and Al distribution with the common occurrence of aluminosilicates in soils.

A number of elements showed an increase in concentration with increasing distance from the bone-soil interface, suggesting an uptake of such elements from the burial matrix into bone: these elements included iron and manganese (see figures 9.46 and 9.47), common diagenetically introduced elements typically found lining cortical surfaces and filling pores/voids. The vertical scale on figure 9.46 was not constant but was adjusted to accommodate the wide range of iron values measured across soil samples. Values for iron were much higher in Watchfield samples because of its iron pan character. The soil profiles plotted for iron and manganese showed highest concentrations in Watchfield samples and lowest in Hartlepool (whose elemental gradients were less evident), and demonstrated that

(1) the rate and pattern of elemental distribution in the vicinity of buried bone could be different both *between* and *within* sites: manganese profiles for Watchfield soils, for example, possessed quite different rates and patterns of change across dis-

tance despite observing the same fundamental trend of an increase with increasing distance, and

(2) the variability of elemental concentrations at the bone-soil interface between and within sites: again, manganese levels for Watchfield are a good example because they were very high in comparison to the other two sites but were also variable at the bone-soil interface (distance = 0 on the x-axis).

This variability at the soil-bone interface was also evident in calcium measurements at Hartlepool and Canterbury (figure 9.48). For example, soil measurements of calcium around skeleton 23 (SK#23) were higher than the corresponding measurements in the other two graves. Skeleton 23 was not located in one of the few limestone burials found at this site and there were no outstanding features in/around this grave to explain these clear differences in soil chemistry; such differences were probably factors of variation in local geology within the site location. Such geochemical variation over relatively small distances limit the potential of these soil studies in and around graves because any elemental patterns/gradients observed could be explained by this natural variation (particularly at boundaries of change) rather than caused by any bone-soil interaction. Nevertheless, consistent patterns of elemental distribution in graves disparately located across a site can confidently be assigned to chemical interaction between bone and its immediate burial matrix.

For example, measurements for zinc in soils from Hartlepool consistently followed a pattern of decline moving toward the bone (Appendix Vf), which may be indicative of the uptake of this element into the bone matrix.

Calcium measurements of soil at Canterbury consistently indicated a decrease in concentration moving nearer to the bone, suggesting possible uptake of calcium into the bone matrix under these burial conditions. The gradient of change was more dramatic near humerus bone than radius and, lastly, femur bone. This might be explained by the fact that the dense, compact cortex of the larger more sturdy femur bone was less prone to diagenetic influences than the more fragile, less compact humerus and radius bone; however, if this were the case, one might equally have expected, for similar reasons, smaller changes in the vicinity of humerus bone compared to that of the radius.

Only soil located near *femora* was analysed for Watchfield. Calcium measurements revealed a general decrease in concentration moving *away* from the bone, suggesting the possibility of a loss of calcium from bone matrices under these relatively acidic conditions.

No clear trends in calcium distribution were apparent in material collected from the Hartlepool site. Patterns were irregular. Calcium levels were much higher here than for Watchfield and Canterbury sites, reflecting the fact that the soil at Hartlepool was derived from a magnesian limestone bedrock. In one sample, a relatively low calcium concentration was found at the bone-soil interface. This corresponded to a relatively high level of strontium in this soil sample. Plots of strontium distribution are found in Figure 9.49. A decline in strontium concentration was observed for this sample suggesting a loss of strontium from bone and its subsequent deposition in surrounding soil. Moreover, the corresponding high strontium and low calcium at the interface in this sample run might suggest a preferential uptake of calcium replacing indigenous strontium in the bone under these alkaline conditions. However, the patterns of distribution for the other two examples at this site were unclear.

A decrease in strontium concentration with increasing distance from the bone was observed in all three examples from Watchfield, suggesting a loss of this element from bone under these burial conditions, and its subsequent deposition in the surrounding soil. This is contrary to XRF analysis of the bone material (subsection 9.4.6.2) from Watchfield which indicated relatively higher strontium uptake at this site compared to Canterbury and, lastly, Hartlepool. Strontium levels were found to increase with increasing distance from the bone in Canterbury examples, suggesting its uptake into the bone from the surrounding burial matrix.

Uranium was only detected in soils from Hartlepool. XRF was not sufficiently sensitive to detect the low concentrations present in Watchfield and Canterbury soils, and while values ranging between 1 and 3 ppm were measured for Hartlepool samples, these are below the acceptable minimum limit of detection. For this reason, uranium distribution at these sites was not plotted.

Figure 9.46: Distribution profiles of iron in soil located around bone material buried in three archaeological sites.

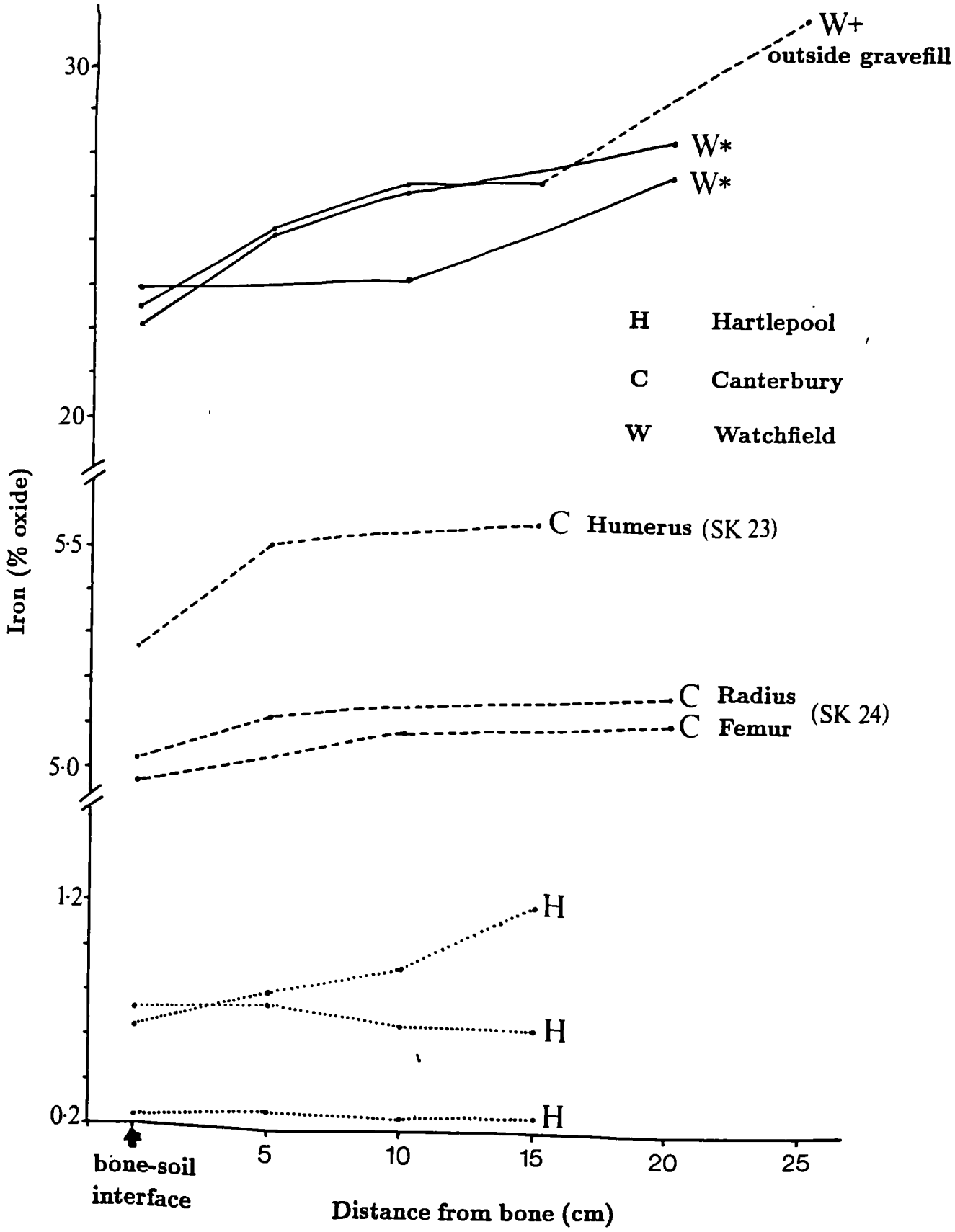

Figure 9.47: Distribution profiles of manganese in soil located around bone material buried in three archaeological sites.

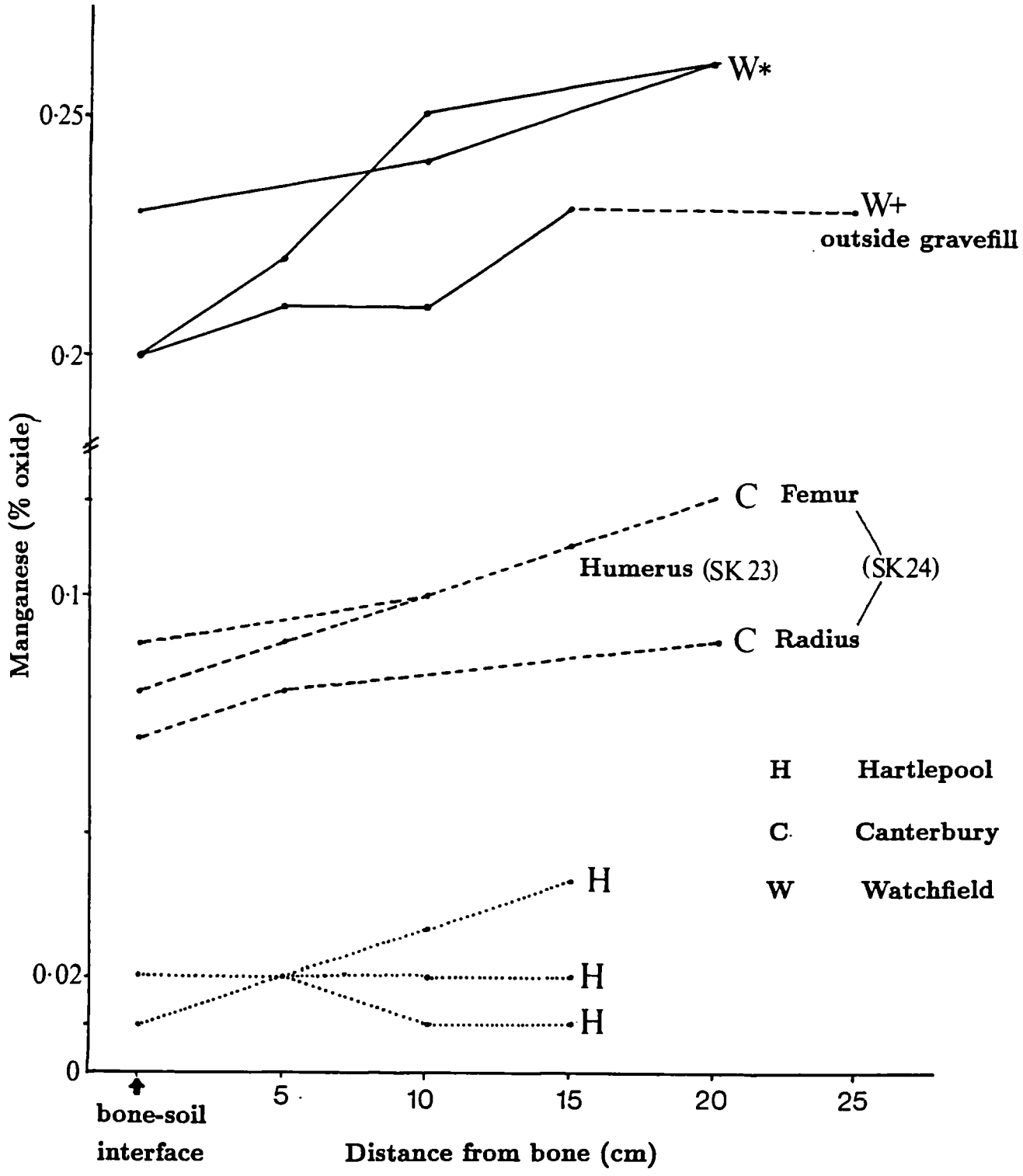

Figure 9.48: Distribution profiles of calcium in soil located around bone material buried in three archaeological sites.

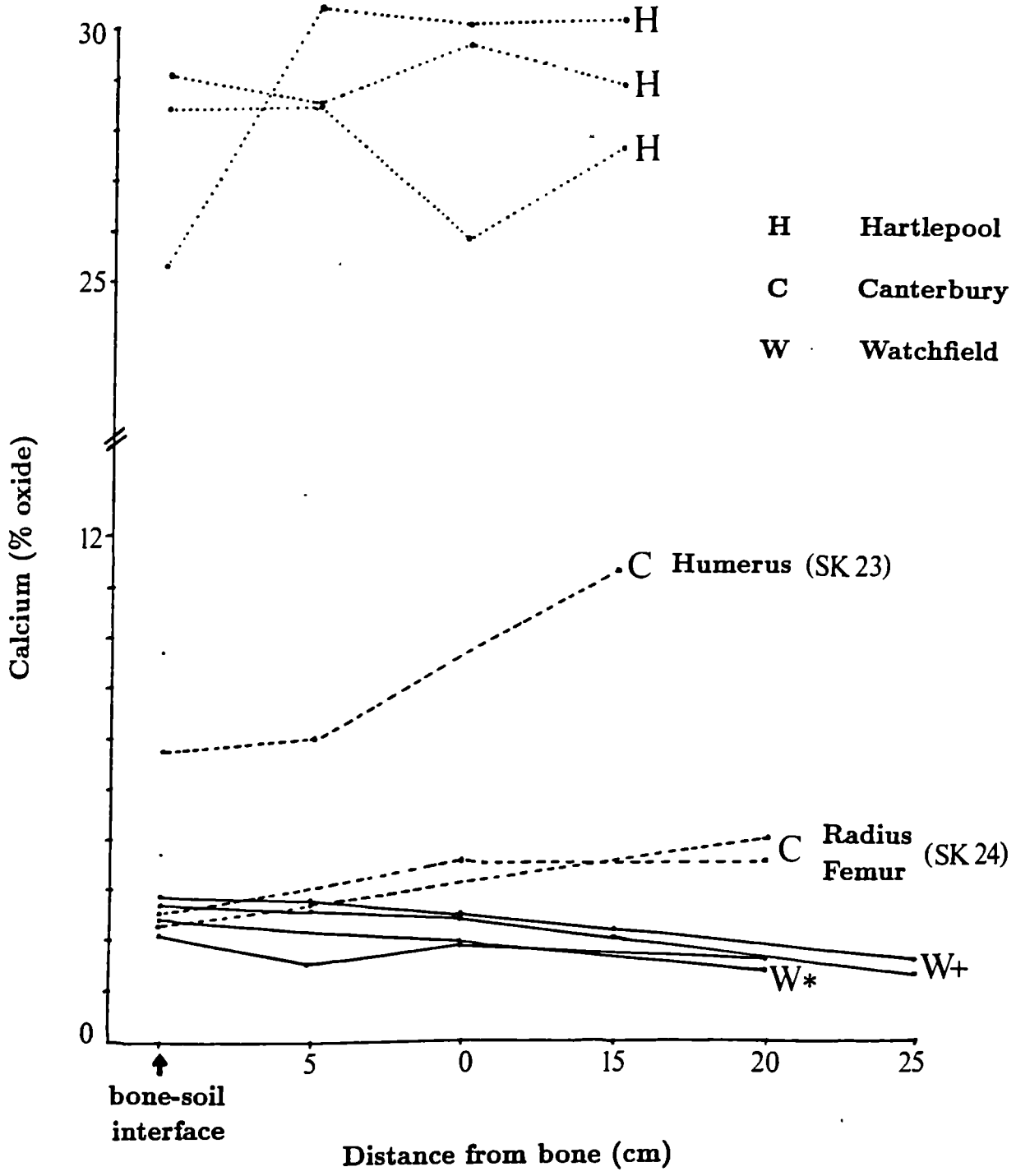

Figure 9.49: Distribution profiles of strontium in soil located around bone material buried in three archaeological sites.

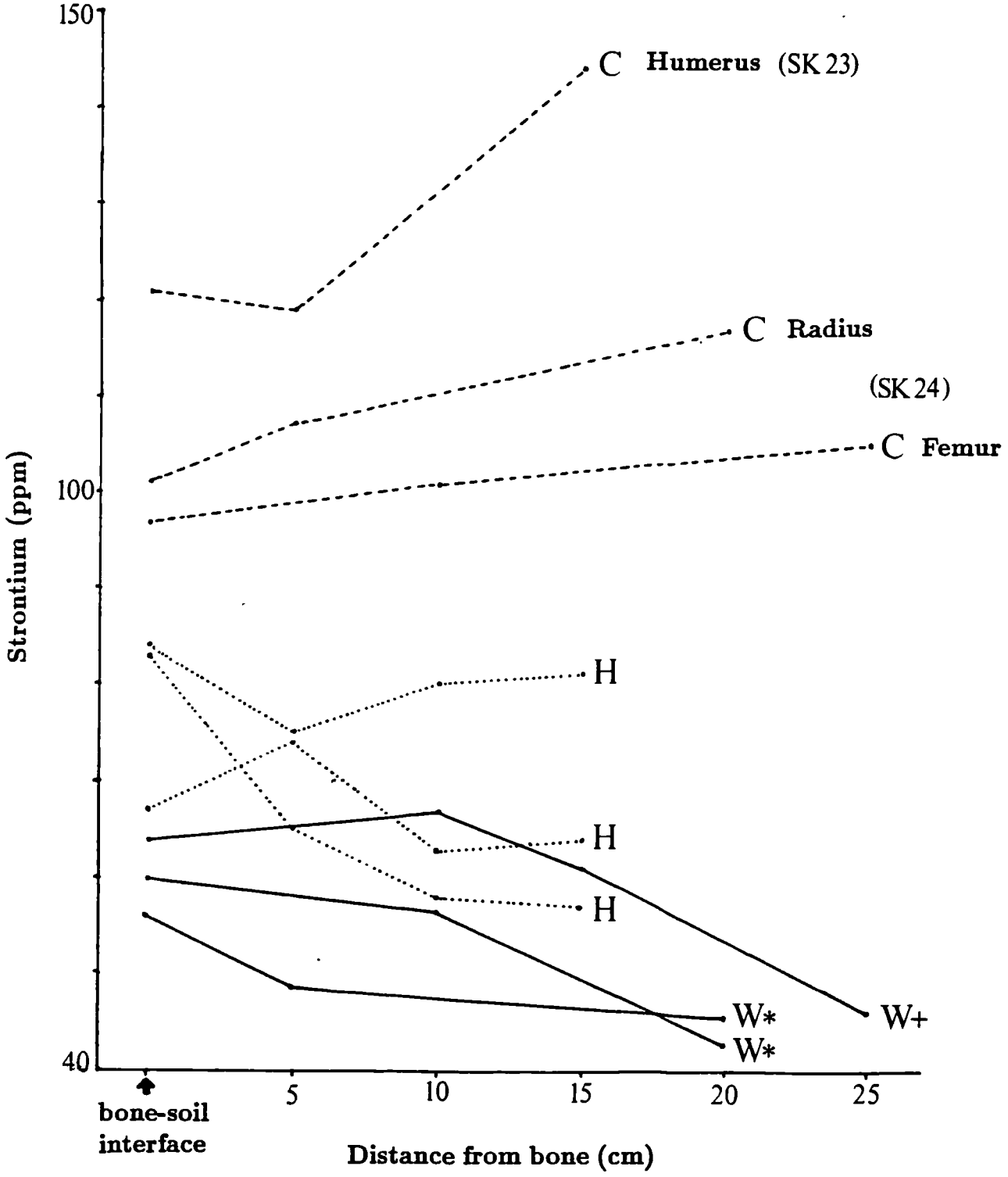

9.5 Summary.

XRF analysis of soils located in the immediate vicinity of bone lying *in situ* has revealed distribution profiles for a number of elements (Fe, Mn, Zn, Sr, Ca) that are indicative of potential soil-bone chemical interaction, and largely support observations based on complementary bone analyses However, elements such as Al, Ba, Mg, Cu and Pb showed no apparent trends/consistent patterns of distribution, despite, in some cases, clear indications of diagenetic activity in corresponding bone material.

Certainly, microPIXE analysis has proved an effective means of detecting the diagenetic alteration of a broad range of elements. Both qualitative and quantitative analyses of bone and corresponding physicochemical measurements of associated soils have demonstrated a number of patterns in elemental uptake and the burial environment. These are discussed in Chapter 10, where fieldwork and uptake studies are compared.

Part IV

Discussion

Chapter X

Discussion and Conclusions.

10.1 Summary of Research Aims.

To re-iterate the aims of the present study, defined at the outset: experiments were conducted to simulate, using simple models, the uptake and deposition of strontium and uranium in bone under specific conditions. Strontium and uranium were studied because of their routine applications in archaeological studies attempting (1) palaeodietary reconstruction, and (2) chronological determination and the identification of diagenesis, respectively. It was anticipated that such an approach would elucidate mechanisms of interaction and investigate environmental conditions promoting them.

The relationship between diagenetic activity and environment was explored in more detail with field studies. These provided "real" archaeological examples of bone from a variety of burial environments (representing both terrestrial and marine contexts), some of which were chemically and physically characterised. Field studies served both to compare and supplement experimental data describing the diagenetic activity of strontium and uranium. Furthermore, general examples of the diagenesis of a wider suite of elements were illustrated using predominantly proton microprobe analysis, a novel technique for such application.

This chapter comprises a critical assessment of the research methodology in terms of experimental approach/strategy and the analytical techniques employed, and evaluates the respective data collected from each. Having considered the merits and limitations of these approaches, observations are subsequently interpreted.

Data from these contrasting studies are collated for discussion of specifically (1) strontium, and (2) uranium uptake into bone, and (3) elemental uptake and deposition in general, derived largely from field studies on diagenesis. The implications of

these findings are considered, together with recommendations on potential future studies arising from this work.

10.2 Critique of Methodology: Design and Analysis.

(i) Analysis: reproducability and reliability.

In the present study, only a few of the many influential variables were isolated so that the influence of pH, for example, could be clearly identified. Thus, it was possible to monitor trends in strontium and uranium uptake with environmental pH, and make deductions about mechanisms of bone-element interaction (uptake and deposition). These interpretations are largely the result of collating data from a wide range of analytical sources. However, such interpretation was not facilitated by the incongruence of the observations based on respective methods of analysis. In many cases, qualitative data derived from microprobe analyses of bone did not agree with quantitative data from XRF and AAS analyses of bone and solution, respectively. Consequently, while temporal patterns of uptake were largely consistent, trends against pH more often than not depended on the analytical method used.

The reasons for such discrepancies are unclear. Certainly differences in elemental yield across quantitative probe analyses can largely be attributed to the inhomogeneity (or heterogeneity) of the porous bone matrix. Indeed, matrix variations were probably responsible for the poor reproducibility of data observed where more than one probe analysis was carried out for each cortical region (Tables 6.6a/b, p175-6). Generally, absolute % oxide/ppm values were less reliable than elemental ratios, and values given to 2 decimal places with standard errors to 1 decimal place, for example in table 6.6a (p175), were not wholly realistic: rather, whole values would have been more appropriate. Indeed, this was the case for quantitative data collected from other sources. XRF % oxide data, for example, were quoted to 2 decimal places (e.g. Table 6.10, p192) and ppm values to 1ppm, rather than being rounded to the nearest multiple of, say, 10ppm, as might be warranted by variability imposed by matrix effects. Similarly, AAS/AES data were quoted to 2 decimal places, but here readings were averaged over 5 measurements to enhance the reliability of data. The spectrophotometric instrumentation was calibrated

using standard "Spectrosol" solutions for all elements measured and these solutions were measured every 8 samples to check for any instrumental drift from the original calibration. Thus, standard solutions representing an appropriate range of elemental concentrations served as both calibration and reference material: since bone dissolution procedures were not carried out, bone reference material was not used for wet chemical analysis. Similarly, bone reference material was not available for the majority of qualitative and quantitative dry bone analyses. Rather, a range of geological reference materials, including apatite, were used to calibrate XRF and microprobe instrumentation, and, in the case of the former, these were cross-referenced throughout sample runs.

The reproducibility of qualitative EPMA line profile data was tested across samples. Four cross-cortical scans were carried out per sample to assess the reproducibility of the profile. Only one profile was recorded, however, due to limited instrument time. Nevertheless, this protocol was able to ascertain that each profile plotted was indeed an accurate representation of the sample as a whole, both in the pattern of elemental distribution and in signal strength (the latter showed some variation).

The analytical discrepancies observed in this study highlight the importance of consistency in experimental approach by ideally employing similar instrumentation for any batch of samples that are to be cross-compared. Moreover, it emphasises the limitations of correlating data obtained in different studies by different workers using either similar instrumentation or, in particular, different analytical techniques. Indeed, IAEA data† for reference materials illustrate the enormous variability in data collected from numerate studies by indicating the wide range of "acceptable values" for each element measured. Such values are collated from a variety of analytical techniques, but also demonstrate a considerable variability within a particular technique. Therefore, it is necessary to exercise caution when utilising the *average* value of these ranges which provide the quoted values for reference materials.

Of course this problem applies for quantitative analysis in any discipline. Bone archaeology is particularly poorly served with regard to available reference mate-

† produced by the Analytical Quality Control Services, International Atomic Energy Agency, P.O. Box 100, A-1400 Vienna, Austria.

rial for bone, or indeed similar phosphate matrices, especially material containing an extensive suite of elements pertinent to archaeological bone. In the present study, I have attempted to overcome this hurdle by employing a number of standard materials during quantitative analysis of powdered bone. These include my own "standard" (ovine bone), synthetic hydroxyapatite, rock phosphate (containing relatively more extraneous mineral phases), and a range of soil standards to provide the required minor and trace elements. In adopting this strategy, however, materials (the soils) with contrasting matrices to biological/geological apatite are introduced, and matrix effects may indeed account for some of the discrepancies between XRF and microprobe data.

Generally, the interpretation of data, discussed later in this chapter, focuses on qualitative microprobe analyses in the form of line-profiles and maps; these offer a greater range of information regarding cross-cortical and microdistribution detail, simultaneously for a number of elements. These qualitative methods have been effective in detecting a number of trends in both the uptake and deposition of strontium and uranium, which are discussed in detail in sections 10.3.1/2.

(ii) Design.

10.2.1 Immersion Studies.

The majority of uptake simulation experiments consisted of immersing bone samples, with variable composition, in solutions maintained at different pH for variable duration. Both bone and immersing solution were analysed after exposure using a variety of analytical instrumentation yielding qualitative and quantitative information about various aspects of the uptake process.

As a consequence of maintaining the simulation system as simple as possible in order to limit the number of variables operating on elemental uptake at any one time and thus make subsequent interpretation more comprehensible, a number of problems associated with experimental design can be highlighted. Indeed, the system arguably lacks sophistication in design. The immersion procedure more closely simulates waterlogged environments in which bone is submerged for long periods of time, in contrast to the majority of burial environments that yield bone

where the inhumed material is more typically subject to alternate wet and dry periods reflecting seasonal variation.

Furthermore, the system, other than varying pH, takes no account of physicochemical or biological factors that may be found in a real burial environment and which can influence diagenesis (Williams, 1988). [refer to Ch.3]

The use of pure water as the bulk solution of the immersing medium, rather than natural groundwaters, meant that models using different anionic complexing of strontium and uranium could not be explored fully. Dissolved carbon dioxide, for instance, in the form of a variety of carbonate complexes is an important and ubiquitous constituent in groundwaters. Taking uranium as an example, since it is most documented: uranium exists largely as a fluoride complex below pH 4, a phosphate complex around neutral pH and a carbonate complex in alkaline conditions (Hostetler and Garrels, 1962). The presence of phosphate and carbonate ions at intermediate Eh and neutral to alkaline pH results in the formation of uranyl phosphate or carbonate complexes which increase the solubility by several orders of magnitude (Hostetler and Garrels, 1962); fluoride ions have little effect on solubility in oxidising conditions (those of the experimental set-up). These solubility effects may have important connotations for the trends in uranium uptake observed in the present study. Results indicate that uranium uptake is enhanced in more alkaline conditions of immersion, predominantly by surface adsorption mechanisms [see section 10.3.2]. However, in the presence of phosphate and particularly carbonate ions, a reduction in surface adsorption mechanisms at the bone-solution interface is likely to occur as uranium is less readily removed from solution. If uranium uptake into bone was still found to increase at higher pH in the presence of these anionic forms, this would corroborate work described here and further reinforce the importance of alkaline environments in uranium uptake mechanisms. In the meantime, this omission provides a limitation in the present study.

Similarly, the absence of cationic forms commonly found in groundwaters (e.g. calcium, magnesium) may influence the uptake patterns observed here as other cations compete with strontium and uranium for sites of interaction on the bone matrix. Calcium ions in groundwaters are probably the most important of these cations; indeed, White and Hannus (1983) state that calcium ions in soil solutions

are one of the controlling factors in bone weathering. In a burial environment, calcium and phosphate ions in soil solution are in equilibrium with corresponding ions on the hydroxyapatite surface (White and Hannus, 1983). To establish such an equilibrium in simulated studies, it can be argued that the immersion arrangement automatically favoured the leaching of inorganic ions from the bone surface. Similarly, the ionic strength of immersing solutions was not taken into account. Variability in buffer composition and in the strontium and uranium salts effected differences in ionic concentration across solutions. Millard (pers.comm.) uses potassium chloride to make up the ionic strength of solutions to a standard constant value. However, the addition of such internal standards may itself complicate the system: this is demonstrated in Series II experiments where the chloride ion was found to react with bone, hence the use of the relatively inert nitrate anion in subsequent studies.

With regard to the bone material itself, laboratory experiments focused on a particular calcified tissue - ovine metacarpal cortical bone - although it was acknowledged that tissue type is an intrinsic factor influencing the extent of diagenesis. Furthermore, subsequent analysis tended to concentrate on the elemental character of the *inorganic* component, with the role of the organic component largely being investigated indirectly, by exploring its differential removal and the effect on the inorganic matrix.

Therefore, the adoption of a rather elementary simulation design does impose a number of limitations on the system, which must be appreciated on subsequent interpretation of the data. Nevertheless, the present study has served to isolate a few of the multifarious factors in the burial environment that influence bone diagenesis, and in doing so has successfully identified trends in the uptake and deposition of both strontium and uranium. [sections 10.3.1/2]

10.2.2 Chemical Separation Study.

Chemical separation data did not agree entirely with EPMA data. Discrepancies arose with the uptake patterns against pH, though generally the fractions to which strontium and uranium were associated concurred with EPMA data.

The interpretation of analytical results obtained in this study were limited by the separation procedures themselves. During demineralisation, nitric acid probably dissolved some of the bone's collagen and other proteins, and thus may also have removed loosely bound ions associated with the organic matrix, as well as exposing protein to the dissolved minerals. Similarly, during deproteinisation, hydrazine may have dissolved some of the mineral; an alternative explanation may be that hydrazine is able to sequester or chelate loosely bound ions associated with the inorganic matrix in much the same way as Spadaro *et al.*(1970) found for ethylenediamine (the predecessor of hydrazine) during the chemical separation of bone. This may explain why strontium was found in one of the organic extractions while predominantly associated with inorganic fractions.

Nevertheless, the separation procedure here could be expected to localise the more tenaciously bound (incorporated?) ions and identify the more weakly bound ions, and is therefore considered a pertinent study.

10.2.3 Crystallinity Studies.

XRD studies have been successful in demonstrating a number of different trends in the crystallinity of bone, according to the respective inorganic:organic ratio and the conditions of immersion treatment when applicable. The accuracy in the measurement and interpretation of data depended on assessing the true position of backgrounds and peak maxima as a function of poorly crystalline specimens, in some cases; macroscopic variation due to the multiphase (impure) nature of the material; and the limitations imposed by instrumental resolution. In Chapter 1, I anticipated that this study would discriminate between adsorption and incorporation mechanisms. However, the sensitivity and detection limits (typically 1-5 %) of XRD are not adequate to achieve this discrimination, and other workers have similarly found that minerals such as calcite occurring as minor inclusions in bone are not detectable by XRD, despite being clearly present on the basis of elemental ratios (e.g. Sillen, 1989).

The crystallinity of the inorganic phase of whole bone is predictably poor, due to the non-stoichiometric nature of biologic hydroxyapatite together with small crystal size. Furthermore, the diffuse nature of bone diffraction profiles is largely

a property of the hydroxyapatite crystals being located in an amorphous organic matrix. This was illustrated by observing crystallinity enhancement in samples possessing a lower organic content, although it was appreciated that the crystallinity of ashed samples reflected the effects of heating on crystal size (Shipman *et al.*, 1984) rather than the absence of organic material. The effects of hydrazine on the diffraction pattern are negligible (Termine *et al.*, 1973; Walters *et al.*, 1990). This trend with organic content underlines the caution that must be taken when interpreting the diffraction profiles of archaeological bone in distinguishing between real crystallographic changes in the inorganic matrix and the reduction in background noise as the amorphous collagen matrix is removed over time. Of course these two processes are undoubtedly interrelated. It has been suggested that crystallographic changes in buried bone may be accelerated during and after organic decomposition as hydroxyapatite crystallites become increasingly exposed to percolating groundwater action, and that, in the early post-depositional period, mineral may to some extent be shielded from diagenesis by the organic matrix (Sillen, 1989; Pate and Hutton, 1988). Data presented here supports this model:

The immersion process itself effected an increase in crystallinity by demonstrating improvements in crystallinity for all bone immersed in buffered solutions. This supports early studies by Termine and Posner (1967) who reported that *in vitro* exposure to water decreased the size of the amorphous bone mineral fraction and simultaneously increased that of the crystalline apatite fraction. The immersion of bone in solution here has therefore promoted crystallinity changes by causing the leaching of amorphous mineral and smaller crystallites, together with early indications of recrystallisation processes promoted by the elevated temperatures of immersion. Hence, the present study has successfully demonstrated an acknowledged diagenetic process in buried bone by artificial/simulated method.

Furthermore, bone immersed in an acidic environment demonstrates greater improvements in crystallinity as a result of the acid leaching of both organic (where appropriate) and inorganic matrices by amide hydrolysis and dissolution respectively. The former will reduce the "shielding effect" of the organic matrix and further expose the apatite lattice, whose smaller crystallites located at the crystal surface will be washed out, thereby increasing the average crystal size (crystallinity).

Whole bone shows least change in crystallinity at neutral pH, when the organic component is most stable and the intimate association of the organic and inorganic matrices is preserved relative to acid and alkaline conditions. This fact is supported by CHN analysis, which demonstrated relatively little organic loss over time at pH 7 compared to pH 4 and pH 10. In contrast, both ashed and hydrazine-treated bone show least alteration at pH 10, where the predominantly/exclusive inorganic matrix is most stable (Lindsay, 1979).

Therefore, in its examination of pH effects, the present study demonstrates the importance of the burial environment in influencing the degree of crystallinity change in buried bone. This challenges the work of Bartsiokas and Middleton (1992) who propose the potential application of crystallinity measurements on bone as a method for relative dating. They found this suggestion on observations indicating that crystallinity is time-dependent, a phenomenon which is further discussed in the fieldwork section. Such a potential chronometric method, however, must simultaneously account for differences in the physicochemical description of the burial environment. Indeed, cation exchange experiments described here illustrate the inverse relationship between crystallinity and reactivity i.e. the ability to incorporate cations into the matrix, which, depending on the chemical description of the burial matrix, will in turn influence the crystallinity of bone.

On the basis of cation exchange data, one might expect the uptake of cations by incorporation/adsorption to the inorganic matrix to be promoted in alkaline conditions, where the non-stoichiometry of biologic apatite (low crystallinity) is most stable. Cation-bone interactions were explored in the present study, focusing on the uptake of strontium and uranium into bone. These investigations are discussed in detail in sections 10.3.1/2.

With regard to crystallinity changes induced by exposure to strontium or uranium, little change was apparent over and above pH/immersion effects. In an attempt to separate the respective effects of immersion pH, organic content and strontium/uranium exposure, statistical analyses were conducted to identify respective variabilities. Statistical analysis of crystallinity measurements found no significant variability for any of these factors, despite clear visible effects on profiles, and

this can be attributed to the small dataset analysed and inappropriate pooling of samples attempting to compensate for small sample size.

10.2.4 Field Studies.

The objectives for conducting field work in parallel with laboratory-based simulation studies were to explore the diagenetic alteration of trace elements in general by examining both bone and associated soils (where possible). Furthermore, the application of the proton microprobe in the study of archaeological bone was investigated. Patterns of uptake in different burial environments were recorded and their findings compared with observations derived from uptake experiments.

To this effect, and with the employment of a variety of analytical instrumentation, field studies have been successful in illustrating a diversity of diagenetic activity in bone material excavated from a broad range of burial environments.

Microscopic examination of archaeological bone structure proved to be a useful means of physical characterisation to assess the extent of diagenetic alteration (reviewed by Garland, 1988). Examination under polarising light was able to reveal any structural disruption by post-depositional activity (microbial for example); in particular, the relative decomposition of the organic matrix indicated a greater exposure of the inorganic matrix, so that the loss of orientation in the optical pattern could be correlated with the degree of chemical alteration of the inorganic matrix. This was most clearly illustrated by material from Watchfield whose microstructure was considerably disrupted (lack of osteonal structures and birefringence) and whose crystallinity was correspondingly most altered.

Relative crystallinity provides a measure of the degree of chemical/structural change, caused by recrystallisation, reprecipitation, leaching etc. XRD analysis contributed a number of important observations. Crystallinity measurements of archaeological material corresponded with simulation experiments in finding a trend of increasing crystallinity with the acidity of the burial environment. Furthermore, crystallinity changes, although small, were observed early on in the inhumation period. Further discussion can be found in section 10.3.3.

EPMA was carried out on a limited number of samples and was able to demonstrate contamination by a variety of trace elements in bone from Hartlepool, Pompeii and the "Mary Rose". However, while the spatial resolution of EPMA is good (2-3 microns), instrumental sensitivity is poor for most of the palaeodietary indicator elements, being of the same order of magnitude as expected biogenic levels. Therefore, in this and in a number of past studies, EPMA was unable to discriminate, for example, diagenetically introduced strontium and zinc from biogenic concentrations. In contrast, microPIXE analysis was able to effectively plot the cross-cortical and micro-distributions of palaeodietary significant elements due to the sensitivity and detection limits (at least an order of magnitude higher than EPMA) combined with the sub-micron spatial resolution of the proton microprobe. The SPM, combining PIXE and RBS analyses, has indeed proved its worth in the study of archaeological bone (Elliott and Grime, 1993).

In the present study, microPIXE analysis has illustrated that bone is subject to contamination from disparate trace elements. While many of the observations made here support those of EPMA in previous literature, PIXE has also demonstrated the diagenetic alteration of elements whose diagenetic behaviour is less understood and less widely acknowledged: of particular importance to the anthropologist are the strontium and zinc findings because of the implications for palaeodietary analysis. Unfortunately, barium was not measured in the present study because it was not significantly detected in preliminary (exploratory) probe analyses. The l-lines for barium are adjacent to the main calcium peaks, and thus masked in a calcium phosphate matrix, particularly when, as in this case, a filter is used to reduce the calcium signal; high energy k-lines for barium do come off fairly weakly but the detection limit for these is quite poor, ranging from 100 to 1000 ppm (Grime, pers.comm.). Thus, the apparent lack of barium in these samples may be a function of the relative insensitivity of PIXE to barium, or it may indicate a lack of barium contamination in exhumed bone, thereby repropounding its use as a reliable palaeodietary indicator.

Quantitative analyses using PIXE underline the importance of simultaneous RBS analysis, as described by Grime *et al.*(1991b). Data from PIXE analysis alone were not reliable and produced spurious results when compared with XRF data

for similar samples. In contrast, XRF analysis of bone and soils was able to demonstrate the diagenetic activity of a diversity of elements and provided an effective supplement to microPIXE data. In addition to demonstrating the differential diagenetic susceptibility of femora and ribs, trends in uptake of respective elements against environmental pH were demonstrated and those of strontium and to some extent uranium confirmed patterns revealed by simulation experiments: these are discussed in detail in subsequent sections.

Simultaneous analysis of corresponding soils has established that elemental uptake into bone is not necessarily and exclusively a property of their respective concentrations in the surrounding soil. For example, in the British terrestrial examples, strontium values were highest in Watchfield material despite the fact that Watchfield soils possessed lower strontium values than those of Hartlepool and Canterbury. This would suggest that an active process of selection/preferential uptake for strontium was occurring, probably as a function of the physicochemical properties of the environment, of which the importance of pH has been illustrated in the present study. Furthermore, this highlights the importance of measuring *exchangeable* cations in the burial matrix rather than total elemental content (Pate and Hutton, 1989).

Nevertheless, taking average elemental yields obtained by XRF analysis of soils, significant variability in elemental composition within and between sites, and at bone-soil interfaces, has demonstrated that the rate and pattern of elemental change and distribution is dependent on the bone type studied and on localised variation in the geology and physicochemical character of the burial environment. Such variability undoubtedly accounts for the past discrepancies in identifying and assessing the diagenetic alteration of trace elements, and challenges the validity of studies that identify diagenesis on the basis of elemental soil profiles (Lambert *et al.*, 1983).

The quantification of uranium here was limited by the fact that concentrations in bone and soil examples, particularly from British terrestrial sites, were around the limits of detection for this element using XRF i.e. a few ppm. Therefore, quantitative analyses of uranium were interpreted with caution. A more sensitive analytical technique would have been neutron activation analysis, or fission track radiography.

Field studies have also introduced the phenomenon of elemental depletion caused by leaching, either of intrinsic or diagenetically introduced elements. Depletion is evident for a number of elements (calcium, magnesium, sodium, for example) in sea-water samples only. The Bay of Agay sample, and to less extent the "Mary Rose" example, has revealed declining elemental profiles in the peripheral cortices. Certainly in the former, this can be explained largely by microbial activity in these 'zones', whose tunnelling action increased the accessibility of permeating waters. It is also possible that, since both burials were located in relatively shallow waters, they were subject to tidal action which may have enhanced both leaching and depositional processes by agitation. This may also explain the wider suite of elements detected in bone from sea-water burials.

Therefore, fieldwork presented here has tackled a number of diagenetic issues using a broad range of analytical techniques and approaches, both routine and novel in such application. The implications of their findings are discussed in more detail in section 10.3.3.

10.3 Summary and Discussion of Results.

10.3.1 The Uptake of Strontium into Bone.

Strontium uptake simulation experiments have demonstrated trends in elemental uptake and distribution over time and with varying pH conditions. The potential for strontium uptake into bone is considerable, the affinity for strontium-bone interaction is demonstrated by finding that up to 78 % of strontium was taken up from a near-saturated solution. Strontium uptake, at least under experimental conditions, is apparently a two-stage process: uptake is initially rapid and exhibits a 'U'-shaped cross-cortical distribution profile indicative of elemental diffusion. With time, the rate of uptake declines, and a relatively homogeneous profile is observed across the cortex.

Therefore, the cross-cortical distribution of strontium over 1, 6 and 10 week periods has demonstrated a temporal sequence of uptake that is consistent over a range of strontium concentrations. Under the experimental conditions employed, the rate

of strontium uptake declined after about six weeks. After this period, strontium redistribution and/or equilibration predominated over continued uptake, resulting in a relatively homogeneous cross-cortical strontium profile. This would indicate that strontium uptake in buried bone may reach a 'climax', after which a typical 'U'-shaped diffusion profile is lost as strontium levels are distributed homogeneously throughout the cortex. The repeatability of this temporal sequence of uptake over a range of strontium concentrations demonstrates that this pattern does not simply reflect saturation phenomena.

The trend in strontium uptake over time thus compromises the validity of studies that attempt to establish the existence of contaminant strontium on the basis of diffusion profiles/gradients, assuming little or no diagenetic activity where strontium is homogeneously distributed through bone e.g. Lambert *et al.*(1983). Indeed, such a temporal phenomenon may apply to any element, and thus explain why Klepinger *et al.*(1986), for example, were unable to document characteristic profiles of contaminant elements in the face of apparent diagenesis. It also challenges work by Lambert *et al.*(1989, 1990) who attempt to decrease the effect of post mortem contamination on inorganic bone analysis by surface removal of the bone. Uptake studies presented here demonstrate strontium penetration across the whole cortical width over a period of only two weeks even in relatively low concentration (5ppm) strontium solutions: so it would seem that surface removal is not a sufficiently effective or appropriate measure to remove diagenetic strontium.

The temporal pattern of strontium uptake may explain the *apparent* lack of contamination in many archaeological samples, including a sea-water burial - the Mary Rose - where strontium levels in sea-water (8-13 ppm) are much higher than those in average groundwaters (0.03-0.07 ppm): whereas cross-cortical distribution profiles of strontium indicate little contamination, based on their homogeneity, corresponding quantitative analysis by XRF clearly demonstrates contamination. In contrast, another sea-water burial - in the Bay of Agay - illustrates clear strontium contamination: this may be the result of fungal activity, or simply reflect enhanced sea-water percolation in areas made more permeable by microbial tunnelling.

The effect of environmental pH on strontium uptake and deposition has also been explored. I am confident that, in contrast to past uptake studies, immersing so-

lutions were buffered effectively and able to counteract any buffering capacity of the bone and thus more closely represent the buffering influence exerted by the (continuous) percolation of groundwater at a particular pH. Discrepancies in data arising from different analytical techniques have made interpretation difficult, but several patterns have emerged in uptake versus environmental pH. For the reasons outlined earlier, data interpretation has focused on observations derived from electron microprobe analyses.

EPMA found that trends in strontium uptake against pH were not particularly clear at low magnification. At higher magnification of the periosteal edge, strontium uptake was more pronounced under acidic conditions in *whole* bone. The trend in uptake against pH observed here agrees with uptake studies by Lambert *et al.*(1985) who revealed extensive strontium uptake into bone under slightly acidic conditions, while apparently finding no such archaeological evidence where soil was neutral-slightly alkaline. They suggested that strontium may be more subject to contamination in acidic soils. However, this study and EPMA data presented here are contrary to the work of LeGeros *et al.*(1979), who observed an increase in strontium uptake into hydroxyapatite with increasing alkalinity - arguing that strontium ions are attracted by increasingly more negative bone surfaces caused by the presence of hydroxyl ions at high pH.

It is not unreasonable to suggest that different mechanisms of interaction predominate according to the pH regime and organic content of the bone. The mechanism of strontium-bone interaction appears to be predominantly by strontium-calcium exchange in *whole* bone: strontium/calcium ratios in bone were found to increase over time in whole but not in ashed bone and this was supported by a decrease in strontium and a corresponding increase in calcium levels in immersing solutions over time. Ashed bone immersions did not demonstrate this trend, despite clear strontium association with this bone. This would indicate the predominance of adsorption mechanisms in ashed bone and heterionic exchange in whole bone. Indeed, there was clear evidence of the adsorption of chloride ions in ashed bone, particularly at the cortical surfaces.

Strontium-calcium heterionic exchange clearly occurs in whole bone and is promoted under relatively acidic conditions. Thus, in an acidic environment, where

the molecular breakdown of both organic and inorganic tissue occurs, the organic-inorganic tissue integrity is compromised so that more sites are available in the apatite matrix for strontium ions, as apatite ions are leached away.

In contrast, strontium uptake into hydrazine-treated and ashed bone is predominantly by surface adsorption and/or pore-filling mechanisms (both revealed by EPMA) and enhanced in more alkaline conditions. Certainly it is likely that in alkaline conditions, where the hydroxyapatite surface has a higher anionic charge, ions that react with this surface and settle into voids, thereby adding positive charge to bone, may have easier access than those that engage in heterionic exchange with little change in net charge (Lambert *et al.*, 1985). Moreover, it is possible that the two-stage uptake process observed here in whole bone represents the predominance of surface adsorption mechanisms, followed by incorporation. Diffusion and surface exchange reactions have been reported as the dominant processes operating over relatively short periods of exposure (Johnson *et al.*, 1970). This would explain the cross-cortical distribution pattern of strontium over time; it is initially taken up predominantly into the cancellous bone of the endosteal cortex, offering a relatively large surface area, and with time is focused in the dense bone of the periosteal cortex, where there are more potential exchange sites.

Correlations have been found between strontium concentration and the increasing crystallinity of bone observed over time (Tuross *et al.*, 1989b). Strontium levels are thought to increase as hydroxyapatite recrystallises during diagenetic growth - as strontium is incorporated into the inorganic matrix. It is able to heterionically exchange with calcium because its valency and ionic radius is similar to that of calcium (0.113 nm cf. calcium's 0.99 nm).

The duration of exposure to strontium ions was explored in the present study. Over time, crystallinity was found to increase, but was observed to differentially affect reflections. Peak 002 did not demonstrate any change, suggesting that the effect of immersion *and/or* strontium exposure had no influence on the c-axis of the crystal lattice (the largest dimension), but rather expansion occurred in the a- and/or b-axes (recorded by 112/211 and 310 reflections).

However, XRD studies presented here do not find any clear correlation between strontium exposure and crystallinity: neither peaks representing strontium incor-

poration in the apatite matrix nor the sharpening of peaks associated with recrystallisation processes permitting its incorporation were evident. This may be a function of the low sensitivity of the instrument. Nevertheless, bone immersed at pH 4 demonstrates greater crystallinity than bone immersed at pH's 7 and 10, presumably reflecting early recrystallisation and, more predominantly, the leaching out of smaller, irregular crystallites. In turn, these processes may enhance strontium uptake (1) by incorporation, strontium ions replacing calcium ions in the apatite lattice during recrystallisation, and (2) by surface adsorption as the smaller crystallites are washed predominantly from the surface. EPMA indicated relatively more strontium associated with whole bone immersed in acidic conditions and this may be correlated with the aforementioned crystallinity changes together with the relatively higher removal of the organic matrix, further exposing hydroxyapatite to ambient solutions. However, one might expect this to be a transient process as hydroxyapatite is also more prone to acidic attack, so that strontium taken up into bone may subsequently be lost as inorganic decay proceeds. This may partly explain the discrepancies in strontium diagenesis across different studies. On the other hand, the relatively low crystallinity in alkaline conditions, where the inorganic matrix is most stable, might at the same time suggest it is more prone to interaction with strontium since CEC data has indicated an increase in reactivity with relative acrystallinity. Indeed, alkaline conditions would favour strontium interaction because of the attraction for this cation by the negatively-charged bone surface that exists in such an environment.

Certainly, the heterionic exchange of calcium and strontium is well-documented in medical (*in vivo*) literature, and is a phenomenon increasingly recognised in palaeochemistry studies e.g. Nelson *et al.*(1986). Chemical separation studies described here have shown little evidence of strontium interaction with the organic component. There are references to strontium interaction with organic tissue: Spadaro (1969, 1970), for example, refers to strontium complexing with tendon tissue via coordination covalent bonding to amino acids. However, such a mechanism would require increased strontium-organic interaction at higher pH. The results from these laboratory experiments fail to show such a trend, and no clear pattern in strontium uptake with organic content at varying pH was observed. The pattern of strontium distribution for each respective pH followed a similar trend in profile with different organic content: a "flattening out" of the profiles with decreasing

organic content. This was particularly evident at pH 4, and could perhaps be paralleled with the temporal trend i.e. shifts in cortical distribution occurring as the organic component of the bone is removed over time in more extreme pH conditions.

The relationship between strontium uptake and environmental pH was further explored in field studies. Both qualitative and quantitative data for British archaeological bone examples largely confirm experimental observations. Strontium contamination was most evident in bone from Watchfield, where the soil pH was relatively acidic in comparison to those of Canterbury and Hartlepool. Watchfield bone, whose organic matrix and microstructural integrity were poorly preserved, demonstrated both higher strontium/calcium ratios in quantitative analyses and elevated levels in the peripheral cortices in microprobe analyses. There was little evidence of diffusion profiles or pore-filling in Canterbury and Hartlepool material, despite the higher concentrations of strontium measured in their soils. This would suggest an active, preferential uptake mechanism in Watchfield material rather than simply a consequence of higher strontium exposure.

The pattern of strontium distribution observed in modern mammalian bone recovered from Olduvai confirms work by Williams (1988). Strontium levels are clearly elevated in the periosteal and endosteal edges, and may represent the early stages of strontium uptake, predominantly by surface adsorption, and reflecting its short duration of interment (approximately 2 years). Alternatively, it may be a property of the alkalinity of the burial environment reducing the rate of its interaction with bone. Whatever the mechanism, clear indications of strontium contamination in such recent bone material with little depositional history demonstrates the affinity of strontium for bone and underlines the hazards in its use as a biogenic signal.

Therefore, the present study has further elucidated the potential diagenetic activity of strontium in buried bone by proposing mechanisms of interaction based on observations derived from uptake simulation studies and fieldwork.

10.3.2 The Uptake of Uranium into Bone.

Uptake studies on uranium have shown that, under experimental conditions, uranium was present only at the immediate cortical edges of the bone, even after twelve weeks immersion. PIXE analysis at the periosteal edge, moving 3 microns incrementally into the cortex, confirmed uranium penetration up to a maximum 165 microns. Uranium enrichment in the outer rim and inner medulla cavity is supported by a number of reports on archaeological material e.g. Szabo *et al.*(1970), Matsu'ura (1978), Williams and Marlow (1987). By examining these cortical edges at higher magnification trends in uranium uptake have become apparent. Such investigation has been able to reveal that uranium uptake is dependent on environmental pH and, in accordance with Rae's (1987) uptake studies, is distributed in both organic and inorganic matrices. Furthermore, the relative distribution in these fractions is also dependent on pH.

Therefore in the present study, both qualitative EPMA and quantitative PIXE/RBS found that uranium uptake was more pronounced under alkaline conditions, with very little uranium detected in bone immersed at pH 4. This is contrary to the classic studies of Neuman *et al.*(1949) who found that uranium uptake decreased with increasing pH, and argued that in more alkaline conditions uranium would complex as a carbonate, and that hydroxyl ions would compete for surface phosphate groups. In contrast, results in the present study would suggest that the increasing presence of negatively charged sites in the bone matrix, as hydroxyl ion concentration increases (or as hydrogen ion concentration decreases) favours the adsorption of large cationic complexes: this includes uranyl complexes in which uranium exists in its oxidised state.

In the experimental simulation, where conditions were oxic and where significant carbonate concentration was absent, uranyl hydroxide – $(UO_2)_3(OH)^{5+}$ – was probably the dominant uranyl (VI) species. Uranium association with the periosteal and endosteal cortices increased with increasing alkalinity, correlating with the decreasing solubility of uranyl hydroxide: this would suggest the predominance of a surface adsorption phenomenon at high pH, and arguably simulates the uptake mechanism proposed by the formation of insoluble uranous (IV) ions via reduction.

Uranium in its reduced state exists as uranium IV, which is sufficiently small to ionically exchange with calcium in the hydroxyapatite crystal: the ionic radius of tetravalent uranium is 0.097 nm cf Ca's 0.099 nm. However, there is some debate as to the mechanism of interaction of the hexavalent uranyl ion with hydroxyapatite. It is largely believed to be restricted to the crystal surface, because of its relatively large size (Altschuler *et al.*, 1958). However, there is evidence to suggest that apatite can incorporate uranium ions from solution without its prior reduction to the uranium IV ion. Studies by Neuman *et al.*(1949), and Kolodny and Kaplan (1970), for example, have suggested that both the uranium IV and the uranium VI can be structurally bound to apatite, the latter being more loosely bound than the former, probably substituting two calcium ions and possibly being able to exchange with water. However, analysis of the immersing solutions by AAS in the present study would indicate that surface adsorption rather than direct incorporation of the uranium VI ion is the predominant mechanism in operation here since calcium levels in alkaline solutions after immersion were not clearly correlated with corresponding uranium removal from solution.

In fact, temporal patterns of uranium uptake would suggest that surface adsorption processes are relatively rapid and preliminary to those of incorporation, which may be a much slower mechanism. This is indicated by EPMA which monitored both the extent of uranium association with peripheral cortices and calcium/uranium profiles in these cortical areas: while uranium peaks at the surface increased with time, calcium-uranium exchange was only apparent after at least 6 weeks immersion.

Uranium concentrations were most significant in bone immersed at pH 10, but proportionately less uranium had penetrated into the cortical tissue. The depth of penetration was generally higher in samples at pH 7. Moreover, uranium/calcium ratios indicated calcium-uranium exchange at this pH. Therefore, it is not unreasonable to suggest that alkaline conditions promote surface adsorption, predominantly to hydroxyapatite which is most stable in these conditions, while neutral conditions may promote both surface adsorption and incorporation.

Temporal trends in uptake highlight the time-limiting factor that may define the pattern and distribution of uranium recorded. Fission track analysis of bone ex-

posed to a higher uranium dose for prolonged duration demonstrates the potential for experimentally inducing uranium deposition in bone: uranium is able to (1) penetrate the full cortical width of bone, (2) demonstrate considerable pore-filling, particularly in trabecular bone, (3) concentrate in peripheral cortices, and (4) associate with remnant organic tissue (see later discussion).

These modes of association were further illustrated in archaeological examples. Fission track analysis of British material demonstrated extensive pore-filling and concentration in peripheral cortices in Watchfield and Hartlepool bone, while a fairly homogeneous distribution with little pore-filling in Canterbury bone. This may partly confirm simulation experiments by suggesting that neutral pH may promote incorporation while pore-filling and surface adsorption phenomena are predominant at more extreme pH. PIXE analysis of these samples could only detect elevated surface uranium in Hartlepool material, whose burial environment was relatively alkaline. At the same time, it must be pointed out that uranium was detectable only in soil from Hartlepool, so that the trend in uptake may simply reflect the chemical rather than physical character of the burial environment.

So, experiments here have demonstrated that the pH conditions of the burial environment influence the degree of uranium-bone interaction. To date most workers have focused on the redox conditions determining the mobility and transport of uranium by altering its oxidation state (Rae, 1987; Williams and Marlow, 1987).

The redox model of uranium uptake is dependent on the physical properties of the *microenvironment* of the bone (Rae, 1987), together with the general *depositional environment* (Williams and Marlow, 1987; Henderson *et al.*, 1987): both form major factors in determining uranium concentrations in fossil bone. Studies of fossil bone from Olduvai Gorge and Kanam describe higher uranium concentrations in fossil bone recovered from a relatively anoxic lacustrine sedimentary environment, while lower concentrations in bone from a more oxic, less alkaline, subaerial sedimentary environment.

The present study recommends a re-evaluation of the environmental influence on uranium uptake into bone. The depositional environments, on which most of the redox model of uranium uptake have been founded, are all *alkaline* environments: the Springs at Kanam contributing to the groundwater range pH 7.3 - 8.1, while

the presence of an alkaline and saline lake during the deposition of fossil bearing sediments at Olduvai Gorge indicates an alkaline groundwater.

The uranium uptake model, first proposed by Rae (1987), relies on buried bone controlling its own immediate burial environment or microenvironment, independent of the physical characteristics of the percolating groundwater. Rae states that "the most important function of free amino-acids is as reducing agents." Based on observations made here, I would add that the effect of organic acids on the pH of the local environment is equally important. These observations therefore demand a more careful consideration of the balance between bone's ability to control and maintain the physical conditions of its own microenvironment against the influence of sedimentary conditions.

It seems plausible that in the early stages of burial a cross-cortical pH gradient will exist: the outer layers, under the overriding influence of alkaline groundwaters, are predominantly alkaline, as organic acids produced during organic decay are more likely to be leached away under groundwater action at these exposed surfaces. In contrast, the inner medullary cortex under the influence of local organic decay and slower removal of the organic acids produced, is more likely to maintain or "self-buffer" a pH 4 - 6 range.

Therefore, it is proposed that the high levels of uranium in Olduvai and Kanam may be the result of both an anoxic and an alkaline environment. Moreover, in the early stages of fossilization uranium may be taken up in both its oxidised and reduced forms, largely by surface adsorption and incorporation mechanisms respectively, and dependent on local pH and redox conditions at the sedimentary- and micro- environmental levels. It is feasible that during these early stages, while uranium is largely taken up via incorporation in its reduced form in the medullary cortex, the proportion of uranium taken up as the uranyl ion by adsorption and the uranous ion by incorporation at the cortical edges will depend on the redox and pH conditions of the groundwater: alkaline oxic environments favouring adsorption, while alkaline anoxic environments, and possibly neutral oxic conditions, favouring incorporation at the outer edges. As groundwater alkalinity declines, so do uranium adsorption mechanisms, as the inorganic matrix becomes less stable. In fact, in acid oxic solutions, uranium is transported predominantly as the uranyl ion and

uranyl hydroxide: the affinity of uranium hydroxide for apatite adsorption has been demonstrated here, and would suggest surface adsorption mechanisms might operate under natural neutral/acidic conditions.

In neutral and alkaline oxidising conditions, uranium is commonly transported as a uranyl dicarbonate and uranyl tricarbonate complex respectively. As the partial pressure of carbon dioxide increases in solution, as would occur in increasingly alkaline conditions, stronger reducing agents are required to remove uranium from solution as uraninite or schoepite (the only possible solid phases expected to be stable in the presence of water and variable oxygen). Under such conditions, it is possible that the reducing level in the microenvironment at the outer surface is not sufficient for the formation of uranium (IV) and reactions of the uranyl ion with bone predominate.

When the rate of organic decay has dropped off and the cross-cortical pH has equilibrated with the pH of the sedimentary environment, then the redox conditions of the burial environment may determine whether adsorbed ions are subsequently incorporated, or whether there is further uptake or, conversely, leaching of uranium. The latter may explain the pattern of younger ages for surface bone obtained by Uranium-Series dating, where uranium depletion in cortical rims may be a property of both the vulnerability of these edges to environmental influences and of the relative predominance of adsorbed rather than incorporated uranium ions.

Environmental pH clearly has an effect on the role of the organic component of bone on uranium uptake. The organic complexing of uranium, as uranium ions form weak ionic bonds with organic ligands of the degrading collagen, is substantiated by numerous geological examples: carbonaceous matter, in particular humic and fulvic acids, is an important material for uranium fixation in geology, being a good absorbent of uranium solutions over a wide pH range (Doi, 1975; Szalay, 1969). Amino acids are presumed to behave in a similar manner to humic and fulvic acids; indeed, they have been observed to form complexes with uranium (Cefola *et al.*, 1962).

In this study, no detectable uranium uptake was observed at pH 4 in any of the bone samples, whatever their organic content. At pH 7 uptake increased with decreasing organic content, and at pH 10 uptake increased with increasing organic

content. This would agree with work by Spadaro (1970) who reports that at higher pH's, whole bone appears to behave more like bone collagen than bone mineral in its ion uptake behaviour, suggesting that negatively charged or polar groups may be involved in the organic complexing of ions. However, in contrast, this trend is contrary to proposed mechanisms of organic binding which favour acidic environments for uranium complexing: the adsorption of uranium to humic acids, for example, is caused by reaction of cations with carboxylic groups on the surface polyaromatic skeleton of these acids i.e. the uranyl ion is fixed by acid groups on humic acids. Szalay (1969) in his study on humic acids conducted his laboratory experiments at pH 5. Similarly Doi (1975) plotted uranium adsorption ratios against pH and found greatest adsorption at pH 3.5 to 8.5. Alkaline conditions are generally thought to have a mobilising effect, and at high pH the degradation products formed as organics are hydrolysed are known to enhance the solubility of actinides in solution.

However, Gascoyne in 1980 reported that the uranium concentration of speleothems (cave calcite deposits) with high organic content is often nominal (0.5 to 5ppm) while higher (> 10ppm) in those with less organic content. This implies that the complexing ability of organics for uranium is inferior to that of phosphates (and carbonates) at the pH of calcite deposition i.e. at pH 7-8. This may partly explain the relative redundance of organics observed here at pH 7, compared to pH 10. Indeed, Gindler (1973) reported that protein-uranium complexes are formed at pH's > 7. Protein complexation does not require the prior reduction of the uranyl ion (Szalay 1969, Chapman 1976), thus allowing the adsorption of uranium (+VI) to the organic as well as the inorganic matrix of bone.

If the two-stage process of uranium uptake occurs, as suggested by Rae (1987), whereby organic components effectively concentrate uranium while inorganic fractions provide the matrix where uranium is deposited permanently, then this may explain the lack of uranium uptake observed here at pH 4. Under acidic conditions, both inorganic and organic matrices are subject to degradation. It is possible that the organic component is being degraded and leached too quickly to maintain an anoxic microenvironment, thus taking any uranium adsorbed with it into solution. If this is the case, then rapid degradation of the organic component

prevents the first stage of uranium complexing prior to apatite incorporation/ adsorption. This would also explain the contrast in uptake behaviour at pH 7 and pH 10. Incorporation of uranium, together with adsorption, is evidently occurring at neutral pH where organic-inorganic matrix integrity is most intact and stable, thereby allowing this two-stage process to occur. At pH 10, the organic matrix is compromised to some extent by basic hydrolysis, but this activity evidently enhances uranium-complexing. The slower process of uranium (VI) incorporation into the inorganic matrix in alkaline conditions may be a function of the challenged organic-inorganic integrity (mild in comparison to acidic conditions), or a property of the relative stability of hydroxyapatite to recrystallisation, thus maintaining its non-stoichiometric character: certainly, CEC data indicate an enhanced exchange capacity with apatite acrystallinity.

The relationship between uranium uptake and bone crystallinity is unclear. This may reflect the level of sensitivity of XRD, or it may indicate little correlation between crystallinity and uranium deposition in bone. According to the present study, crystallinity over time increases with acidity i.e. in conditions that do not promote uranium uptake. Moreover, uranium uptake in the early stages appears to be predominantly by adsorption rather than incorporation, which may be a consequence of the former (the two-stage process). This may explain the reported early uptake of uranium into younger bone when the organic-inorganic matrices are relatively intact. As crystallinity increases, which (as earlier observations point out) may occur early in burial, and is often correlated with decreasing organic content (1) there is no organic "substrate" for adsorption/complexation, and (2) hydroxyapatite is less prone to adsorption/incorporation (CEC data) because of its relative stability. Uranium uptake as the smaller uranous ion may be favoured during recrystallisation, while uranyl ions, reacting predominantly by adsorption and more slowly by incorporation, are not.

To conclude, simulation studies examining uranium uptake into bone have exposed a highly complex, interactive process that is dependent, at least, on the physico-chemical character of both bone and burial environment.

10.3.3 Case Examples of Bone Diagenesis.

Samples of ancient bone buried under a wide range of conditions have been analysed using microPIXE. This method of analysis has successfully illustrated that bone is subject to contamination from disparate trace elements. Furthermore, the distribution of particular elements may be correlated, so that the presence of one may indicate a high probability of similar contamination by others. This appears to be the case for iron, manganese and zinc (copper is possible) which are found to be common and extensive contaminants of exhumed bone. Such observations might suggest that, with further similar investigations conducted on material from a wider range of burial environments, a database of typical associations or correlations of two or more elements could provide a crude identification system: this could potentially afford a more economical means of assessing the extent of diagenesis using relatively few 'marker' elements as a guide for deducing the behaviour of many. Katzenberg (1984) employed a similar strategy in defining a formula to correct for strontium values deposited in soil particles, acting on a significant correlation between strontium and zirconium. However, such an approach is highly dubious because of the inconsistent and thus unpredictable nature of diagenesis (Klepinger *et al.*, 1986; Runia, 1987,1988).

The crystallinity of archaeological bone examples presented here corroborates experimental studies in demonstrating the importance of the burial environment in determining the degree of inorganic matrix alteration. The acidity of the depositional environment will influence (1) the rate of organic decay, and thus the degree of exposure of the inorganic matrix to percolating groundwaters, and (2) the extent of leaching of amorphous mineral and smaller crystallite components of the inorganic matrix itself. This further reinforces the weakness in the use of crystallinity as a chronometric tool (Bartsiokas and Middleton, 1992). At the same time, it might be argued that the Watchfield material is the oldest sample (Saxon) from the British examples and therefore possesses the most crystalline form because it has been exposed to groundwater action for relatively longer. However, there is also a flaw in the assumption that the duration of burial is proportional to the extent of groundwater action: this argument, in addition to overlooking physicochemical differences (as demonstrated), does not account for differences in

hydrological regime, which can range from permanently saturated to arid conditions, depending on water availablility and the drainage properties of the burial matrix.

An important consideration arising from XRD analysis is that crystallinity changes have been observed in bone up to 1,500 years old and, furthermore, in recent bone material (Olduvai) that has only been partially buried for a few years. This suggests that crystallinity changes may occur early in the inhumation period, a theory that contrasts observations made by Sillen (1989), Schoeninger (1982) and Hassan (1975). These workers found little evidence of increasing crystallinity in bones up to 15,000 years b.p. and conclude that crystallinity changes may take a long time to manifest themselves, perhaps after some thousands of years of interment (Sillen, 1989). Such discrepancies are again likely to be attributable to differences in respective burial environments.

The variability across burial environments in different geographical locations was further highlighted in soil analyses presented here. The rate and pattern of elemental distribution was found to be highly variable both between and within respective sites. Such variation, particularly at the local level, challenges the validity of assessing diagenetic activity on the basis of elemental gradient patterns in the soil matrix. Similarly, the variability in elemental content of bone within and between (1) bone type and (2) site, challenges the validity of the intercomparison of sites on the basis of quantitative analyses, unless a significantly representative number of samples are analysed from each (a major limitation of the present study was the sample size).

Finally, field studies have demonstrated the diagenetic alteration of three elements of palaeodietary significance: strontium (discussed in detail in section 10.3.1), zinc and copper. Barium, the other major palaeodietary indicator element, was not measured in bone because it was not present in sufficiently high (detectable) levels. While this might suggest its relative stability during postmortem alteration of bone, it may also simply be explained by the comparative insensitivity of the adopted analytical instrumentation or be defined by the type of burial environments presented here. Certainly, it seems unlikely that barium is unaffected by

diagenesis when other divalent ions with similar ionic size (e.g. strontium and calcium) are clearly diagenetically active.

10.3.4 Practical Implications.

(i) Strontium.

The present study concludes that the diagenetic alteration of strontium in buried bone is inevitable and, as a consequence, the use of strontium as a palaeodietary indicator must be practised with extreme caution: the biological anthropologist cannot assume its geochemical stability and thus reliability as a biogenic signal. Furthermore, the degree of strontium diagenesis is dependent on the pH of the burial environment, which in turn determines the mechanism(s) of strontium-bone interaction. Strontium diagenesis is usually a contamination phenomenon, since there is little evidence of its depletion in the archaeological examples or in crude leaching experiments presented here.

The validity of studies that attempt to identify diagenesis on the basis of elemental gradient profiles across the bone cortex is challenged here on discovering that homogeneous distribution does not necessarily exclude the occurrence of cross-cortical diffusion. It is recommended that at least a second analytical method is conducted in conjunction with such microprobe studies, in much the same way as quantitative analysis of the "Mary Rose " bone identified clear strontium contamination that was not evident on the basis of microPIXE analysis.

(ii) Uranium.

Uranium findings confer further complications on the use of uranium in dating and palaeoenvironmental applications caused by the complexity of uranium interaction with bone.

Uranium uptake into bone and any subsequent leaching/removal will be affected not only by changes in redox conditions, a fact that forms the basis of deriving information about the palaeoenvironment, but also on pH fluctuations over time (within the limits of uranium availability in the local geochemistry). This raises

further potential, with a simultaneously more difficult interpretation, for exploiting uranium distribution as a means of defining the palaeoenvironment; it also introduces scope for further inaccuracies in Uranium-Series dating measurements. Moreover, its absence in bone, caused perhaps by acidic conditions, despite an oxic environment, does not exclude the diagenetic alteration of other elements, thereby highlighting caution when using uranium as a diagenetic indicator.

(iii) How effective are methods designed to minimise the effects of diagenesis ?

Both fieldwork and strontium uptake data demonstrate elemental distribution that is not exclusive to surface cortical regions; rather, adsorption and/or cation exchange phenomena are observed to penetrate deeper into the cortex, as elements in groundwaters/immersing solutions have diffused through the natural porosities of bone. This is even demonstrated in modern Olduvai bone where elevated strontium and Sr/Ca ratios are observed at least 1 mm into the bone cortex. These observations would indicate that while removing the most strongly contaminated regions of bone in many cases, mechanical abrasive cleaning of bone surfaces, typically a few millimetres depth, is not an effective means of removing contaminant material. Simulation studies, and to a large extent fieldwork, find uranium association at the cortical surfaces and in the immediate outer cortices, suggesting mechanical cleaning is an effective treatment. However, this contrasts with work by other researchers that report more extensive uranium distribution throughout bone e.g. Henderson *et al.*(1983), Williams and Marlow (1987), Williams (1988), Williams and Potts (1988).

Chemical (acid) cleaning, on the other hand, is probably effective in removing strontium and similarly bound elements, and possibly elements that behave in a similar way to uranium; the latter depends on whether this treatment is able to account for organically complexed elements by acid mobilisation. This may certainly be significant in the effective removal of zinc, which has been demonstrated as a potential diagenetic contaminant, and whose association with bone may largely be attributable to the organic fraction (Spadaro, 1970).

The degree of effectiveness in removing strontium by chemical cleaning may be dependent on the pH character of the burial environment, which, according to data

presented here, will determine whether strontium is incorporated or adsorbed. However, work by Price *et al.*(1992) suggests that this procedure is able to remove relatively soluble contaminants incorporated within the crystalline apatite structure as well as those on the crystal surface. This would indicate successful removal of uranium (or similar) contamination of the inorganic matrix, observed here largely as adsorption, and also of strontium, whether taken up by adsorption or incorporation. Removal of incorporated material may require a longer period of treatment according to experiments on the acid washing of ashed bone, where elements are firmly incorporated during recrystallisation induced by the high ashing temperatures (Price *et al.*, 1992).

10.4 Summary and Recommendations for Further Study.

10.4.1 Summary

Strontium uptake simulation experiments highlight the affinity of strontium for bone by demonstrating its rapid and extensive uptake, penetrating the full cortical width after only a short period of exposure. Temporal patterns of uptake are discussed and show that homogeneous cross-cortical distribution profiles do not necessarily indicate the absence of diagenetic activity. Strontium uptake into whole bone is apparently more pronounced under acidic conditions, while alkaline conditions promote uptake into ashed and hydrazine-treated bone. Furthermore, it is proposed that strontium incorporation into the apatite matrix is the predominant mechanism of interaction in acidic conditions, while surface adsorption and pore-filling are dominant in alkaline conditions. Certainly, strontium uptake and deposition in buried bone is largely a function of the inorganic matrix, since there is little evidence for strontium-organic complexing.

Uptake experiments demonstrate **uranium** uptake only at the immediate cortical edges, as opposed to strontium's penetration across the full cortical width. Uranium uptake is more pronounced under alkaline conditions, with very little uranium detected at pH 4. Results suggest that, in addition to the redox potential, the alkalinity of the burial environment may be important in the uptake mechanisms of uranium into bone. In addition, the environmental pH apparently has an effect on the relative roles of the organic and inorganic components of bone

in uranium interaction. Moreover, since no attempt is made to alter the redox environment of the experiment i.e. the hexavalent ion of uranium is being studied, results suggest that uranium is taken up into bone in both its reduced *and* oxidised forms, probably by incorporation and adsorption mechanisms, respectively.

The **proton microprobe** has proved a very successful analytical instrument in the study of bone diagenesis. Further investigations using the technique of microPIXE on archaeological bone material from a wider range of burial environments, and in parallel with contextual soil analyses, will provide a better understanding of diagenesis.

Certainly, the uptake and distribution of elements are dependent on the burial conditions: both fieldwork and laboratory-based uptake experiments presented here confirm that the validity of trace element studies on bone depends essentially on the geological environment of the burial. This study has shown that the physical and chemical properties of the burial matrix play a fundamental part in determining bone interaction with its immediate burial environment, and complements other studies which have discussed the biological aspects of bone fossilization and diagenesis (e.g. Grupe and Piepenbrink, 1988; Hanson and Buikstra, 1987).

10.4.2 Recommendations for Further Study.

While these interpretations can be formed justifiably on the basis of observations presented here, it is appreciated that the cumulative effects of experimental simplifications and evasions are not dismissable. Nevertheless, the present research provides one of several preliminary studies that have explored diagenesis by experimental simulation: these data can be built upon with improved methods in the future that incorporate more complex and contextually accurate experimental design.

The present study thus forms a small but significant branch of a ramifying and systematic study of the many aspects of elemental uptake into buried bone, derived largely from the complexity of the burial environment, and generating a wealth of experimental work potential.

A systematic study of all aspects of uptake is essential. In particular, detailed investigations of specific uptake mechanisms are required to elucidate what is clearly a complicated multi-factorial uptake process incorporating diffusion, adsorption and desorption, ion exchange and leaching. The latter was not considered in detail here. Nevertheless, it is important to explore (1) the *removal* of intrinsic elements in bone, and (2) the readiness/probability of the subsequent loss of diagenetically introduced elements i.e. the extent of *reversibility* of uptake under variable conditions; such an exploration may illuminate the nature of differential leaching processes, particularly in more acidic pH conditions when the dissolution of hydroxyapatite is effected. An investigation of this kind could be conducted by modifying the percolation system employed in cation exchange experiments described here. Ammonium acetate solution, or 'leaching' solutions of variable pH, could be percolated through (a) experimental bone, previously exposed to a variety of elements, or (b) archaeological bone material, and the chemistry of the leachates measured. This would identify potentially exchangeable cations, either intrinsic to or diagenetically introduced into bone, and provide an indication of the liability of their subsequent leaching out of bone.

Furthermore, the effect of competing ions could be explored by progressively introducing into the experimental system a variety of cations typically found in groundwaters to monitor cation competition. In this way, the chemistry of the experimental solution could gradually be built up to effectively simulate real groundwaters. The presence of calcium in solution enabling an equilibrium to be set up with calcium in bone, together with variations in the physical and biological characteristics of groundwater all play a role in determining the rate of hydroxyapatite alteration.

Post-mortem alteration of the organic matrix requires further investigation. A more thorough analysis of the organic matrix itself after exposure to a range of elements could be conducted, yielding detailed information about the nature of its diagenetic alteration and interactive consequences for that of the inorganic matrix. The biological (microbial) character of the burial environment must be considered in this context.

Further investigation of the physical parameters of the burial environment are

also worthy of consideration in *in vitro* simulation studies. Eh, for example, is an essential factor in determining the diagenetic contribution of di-/multi-valent ions. The control of *in vitro* redox conditions, requiring the use of potentiometer instrumentation, is essential in elucidating the comparative rate and mechanism of uptake of uranous and uranyl ions. Subsequent infra-red spectroscopy may provide a means of identifying the nature of uranium-bone bonding.

Certainly, it is important to discriminate between surface adsorption and incorporation mechanisms, which requires knowledge of the surface chemistry of bone and how it is affected by changes in the ionic strength and pH of groundwaters.

Environmental conditions and trace element availability in the burial matrix during fossil bone interment are undoubtedly the main controls on elemental uptake and distribution. Further knowledge of how the physical, chemical and biological character of the burial environment affects the mobility and fixation of these elements is essential before the archaeometric significance of the trace element content of exhumed bone is truly realised.

Bibliography

Ahlgren, L., Christofferson, J.O., Mattsson, S. (1981) Lead and Barium in Archaeological Roman Skeletons Measured by Non-Destructive X-Ray Fluorescence. In (D.K. Smith, C. Barrett, eds.) Advances in X-Ray Analysis. pp377-382.

Allaway, W.H.(1986) Soil-Plant-Animal and Human Interrelationships in Trace Element Nutrition. In (W.Mertz, ed.) Trace Elements in Human and Animal Nutrition. 5th Edition. Orlando, FL: Academic Press. pp465-488.

Altschuler, Z.S., Clarke, R.S., Young, E.J. (1958) Geochemistry of Uranium in Apatite and Phosphorite. Geological Survey Professional Paper 314D. 45-90.

Ames, (1960) Some Cationic Substitutions During the Formation of Phosphate from Calcite. Economic Geology 55. 354-362.

Anderson, A.J., Clark, A.H., Ma, X-P, Palmer, G.R., MacArthur, J.D. and Roedder, E. (1989) Proton-Induced X-Ray and Gamma-Ray Emission Analysis of Unopened Fluid Inclusions. Economic Geology 84. 924-939.

Armstrong, W.D., Singer, L. (1965) Composition and Constitution of Mineral Phase of Bone. Clinical Orthopaedics 38. 179-190.

Arnaud, G., Arnaud, S., Ascenzi, A., Bonucci, E., Graziani, G. (1978) On the Problem of the Preservation of Human Bone in Sea-water. Journal of Human Evolution 7. 409-420.

Ascenzi, A. (1969) Microscopy and Prehistoric Bone. In (D.Brothwell, E.Higgs, ed.s) Science in Archaeology : A Survey of Progress and Research. 2nd Edition.

Ascenzi,A., Silvestrini,G.(1984) Bone-boring Micro-organisms: Experimental Investigation. Journal of Human Evolution 13 (6). 531-537.

Bacon, G.E., Bacon, P.J., Griffiths, R.K. (1979) The Orientation of Apatite Crystals in Bone. Journal of Applied Crystallography 12. 99-103.

Bada, J.L. (1985) Amino Acid Racemization Dating of Fossil Bones. Annual Review Earth Planetary Science 13. 241-268.

Bada, J.L., Schoeninger, M.J., Schimmelman, A.(1989) Isotopic Fractionation during Peptide Bone Hydrolysis. *Geochimica et Cosmochimica Acta* 53. 3337-3341.

Badone, E., Farquhar, R.M. (1982) Application of Neutron Activation Analysis to the Study of Element Concentration and Exchange in Fossil Bones. Journal of Radioanalytical Chemistry 69. 291-311.

Bartsiokas, A., Middleton, A.P.(1992) Characterization and Dating of Recent and Fossil Bone by X-Ray Diffraction. Journal of Archaeological Science 19(1). 63-72.

Basham, I.R., Easterbrook, G.D. (1977) Alpha-Particle Autoradiography of Geological Specimens by Use of Cellulose Nitrate Detectors. Instrumental Mineral Metallurgy Bulletin 86. B96-B98.

Bear, F.E.(1964) Chemistry of the Soil. 2nd Edition. Chapman and Hall Ltd., London.

Beaty, R.D. (1978) Concepts, Instrumentation and Techniques in Atomic Absorption Spectroscopy. Perkin Elmer.

Behrensmeyer, A.K. (1978) Taphonomic and Ecological Information from Bone Weathering. Paleobiology 4. 150-162.

Berry, J.A., Cowper, M.M., Green, A., Jefferies, N.L., Linklater, C.N.(1991) Sorption of Radionuclides on Mineral Surfaces. Proceedings of the Third International Conference on Nuclear Fuel Reprocessing and Waste Management, Japan (RECOD 91) Vol.2. p998.

Blakely, R.L. (1989) Bone Strontium in Pregnant and Lactating Females From Archaeological Samples. American Journal of Physical Anthropology 80. 173-185.

Blank, H. and Traxel, K. (1984) Proton Induced X-Ray Emission in Micro-Regions Applied in Mineralogy. Scanning Electron Microscopy Part III. 1089-1096.

Blumenthal, N.C., Betts, F., Posner, A.S. (1975) Effect of Carbonate and Biological Macromolecules on the Formation and Properties of Hydroxyapatite. Calcified Tissue Research 18. 81-90.

Bonar, L.C., Roufosse, A.H., Sabine, W.K., Grynpas, M.D., Glimcher, M.J.(1983) X-Ray Diffraction Studies of the Crystallinity of Bone Mineral in Newly Synthesized and Density Fractionated Bone. Calcified Tissue International 35. 202-209.

Boskey, A.L., Posner, A.S. (1984) Structure and Formation of Bone Mineral. In (G.W.Hastings, P.Ducheyne, eds.) Natural and Living Biomaterials. CRC Press. pp27-41.

Bourne, G.H.(Ed.) (1971) Biochemistry and Physiology of Bone I. Academic Press, New York.

Bourne, G.H.(Ed.) (1972) Biochemistry and Physiology of Bone I. 2nd Edition.

Academic Press, New York.

Bowen, H.J.M.(1979) Environmental Chemistry of the Elements. Academic Press, New York.

Bowie, S.H.U., Atkin, D. (1956) An Unusually Radioactive Fossil Fish form Thurso, Scotland. Nature 177. 487-488.

Bowie, S.H.U., Plant, J.A. (1983) Natural Radioactivity in the Environment. In (I.Thornton,ed.) Applied Environmental Geochemistry. Ch.16. Academic Press, New York.

Broadway, J.A., Strong, A.B. (1983) Radionuclides in Human Bone Samples. Health Physicist 45. 765-768

Brophy, G.P., Nash, J.T. (1968) Compositional, Infra-red, and X-ray Analysis of Fossil Bone. American Mineralogist 53. 445-454.

Brown, A.B. (1973) Bone Strontium Content as a Dietary Indicator in Human Skeletal Populations. Ph.D Thesis, Department of Anthropology, University of Michigan, Ann Arbor, U.S.A. Publication No. 74-15.

Brown, S.B. (1980) An Introduction to Spectroscopy for Biochemists. Academic Press, New York.

Brown, W.E., Chow, L.C. (1976) Chemical Properties of Bone Mineral. Annual Review Materials Science 6. 213-236

Buikstra, J.E., Frankenberg, S., Lambert, J.B., Xue, L. (1989) Multiple Elements: Multiple Expectations. In (T.D.Price, ed.) The Chemistry of Prehistoric Human Bone. Cambridge University Press. pp154-210

Burgess, J. (1978) Metal Ions in Solution. Wiley and Sons, London.

Burnett, D.S., Woolum, D.S. (1983) *In Situ* Trace Element Microanalysis. Annual Review of Earth and Planetary Science 11. 329-358.

Byrne, K., Parris, D.C.(1987) Reconstruction of the diet of the Middle Woodland Amerindian Population at Abbott Farm by Trace Element Analysis. American Journal of Physical Anthropology 74. 373-384.

Cabri, L.J. (1988) Applications of Proton and Nuclear Microprobes in Ore Deposit Mineralogy and Metallurgy. Nuclear Instruments and Methods in Physics Research B30. 459-465. North-Holland Publishing, Amsterdam.

Cameron, D.A.(1972) The Ultrastructure of Bone.In (G.H.Bourne, ed.) The Biochemistry and Physiology of Bone. 2nd Edition Volume I. Chapter 6. pp191-236. Academic Press, New York.

Campbell, J.L. and Cookson, J.A. (1984) PIXE Analysis of Thick Targets. Nuclear Instruments and Methods in Physics Research B3. 185-197.

Cefola, M., Taylor, R.C., Gentile, P.S, Celiano, A. (1962) Coordination Compounds III. Chelate Compounds of the Uranyl Ion with Hydroxy-, Mercapto- and Amino Acids. Journal of Physical Chemistry 66. 760-761.

Chander, S., Fuerstenau, D.W. (1982) On the Dissolution and Interfacial Properties of Hydroxyapatite. Colloids Surface 4. 101-120.

Chander, S., Fuerstenau, D.W. (1983) Solubility and Interfacial Properties of Hydroxyapatite. A Review. In (D.N.Mishra, ed.) Adsorption on and Surface Chemistry of Hydroxyapatite. Plenum Press. pp29-50.

Chapman, J.A. (1976) Preparation of Fibrous Long Spacing Collagen. In (D.A.Hall, ed.) The Methodology of Connective Tissue Research. Jaynson-Bruvvers, Oxford. pp65-72.

Christensen, M., Walter, Ph., Menu, M. (1992) Usewear Characterisation of Prehistoric Flints with IBA. Nuclear Instruments and Methods in Physics Research B64. 488-493.

Cichocki, T., Divoux, S., Gonsior, B., Hofert, M., Jarczyk, L., Raith, B., Rokita, E., Strzalkowski, A., Sych, M. (1990) Intramembranaceous Ossification Analyses by a Proton Microprobe. Histochemistry 94. 171-177.

Clayton, E.J. (1986) Australian Atomic Energy Commission Report AAEC/M1 13.

Comar, C.L., Russell, R.S., Wasserman, R.H. (1957) Strontium-Calcium Movement from Soil to Man. Science 126. 485-496.

Comar, C.L., Wasserman, R.H.(1964) Strontium. In: Mineral Metabolism, Vol.2A. pp523-572. Academic Press, New York.

Cook, S.F.(1960) Dating Prehistoric Bone by Chemical Analysis. In (R.F.Heizer, S.F.Cook, eds.) The Application of Quantitative Methods in Archaeology. Publ. Quandrangle and Tavistock.

Coote, G.E., Holdaway, S.(1982) Archaeometry: An Australasian Perspective. Australian National University Press. pp251-261.

Curran, S.C. (1953) Luminescence and the Scintillation Counter. London, Butterworths Scientific Publications.

Daniels, R. (1986) The Excavation of the Church of Franciscans, Hartlepool, Cleveland. The Archaeological Journal 143.

David, D.J. (1962) Determination of Strontium in Biological Materials and Exchangeable Strontium in Soils by Atomic Absorption Spectrophotometry. The Analyst 87. 576-585.

Dawson, R.M.C., Elliot, D.C, Elliott, W.H., Jones, K.M. (1986) Data for Biochemical Research 3rd Edition. Clarendon Press, Oxford.

Demortier, G.(1987) Microbeam Applications in Archaeology. In (F.Watt, G.W.Grime, eds.) Principles and Applications of High-Energy Ion Microbeams. Chapter 10. pp 333-377. Hilger, Bristol. IOP Publishing Ltd.

DeNiro, M.J. (1985) Postmortem Preservation and Alteration of *in vivo* Bone Collagen Isotope Ratios in Relation to Palaeodietary Reconstruction. Nature 317. 806-809.

DeNiro, M.J., Epstein, S.(1981) Influence of Diet on the Distribution of Nitrogen Isotopes in Animals. *Geochimica et Cosmochimica Acta* 45. 341-351.

Doi, K., Shuichiro, H., Sokamaki, Y.(1975) Uranium Mineralisation by Groundwater in Sedimentary Rocks, Japan. Economic Geology 70. 628-646.

Driessens, F.C.M. (1980) The Mineral in Bone, Dentine and Tooth Enamel. Bulletin Societe Chimica Belgique 89. 663-689.

Dry, M.E., Beebe, R.A. (1960) Adsorption Studies on Bone Mineral and Synthetic Hydroxyapatite. Journal of Physical Chemistry 64. 1300-1304.

Duane, M.J., Williams, C.T. (1980) Some Applications of Autoradiographs in Textural Analysis of Uranium-Bearing Samples. Economic Geology 75. 766-770.

Eastoe, J.E. (1961) The Chemical Composition of Bone. In (C.Long, ed.) Biochemists' Handbook. Princeton: Van Nostrand. pp715-720.

Edward, J.B, Benfer, R.A, Morris, J.S.(1990) The Effects of Dry Ashing on the Composition of Human and Animal Bonen. Biological Trace Element Research 25. 219-231.

Eidt, R.C.(1977) Detection and Examination of Anthrosols by Phosphate Analysis. Science 197. 1327-1333.

El-Kammar, A., Hancock, R.G.V., Allen, R.O.(1989) Human Bones as Archaeological Samples: Changes Due to Contamination and Diagenesis. In: Archaeological Chemistry. Chapter 18, pp337-352. American Chemical Society.

Elliott, T.A., Grime, G.W.(1993) Examining the Diagenetic Alteration of Human Bone Material from a Range of Archaeological Burial Sites using Nuclear Microscopy. Nuclear Instruments and Methods in Physics Research B *in press.*

Everson Pearse, A.G. (1972) Histochemistry Theoretical and Applied. Vol.2, Third Edition. Churchill Livingstone, London.

Ezzo, J.A.(1992) A Test of Diet Versus Diagenesis at Ventana Cave, Arizona. Journal of Archaeological Science 19(1). 23-37.

Fairbridge, R.W. (1972) The Encyclopaedia of Geochemical and Environmental Sciences Vol IVA. New York: Van Nostrand Reinhold.

Fazekas, I, Kosa, F.(1978) Forensic Fetal Osteology. Ch.4: Preparation of Foetal

Bones. pp37-40. Akademiai Kiado, Budapest.

Fleischer, R.L., Price, P.B., Walker, R.M. (1975) Nuclear Tracks in Solids. Principles and Applications. London: University of California Press.

Fornaciari, G., Mallegni, F., Bertini, D., Nuti, V.(1981) Cribra Orbitalia and Elemental Bone Iron in the Punics of Carthage. Ossa 8. 63-77.

Francalacci, P. (1989) Dietary Reconstruction at Arene Candide Cave (Liguria, Italy) by Means of Trace Element Analysis. Journal of Archaeological Science 16. 109-124.

Francalacci, P., Tarli, S.B. (1988) Multielementary Analysis of Trace Elements and Preliminary Results on Stable Isotopes in two Italian Prehistoric Sites. Methodological Aspects. In (G.Grupe, B.Herrmann, eds.) Trace Elements in Environmental History. Springer-Verlag, Berlin. pp41-52.

Freeze, R.A, Cherry, J.A.(1979) Groundwater. Prentice-Hall, Inc., New Jersey.

Freshney, R.I.(1987) Culture of Animal Cells. 2nd Edition.

Frost, H.M.(1980) In (M.R.Urist, ed.) Fundamental and Clinical Bone Physiology. Chapter 7 pp208-242. J.B.Lippincott Co., Philadelphia.

Frost, H.M.(1987) Secondary Osteon Populations. Yearbook of Physical Anthropology 30. 221-238.

Fulton, B.A., Meloan, C.E., Finnegan, M.(1986) Reassembling Scattered and Mixed Bones by Trace Element Ratios. Journal of Forensic Sciences JFSCA 31(4). 1455-1462.

Ganzorig, Z., Darhzeveg, L., Otgonsuren, O., Khuukhenkhun, G., Chadraabal, I., Chultem, D. (1974) Non-Destructive Determination of a Trace Amount of U and Th in Materials of Complex Chemical Composition. Radiokhimiya 16 (2). 247-253.

Garland, A.N.(1988) A Histological Study of Archaeological Bone Decomposition. In (A.Boddington, A.N.Garland, R.C.Janaway, eds.) Death, Decay and Reconstruction. Manchester: Manchester University Press. pp109-126.

Gascoyne, M. (1977) Uranium Series Dating of Speleothem: an Investigation of Technique, Data Processing and Precision. McMaster University Memo. pp74-77.

Gascoyne, M. (1980) Pleistocene Climates Determined from the Stable Isotopic and Geochronological Studies of Speleothem. Unpublished Ph.D Thesis, McMaster University, Ontario, Canada.

Gascoyne,M. (1982) Geochemistry of the Actinides and their Daughters. In (M.Ivanovich, R.S.Harmon, eds.) Uranium Series Disequilibrium: Applications to Environmental Problems. Clarendon Press, Oxford.

Gilbert, R.I.(1985) Stress, Palaeonutrition, and Trace Elements. In (Gilbert, R.I., Mielke, J.H. eds.) The Analysis of Prehistoric Diets. Academic Press, Orlando. p339

Gindler, J.E. (1973) Physical and Chemical Properties of Uranium. In (H.C.Hodge, J.N.Stannard, eds.) Uranium-Plutonium Transplutonic Elements. Chapter 2, pp69-152. Springer-Verlag, Berlin-Heidelberg.

Glimcher, M.J.(1984) Recent Studies of the Mineral Phase in Bone and its Possible Linkage to the Organic Matrix by Protein-Bound Phosphate Bonds. Philos.Trans.R.Soc.Lond. (Biol) 301 (9121) Feb 13. 479-508.

Goldschmidt, V.M. (1954) Geochemistry. Clarendon Press, Oxford.

Good, N.E., Izawa, S. (1972) Hydrogen Ion Buffers. Methods in Enzymology 24(B). 53-68.

Good, N.E., Winget, G.D., Winter, W., Connolly, T.N., Izawa, S., Singh, R.M.M. (1966) Hydrogen Ion Buffers for Biological Research. Biochemistry 5(2). 467-477.

Gordon, C.C, Buikstra, J.E.(1981) Soil pH, Bone Preservation and Sampling Bias at Mortuary Sites. American Antiquity 46. 566-571.

Greenland, D.J., Hayes, M.H.B.(Eds.) (1981) The Chemistry of Soil Processes. Wiley and Sons Ltd., Chichester.

Greenwood, N.N., Earnshaw, A.(1984) Chemistry of the Elements. Pergamon Press, Oxford. pp1450-1486.

Grime, G.W., Dawson, M., Marsh, M., McArthur, I.C., and Watt, F. (1991a) The Oxford Submicron Nuclear Microscopy Facility. Nuclear Instruments and Methods in Physics Research B54. pp52-63. North-Holland Physics Publishing.

Grime, G.W., Watt, F., Duval, A.R. and Menu, M. (1991b) Nuclear Microscopy of Inhomogeneous Thick Samples. Nuclear Instruments and Methods in Physics Research B54. pp353-362. North-Holland Physics Publishing.

Grime, G.W., Watt, F. and Sutton, C. (1991c) Microscopes with Proton Power. New Scientist (June 1)

Grupe, G. (1988) Impact of the Choice of Bone Samples on Trace Elemental Data in Excavated Human Skeletons. Journal of Archaeological Science 15. 123-129.

Grupe, G., Hummel, S.(1991) Trace Elements Studies on Experimentally Cremated Remains. I. Alteration of the Chemical Composition at High Temperatures. Journal of Archaeological Science 18. 177-186.

Grupe, G., Piepenbrink, H. (1988) Trace Element Contamination in Excavated

Bones by Microorganisms. In (G.Grupe, B.Herrmann, eds.) Trace Elements in Environmental History. Springer-Verlag, Berlin. pp103-112.

Gude, W.D. (1968) Autoradiographic Techniques : Localisation of Radioisotopes in Biological Material. Prentice-Hall: Biological Technique Series.

Hackett, C.J.(1981) Microscopical Focal Destruction (Tunnels) in Exhumed Human Bones. Medicine, Science and the Law 21. 243-265.

Hancock R.G.V., Grynpas, M.D., Pritzker, K.P.H. (1989) Abuse of Bone Analysis for Archaeological Dietary Studies. Archaeometry 31. 169-179.

Hancox, N.M.(1972) Biology of Bone: Biological Structure and Function. No.1. Cambridge University Press.

Hanson, D.B., Buikstra, J.E.(1987) Histomorphological Alteration in Buried Human Bone from the Lower Illinois Valley: Implications for Palaeodietary Research. Journal of Archaeologiacl Science 14. 549-563.

Hardy, R., Tucker, M.(1988) X-Ray Powder Diffraction of Sediments. In (M.Tucker, ed.) Techniques in Sedimentology. Chapter 7, pp191-228. Blackwell, Oxford.

Hare, P.E. (1980) Organic Geochemistry of Bone and its relation to the Survival of Bone in the Natural Environment. In (A.K.Behrensmeyer, A.P.Hill, eds.) Fossils in the Making. Chicago: University of Chicago Press. pp208-219.

Hare, P.E., Fogel, M.L., Stafford Jr., T.W., Mitchell, A.D., Hoering, T.C.(1991) The Isotopic Composition of Carbon and Nitrogen in Individual Amino Acids Isolated from Modern and Fossil Proteins. Journal of Archaeological Science 18. 277-282.

Harrison, G.E., Howells, G.R., Pollard, J. (1967) Comparative Uptake and Elution of Ca-45, Sr-85, Ba-133 and Ra-223 in Bone Powder. Calcified Tissue Research 1. 105-113.

Hassan, A.A.(1975) Geochemical and Mineralogical Studies on Bone and their Implications for Radiocarbon Dating. Unpublished Ph.D Thesis, Southern Methodist University, Texas.

Hassan, A.A., Ortner, D.J.(1977) Inclusions in Bone Material as a Source of Error in Radiocarbon Dating. Archaeometry 19. 131-135.

Hassan, A.A., Termine, J.D., Haynes, Jr, C.V. (1977) Mineralogical Studies on Bone Apatite and their Implications for Radiocarbon Dating. Radiocarbon 19. 364-374.

Hatch, J.W., Geidel, R.A.(1985) Status-Specific Dietary Variation in Two World Cultures. Journal of Human Evolution 14. 469-476.

Henderson, P., Marlow, C.A., Molleson, T.I., Williams, C.T. (1983) Patterns of Chemical Change During Bone Fossilisation and their Significance. Nature

306. 358-360.

Henderson, P., Pickford, M., Williams, C.T. (1987) A Geochemical Study of Rocks and Spring Waters at Kanam and Kanjera, Kenya, and the Implications Concerning Element Mobility and Uptake. Journal of African Earth Sciences 6. 221-227.

Hendry, G.L. (1975) X-Ray Fluorescence. In (Nicol, ed.) Physicochemical Methods of Mineral Analysis. Chapter 3, pp87-153. A.W. Plenum Press, New York.

Hennig,C.J, Grun,R. (1983) Electron Spin Resonance Dating in Quaternary Geology. Quaternary Science Review 2. 157-238.

Hill, A.P.(1980) Post-Mortem Damage to the Remains of Contemporary E.African Mammals. In (A.K.Behrensmeyer, A.P.Hill, eds.) Fossils in the Making. Part 3, Chapter 8. pp131-156. University of Chicago Press.

Hodge, A.J., Petruska, J.A.(1963). In (G.N.Ramachandran, ed.) Aspects of Protein Structure. pp289-300. Academic Press, London.

Hodges, R.M., Macdonald, N.S., Nusbaum, R., Stearns, R., Ezmerlain, F., Spain, P., MacArthur, C. (1950) The Strontium Content of Human Bones. Journal of Biological Chemistry 185. 519-524.

Holloway, J.R., Drake, M.J. (1977) Quantitative Microautoradiography by X-Ray Emission Microanalysis. *Geochimica et Cosmochimica Acta* 41. 1395-1397.

Hostleter, P.B., Garrels, R.M.(1962) Transport and Precipitation of Uranium and Vanadium at Low Temperatures, with Special Reference to Sandstone Type Uranium Deposits. Economic Geology 57. 137-167.

Ivanovich, M. (1982) Uranium Series Disequilibria Applications in Geochronology. In (M.Ivanovich, R.S.Harmon, eds.) Uranium Series Disequilibrium: Applications to Environmental Problems. Clarendon Press, Oxford.

Jackson, S.A., Cartwright, A.G., Lewis,D.(1978) The Morphology of Bone Mineral Crystals. Calcified Tissue Research 25. 217-222.

Jaksic, M., Grime, G.W., Henderson, J., Watt, F.(1991) Quantitative PIXE Analysis using a Scanning Proton Microbeam. Nuclear Instruments and Methods in Physics Research B54. 491-498.

Jenkins and deVries (1978) Worked examples in X-ray analysis.

Johnson, A.R., Armstrong, W.D., Singer, L. (1970) The Exchangeability of Calcium and Strontium of Bone *in vitro* . Calcified Tissue Research 6. 103-112.

Kamen, M.D. (1947) Radioactive Tracers in Biology : An Introduction to Tracer Methodology. Organic and Biological Chemistry I. Academic Press, New York.

Katzenberg, M.A. (1992) Advances in Stable Isotope Analysis of Prehistoric Bones.

In (S.R.Saunders and M.A.Katzenberg, eds.) Skeletal Biology of Past Peoples: Research Methods. Chapter 6, pp105-119. Wiley-Liss, Inc.

Kibby, C.L., Hall, W.K.(1972) Surface Properties of Calcium Phosphates. In (M.L.Hair, Ed.) Biochemical Surfaces Vol.2. Dekker, New York.

Kleeman, J.D., Lovering, J.F. (1967) Uranium Distribution Studies by Fission Track Registration in Lexan Plastic Prints. Sydney, Atomic Energy in Australia, 10. pp3-8.

Klepinger, L.L. (1984) Nutritional Assessment from Bone. Annual Review of Anthropology 13. 75-96.

Klepinger, L.L.(1992) Innovative Approaches to the Study of Past Human Health and Subsistence Strategies. In (S.R.Saunders, M.A.Katzenberg, eds.) Skeletal Biology of Past Peoples: Research Methods. Chapter 7 pp121-130. Wiley-Liss, Inc., New York.

Klepinger, L.L., Kuhn, J.K., Wendell, S. (1986) An Elemental Analysis of Archaeological Bone From Sicily as a Test of Predictability of Diagenetic Change. American Journal of Physical Anthropology 70. 325-331.

Klug, H.P.,Alexander, L.E. (1962) X-Ray Diffraction Procedures. Wiley, New York.

Kolodny, Y., Kaplan, I.R. (1970) Uranium Isotopes in Sea-Floor Phosphorites. *Geochimica Cosmochimica Acta* 34. 3-24.

Kyle, J.H. (1986) Effects of Post-Burial Contamination on the Concentrations of Major and Minor Elements in Human Bones and Teeth - the Implications for Paleodietary Research. Journal of Archaeological Science 13. 403-406.

Lally, A.E. (1982) Uranium Series Disequilibrium: Applications to Environmental Problems (M.Ivanovich, R.S.Harmon, eds.). Clarendon Press, Oxford.

Lambert, J.B., Simpson, S.V., Buikstra, J.E., Hanson, D. (1983) Electron Microprobe Analysis of Elemental Distribution in Excavated Human Femurs. American Journal of Physical Anthropology 62. 409-423.

Lambert, J.B., Simpson, S.V., Buikstra, J.E. Charles, D.K. (1984) Analysis of Soil Associated with Woodland Burials. In (J.B.Lambert, Ed) Archaeological Chemistry III, Advances in Chemistry, No.208. Washington,D.C.: American Chemical Society. pp97-113.

Lambert, J.B., Simpson, S.V., Szpunar, C.B., Buikstra, J.E. (1984) Ancient Human Diet from Inorganic Analysis of Bone. Accounts of Chemical Research 17. 298-305.

Lambert, J.B., Simpson, S.V., Szpunar, C.B., Buikstra, J.E. (1984) Copper and Barium as Dietary Discriminants: the Effects of Diagenesis. Archaeometry

26. 131-138.

Lambert, J.B., Simpson, S.V., Szpunar, C.B., Buikstra, J.E. (1985) Bone Diagenesis and Dietary Analysis. Journal of Human Evolution 14. 477-482.

Lambert, J.B., Simpson, S.V., Weiner, S.G., Buikstra, J.E. (1985) Induced Metal-Ion Exchange in Excavated Human Bone. Journal of Archaeological Science 12. 85-92.

Lambert, J.B., Szpunar, C.B., Buikstra, J.E. (1979) Chemical Analysis of Excavated Human Bone from Middle and Late Woodland Sites. Archaeometry 21. 115-129.

Lambert, J.B., Vlasak, S.M., Thometz, A.C., Buikstra, J.E. (1982) A Comparative Study of the Chemical Analysis of Ribs and Femurs in woodland Populations. American Journal of Physical Anthropology 59. 289-294.

Lambert, J.B., Xue,L., Buikstra, J.E. (1989) Physical Removal of Contaminative Inorganic Material from Buried Human Bone. Journal Archaeological Science 16. 427-436.

Lambert, J.B., Weydert, J.M., Williams, S.R., Buikstra, J.E. (1990) Comparison of Methods for the Removal of Diagenetic Material in Buried Bone. Journal Archaeological Science 17. 453-468.

Lambert, J.B., Xue, L., Buikstra, J.E. (1991) Inorganic Analysis of Excavated Human Bone after Surface Removal. Journal of Archaeological Science (3) 363-384.

Langmuir, D.(1978) Uranium Solution-Mineral Equilibria at Low Temperatures with Applications to Sedimentary Ore Deposits. *Geochimica et Cosmochimica Acta* 42. 547-569.

Lee-Thorp, J.A., van der Merwe, N.J. (1991) Aspects of the Chemistry of Modern and Fossil Biological Apatites. Journal of Archaeological Science 18. 343-354.

LeGeros, R.Z. (1981) Apatites in Biological Systems. Progress in Crystal growth Characteristics 4. 1-45.

LeGeros, R.Z., Kijowski, R., LeGeros, J.P. (1989) Effect of Strontium on some Properties of Apatites. In (R.W.Fearnhead, ed.) Proceedings of the Fifth International Symposium on Tooth Enamel (Tooth Enamel V) Tsurimi: Florence pp383-401.

LeGeros, R.Z., Quirolgico, G., Taheri, H. (1979) Consequences of Strontium Incorporation in Apatites. Journal Dental Research 58A, 168(abstract no. 301).

LeGeros, R.Z., Taheri, M.H., Quirolgico, G.B., LeGeros, J.P. (1980) Formation and Stability of Apatites: Effects of some Cationic Substituents. In: Proceedings of the 2nd International Congress on Phosphorus Compounds. Boston:

IMPHOS. pp89-103.

Legros, R., Bonel, G., Montel, G., Balmain-Oligo, N., Juster, M.(1977) Etude Systematique des Variations de Composition du Constituant Mineral de Differents Os de Divers Animaux Suivant sa Localisation. Comptes Rendus d'Academie des Sciences, Paris 285D. 1519-1522.

Lindsay, W.L.(1979) Chemical Equilibria in Soils. Wiley and Sons, New York.

March, J. (1977) Advanced Organic Chemistry: Reactions, Mechanisms and Structure. 2nd Edition. pp353-356. McGraw Hill Int. Book Co.

Marchiafava, V., Bonucci, E., Ascenzi, A. (1974) Fungal osteoclasia: a Model for Dead bone Resorption. Calcified Tissue Research 14. 195-210.

Mason, B., Moore, C.B. (1982) Principles of Geochemistry (4th Edition) Chichester, New York: John Wiley and Sons.

Masters, P.M.(1987) Preferential Preservation of Noncollagenous Protein During Bone Diagenesis: Implications for Chronometric and Stable Isotope Measurements. *Geochimica et Cosmochimica Acta* 51. 3209-3214.

Matsu'ura, S. (1978) Uranium Analysis of Fossil Bones using Fission Track Techniques and its Applications to Archaeological Science. Quaternary Research 17. 95-104.

McLean, F.C., Urist, M.R.(1955) Bone: An Introduction to the Physiology of Skeletal Tissue. Chicago: University of Chicago Press.

McConnell, D. (1973) Apatite. Its Crystal Chemistry, Mineralogy, Utilisation, and Geologic and Biologic Occurrences. Springer-Verlag, New York.

Nancollas, G.H., Mohan, M.S.(1970) The Growth of Hydroxyapatite Crystals. Archives of Oral Biology 15. 731-745.

Nelson, B.K., DeNiro, M.J., Schoeninger, M.J.,DePaolo, D.J., Hare, P.E. (1986) Effects of Diagenesis on Strontium, Carbon, Nitrogen and Oxygen Concentration and Isotopic Composition of Bone. *Geochimica et Cosmochimica Acta* 50. 194-199.

Nelson, D.A., Sauer, N.J. (1984) An Evaluation of Postdepositional Changes in the Trace Element Content of Human Bone. American Antiquity 49. 141-147

Neiler, J.H., Bell, P.R. (1965) The Scintillation Method. In (K.Siegbahn, ed.) Alpha-, Beta- and Gamma-Spectroscopy Vol.1. Chapter 5, pp245-302. North-Holland Publications.

Neuman, W.F.(1980) In (M.R.Urist, ed.) Fundamental and Clinical Bone Physiology. Chapter 4. pp83-107. J.B.Lippincott Co., Philadelphia.

Neuman, W.F., Neuman, M.W.(1958) The Chemical Dynamics of Bone Mineral.

Chicago: University of Chicago Press.

Neuman, W.F., Neuman, M.W., Mulyran, B.J. (1948a) The Deposition of Uranium in Bone. I Animal Studies. Journal Biological Chemistry 175. 705-709.

Neuman, W.F., Neuman, M.W.(1948b) The Deposition of Uranium in Bone. II Autoradiographic Studies. Journal Biological Chemistry 175. 710-714.

Neuman, W.F., Neuman, M.W., Main, E.R., Mulyran, B.J. (1948c) The Deposition of Uranium in Bone. III The Effect of Diet. Journal Biological Chemistry 175. 715-719.

Neuman, W.F., Neuman, M.W., Main, E.R., Mulyran, B.J. (1949a) The Deposition of Uranium in Bone. IV Adsorption Studies In Vitro. Journal Biological Chemistry 179. 325-334.

Neuman, W.F., Neuman, M.W., Main, E.R., Mulyran, B.J. (1949b) The Deposition of Uranium in Bone. V Ion Exchange Studies. Journal Biological Chemistry 179. 335-340.

Neuman, W.F., Neuman, M.W., Main, E.R., Mulyran, B.J. (1949c) The Deposition of Uranium in Bone. VI Ion Competition Studies. Journal Biological Chemistry 179. 341-348.

Newesely, H.(1989) Chemical Stability of Hydroxyapatite under Different Conditions. In (G.Grupe and B.Herrmann, eds) Trace Elements in Environmental History. Heidelberg: Springer-Verlag. pp1-16.

Norrish, K., Chappell, P.W. (1967) XRF Spectrography. In (J.Zussman, ed.) Physical Methods in Determinative Mineralogy. Academic Press, London.

Nriagn, J.O., Moore, P.B.(Eds.) (1984) Phosphate Minerals. Springer-Verlag, Berlin.

Osmond, J.K., Cowart, J.B. (1982) Ground Water. In (M.Ivanovich, R.S.Harmon, eds.) Uranium Series Disequilibrium: Applications to Environmental Problems. Clarendon Press, Oxford.

Parker, R.B.(1967) Electron Microprobe Analysis of Fossil Bones and Teeth. Geological Society of America Special Paper 101. 415-6

Parker, R.B., Toots, H.(1970) Minor Elements in Fossil Bone. Geological Society American Bulletin 81. 25-32.

Parker, R.B., Toots, H.(1972) Hollandite-Coronite in Fossil Bone. American Mineralogist 57. 1527.

Parker, R.B., Toots, H. (1980) Trace Elements in Bones as Palaeobiological Indicators. In (A.K.Behrensmeyer, A.P.Hill, eds.) Fossils in the Making. University of Chicago Press. pp197-207.

Pate, F.D., Brown, K.A. (1985) The Stability of Bone Strontium in the Geochemical Environment. Journal of Human Evolution 14. 483-491.

Pate, F.D., Hutton, J.T. (1988) The Use of Soil Chemistry Data to Address Post-Mortem Diagenesis in Bone Mineral. Journal of Archaeological Science 15. 729-739.

Pate, F.D., Hutton, J.T., Norrish, K. (1989) Ionic Exchange Between Soil Solution and Bone : Toward a Predictive Model. Applied Geochemistry 4. 303-316.

Perrin, D.D., Dempsey, B. (1974) Buffers for pH and Metal Ion Control. Chapman and Hall Laboratory Manuals, London.

Piepenbrink, H.(1986) Two Examples of Biogenous Dead Bone Decomposition and Their Consequences for Taphonomic Interpretation. Journal of Archaeological Science 13. 417-430.

Plant, J.A., Raiswell, R.(1983) Principles of Environmental Geochemistry. In (I.Thornton, ed.) Applied Environmental Geochemistry. Chapter 1, pp1-38. Academic Press, London.

Posner, A.S.(1969) Crystal Chemistry of Bone Mineral. Physics Review 49. 760-792.

Posner, A.S. (1985) The Mineral of Bone. Clinical Orthopaedics and Related Research 200. 87-99.

Posner, A.S.(1985) The Structure of Bone Apatite Surfaces. Journal of Biomedical Material Research. Mar.19 (3). 241-250.

Posner, A.S., Betts, F., Blumenthal, N.C.(1981) Formation and Structure of Synthetic and Bone Hydroxyapatites. In (B.R.Pamplin, ed.) Progress in Crystal Growth and Characterisation Vol.3. pp49-65. Pergamon Press Ltd.

Potts, P.J.(1987) Handbook of Silicate Rock Analysis.

Potts, P.J. (1984) Neutron Activation-Induced Beta Autoradiography as a Technique for Locating Minor Phases in Thin Section: Application to Rare Earth Element and Platinum-Group Element Analysis. Economic Geology 79. 738-747.

Potts, P.J. (1986) Neutron Activation-Induced Beta Autoradiography as a Technique for Locating Minor Phases in Thin Section: Emulsion Response Characteristics. In (R.Freer, P.F.Dennis, eds.) Mass Transport in Silicate and Oxide Systems. Material Science Forum 7. pp35-44. Aedermannsdorf, Switzerland: Trans. Technical Publications.

Price, T.D.(1989) The Chemistry of Prehistoric Human Bone. Cambridge University Press.

Price, T.D. (1989) Multi-element Studies of Diagenesis in Prehistoric Bone. In

(T.D.Price, ed.) The Chemistry of Prehistoric Human Bone. Cambridge University Press. pp126-154.

Price, T.D., Kavanagh, M.(1982) Bone Composition and the Reconstruction of Diet: Examples from the Mid-Western United States. Mid-Continent Journal of Archaeology 7. 61-79.

Price, T.D., Blitz, J., Burton, J., Ezzo, J.A.(1992) Diagenesis in Prehistoric Bone: Problems and Solutions. Journal of Archaeological Science 19. 513-529.

Price, T.D., Schoeninger, M.J., Armelagos, G.J. (1985). Bone Chemistry and Past Behaviour: an overview. Journal of Human Evolution 14. 419-447.

Priest, N.D., Howells, G.R., Green, D., Haines, J.W. (1982) Uranium in Bone: Metabolic and Autoradiographic Studies in the Rat. Human Toxicology 1. 97-114.

Rae, A.M. (1987) Uranium Series Dating of Bone and Cave Deposits. D.Phil.Thesis, University of Oxford.

Rae, A.M., Hedges, R.E.M., Ivanovich, M.(1989) Further Studies for Uranium-Series Dating of Fossil Bone. Applied Geochemistry 4. 331-337.

Rae, A.M., Ivanovich, M. (1986) Successful Application of Uranium Series Dating of Fossil Bone. Applied Geochemistry 1. 419-426.

Rae, A.M., Ivanovich, I., Schwarcz, H.P.(1987) Absolute Dating by Uranium Series Disequilibrium of Bones from the Cave of La Chaise-De-Vouthon (Charente), France. Earth Surface Processes and Landforms 12. 543-550.

Raisanen, J. (1986) Detection Limits of External Beam PIXE in the Analysis of Thick Samples for Elements with $Z > 26$. X-Ray Spectrometry 15. 159-166.

Randall, J.T., Fraser, R.D.B., Jackson, S., Martin, A.V.W., North, A.C.T. (1952) Aspects of Collagen Structure. Nature 169. 1029-1033.

Rankama, K., Sahama, Th.G. (1950) Geochemistry. University of Chicago Press.

Rheingold, A.L., Hues, S.,Cohen, M.N. (1983) Strontium and Zinc Content in Bones as as Indication of Diet. Journal of Chemical Education 60. 233-234.

Roeder, P.L., MacArthur, D., Ma, X.P., Palmer, G.R. and Mariano, A.N. (1987) Cathodoluminescence and Microprobe Study of Rare-Earth Elements in Apatite. American Mineralogist 72. 801-811.

Reeder, R.J., Grams, J.C. (1987) Sector Zoning in Calcite Cement Crystals: Implications for Trace Element Distributions in Carbonates. *Geochimica et Cosmochimica Acta* 51. 187-194.

Rogers, A.W. (1979) Techniques of Autoradiography. Elsevier/North-Holland Biomedical Press, Amsterdam.

Rokita, E.(1991) Physicochemical Studies of Aortic Wall Mineralization. Life Chemistry Reports 8. 185-242.

Rootare, H.M., Dietz, V.R., Carpenter, F.C. (1962) Solubility-Product Phenomena in Hydroxyapatite-Water Systems. Journal of Colloid Science 17. 179-206.

Rosholt, J.J. (1957) Quantitative Radiochemical Methods for the Determination of the Sources of Natural Radioactivity. Analytical Chemistry 29. 1398-1408.

Runia, L.T. (1987) Strontium and Calcium Distribution in Plants: Effect on Paleodietary Studies. Journal of Archaeological Science 14. 599-608.

Runia, L.T. (1987) The Chemical Analysis of Prehistoric Bones: A Palaeodietary and Ecoarchaeological Study of Bronze-Age West-Friesland. B.A.R. International Series 363.

Runia, L.T. (1988) Discrimination Factors on Different Trophic Levels in Relation to the Trace Element Content in Human Bones. In (G.Grupe, B.Herrmann, eds.) Trace Elements in Enviromental History. Springer-Verlag, Heidelberg. pp53-66.

Sandford, M.K. (1992) A Reconsideration of Trace Element Analysis in Prehistoric Bone. In (S.R.Saunders, M.A.Katzenberg, eds.) Skeletal Biology of Past Peoples: Research Methods. Chapter 5, pp79-103. Wiley-Liss, Inc., New York.

Santschi, P.H.(1988) Factors Controlling the Biogeochemical Cycles of Trace Elements in Fresh and Coastal Marine Waters as Revealed by Artificial Radioisotopes. Limnology and Oceanography 33(4). 848-866.

Schoeninger, M.J. (1979) Diet and Status at Chalcatzingo : some Empirical and Technical Aspects of Strontium Analysis. American Journal of Physical Anthropology 51. 295-310.

Schoeninger, M.J. (1985) Trophic Level Effects on 15N/14N and 13C/12C Ratios in Bone Collagen and Strontium Levels in Bone Mineral. Journal of Human Evolution 14. 515-526.

Schoeninger, M.J. (1989) Reconstructing Human Diet. In (T.D.Price, ed.) The Chemistry of Prehistoric Human Bone. Cambridge University Press. pp38-67.

Schoeninger, M.J., DeNiro, M.J.(1984) Nitrogen and Carbon Isotopic Composition of Bone Collagen from Marine and Terrestrial Animals. *Geochimica et Cosmochimica Acta* 48. 625-639.

Schoeninger, M.J., Moore, K.M., Murray, M.L., Kingston, J.D. (1989) Detection of Bone Preservation in Archaeological and Fossil Samples. Applied Geochemistry 4. 281-292.

Schoeninger, M.J., Peebles,C.S. (1981) Effects of Mollusc Eating on Human Bone

Strontium Levels. Journal of Archaeological Science 8. 391-397.

Schutkowski, H., Hummel, S. (1987) Variabilitatsvergleich von Wandstarken fur die Geschleechtszuweisung an Leichenbranden. Anthrologischer Anzeiger 45. 43-47.

Schutkowski, H., Hummel, S., Nitsch, K.H., Herrmann, B (1987). Struktur-und Elementanalysen sogenannter Clinker aus Brandgrabern. Archaologisches Korrespondenzblatt 17. 401-404.

Schwarcz, H.P. (1982) Applications of Uranium-Series Dating to Archaeometry. In (M.Ivanovich, R.S.Harmon, eds.) Uranium Series Disequilibrium: Applications to Environmental Problems. Clarendon Press, Oxford. pp302-325.

Sealy, J.C., Sillen, A. (1988) Sr and Sr/Ca in Marine and Terrestrial Foodwebs in the Southwestern Cape, South Africa. Journal of Archaeological Science 15. 425-438.

Sealy, J.C., van der Merwe, N.J., Sillen, A., Kruger, F.J., Krueger, H.W. (1991) Sr-87/Sr-86 as a Dietary Indicator in Modern and Archaeological Bone. Journal of Archaeological Science 18. 399-416.

Seitz, M.G., Taylor, R.E. (1974) Uranium Variations in Dated Fossil Bones. Archaeometry 16. 129-135.

Sharma, K.K., Choubey, V.M., Sharma, O.P., Nagpaul, K.K. (1981) Uranium Distribution in Siwalik Vertebrates using Fission Track Technique. Journal of the Geological Society of India 22. 92-97

Shemesh, A.(1990) Crystallinity and Diagenesis of Sedimentary Apatites. *Geochimica et Cosmochimica Acta* 54. 2433-2438.

Shinoda, G.(Ed.) (1972) Proceedings of the 6th International Conference on X-Ray Optics and Microanalysis. Tokyo University Press.

Shipman, P., Foster, G., Schoeninger, M. (1984) Burnt Bones and Teeth: an Experimental Study of Color, Morphology, Crystal Structure and Shrinkage. Journal of Archaelogical Science 11. 307-325.

Shipman, P., Walker, A., Bichell, D.(1985) The Human Skeleton. Cambridge, MA: Harvard University Press.

Sillen, A. (1981) Strontium and Diet at Hayonim Cave. American Journal of Physical Anthropology 56. 131-137.

Sillen, A. (1986) Biogenic and Diagenetic Sr/Ca in Plio-Pleistocene Fossils of the Omo Shngura Formation. Paleobiology 12. 311-323.

Sillen, A. (1989) Diagenesis of the Inorganic Phase of Cortical Bone. In (T.D.Price, ed.) The Chemistry of Prehistoric Human Bone. Cambridge University Press. pp211-229.

Sillen, A.(1992) Strontium-Calcium Ratios (Sr/Ca) of *Australopithecus Robustus* and Associated Fauna from Swaartkrans. Journal of Human Evolution 23. 495-516.

Sillen, A., Kavanagh, M. (1982) Strontium and Paleodietary Research: a Review. Yearbook of Physical Anthropology 25. 67-90.

Sillen, A., LeGeros, R. (1991) Solubility Profiles of Synthetic Apatites and of Modern and Fossil Bones. Journal of Archaeological Science 18. 385-397.

Sillen, A., Sealy, J.C., van der Merwe, N.J.(1989) Chemistry and Palaeodietary Research: no more easy answers. American Antiquity 54. 3.

Sissons, H.A.(1971) The Growth of Bone. In (G.H.Bourne, ed.) Biochemistry and Physiology of Bone Vol. III. Chapter 4 pp145-180. Academic Press, New York.

Smith, K.C., Bradley, D.A.(1952) Radioactive Dinosaur Bones from the Camp Davies Region, Western Wyoming. Michigan Academic Science Papers 37. 257-263.

Spadaro,J.A. (1969) Trace Metal Ions in Bone and Collagen. Unpublished Ph.D.Dissertation. Department of Physics, Syracuse University, Syracuse, New York.

Spadaro, J.A., Becker, R.O.(1970) Size-specific Metal Complexing Sites in Native Collagen. Nature 225. 1134-1136.

Spadaro, J.A., Becker, R.O., Bachman, C.H.(1970) The Distribution of Trace Metal Ions in Bone and Tendon. Calcified Tissue Research 6. 49-54.

Stevens, W., Bruenger, F.W., Atherton, D.R., Smith, J.M., Taylor, G.N. (1980) The Distribution and Retention of Hexavalent U-233 in the Beagle. Radiation Research 83. 109-126.

Storey, J.M.V., Symonds, R.P., Hart, F.A., Walsh, J.N. (1988) The Chemical Investigation of "Colchester" Samian by Means of Inductively Coupled Plasma Emission Spectrometry. Journal of Roman Pottery Studies 2.

Stumm, W., Morgan, J.J.(1970) Aquatic Chemistry: An Introduction Emphasizing Chemical Equilibria in Natural Waters. Wiley-Interscience.

Sullivan, C.H., Krueger, H.W.(1981) Carbon Isotope Ratios of Bone Apatite and Animal Diet Reconstruction. Nature 301. 177

Swedlow, D.B., Harper, R.A., Katz, J.L. (1972) Evaluation of a New Preparative Technique for Bone Examination in the S.E.M. In: Scanning Electron Microscopy Part III. Proceedings, Workshop on Biological S.E.M. pp335-342. Chicago: IIT Research Institute.

Szabo, B.J. (1980) Results and Assessment of Uranium Series Dating of Vertebrate Fossils from Quaternary Alluviums in Colorado. Arctic and Alpine Research

12 (1). 95-100.

Szabo, B.J., Dooley, Jr.J.R., Taylor, R.B., Rosholt, J.N. (1970) Distribution of Uranium in Uranium-Series Dated Fossil Shells and Bones shown by Fission Tracks. U.S. Geological Survey Professional Paper 700B. B90-B92.

Szalay, A. (1969) Accumulation of Uranium and Other Organic Shales and the Role of Humic Acids in these Geochemical Enrichments. Archiv.for Mineralogi Och Geologi 5. 23-36.

Szpunar, C.B., Lambert, J.B., Buikstra, J.E. (1978) Analysis of Excavated Bone by Atomic Absorption. American Journal of Physical Anthropology 48. 199-202.

Termine, J.D., Eanes, E.D., Greenfield, D.S., Nylen, M.U., Harper, R.A. (1973) Hydrazine-Deproteinated Bone Mineral: Physical and Chemical Properties. Calcified Tissue Research 12. 73-90.

Termine, J.D., Posner, A.S.(1967) Amorphous/Crystalline Interrelationships in Bone Mineral. Calcified Tissue Research 1. 8-23.

Thompson, M., Bush, P.R, Ferguson, J. (1987) The Analysis of Flint by Inductively Coupled Plasma Atomic Emission Spectrometry as a Method of Source Determination. Scientific Study of Flint, Proceedings of the International Symposium., Brighton. (Ed. G.de G. Sieveking). pp243-247.

Thompson, M., Walsh, J.N.(1989) Handbook of Inductively Coupled Plasma Spectrometry. 2nd Edition. London: Blackie and Son Ltd.

Thornton, I.(1983) Applied Environmental Geochemistry. Academic Press, London.

Tiemei, C., Sixun, Y.(1988) Uranium-Series Dating of Bones and Teeth from Chinese Palaeolithic Sites. Archaeometry 30(1). 59-76.

Toots, H., Voorhies, M.R. (1965) Strontium in Fossil Bones and the Reconstruction of Food Chains. Science 149. 854-855.

Traxel, K.(1990) Nuclear Microbeams: Realization and Use as Scientific Tool. Nuclear Instruments and Methods in Physics Research B50. 177-188.

Tripathi, V.S.(1979) Uranium Solutions - Mineral Equilibrium at Low Temperatures with Application to Sedimentary Core Deposits. *Geochimica et Cosmochimica Acta 43.* 1989-1990.

Turekian, K.K., Kulp, J.L. (1956) The Geochemistry of Strontium. *Geochimica et Cosmochimica Acta* 10. 248-296.

Tuross, N., Behrensmeyer, A.K., Eanes, E.D., Fisher, L.W., Hare, P.E. (1989a) Molecular Preservation and Crystallographic Alterations in a Weathering Sequence of Wildebeest Bones. Applied Geochemistry 4. 261-270.

Tuross, N., Behrensmeyer, A.K., Eanes, E.D. (1989b) Strontium Increases and Crystallinity Changes in Taphonomic and Archaeological Bone. Journal of Archaeological Science 16. 661-672.

Underwood, E.J.(1977) The Trace Elements in Human and Animal Nutrition. 4th Edition. Academic Press, New York.

Urist, M.R.(1976) Biochemistry of Calcification. In (G.H.Bourne, ed.) Biochemistry and Physiology of Bone. 2nd Ed. Vol IV. pp2-53. Academic Press, New York.

van der Merwe, N.J.(1982) Carbon Isotopes, Photosynthesis, and Archaeology. American Scientist 70. 596-606.

Vaughan, J.M. (1970) The Physiology of Bone. Clarendon Press, Oxford.

Vaughan, J.M.(1975) The Physiology of Bone. 2nd Edition. Clarendon Press, Oxford.

Vinogradov, A.P.(1959) The Geochemistry of Rare and Dispersed Chemical Elements in Soils. 2nd Edition. Chapters 9, 16. Consultants Bureau Inc., New York.

Vlasak, S.M.(1982) Elemental Analysis of Excavated Human Bone: A Study of Post-Mortem Deterioration. Ph.D. dissertation, Northwestern University.

Von Endt, D.W., Ortner, D.J.(1984) Experimental Effects of Bone Size and Temperature on Bone Diagenesis. Journal of Archaeological Science 11. 247-253.

Vuorinen, H.S., Tapper, U., Mussalo-Rauhamaa, H.(1990) Trace and Heavy Metals in Infants, Analysis of Long Bones from Ficana, Italy, 8-6th Century B.C. Journal of Archaeological Science 17. 237-254.

Waldron, H.A., Khera, A., Walker,G., Wibberly, G., Green, C.J.S. (1979) Lead Concentrations in Bones and Soil. Journal of Archaeological Science 6. 35-40.

Walser, M., Robinson, B.(1963) Renal Excretion and Tubular Reabsorption of Calcium and Strontium. In (R.H.Wasserman, ed.) The Transfer of Calcium and Strontium across Biological Membranes. Academic Press, New York. pp211-228.

Walter, Ph., Menu, M., Dran, J.C.(1992) Dating of Archaeological Flints by Fluorine Depth Profiling: New Insights into the Mechanism of Fluorine Uptake. Nuclear Instruments and Methods in Physics Research B64. 494-498.

Walters, M.A., Leung, Y.C., Blumenthal, N.C., LeGeros, R.Z., Konsker, K.A.(1990) A Raman and Infra-red Spectroscopic Investigation of Biological Hydroxyapatite. Journal of Inorganic Biochemistry 39. 193-200.

Watt, F., Grime, G.W., Brook, A.J., Gadd, G.M., Perry, C.C., Pearce, R.B., Turnau, K., and Watkinson, S.C. (1991) Nuclear Microscopy of Biological

Specimens. Nuclear Instruments and Methods in Physics Research B54. 123-143. North-Holland Physics Publishing.

Watt, F. and Grime, G.W. (1987) Principles and Applications of High-Energy Ion Microbeams. Adam Hilger, Bristol. IOP Publishing Ltd.

Wedepohl, K.H. (1978) Handbook of Geochemistry. Springer-Verlag, Berlin.

White, E.M., Hannus, L.A. (1983) Chemical Weathering of Bone in Archaeological Soils. American Antiquity 48. 316-322.

White, C.D., Schwarcz, H.P.(1989) Ancient Maya Diet: as Inferred from Isotopic and Elemental Analysis of Human Bone. Journal of Archaeological Science 16. 451-474.

Willans, S.M., McCarthy, I.D.(1986) Distributed Model of Blood-Bone Exchange. Journal of Biomedical Engineering. Jul.8(3). 235-243.

Williams, C.T. (1988) Alteration of Chemical Composition of Fossil Bones by Soil Processes and Groundwater. In (G.Grupe, ed.) Trace Elements in Environmental History. Springer-Verlag, Berlin. pp27-40.

Williams, C.T., Marlow, C.A. (1987) Uranium and Thorium Distributions in Fossil Bones From Olduvai Gorge, Tanzania and Kanam, Kenya. Journal of Archaeological Science 14. 297-309.

Williams, C.T., Potts, P.J. (1988) Element Distribution Maps in fossil bones. Archaeometry 30 (2).237-247.

Winter, L.C., Marlow, M (1991) Kitchen Chemistry? The Use of Microwaves in the Analysis of Human Bone. Proceedings of the Archaeological Sciences Conference Bradford, 20-22 Sept. 1989. Oxbow Books.

Wood, E.J. (1980) Atomic Absorption Spectroscopy. In (S.B.Brown, ed.) An Introduction to Spectroscopy for Biochemists. Chapter 8. Academic Press, London.

Wyckoff, R.W.G.(1972) The Biochemistry of Animal Fossils. Scientifica Publ.Ltd, Bristol.

Wyckoff, R.W.G., Doberenz, A.R. (1968) The Strontium Content of Fossil Teeth and Bones. *Geochemica Cosmochimica Acta* 32. 109-115

Zipkin,I. (1973) Biological Mineralization. Wiley, New York.

APPENDICES

APPENDIX I.

APPENDIX Ia: XRF DATA AGAINST ASHING TEMPERATURE

(values in ppm)

Ashing temperature 500 C :

Si	300	Mn	n.d	Sr	356	V	52
Al	100	P	417800	Rb	11	Cr	n.d
Fe	100	S	300	Zn	118	Nd	1
Mg	13300	Ba	80	Cu	5	Ga	4
Ca	518300	Nb	n.d	Ni	n.d	La	10
Na	15500	Zr	26	Pb	9	Ce	21
K	2200	Y	n.d	U	1		
Ti	n.d			Th	2	(H2O	52500)

Loss-on-ignition : 37.83 %

Ashing temperature 800 C :

Si	500	Mn	100	Sr	370	V	54
Al	100	P	439800	Rb	9	Cr	n.d
Fe	100	S	200	Zn	110	Nd	n.d
Mg	15300	Ba	83	Cu	18	Ga	n.d
Ca	525800	Nb	n.d	Ni	n.d	La	n.d
Na	15100	Zr	27	Pb	10	Ce	13
K	600	Y	n.d	U	1		
Ti	100			Th	0	(H2O	10500)

Loss-on-ignition : 39.16 %

Ashing temperature 1000 C :

Si	400	Mn	100	Sr	356	V	49
Al	100	P	431500	Rb	8	Cr	n.d
Fe	100	S	300	Zn	24	Nd	n.d
Mg	14400	Ba	76	Cu	79	Ga	2
Ca	524800	Nb	n.d	Ni	n.d	La	5
Na	9900	Zr	26	Pb	7	Ce	26
K	400	Y	n.d	U	2		
Ti	100			Th	2	(H2O	5000)

Loss-on-ignition : 41.42 %

where n.d = not detected (either not present, or in quantities below detection limit).

APPENDIX Ib

Experimental studies on the effects of hydrazine treatment of bone.

(1) % LOI and CHN.

Sample	Treatment (hrs)	Weight loss (%)	% LOI	% Carbon	% Hydrogen	% Nitrogen
1	000	00.00	36.00	n.m	n.m	n.m
2	002	08.57	31.00	n.m	n.m	n.m
3	005	08.65	30.00	13.41	2.50	05.49
4	009	08.69	29.00	n.m	n.m	n.m
5	017	08.76	28.37	n.m	n.m	n.m
6	024	08.95	19.00	05.29	1.15	01.28
7	048	09.90	15.70	n.m	n.m	n.m
8	072	10.90	05.16	01.43	0.58	00.18

where n.m = not measured.

(2) Chemical effects : XRF analysis.

Sample treatment(hrs)	% Ca (oxide)	% P (oxide)	Sr ppm	U ppm
26	54.17	41.28	350.88	1.80
48	49.33	44.00	354.45	0.00
72	49.95	43.12	322.49	0.39
144	48.69	43.62	345.45	7.28

APPENDIX Ic

IMMERSION SERIES I.

Dose Calculations

(I) U

100 mg $UO_2(NO_3)_2$ was added to 1 ml distilled water to make a stock solution. 1, 2, 5, and 10 μl of stock solution were then placed in separate scintillation tubes containing 10 ml scintillation filter solution. The number of counts per solution is shown in the table below :

Volume	Conc. (ppm)	Counts
1 μl	10	108
2 μl	20	226
5 μl	50	603
10 μl	100	1331

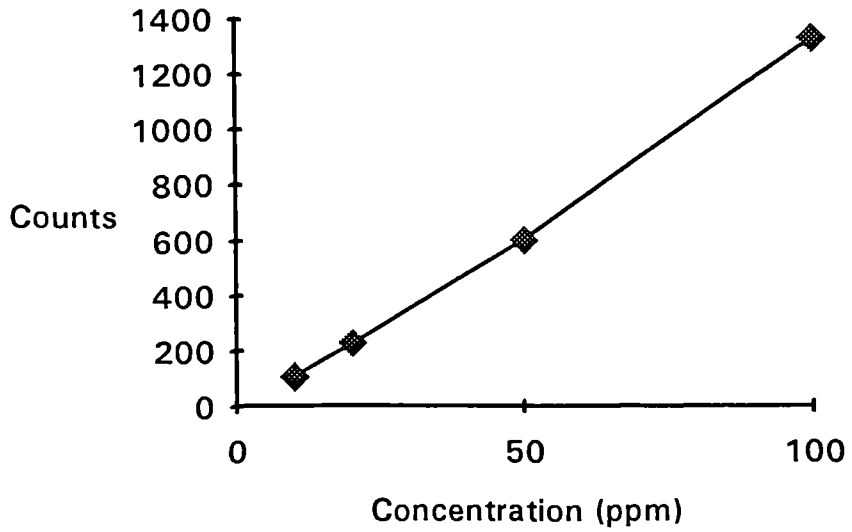

From the graph, the following concentrations were calculated :

1 μl of a 100,000 ppm uranium solution (100 mg uranium salt in 1 ml solution) $\equiv$ 108 counts.

$\therefore$ mass $UO_2(NO_3)_2$ in 1 μl = $100/10^6$ = 0.1 mg

$\therefore$ 0.1 mg $UO_2(NO_3)_2$ $\equiv$ 108 counts.

So, mass $UO_2(NO_3)_2$ required for 1 M counts = $0.1/108 \times 1$ M = 926 mg

Similarly, from the graph , 10 μl of solution $\equiv$ 1331 counts
$\therefore$ 1 mg $UO_2(NO_3)_2$ $\equiv$ 1331 counts.
$\therefore$ For 1 M counts, 751 mg required.

So, approx. **1g** $UO_2(NO_3)_2$ required for each sample to give **1M** counts.

APPENDIX II.

APPENDIX IIa : QUANTITATIVE ANALYSIS OF REFERENCE BONE AND PHOSPHATE MATERIALS BY XRF.

(1) Reference Materials.

Reference Material	% oxide % Ca	% P	ppm Sr	U
Ashed ovine bone	50.69	42.99	130.22	9.44
Ashed ovine bone	49.82	41.88	130.97	0.96
Ashed ovine bone	49.69	42.68	35.64	10.27
Phosphate rock (SARM32)	54.39	39.44	5206.79	27.00
Phosphate rock	55.13	37.63	4687.49	16.84
Phosphate rock	55.20	37.53	4555.86	15.54
CERTIFIED VALUES*	54.44	39.96	5200.00	
Modern human bone	48.31	44.16	81.97	7.62
IAEA-H5 bone std	49.44	43.91	270.50	6.27
IAEA-H5 bone std	50.54	42.17	220.41	4.50
IAEA-H5 bone std	51.01	42.09	224.67	4.03
CERTIFIED VALUES**	21.20	10.20	96.00	-

Reference authorities:
*British Chemical Standards **International Atomic Energy Authority.

APPENDIX IIb : QUANTITATIVE DATA FOR IMMERSION SERIES II STRONTIUM UPTAKE OVER TIME

where original [strontium] in immersing solution = 4M or 555800 ppm
bone analysed by XRF.

Duration of Immersion (weeks)	Whole/Ashed Bone	XRF Analysis of bone % CaO	% P2O5	Sr(ppm)
1	Whole	50.24	38.71	78156.20
6	Whole	52.02	34.97	090256.72
6	Whole	49.57	40.08	086389.45
10	Whole	49.73	24.81	100120.70
1	Ashed	36.94	24.28	122530.70
6	Ashed	36.47	21.70	143461.80
6	Ashed	46.43	27.68	111807.40
10	Ashed	35.35	23.36	136422.70

APPENDIX IIc : QUANTITATIVE DATA FOR CONTROL IMMERSIONS

AIM : To examine the effects of pH on the Ca, P, Sr and U levels in bone of variable organic:inorganic ratio in buffered water for 2 weeks.

Bone analysed by XRF ; solutions by AAS (Ca), AES (Sr) and LSC (U).

		XRF Analysis of bone				AAS Analysis of solution	AES	LSC
Desc. of bone	pH	% CaO	% P2O5	Sr(ppm)	U(ppm)	Ca (ppm)	Sr (ppm)	U(cts) *
Whole	4	49.83	43.07	289.57	2.86	060	9.0	27.60
Whole	7	48.80	43.53	320.05	2.25	006	5.0	25.70
Whole	10	50.00	43.72	347.11	0.00	000	0.0	25.00
Ashed	4	49.99	43.58	188.32	2.27	166	8.0	20.40
Ashed	7	49.42	43.70	167.34	6.39	095	5.0	19.20
Ashed	10	50.12	42.30	125.05	0.12	000	0.0	23.60
Hydrazine	4	53.39	41.17	271.07	1.60	079	7.0	25.60
Hydrazine	7	50.13	43.22	282.81	0.00	076	5.0	25.00
Hydrazine	10	48.44	44.15	285.59	0.48	000	0.0	21.80 *

* see Appendix IIIb for conversion of scintillation counts to ppm.

APPENDIX IId : QUANTITATIVE DATA FOR IMMERSION SERIES III
STRONTIUM UPTAKE AGAINST pH OF IMMERSION.

where original [strontium] in immersing solution = 1 M or 139,000 ppm (2 weeks); bone analysed by XRF ; solutions by AAS (Ca) and AES (Sr).

(1) Whole bone immersions.

pH of Immersion	Analysis of bone			Analysis of solution	
	% CaO	% P2O5	Sr(ppm)	Ca (ppm)	Sr (ppm)
4	48.98	43.97	13300.90	166	639
4	51.17	42.36	15157.82	189	600
6	49.22	31.02	16001.60		
7	50.58	42.70	17849.07	037	602
7	52.61	42.76	21252.22	044	550
8	51.53	34.96	17539.30		
10	50.03	43.03	17429.52	002	230
10	52.83	40.02	17647.14	002	185

(2) Hydrazine-treated bone immersions.

pH of Immersion	Analysis of bone			Analysis of solution	
	% CaO	% P2O5	Sr(ppm)	Ca (ppm)	Sr (ppm)
4	48.60	43.98	18545.35	244	nm
4	50.82	42.69	18831.74	247	nm
4	50.39	43.50	19855.79	260	nm
7	50.30	42.93	19842.29	043	nm
7	50.62	42.90	22690.03	048	nm
7	50.23	42.53	23138.00	051	nm
10	50.48	41.81	22306.80	000	nm
10	50.77	42.44	24299.64	001	nm
10	51.82	41.08	23525.54	001	nm

(3) Ashed bone immersions.

pH of Immersion	Analysis of bone			Analysis of solution	
	% CaO	% P2O5	Sr(ppm)	Ca (ppm)	Sr (ppm)
4	49.83	43.93	14005.87	292	nm
4	48.88	43.84	12927.85	270	nm
4	50.46	43.12	12617.37	259	nm
7	51.40	42.18	15615.81	081	nm
7	49.16	43.85	15837.67	082	nm
10	51.81	42.16	20703.77	000	nm
10	51.18	42.01	17518.35	000	nm

where nm = not measured.

APPENDIX III.

APPENDIX IIIa : QUANTITATIVE DATA FOR IMMERSION SERIES III URANIUM UPTAKE AGAINST pH OF IMMERSION.

where original [uranium] in solution = 2240 ppm, 2 weeks immersion.
bone analysed by XRF ; solutions by AAS (Ca), AES (Sr), LSC (U).

(1) Whole bone immersions.

pH of Immersion	XRF Analysis of bone				AAS Analysis of sol.	LSC Analysis of sol.
	% CaO	% P2O5	Sr(ppm)	U(ppm)	Ca (ppm)	U (cts) *
4	50.64	43.08	251.24	93.51	142	23.80
4	51.36	42.81	270.52	117.01	168	27.60
6	49.60	43.22	87.95	8253.73		
7	50.56	43.69	231.58	7479.96	013	44.00
7	50.86	40.81	128.53	6262.07	011	37.00
8	51.17	40.85	55.08	4173.45		
10	50.97	41.40	129.94	2772.88	001	40.40
10	52.14	41.84	172.92	7328.88		38.00
10	49.09	43.95	104.93	2439.58		43.00 *

(2) Hydrazine-treated bone immersions.

pH of Immersion	XRF Analysis of bone				Analysis of sol.	
	% CaO	% P2O5	Sr(ppm)	U(ppm)	Ca (ppm)	U (cts) *
4	51.27	40.92	61.67	13608.72	146	21.40
4	48.67	43.86	69.13	12275.56	131	20.20
4	53.59	39.51	65.33	10793.22	115	22.20
7	50.91	41.90	98.85	10577.57	014	22.40
7	48.17	38.00	18.64	9213.17	012	25.80
7	50.94	40.82	68.41	11682.54	015	28.40
10	51.18	42.50	56.99	11804.92	000	26.40
10	51.10	42.27	63.15	11890.48	001	20.20
10	50.86	42.08		10748.05	000	23.80 *

(3) Ashed bone immersions.

pH of Immersion	XRF Analysis of bone				Analysis of sol.	
	% CaO	% P2O5	Sr(ppm)	U(ppm)	Ca (ppm)	U (cts) *
4	50.44	41.96		10019.35	220	25.00
4	48.77	43.47		10837.82	237	21.60
4	50.65	43.03		11145.60	245	21.40
7	50.73	41.82		9733.90	034	23.80
7	52.08	41.00		11002.39	038	24.20
7	49.52	43.39		9998.39	034	26.40
10	51.99	41.41		9927.61	000	26.00
10	52.01	41.76		10324.02	001	18.80
10	52.53	42.11		7851.62	000	27.20

* see Appendix IIIb for conversion of scintillation counts to ppm.

APPENDIX IIIb : LIQUID SCINTILLATION COUNTS.

* Count readings for standard solutions and background for conversion of scintillation counts to ppm.

(All count readings for uranium in Appendices II and III represent counts/minute/100 microlitres of solution, counting period 5 minutes, where background has not been subtracted).

Standard U solution	Counts (cpm)	Counts - B
Background (B)	24.80	N/A
22.4 ppm	25.40	0.6
224.0 ppm	79.40	54.6
1000.0 ppm	168.00	143.2
2240.0 ppm	581.60	556.8
4480.0 ppm	1150.60	1125.8

APPENDIX IIIc : PIXE AND RBS DATA FOR PROTON MICROPROBE ANALYSIS OF BONE IMMERSED IN URANIUM SOLUTION.

Variables : organic:inorganic ratio of bone (whole, ashed, hydrazined)
pH of immersion

(i) A Comparison of U/Ca atomic % ratio by PIXE and RBS analyses to determine Scale Factor (plotted in Figure 7.21)

Selected spectra	R B S DATA			P I X E D A T A	
	Average height of		R RBS % (R1)	R PIXE (R2)	Scale
	ch.401-420 U (HU)	ch.379-388 Ca (HCa)	20 x HU x 8.41 / 92 HCa 8.331	%	factor (R1/R2)
Hydrazined	52.0	25.0	9.9	15.57	0.64
pH 7	19.6	15.5	6.03	7.90	0.76
	4.75	31.15	0.73	0.70	1.04
Ashed, pH7	33.75	54.85	2.89	3.00	0.96
Hydrazined,pH10	24.25	25.75	4.49	3.72	1.21
	15.7	23.4	3.20	3.33	0.96
Whole,pH7	4.8	22.6	1.01	4.15	0.24
Ashed,pH10	7.95	17.75	2.14	1.41	1.52
	6.35	18.85	1.61	1.20	1.34
	7.65	14.95	2.44	1.63	1.50

APPENDIX IIIc cont.

(ii) PIXE Data : U/Ca atomic % measured with incremental distance into periosteal cortical tissue of bone sample.

(12 micron proton beam diameter, generally scanning every 3 microns into sample).

A. pH 4 Immersions.

(1) Whole Bone immersed at pH 4.

Distance from starting point of scan (microns)	U/Ca atomic %
0	n.d
3	n.d
12	n.d
24	n.d
30	n.d
51	n.d
57	n.d

(2) Hydrazine-treated bone at pH 4.

Distance from starting point of scan (microns)	U/Ca atomic %
0	n.d
3	n.d
6	n.d
12	n.d
24	n.d
30	n.d
57	n.d

(3) Ashed bone immersed at pH 4.

Distance from starting point of scan (microns)	U/Ca atomic %
0	n.d
3	n.d
9	n.d
15	n.d
21	n.d
33	n.d
51	n.d

where n.d = not detected.

APPENDIX IIIc cont. B. pH 7 Immersions.

(1) Whole bone immersed at pH 7. (plotted in figure 7.26)

Distance from starting point of scan (microns)	U/Ca atomic %
0	1.88
3	2.01
6	1.98
9	1.68
12	2.22
15	1.12
18	0.77
21	0.80
24	0.29
27	0.26
30	0.15
33	0.02

(2) Hydrazine-treated bone at pH 7 -linescan #1 (plotted in fig. 7.27)

Distance from starting point of scan (microns)	U/Ca atomic %
0	12.55
3	13.49
6	12.94
12	15.84
18	18.29
24	15.57
30	19.87
36	23.01
42	35.22
48	23.85
54	7.90
60	3.28
66	2.04
72	0.70
78	0.11

(2a) Hydrazine-treated bone at pH 7 -linescan #2

Distance from starting point of scan (microns)	U/Ca atomic %
0	13.85
3	14.40
6	15.06
12	15.98
39	1.79
45	0.80
51	0.28
57	0.12

(2b) Hydrazine-treated bone at pH 7 -linescan #3

Distance from starting point of scan (microns)	U/Ca atomic %
0	0.43
15	3.07
21	3.29
27	9.01
30	24.79
33	39.45
36	51.17
39	24.16

(3) Ashed bone immersed at pH 7 -linescan #1 (plotted in fig.7.28)

Distance from starting point of scan (microns)	U/Ca atomic %
0	30.06
3	27.65
6	20.09
9	15.14
12	11.91
18	6.99
24	5.60
30	5.04
39	4.89
51	3.60

(3a) Ashed bone immersed at pH 7 -linescan #2

Distance from starting point of scan (microns)	U/Ca atomic %
0	45.76
3	35.74
6	25.59
9	13.50
15	4.01
21	3.30
30	2.53
39	2.07
54	1.66
69	1.41

63	3.33		84	2.11
75	3.00		99	-
90	2.80		129	1.86
96	3.44		144	1.06

C. pH 10 Immersions.

(1) Whole bone immersed at pH 10
(plotted in figure 7.29)

Distance from starting point of scan (microns)	U/Ca atomic %
0	10.62
3	11.92
6	7.55
9	6.68
12	5.68
15	4.15
18	2.21
21	0.95
24	0.43
30	0.21
45	0.03

(2) Hydrazine-treated bone at pH 10
(plotted in figure 7.30)

Distance from starting point of scan (microns)	U/Ca atomic %
0	39.02
3	24.20
6	15.11
9	8.29
12	5.40
15	4.19
18	3.72
21	3.72
24	3.30
30	3.49
36	3.33
42	3.05
51	3.01
60	2.62
69	2.02
81	1.83
96	1.54
111	0.60
141	0.12

(3) Ashed bone immersed at pH 10
(plotted in figure 7.31)

Distance from starting point of scan (microns)	U/Ca atomic %
0	2.00
3	2.08
6	1.78
9	1.77
12	1.63
15	1.66
18	1.69
30	1.41
42	1.39
54	1.24
78	1.15
108	0.63
153	0.03

APPENDIX IV.

APPENDIX IVa

CRYSTALLINITY MEASUREMENTS USING XRD TO EXAMINE THE EFFECTS OF IMMERSION.

Variables : bone (hydrazine-treated and ashed material)
chemistry of immersing solution (buffered H2O, Sr and U)
pH of immersing solution
parameters of crystallinity measurements
(peaks of profile, type of measurement)

(1) Hydrazine-treated Bone.

(i) Control : no immersion.

Sample #	Peak (hkl) of diffraction profile	Crystallinity measurements D	B/H	I
1	002	0.167	0.220	0163.64
1	112/211	0.060	0.214	1300.62
1	310	0.062	1.000	0016.00
2	002	0.200	0.135	0185.19
2	112/211	0.059	0.181	1587.13
2	310	0.071	0.824	0238.06
3	002	0.167	0.167	0216.00
3	112/211	0.071	0.146	1344.00
3	310	0.067	0.833	0270.00

(ii) Buffered Water Immersions (1 sample represents each pH)

pH of immersion	Peak (hkl) of diffraction profile	Crystallinity measurements D	B/H	I
4	002	0.250	0.082	0195.12
4	112/211	0.074	0.116	1572.70
4	310	0.083	0.545	0266.34
7	002	0.250	0.082	0175.82
7	112/211	0.070	0.119	1715.00
7	310	0.083	0.667	0217.63
10	002	0.250	0.103	0155.34
10	112/211	0.083	0.112	1296.04
10	310	0.070	0.636	0320.89

APPENDIX IVa cont.

(iii) Strontium Immersions.

pH of immersion	Peak (hkl) of diffraction profile	Crystallinity measurements D	B/H	I
4	002	0.233	0.096	0193.50
4	112/211	0.077	0.117	1443.00
4	310	0.083	0.545	0264.00
(1) 7	002	0.222	0.115	0175.50
(1) 7	112/211	0.083	0.119	1212.00
(1) 7	310	0.077	0.765	0221.00
(2) 7	002	0.220	0.105	0196.77
(2) 7	112/211	0.077	0.120	1405.52
(2) 7	310	0.072	0.778	0247.95
10	002	0.250	0.114	0140.00
10	112/211	0.087	0.115	1150.00
10	310	0.067	0.882	0255.00

(iii) Uranium Immersions.

pH of immersion	Peak (hkl) of diffraction profile	Crystallinity measurements D	B/H	I
4	002	0.200	0.156	0160.00
4	112/211	0.071	0.156	1260.00
4	310	0.083	0.667	0216.00
(1) 7	002	0.250	0.098	0164.00
(1) 7	112/211	0.077	0.126	1339.00
(1) 7	310	0.083	0.667	0216.00
(2) 7	002	0.200	0.143	0174.83
(2) 7	112/211	0.071	0.163	1203.45
(2) 7	310	0.083	0.632	0229.68
10	002	0.182	0.183	0165.00
10	112/211	0.071	0.149	1316.00
10	310	0.105	0.500	0180.50

APPENDIX IVa cont.

(2) Ashed Bone

(i) Control : no immersion.

Sample #	Peak (hkl) of diffraction profile	Crystallinity measurements D	B/H	I
1	002	0.250	0.091	0175.82
1	112/211	0.080	0.139	1124.10
1	310	0.091	0.579	0208.56
2	002	0.248	0.092	0176.73
2	112/211	0.080	0.139	1124.10
2	310	0.088	0.582	0221.88
3	002	0.250	0.089	0179.78
3	112/211	0.091	0.129	0936.11
3	310	0.091	0.577	0209.34

(ii) Buffered Water Immersions (1 sample represents each pH)

pH of immersion	Peak (hkl) of diffraction profile	Crystallinity measurements D	B/H	I
4	002	0.250	0.093	0172.04
4	112/211	0.091	0.086	1404.17
4	310	0.100	0.371	0269.54
7	002	0.200	0.143	0174.83
7	112/211	0.069	0.146	1438.36
7	310	0.091	0.524	0230.45
7	002	0.222	0.102	0198.73
7	112/211	0.083	0.104	1395.74
7	310	0.083	0.600	0241.93

APPENDIX IVa cont.

(iii) Strontium Immersions.

pH of immersion	Peak (hkl) of diffraction profile	Crystallinity measurements D	B/H	I
4	002	0.200	0.143	0175.00
4	112/211	0.074	0.125	1458.00
4	310	0.067	0.833	0270.00
(1) 7	002	0.182	0.153	0198.00
(1) 7	112/211	0.080	0.113	1387.50
(1) 7	310	0.077	0.619	0273.00
(2) 7	002	0.200	0.119	0210.08
(2) 7	112/211	0.083	0.106	1219.80
(2) 7	310	0.125	0.296	0216.22
10	002	0.200	0.135	0185.00
10	112/211	0.083	0.112	1284.00
10	310	0.067	0.750	0300.00

(iii) Uranium Immersions.

pH of immersion	Peak (hkl) of diffraction profile	Crystallinity measurements D	B/H	I
4	002	0.222	0.125	0162.00
4	112/211	0.083	0.118	1224.00
4	310	0.091	0.524	0231.00
(1) 7	002	0.200	0.139	0180.00
(1) 7	112/211	0.080	0.118	1325.00
(1) 7	310	0.077	0.619	0273.00
(2) 7	002	0.200	0.135	0185.19
(2) 7	112/211	0.070	0.147	1384.54
(2) 7	310	0.031	0.647	0186.64
10	002	0.222	0.136	0148.50
10	112/211	0.080	0.137	1137.50
10	310	0.091	0.611	0198.00

Values in brackets are given to denote sample # where more than one sample analysed for a particular variable.

APPENDIX IVa.i

HISTOGRAM PLOTS OF THE THREE CRYSTALLINITY MEASUREMENTS TAKEN FOR ALL BONE SAMPLES SUBJECTED TO IMMERSION TREATMENT.

AIM : To investigate the normality of frequency distributions in the dataset and thus determine its suitability for subsequent ANOVA statistical tests. Crystallinity measurements are examined in turn: D (M1), B/H (M2) and I (M3).

M1 : D - reciprocal of peak breadth

```
   COUNT    MIDPOINT     ONE SYMBOL EQUALS APPROXIMATELY   .50 OCCURRENCES

       0      -.010
       0       .005
       0       .020
       1       .035   **
       0       .050
      11       .065   **********************
      25       .080   **************************************************
       5       .095   **********
       1       .110   **
       1       .125   **
       0       .140
       0       .155
       0       .170
       2       .185   ****
       8       .200   ****************
       5       .215   **********
       1       .230   **
       6       .245   ************
       0       .260
       0       .275
       0       .290
                      I....+....I....+....I....+....I....+....I....+....I
                      0         5         10        15        20        25
                                HISTOGRAM FREQUENCY
```

MEAN	.126	STD DEV	.068	MINIMUM	.031
MAXIMUM	.250				
VALID CASES	66	MISSING CASES	0		

APPENDIX IVa.i cont.

M2 : Peak breadth:height ratio

```
  COUNT    MIDPOINT    ONE SYMBOL EQUALS APPROXIMATELY    .60 OCCURRENCES

      6         .08  **********
     27         .12  *********************************************
     10         .16  ****************
      1         .20  **
      0         .24
      1         .28  **
      0         .32
      1         .36  **
      0         .40
      0         .44
      0         .48
      3         .52  *****
      2         .56  ***
      4         .60  *******
      3         .64  *****
      3         .68  *****
      0         .72
      3         .76  *****
      0         .80
      1         .84  **
      1         .88  **
                 I....+....I....+....I....+....I....+....I....+....I....+....I
                 0         6         12        18        24        30
                           HISTOGRAM FREQUENCY
```

MEAN	.289	STD DEV	.250	MINIMUM	.082
MAXIMUM	.882				
VALID CASES	66	MISSING CASES	0		

APPENDIX IVa.i cont.

M3 : Intensity

```
  COUNT    MIDPOINT    ONE SYMBOL EQUALS APPROXIMATELY    .60 OCCURRENCES

      0          28
      5         118  ********
     30         208  **************************************************
      9         298  ***************
      0         388
      0         478
      0         568
      0         658
      0         748
      0         838
      0         928
      0        1018
      2        1108  ***
      4        1198  *******
      5        1288  ********
      6        1378  **********
      3        1468  *****
      1        1558  **
      0        1648
      1        1738  **
      0        1828

                     I....+....I....+....I....+....I....+....I....+....I....+....I
                     0          6         12         18         24         30
                               HISTOGRAM FREQUENCY
```

MEAN	587.577	STD DEV	545.831	MINIMUM	140.000
MAXIMUM	1715.000				
VALID CASES	66	MISSING CASES	0		

APPENDIX IVb : MULTI-WAY ANOVA OF CRYSTALLINITY MEASUREMENTS

* * * A N A L Y S I S O F V A R I A N C E * * *

AIM : To examine the combined effects of pH, organic:inorganic ratio, and immersion treatment on the three measurements of crystallinity - D (M1), B/H (M2), and I (M3).

M1 D - reciprocal of peak breadth
by NEWPH
NEWBONE
NEWTR

Source of Variation	Sum of Squares	DF	Mean Square	F	Sig of F
Main Effects	.002	5	.000	.073	.996
NEWPH	.000	2	.000	.029	.971
NEWBONE	.000	1	.000	.065	.799
NEWTR	.001	2	.001	.102	.903
2-Way Interactions	.001	8	.000	.024	1.00
NEWPH NEWBONE	.000	2	.000	.036	.964
NEWPH NEWTR	.001	4	.000	.023	.999
NEWBONE NEWTR	.000	2	.000	.012	.988
3-Way Interactions	.002	4	.000	.077	.989
NEWPH NEWBONE NEWTR	.002	4	.000	.077	.989
Explained	.005	17	.000	.051	1.00
Residual	.296	48	.006		
Total	.301	65	.005		

APPENDIX IVb cont.

* * * A N A L Y S I S O F V A R I A N C E * * *

M2 Peak breadth:height ratio
by NEWPH
NEWBONE
NEWTR

Source of Variation	Sum of Squares	DF	Mean Square	F	Sig of F
Main Effects	.048	5	.010	.116	.988
NEWPH	.010	2	.005	.059	.943
NEWBONE	.011	1	.011	.132	.718
NEWTR	.027	2	.014	.167	.847
2-Way Interactions	.032	8	.004	.049	1.00
NEWPH NEWBONE	.006	2	.003	.035	.966
NEWPH NEWTR	.026	4	.006	.078	.989
NEWBONE NEWTR	.002	2	.001	.009	.991
3-Way Interactions	.049	4	.012	.149	.963
NEWPH NEWBONE NEWTR	.049	4	.012	.149	.963
Explained	.129	17	.008	.093	1.00
Residual	3.933	48	.082		
Total	4.062	65	.062		

M3 Intensity
by NEWPH
NEWBONE
NEWTR

Source of Variation	Sum of Squares	DF	Mean Square	F	Sig of F
Main Effects	97483	5	19496.544	.049	.998
NEWPH	26294	2	13147.223	.033	.968
NEWBONE	170	1	169.921	.000	.984
NEWTR	75019	2	37509.473	.094	.911
2-Way Interactions	29621	8	3702.650	.009	1.00
NEWPH NEWBONE	2803	2	1401.539	.004	.997
NEWPH NEWTR	15476	4	3868.996	.010	1.00
NEWBONE NEWTR	11295	2	5647.562	.014	.986
3-Way Interactions	21424	4	5356.057	.013	1.00
NEWPH NEWBONE NEWTR	21424	4	5356.057	.013	1.00
Explained	148528	17	8736.950	.022	1.00
Residual	19217031	48	400354.805		
Total	19365559	65	297931.673		

APPENDIX IVc : 1-Way ANOVA of Crystallinity Measurements

AIM : To examine the individual effects of (a) pH,
(b) organic:inorganic ratio of bone, and (c) immersion treatment
on the three crystallinity mesurements- D (M1), B/H (M2), and I (M3).

(a) The effects of pH : O N E W A Y A N O V A

Variable M1 D - reciprocal of peak breadth
By Variable PH

ANALYSIS OF VARIANCE

SOURCE	D.F.	SUM OF SQUARES	MEAN SQUARES	F RATIO	F PROB.
BETWEEN GROUPS	2	.0006	.0003	.0612	.9407
WITHIN GROUPS	63	.3008	.0048		
TOTAL	65	.3013			

Variable M2 Peak breadth:height ratio
By Variable PH

ANALYSIS OF VARIANCE

SOURCE	D.F.	SUM OF SQUARES	MEAN SQUARES	F RATIO	F PROB.
BETWEEN GROUPS	2	.0095	.0048	.0742	.9286
WITHIN GROUPS	63	4.0524	.0643		
TOTAL	65	4.0619			

Variable M3 Intensity
By Variable PH

ANALYSIS OF VARIANCE

SOURCE	D.F.	SUM OF SQUARES	MEAN SQUARES	F RATIO	F PROB.
BETWEEN GROUPS	2	22293.8531	11146.9266	.0363	.9644
WITHIN GROUPS	63	19343264.92	307035.9512		
TOTAL	65	19365558.78			

Appendix IVc cont.

(b) The effects of organic:inorganic ratio of bone.

Variable M1 D - reciprocal of peak breadth
By Variable NEWBONE

ANALYSIS OF VARIANCE

SOURCE	D.F.	SUM OF SQUARES	MEAN SQUARES	F RATIO	F PROB.
BETWEEN GROUPS	1	.0004	.0004	.0856	.7708
WITHIN GROUPS	64	.3009	.0047		
TOTAL	65	.3013			

Variable M2 Peak breadth:height ratio
By Variable NEWBONE

ANALYSIS OF VARIANCE

SOURCE	D.F.	SUM OF SQUARES	MEAN SQUARES	F RATIO	F PROB.
BETWEEN GROUPS	1	.0108	.0108	.1705	.6810
WITHIN GROUPS	64	4.0511	.0633		
TOTAL	65	4.0619			

Variable M3 Intensity
By Variable NEWBONE

ANALYSIS OF VARIANCE

SOURCE	D.F.	SUM OF SQUARES	MEAN SQUARES	F RATIO	F PROB.
BETWEEN GROUPS	1	169.9214	169.9214	.0006	.9812
WITHIN GROUPS	64	19365388.85	302584.2009		
TOTAL	65	19365558.78			

APPENDIX IVc cont.

(c) The effects of immersion treatment (exposure to Sr, U, H20)

Variable M1 D - reciprocal of peak breadth
By Variable TR

ANALYSIS OF VARIANCE

SOURCE	D.F.	SUM OF SQUARES	MEAN SQUARES	F RATIO	F PROB.
BETWEEN GROUPS	2	.0015	.0007	.1557	.8561
WITHIN GROUPS	63	.2999	.0048		
TOTAL	65	.3013			

Variable M2 Peak breadth:height ratio
By Variable TR

ANALYSIS OF VARIANCE

SOURCE	D.F.	SUM OF SQUARES	MEAN SQUARES	F RATIO	F PROB.
BETWEEN GROUPS	2	.0272	.0136	.2123	.8093
WITHIN GROUPS	63	4.0347	.0640		
TOTAL	65	4.0619			

Variable M3 Intensity
By Variable NEWTR

ANALYSIS OF VARIANCE

SOURCE	D.F.	SUM OF SQUARES	MEAN SQUARES	F RATIO	F PROB.
BETWEEN GROUPS	2	71018.3535	35509.1768	.1159	.8907
WITHIN GROUPS	63	19294540.42	306262.5464		
TOTAL	65	19365558.78			

APPENDIX IVd : CHN DATA FOR IMMERSED BONE.

Monitoring the Organic Content of Bone Immersed at Different pH over Variable Periods of Time.

Variables : state of bone (sliced v. powdered)
organic:inorganic content of bone (hydrazine-treated, ashed)
pH of immersion
duration of immersion

(i) Powdered Whole Bone.

pH of immersion	Duration of immersion (weeks)	% Nitrogen	% Carbon	% Hydrogen	Total % CHN
N/A	N/A	3.56	20.49	3.28	27.33
4	2	1.41	06.57	1.31	09.29
6	2	1.59	06.86	1.34	09.79
7	2	1.64	06.99	1.36	09.99
8	2	1.20	05.66	1.19	08.05
10	2	0.31	03.27	0.77	04.35
4	12	0.83	05.36	1.01	07.20
7	12	0.39	04.21	0.86	05.46
10	12	0.14	03.23	0.85	04.22

(ii) Sliced Whole Bone.

pH of immersion	Duration of immersion (weeks)	% Nitrogen	% Carbon	% Hydrogen	Total % CHN
4	2	4.39	15.29	2.63	22.31
7	2	3.45	11.59	2.05	17.09
10	2	3.97	12.98	2.36	19.31
4	5	3.75	12.59	2.10	18.44
7	5	4.10	13.53	2.21	19.84
10	5	4.33	14.57	2.57	21.47
4	12	3.16	11.31	1.88	16.35
7	12	2.13	08.09	1.45	11.67
10	12	3.17	11.13	1.97	16.27

APPENDIX IVd cont.

(iii) Sliced Hydrazine-treated Bone.

pH of immersion	Duration of immersion (weeks)	% Nitrogen	% Carbon	% Hydrogen	Total % CHN
N/A	N/A	1.28	05.29	1.15	07.72
7	2	0.29	03.08	0.77	04.14
10	2	0.08	01.98	0.69	02.75
4	5	0.42	02.88	0.75	04.05
7	5	0.34	02.71	0.75	03.80
10	5	0.04	01.62	0.60	02.26
4	12	0.20	02.09	0.63	02.92
7	12	0.16	01.99	0.67	02.82
10	12	0.06	01.93	0.69	02.68

where N/A represents control bone - not subjected to immersion procedure.

APPENDIX IVe : CATION EXCHANGE CAPACITY DATA

Sample	% Organic	Total CEC	Average Total CEC (meq/100g bone)
Collagen	100	42.8	
Collagen	100	42.8	43.07
Collagen	100	43.6	
Whole	37	68.57	
Whole	37	66.29	67.05
Whole	37	66.29	
Hydrazine(4)	30	34.1	
Hydrazine(4)	30	33.7	33.77
Hydrazine(4)	30	33.5	
Hydrazine(17)	25	32.0	
Hydrazine(17)	25	33.3	32.6
Hydrazine(17)	25	32.5	
Hydrazine(72)	5	32.4	
Hydrazine(72)	5	33.5	32.8
Hydrazine(72)	5	32.6	
Ashed	0	28.6	
Ashed	0	27.4	28.0
Ashed	0	28.0	
CaPO4 Std	0	16.0	
CaPO4 Std	0	15.0	15.6
CaPO4 Std	0	15.8	
Rock PO4	0	4.4	
Rock PO4	0	5.6	5.13
Rock PO4	0	5.4	

(Values in brackets for hydrazine-treated samples represent no. of hours of hydrazine treatment)

APPENDIX IVf : DETERMINATION OF EXCHANGEABLE CATIONS.

Bone description	Ca	Na	Mg	K	Ca	Na	Mg	K	
	ppm measured in soln.				cmol (+) per kg sample				
Whole bone	130.6	20.1	13.2	3.2	65.3	8.7	11.0	0.8	
Collagen	6.2	4.0	0.6	1.2	3.1	1.7	0.6	0.3	
Hydrazine (17hrs)	128.4	44.6	29.0	4.1					
Hydrazine (17hrs)	126.2	44.0	30.6	4.1	3.7	19.4	24.2	1.1	(av)
Hydrazine (72hrs)	115.3	39.9	25.8	3.6					
Hydrazine (72hrs)	116.3	21.0	20.8	2.4	57.9	13.2	19.4	0.8	(av)
Ashed bone	112.7	12.3	16.4	1.8	56.4	5.3	13.7	0.5	
Phosphate rock	108.4	0.30	9.6	0.9	54.2	0.1	8.0	0.2	
Synthetic HA	27.7	0.27	5.2	0.7	13.9	0.1	4.3	0.2	

APPENDIX V.

APPENDIX Va : EPMA DATA FOR ARCHAEOLOGICAL BONE MATERIAL FROM HARTLEPOOL.

Spectrum: TE1 SPOT A

ELMT	ZAF	%ELMT	+-	Error	ATOM.%		%OXIDE	FORMULA
CaK : 1	1.018	22.038	+-	.232	26.338	CaO	30.836	3.519
P K : 1	1.224	8.489	+-	.155	13.130	P2O5	19.454	1.754
NaK : 2	.618	< .499	+-	.249				
MgK : 1	.797	< .144	+-	.072				
AlK : 1	.885	< .109	+-	.055				
ClK : 1	.952	< .110	+-	.055				
K K : 1	1.130	< .133	+-	.067				
FeK : 1	.820	< .220	+-	.110				
S K : 1	.923	.266	+-	.071	.397	SO	.398	.053
SrL : 1	.856	< .323	+-	.162				
MnK : 1	.800	< .180	+-	.090				
PbM : 1	.661	< .326	+-	.163				
CuK : 1	.793	< .342	+-	.171				
ZnK : 1	.791	< .510	+-	.255				
O K : 1	.000	20.002			59.880			8.000
TOTAL		50.795			100.000		50.688	5.326

Spectrum: TE1 SPOT B

ELMT	ZAF	%ELMT	+-	Error	ATOM.%		%OXIDE	FORMULA
CaK : 1	1.018	13.914	+-	.187	26.479	CaO	19.469	3.552
P K : 1	1.221	5.181	+-	.125	12.760	P2O5	11.873	1.712
NaK : 2	.617	< .410	+-	.205				
MgK : 1	.795	< .121	+-	.060				
AlK : 1	.882	.111	+-	.052	.313	Al2O3	.209	.042
ClK : 1	.954	< .096	+-	.048				
K K : 1	1.131	< .115	+-	.057				
FeK : 1	.821	< .192	+-	.096				
S K : 1	.925	.180	+-	.060	.428	SO	.269	.057
SrL : 1	.853	< .265	+-	.133				
MnK : 1	.801	< .158	+-	.079				
PbM : 1	.662	< .276	+-	.138				
CuK : 1	.794	< .306	+-	.153				
ZnK : 1	.791	< .418	+-	.209				
O K : 1	.000	12.509			59.632			8.000
TOTAL		31.895			100.000		31.820	5.364

Spectrum: TE1 SPOT C

ELMT	ZAF	%ELMT	+-	Error	ATOM.%		%OXIDE	FORMULA
CaK : 1	1.016	24.429	+-	.245	24.951	CaO	34.181	3.362
P K : 1	1.212	9.730	+-	.166	12.861	P2O5	22.297	1.733
NaK : 2	.620	< .493	+-	.247				
MgK : 1	.785	< .149	+-	.075				
AlK : 1	.872	.201	+-	.067	.306	Al2O3	.381	.041
ClK : 1	.947	< .114	+-	.057				
K K : 1	1.123	< .140	+-	.070				
FeK : 1	.823	< .223	+-	.112				
S K : 1	.919	.425	+-	.075	.543	SO	.637	.073
SrL : 1	.846	< .342	+-	.171				
MnK : 1	.802	< .191	+-	.096				
PbM : 1	.659	< .342	+-	.171				
CuK : 1	.794	< .378	+-	.189				
ZnK : 1	.791	< .531	+-	.265				
O K : 1	.000	23.207			59.376			8.000
TOTAL		57.993			100.000		57.495	5.209

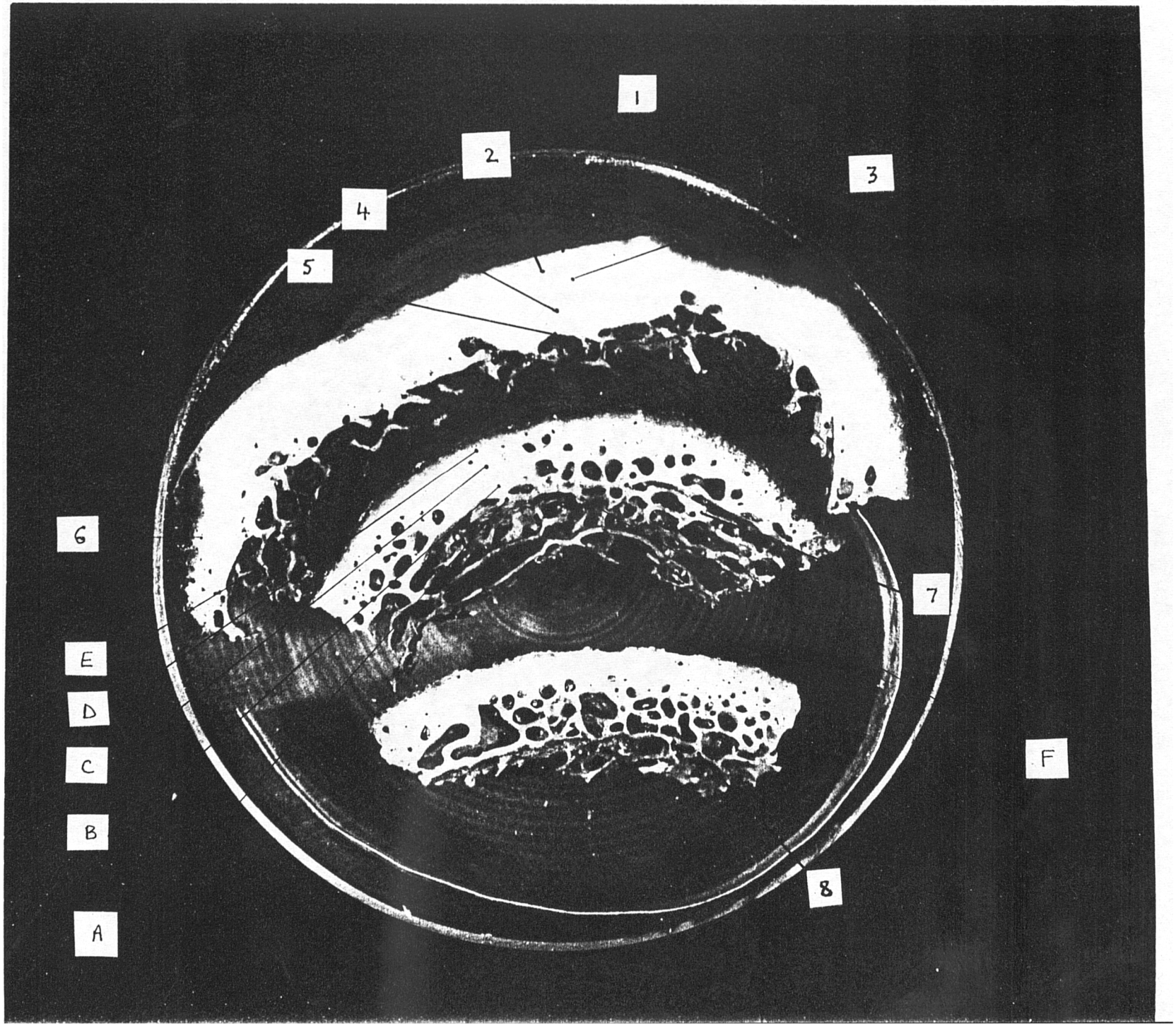
1
2
3
4
5
6
7
8
A
B
C
D
E
F

Spectrum: TE1 SPOT D

ELMT	ZAF	%ELMT	+-	Error	ATOM.%		%OXIDE	FORMULA
CaK : 1	1.017	23.875	+-	.241	26.173	CaO	33.406	3.517
P K : 1	1.221	9.017	+-	.160	12.792	P2O5	20.663	1.719
NaK : 2	.620	< .503	+-	.251				
MgK : 1	.796	< .145	+-	.072				
AlK : 1	.883	.193	+-	.063	.315	Al2O3	.365	.042
ClK : 1	.952	< .115	+-	.058				
K K : 1	1.129	< .136	+-	.068				
FeK : 1	.820	< .226	+-	.113				
S K : 1	.924	.418	+-	.074	.573	SO	.626	.077
SrL : 1	.853	< .330	+-	.165				
MnK : 1	.800	< .188	+-	.094				
PbM : 1	.662	< .342	+-	.171				
CuK : 1	.793	< .372	+-	.186				
ZnK : 1	.791	< .506	+-	.253				
O K : 1	.000	21.680			59.536			8.000
TOTAL		55.183			100.000		55.061	5.355

Spectrum: TE1 SPOT E

ELMT	ZAF	%ELMT	+-	Error	ATOM.%		%OXIDE	FORMULA
CaK : 1	1.018	27.514	+-	.258	26.778	CaO	38.498	3.593
P K : 1	1.224	10.156	+-	.167	12.793	P2O5	23.274	1.717
NaK : 2	.617	< .502	+-	.251				
MgK : 1	.795	< .149	+-	.074				
AlK : 1	.884	< .113	+-	.057				
ClK : 1	.953	< .118	+-	.059				
K K : 1	1.132	< .143	+-	.071				
FeK : 1	.821	< .237	+-	.118				
S K : 1	.926	.500	+-	.077	.608	SO	.750	.082
SrL : 1	.856	< .342	+-	.171				
MnK : 1	.800	< .193	+-	.096				
PbM : 1	.663	< .354	+-	.177				
CuK : 1	.793	< .383	+-	.191				
ZnK : 1	.791	< .550	+-	.275				
O K : 1	.000	24.453			59.618			8.000
TOTAL		62.624			100.000		62.522	5.392

Spectrum: TE1 SPOT F

ELMT	ZAF	%ELMT	+-	Error	ATOM.%		%OXIDE	FORMULA
CaK : 1	1.017	27.020	+-	.258	25.937	CaO	37.806	3.493
P K : 1	1.219	10.386	+-	.170	12.902	P2O5	23.800	1.738
NaK : 2	.622	< .507	+-	.254				
MgK : 1	.793	< .151	+-	.075				
AlK : 1	.879	< .115	+-	.058				
ClK : 1	.951	< .118	+-	.059				
K K : 1	1.128	< .143	+-	.072				
FeK : 1	.820	< .238	+-	.119				
S K : 1	.922	.332	+-	.076	.398	SO	.497	.054
SrL : 1	.852	< .348	+-	.174				
MnK : 1	.800	< .194	+-	.097				
PbM : 1	.661	< .347	+-	.173				
CuK : 1	.793	< .389	+-	.194				
ZnK : 1	.790	< .546	+-	.273				
O K : 1	.000	24.703			59.401			8.000
TOTAL		62.441			100.000		62.103	5.284

APPENDIX Vb : ADDITIONAL PIXE DATA FOR ARCHAEOLOGICAL BONE MATERIAL.

Hartlepool femur

(2500um)

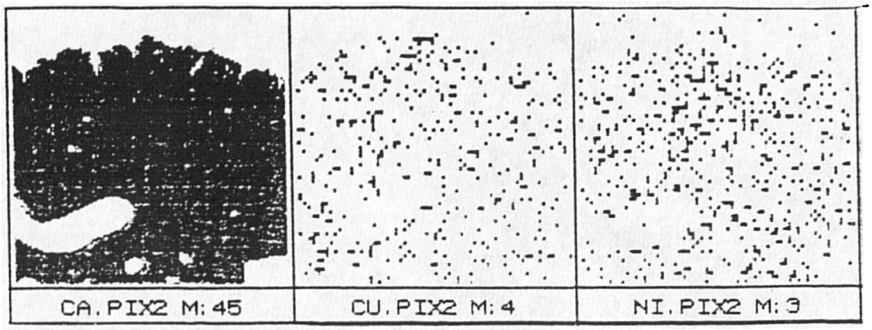

Canterbury femur

(2500um)

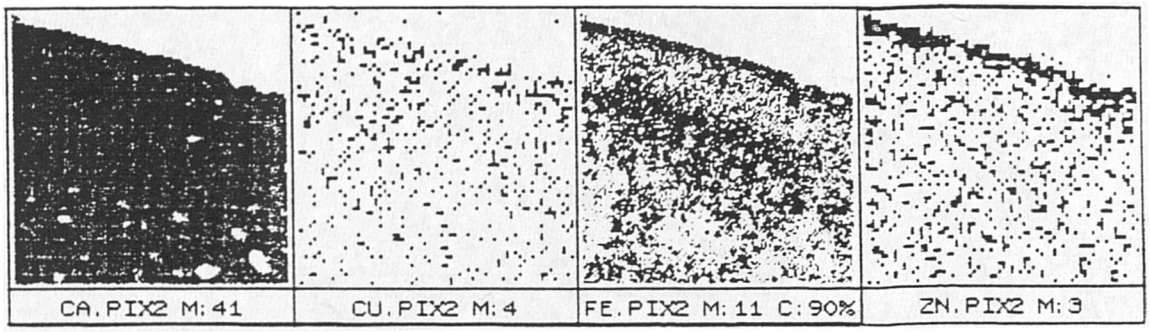

Watchfield femur

(125um)

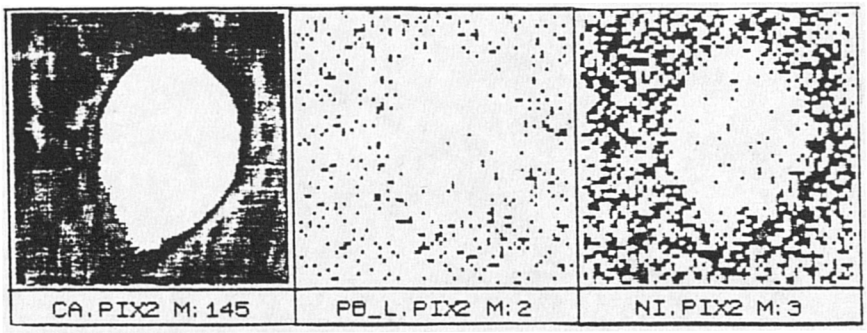

Mary Rose clavicle

(2500um)

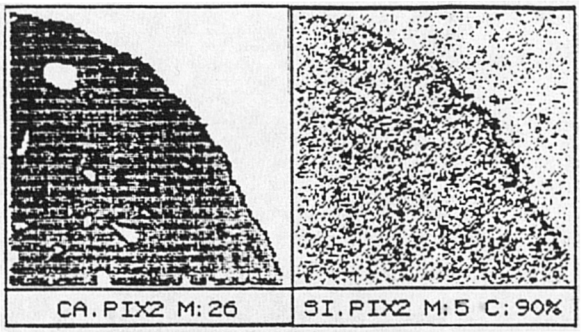

Bay of Agay

(2500um)

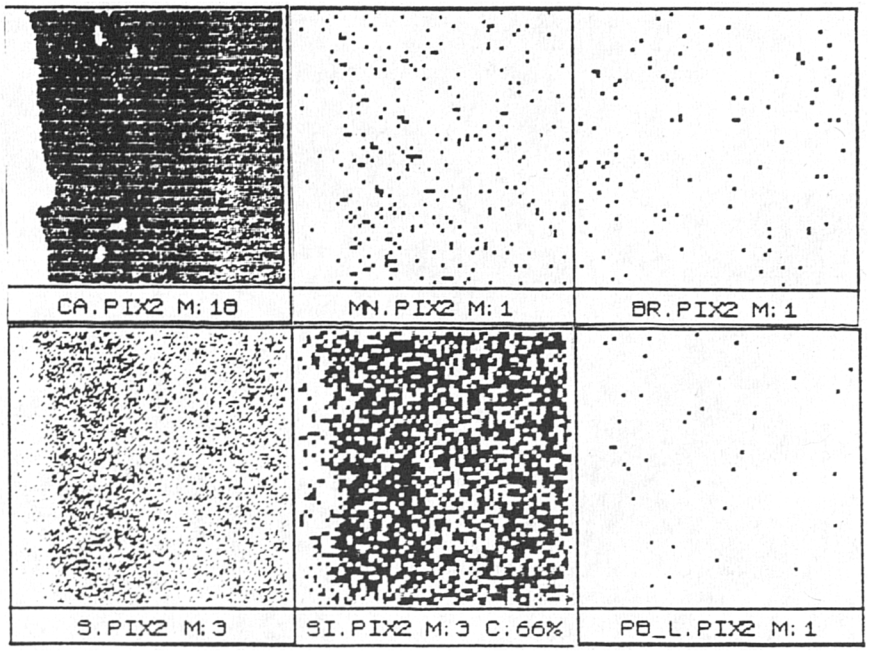

Pompeii

(2500um)

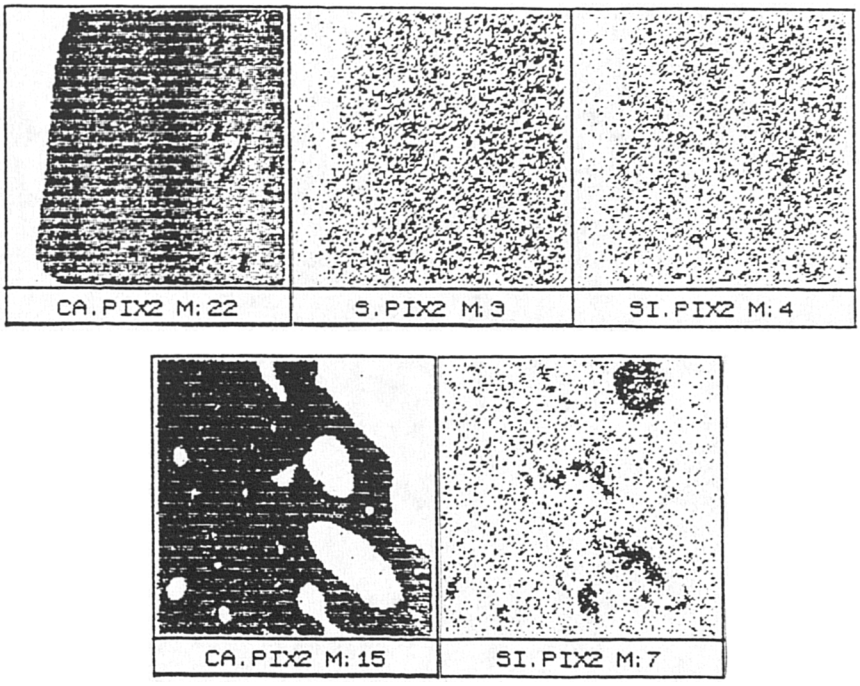

APPENDIX Vc : QUANTITATIVE ANALYSIS OF HARTLEPOOL BONE BY PIXE.

PIXE RESULTS FOR RUN S119009.PIX2

SPM233: Hartlepool femur (11-OCT-90)

<<<<<<<<<<<<<<<<<<<<<<<<<<<<<<<<<<<<<<<<<<<<<<<<<<<< Oxford University SPM Unit >>

Proton beam:
Energy: 3.000 MeV
Dose: 0.3171E-01 uC (1.97917E+11 particles)

Detector:
Area: 80.000 mm2 Be window : 8.0um
Dist to sample: 17.000 mm Thickness : 4.0mm
Solid angle: 276.817 msr Au layer : 0.000um
Angle to beam: 60.00 deg Dead layer: 0.100um
Ice layer : 2.750um

Scan size: 2500 x 2500 micron

Filter :Z thick hole(mm2)
Perspex (mm) 0.800 ******

Target: Thickness: 200. um
Density: 1.75 gm/cm3
Areal dens: 34.960 mg/cm2
Matrix construction for sample (by wt)
CA ... 40.0 %
C ... 12.0 %
O ... 48.0 %

>>>>>> Please note that the calculated concentrations assume the target composition and thickness quoted above <<<<<<

Element		Concentration (see above)	Stat. error	Minimum detectable limit	Peak counts	Molar conc. (mole/l)	Det. effic (%)	Approx. self abs. effect (%)	Areal density
Bromine	:	14.71 ppm+-	23.8%	6.6 ppm	51.9	322. uM/l	72.26	16.42	514. ng/cm2
Calcium	:	5.75 % +-	0.1%	41.9 ppm	570177.6	2.51 M/l	9.82	50.90	2.01 mg/cm2
Chlorine	:	66.00 ppm+-	21.3%	32.0 ppm	471.3	3.25 mM/l	8.77	74.30	2.31 ug/cm2
Chromium	:	19.19 ppm+-	44.0%	19.1 ppm	93.2	645. uM/l	20.29	65.06	671. ng/cm2
Copper	:		<	8.2 ppm	15.4		51.41	100.00	8.50 ng/cm2
Iron	:		<	11.2 ppm	22.1		32.74	100.00	9.53 ng/cm2
Manganese	:	15.29 ppm+-	41.6%	14.3 ppm	91.4	486. uM/l	26.21	59.30	534. ng/cm2
Nickel	:		<	10.3 ppm			45.66	42.33	
Phosphorus	:	3.32 % +-	0.3%	93.6 ppm	145209.5	1.87 M/l	7.30	86.20	1.16 mg/cm2
Lead	L:	95.00 ppm+-	11.0%	17.3 ppm	165.2	801. uM/l	73.86	21.63	3.32 ug/cm2
Rubidium	:		<	8.4 ppm			75.16	12.47	
Sulphur	:	729.77 ppm+-	7.3%	121.2 ppm	4346.2	39.8 mM/l	8.16	80.80	25.5 ug/cm2
Strontium	:	155.28 ppm+-	6.2%	7.8 ppm	293.1	3.10 mM/l	76.10	11.01	5.43 ug/cm2
Thorium	L:						74.52	100.00	
Uranium	L:		<	21.0 ppm			75.49	11.99	
Yttrium	:						76.76	100.00	
Zinc	:	97.09 ppm+-	4.9%	7.3 ppm	749.2	2.60 mM/l	56.49	32.69	3.39 ug/cm2
TOTAL	:	9.18 %							

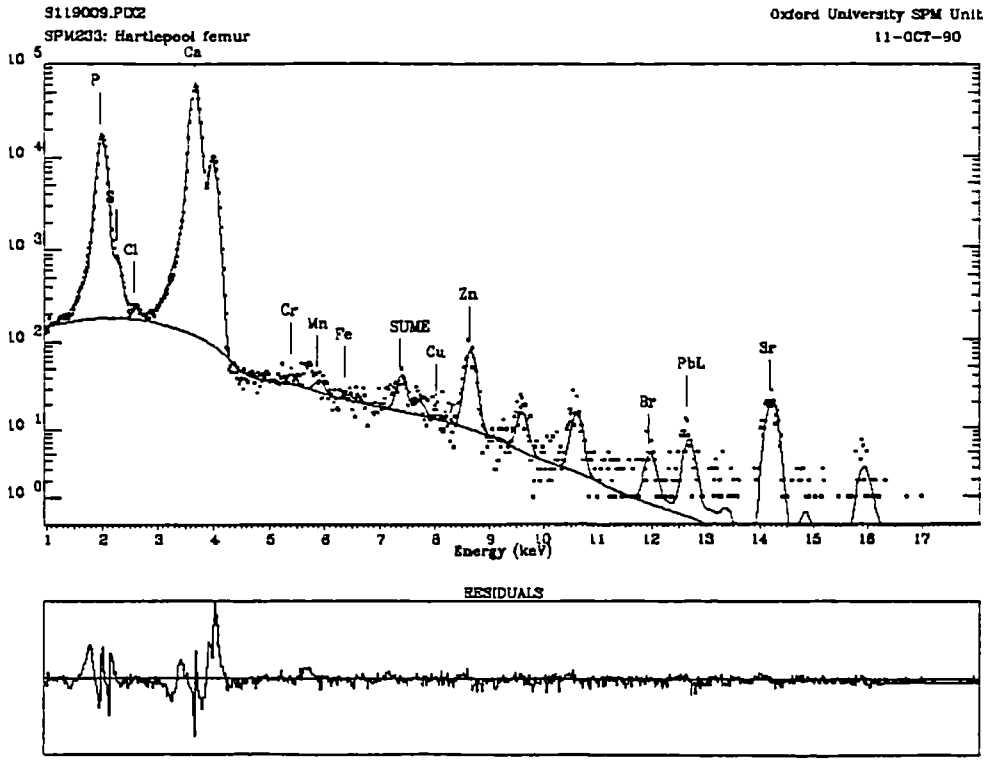

APPENDIX Vd : QUANTITATIVE ANALYSIS OF "MARY ROSE" BONE BY PIXE/RBS.

Run 181.015 SPM325 Mary Rose Clavicle t: 0:06:45 Beam Q: 0.0294uC

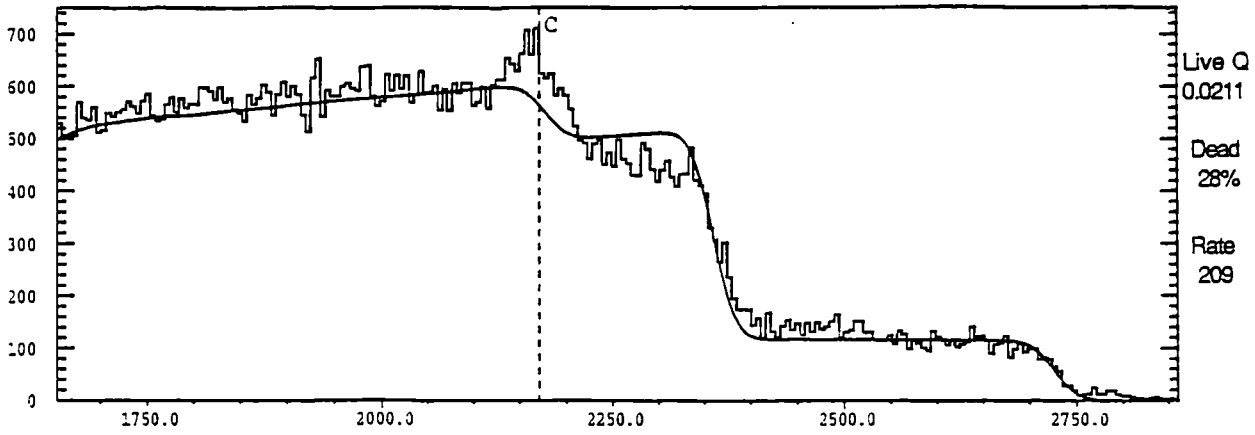

ADC3: RBS spectrum (keV) Detector: BIG

Matrix Composition for RUMP simulation

Layer 1: CaCO3 80.00um 1.75g/cm3 13.98mg/cm2 5.257E+22at/cm3

Q correction factor = 0.7500

Oxford University SPM Facility

Run 181.015 SPM325 Mary Rose Clavicle t: 0:06:45 Beam Q: 0.0176uC

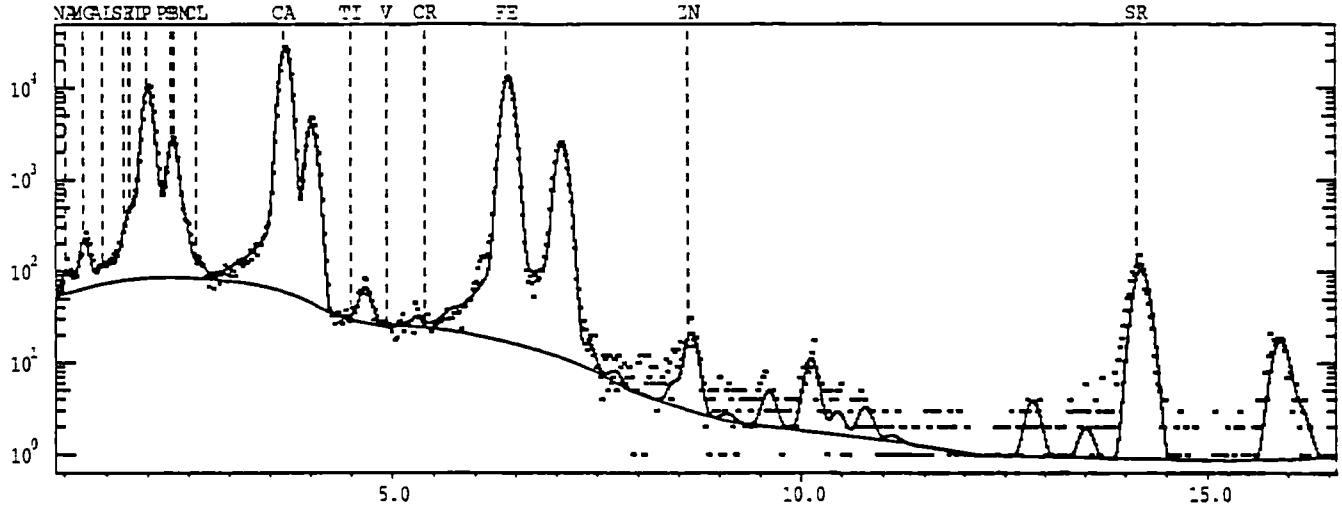

ADC2: PIXE spectrum (keV) Detector: LS3N d=23.0mm Filter:Perspx

RESIDUALS

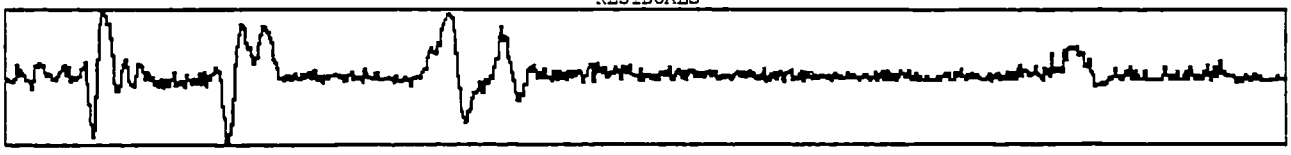

Peak	Counts	ppm or %	MDL	Peak	Counts	ppm or %	MDL
NA	263	7839.3 +- 14%	2473.8	TI	28	80.2 +-100%	207.5
MG	905	8817.7 +- 5%	983.0	V	13	23.9 +-100%	120.0
AL	206	1003.8 +- 25%	577.0	CR	21	23.1 +-100%	72.6
SI	581	1651.4 +- 15%	591.7	MN	-		68.5
SRL	1349	0.0 +- 10%	0.0	FE	99401	5.3%+- 0%	0.0%
P	61328	13.5%+- 0%	0.0%	NI	-		25.3
S	14333	2.3%+- 1%	0.1%	CU	-		12.6
PBM	1331	0.0 +- 15%	0.0	ZN	152	64.1 +- 11%	11.6
CL	210	286.6 +- 36%	237.9	PBL	-		38.0
K	-		184.5	SR	1077	1824.0 +- 3%	22.8
CA	192179	20.6%+- 0%	0.0%				

APPENDIX Ve: XRF ANALYSIS OF ARCHAEOLOGICAL/EXHUMED BONE.
(Ca, P, Sr and U)

Bone description	Ca	P	Sr ppm	U ppm	Sr/Ca	U/Ca
	% oxide				x 10	
Mary Rose	50.24	42.47	1899.15	28.27	378.00	5.63
Olduvai 2.1	52.21	42.29	3983.37	22.18	762.95	4.24
Olduvai 13.3 (whole)	50.71	43.08	1575.44	9.56	310.68	1.89
Olduvai 13.3 (B)	52.35	40.04	1461.62	17.20	279.20	3.29
Olduvai 13.3 (T)	51.20	43.43	1816.62	6.77	354.81	1.32
Watchfield SK#304	54.43	40.39	384.74	8.38	70.69	1.53
Watchfield SK#304 rib	52.04	41.21	400.83	9.14	77.02	1.76
Watchfield SK#108	50.84	43.56	444.38	2.67	87.41	0.53
Watchfield SK#108 rib	51.29	42.86	514.96	2.05	100.40	0.39
Watchfield SK#321	52.02	42.75	553.27	4.81	106.40	0.92
Canterbury SK#23	53.70	31.94	400.00	2.13	74.49	0.40
Canterbury SK#24	52.45	30.33	350.80	3.01	66.73	0.57
Canterbury SK#24 rib	47.84	26.49	389.00	6.26	81.31	1.31
Canterbury SK#13	52.97	31.39	347.00	2.03	65.51	0.38
Canterbury SK#10	49.35	30.37	372.00	4.72	75.38	0.96
Canterbury SK#71	53.56	31.43	288.00	2.51	53.77	0.46
Hartlepool	52.76	37.43	221.00	4.97	41.90	0.94
Hartlepool	53.80	38.98	239.00	3.00	44.40	0.56
Hartlepool	53.60	38.70	215.00	9.91	40.11	1.85
Hartlepool rib	51.89	36.47	247.00	13.78	47.60	2.66

APPENDIX Vf : QUANTITATIVE ANALYSIS OF SOILS BY XRF.

APPENDIX Vf.i : XRF ANALYSIS OF MAJOR ELEMENTS IN SOILS.
(All values quoted as % oxides.)

(a) Soils collected from Hartlepool, Cleveland.

(i) Soils found near femoral bone

Distance from bone (cm)	% oxides									
	Si	Al	Fe	Mg	Ca	Na	K	Mn	P	S
0	17.65	03.17	00.25	14.41	25.33	00.02	00.36	00.01	00.52	00.03
5	01.27	00.32	00.27	20.24	30.39	00.01	00.06	00.02	00.39	00.01
10	01.38	00.31	00.26	20.31	30.00	00.01	00.06	00.01	00.03	00.01
15	01.40	00.32	00.27	20.56	30.10	00.01	00.06	00.01	00.05	00.01

(ii) Soils found near tibial bone

Distance from bone (cm)	% oxides									
	Si	Al	Fe	Mg	Ca	Na	K	Mn	P	S
0	05.38	00.90	00.71	18.75	28.29	00.01	00.13	00.02	00.11	00.01
5	04.94	01.04	00.75	19.14	28.45	00.01	00.16	00.02	00.12	00.01
10	03.84	00.91	00.67	19.11	29.61	00.01	00.13	00.02	00.04	00.01
15	04.39	00.87	00.67	19.66	28.79	00.01	00.13	00.02	00.04	00.02
0	04.85	00.86	00.64	20.85	29.00	00.00	00.21	00.02	00.05	-
5	05.23	01.06	00.81	20.13	28.49	00.00	00.23	00.02	00.04	-
10	09.80	02.00	01.22	18.95	25.75	00.01	00.43	00.03	00.04	-
15	07.22	01.45	00.93	20.10	27.61	00.00	00.34	00.04	00.03	-

APPENDIX Vf.i cont.

(b) Soils collected from Canterbury, Kent.

(i) Soils found near humeral bone.

Distance from bone (cm)	% oxides									
	Si	Al	Fe	Mg	Ca	Na	K	Mn	P	S
0	70.81	10.61	05.27	02.10	05.76	00.47	01.92	00.08	00.86	-
5	70.00	10.56	05.51	02.11	06.00	00.47	01.94	00.09	00.92	-
15	65.48	10.19	05.58	02.56	09.27	00.45	01.96	00.11	00.59	-
General	64.11	08.29	03.89	02.11	12.19	00.43	01.53	00.08	00.50	-

(ii) Soils found near rib bone.

Distance from bone (cm)	% oxides									
	Si	Al	Fe	Mg	Ca	Na	K	Mn	P	S
0	77.91	10.66	05.02	01.86	02.31	00.47	01.85	00.07	01.01	-
5	77.05	10.82	05.12	01.87	02.71	00.47	01.87	00.08	01.02	-
20	74.53	10.25	05.20	01.79	03.98	00.44	01.80	00.09	01.10	-

(iii) Soils found near femoral bone.

Distance from bone (cm)	% oxides									
	Si	Al	Fe	Mg	Ca	Na	K	Mn	P	S
0	77.10	10.74	04.97	01.85	02.61	00.46	01.87	00.09	00.98	-
10	74.05	10.04	05.09	01.81	03.35	00.47	01.82	00.10	00.98	-
20	76.50	10.51	05.14	01.84	03.54	00.47	01.83	00.12	00.95	-
40	77.72	09.68	04.92	01.75	02.26	00.48	01.76	00.14	00.97	-
0	68.85	10.30	04.52	02.11	07.70	00.43	01.81	00.07	00.98	-
0	73.29	10.69	05.76	01.99	03.69	00.45	01.87	00.11	01.30	-

APPENDIX Vf.i cont.

(c) Soils collected in Watchfield, Oxfordshire.

(i) Soils found near femoral bone.

Distance from bone (cm)	% oxides									
	Si	Al	Fe	Mg	Ca	Na	K	Mn	P	S
0	57.69	05.98	22.40	01.47	02.70	00.32	00.99	00.20	01.57	-
5	56.95	06.37	24.27	01.53	02.60	00.33	01.04	00.21	01.57	-
10	53.90	06.56	25.35	01.56	02.55	00.32	01.09	00.21	01.58	-
15	56.81	06.65	25.48	01.54	02.14	00.33	01.08	00.23	01.56	-
25	52.88	06.32	29.10	01.49	01.47	00.35	01.05	00.23	01.26	-
0	-	-	-	-	02.91	-	-	-	-	-
5	-	-	-	-	02.84	-	-	-	-	-
15	-	-	-	-	02.25	-	-	-	-	-
25	66.68	06.11	21.62	01.37	01.73	00.32	00.95	00.24	01.10	-
0	61.60	06.44	22.00	01.54	02.18	00.36	01.09	00.20	01.33	-
5	58.74	06.26	24.19	01.46	01.58	00.34	00.96	00.22	01.27	-
10	57.31	06.07	25.22	01.47	02.00	00.36	01.01	00.25	01.29	-
20	55.69	05.97	26.38	01.48	01.98	00.37	01.03	00.26	01.29	-
15	59.56	06.76	22.65	01.54	02.48	00.33	01.13	00.25	01.42	-
0	59.42	06.35	22.86	01.49	02.45	00.32	01.08	00.23	01.45	-
10	57.76	06.58	23.17	01.53	02.13	00.34	01.10	00.24	01.53	-
20	55.48	06.49	25.62	01.53	01.70	00.37	01.08	00.26	01.27	-

where distance = 0 refers to soil immediately adjacent to bone in situ.
'general'= soil sample taken from the site (not associated with grave contexts) as a general example.
- = value not measured.

APPENDIX Vf.ii : XRF ANALYSIS OF MINOR/TRACE ELEMENTS IN SOILS.
(All values quoted in ppm.)

(a) Soils collected from Hartlepool, Cleveland.

(i) Soils found near femoral bone.

Distance from bone (cm)	Ba	Sr	Rb	Zn	Cu	Ni	Pb	U	Th
0	140.0	083.0	025.0	043.0	016.0	014.0	031.0	001.0	010.0
5	053.0	065.0	009.0	043.0	005.0	005.0	017.0	003.0	011.0
10	052.0	058.0	009.0	052.0	008.0	005.0	016.0	002.0	011.0
15	052.0	057.0	008.0	089.0	008.0	200.0	018.0	003.0	010.0

(ii) Soils found near tibial bone.

Distance from bone (cm)	Ba	Sr	Rb	Zn	Cu	Ni	Pb	U	Th
0	061.0	067.0	015.0	049.0	008.0	001.0	020.0	001.0	009.0
5	062.0	074.0	017.0	054.0	008.0	001.0	019.0	002.0	008.0
10	061.0	063.0	016.0	053.0	010.0	002.0	019.0	002.0	009.0
15	065.0	064.0	015.0	067.0	008.0	006.0	018.0	003.0	010.0
0	069.0	084.0	002.0	038.0	006.0	009.0	019.0	001.0	006.0
5	071.0	075.0	006.0	040.0	008.0	012.0	022.0	001.0	007.0
10	118.0	080.0	013.0	042.0	008.0	013.0	019.0	001.0	007.0
15	110.0	081.0	015.0	043.0	005.0	012.0	021.0	002.0	005.0

APPENDIX Vf.ii cont.

(b) Soils collected from Canterbury, Kent.

(i) Soils found near humeral bone.

Distance from bone (cm)	Ba	Sr	Rb	p p m Zn	Cu	Ni	Pb	U	Th
0	339.0	121.0	-	-	-	-	-	000.0	-
5	346.0	119.0	-	-	-	-	-	000.0	-
15	329.0	144.0	-	-	-	-	-	000.0	-
General	252.0	136.0	-	-	-	-	-	000.0	-

(ii) Soils found near rib bone.

Distance from bone (cm)	Ba	Sr	Rb	p p m Zn	Cu	Ni	Pb	U	Th
0	369.0	101.0	-	-	-	-	-	000.0	-
5	366.0	107.0	-	-	-	-	-	000.0	-
20	352.0	117.0	-	-	-	-	-	000.0	-

(iii) Soils found near femoral bone.

Distance from bone (cm)	Ba	Sr	Rb	p p m Zn	Cu	Ni	Pb	U	Th
0	363.0	097.0	-	-	-	-	-	000.0	-
10	355.0	101.0	-	-	-	-	-	000.0	-
20	347.0	105.0	-	-	-	-	-	000.0	-
40	419.0	099.0	-	-	-	-	-	000.0	-
0	350.0	130.0	-	-	-	-	-	000.0	-
0	392.0	117.0	-	-	-	-	-	000.0	-

APPENDIX Vf.ii cont.

(c) Soils collected from Watchfield, Oxfordshire.

(i) Soils found near femoral bone.

Distance from bone (cm)	Ba	Sr	Rb	p p m Zn	Cu	Ni	Pb	U	Th	
0	137.0	064.0	-	-	-	-	-	000.0		-
10	138.0	067.0	-	-	-	-	-	000.0		-
15	137.0	061.0	-	-	-	-	-	000.0		-
25	121.0	046.0	-	-	-	-	-	000.0		-
25	144.0	049.0	-	-	-	-	-	000.0		-
0	173.0	056.0	-	-	-	-	-	000.0		-
5	134.0	049.0	-	-	-	-	-	000.0		-
20	146.0	046.0	-	-	-	-	-	000.0		-
15	172.0	060.0	-	-	-	-	-	000.0		-
5	165.0	060.0	-	-	-	-	-	000.0		-
10	166.0	057.0	-	-	-	-	-	000.0		-
20	148.0	043.0	-	-	-	-	-	000.0		-

where distance = 0 refers to soil immediately adjacent to bone in situ.
'general'= soil sample taken from the site (not associated with grave contexts) as a general example.
- = value not measured.

APPENDIX Vg
QUANTITATIVE DATA FOR REFERENCE BONE AND SOILS.

1. Average measured values using XRF spectrometry

2. Certified values by reference authorities.

Note: In addition to these reference standards, a range of geological materials were used to calibrate the instrumentation: these include basalts (specifically BE-N, BR), dolomitic limestone (NBS88A), argillaceous limestones (NBS1a, NBS1c), granites (NIM-G, NIM-L) and syenite (SY-3). These are provided by the National Bureau of Standards and British Chemical Standards.

REF.MATERIAL	SOURCE	CaO	P2O5	Fe2O3	MnO	SiO2	Al2O3	MgO	Na2O	K2O	Sr	Zn	U	Cu
H5 animal bone	IAEA	40.4%	25.0%	0.02%	N/K	N/K	N/K	N/K	N/K	N/K	129ppm	120ppm	N/K	N/K
certified values		21.2%	10.2%	0.008%	N/K	N/K	N/K	0.36%	0.5%	0.07%	96ppm	89ppm	N/K	N/K
SARM-32 rock phosphate	BCS	55.20%	37.53%	N/K	N/K	N/K	N/K	N/K	N/K	N/K	4555ppm	N/K	N/K	N/K
certified values		54.44%	39.96%	N/K	N/K	N/K	N/K	N/K	N/K	N/K	5200ppm	N/K	N/K	N/K
Soil-7	IAEA	21.78%	0.13%	3.33%	0.48%	39.21%	9.89%	1.95%	0.33%	1.52%	103ppm	94ppm	3ppm	13ppm
certified values		20.9%	0.05%	3.7%	0.63%	38.5%	8.9%	1.9%	0.6%	2.9%	108ppm	104ppm	2.6ppm	11ppm
SO-3 Soil	BCS	53.13%	0.16%	5.66%	1.03%	30.05%	5.37%	5.89%	-	-	196ppm	35.6ppm	1.11ppm	5ppm
certified values		20.71%	0.11%	-	0.07%	33.72%	5.80%	8.42%	1.01%	1.40%	222ppm	48.3ppm	1.11ppm	17ppm

BCS= British Chemical Standards issued by the Bureau of Analysed Samples Ltd.

IAEA= International Atomic Energy Agency.

N/K= values not measured